

STRUCTURAL DESIGN FOR
FIRE SAFETY

ANDREW H. BUCHANAN
ANTHONY K. ABU

SECOND EDITION

WILEY

STRUCTURAL DESIGN FOR FIRE SAFETY

STRUCTURAL DESIGN FOR FIRE SAFETY

Second Edition

Andrew H. Buchanan & Anthony K. Abu
University of Canterbury, New Zealand

WILEY

This edition first published 2017
© 2017 John Wiley & Sons, Ltd

First Edition published in 2001

Registered Office

John Wiley & Sons, Ltd, The Atrium, Southern Gate, Chichester, West Sussex, PO19 8SQ, United Kingdom

For details of our global editorial offices, for customer services and for information about how to apply for permission to reuse the copyright material in this book please see our website at www.wiley.com.

The right of the author to be identified as the author of this work has been asserted in accordance with the Copyright, Designs and Patents Act 1988.

All rights reserved. No part of this publication may be reproduced, stored in a retrieval system, or transmitted, in any form or by any means, electronic, mechanical, photocopying, recording or otherwise, except as permitted by the UK Copyright, Designs and Patents Act 1988, without the prior permission of the publisher.

Wiley also publishes its books in a variety of electronic formats. Some content that appears in print may not be available in electronic books.

Designations used by companies to distinguish their products are often claimed as trademarks. All brand names and product names used in this book are trade names, service marks, trademarks or registered trademarks of their respective owners. The publisher is not associated with any product or vendor mentioned in this book.

Limit of Liability/Disclaimer of Warranty: While the publisher and author have used their best efforts in preparing this book, they make no representations or warranties with respect to the accuracy or completeness of the contents of this book and specifically disclaim any implied warranties of merchantability or fitness for a particular purpose. It is sold on the understanding that the publisher is not engaged in rendering professional services and neither the publisher nor the author shall be liable for damages arising herefrom. If professional advice or other expert assistance is required, the services of a competent professional should be sought.

Library of Congress Cataloging-in-Publication Data

Names: Buchanan, Andrew Hamilton, 1948– author. | Abu, Anthony Kwabena, 1980– author.

Title: Structural design for fire safety / Andrew H. Buchanan, Anthony K. Abu.

Description: Second edition. | Chichester, West Sussex, United Kingdom : John Wiley & Sons Inc., 2017. |

Includes bibliographical references and index.

Identifiers: LCCN 2016032579 | ISBN 9780470972892 (cloth) | ISBN 9781118700396 (epub)

Subjects: LCSH: Building, Fireproof. | Structural engineering.

Classification: LCC TH1065 .B89 2017 | DDC 693.8/2–dc23

LC record available at <https://lccn.loc.gov/2016032579>

A catalogue record for this book is available from the British Library.

Cover image: AUSTRIA FIRE RETIREMENT HOME

(Media ID: 20080209000077529215)

Credit: EPA | Source: APA | Trans Ref: EGG03

Set in 10/12pt Times by SPi Global, Pondicherry, India

10 9 8 7 6 5 4 3 2 1

Contents

Preface	xv
List of Notations	xvi
1 Introduction	1
1.1 Objective and Target Audience	1
1.2 Fire Safety	2
1.3 Performance-based Design	2
<i>1.3.1 Fundamentals of Performance-based Design</i>	2
<i>1.3.2 Documentation and Quality Control</i>	4
<i>1.3.3 Risk Assessment</i>	4
1.4 Structural Fire Engineering	5
1.5 Purpose of this Book	5
1.6 Units	6
1.7 Organization of Chapters	6
2 Fire Safety in Buildings	8
2.1 Fire Safety Objectives	8
<i>2.1.1 Life Safety</i>	8
<i>2.1.2 Property Protection</i>	9
<i>2.1.3 Environmental Protection</i>	9
2.2 Process of Fire Development	9
<i>2.2.1 Fire Behaviour</i>	10
<i>2.2.2 Human Behaviour</i>	11
<i>2.2.3 Fire Detection</i>	12
<i>2.2.4 Active Control</i>	12
<i>2.2.5 Passive Control</i>	12
2.3 Conceptual Framework for Fire Safety	13
<i>2.3.1 Scenario Analysis</i>	13
<i>2.3.2 Quantitative Risk Assessment</i>	13
<i>2.3.3 Fire Safety Concepts Tree</i>	14

2.4	Fire Resistance	17
2.4.1	<i>Examples of Fire Resistance</i>	17
2.4.2	<i>Objectives for Fire Resistance</i>	19
2.4.3	<i>Fire Design Time</i>	20
2.4.4	<i>Trade-offs</i>	21
2.4.5	<i>Repairability and Reserviceability</i>	22
2.5	Controlling Fire Spread	22
2.5.1	<i>Fire Spread within Room of Origin</i>	22
2.5.2	<i>Fire Spread to Adjacent Rooms</i>	23
2.5.3	<i>Fire Spread to Other Storeys</i>	25
2.5.4	<i>Fire Spread to Other Buildings</i>	27
2.6	Building Construction for Fire Safety	29
2.6.1	<i>Fire during Construction and Alterations</i>	29
2.6.2	<i>Fire following Earthquake</i>	30
2.7	Assessment and Repair of Fire Damage	31
2.7.1	<i>Inspection</i>	32
2.7.2	<i>Steel</i>	32
2.7.3	<i>Concrete and Masonry</i>	33
2.7.4	<i>Timber</i>	33
3	Fires and Heat	35
3.1	Fires in General	35
3.2	Combustion	37
3.3	Fire Initiation	39
3.3.1	<i>Sources and Mechanisms</i>	39
3.3.2	<i>Pilot Ignition and Auto-ignition</i>	39
3.3.3	<i>Flame Spread</i>	39
3.4	Pre-flashover Fires	40
3.4.1	<i>Burning Items in Open Air</i>	40
3.4.2	<i>Burning Items in Rooms</i>	42
3.4.3	<i>t-Squared Fires</i>	44
3.4.4	<i>Fire Spread to Other Items</i>	46
3.4.5	<i>Pre-flashover Fire Calculations</i>	46
3.5	Flashover	48
3.5.1	<i>Conditions Necessary for Flashover</i>	48
3.6	Post-flashover Fires	49
3.6.1	<i>Ventilation Controlled Burning</i>	49
3.6.2	<i>Fuel Controlled Burning</i>	53
3.6.3	<i>Fire Temperatures</i>	54
3.6.4	<i>Computer Models</i>	58
3.7	Design Fires	60
3.7.1	<i>Hand Methods</i>	60
3.7.2	<i>Published Curves</i>	61
3.7.3	<i>Eurocode Parametric Fires</i>	62

3.8	Other Factors	66
3.8.1	<i>Additional Ventilation Openings</i>	66
3.8.2	<i>Progressive Burning</i>	66
3.8.3	<i>Localized Fires</i>	69
3.9	Heat Transfer	69
3.9.1	<i>Conduction</i>	69
3.9.2	<i>Convection</i>	72
3.9.3	<i>Radiation</i>	72
3.9.4	<i>Design Charts for Fire Resistance Calculation</i>	74
3.10	Worked Examples	75
4	Fire Severity and Fire Resistance	84
4.1	Providing Fire Resistance	84
4.1.1	<i>Background</i>	84
4.1.2	<i>Fire Exposure Models</i>	88
4.1.3	<i>Design Combinations</i>	89
4.2	Fire Severity	89
4.3	Equivalent Fire Severity	90
4.3.1	<i>Equal Area Concept</i>	90
4.3.2	<i>Maximum Temperature Concept</i>	91
4.3.3	<i>Minimum Load Capacity Concept</i>	92
4.3.4	<i>Time Equivalent Formulae</i>	92
4.4	Fire Resistance	95
4.4.1	<i>Definition</i>	95
4.4.2	<i>Assessing Fire Resistance</i>	95
4.5	Fire Resistance Tests	96
4.5.1	<i>Standards</i>	96
4.5.2	<i>Test Equipment</i>	97
4.5.3	<i>Failure Criteria</i>	97
4.5.4	<i>Standard of Construction</i>	101
4.5.5	<i>Furnace Pressure</i>	101
4.5.6	<i>Applied Loads</i>	101
4.5.7	<i>Restraint and Continuity</i>	102
4.5.8	<i>Small-scale Furnaces</i>	103
4.6	Specifying Fire Resistance	103
4.6.1	<i>Approved Fire Resistance Ratings</i>	103
4.6.2	<i>Fire Resistance by Calculation</i>	104
4.7	Fire Resistance of Assemblies	107
4.7.1	<i>Walls</i>	107
4.7.2	<i>Floors</i>	108
4.7.3	<i>Beams</i>	108
4.7.4	<i>Columns</i>	108
4.7.5	<i>Penetrations</i>	109
4.7.6	<i>Junctions and Gaps</i>	110

4.7.7	<i>Seismic Gaps</i>	110
4.7.8	<i>Fire Doors</i>	110
4.7.9	<i>Ducts</i>	111
4.7.10	<i>Glass</i>	112
4.7.11	<i>Historical Buildings</i>	112
4.8	Worked Examples	113
5	Design of Structures Exposed to Fire	115
5.1	Structural Design at Normal Temperatures	115
5.2	Loads	116
5.2.1	<i>Types of Load</i>	116
5.2.2	<i>Load Combinations</i>	116
5.2.3	<i>Structural Analysis</i>	116
5.2.4	<i>Non-linear Analysis</i>	117
5.2.5	<i>Design Format</i>	117
5.2.6	<i>Working Stress Design Format</i>	118
5.2.7	<i>Ultimate Strength Design Format</i>	119
5.2.8	<i>Material Properties</i>	120
5.2.9	<i>Probability of Failure</i>	121
5.3	Structural Design in Fire Conditions	122
5.3.1	<i>Design Equation</i>	123
5.3.2	<i>Loads for Fire Design</i>	124
5.3.3	<i>Structural Analysis for Fire Design</i>	125
5.4	Material Properties in Fire	126
5.4.1	<i>Testing Regimes</i>	126
5.4.2	<i>Components of Strain</i>	127
5.5	Design of Individual Members Exposed to Fire	130
5.5.1	<i>Tension Members</i>	130
5.5.2	<i>Compression Members</i>	130
5.5.3	<i>Beams</i>	131
5.6	Design of Structural Assemblies Exposed to Fire	135
5.6.1	<i>Frames</i>	135
5.6.2	<i>Redundancy</i>	135
5.6.3	<i>Disproportionate Collapse</i>	136
5.6.4	<i>Continuity</i>	136
5.6.5	<i>Plastic Design</i>	142
5.6.6	<i>Axial Restraint</i>	143
5.6.7	<i>After-fire Stability</i>	149
5.7	Worked Examples	149
6	Steel Structures	154
6.1	Behaviour of Steel Structures in Fire	154
6.1.1	<i>Structural Steel Design Process</i>	155

6.2	Steel Temperature Prediction	157
6.2.1	<i>Fire Exposure</i>	157
6.2.2	<i>Calculation Methods</i>	158
6.2.3	<i>Section Factor</i>	158
6.2.4	<i>Thermal Properties</i>	159
6.2.5	<i>Temperature Calculation for Unprotected Steelwork</i>	161
6.2.6	<i>Temperature Calculation for Protected Steelwork</i>	163
6.2.7	<i>Typical Steel Temperatures</i>	164
6.2.8	<i>Temperature Calculation for External Steelwork</i>	165
6.3	Protection Systems	166
6.3.1	<i>Concrete Encasement</i>	167
6.3.2	<i>Board Systems</i>	167
6.3.3	<i>Spray-on Systems</i>	169
6.3.4	<i>Intumescent Paint</i>	169
6.3.5	<i>Protection with Timber</i>	170
6.3.6	<i>Concrete Filling</i>	170
6.3.7	<i>Water Filling</i>	171
6.3.8	<i>Flame Shields</i>	171
6.4	Mechanical Properties of Steel at Elevated Temperature	171
6.4.1	<i>Components of Strain</i>	171
6.4.2	<i>Thermal Strain</i>	172
6.4.3	<i>Creep Strain</i>	173
6.4.4	<i>Stress-related Strain</i>	174
6.4.5	<i>Proof Strength and Yield Strength</i>	174
6.4.6	<i>Design Values</i>	175
6.4.7	<i>Modulus of Elasticity</i>	178
6.4.8	<i>Residual Stresses</i>	179
6.5	Design of Steel Members Exposed to Fire	179
6.5.1	<i>Design Methods</i>	179
6.5.2	<i>Design of Steel Tensile Members</i>	180
6.5.3	<i>Design of Simply Supported Steel Beams</i>	181
6.5.4	<i>Lateral-torsional Buckling</i>	184
6.5.5	<i>Design for Shear</i>	184
6.5.6	<i>Continuous Steel Beams</i>	185
6.5.7	<i>Steel Columns</i>	186
6.6	Bolted and Welded Connections	187
6.7	Cast-iron Members	188
6.8	Design of Steel Buildings Exposed to Fire	188
6.9	Worked Examples	188
7	Concrete Structures	195
7.1	Behaviour of Concrete Structures in Fire	195
7.2	Concrete Materials in Fire	196
7.2.1	<i>Normal Weight Concrete</i>	196

7.2.2	<i>High Strength Concrete</i>	196
7.2.3	<i>Lightweight Concrete</i>	198
7.2.4	<i>Steel-fibre Reinforced Concrete</i>	199
7.2.5	<i>Masonry</i>	199
7.2.6	<i>Prestressed Concrete</i>	199
7.2.7	<i>External Reinforcing</i>	200
7.3	Spalling of Cover Concrete	201
7.3.1	<i>Cover</i>	201
7.3.2	<i>Spalling</i>	201
7.4	Concrete and Steel Reinforcing Temperatures	202
7.4.1	<i>Fire Exposure</i>	202
7.4.2	<i>Calculation Methods</i>	202
7.4.3	<i>Thermal Properties</i>	204
7.5	Mechanical Properties of Concrete at Elevated Temperatures	207
7.5.1	<i>Test Methods</i>	207
7.5.2	<i>Components of Strain</i>	207
7.5.3	<i>Thermal Strain</i>	208
7.5.4	<i>Creep Strain and Transient Strain</i>	209
7.5.5	<i>Stress Related Strain</i>	209
7.6	Design of Concrete Members Exposed to Fire	213
7.6.1	<i>Member Design</i>	215
7.6.2	<i>Simply Supported Concrete Slabs and Beams</i>	215
7.6.3	<i>Shear Strength</i>	217
7.6.4	<i>Continuous Slabs and Beams</i>	218
7.6.5	<i>Axial Restraint</i>	220
7.6.6	<i>Reinforced Concrete Columns</i>	223
7.6.7	<i>Reinforced Concrete Walls</i>	223
7.6.8	<i>Reinforced Concrete Frames</i>	224
7.7	Worked Examples	224
8	Composite Structures	234
8.1	Fire Resistance of Composite Elements	234
8.2	Assessing Fire Resistance	237
8.2.1	<i>Tabulated Data for Beams and Columns</i>	237
8.2.2	<i>Simple Calculation Methods</i>	237
8.2.3	<i>Advanced Calculation Methods</i>	238
8.3	Behaviour and Design of Individual Composite Members in Fire	238
8.3.1	<i>Composite Slabs</i>	238
8.3.2	<i>Composite Beams</i>	240
8.3.3	<i>Composite Columns</i>	243
8.4	Design of Steel and Composite Buildings Exposed to Fire	248
8.4.1	<i>Multi-storey Steel Frame Buildings</i>	248
8.4.2	<i>Car Parking Buildings</i>	251
8.4.3	<i>Single-storey Portal Frame Buildings</i>	252
8.5	Worked Example	255

9	Timber Structures	257
9.1	Description of Timber Construction	257
9.1.1	<i>Heavy Timber Construction</i>	257
9.1.2	<i>Laminated Timber</i>	258
9.1.3	<i>Behaviour of Timber Structures in Fire</i>	259
9.1.4	<i>Fire Resistance Ratings</i>	260
9.1.5	<i>Fire Retardant Treatments</i>	261
9.2	Wood Temperatures	261
9.2.1	<i>Temperatures Below the Char</i>	262
9.2.2	<i>Thermal Properties of Wood</i>	262
9.3	Mechanical Properties of Wood	264
9.3.1	<i>Mechanical Properties of Wood at Normal Temperatures</i>	264
9.3.2	<i>Mechanical Properties of Wood at Elevated Temperatures</i>	266
9.4	Charring Rate	273
9.4.1	<i>Overview of Charring</i>	273
9.4.2	<i>Corner Rounding</i>	275
9.4.3	<i>Charring Rate of Protected Timber</i>	276
9.4.4	<i>Effect of Heated Wood Below the Char Line</i>	277
9.4.5	<i>Design for Realistic Fires</i>	279
9.5	Design for Fire Resistance of Heavy Timber Members	280
9.5.1	<i>Design Concepts</i>	280
9.5.2	<i>Timber Beams</i>	280
9.5.3	<i>Timber Tensile Members</i>	283
9.5.4	<i>Timber Columns</i>	283
9.5.5	<i>Empirical Equations</i>	284
9.5.6	<i>Timber Beam-columns</i>	285
9.5.7	<i>Timber Decking</i>	286
9.5.8	<i>Hollow Core Timber Floors</i>	288
9.5.9	<i>Timber-concrete Composite Floors</i>	288
9.5.10	<i>Cross Laminated Timber</i>	288
9.5.11	<i>Reinforced Glulam Timber</i>	289
9.5.12	<i>Post-tensioned Timber Structures</i>	289
9.6	Timber Connections in Fire	290
9.6.1	<i>Geometry of Timber Connections</i>	291
9.6.2	<i>Steel Dowel-type Fasteners</i>	292
9.6.3	<i>Connections with Side Members of Wood</i>	293
9.6.4	<i>Connections with External Steel Plates</i>	295
9.6.5	<i>Glued Timber Connections</i>	296
9.7	Worked Examples	297
10	Light Frame Construction	301
10.1	Summary of Light Frame Construction	301
10.2	Gypsum Plaster Board	304
10.2.1	<i>Manufacture</i>	304

10.2.2	<i>Types of Gypsum Board</i>	305
10.2.3	<i>Chemistry</i>	306
10.2.4	<i>Thermal Properties</i>	306
10.2.5	<i>Fire Resistance</i>	306
10.2.6	<i>Ablation</i>	308
10.2.7	<i>Cavity Insulation</i>	308
10.3	Fire Behaviour	309
10.3.1	<i>Walls</i>	310
10.3.2	<i>Floors</i>	310
10.3.3	<i>Buildings</i>	310
10.4	Fire Resistance Ratings	311
10.4.1	<i>Failure Criteria</i>	311
10.4.2	<i>Listings</i>	312
10.4.3	<i>Generic Ratings</i>	312
10.4.4	<i>Proprietary Ratings</i>	312
10.4.5	<i>Typical Fire Resistance Ratings</i>	312
10.4.6	<i>Fire Severity</i>	313
10.5	Design for Separating Function	314
10.5.1	<i>Temperatures Within Light Frame Assemblies</i>	314
10.5.2	<i>Insulation</i>	315
10.5.3	<i>Component Additive Methods</i>	316
10.5.4	<i>Finite Element Calculations</i>	317
10.6	Design for Load-bearing Capacity	318
10.6.1	<i>Verification Methods</i>	318
10.6.2	<i>Calculation Methods</i>	318
10.6.3	<i>Onset of Char Method</i>	318
10.6.4	<i>Fire Test Performance</i>	319
10.6.5	<i>Timber Stud Walls</i>	320
10.6.6	<i>Calculation of Structural Performance</i>	320
10.6.7	<i>Buckling of Studs</i>	322
10.6.8	<i>End Restraint</i>	323
10.6.9	<i>Steam Softening</i>	324
10.6.10	<i>Finite Element Calculation Methods</i>	324
10.7	Steel Stud Walls	325
10.7.1	<i>Design of Steel Stud Walls</i>	325
10.8	Timber Joist Floors	327
10.9	Timber Trusses	328
10.10	Construction Details	329
10.10.1	<i>Number of Layers</i>	329
10.10.2	<i>Fixing of Sheets</i>	329
10.10.3	<i>Resilient Channels</i>	331
10.10.4	<i>Penetrations</i>	332
10.10.5	<i>Party Walls</i>	333
10.10.6	<i>Fire Stopping, Junctions</i>	334
10.10.7	<i>Conflicting Requirements</i>	335

10.11	Lightweight Sandwich Panels	335
	10.11.1 Description	335
	10.11.2 Structural Behaviour	335
	10.11.3 Fire Behaviour	336
	10.11.4 Fire Resistance	337
	10.11.5 Design	339
11	Advanced Calculation Methods	340
11.1	Types of Advanced Calculation Methods	340
11.2	Fire Models	341
	11.2.1 Plume Models	342
	11.2.2 Zone Models	342
	11.2.3 CFD Models	343
	11.2.4 Post-flashover Fire Models	343
11.3	Thermal Response Models	344
	11.3.1 Test Data and Simple Calculation Methods	344
	11.3.2 Thermal Modelling with Advanced Calculation Methods	344
11.4	Advanced Structural Models	348
11.5	Advanced Hand Calculation Methods	349
	11.5.1 Steel-concrete Composite Floors	349
	11.5.2 Tensile Membrane Action	349
	11.5.3 The Membrane Action Method	350
	11.5.4 The Slab Panel Method	353
	11.5.5 Failure Mechanisms of Composite Slabs	353
11.6	Finite Element Methods for Advanced Structural Calculations	355
	11.6.1 Structural Behaviour Under Fire Conditions	355
	11.6.2 Finite Element Analysis Under Fire Conditions	358
	11.6.3 Material Properties	359
	11.6.4 Structural Properties	364
11.7	Software Packages for Structural and Thermal Fire Analysis	369
	11.7.1 Generic Software Packages	369
	11.7.2 Specific Structural Fire Engineering Software	370
12	Design Recommendations	371
12.1	Summary of Main Points	371
	12.1.1 Fire Exposure	371
	12.1.2 Fire Resistance	372
12.2	Summary for Main Materials	372
	12.2.1 Structural Steel	372
	12.2.2 Reinforced Concrete	373
	12.2.3 Steel-concrete Composite Construction	374
	12.2.4 Heavy Timber	374
	12.2.5 Light Frame Construction	375
12.3	Thermal Analysis	375
12.4	Conclusions	376

Appendix A: Units and Conversion Factors	377
Appendix B: Section Factors for Steel Beams	381
References	394
Index	411

Preface

Fires in buildings have always been a threat to human life and property. The threat increases as larger numbers of people live and work in bigger buildings throughout the world. Professor Buchanan's interest in structural fire engineering was initiated by Professor Brady Williamson in the 1970s at the University of California at Berkeley, and developed during his subsequent career as a practising structural engineer, then as an academic. Dr Abu was introduced to the subject by Professor Ian Burgess and Professor Roger Plank at the University of Sheffield in 2004, and has since worked with a number of consultants in the field.

New Zealand became one of the first countries to adopt a performance-based building code in the late 1980s, stimulating a demand for qualified fire engineers. This led to the establishment of a Master's Degree in Fire Engineering at the University of Canterbury, where one of the core courses is structural fire engineering, now taught by Dr Abu. The lecture notes for that course have grown into this book. Many masters and PhD students have conducted research which has contributed to our knowledge of fire safety, and much of that is reported here.

Professor Buchanan and Dr Abu have both been involved in many problems of fire safety and fire resistance, designing fire resisting components for buildings, assisting manufacturers of fire protecting materials, and serving on national fire safety committees.

Preparation of this book would not have been possible without the help of many people. We wish to thank Charley Fleischmann, Michael Spearpoint, Peter Moss, Rajesh Dhakal and other colleagues in the Department of Civil and Natural Resources Engineering at the University of Canterbury, and a large number of graduate students.

Many people provided helpful comments on the text, figures, and underlying concepts, especially Philip Xie, Melody Callahan, and a large number of friends and colleagues in the international structural fire engineering community.

This book is only a beginning; the problem of fire safety is very old and will not go away. We hope that this book helps to encourage rational improvements to structural fire safety in buildings throughout the world.

The second edition has been a long time coming because of devastating earthquakes in Christchurch and other unforeseen difficulties. We hope that it has been worth the wait.

Andrew H. Buchanan and Anthony K. Abu
University of Canterbury, New Zealand

List of Notations

α	Fire intensity coefficient	MW/s ²
α	Thermal diffusivity	m ² /s
α	Ratio of hot wood strength to cold wood strength	
α_h	Horizontal openings ratio	
α_v	Vertical openings ratio	
β	Target reliability	
β	Measured charring rate	mm/min
β_1	Effective charring rate if corner rounding ignored	mm/min
β_n	Nominal charring rate	mm/min
β_{par}	Charring rate for parametric fire exposure	mm/min
δ	Beam deflection	mm
Δ	Deflection	mm
Δ_L	Maximum permitted displacement	mm
Δ_0	Mid-span deflection of the reference specimen	mm
χ	Buckling factor	
ε	Strain	
ε_i	Initial strain	
ε_σ	Stress-related strain	
ε_{cr}	Creep strain	
ε_{th}	Thermal strain	
ε_{tr}	Transient strain	
ε	Resultant emissivity	
ε_e	Emissivity of the emitting surface	
ε_r	Emissivity of the receiving surface	
ϕ	Configuration factor	
Φ	Strength reduction factor	
Φ_f	Strength reduction factor for fire design	
k	Elastic curvature	1/m
γ_M	Partial safety factor for material	
γ_G	Partial safety factor for dead load	
γ_Q	Partial safety factor for live load	

η	Temperature ratio	
θ	Plastic hinge rotation	rad
θ	Radiating angle	rad
ρ	Density	kg/m ³
σ	Stefan–Boltzmann constant	kW/m ² K ⁴
σ	Stress	MPa
ν_p	Regression rate	m/s
ξ	Reduction coefficient for charring of decks	
a	Depth of heat affected zone below char layer	mm
a	Depth of rectangular stress block	mm
a	Distance of the maximum positive moment from the support	m
a_f	Depth of stress block, reduced by fire	mm
a_{fi}	Thickness of wood protection to connections	mm
A	Cross-sectional area	mm ² , m ²
A_f	Floor area of room	m ²
A_{fi}	Area of member, reduced by fire	mm ² , m ²
A_{fuel}	Exposed surface area of burning fuel	m ²
A_h	Area of horizontal ceiling opening	m ²
A_1	Area of radiating surface 1	m ²
A_r	Cross-sectional area reduced by fire	mm ² , m ²
A_s	Area of reinforcing steel	mm ²
A_t	Total internal surface area of room	m ²
A_w	Window area	m ²
b	Breadth of beam	mm
b_f	Breadth of beam reduced by fire	mm
b	$\sqrt{\text{Thermal inertia}} = \sqrt{(k\rho c_p)}$	Ws ^{0.5} /m ² K
b_v	Vertical opening factor	
B	Breadth of window opening	m
c	Thickness of char layer	mm
c_p	Specific heat	J/kg K
c_v	Concrete cover to reinforcing	mm
C	Compressive force	kN
C	Contraction	mm
d	Depth of beam, effective depth of concrete beam	mm
d	Thickness of timber deck	mm
d	Diameter of circular column or width of square column	mm
d_f	Depth of beam reduced by fire	mm
d_i	Thickness of insulation	mm
D	Length of short side of compartment	m
D	Deflection	mm
D	Thickness of slab of burning wood	m
D_b	Reinforcing bar diameter	mm
e	Eccentricity	mm
e_f	Fuel load energy density (per unit floor area)	MJ/m ²
e_t	Fuel load energy density (per unit area of internal room surfaces)	MJ/m ²
E	Modulus of elasticity	GPa
E	Total energy contained in fuel	MJ

E_k	Characteristic earthquake load	
f	Factor in concrete-filled steel column equation	
f	Stress	MPa
f^m	Calculated stress in member	MPa
f_t^m	Calculated tensile stress for working stress design	MPa
f_a	Allowable design stress for working stress design	MPa
f_b	Characteristic flexural strength	MPa
$f_{b,f}$	Characteristic flexural strength in fire conditions	MPa
f_c	Crushing strength of the material	MPa
f_c'	Characteristic compressive strength	MPa
$f_{c,T}'$	Compressive strength at elevated temperature	MPa
f_t	Characteristic tensile strength	MPa
f_{tv}	Long term allowable tensile strength	MPa
$f_{t,f}$	Characteristic tensile strength in fire conditions	MPa
f_y	Yield strength at 20 °C	MPa
$f_{y,T}$	Yield strength at elevated temperature	MPa
F	Surface area of unit length of steel	m ²
F_c	Crushing load of column	kN
F_{crit}	Critical buckling load of column	kN
F_v	Ventilation factor ($A_v\sqrt{H_v}/A_t$)	m ^{0.5}
g	Acceleration of gravity	m/s ²
g	Char parameter	
G	Dead load	
G_k	Characteristic dead load	
h	Slab thickness	mm
h	Initial height of test specimen	mm
h	Height from mid-height of window to ceiling	m
h_c	Convective heat transfer coefficient	W/m ² K
h_r	Radiative heat transfer coefficient	W/m ² K
h_t	Total heat transfer coefficient	W/m ² K
H	Height of radiating surface	m
H_p	Heated perimeter of steel cross section	m
H_r	Height of room	m
H_v	Height of window opening	m
ΔH_c	Calorific value of fuel	MJ/kg
ΔH_c	Heat of combustion of fuel	MJ/kg
$\Delta H_{c,n}$	Effective calorific value of fuel	MJ/kg
I	Moment of inertia	mm ⁴
jd	Internal lever arm in reinforced concrete beam	mm
k	Growth parameter for t ² fire	s/ \sqrt{MW}
k	Thermal conductivity	W/mK
k_i	Thermal conductivity of insulation	W/mK
k_a	Ratio of allowable strength to ultimate strength	
k_b	Compartment lining parameter	min m ² /MJ
k_c	Compartment lining parameter	min m ^{2.25} /MJ
k_f	Strength reduction factor for heated wood	
k_{mean}	Factor to convert allowable stress to mean failure stress	
$k_{c,T}$	Reduction factor for concrete strength	
$k_{E,T}$	Reduction factor for modulus of elasticity	

$k_{y,T}$	Reduction factor for yield strength	
k_d	Duration of load factor for wood strength	
k_{sh}	Correction factor for shadow effect	
k_{20}	Factor to convert 5th percentile to 20th percentile	
K	Effective length factor for column	
l_1, l_2	Dimensions of floor plan	m
L	Fire load (wood mass equivalent)	kg
L	Length of structural member	mm
L_f	Factored load for fire design	
L_u	Factored load for ultimate limit state	
L_w	Load for working stress design	
L_v	Heat of gasification	MJ/kg
m_c	Moisture content as percentage by weight	%
\dot{m}	Rate of burning	kg/s
M	Mass per unit length of steel cross section	kg
M	Mass of fuel	kg
M	Bending moment	kN.m
M^-	Negative bending moment	kN.m
M^{*cold}	Design bending moment in cold conditions	kN.m
M^{*fire}	Design bending moment in fire conditions	kN.m
$M^{*fire,red}$	Design bending moment of plastic hinge in fire conditions	kN.m
M_f	Total mass of fuel available for combustion	kg
M_f	Flexural capacity in fire conditions	kN.m
M_n	Flexural capacity in cold conditions	kN.m
M_y	Moment capacity at the start of yielding	kN.m
M_p	Moment capacity of plastic hinge	kN.m
M_p^+	Positive moment capacity of plastic hinge	kN.m
M_p^-	Negative moment capacity of plastic hinge	kN.m
M_u	Moment capacity	kN.m
N	Axial load, axial load capacity	kN
N_c	Crushing strength capacity	kN
N_{crit}	Critical buckling strength	kN
N_n	Axial load capacity	kN
N_w	Axial tensile force for working stress design	kN
N_u	Axial load capacity	kN
N_f	Axial load capacity in fire conditions	kN
N^*	Design axial force	kN
N^{*fire}	Design axial force in fire conditions	kN
p	Perimeter of fire exposed cross section	m
q_p	Surface burning rate	kg/s/m ²
\dot{q}	Heat flux	W/m ²
q_i	Incident radiation reaching fuel surface	kW/m ²
\dot{q}_C	Heat produced by combustion of fuel	kW
\dot{q}_L	Heat carried out of the opening by convection of hot gases and smoke	kW
\dot{q}_R	Heat radiated through the opening	kW
\dot{q}_W	Heat conducted into the surrounding structure	kW
Q	Rate of heat release	MW
Q_{fo}	Critical heat release rate for flashover	MW
Q_p	Peak heat release rate	MW

Q_{fuel}	Rate of heat release for fuel controlled fire	MW
Q_{vent}	Rate of heat release for ventilation controlled fire	MW
Q	Live load	
Q_k	Characteristic live load	
r	Radius of gyration	mm
r	Radius of charred corner	mm
r	Distance from radiator to receiver	m
r_{load}	Load ratio	
R	Load capacity	
R_a	Ratio of actual to allowable load at normal temperature	
R_f	Minimum load capacity reached during the fire	
R_{code}	Load capacity reached at time t_{code}	
R_{cold}	Load capacity in cold conditions	
R_{fire}	Load capacity in fire conditions	
s	Thickness of compartment lining material	m
s_{lim}	Limit thickness	m
s	Heated perimeter	mm
S	Plastic section modulus	mm ³
S_k	Characteristic snow load	
SW	Self-weight	
t	Thickness of steel plate	mm
t	Time	h, min or s
t^*	Fictitious time	h
t_e	Equivalent duration of exposure to the standard fire to a complete burnout of a real fire in the same room	min
t_{fail}	Time to failure of the element when exposed to the standard fire	
t_b	Duration of burning	min
t_d	Duration of burning period (ventilation controlled)	h
t_{fo}	Time to flashover	s
t_{lim}	Duration of burning period (fuel controlled)	h
t_{max}	Time to reach maximum temperature	h
t_{max}^*	Fictitious time to reach maximum temperature	h
t_{code}	Time of fire resistance required by the building code	min
t_r	Time of fire resistance	min
t_s	Time of fire severity	min
T	Thermal thrust	kN
T	Temperature	°C
T_e	Absolute temperature of the emitting surface	K
T_r	Absolute temperature of the receiving surface	K
T_g	Gas temperature	°C
T_i	Initial temperature of wood	°C
T_{lim}	Limiting temperature	°C
T_{code}	Temperature reached at time t_{code}	°C
T_{fail}	Temperature of failure	°C
T_{max}	Maximum temperature	°C
T_p	Temperature of wood at start of charring	°C
T_0	Ambient temperature	°C
T_y	Tensile force at yield	kN
U	Load effect	

U_f	Load effect in fire conditions	
U_f^*	Design force for ultimate limit state design	
U_f^*	Design force in fire conditions	
V_{fire}	Volume of unit length of steel member	m^3
V_f	Shear capacity in fire conditions	kN
V	Shear capacity	kN
V^*	Design shear force	kN
V_f^*	Design shear force in fire conditions	kN
w	Ventilation factor	
w	Uniformly distributed load on beam	kN/m
w_c	Uniformly distributed load on beam, in cold conditions	kN/m
w_f	Uniformly distributed load on beam, in fire conditions	kN/m
\bar{W}	Length of long side of compartment	m
W	Width of radiating surface	m
W_k	Characteristic wind load	
x	Distance in the direction of heat flow	m
x	Height ratio	
y	Width ratio	
y_b	Distance from the neutral axis to the extreme bottom fibre	(mm)
z	Thickness of zero strength layer	mm
z	Load factor	
Z	Elastic section modulus	mm^3
Z_f	Elastic section modulus in fire conditions	mm^3

1

Introduction

This book is an introduction to the structural design of buildings and building elements exposed to fire. Structural fire resistance is discussed in relation to overall concepts of building fire safety. The book brings together, from many sources, a large volume of material relating to the fire resistance of building structures. It starts with fundamentals, giving an introduction to fires and fire safety, outlining the important contribution of structural fire resistance to overall fire safety.

Methods of calculating fire severity and achieving fire resistance are described, including fire performance of the main structural materials. The most important parts of the book are the design sections, where the earlier material is synthesised and recommendations are made for rational design of building elements and structures exposed to fires.

This book refers to codes and standards as little as possible. The emphasis is on understanding structural behaviour in fire from first principles, allowing structural fire safety to be provided using rational engineering methods based on national structural design codes.

1.1 Objective and Target Audience

This book is primarily written for practising structural engineers and students in structural engineering who need to assess the structural performance of steel, concrete or timber structures exposed to unwanted fires. A basic knowledge of structural mechanics and structural design is assumed. The coverage of fire science in this book is superficial, but sufficient as a starting point for structural engineers and building designers. For more detail, readers should consult recognised texts such as Quintiere (1998), Karlsson and Quintiere (2000) and Drysdale (2011), and the Handbook of the Society of Fire Protection Engineers (SFPE, 2008). This book will help fire engineers in their discussions with structural engineers, and will also be

useful to architects, building inspectors, code officials, firefighters, students, researchers and others interested in building fire safety.

A structural engineer who has followed this book should be able to:

- interpret the intentions of code requirements for structural fire safety;
- understand the concepts of fire severity and fire resistance;
- estimate time–temperature curves for fully developed compartment fires;
- design steel, concrete, steel-concrete composite, or timber structures to resist fire exposure;
- assess the fire performance of existing structures.

1.2 Fire Safety

Unwanted fire is a destructive force that causes many thousands of deaths and billions of dollars of property loss each year. People around the world expect that their homes and workplaces will be safe from the ravages of an unwanted fire. Unfortunately, fires can occur in almost any kind of building, often when least expected. The safety of the occupants depends on many factors in the design and construction of buildings, often focusing on the escape of people from burning buildings. Occupant escape and firefighter access is only possible if buildings and parts of buildings will not collapse in a fire or allow the fire to spread. Fire safety science is a rapidly expanding multi-disciplinary field of study. It requires integration of many different fields of science and engineering, some of which are summarized in this book.

Fire deaths and property losses could be eliminated if all fires were prevented, or if all fires were extinguished at the size of a match flame. Much can be done to reduce the probability of occurrence, but it is impossible to prevent all major fires. Given that some fires will always occur, there are many strategies for reducing their impact, and some combination of these will generally be used by designers. The best proven fire safety technology is the provision of automatic fire sprinklers because they have been shown to have a very high probability of controlling or extinguishing any fire. It is also necessary to provide facilities for the detection and notification of fires, safe travel paths for the movement of occupants and firefighters, barriers to control the spread of fire and smoke, and structures which will not collapse prematurely when exposed to fire. The proper selection, design and use of building materials is very important, hence this book.

1.3 Performance-based Design

1.3.1 *Fundamentals of Performance-based Design*

Until recently, most design for fire safety has been based on *prescriptive* building codes, with little or no opportunity for designers to take a rational engineering approach. Many countries have recently adopted *performance-based* building codes which allow designers to use any fire safety strategy they wish, provided that adequate safety can be demonstrated (Hurley and Bukowski, 2008). In general terms, a prescriptive code states how a building is to be constructed whereas a performance-based code states how a building is to perform under a wide range of conditions (Custer and Meacham, 1997).

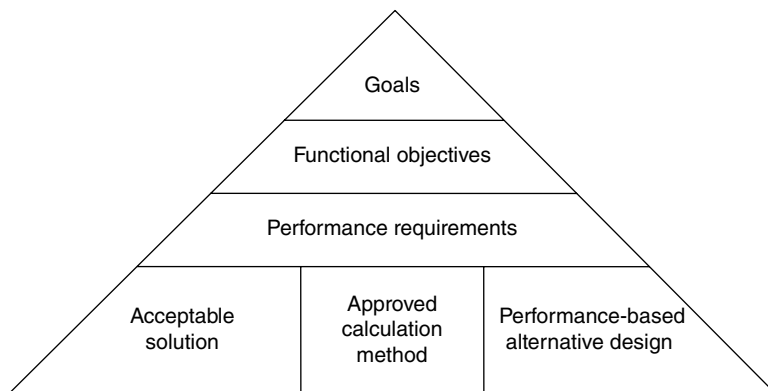


Figure 1.1 Typical hierarchical relationship for performance-based design

Some prescriptive building codes give the opportunity for performance-based selection of structural assemblies. For example, if a code specifies a floor with a fire resistance rating of two hours, the designer has the freedom to select from a wide range of approved floor systems which have sufficient fire resistance. This book provides tools for assessing the fire performance of structural elements which have been tested, as well as those with different geometry, loads or fire exposure from those tested.

In the development of new codes, many countries have adopted a multi-level hierarchical performance-based code format as shown in Figure 1.1. At the highest levels, there is legislation specifying the overall goals, functional objectives and required performance which must be achieved in all buildings. At a lower implementation level, there is a selection of alternative means of achieving those goals. The three most common options are:

1. A prescriptive 'Acceptable Solution' (sometimes call a 'deemed-to-satisfy' solution).
2. An approved standard calculation method.
3. A performance-based 'Alternative Design' which is a more comprehensive fire engineering design from first principles.

Standard calculation methods are still being developed for widespread use, so compliance with performance-based codes in most countries is usually achieved by simply meeting the requirements of the Acceptable Solution, with options 2 and 3 being used for special cases or very important buildings. Alternative Designs can sometimes be used to justify variations from the Acceptable Solution in order to provide improved safety, cost savings, or other benefits.

The code environment in New Zealand (described by Spearpoint, 2008), is similar to that in England, Australia and some Scandinavian countries. Moves towards performance-based codes are being taken in the United States (SFPE, 2000). Codes are different around the world, but the objectives are similar; that is to protect life and property from the effects of fire (ABCB, 2005). It is not easy to produce or use performance-based fire codes for many reasons; fire safety is part of a complex system of many interacting variables, there are so many possible strategies that it is not simple to assess performance in quantitative terms, and there is lack of

information on behaviour of fires and the performance of people and buildings exposed to fires. A number of useful documents have been produced to assist users of performance-based codes, including Custer and Meacham (1997), BS7974 (BSI, 2001), ABCB (2005), Spearpoint (2008) and ISO 23932 (2009). This book provides useful additional information, addressing the design of structures for fire safety, which is a small but important segment of the overall provision of fire safety.

1.3.2 Documentation and Quality Control

As the provision of fire safety in buildings moves away from blind adherence to prescriptive codes towards rational engineering which meets specified performance goals, the need for comprehensive documentation and quality control becomes increasingly important. It is recommended (ABCB, 2005; ISO, 2009) that quantitative calculations be put in context with a 'qualitative design review' which defines the objectives and acceptance criteria for the design, identifies potential hazards and fire scenarios, and reviews the overall design and fire safety features. The review and accompanying calculations should be included in a comprehensive report which describes the building and the complete fire design process (Caldwell *et al.*, 1999). The report should address installation and maintenance of the fire protection features, and management of the building to ensure fire safety, with reference to drawings and documentation from other consultants.

It is important to consider quality control of fire safety throughout the design, construction and eventual use of the building, starting as early as possible in the planning process. Changes to the design often occur during construction, and these may affect fire safety if the significance of the original details is not well documented and well understood on the job site. The approving or checking authorities should also prepare a comprehensive report describing the design and the basis on which it is accepted or rejected. Those taking responsibility for design, approval and site inspection must be suitably qualified. The reliability of active and passive fire protection will depend on the quality of the construction, including workmanship and supervision.

1.3.3 Risk Assessment

Fire safety is all about risk. The probability of a serious fire in any building is low, but the possible consequences of such a fire are enormous. The objectives of design for fire safety are to provide an environment with an acceptably low probability of loss of life or property loss due to fire. Tools for quantitative risk assessment in fire safety are still in their infancy, so most fire engineering design is deterministic. The design methods in this book are deterministic, and must be applied with appropriate safety factors to ensure that they produce an acceptable level of safety.

Fire safety engineering is not a precise discipline, because any assessment of safety requires judgement as to how fire and smoke will behave in the event of an unplanned ignition, and how fire protection systems and the occupants of the building will respond. Design to provide fire safety is based on scenario analysis. For any scenario it is possible to calculate some responses, but the level of accuracy can only be as good as the design assumptions, the input data and the analytical methods available. Fire safety engineering is a very new discipline, so the precision of calculation methods will improve as the discipline matures, but it will always

be necessary to exercise engineering judgement based on experience and logical thinking, using all the information that is available. Analysis of past fire disasters and visits to actual fires and fire damaged buildings are excellent ways of gaining experience.

1.4 Structural Fire Engineering

Traditional fire resistance has been simply achieved by designing buildings for room-temperature conditions, then wrapping individual structural elements in protective insulation (for steel construction) or in sacrificial material (for concrete or timber construction). The primary reason for this approach is to limit temperatures in the interior of structural components, so that there is sufficient cold cross-section to provide the required structural resistance in fire conditions.

The new discipline of *structural fire engineering* is leading to major advances in the provision of fire resistance, as an important component of overall building fire safety. Structural fire engineering is an amalgamation of the two older disciplines of *structural engineering* and *fire engineering* to ensure better prediction of building behaviour in the event of a fire, and better overall design for fire safety (Lennon, 2011).

Structural fire engineering follows a scientific approach to the design of any building for fire conditions, requiring the identification of objectives and establishing the criteria that need to be met. Based on the potential fires that can develop, an estimate of material and structural response of the structure is made, ensuring a rational level of sophistication is applied to each design scenario to accurately predict structural behaviour (IStructE, 2003, 2007). The improved understanding of fire and structural behaviour has meant that designers can now take advantage of fire resistance that is inherent in buildings due to their structural form, and use innovative methods and materials to provide structural fire safety at reasonable cost (Newman *et al.*, 2006). The design of structural connections has been largely ignored in the traditional design approach, but the collapse of major buildings such as the World Trade Center towers (Gann, 2008) has shown that it is important to tie buildings together to ensure that failure of one element does not result in collapse of other elements or even collapse of the entire building. An understanding of load paths in structures exposed to fires is critical because these are often different from load paths at ambient temperature, requiring an appreciation of global structural behaviour in all scenarios.

There is increasing international collaboration in the field of structural fire engineering, including development of the Eurocodes, new international journals, and regular international conferences such as the bi-annual Structures in Fire (SiF) conference (www.structuresinfire.com).

With all the advantages of structural fire engineering, it is desirable to incorporate it into building design at the conceptual stage, to ensure economic options that produce safe buildings. This book introduces the fundamentals of structural design for fire conditions and the advantages that structural fire engineering can provide.

1.5 Purpose of this Book

Structural design for fire safety concentrates on fire resistance, which is an important part of any design for fire safety. In most buildings, selected structural members and non-structural barriers are provided with fire resistance in order to prevent the spread of fire and smoke, and

to prevent structural collapse during an uncontrolled fire. The provision of fire resistance is just one part of the overall fire design strategy for protecting lives of occupants and fire-fighters, and for limiting property losses. Fire resistance is often described as *passive* fire protection, which is always ready and waiting for a fire, as opposed to *active* fire protection such as automatic sprinklers which are required to activate after a fire is detected. Design strategies often incorporate a combination of active and passive fire protection measures.

Fire resistance is of little significance in the very early stages of a fire, but becomes increasingly important as a fire gets out of control and grows beyond flashover to full room involvement. The importance of fire resistance depends on the size of the building and the fire safety objectives. To provide life safety, fire resistance is essential in all buildings where a fire could grow large before all the occupants have time to escape. This is especially important for large and tall buildings and those where the occupants have difficulty in moving. Fire resistance is also important for Fire Service access and rescue, because firefighters may need to be inside a building well after all the occupants have escaped. Fire resistance is also most important for property protection in buildings of any size, especially if the fire is not controlled with a fire suppression system.

1.6 Units

This book uses metric units throughout. These are generally SI (Système International) units. The basic SI unit for length is the *metre* (m), for time the *second* (s), and for mass the *kilogram* (kg). Weight is expressed using the *newton* (N) where one newton is the force that gives a mass of one kilogram an acceleration of one metre per second per second. On the surface of the earth, one kilogram weighs approximately 9.81 N because the acceleration due to gravity is 9.81 m/s^2 . The basic unit of stress or pressure is the *pascal* (Pa) which is one newton per square metre (N/m^2). It is more common to express stress using the megapascal (MPa) which is one meganewton per square metre (MN/m^2) or identically one newton per square millimetre (N/mm^2).

The basic unit of heat or energy or work is the *joule* (J) defined as the work done when the point of application of one newton is displaced one metre. Heat or energy is more often expressed in thousands of joules [kilojoules (kJ)] or millions of joules [megajoules (MJ)]. The basic unit for rate of power or heat release rate is the *watt* (W). One watt is one joule per second, hence a kilowatt (kW) is a thousand joules per second and a megawatt (MW) is a megajoule per second.

Temperature is most often measured in degrees *Celsius* ($^{\circ}\text{C}$), but for some calculations the temperature must be the *absolute* temperature in *Kelvin* (K). Zero degrees Celsius is 273.15 Kelvin, with the same intervals in each system. A list of units and conversion factors is included in Appendix A. A more extensive list of units and conversion factors can be found in the SFPE Handbook (SFPE, 2008).

1.7 Organization of Chapters

This book is organized in a form suitable for teaching a fire safety design course to structural engineering students. Chapter 2 is a discussion of fire safety in buildings, looking at overall strategies and the importance of preventing spread of fire or structural collapse within the

whole context of fire safety. Chapter 3 is an elemental review of combustion and heat transfer for those with no background in those subjects, and it also describes fire behaviour in rooms in order to give an indication of the impact of an uncontrolled fire on the building structure. Chapter 4 describes fire severity by comparing post-flashover fires with standard test fires. It further describes methods of achieving fire resistance, including standard tests and calculation methods.

The structural engineering section of the book starts in Chapter 5 where structural design for fire conditions is contrasted with structural design at normal temperatures, and important concepts such as flexural continuity, moment redistribution and axial restraint are introduced. The subsequent chapters address the fire behaviour and design of structural materials and assemblies. Chapters 6, 7 and 8 describe steel, reinforced concrete and composite steel construction, while Chapters 9 and 10 cover timber structures and light frame structures. Advanced calculation methods are covered in Chapter 11, and Chapter 12 gives a summary of the recommended fire design methods for structures of different materials.

2

Fire Safety in Buildings

This chapter gives an introduction to the overall strategy for providing fire safety in buildings, and identifies the roles of fire resistance and structural performance as important parts of that strategy.

2.1 Fire Safety Objectives

The primary goal of fire protection is to limit, to acceptable levels, the probability of death, injury, property loss and environmental damage in an unwanted fire. The balance between life safety and property protection varies in different countries, depending on the type of building and its occupancy. The earliest fire brigades and fire codes were promoted by insurance companies who were more interested in property protection than life safety; this was certainly the case at the time of the great fire of London in 1666.

A recent trend has been for national codes to give more emphasis to life safety than to property protection. Some codes assume that fire damage to a building is the problem of the building owner or insurer, with the code provisions only intended to provide life safety and protection to the property of other people. Many fire protection features such as automatic sprinkler systems provide both life safety and property protection. The distinction between life safety and property protection becomes important if the owner is unaware of the likely extent of fire damage to the building and contents, even if the building complies with minimum code requirements.

2.1.1 Life Safety

The most common objective in providing life safety is to ensure safe escape. To do this it is necessary to alert people to the fire, provide suitable escape paths, and ensure that people are not affected by fire or smoke while escaping through those paths to a safe place. In some

buildings it is necessary to provide safety for people unable to escape, such as those under restraint, in a hospital, or in a place of refuge within the building. People in adjacent buildings must also be protected, and it is essential to provide for the safety of firefighters who enter the fire building for rescue or fire control.

2.1.2 *Property Protection*

The objective of protecting property starts with protecting the structure, fabric, and contents of the building. Additional objectives relate to fire protection of neighbouring buildings. An extra level of protection may be necessary if rapid repair and re-use after a fire are important. In many cases an important objective may be to protect intangible items such as possible loss of business or irreplaceable loss of heritage values. A loss disproportionate to the size of the original fire can occur if there is major damage to ‘lifelines’ such as energy distribution or telecommunications facilities.

2.1.3 *Environmental Protection*

In many countries an additional objective is to limit environmental damage in the event of a major fire. The primary concerns are emissions of gaseous pollutants in smoke, and liquid pollution in fire-fighting run-off water, both of which can cause major environmental impacts. The best way to prevent these emissions is to extinguish any fire while it is small. All of the above objectives can be met if any fire is extinguished before growing large, which can be accomplished most easily with an automatic sprinkler system.

2.2 **Process of Fire Development**

Fire safety objectives are usually met with a combination of active and passive fire protection systems. Depending on the design, *Active systems* limit fire development and its effects by some action taken by a person or an automatic device. *Passive systems* on the other hand control the fire or its effects by systems that are built into the structure or fabric of the building, not requiring specific operation at the time of a fire. Some building elements or materials cannot be easily classified as either active or passive systems, for example intumescent coatings which will react automatically in a fire, while fire doors may be shut automatically or by the occupants after a fire is detected. The typical development of a fire in a room is described in Figure 2.1 to emphasize the need for fire protection systems.

Figure 2.1 shows a typical time–temperature curve for the complete process of fire development inside a typical room, assuming no fire suppression. Not all fires follow this development because some fires go out naturally and others do not reach flashover, especially if the fuel item is small and isolated or if there is not enough air to support continued combustion. If a room has very large window openings, too much heat may flow out of the windows for flashover to occur. Complementary to Figure 2.1, Table 2.1 is a summary of the main periods of fire behaviour relative to the active or passive actions that can take place in those periods. The brief discussions that follow relate to Figure 2.1 and Table 2.1, and serve as an introduction to the discussion of fire safety strategies later in this chapter and the description of fire behaviour in Chapter 3.

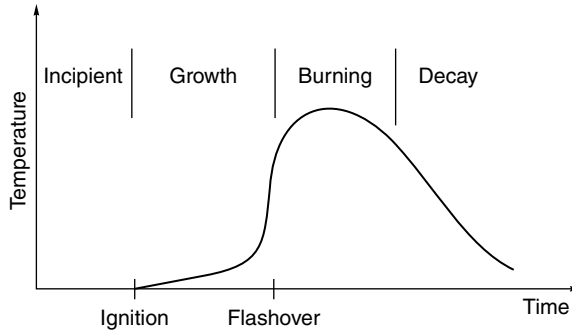


Figure 2.1 Time–temperature curve for full process of fire development

Table 2.1 Summary of periods of typical fire development

	Incipient period	Growth period	Burning period	Decay period
Fire behaviour	Heating of fuel	Fuel controlled burning	Ventilation controlled burning	Fuel controlled burning
Human behaviour	Prevent ignition	Extinguish by hand, escape	Death	
Detection	Smoke detectors	Smoke detectors, heat detectors, etc.	External smoke and flame	
Active control	Prevent ignition	Extinguish by sprinklers or firefighters. Control smoke	Control by fire fighters	
Passive control	Control of materials	Select materials with resistance to flame spread	Provide fire resistance, to contain the fire and prevent collapse	

2.2.1 Fire Behaviour

In the *incipient* period of fire development, heating of potential fuel is taking place. *Ignition* is the start of combustion, marking the transition to the *growth* period. In the growth period, most fires spread slowly at first on combustible surfaces, then more rapidly as the fire grows and there is radiant feedback from flames and hot gases to other fuel items. Hot gases rise by convection and spread across the ceiling, forming a hot upper layer which radiates heat to fuel items lower in the room. If upper layer temperatures reach about 600 °C, the burning rate increases rapidly, leading to *flashover* which is the transition to the *burning* period (often referred to as ‘full room involvement’ or ‘fully developed fire’). The rate of burning in the growth period is generally controlled by the nature of the burning fuel surfaces, whereas in the burning period the temperatures and radiant heat flux within the room are so great that all exposed surfaces are burning and the rate of heat release is usually governed by the available ventilation. It is the burning period of the fire which predominantly impacts on structural elements and compartment boundaries. If the fire is left to burn, eventually the fuel burns out and temperatures drop in the *decay* period, where the rate of burning again becomes a function of the fuel itself rather than the ventilation.



Figure 2.2 Hotel fire where spread of smoke remote from the fire killed 84 people (MGM Grand Hotel, Las Vegas, 1980). Reproduced from Coakley *et al.*, 1982

2.2.2 Human Behaviour

People in the room of origin may see or smell signs of the potential fire during the pre-ignition period when the fuel is being heated by some heat source. Many fires are averted by occupants who prevent ignition by removing the fuel or eliminating the ignition source in the incipient period. After ignition the fire will be more obvious, giving occupants the opportunity to extinguish it while it is very small if they are awake and mobile. Once the fire grows to involve a whole item of furniture or more, it becomes more difficult to be extinguished by hand, but active occupants may have time for escape, provided that smoke has not blocked the escape routes.

Conditions in a room fire become life-threatening during the growth period. After flashover, survival is not possible because of the extreme conditions of heat, temperature and toxic gases. People elsewhere in the building may not know about the fire until it is large, leading to hazardous conditions (Figure 2.2). In order to ensure life safety in the event of a fire, it is essential that the fire be detected, and the occupants be alerted with sufficient information to make a

decision to move, and with sufficient time to reach a safe place before conditions become untenable. The SFPE Handbook (SFPE, 2008) gives more information on human behaviour and tenability limits.

2.2.3 *Fire Detection*

In the incipient period of a fire, human detection is possible by sight or smell. Automatic detection before ignition is possible if a very sensitive aspirating smoke detector has been installed, which is only likely in special buildings containing very valuable items or equipment. After ignition, a growing fire can be detected by the occupants, or by a smoke detector, heat detector or other detectors (Spearpoint, 2008) usually located on the ceiling. Smoke detectors are more sensitive than heat detectors, especially for smouldering fires where there may be life threatening smoke but little heat. Automatic sprinkler systems are activated by heat detecting devices. After flashover, neighbours may detect smoke and flames coming out of windows or other openings.

2.2.4 *Active Control*

Active control refers to control of the fire by some action taken by a person or an automatic device. The best form of active fire protection is an automatic sprinkler system, which discharges water over a local area under one sprinkler head when it is activated by local high temperatures. More sprinkler heads will be activated if local temperatures increase. Sprinkler systems will prevent small fires from growing larger, and may extinguish some fires. A sprinkler system must operate early in a fire to be useful because the water supply system is designed to tackle only a small or moderate fire, well before flashover occurs.

Active control of smoke movement requires the operation of fans or other devices to remove smoke from certain areas or to pressurize stairwells. This may require sophisticated control systems to ensure that smoke and toxic products are removed from the building and not circulated to otherwise safe areas.

Occupants can prevent ignition if they are aware of hazardous situations, and they can extinguish very small fires before they get out of control. Firefighters can actively control or extinguish a fire, but they can only do so if they arrive before it gets too large. Time is critical because it takes time for detection, time for notification of the firefighters, time for travel to the fire and time for locating the fire in the building and setting up water supplies. Firefighters usually have insufficient water to extinguish a large post flashover fire, in which case they can only prevent further spread of fire and extinguish it during the decay period.

2.2.5 *Passive Control*

Passive control refers to fire control by systems that are built into the structure or fabric of the building, not requiring operation by people or automatic controls. For pre-flashover fires, passive control includes selection of suitable materials for building construction and interior linings that do not support rapid flame spread or smoke production in the growth period. In post-flashover fires, passive control is provided by structures and assemblies which have sufficient fire resistance to prevent both spread of fire and structural collapse.

2.3 Conceptual Framework for Fire Safety

Building codes are different in every country. In a prescriptive code environment, designers have little choice but to follow a book of rules. With more modern performance-based codes, designers have the freedom to design innovative solutions to fire safety problems, provided that the required levels of safety and performance can be demonstrated to the satisfaction of the approving authorities. Whatever type of code is used, design for fire safety will include a combination of reducing the probability of ignition, controlling the spread of fire and smoke, allowing for occupant escape and firefighter access, and preventing structural collapse. It is difficult to visualize or demonstrate safety without a conceptual framework because of the large number of interacting variables. Several related frameworks are described briefly below. Even a simple ‘checklist’ of fire safety and fire protection items can be of considerable assistance in seeing the big picture (ISO, 1999b; Spearpoint, 2008).

2.3.1 Scenario Analysis

One framework for demonstrating fire safety is scenario analysis. In this method a number of reasonable ‘worst case’ scenarios are analysed. In each scenario the likely growth and spread of fire and smoke is compared with detection and occupant movement, taking into account all the active and passive fire protection features and structural behaviour, to establish whether the performance requirements have been satisfied. An overview of scenario analysis is shown in Figure 2.3. This type of scenario analysis is the most often used basis of fire engineering design (ABCB, 2005; Spearpoint, 2008). Within the selected scenarios it is possible to ask a large number of ‘what if?’ questions to find the worst cases and optimize the design.

2.3.2 Quantitative Risk Assessment

In any study of safety there is a need for quantification, in order to answer the question ‘how safe?’ Quantitative risk assessment is a rapidly growing discipline which is increasingly being applied to fire safety, although most current performance-based design does not quantify the level of safety. A risk analysis can be based on existing historical data for the type of building under consideration, but such data are extremely limited. Safety can be quantified using fault tree analysis or event tree analysis if sufficient input data can be derived or estimated. A summary of risk assessment methods for fire safety is given by Watts (2003).

There are a number of computational fire risk assessment programs under development which are able to carry out probabilistic calculations of the scenario analyses described above, in order to quantify the overall expected fire loss and expected risk-to-life (e.g. Beck and Yung, 1994). Such programs are more useful for research and code-writing than for design.

In the absence of simple probabilistic design methods, most design calculations will be made deterministically, with appropriate safety factors applied to provide the required level of safety. Structural designers are very familiar with this process, where design codes provide partial safety factors for applied loads and material strength, calibrated so that the deterministic design process provides sufficient safety. The determination of suitable safety factors for fire design is in its infancy, so there may be occasions when a large degree of professional judgement is required by the fire designer and consequently by the approving authority.

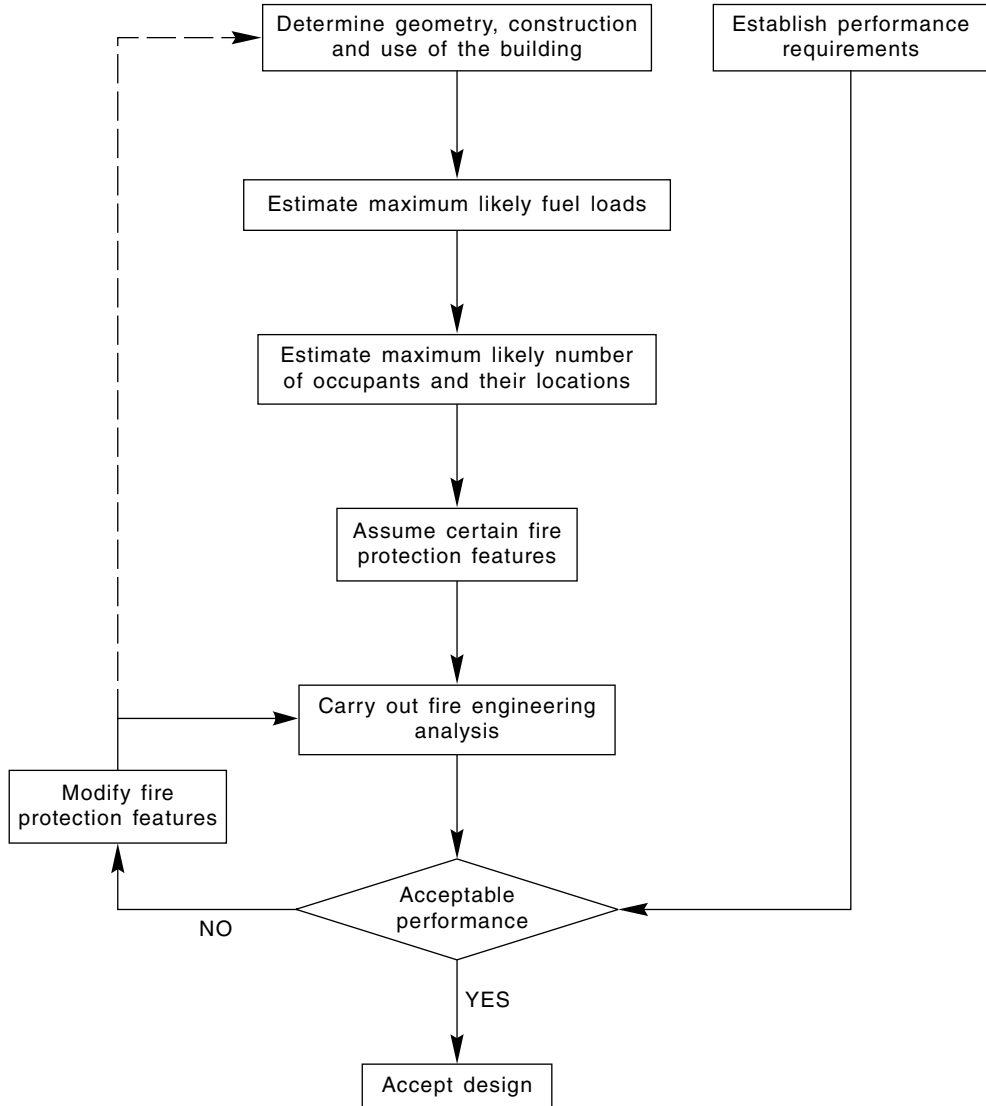


Figure 2.3 Overview of scenario analysis

2.3.3 Fire Safety Concepts Tree

One of the more durable frameworks for fire safety assessment is the Fire Safety Concepts Tree developed by the National Fire Protection Association (NFPA, 2003). Figure 2.4 shows an edited summary of the Fire Safety Concepts Tree. The following paragraphs give a brief explanation of the tree, as a guide to establishing the relative importance of the various components of a fire safety strategy.

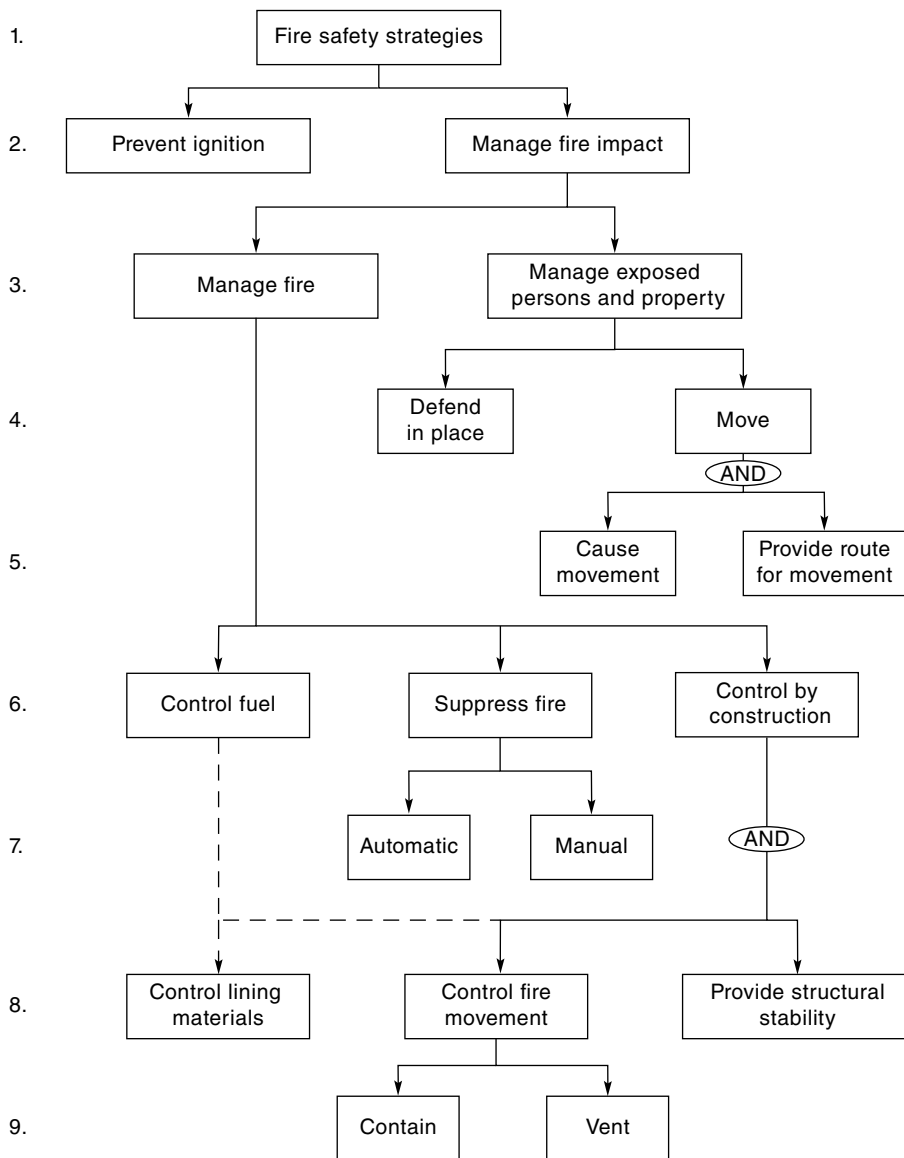


Figure 2.4 Fire Safety Concepts Tree. Adapted with permission from NFPA (2010a). © 2010 National Fire Protection Association, all rights reserved

2.3.3.1 Prevention versus Management

Line 2 of the tree states the obvious; fire management is unnecessary if ignition can be prevented, but if not, the impact of the fire must be managed. In reality there will always be unplanned ignitions, but the probability of these can be reduced with fire prevention programmes. Arson is a growing cause of fires which cannot easily be controlled by building designers. Unless stated

otherwise, this tree shows alternative strategies, whereby the objectives on one line can be met by any one of the items on the following line. Line 3 shows that managing the impact of a fire can be achieved either by managing the fire itself or by management of exposed persons and property.

2.3.3.2 Management of Exposed Persons and Property

Line 4 shows that exposed persons and property can be managed by moving them from the building or by defending them in place. The usual strategy is to move people from a building, unless they are incapacitated or under restraint. An intermediate position for very large buildings is to move people to a place of refuge within the building. Most exposed property must be defended in place because it is impossible for it to be moved quickly.

In order for people to move, the fire must be detected, the people must be notified, *and* there must be a suitable safe path for movement (Line 5). The ‘AND’ symbol indicates that success in both boxes is required to meet the objective. Human behaviour and escape route design is beyond the scope of this book. Refer to the SFPE Handbook (SFPE, 2008) for more information.

2.3.3.3 Manage the Fire

Line 6 shows three options for managing a fire. In the first case the fuel source can be controlled, by limiting the quantity or geometry of the available fuel. For example, this could be a limit on the amount of combustible material stored in a space. The second option is to suppress the fire and the third is to control the fire by construction. Fire suppression is a huge topic beyond the scope of this book, but as shown in Line 7, suppression can either be automatic or manual. In either case suppression depends on early detection of the fire and application of sufficient quantities of appropriate suppressant, usually water.

2.3.3.4 Control by Construction

Control of fire by construction is the subject of this book. Line 8 of the concepts tree shows that in order to control fire by construction it is necessary to both control the movement of the fire and provide structural stability. The left-hand box in Line 8 indicates that fire growth and severity can be controlled by limiting the fuel in combustible room linings. This box is connected by dotted lines because, strictly speaking, it should be a subset of “control fuel” from Line 6, but it has been placed in Line 8 because selection and installation of the linings is part of the construction process, rather than a building management issue.

2.3.3.5 Provide Structural Stability

The provision of structural stability is essential if buildings or part of buildings are to remain standing during a fire (depending on the importance of the individual building), and be easily repaired for subsequent use. Structural stability is also essential to protect people or property elsewhere in the building at the time of the fire. Some elements such as walls and floors may

have a separating function as well as a load-bearing function. Building elements such as beams and columns only have a load-bearing function. Structural stability in fire is covered in later chapters.

2.3.3.6 Control Fire Movement

The two strategies for controlling fire movement are either to contain the fire or vent it to the outside (Line 9). Fire venting is a useful strategy for reducing the impact of fires, especially in single storey buildings (or the top storey of taller buildings). Venting can be by an active system of mechanically operated vents, or a passive system that relies on melting of plastic skylights. In either case, the increased ventilation may increase the local severity of the fire, but fire spread within the building and the overall thermal impact on the structure will be reduced.

Containment of a fire to prevent spread is a principal tool of passive fire protection. Fire resistance helps to limit fire spread from the room of origin while ensuring structural integrity of the compartment. Thus walls and floors of most buildings are provided with fire resistance primarily to contain any fire to the room of origin. Preventing fires growing to a large size is one of the most important components of a fire safety strategy. Radiant spread of fire to neighbouring buildings must also be prevented, by limiting the size of openings in exterior walls. Fire resistance of walls and floors is covered in detail elsewhere in this book.

Smoke movement can also be controlled by venting or containment. Smoke removal is an important strategy in fires whose size has been limited by automatic sprinkler systems. Pressurization and smoke barriers can both be used to contain the spread of smoke in a building (Spearpoint, 2008; Klote *et al.*, 2012).

2.4 Fire Resistance

Fire safety objectives are usually met with a combination of active and passive fire protection systems. *Active systems* control the fire or fire effects by some action taken by a person or an automatic device. *Passive systems* control the fire or fire effects by systems that are built into the structure or fabric of the building, not requiring specific operation at the time of a fire. The most important component of passive fire protection is *fire resistance*, which is designed to prevent spread of fire and structural collapse.

2.4.1 Examples of Fire Resistance

An example of fire resistance is shown in Figure 2.5, where Figure 2.5(a) shows a fully developed fire burning in a warehouse which stored foamed plastic materials. It can be seen that the fire has not spread into the offices at the left end of the building. The aftermath of the fire is shown in Figure 2.5(b), which shows the collapsed steel beams which had inadequate fire resistance, and the damaged concrete masonry wall which had sufficient fire resistance to remain standing. All of the fuel and the timber roof purlins have burned away. Figure 2.5(c) is a view of the light timber framed wall which had sufficient fire resistance to prevent the fire from spreading from the warehouse into the offices. The gypsum board on the fire side has been removed by firefighters while the gypsum board on the office side is undamaged.

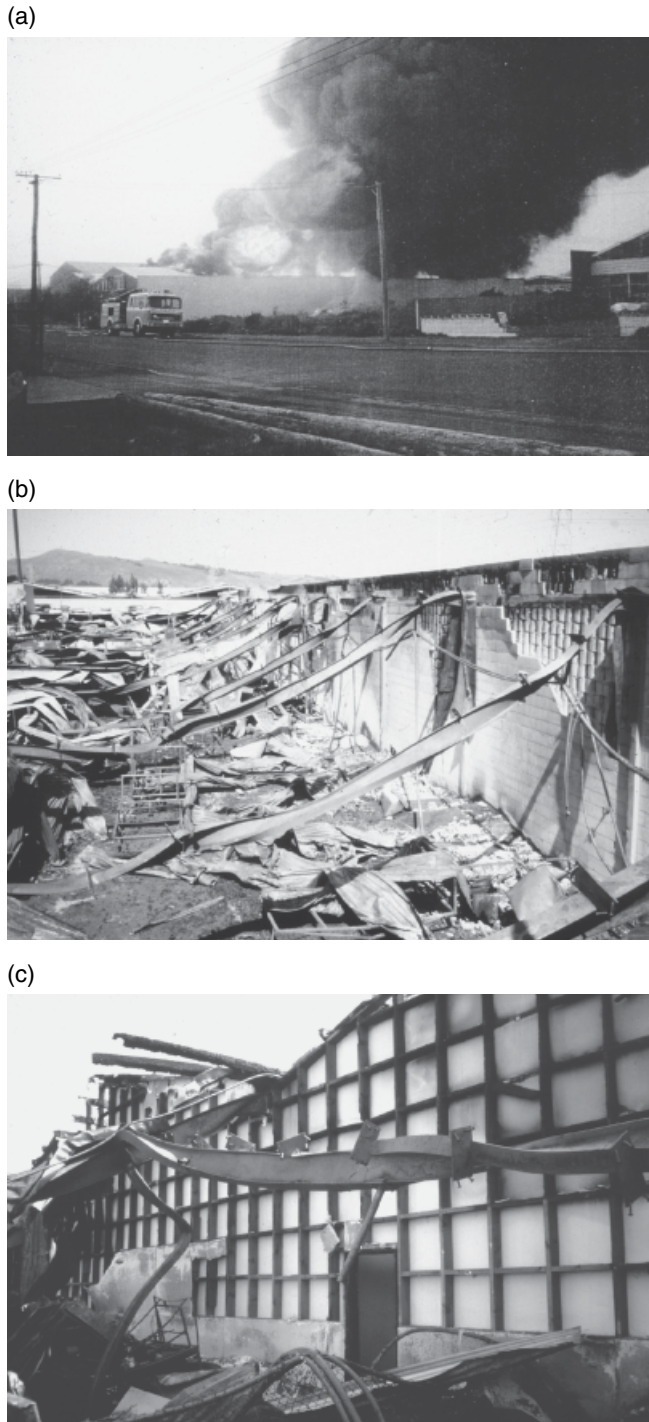


Figure 2.5 Example of fire resistance in a severe warehouse fire: (a) view of the fire after roof collapse; (b) collapsed steel beams and damaged concrete masonry wall after the fire; and (c) light timber framed wall separating the warehouse from the offices



Figure 2.6 Fire on the 12th floor of a 62 storey building, illustrating the importance of providing both containment and structural stability. Reproduced by permission of Boris Yaro

Another example is given in Figure 2.6 which shows a fire in the 12th storey of the 62 storey Interstate Bank building in Los Angeles in 1988. This photograph vividly demonstrates the importance of providing both containment and structural stability to protect the occupants and the property in the 50 storeys above the level of the fire.

2.4.2 Objectives for Fire Resistance

The objectives for providing fire resistance need to be established before making any design, recognizing that fire resistance is only one component of the overall fire safety strategy. Structural elements can be provided with fire resistance for controlling the spread of fire or to prevent structural collapse, or both, depending on their function. Modern performance-based

codes (NKB, 1994; MBIE, 2007; ABCB, 2015) show a similar approach to the requirements for fire resistance, as outlined below:

- To prevent internal spread of fire, a building can be divided into ‘fire compartments’ or ‘firecells’ with barriers which prevent fire spread for the *fire design time*. The many reasons for providing compartmentation include increasing the time available for escape, limiting the area of possible loss, reducing the fire impact on the structure, separating different occupancies, isolating hazards, and protecting escape routes. The separating barriers are usually floors or walls.
- To reduce the probability of fire spread to other buildings, boundary walls must have sufficient fire resistance to remain standing and to contain a fire for the *fire design time*.
- To prevent structural collapse, structural elements must be provided with sufficient fire resistance to maintain stability for the *fire design time*. Prevention of collapse is essential for load-bearing structural members and for load-bearing barriers which also provide containment. Structural fire resistance must be provided to the main load-bearing structural elements, and to secondary elements which support or provide stability to barriers or main members.
- Prevention of collapse is also essential if there are people or property to be protected elsewhere in the building, and for a building which is to be repaired after a fire.

2.4.3 Fire Design Time

The term *fire design time* is not precisely defined. Depending on the importance of the building, the requirements of the owner, and the consequences of a structural collapse or spread of fire, the *fire design time* will be selected by the designer as one or more of the following:

1. The time required for occupants to escape from the building.
2. The time for firefighters to carry out rescue activities.
3. The time for firefighters to surround and contain the fire.
4. The duration of a burnout of the fire compartment with no intervention.

Codes in various countries use these times in different ways for different occupancies. Many small single storey buildings may be designed to protect the escape routes and to remain standing only long enough for the occupants to escape (Time 1) after which the fire will destroy the building. Alternatively, very tall buildings, or buildings where people cannot easily escape, should be designed to prevent major spread of fire and structural collapse for a complete burnout of one or more fire compartments (Time 4). Times 2 and 3 are intermediate times which may be applied to medium sized buildings, to provide life safety or property protection, respectively.

It can be seen that the provision of structural fire resistance may be essential, or unimportant, or somewhere between these two extremes (Almand, 1989). On one hand there may be a major role for the structure so that collapse is unacceptable even in the largest foreseeable fire. This may occur where evacuation is likely to be slow or impossible, or where great value is placed on the building or its contents. On the other hand, there may be virtually no role for the

structure so that structural collapse is acceptable after some time of fire exposure, where the building can be readily evacuated, or there is little value placed on the building and there is no fire threat to adjoining properties.

Design for burnout of a fire compartment is a conservative approach which is likely to be used in many situations. Many modern codes require design of certain buildings for burnout. This book gives design methods which can be used for calculating structural fire resistance for complete burnout, or partial burnout with intervention from firefighters or suppression systems.

The *fire design time* must be assessed carefully, because it is not the same as the *fire resistance* time specified by a building code or measured in a fire resistance test. The *fire design time* includes time for ignition, growth and fire spread before flashover. The *fire design time* should include a safety factor to allow for the number of people in the building, the size of the building and the consequences of failure of the building. Schleich (1996) proposes safety factors ranging from 1.0 for small, single storey buildings to 2.5 for large, multi-storey buildings.

2.4.4 Trade-offs

One of the difficulties in assessment of fire safety is the extent to which some fire protection measures can be ‘traded off’ against others. For example, some prescriptive codes allow fire resistance ratings or fire compartment areas to be reduced if an automatic sprinkler system is installed, or they allow travel distances to be increased when smoke or heat detectors or sprinklers are installed. Trade-offs do not apply in a totally performance-based environment, because the designer will produce a total package of fire protection features contributing to the required level of safety. However, in practice, most designs are based on prescriptive codes, so it is often useful to make trade-offs.

It is often difficult to justify trade-offs, especially reductions of fire resistance if automatic sprinkler systems are installed, for the following reasons. If an automatic suppression system can be relied on to control a fire with total certainty, no fire resistance or passive fire protection is necessary. However, no system is 100% effective, so the question is how much fire resistance should be provided for the remote probability that the suppression system fails to operate or fails to control the fire. As an example, it could be argued that if the suppression system fails when street water supplies are destroyed by an earthquake or explosion, the resulting fire will have the same severity as if there had been no suppression system at all, so there should be no trade-off for sprinklers.

No codes allow a total trade-off for sprinklers, but many national codes allow a partial trade-off, assuming that in a sprinklered building, the probability of an uncontrolled fire is much less likely than the probability of a sprinkler-controlled fire. Quantitative justification for partial trade-offs is not easy, but two possible probabilistic arguments are as follows:

1. Many national codes allow a reduction in fire resistance of structural members if the building is sprinklered. A possible justification for this approach is based on safety factors. If, for example, the fire resistance normally specified for a burnout of a fire compartment in an unsprinklered building has an inherent safety factor of 2.0, then in the unlikely event of a fire and a sprinkler failure, that safety factor could be reduced to as low as 1.0, hence the 50% reduction. Such an argument can only be used if the method of specifying fire resistance for unsprinklered buildings is sufficiently conservative in the first instance.

2. The Eurocode 1 Part 1.2 (CEN, 2002b) suggests that for calculating fire resistance, the fuel load in a sprinklered building be taken as 60% of the design fuel load. This approach could be justified by considering sprinkler failure to be such an unlikely event that the design fuel load should be the most likely fuel load rather than the 90 percentile fuel load used for design of unsprinklered buildings.

2.4.5 *Repairability and Reserviceability*

Repair and reserviceability may be important for some building owners. A building designed to resist a complete burnout will be severely damaged, even if the fire is contained and the structure is intact. Most performance-based codes do not require that the structure should be undamaged following a fire. For example, Eurocode 1 Part 1.2 (CEN, 2002b) states that when designing for a required fire resistance period, the performance of the structure beyond that time need not be considered. A requirement for little or no damage to the building structure may be requested by some codes or some building owners, but this will require a greater level of passive fire protection than required to only prevent collapse.

A reserviceability requirement would limit damage so that the building could be reoccupied with no (or very little) time for repairs. Such a requirement might be imposed on buildings of social, cultural or economic importance. This is only possible with the use of active fire suppression systems such as sprinklers to prevent the fire from becoming large and destructive.

2.5 **Controlling Fire Spread**

The larger a fire, the greater its destructive potential. Many facets of fire protection are aimed at preventing small fires from becoming large ones. The control of fire movement, or fire spread, is discussed here in four categories: within the room of origin; to other rooms on the same level; to other storeys of the same building; and to other buildings.

2.5.1 *Fire Spread within Room of Origin*

Fire spread within the room of origin depends largely on the heat release rate of the initially burning object. Initial fire spread can be by flame impingement or radiant heat transfer from one burning item to another. As the fire grows, the movement of buoyant hot gases under the ceiling can cause the fire to spread to other parts of the room. Vertical and horizontal fire spread will be greatly increased if the room is lined with combustible materials susceptible to rapid flame spread on the walls and especially on the ceilings. Most countries have prescriptive codes which place limits on the combustibility or flame spread characteristics of linings in particular buildings or parts of buildings.

The properties of interest are ignitability, heat release, flame spread and the amount of smoke produced. These are often called the 'early fire hazard' properties or 'reaction to fire' properties. There are many different test methods for assessing the early fire hazard properties of materials in different countries, which makes international comparisons very difficult. In North America the principal test is the ASTM E-84 Steiner Tunnel test using a 7.6 m long tunnel (ASTM, 2015). Most other countries have a variety of tests which expose materials in

various sizes to heating by a radiant panel. Recent international developments include the cone calorimeter test of small specimens (100×100 mm) and the full-scale room fire test for evaluating the fire performance of room lining materials. Another international test method is the Single Burning Item test which has become the test procedure for classifying building products in the harmonized European system. This is an intermediate-scale test where two test samples are mounted in a corner configuration, subjected to a gas flame ignition source, and the rates of heat release and smoke production are measured. All of the above tests have been the subject of much research and international standardization.

With regard to ignition and fire spread, unprotected wood-based materials are safer than many plastic or synthetic materials, but are less safe than materials such as paper-faced gypsum plaster or completely non-combustible materials such as concrete. The early fire hazard properties of wood building elements can be improved with the use of special paints or chemical treatment.

2.5.2 Fire Spread to Adjacent Rooms

Spread of fire and smoke to adjacent rooms is a major contributor to fire deaths. The movement of fire and smoke depends very much on the layout of the building. Open doors can provide a path for smoke and toxic combustion products to travel from the hot upper layer of the fire room into the next room or corridor. These hot gases can pre-heat the next area leading to subsequent rapid spread of fire.

Keeping doors closed is essential to preventing fire spread from room to room. Doors through fire barriers must maintain the containment function of the barrier through which they pass, whether for smoke control or fire resistance. Door closing devices which operate automatically when a fire is detected are very effective. Other innovations to improve door performance include smoke control strips to reduce spread of smoke, and strips of intumescent material that will swell when heated to prevent fire spreading through gaps around the door.

Concealed spaces are one of the most dangerous paths for spread of fire and smoke. A hazardous situation occurs if there are concealed spaces which allow spread of fire and smoke to adjacent rooms, or even to rooms some distance from the fire. Figure 2.7 shows spread of smoke through a concealed ceiling cavity. Concealed cavities are a particular problem in old buildings, especially if a number of new ceilings or partitions have been added over the years.

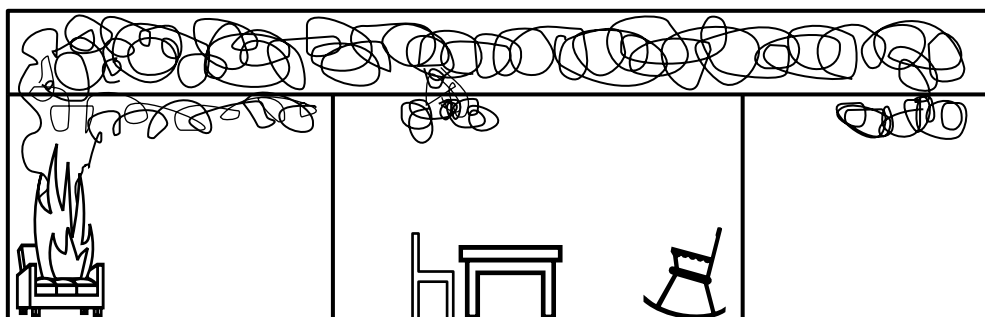


Figure 2.7 Spread of smoke and fire through a ceiling cavity

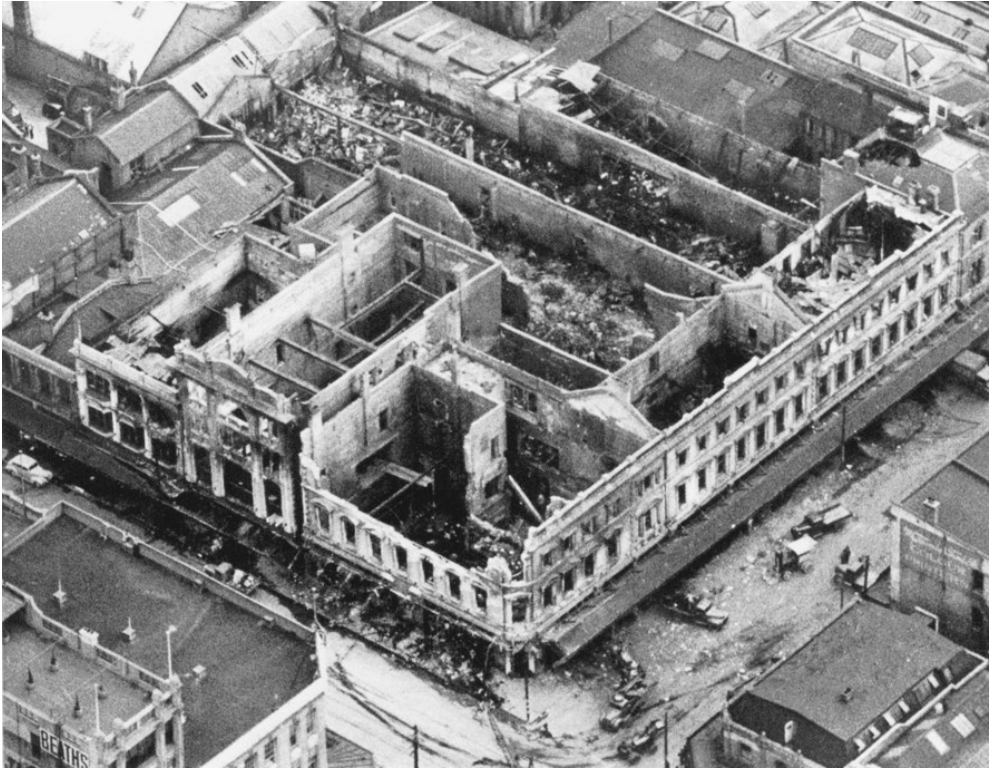


Figure 2.8 The masonry walls of a large department store after a severe fire (Ballantynes department store, New Zealand, 1947). Reproduced by permission of The New Zealand Herald/newspix.co.nz

Fire can also spread to adjacent rooms by penetrating the surrounding walls, as occurred in the building shown in Figure 2.8. Walls can be designed with sufficient fire resistance to prevent the spread of fully developed fires, but they must be constructed with attention to detail if fire performance is to be ensured. Fire resisting walls must extend through suspended ceilings to the floor or roof above so that the fire cannot spread through a concealed space above the wall. In order to prevent fire spreading over the top of a fire resisting wall at roof level, the wall can be extended above the roof line to form a parapet, or the roof can be fire-rated for some distance either side of the top of the wall.

A severe fire will find any weakness in a separating barrier, and many such weaknesses are not visible during normal operation of the building. Care must be taken to ensure that poor quality workmanship or penetrations for services and fittings do not compromise the performance of fire resisting walls. The term ‘fire stopping’ refers to the sealing of penetrations and cavities through which fire might spread (O’Hara, 1994). There are many techniques for fire stopping of penetrations, construction joints and seismic gaps (Abrams and Gustafarro, 1971). Materials for fire stopping include mineral wool, wood blocks, gypsum board, metal brackets and a wide array of proprietary products such as fire resisting putty, board materials and intumescent pillows and collars (Figure 2.9).



Figure 2.9 Fire protection to service penetrations through a fire resisting floor

Air-handling ducts which pass through fire resistant walls and floors can create paths for spread of fire. This can be prevented by the use of fire resistant insulating duct materials and internal ‘fire dampers’ which are designed to close off the opening in the event of a fire.

2.5.3 *Fire Spread to Other Storeys*

Fire can spread to other storeys by a variety of paths, inside and outside the building. Internal routes for fire spread include failure of the floor/ceiling assembly, and fire spread through vertical concealed spaces, service ducts, shafts or stairways. Vertical services must either be enclosed in a protected duct or have fire resistant penetration closers at each floor level, as shown in Figure 2.10. Vertical shafts and stairways must be fire-stopped or separated from the occupied space at each level to avoid creating a path for spread of fire and smoke from floor to floor. A particularly dangerous situation can arise if there are interconnected horizontal and vertical concealed spaces, within the building or on the façade.

Another potential path for vertical fire spread is through gaps at the junction of the floor and the exterior wall, just inside the façade, as shown on the left-hand side of Figure 2.11. This is particularly important for ‘curtain-wall’ construction where the exterior panels are not part of the structure. A possible detail to prevent such fire spread is shown in Figure 2.12. Careful detailing and installation is necessary to ensure that the entire gap is sealed, especially at corners and junctions, to eliminate any possible path for fire spread (Gustaferrero and Martin, 1988).

Gaps such as these between structural and non-structural elements are often filled with non-rigid fire-stopping materials to allow for seismic or thermal movement. The filling

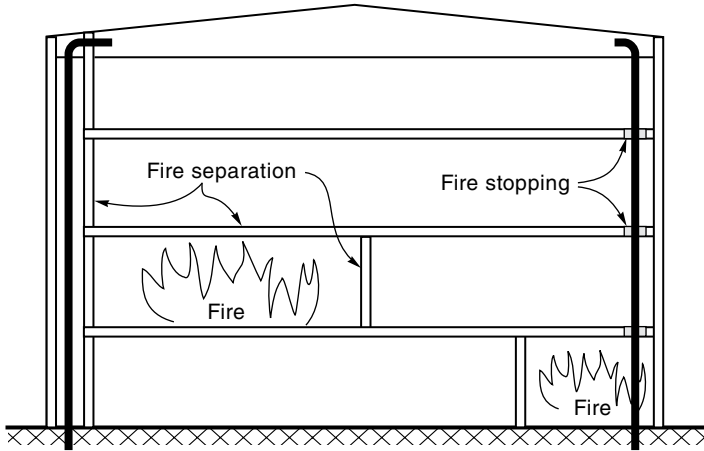


Figure 2.10 Fire separation of vertical services

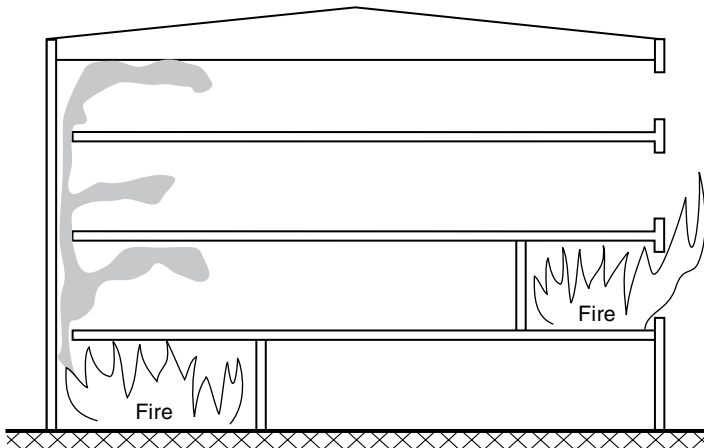


Figure 2.11 Fire spread from storey to storey

material must be able to provide the necessary fire resistance both before and after the anticipated movement (including earthquake movement in seismic areas). Filling material may be mineral or ceramic fibre batts or blankets, which must be adequately held in place. Glass fibre materials are not suitable for fire stopping because they shrink and melt at temperatures over about 300 °C. Metal brackets or angles supporting the filling material must not be made from aluminium alloys because they melt at temperatures over 500 °C. If made from steel, the brackets should be fire protected with intumescent paint or other suitable material.

Vertical fire spread can also occur outside the building envelope, via combustible cladding materials or exterior windows as shown on the right-hand side of Figure 2.11. Combustible cladding susceptible to rapid flame spread should not be used on the exterior of tall buildings. Vertical spread of fire from window to window is a major hazard in multi-storey buildings. This hazard can be partly controlled by keeping windows small and well separated, and by

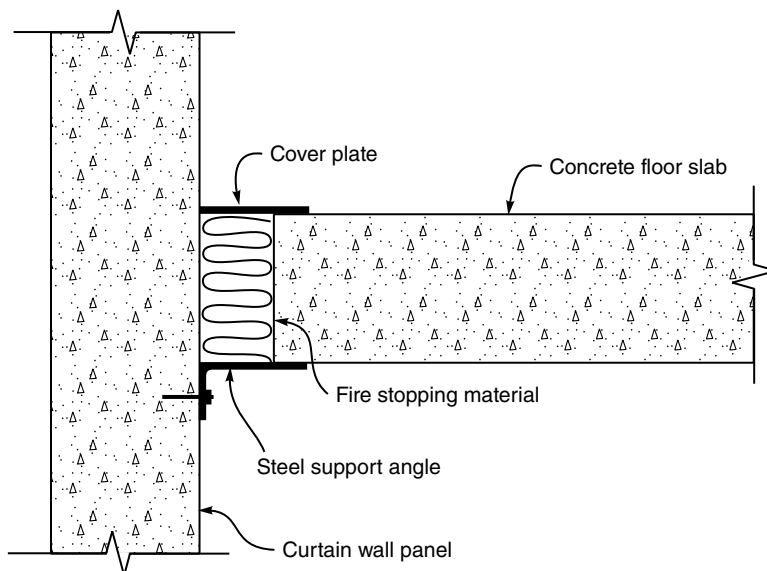


Figure 2.12 Fire stopping between slab and curtain wall

using horizontal aprons which project above window openings (Oleszkiewicz, 1991). Flames from small narrow windows tend to project further away from the wall of the building than flames from long wide windows, leading to lower probability of storey to storey fire spread (Drysdale, 2011).

2.5.4 Fire Spread to Other Buildings

Fire can spread from a burning building to adjacent buildings by flame contact, by radiation from windows, or by flaming brands. Fire spread can be prevented by providing a fire resisting barrier or by providing sufficient separation distances. Figure 2.13 shows a severe fire in a department store, where the entire building is fully involved in the fire and the roof framing is about to collapse, but the fire is prevented from spreading to adjacent properties by fire resisting boundary walls. If there are openings in the external wall, the probability of fire spread depends greatly on the distances between the buildings and the size of the openings. Exterior fire resisting walls must have sufficient structural fire resistance to remain in place for the duration of the fire. This becomes a particular problem if the structure which normally provides lateral support to the walls is damaged or destroyed in the fire. Outwards collapse of exterior walls can be a major hazard for firefighters and bystanders, and can lead to further spread of fire to adjacent buildings.

Fire spread by flame contact is only possible if the buildings are quite close together, whereas fire spread by radiation can occur over many metres. Radiant heat flux from the window of a building fire can ignite combustible cladding on a nearby building, or combustible products inside the windows. The calculation of radiant heat flux from one building to another is described in Chapter 3. Fire can also travel large distances between buildings if combustible vegetation is present.



Figure 2.13 Severe fire in a department store. Reproduced from Euskonews magazine

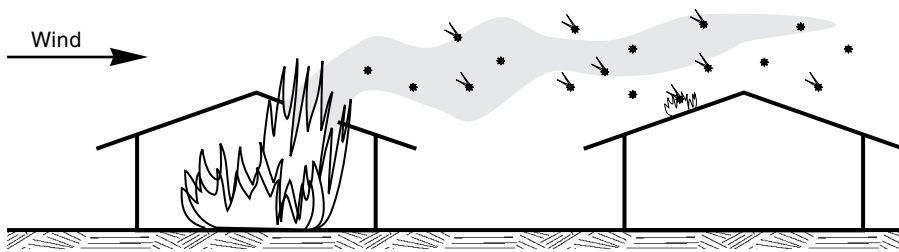


Figure 2.14 Fire spread by flaming brands

Flaming brands carried by the wind can cause fire spread between buildings with combustible roofing materials as shown in Figure 2.14. This can be controlled by restricting the use of combustible roofing materials. Fire spread between adjacent buildings also depends on the relative heights of the buildings. A fire burning through the roof of a low

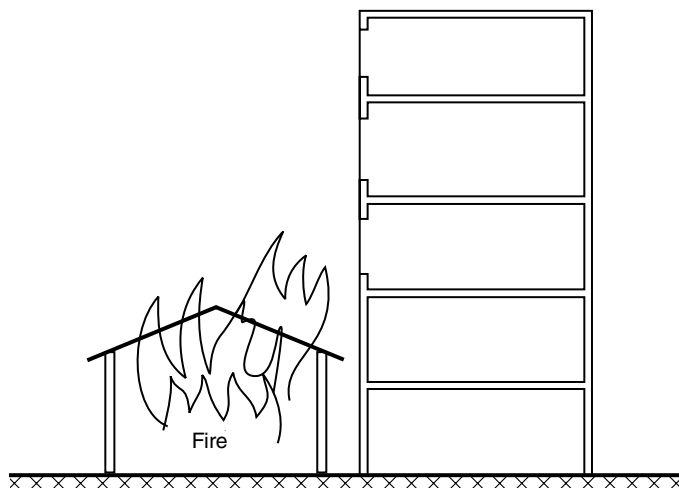


Figure 2.15 Fire spread from a low building to a taller building

building can spread into windows of an adjacent tall building as shown in Figure 2.15 unless adequate fire resistance is provided.

2.6 Building Construction for Fire Safety

2.6.1 Fire during Construction and Alterations

The possibility of a fire occurring during the construction process, or during alterations, is often overlooked, despite many serious fire losses. The fire hazard is usually much greater during construction than at any other time in the life of the building, because of the increased number of ignition sources and incomplete fire protection features. There are many recorded cases of ignition from cutting or welding during construction, some leading to massive fire losses. Most active fire protection systems are not commissioned until a building is completed, and most passive fire protection such as fire stopping and structural fire cladding is not finished until late in the building process.

The probability of fire losses during construction can be reduced by the implementation of a safety plan which recognizes the hazards and the condition of the building at each stage in the construction process, and brings active and passive fire protection systems on line as soon as possible. This is particularly important for buildings using combustible building materials such as wood (Bregulla *et al.*, 2010).

Poorly executed alterations may reduce the fire safety of a building. There are many documented cases of fires spreading through unprotected concealed spaces which were created during alterations. The persons carrying out repairs may damage or remove passive fire safety features because they are not aware of their importance. For example, new building services installed above suspended ceilings may penetrate important fire walls or floors without fire stopping, creating paths for unseen spread of fire and smoke. Weaknesses such as these are not obvious without careful inspection.



Figure 2.16 Fire damage following the San Francisco earthquake, 1906. Reproduced from Walker (1982) by permission of the Bancroft Library

2.6.2 *Fire following Earthquake*

The possibility of fire following earthquake is a major threat in seismic regions of the world. There are many examples of serious fires following earthquakes. Figure 2.16 shows fire damage following the 1906 San Francisco earthquake, and the 1986 earthquake in the same city also caused serious fire damage. Figure 2.17 shows fire damage following the 1995 Kobe earthquake. Major fire damage has followed many other earthquakes including Tokyo in 1923 and Napier, New Zealand in 1931 (Steinbrugge, 1982; Botting, 1998).

There are three main factors increasing the danger of fire after earthquake. The probability of ignition is high because of toppled furniture, electrical malfunction and movement of hot equipment. Active and passive fire protection systems may be damaged by the earthquake, and the probability of prompt Fire Service attention is much lower than in normal conditions (Scawthorn, 1992).

Active suppression such as automatic sprinkler systems will not work after an earthquake if there is damaged pipework in the building or complete loss of city water supplies. For these reasons greater attention should be given to passive containment and structural fire resistance



Figure 2.17 One of many severe fires which destroyed buildings after the Hanshin-Awaji earthquake, Kobe, Japan, 1995

in seismic regions than in non-seismic regions, especially in tall or large buildings where there could be significant danger to life or property.

2.7 Assessment and Repair of Fire Damage

This section gives basic advice on the assessment and repair of fire damaged buildings, because structural engineers are often engaged to report on options for re-use or repair. If there is a danger of local collapse, immediate concerns about the stability of free-standing residual parts of a fire damaged building will have to be addressed very quickly. More often the owner will want to know if the damaged building can be rehabilitated, in which case there will be time for a more complete investigation.

2.7.1 Inspection

It is important to visit the fire scene as soon as possible after the fire, while all the fire debris and non-structural damage is visible. This visit can provide essential information on the extent of the fire, the location of the most severe burning and the maximum temperatures reached during the fire. It is also important to revisit the fire scene after debris and non-structural items have been removed, when it becomes possible to inspect structural members in more detail. It is very important to inspect the details of connections between structural members for cracking of concrete, damage to welded connections or distortion of bolts.

Maximum local temperatures reached in a fire can be estimated from an inspection of materials which have melted. The approximate melting temperatures of several materials are given in Table 2.2. The duration of the fully developed period of the fire can be roughly estimated from the residual size of heavy timber members which will have charred at approximately 0.7 mm per minute as described in Chapter 9.

Most of the significant fire damage in a structure will be readily visible. With the exception of temperature-related loss of material strength, significant damage will usually be visible as large deflections, local deformations, spalling of concrete or charring of timber. Most members which have deformed during the fire will have to be replaced, unless the deformations do not affect the future use of the building. Allowance must be made for deflections which may have existed before the fire. If a large number of members have significant distortion the entire structure may have to be demolished.

2.7.2 Steel

Unprotected steel members often suffer large deformations in fully developed fires, whereas well protected members usually exhibit little or no damage. In most cases no further assessment is necessary for fire-exposed steel members which remain straight after cooling (Tide, 1998). The most common grades of structural steel do not suffer significant loss of strength when

Table 2.2 Approximate melting temperature of materials

Material	Approximate melting temperature (°C)
Polyethylene	110–120
Lead	330
Zinc	420
Aluminium alloys	500–650
Aluminium	650
Glass	600–750
Silver	950
Brass and bronze	850–1000
Copper	1100
Cast iron	1150–1300
Steel	>1400

Source: Reproduced from Gustaferrero and Martin (1988) by permission of Precast/Prestressed Concrete Institute.

cooled after heating up to about 600 °C. Heating to higher temperatures can result in a strength reduction of up to 10% after cooling. The reduction in strength is much greater for high strength steels containing alloys such as vanadium and niobium. If necessary, hardness tests or small tensile test specimens can be used to determine whether there has been a reduction in strength. Many types of high strength bolts have been heat-treated during manufacture which makes them susceptible to loss of strength after heating, in which case they should be replaced. Extensive guidance is given by Kirby *et al.* (1993).

2.7.3 Concrete and Masonry

Concrete structures generally behave well in fires. Concrete slabs or beams which have excessive deflections will have to be replaced. Cover concrete which has spalled off, or which is badly cracked, can be replaced with poured or sprayed concrete, incorporating additional reinforcing if necessary. Concrete members exhibiting no visible damage may have reduced strength due to elevated temperatures of the concrete or the reinforcing. Typical mild steel reinforcing regains any lost strength when it cools. High strength steels, especially cold-drawn prestressing tendons, are susceptible to strength loss if they are heated to temperatures above 400 °C. Prestressing steels cooled after heating to 500 °C can have a 30% loss of strength and heating to 600 °C can result in a 50% loss of strength (Gustaferro and Martin, 1988).

Loss of strength of the concrete itself is usually of less concern than loss of strength of the steel reinforcing. The heat affected region is often not very thick because of the low thermal conductivity of concrete. In simply supported flexural members, the compression zone on the top of the slab or beam is often not exposed to very high temperatures. Loss of strength of concrete near the surface can be estimated with an impact rebound hammer. Some types of concrete change colour after heating to elevated temperatures, depending on the aggregate. Marchant (1972) describes a design procedure for reinstatement of fire damaged reinforced concrete buildings, and reports that typical concrete heated to less than 300 °C will have no colour change, concrete heated to 300–600 °C may be pink, concrete heated to 600–950 °C may be whitish-grey and concrete heated over 950 °C may be a buff colour. Fire-exposed concrete suffers no significant loss of residual strength when heated below 300 °C, whereas for higher temperatures the strength loss will depend on the concrete temperature as described in Chapter 7. When the concrete cools after heating, it regains strength slowly but never reaches the original strength (Lie, 1992).

Ceramic clay bricks lose very little strength after heating to temperatures as high as 1000 °C, but the mortar may suffer some damage. Reinforced concrete masonry will need to be assessed in the same way as normal reinforced concrete.

2.7.4 Timber

Because wood burns, fire damage to exposed timber surfaces is immediately visible. Heavy timber structural members such as beams, columns, or solid wood floors will be charred on the surface, with undamaged wood in the centre, as described in Chapter 9. The residual wood under the charred layer can be assumed to have full strength. The size of the residual cross section can be determined by scraping away the charred layer and any wood which is significantly discoloured. Fire-exposed heavy timber members tend to deform much less than

unprotected steel members. Fire-damaged timber members do not need to be replaced if the residual cross section has sufficient strength to carry the design loads. For future fire resistance it may be necessary to apply additional protection such as new layers of wood, or gypsum board, because of loss of the sacrificial wood. Severely damaged members will need to be replaced.

Light timber frame structures are protected from fire by linings of non-combustible material such as gypsum board, as described in Chapter 10. After a severe fire, the linings on the underside of ceilings and the fire side of walls will certainly be damaged. Some linings may have fallen off due to the effects of the fire or fire-fighting activities. All damaged linings should be removed to inspect damage to the studs or joists. Any charred timber will have reduced load capacity. Calculations will be necessary to assess the strength of the residual members.

Inspection of gypsum board can give an indication of the duration of fully developed burning. When gypsum board is exposed to fire it dehydrates steadily from the hot surface. The depth of dehydration can be observed by breaking open a small piece of board to locate the transition between the soft dehydrated plaster and the solid gypsum of the original board. Typical gypsum board dehydrates at approximately 0.5 mm per minute.

3

Fires and Heat

This chapter discusses fires in rooms and heat transfer to structural members. It reviews the combustion of fuels in typical building fires, and the factors that affect fire growth. It also provides simple descriptions of pre- and post-flashover fires. For more information on these topics, refer to Quintiere (1998), Karlsson and Quintiere (2000) or Drysdale (2011).

3.1 Fires in General

A fire occurs when a combustible item comes into contact with oxygen in the presence of heat. The fire, which usually starts with the burning of one item, gradually spreads to other nearby items and grows in size and intensity as a *pre-flashover fire*. In an open environment, a peak intensity is reached very rapidly, then the rate of combustion gradually decreases until the available fuel has been consumed. In a closed environment, on the other hand, the size and intensity of the fire can increase until all items in the enclosed space are fully engulfed in flame at the time of *flashover*, which is a transition to the burning period, during which the peak intensity is maintained while the rate of burning is controlled by the availability of oxygen through ventilation openings. After most of the fuel has been consumed, the fire decays gradually. *Post-flashover fires* are the main concern for the design of structures in fire conditions.

Most of the potential fuel in building fires is organic material originally derived from plants, animals or petrochemicals. The material available as fuel may be part of the building structure, lining materials, or the permanent or temporary contents of the building. Plant-based materials include wood-based materials, cotton, jute, straw, food crops or trees. Animal-based materials include wool, meat and many food products. Petrochemicals include many liquid and gaseous fuels, and almost all plastic materials, also known as polymers. All of these materials are

Table 3.1 Net calorific values of some combustible materials (in MJ/kg)

Solids	
Wood	17.5
Other cellulosic materials	20.0
Clothes, Cork, Cotton, Paper, Cardboard, Silk, Straw, Wool	
Carbon	30.0
Anthracite, Charcoal, Coal	
Chemicals	
Alcohols	30.0
Methanol, Ethanol, Ethyl alcohol	
Fuels	45.0
Gasoline, Petroleum, Diesel	
Pure hydrocarbon plastics	40.0
Polyethylene, Polystyrene, Polypropylene	
Other products	
Polyester (plastic)	30.0
Polyisocyanurate and polyurethane (plastics)	25.0
Polyvinylchloride, PVC (plastic)	20.0
Rubber tyre	30.0

Source: Extracted from CEN (2002b). © CEN, reproduced with permission.

organic compounds, their molecules consisting mainly of carbon and hydrogen atoms, with the addition of oxygen, nitrogen and other atoms in some cases.

Energy is released in the form of heat, from the start of the fire. The rate of heat release from a combustion reaction depends on the nature of the burning material, the size of the fire, and the amount of air available. The *calorific value* or *heat of combustion* is the amount of heat released during complete combustion of a unit mass of fuel. Most solid, liquid and gaseous fuels have a calorific value between 15 and 50 MJ/kg. Net calorific values ΔH_c (MJ/kg) for a range of common fuels are shown in Table 3.1. For materials such as wood which contain moisture under normal conditions, the effective calorific value $\Delta H_{c,n}$ (MJ/kg) can be calculated from:

$$\Delta H_{c,n} = \Delta H_c (1 - 0.01 m_c) - 0.025 m_c \quad (3.1)$$

where m_c is the moisture content as a percentage of weight.

The maximum possible energy that can be released when fuel burns is the energy contained in the fuel, E (MJ) given by:

$$E = M \Delta H_c \quad (3.2)$$

for dry fuel, or

$$E = M \Delta H_{c,n}$$

for fuels containing moisture, where M is the mass of the fuel (kg).

The amount of combustible materials in buildings is most often expressed as the *Fire Load Energy Density* (FLED) per square metre of floor area. For each room, the fire load energy density e_f (MJ/m² floor area) is given by:

$$e_f = E/A_f \quad (3.3)$$

where A_f is the floor area of the room (m²).

Many European references express fire load as energy density per square metre of total bounding surfaces of the room. This energy density e_t (MJ/m² total room surface area) is given by:

$$e_t = E/A_t \quad (3.4)$$

where A_t is the total area of the bounding surfaces of the room (m² floor, ceiling and walls, including window openings).

Values of fire load energy density range from 100 to 10,000 MJ/m² of floor area. The fire design verification method of the New Zealand Building Code (MBIE, 2012) gives design values of 400, 800 and 1200 MJ/m² for residential, office and retail occupancies respectively, requiring storage areas to be assessed separately. These values compare closely with the Eurocode 1 Part 1.2 (CEN, 2002b), which also provides fire load densities based on the type of occupancy, ranging from 100 to 1500 MJ/m² of floor area.

Design fire loads should be determined in a similar way to design loads for other extreme events such as wind or earthquake, so that the design fire represents an extreme value of the likely fire scenarios. The design fire load is often defined as having less than 10% probability of being exceeded in 50 years, so it will be close to the maximum fire load expected in the life of the building. Both fixed and moveable fire loads should be included. When the fire load is determined from representative surveys, the design load should be the 90 percentile value of surveyed loads, which will be much larger than the typical average fire load at a random point in time. For a coefficient of variation of 50–80% of the average value, the 90 percentile value will be 1.65–2.0 times the average value.

The single most important descriptor of the intensity of a fire is the *heat release rate* (Babrauskas and Peacock, 1992) which can be calculated as the amount of energy released (MJ) in a certain time (in seconds) with units of megawatts (MW). The rate of heat release typically builds up gradually to a peak and then dies out when sufficient fuel has been consumed. An average heat release rate Q (MW) can be calculated by:

$$Q = E/t \quad (3.5)$$

where E is the total energy contained in the fuel (MJ), and t is the duration of the burning (s).

3.2 Combustion

In its most simple form, the combustion of organic material is an exothermic chemical reaction involving the oxidation of hydrocarbons to produce water vapour and carbon dioxide. For example the chemical reaction for the complete (stoichiometric) combustion of propane is given by:



This is a simplification of the chemistry. There are many chemical processes involved, depending on temperatures, pressures and the availability of the materials. Intermediate reactions involve a large number of atoms and free radicals. In many fire situations there will be incomplete combustion, leading to the production of carbon monoxide gas (CO) or solid carbon (C) as soot particles in the flames or smoke. The chemistry changes continually throughout the combustion process.

At room temperatures, some fuels are gases but most are solids or liquids. Gases can mix with air to burn directly without any phase change, but all solid and liquid fuels must be converted to the gaseous phase before they can burn. For most liquids, the transition from liquid to the gaseous phase under the application of heat is by *evaporation*. For some polymers the process is by *thermal decomposition* into new volatile products. Many solid fuels *melt* when heated, producing a liquid which can then evaporate or thermally decompose into a gas. Some other fuels, including most wood products, thermally decompose with a transition directly from solid to gaseous phase. This thermal decomposition of wood is known as *pyrolysis*.

The combustion process for any material requires the availability of oxygen for the oxidation reaction to occur. The most efficient combustion is *premixed burning* where the gaseous fuel is mixed with oxygen or air containing oxygen before ignition (as in a Bunsen burner). Combustion will be very rapid if the gases are mixed in the right proportions (e.g. in an internal combustion engine). Combustion will not occur if the mixture has too much or too little oxygen for the given conditions of temperature and pressure. The limiting conditions are called the limits of flammability. In most building fires there is no premixed burning, and the rate of combustion depends on the rate of mixing of air with the gaseous fuels as they become available. The combustion takes place in the region where the gases mix. The mixing is usually driven by buoyancy and turbulence resulting from the convective movement of the flame and combustion products in the plume above the fire.

The maximum temperature that can be reached in a flame is known as the *adiabatic flame temperature*. This is the theoretical maximum temperature that can be reached when the combustion products are heated from their initial temperature by the heat released in the combustion reaction, with no losses. In flames from a typical burning object, the adiabatic flame temperature may be reached in a small region in the centre of the flame, but the average temperature of the flame will be considerably less.

For an object to be first ignited, there must be an external source of heat to raise the temperature of the object to its ignition temperature. If the fire grows after ignition, it may reach *established burning* after which the flames are large enough to sustain the combustion reaction with no assistance from any external source of heat. The burning is driven by heat from the flames which heats the remaining fuel to a sufficient temperature for the production of volatile combustible gases which burn in a dynamic process, producing more volatiles and more flames.

Smouldering is the term given to flameless combustion such as in a cigarette. *Smouldering combustion* is much slower than flaming combustion, and temperatures are also lower (Ohlemiller, 2008). Smouldering combustion is a particular hazard in residential buildings, because insufficient heat or noise is generated to wake sleeping occupants who can be overcome by the smoke and toxic combustion products. The smoke from smouldering combustion will activate smoke detectors, but it usually has insufficient temperature to activate heat detectors or automatic sprinkler systems. Smouldering combustion does not produce temperatures sufficient to affect structures, so is not considered further in this book.

A useful similarity between all hydrocarbon-based fuels is that the heat release rate per unit of oxygen consumption is almost constant. This forms the basis of oxygen consumption calorimetry experiments. For almost all fuels, approximately 13 MJ of heat is released for each kilogram of oxygen consumed, which is approximately 3 MJ of heat for each kilogram of air involved in the burning. This relationship allows the rate of heat release in experimental fires to be obtained by sampling the oxygen concentration in the flue gases. This concept is becoming widely used in experimental fire testing; on a small scale in cone calorimeters, on a medium scale in furniture calorimeters and on a larger scale in room calorimeters.

3.3 Fire Initiation

3.3.1 Sources and Mechanisms

Ignition occurs when a combustible mixture of gases is heated to temperatures that will trigger the exothermic oxidation reaction of combustion. Ignition almost always requires the input of heat from an external source. The few cases where self-heating within solid materials can cause *spontaneous combustion* is a special subject that is not covered in this book. There are numerous possible heat sources that cause building fires to ignite. These include flaming sources (matches, candles, gas heaters, and open fires), smouldering sources (cigarettes), electrical sources (arcing, overheating), radiant sources (sunlight, hot items, heaters, fires), also hot surfaces, friction, lightning and others. War and terrorism have also been the cause of many fires in buildings, as evidenced by the World Trade Center collapses in 2001 (Shyam-Sunder, 2005). Many sources of potential ignition can be reduced or controlled by fire prevention strategies, but some unwanted fires will always occur.

The amount of heat and temperature required to cause ignition depends on the material properties of the fuel, the size and shape of the ignited object, and the time of exposure to heat. The time to ignition of materials depends on the *thermal inertia* of the material itself. Thermal inertia is defined later in this chapter as the product of thermal conductivity, density and specific heat. When exposed to the same heat source, the surface of materials with low thermal inertia (e.g. polystyrene foam) will heat more rapidly than materials with higher thermal inertia (e.g. wood) leading to much more rapid ignition.

3.3.2 Pilot Ignition and Auto-ignition

It is useful to distinguish between *pilot ignition* which occurs in the presence of a flame or spark and *auto-ignition* which is the spontaneous ignition of volatile gases from a fuel source in the absence of any flame or spark. Auto-ignition requires the gases to be at a higher temperature than for pilot ignition. For surfaces exposed to radiant heat flux, the heat flux intensity required to cause auto-ignition is higher than that required for pilot ignition.

3.3.3 Flame Spread

After ignition has occurred somewhere in a building, fire safety depends greatly on the rate of fire spread. Initial fire spread is caused by spread of flame on the burning object or adjacent combustible materials. The main factor affecting flame spread is the rate of heating of the fuel

ahead of the flame. This in turn depends on the size and location of the flame (causing radiant heating), the air flow direction (causing convective heating), the thermal properties of the fuel (affecting the rate of temperature rise), and the flammability of the fuel (Drysdale, 2011). Heating ahead of the flame will be more rapid if there are heat sources in addition to the flame itself, such as radiation from a layer of hot gases under the ceiling. Air movement is very important. Flame spread will be much more rapid with air flow in the direction of spread ('wind aided') than air flow in the other direction ('wind opposed'). Upward flame spread is always rapid because the flame can rapidly preheat the material ahead of the burning region. Flames tend to spread most rapidly on surfaces which have a high rate of temperature increase on exposure to heat flux. These are materials with low thermal inertia which are also more susceptible to ignition. Materials such as low density plastic foams experience rapid flame spread and fire growth for this reason.

3.4 Pre-flashover Fires

Fires in rooms are described separately for pre- and post-flashover fires, beginning with pre-flashover fires. An understanding of pre-flashover fires is essential when designing for life safety. Burning objects can behave differently when they burn inside a room rather than in the open air, as described below.

3.4.1 *Burning Items in Open Air*

The rate of heat release from a pool of liquid or a solid item burning in the open depends on the rate at which heat from the flames can evaporate or pyrolyse the remaining fuel, and the rate at which oxygen can mix with the unburned fuel vapour to form diffusion flames. A *plume* of smoke and hot gases rises directly above the fire, cooling as it rises because of the large amount of surrounding air *entrained* into the plume. If an object such as a furniture item is ignited and allowed to burn freely in the open, the heat release rate tends to increase exponentially as the flames get larger and they radiate more heat back to the fuel. A *peak heat release rate* is usually reached, followed by steady state burning and eventual decay. The peak heat release rate for open air burning depends on the geometry and nature of the fuel within the object. There is a large amount of information available on the heat release rate of burning items. Many objects such as furniture and appliances have been burned in furniture calorimeters (Figure 3.1), producing valuable information including the rate of heat release, and production of smoke and combustion gases. The furniture calorimeter simulates free burning in the open air. The burning rate may be very different under a ceiling, or inside a room, as described in the next section. Burning rates of many materials are described by Babrauskas and Grayson (1992) and Babrauskas (2008). For example, heat release rates for some typical items of furniture are given in Figure 3.2. Many studies have attempted to predict the burning of an item of furniture from information on the burning characteristics of the individual components, most often measured in a cone calorimeter (ISO, 2015). These studies have only had limited success because of difficulty scaling the complex phenomena from bench scale to complete items or to whole rooms. For fire engineering design it is preferable to use the results of tests on realistic full size objects to develop fire design curves.



Figure 3.1 A burning sofa in a furniture calorimeter test. If this sofa was burning in a room, the room would be full of toxic smoke

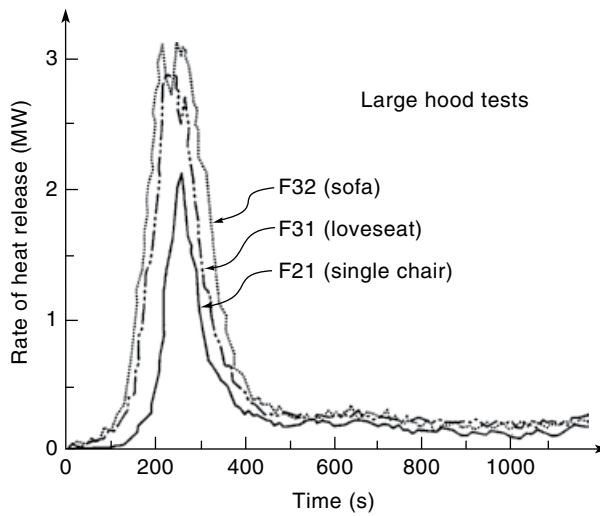


Figure 3.2 Heat release rate for furniture items. Reproduced from Babrauskas (2008) by permission of Society of Fire Protection Engineers

Table 3.2 Burning rates for some liquid and solid fuels

	Density	Regression rate	Mass loss rate	Surface burning rate	Specific surface	Total burning rate	Net calorific value	Heat release rate
	(kg/m ³)	(mm/h)	(kg/h)	(kg/s/m ²) (surface)	(m ² surface m ² floor)	(kg/s/m ²) (floor)	(MJ/kg)	(MW/m ²) (floor)
Liquids								
LPG (C ₃ H ₈)	585	609	356	0.099	1.0	0.099	46.0	4.55
Petrol	740	268	198	0.055	1.0	0.055	43.7	2.40
Kerosene	820	171	140	0.039	1.0	0.039	43.2	1.68
Ethanol	794	68	54	0.015	1.0	0.015	26.8	0.40
Plastics								
PMMA	—	—	—	0.054	1.0	0.054	24.0	1.34
Polyethylene	—	—	—	0.031	1.0	0.031	44.0	1.36
Polystyrene	—	—	—	0.035	1.0	0.035	40.0	1.40
Wood								
Flat wood	500	40	20	0.056	1.0	0.0056	16	0.09
1 m cube	500	40	20	0.056	6.0	0.033	16	0.53
100 mm in	500	40	20	0.056	20	0.11	16	1.8
crib	500	40	20	0.056	47	0.26	16	4.2
25 mm in crib	300	108	32	0.009	1.0	0.009	16	0.14
Softboard								

PMMA, poly(methyl methacrylate).

Burning rates for some liquid and solid fuels are given in Table 3.2 (derived from Babrauskas, 2008). These are based on a constant rate of burning per square metre of exposed surface area. The figures for liquids and plastics are measurements from open-air burning experiments. The figures for liquids are for pool fires over 2 m in diameter. The figures for wood are based on a constant regression rate of 40 mm/h which is typical for burning of wood in a fully developed room fire. The values for wood furniture will be similar to those given for wood cribs. Table 3.2 shows how the surface regression rate, the mass loss rate and the burning rate are all related, and they can be combined with the calorific value of the fuel to give the heat release rate. These figures can be used to estimate the rate of heat release in a large open air fire, such as may occur in an industrial building after the roof has collapsed.

3.4.2 Burning Items in Rooms

The heat release rate of burning items of furniture or other fuel in the open air has been discussed in the previous section. Burning objects can behave differently when they burn inside a room. The convective plume of hot gases above the burning object will hit the ceiling and spread horizontally to form a hot upper layer. In the early stages of the fire, the rate of burning may be significantly enhanced by radiant feedback from this hot upper layer. Later,

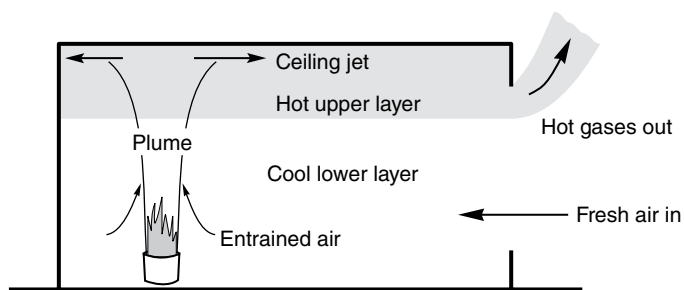


Figure 3.3 Early stages of fire in a room

the rate of burning may be severely reduced because of limited ventilation, which can restrict the transport of incoming air and outgoing combustion products through the openings, and reduce the oxygen concentration in the lower layer.

Figure 3.3 shows a fire in a room, at an early stage when only a single item is burning, before any spread of flame to linings or other items. The room has only one opening for ventilation. The combustion reaction requires the input of oxygen, initially obtained from the air in the room, but later from air coming in through the opening. The energy released by the fire acts like a pump, pulling cool air into the room, entraining it into the fire plume and pushing combustion products out through the top of the opening. The fire plume provides buoyant convective transport of combustion products up to the ceiling. The plume entrains a large amount of cold air which cools and dilutes the combustion products. The diluted combustion products form a hot upper layer within the room. The thickness and temperature of the hot layer increase as the fire grows. The lower layer consists of cooler incoming air which is heated slightly by mixing and radiation from the upper layer (Figure 3.4).

When the plume reaches the ceiling, there is a flow of hot gases radially outwards along the underside of the ceiling, called the ceiling jet. The direction of the ceiling jet will be influenced by the shape of the ceiling. For a smooth horizontal ceiling the flow will be the same in each radial direction. The hot gases in the ceiling jet will activate heat detectors or fire sprinkler heads located near the ceiling. As the fire continues to burn, the volume of smoke and hot gases in the hot upper layer increases, reducing the height of the interface between the two layers. The combustion products will start to flow out the door opening when the interface drops below the door soffit as shown in Figure 3.3. The hot layer thickness depends on the size and duration of the fire and the size of door or window openings. If there are insufficient ventilation openings, the fire will die down and may self-extinguish because of lack of oxygen.

The nature of wall, floor and ceiling linings can have a significant influence on fire growth and development in a room. Combustible lining materials can drastically increase the rate of initial fire growth due to rapid flame spread up walls and across ceilings. Temperatures will be higher and fire growth more rapid in a well-insulated room where less heat can be absorbed by the bounding elements. Computer models that predict fire growth including ignition and flame spread on combustible lining materials have been developed (Wade, 2004a, 2004b). If an automatic sprinkler system is installed, it will operate early in the pre-flashover fire period, and either extinguish the fire or prevent it from growing any larger after that time.



Figure 3.4 Smoke damage following a pre-flashover fire in a room, indicating the thickness of the hot upper layer during the fire

3.4.3 *t*-Squared Fires

The growth rate of a design fire is often characterized by a parabolic curve known as a *t*-squared fire such that the heat release rate is proportional to the time squared. The *t*-squared fire can be thought of in terms of a burning object with a constant heat release rate per unit area, in which the fire is spreading in a circular pattern with a constant radial flame speed. The *t*-squared heat release rate is given by:

$$Q = (t/k)^2 \quad (3.7)$$

where Q is the heat release rate (MW), t is the time (s) and k is a growth constant ($s/\sqrt{\text{MW}}$).

Values of k are given in Table 3.3 for slow, medium, fast and ultrafast fire growth, producing the heat release rates shown in Figure 3.5. The numerical value of k is the time for the fire to reach a size of 1.055 MW. The choice of growth constant depends on the type and geometry of the fuel. Values of k and peak heat release rate for many different burning objects are given

Table 3.3 Fire growth rates for *t*-squared fires

Fire growth rate	Growth constant, <i>k</i> (s/√MW)	Fire intensity coefficient, <i>α</i> (MW/s ²)	Typical real fire
Slow	600	2.93 × 10 ⁻⁶	Densely packed wood products
Medium	300	1.17 × 10 ⁻⁶	Solid wooden furniture such as desks Individual furniture items with small amount of plastic
Fast	150	4.66 × 10 ⁻⁵	Some upholstered furniture High stacked wood pallets Cartons on pallets
Ultrafast	75	1.874 × 10 ⁻⁴	Most upholstered furniture High stacked plastic materials Thin wood furniture such as wardrobes

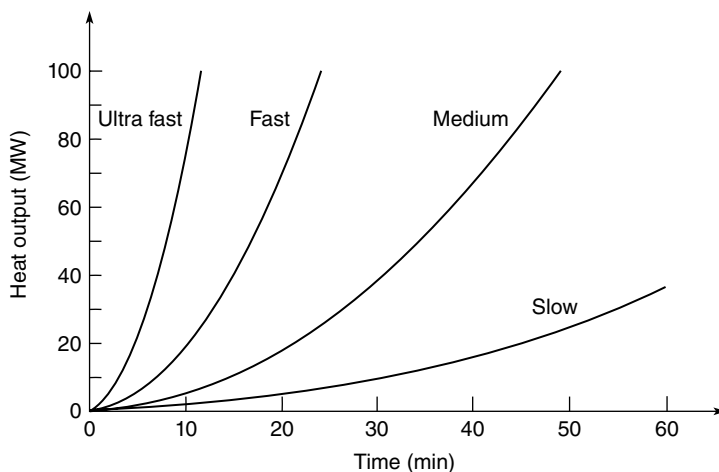


Figure 3.5 Heat release rate for *t*-squared fires

by Babrauskas (2008). An alternative formulation which gives identical results is to describe the heat release rate *Q* (MW) for a *t*-squared fire by:

$$Q = \alpha t^2 \tag{3.8}$$

where *α* is the fire intensity coefficient (MW/s²). Values of *α* are also given in Table 3.3.

Figure 3.6 shows the resulting heat release rates for furniture in an office fire with slow, medium and fast fire growth rates for a peak heat release rate of 9MW. The furniture item weighs 160kg with a calorific value of 20MJ/kg, giving a total energy load of 3200MJ, which is the area under each of the curves shown in Figure 3.6. The *t*-squared fire can be used to construct pre-flashover design fires, as input for calculating the initial fire growth in rooms.

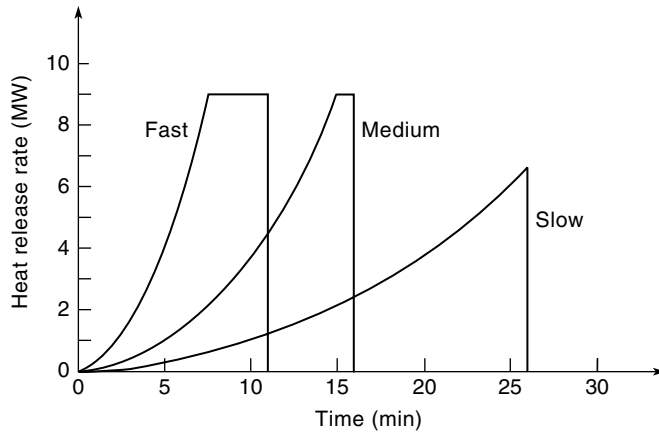


Figure 3.6 Heat release rates for a fire load of 3200 MJ

3.4.4 Fire Spread to Other Items

The fires described above are generally used to describe the heat release rate for burning of a single object. In the very early stages of a fire, before the upper layer gets very hot, fire may spread from the first burning object to a second object by flame contact if it is very close, or by radiant heat transfer. The time to ignition of a second object depends on the intensity of radiation from the flame and the distance between the objects. When the time to ignition of the second object has been calculated, the combined heat release rate can be added at any point in time to give the total heat release rate for these two and subsequent objects. This combined curve then becomes the input design fire for the room under consideration. There may be many more items involved, and the resulting combination may itself be approximated by a t -squared fire for simplicity.

For example, Figure 3.7(a) shows the t -squared heat release rate for two objects. The first burns with medium growth rate for 10 min, followed by 1 min of steady burning at its peak heat release rate of 4.0 MW. The second object ignites after 3 min, burning with fast growth rate for 4 min followed by steady burning at 2.5 MW for 2 min. Figure 3.7(b) shows the combined heat release rate curve for the two objects. The FREEBURN routine in the FPEtool computer package was used to calculate the time of ignition of the second object (Deal, 1993). There are now more sophisticated packages that can generate heat release rates from multiple fuel objects. These are briefly discussed in the sections that follow.

3.4.5 Pre-flashover Fire Calculations

In the fire engineering design process, much effort is expended in calculating the effects of pre-flashover fires, because this stage of the fire has the most influence on life safety. In order to ensure safe egress of building occupants it is necessary for the designer to know the expected rate of fire growth, and the resulting depth and temperature of the hot upper layer in the fire room and adjacent corridors as the fire develops. It is also essential to know the activation time and resulting effects of automatic detection and suppression systems. These calculations

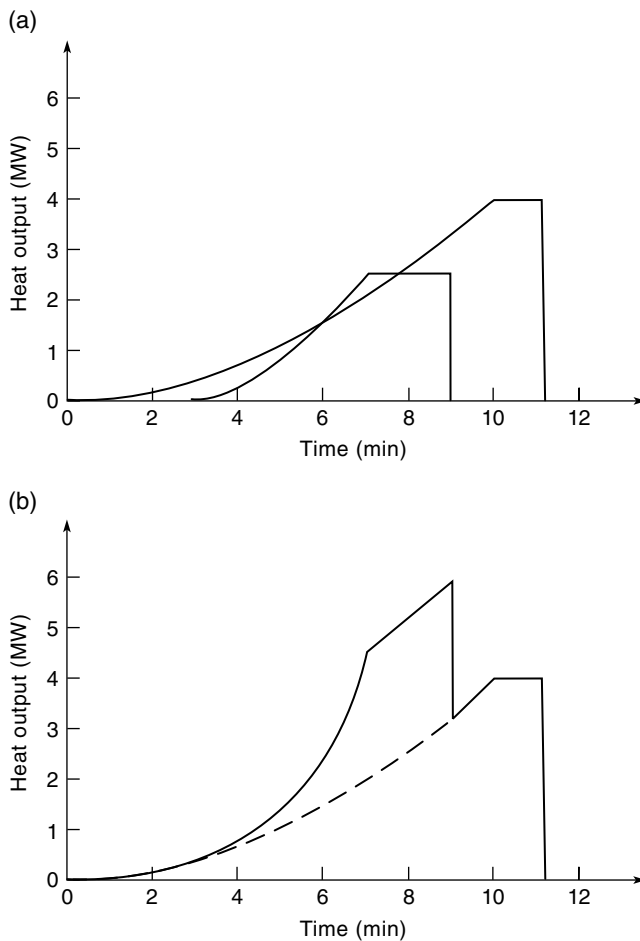


Figure 3.7 Combined design fire for two burning objects

are most often made using computer models such as those described below. For hand calculations of upper layer temperatures, Walton and Thomas (2008) describe equations derived by McCaffrey *et al.* (1981).

3.4.5.1 Zone Models

Zone models are relatively simple computer programs which can model the behaviour of a pre-flashover fire such as that shown in Figure 3.3. Most are *two-zone* models because they consider the room fire in terms of two homogeneous layers, or zones, and the connecting plume (Quintiere, 2008). Conservation equations for mass, momentum and energy are applied to each zone in a dynamic process that calculates the size, temperature and species concentration of each zone as the fire progresses, together with the flow of smoke and toxic products through openings in the walls and ceiling. Zone models do not calculate the growth of fire on objects

or surfaces, so they require input data such as a t -squared fire. Typical output includes the layer height, temperatures and concentrations of gas species in both layers, floor and wall temperatures, and the heat flux at the floor level.

One of the most versatile and widely used zone models is CFAST (Peacock *et al.*, 1993; Portier *et al.*, 1996) which can calculate the movement of smoke and hot gases in interconnected rooms. CFAST is available free of charge on the internet from the Building and Fire Research Laboratory of the National Institute of Standards and Technology (NIST). Wade (2004a, 2004b) has developed B-RISK (formerly BRANZFIRE), which is an enclosure zone model with an optional fire growth model for combustibles linings. It can calculate time-dependent distribution of smoke and heat through a collection of connected compartments during a fire (Spearpoint, 2008).

3.4.5.2 Field Models

The assumption of two distinct layers of gases is a convenient way of describing and calculating pre-flashover fire behaviour in rooms, but in reality there is a gradual three-dimensional transition of temperature, density and smoke between the layers, and this transition limits the accuracy of zone models. *Field models* are much more sophisticated computer programs which use Computational Fluid Dynamics (CFD) to model fires using a large number of discrete zones in a three-dimensional grid. Field models are much more difficult to run and to interpret than zone models, so they are more often used as research tools rather than design tools. NIST has developed Fire Dynamics Simulator (FDS) (McGrattan *et al.*, 2015a, 2015b), which simplifies the CFD modelling process to approximate forms of the Navier–Stokes equations for low-speed, thermally driven flows to simulate the mixing and transport phenomenon of combustible products (Spearpoint, 2008). FDS is increasingly used by designers for modelling pre-flashover fires, but neither zone models nor field models are suitable for accurately modelling post-flashover fires.

3.5 Flashover

If the fire shown in Figure 3.3 is allowed to grow without intervention, assuming sufficient fuel in the burning item, temperatures in the hot upper layer will rise, increasing the level of radiant heat flux to all other objects in the room. At a critical level of heat flux, all exposed combustible items in the room will begin to burn, leading to a rapid increase in both heat release rate and temperatures. This transition is called *flashover*. After flashover the fire is often referred to as a ‘post-flashover fire’, ‘fully developed fire’ or ‘full-room involvement’. It is not possible for flashover to occur in an open unenclosed space because, by definition, flashover can only occur in an enclosed compartment. Drysdale (2011) points out that flashover must be considered as the transition from a localized fire to combustion of all exposed combustible surfaces, rather than a precise event.

3.5.1 Conditions Necessary for Flashover

There are certain pre-conditions necessary for flashover to occur. There must be sufficient fuel and ventilation for a growing fire to develop to a significant size. The ceiling must be

able to trap hot gases, and the geometry of the room must allow the radiant heat flux from the hot layer to reach critical ignition levels at the level of the fuel items. Drysdale (2011) gives a detailed discussion of these factors, with summaries of a number of compartment tests. In a typical room flashover occurs when the hot layer temperature is about 600 °C, resulting in a radiant heat flux of about 20 kW/m² at floor level.

From an analysis of a large number of experimental fires, it has been observed that flashover will only occur if the heat output from the fire reaches a certain critical value, related to the size of the ventilation openings. For a room with one window, the critical value of heat release Q_{fo} (MW) is given by Thomas's flashover criterion (Walton and Thomas, 2008):

$$Q_{fo} = 0.0078 A_t + 0.378 A_v \sqrt{H_v} \quad (3.9)$$

where A_t is the total internal surface area of the room (m²), A_v is the area of the window opening (m²) and H_v is the height of the window opening (m).

Drysdale (2011) derives a similar expression, and points out that this type of correlation is very approximate, depending on the size, shape and lining materials of the room, and even the location of the fire within the room. Walton and Thomas (2008) show a comparison of this and similar expressions. If all the burning objects in a room can be characterized by a t -squared design fire as described in Section 3.4.3, a rough method of calculating the time to flashover is to use the critical value of heat release Q_{fo} from Equation 3.9 in Equation 3.10.

$$t_{fo} = k \sqrt{Q_{fo}} \quad (3.10)$$

where k is the value from Table 3.3.

3.6 Post-flashover Fires

The behaviour of the fire changes dramatically after flashover. The flows of air and combustion gases become very turbulent. The very high temperatures and radiant heat fluxes throughout the room cause all exposed combustible surfaces to pyrolyse, producing large quantities of combustible gases, which burn where there is sufficient oxygen. The most important information for structural design is the temperature in the room during the post-flashover fire. Sometimes the burning rates are also useful, so they are described first.

3.6.1 Ventilation Controlled Burning

In typical rooms, post-flashover fires are ventilation controlled, so the rate of combustion depends on the size and shape of ventilation openings. It is usually assumed that all window glass (other than wired glass or fire resistant glass) will break and fall out at the time of flashover, as a result of the rapid rise in temperature. If the glass does not fall out the fire will burn for a longer time at a lower rate of heat release. This can be detrimental for massive structural elements (or protected elements) as slow heating causes increased thermal exposure. In a ventilation controlled fire, there is insufficient air in the room to allow all the combustible gases to burn inside the room, so the flames extend out the windows and additional combustion takes place where the hot unburned gaseous fuels mix with outside air (Figure 3.8).



Figure 3.8 Post-flashover fire on the top floor of a multi-storey office building. The flames coming out of the windows indicate that this fire is ventilation controlled

3.6.1.1 Rate of Burning

When the fire is ventilation controlled, the rate of combustion is limited by the volume of cold air that can enter and the volume of hot gases that can leave the room. For a room with a single opening, Kawagoe (1958) used many experiments to show that the rate of burning of wood fuel \dot{m} (kg/s) can be approximated by:

$$\dot{m} = 0.092 A_v \sqrt{H_v} \quad (3.11)$$

where A_v is the area of the window opening (m^2) and H_v is the height of the window opening (m). In many references the burning rate \dot{m} is given as $5.5 A_v \sqrt{H_v}$ kg/min or $330 A_v \sqrt{H_v}$ kg/h, which are the same as Equation 3.11 in different units of time. Note that $A_v \sqrt{H_v}$ can be rewritten as $BH_v^{1.5}$ where B is the breadth of the window opening. This shows that the burning rate is largely dependent on the area of the window opening, but more so on its height.

If the total mass of fuel in the room is known, the duration of the burning period t_b (s) can be calculated using:

$$t_b = M_f / \dot{m} \quad (3.12)$$

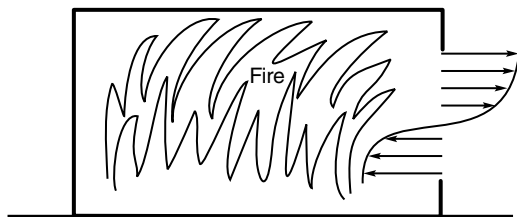


Figure 3.9 Window flows for ventilation controlled fire

where M_f is the total mass of fuel available for combustion (kg). The corresponding ventilation controlled heat release rate Q_{vent} (MW) for steady state burning is:

$$Q_{vent} = \dot{m}\Delta H_c \quad (3.13)$$

where ΔH_c is the heat of combustion of the fuel (MJ/kg).

If the total amount of fuel is known in energy units (MJ), the duration of the burning period t_b (s) can be calculated from:

$$t_b = E/Q_{vent} \quad (3.14)$$

where E is the energy content of fuel available for combustion (MJ).

These calculations all depend on the approximate relationship for burning rate given by Equation 3.11 which is widely used, but not always accurate. Even if the burning rate is known precisely, the calculation of heat release rate is not accurate because an unknown proportion of the pyrolysis products burn as flames outside the window rather than inside the compartment. Other sources of uncertainty arise because some proportion of the fuel may not be available for combustion, and the fire may change from ventilation control to a fuel controlled fire after some time.

Drysdale (2011) shows how Equation 3.11 can be derived by considering the flows of air and combustion products through an opening as shown in Figure 3.9. In a ventilation controlled fire there are very complex interactions between the radiant heat flux on the fuel, the rate of pyrolysis (or evaporation) of the fuel, the rate of burning of the gaseous products, the inflow of air to support the combustion, and the outflow of combustion gases and unburned fuel through openings. The interactions depend on the shape of the fuel (cribs or lining materials), the fuel itself (wood or plastic or liquid fuel) and the ventilation openings.

The empirical dependence of the ventilation controlled burning rate on the term $A_v\sqrt{H_v}$ has been observed in many studies, but some tests have shown departures from Kawagoe's equation. Following a large number of small-scale compartment fires with wood cribs reported by Thomas and Heselden (1972), Law (1983) proposed a slightly more refined equation for burning rate, finding that the burning rate is not directly proportional to $A_v\sqrt{H_v}$ but also depends on the floor shape of the compartment. Law's equation is:

$$\dot{m} = 0.18 A_v \sqrt{\frac{H_v W}{D}} (1 - e^{-0.036\Omega}) \quad (3.15)$$

where

$$\Omega = \frac{A_t - A_v}{A_v \sqrt{H_v}}$$

W is the length of the long side of the compartment width (m), D is the length of the short side of the compartment (m), and A_t is the total area of the internal surfaces of the compartment (m^2). In the calculation above, it is assumed that the opening is in the long side of the compartment.

Equation 3.15 gives approximately the same burning rate as Equation 3.11 for square compartments with a ventilation factor of $A_v \sqrt{H_v} / A_t = 0.05$ ($\Omega=20$). The burning rate is greater than Equation 3.11 for smaller openings and wider shallower compartments. Equation 3.15 only applies directly to compartments with windows in one wall because it is not easy to differentiate the terms W and D if there are windows in two or more walls. Equation 3.15 is used in the Eurocode 1 Part 1.2 (CEN, 2002b) for calculating the rate of burning when assessing the flame height from compartment windows.

Thomas and Bennetts (1999) have cast considerable doubt on the applicability of Kawagoe's equation, showing that the burning rate also depends heavily on the shape of the room and the width of the window in proportion to the wall in which it is located. If the width of the window is less than the full width of the wall, the burning rate is seen to be much higher than predicted by Equation 3.11 because of increased turbulent flow at the edges of the window. Despite these recent findings, Kawagoe's equation is the basis of most post-flashover fire calculations, until further research is conducted.

3.6.1.2 Ventilation Factor

The amount of ventilation in a fire compartment is often described by the ventilation factor F_v ($\text{m}^{0.5}$) given by:

$$F_v = A_v \sqrt{H_v} / A_t \quad (3.16)$$

where A_v is the area of the window opening (m^2), H_v is the height of the window opening (m) and A_t is the total internal area of the bounding surfaces (including openings) (m^2). The ventilation factor F_v has units of $\text{m}^{0.5}$ which has little intuitive meaning. However, if the acceleration of gravity g is introduced, the term $A_v \sqrt{gH_v} / A_t$ has units of metres per second, which is related to the velocity of gas flow through the openings. Considering only a single opening, the term $A_v \sqrt{gH_v}$ has units of cubic metres per second, which is related to the volumetric flow of gases through the opening.

3.6.1.3 Multiple Openings

Equation 3.8, Equation 3.11 and Equation 3.15 have been written for a single window opening in one wall of the compartment. If there is more than one opening, the same equations can be used, with A_v being the total area of all the openings and H_v being the weighted average height of all the window and door openings. Openings can be on several walls, which implies an

assumption that the air flow is similar in all openings and there is no strong wind blowing which would create a cross flow through the room.

Referring to Figure 3.10, the weighted average height of the openings H_v and the area of the internal surfaces of the compartment A_v can be calculated using:

$$H_v = (A_1 H_1 + A_2 H_2 + \dots) / A_v \tag{3.17a}$$

$$A_v = A_1 + A_2 + \dots = B_1 H_1 + B_2 H_2 + \dots \tag{3.17b}$$

$$A_r = 2(l_1 l_2 + l_1 H_r + l_2 H_r) \tag{3.17c}$$

The terms B_i and H_i are the breadth and height of the windows, respectively, l_1 and l_2 are the floor plan dimensions, and H_r is the room height.

3.6.2 Fuel Controlled Burning

Not all post-flashover fires are ventilation controlled. The rate of burning may sometimes be controlled by the surface area of the fuel, especially in large well-ventilated rooms containing fuel items which have a limited area of combustible surfaces. In this case the rate of burning will be similar to that which would occur for the fuel item burning in the open air, with enhancement from radiant feedback from the hot upper layer of gases or hot wall and ceiling surfaces. Most fires become fuel controlled in the decay period.

The average heat release rate from a fuel controlled fire can be calculated if the total fuel load and the duration of burning are both known. For example, Law (1983) has observed many experimental fires from which she concludes that typical domestic furniture fires have a free burning fire duration t_b of about 20 min (1200s), so that the heat release rate Q_{fuel} (MW) is given crudely by:

$$Q_{fuel} = E/1200 \tag{3.18}$$

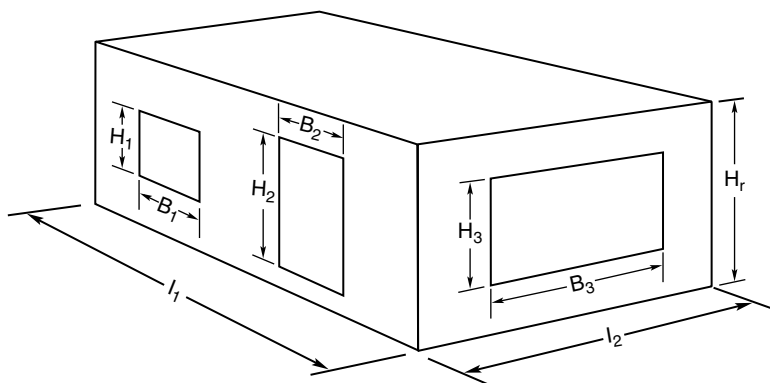


Figure 3.10 Calculation of ventilation factor for more than one window

where E is the total fuel load (MJ). More often the duration is not known, and the heat release rate needs to be estimated from information about the fuel and the temperatures in the fire compartment.

In all the above calculations, not all of the combustible material in the room may be available for immediate combustion. For this reason, many researchers introduce a *fuel fraction* which is an efficiency factor by which the heat of combustion or available fuel is reduced. Babrauskas (1981) suggests a value in the range 0.5–0.9, so 0.7 may be a suitable value for general design purposes. As shown by the worked examples, the various equations for fuel controlled heat release rate can give very different answers, so more research in this area is necessary. This is not of major importance because most post-flashover fire calculations for structural design assume ventilation controlled burning.

3.6.3 Fire Temperatures

Estimation of temperatures in post-flashover fires is an essential part of structural design for fire safety. Unfortunately this cannot be done precisely. This section describes measured and predicted temperatures from various studies, and a range of methods for estimating temperatures for design purposes. Temperatures in post-flashover fires are usually of the order of about 1000 °C. The temperature at any time depends on the balance between the heat released within the room and all the heat losses; through openings by radiation and convection, and by conduction into the walls, floor and ceiling.

3.6.3.1 Measured Temperatures

Several experimental studies have measured temperatures in post-flashover fires. There is considerable scatter between the results of different studies. Figure 3.11 shows the shapes of typical time temperature curves, starting at flashover, measured by Butcher *et al.* (1966) in real rooms with door or window openings and well distributed fuel load. Figure 3.11 also shows the ISO 834 standard curve used for fire resistance testing, as described in Section 3.7.2.

Figure 3.12 shows the maximum recorded temperature during the steady burning period for a large number of wood crib fires in small-scale compartments reported by Thomas and Heselden (1972). The recorded temperature was the average of a number of thermocouple readings within each compartment. An empirical equation for the line in Figure 3.12 has been developed by Law (1983), summarized by Walton and Thomas (2008). The maximum temperature T_{max} (°C) is given by:

$$T_{max} = 6000(1 - e^{-0.1\Omega}) / \sqrt{\Omega} \quad (3.19)$$

where

$$\Omega = \frac{A_t - A_v}{A_v \sqrt{H_v}}$$

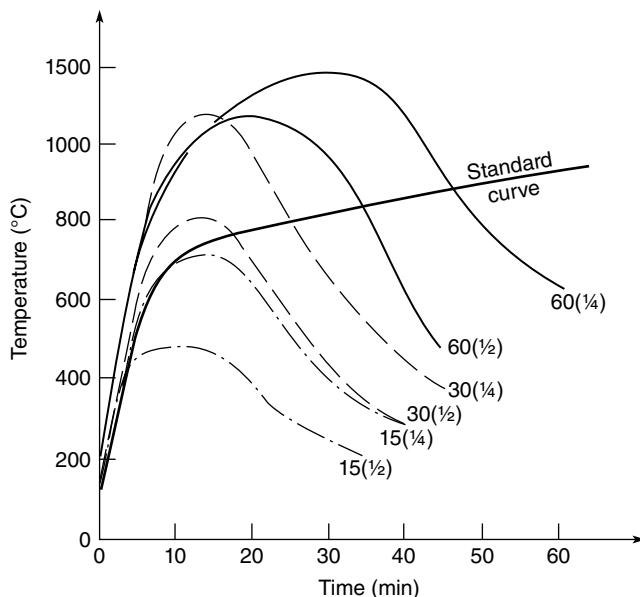


Figure 3.11 Experimental time temperature curves. Reproduced from Butcher *et al.* (1966) under the terms of the Open Government Licence

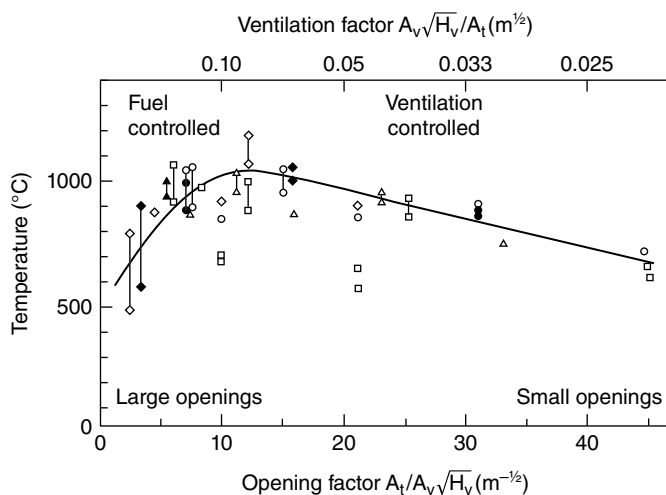


Figure 3.12 Maximum temperature in the burning period of experimental fires. Reproduced from Thomas and Heselden (1972) by permission of Building Research Establishment Ltd

The maximum temperature in Equation 3.19 may not be reached if the fuel load is small. For low fuel loads it can be reduced according to:

$$T = T_{max} (1 - e^{-0.05\psi}) \tag{3.20}$$

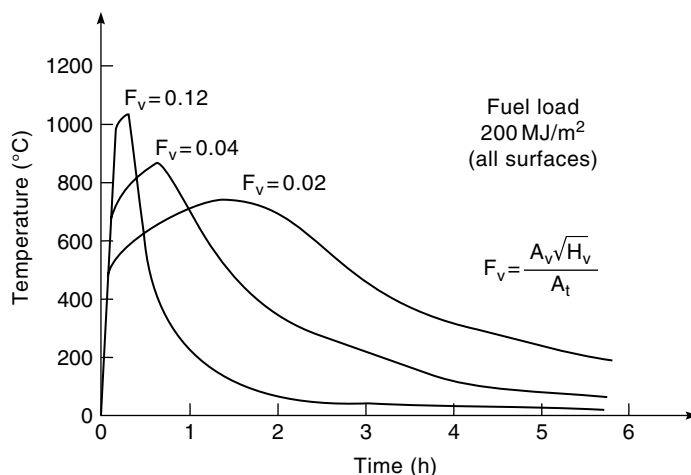


Figure 3.14 Time–temperature curves for varying ventilation and constant fuel load (MJ/m² total surface area)

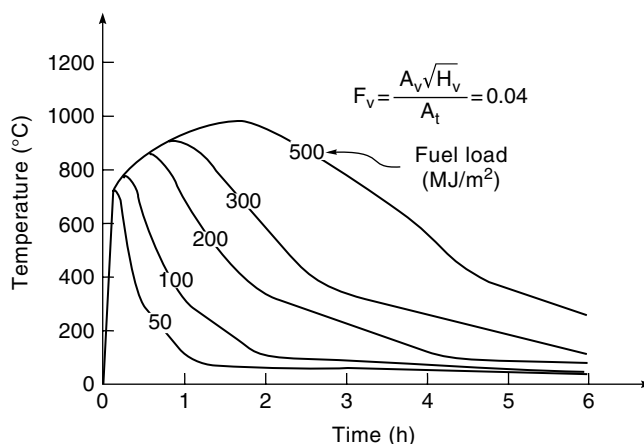


Figure 3.15 Time–temperature curves for varying fuel load (MJ/m² total surface area) and constant ventilation

fires burn faster than poorly ventilated fires, so they burn at higher temperatures, but for a shorter duration.

Figure 3.15 shows the effect of varying the fuel load for a constant size of ventilation opening. The rate of burning is the same in all cases because it is controlled by the window size, but increasing the fuel load leads to longer and hotter fires before the decay period begins.

3.6.3.3 Rate of Temperature Decay

The rate of temperature decay in a post-flashover fire is not easy to predict. The decay rate depends mainly on the shape and material of the fuel, the size of the ventilation openings and the thermal properties of the lining materials. If all the fuel is liquid or molten material in a

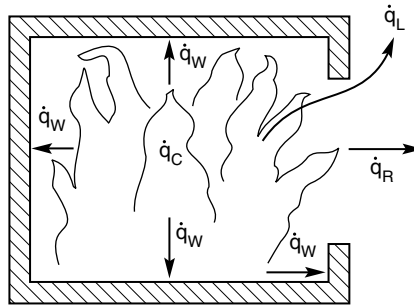


Figure 3.16 Heat balance for a post-flashover room fire

pool, the burning period will end suddenly when all the fuel has been consumed. On the other hand, solid materials like wood will burn at a predictable rate, leading to long decay periods depending on the thickness of the fuel items. The burning rate will be controlled by limited ventilation as long as the area of burning surfaces remains large. After the burning surface area reduces to a certain level, the fire will become fuel controlled and the decay rate will depend on the volume and thickness of the remaining items of fuel. If the fuel has a small ratio of surface area to volume, the fuel controlled burning in the later stages of the fire will lead to a long slow decay rate.

The rate of temperature decay depends on the ventilation openings because large openings will allow rapid heat loss from the compartment by both convection and radiation, whereas small openings will allow the heat to be trapped for much longer. The effect of thermal properties of the construction materials is not easy to quantify. On one hand, materials of low thermal inertia will store less heat and hence transfer less heat back into the compartment after the fire is out, leading to a rapid rate of decay. On the other hand, such materials (which also have low thermal conductivity) will insulate the compartment and result in higher temperatures if any residual burning occurs in the decay period. Of these two contradictory effects, the first is likely to predominate, so that materials of low thermal inertia will likely lead to more rapid decay rates.

3.6.4 Computer Models

A number of computer models have been used for calculating temperatures in post-flashover room fires. Most of these are single-zone models which consider the room to be a well-mixed reactor. It is possible to use two-zone models for post-flashover fires, but these are not generally considered appropriate because many of the pre-flashover assumptions are no longer valid. Field models are not easily applied to post-flashover fires because of excessive turbulence. All computer models for post-flashover fires are based on heat balance. Figure 3.16 shows the main components of heat flow in a simple compartment fire. The heat produced by combustion of the fuel \dot{q}_C is balanced by the heat losses, the main components being heat conducted into the surrounding structure \dot{q}_W , heat radiated through the opening \dot{q}_R , and heat carried out of the opening by convection of hot gases and smoke \dot{q}_L . The computer models consider this heat balance and solve the conservation equations to predict the temperature of the gases within the compartment.

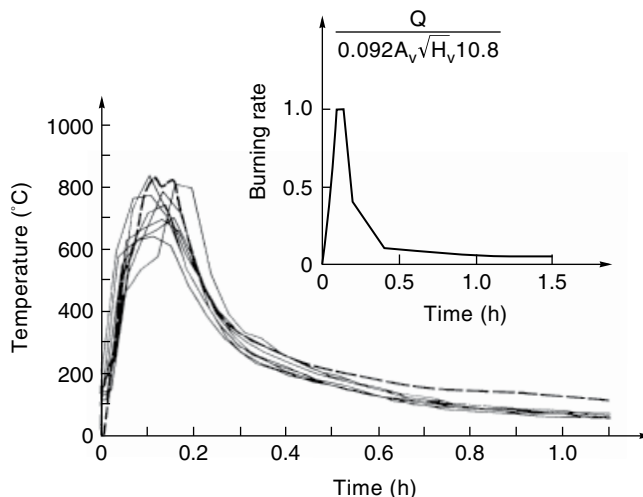


Figure 3.17 Burning rate used for calculating Swedish curves. Reproduced from Magnusson and Thelandersson (1970) by permission of Fire Safety Engineering Department, Lund University

Single-zone models assume that all combustion takes place within the compartment, temperatures are uniform within the compartment, and heat flow into the surrounding structure is identical on all walls and the ceiling. A difficulty for all models is the calculation of the burning rate. Most models simply assume ventilation controlled burning as given by Equation 3.11, but some also include fuel controlled burning. None of the available models is able to accurately include the effects of horizontal openings in the ceiling. More information on computer models is given in Chapter 11.

3.6.4.1 Swedish Method and Lie's Method

The Swedish curves have been shown in Figure 3.13. When calibrating their model, Magnusson and Thelandersson (1970) manipulated the heat release rate to produce temperatures similar to those observed in short duration test fires. The resulting shape of the heat release rate curve used in those calculations is shown in Figure 3.17. The peak rate of heat release is the theoretical rate for ventilation controlled burning given by Equation 3.11, assuming a calorific value of only 10.8 MJ/kg, which is lower than the value used by most other authors. Temperatures in the decay phase are calculated in the computer model using assumed burning rates such as those shown in Figure 3.17. Magnusson and Thelandersson extrapolated their computer model to much higher fuel loads and longer durations than the available test data in order to produce curves such as those shown in Figure 3.13.

In a similar approach to the Swedish method, Lie (1995) used values from Kawagoe's original work to perform heat balance calculations for post-flashover fires with a range of ventilation factors and different wall lining materials, proposing a set of approximate equations for design purposes, including the duration of burning and arbitrary decay rates. Lie's curves are unrealistic for rooms with small windows because the proposed temperatures are not sufficient for flashover to have occurred.

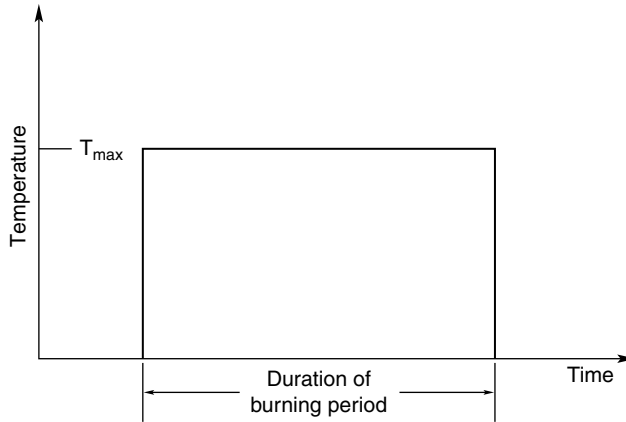


Figure 3.18 Design fire with constant temperature

Other programs that have been used to generate post-flashover fire temperatures are COMPF2 (Babrauskas, 1979, 1981) and FASTLite (Portier *et al.*, 1996). COMPF2 was a single-zone model which solved the heat balance equations to generate gas temperatures. It had several options for calculating the heat release rate, based on ventilation control, fuel control, or the porosity of wood crib fuels. It also had the capacity to calculate the rate of temperature reduction. FASTLite was a two-zone model which used C-FAST to model post-flashover fires using equations for the heat release rate adapted from the FIRE SIMULATOR section of FPEtool. Ozone is a single-zone model developed in Europe as part of a major collaboration investigating the ‘natural fire safety concept’ for competitive design of steel buildings (Cadorin *et al.*, 2001). Ozone is based on similar principles to COMPF2, with improved calculation procedures.

3.7 Design Fires

When designing a structure to resist exposure to fire, it is often necessary to select a design fire. Alternative methods of obtaining design fires include hand calculations, published curves or parametric fire equations. Each of these are discussed in this section.

3.7.1 Hand Methods

A very simple, but crude, method is to assume that the fire has a constant temperature throughout the burning period, giving a time–temperature curve as shown in Figure 3.18. Such a time–temperature curve will often be sufficiently accurate for simple designs. The maximum temperature can be estimated using Equation 3.19 and Equation 3.20. The duration of the burning period can be calculated from Equation 3.14, assuming ventilation control.

Table 3.4 ASTM E119 and ISO 834 time and temperature values

Time (min)	ASTM E119 temperature (°C)	ISO 834 temperature (°C)
0	20	20
5	538	576
10	704	678
30	843	842
60	927	945
120	1010	1049
240	1093	1153
480	1260	1257

3.7.2 Published Curves

For many applications it is possible to scale temperatures off published curves which have been derived from computer calculations. This can be done using the Swedish curves shown in Figure 3.13, using interpolation where necessary. Data points on the curves are also published (Magnusson and Thelandersson, 1970; Drysdale, 2011) but no simple formulae are available. Nominal fire curves are also used. These are the standard fire curve, the external fire curve and the hydrocarbon fire curve.

Most countries around the world rely on full size fire resistance tests to assess the fire performance of building materials and structural elements. The time–temperature curve used in fire resistance tests is called the ‘standard fire’. Full-size tests are preferred over small-scale tests because they allow the method of construction to be assessed, including the effects of thermal expansion and deformation under load. The most widely used test specifications are ISO 834 (ISO, 1999a) and ASTM E119 (ASTM, 2012). Other national standards include British Standard BS 476 Parts 20–23 (BSI, 1987) and Australian Standard AS 1530 Part 4 (SA, 2005).

Most national standards are based on either the ASTM E119 test or the ISO 834 test, which are compared below:

- (i) The standard fire curve

ISO 834 curve: The furnace temperature–time relationship is given by:

$$T_g = 20 + 345 \log(8t + 1) \quad (3.21)$$

- (ii) ASTM E119

ASTM E119 on the other hand is defined by a number of discrete points, which are shown in Table 3.4, with the corresponding ISO 834 temperatures.

There are several equations approximating the ASTM E119 curve; the simplest is given by Lie (1995) as:

$$T_g = 20 + 750 \left(1 - e^{-3.79553\sqrt{t_h}}\right) + 170.41\sqrt{t_h} \quad (3.22)$$

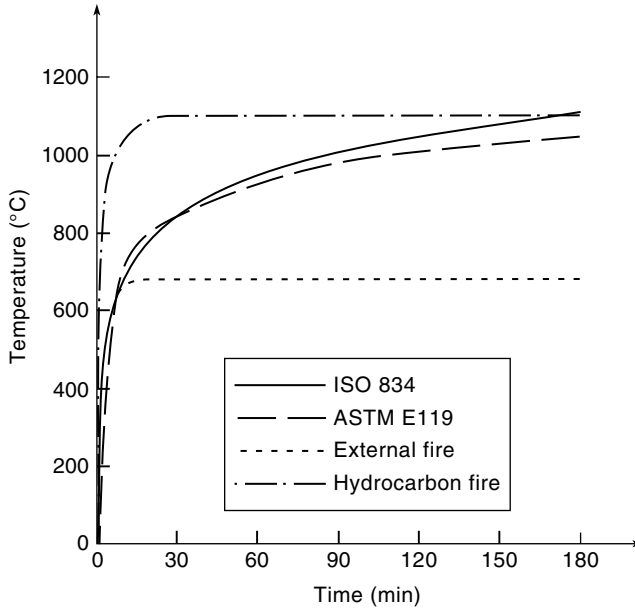


Figure 3.19 Nominal time–temperature curves for post-flashover fires

- (iii) The external fire curve

The external fire curve, given by:

$$T_g = 20 + 660(1 - 0.686e^{-0.32t} - 0.313e^{-3.8t}) \quad (3.23)$$

is a time–temperature relationship that is representative of the reduced exposure experienced by elements on the facade of buildings.

- (iv) The hydrocarbon fire curve

The hydrocarbon fire curve is used for environments where a high degree of hydrocarbons is present. It is given by:

$$T_g = 20 + 1080(1 - 0.325e^{-0.167t} - 0.675e^{-2.5t}) \quad (3.24)$$

In the equations above, T_g is the gas temperature, t is the time in minutes and t_h is the time in hours. These four curves are compared in Figure 3.19.

3.7.3 Eurocode Parametric Fires

The Eurocode 1 Part 1.2 (CEN, 2002b) gives an equation for ‘parametric’ fires, allowing a more realistic time–temperature relationship to be produced for any combination of fuel load, ventilation openings and wall lining materials. The Eurocode parametric fire curves have been derived to give a good approximation to the burning period of the Swedish curves shown in

Figure 3.13. They have been further improved to clearly distinguish between fuel controlled and ventilation controlled post-flashover fires (Franssen *et al.*, 2009).

3.7.3.1 Equation for Burning Period

The Eurocode equation for temperature T (°C) is:

$$T_g = 20 + 1325 \left(1 - 0.324e^{-0.2t^*} - 0.204e^{-1.7t^*} - 0.472e^{-19t^*} \right) \quad (3.25)$$

where t^* is a fictitious time given by:

$$t^* = \Gamma t \quad (3.26)$$

where t is the time (in hours), and

$$\Gamma = \frac{\left(F_v / F_{ref} \right)^2}{\left(b / b_{ref} \right)^2}$$

b is $\sqrt{\text{thermal inertia}} = \sqrt{k\rho c_p}$ (Ws^{0.5}/m²K) and F_v is the ventilation factor ($m^{0.5}$) given by:

$$F_v = A_v \sqrt{H_v} / A_t$$

Equation 3.25 is a good approximation to the ISO 834 standard fire curve for temperatures up to about 1300 °C. Hence the Eurocode parametric fire curve is close to the ISO 834 curve for the special case where $F_v = F_{ref}$ and $b = b_{ref}$. Larger ventilation openings or more highly insulated compartments will result in higher room temperatures. Smaller openings and poorly insulated compartments will result in lower temperatures. In the Eurocode, the value of F_{ref} is 0.04 and the value of b_{ref} is 1160 such that

$$\Gamma = \frac{\left(F_v / 0.04 \right)^2}{\left(b / 1160 \right)^2} \quad (3.27)$$

The above formulation of the parametric fire curve assumes that the walls and ceiling of the fire compartment are made from one layer of material, with thermal inertia $k\rho c_p$. If there are two or more layers of different materials, the Eurocode gives a formula for calculating an effective value of the b term.

For a wall with material 1 on the fire side and material 2 protected by material 1, and thicknesses s_1 and s_2 of the two layers, the thermal properties $b = \sqrt{k\rho c_p}$ are called b_1 and b_2 , respectively. If a heavy material is insulated by a lighter material such that $b_1 < b_2$ the value of the lighter material in layer 1 should be used in the calculations, so that $b = b_1$. If a light material is covered by a heavier material (as in sandwich panel construction) such that $b_1 > b_2$

Table 3.5 Fire growth rate for different occupancies

Occupancy	Fire growth rate	Duration of burning (min)
Dwelling	Medium	20
Hospital (room)	Medium	20
Hotel (room)	Medium	20
Library	Fast	15
Office	Medium	20
Classroom of a school	Medium	20
Shopping centre	Fast	15
Theatre (cinema)	Fast	15
Transport (public space)	Slow	25

Source: Adapted from Eurocode 1 Part 1.2 (CEN, 2002b).

then the b value depends on the thickness of the heavier material and the time of the heating period of the fire. The limiting thickness $s_{lim,1}$ of the fire-exposed material is calculated from:

$$s_{lim,1} = \sqrt{\frac{3600 t_{max} k}{\rho c_p}} \quad (3.28)$$

where t_{max} is the time of the heating period of the fire (in hours) and the thermal properties are for material 1.

If $s_1 > s_{lim,1}$ then $b = b_1$, and if $s_1 < s_{lim,1}$ then $b = (s_1/s_{lim,1}) b_1 + (1 - s_1/s_{lim,1}) b_2$.

3.7.3.2 Duration of Burning Period

For ventilation controlled fires, the duration of the burning period t_d (in hours) in the Eurocode simplifies to:

$$t_d = 0.0002 e_t / F_v = \frac{0.0002 E}{A_v \sqrt{H_v}} \quad (3.29)$$

where e_t is the fuel load (MJ/m² total surface area) and E is the total energy content of the fuel (MJ).

For fuel controlled fire scenarios, the Eurocode sets the duration of burning t_{lim} as 25, 20 or 15 min, depending on a slow, medium or fast fire growth rate, respectively. The typical fire growth rate in various occupancies (hence the duration of burning t_{lim}) is given in Annex E of Eurocode 1 (CEN, 2002b), as shown in Table 3.5.

3.7.3.3 Decay Period

The Eurocode time–temperature relationship in the cooling phase of the parametric fire is given by:

$$T = T_{max} - 625 \left(t^* - t_{max}^* x \right) \quad \text{for } t_{max}^* \leq 0.5 \quad (3.30a)$$

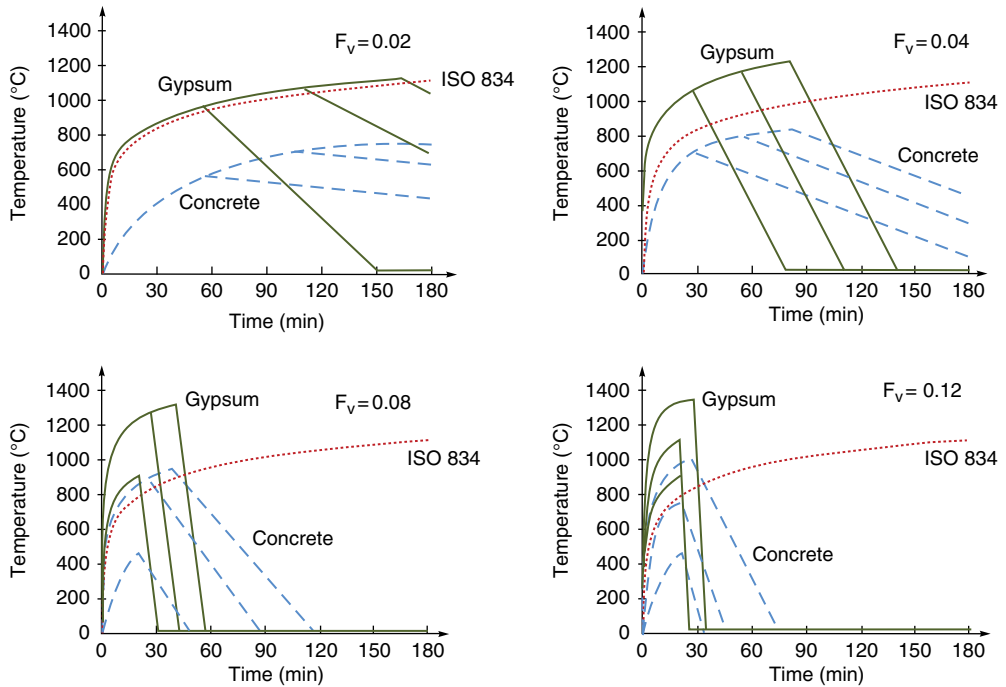


Figure 3.20 Parametric time–temperature curves. Fuel load is 400, 800 and 1200 MJ/m² floor area

$$T = T_{max} - 250(3 - t_{max}^*) (t^* - t_{max}^* x) \quad \text{for } 0.5 < t_{max}^* < 2.0 \tag{3.30b}$$

$$T = T_{max} - 250(t^* - t_{max}^* x) \quad \text{for } t_{max}^* > 2.0 \tag{3.30c}$$

where $t_{max}^* = (0.0002 e_i / F_v) \Gamma$

and $x = \begin{cases} 1.0 & \text{if } t_{max} > t_{lim} \\ t_{lim} \Gamma / t_{max}^* & \text{if } t_{max} = t_{lim} \end{cases}$

with $\Gamma_{lim} = \frac{(F_{v,lim} / 0.04)^2}{(b / 1160)^2}$ and $F_{v,lim} = 0.0001 e_i / t_{lim}$ ($t_{lim} = 25 \text{ min}, 20 \text{ min}, 15 \text{ min}$)

3.7.3.4 Time–temperature Curves

Figure 3.20 shows the Eurocode time–temperature equation plotted for a range of ventilation factors, fuel loads and materials. The temperatures in the burning period have been calculated from the equations described above, from Eurocode 1 Part 1.2 (CEN, 2002b). In each part of Figure 3.20, curves have been drawn for three fire loads and for two types of construction materials, showing the significant dependence of fire temperatures on the thermal properties of the bounding materials. The fire loads are 400, 800 and 1200 MJ/m² floor area, for a room 5 × 5 m in plan and 3 m high. The materials are normal weight concrete ($b = 1900 \text{ W s}^{0.5} / \text{m}^2 \text{ K}$) and gypsum plaster board ($b = 522 \text{ W s}^{0.5} / \text{m}^2 \text{ K}$). A typical commercial office building with a

mixture of these materials on the walls and ceiling would give curves between these two, similar to a building made from lightweight concrete.

It is observed that, with the exception of the fire in the room lined with gypsum and a 400 MJ/m² fuel load, the fires with opening factors 0.02 and 0.04 have the same general shape for concrete or gypsum. The different descending branch is due to t_{max}^* for the 400 MJ/m² case lying between 0.5 h and 2 h while the rest have t_{max}^* values greater than 2 h. For $F_v = 0.08$ and 0.12 there are instances with curves of different shapes. This is because the relative amounts of ventilation are higher so that the fire becomes fuel controlled and therefore burns more rapidly. The temperatures are therefore dictated by the rapid fire growth rates (from Table 3.5); their maximum temperatures are recorded at the time t_{lim} .

3.8 Other Factors

3.8.1 Additional Ventilation Openings

Ventilation controlled fires are very sensitive to the size and location of openings. The presence of a ceiling opening allows combustion products to exit the ceiling opening while cool air enters the window. This significantly increases the ventilation to the fire as shown in Figure 3.21.

Magnusson and Thelandersson (1970) provide an approximate nomogram for allowing for ceiling vents, shown in Figure 3.22. If all of the lines shown are assumed to be straight lines through the origin, the nomogram can be simplified to give a fictitious ventilation factor:

$$\left(A_v \sqrt{H_v}\right)_{fict} = A_v \sqrt{H_v} + 2.3 A_h \sqrt{h} \quad (3.31)$$

where A_h is the area of the horizontal opening in the ceiling (m²), and h is the vertical distance from mid-height of the window opening to the ceiling of the compartment. This approximate expression can only be used for values of $A_v \sqrt{h} / A_v \sqrt{H_v}$ in the range 0.3–1.5. Beyond the upper limit, the expression is not valid because the window opening no longer dominates the flow of gases. According to Magnusson and Thelandersson, their model has been shown to work up to this limit in tests reported by Thomas *et al.* (1963). The term $\left(A_v \sqrt{H_v}\right)_{fict}$ from Equation 3.31 can be used in place of $A_v \sqrt{H_v}$ to calculate the burning rate in Equation 3.11, or to select a time–temperature curve from Figure 3.13.

A room with openings on two opposite walls may have cross ventilation, especially if there is a wind blowing as shown in Figure 3.23, producing increased rates of burning. No research has been done on this type of scenario, other than some estimates for external steel structures exposed to fires from windows (Law and O'Brien, 1989).

3.8.2 Progressive Burning

For large compartments such as open plan offices or industrial buildings, a uniform post-flashover fire will not occupy the whole space at one time. All the time–temperature curves presented for post-flashover fires relate to small rooms which have been tested, up to about 6 m by 6 m in floor area and 3.0 m in height. There is almost no test data for post-flashover

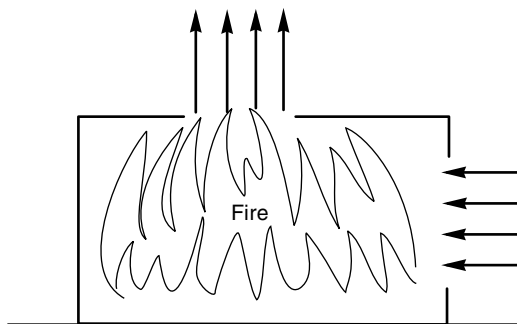


Figure 3.21 Vent flows for room with ceiling opening

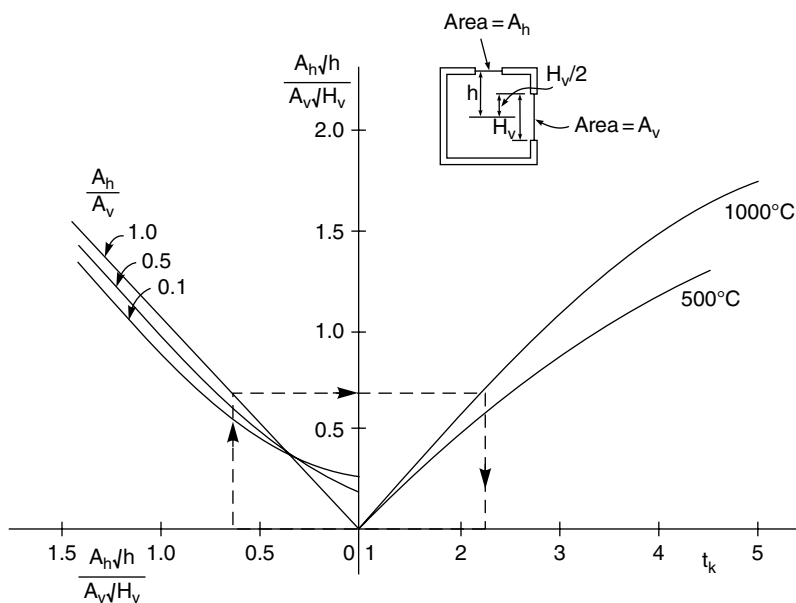


Figure 3.22 Nomogram for calculating the ventilation factor for roof vents. Reproduced from Magnusson and Thelandersson (1970) by permission of Fire Safety Engineering Department, Lund University

fires in compartments with larger floor areas or taller ceilings. In general, it is probably conservative to use the models described above, because the probability of flashover and full-room involvement is less as the size of the compartment increases, and the assumption of full-room involvement for the full burning period is most severe on the structure.

Kirby *et al.* (1994) conducted a series of tests in a narrow room, 20m in length and 6m wide, with uniformly distributed wood cribs as fuel. Even when the fire was ignited at the end farthest from the window, burning moved quickly to the window end, then progressed slowly from that end towards the back as shown in Figure 3.24. Temperatures measured at points A, B and C in Figure 3.24 are shown in Figure 3.25 where it can be seen that the total duration of

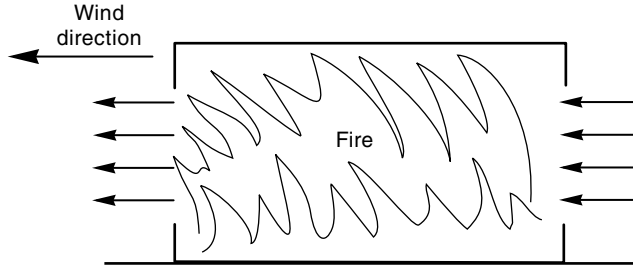


Figure 3.23 Vent flows for two windows, with wind blowing

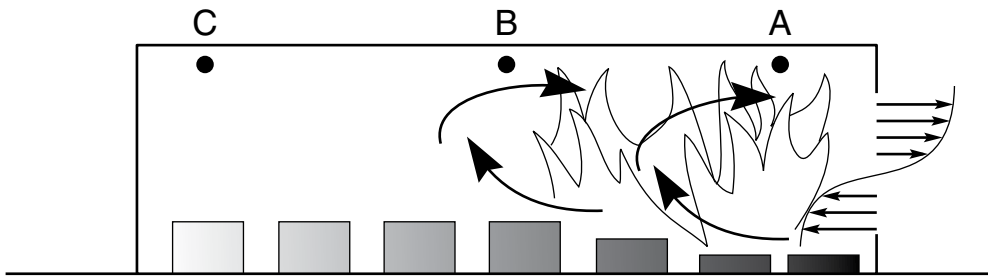


Figure 3.24 Progressive burning in a deep room with one window

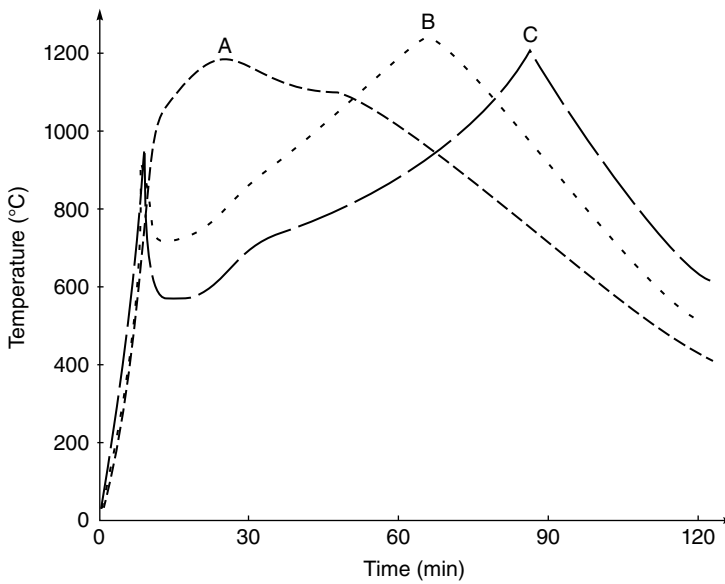


Figure 3.25 Temperatures during progressive burning in a deep room. Reproduced from Kirby *et al.* (1994) by permission of Corus UK Ltd

elevated temperatures is similar at all three points, but the peak temperature progresses back into the compartment as the fuel closest to the window is progressively burned.

Clifton (1996) has proposed a model for fire spreading within a large compartment. Thomas and Bennetts (1999) reported similar behaviour in small-scale experiments, finding that most fires burn progressively with the object nearest the window burning first, and often delaying burning of other items in the room. These findings have significant implications for modelling of post-flashover fires, and have led to the development of the phenomenon of travelling fires (Rein *et al.*, 2007). A methodology that tracks the movement of the fire through the compartment has been proposed. It suggests a near field of peak temperatures for localized burning and a far field of lower temperatures for the areas of the compartment that have either experienced the moving localized fire or are being preheated (Stern-Gottfried *et al.*, 2010).

3.8.3 Localized Fires

The discussion of post-flashover fires in this chapter has been based on the assumption that a fully developed fire occurs and creates the same temperature conditions throughout the fire compartment. In some circumstances, possibly in a large space where there are no nearby combustibles, or in a fire partially controlled by sprinklers, there could be a localized fire which has much less impact on the building structure than a fully developed fire. Tests by Hasemi *et al.* (1995) have been used by Franssen *et al.* (1998) to calculate steel temperatures in steel beams above burning cars in car parking buildings. Structural design calculations can be made in such cases if the member temperatures are known, but it is always conservative to assume a fully developed fire. Bailey *et al.* (1996a) have investigated the structural response of a multi-bay steel frame to a spreading fire including the effects of cooling during the decay period. For design guidance on localized fires refer to Appendix C of Eurocode 1 Part 1.2 (CEN, 2002b).

3.9 Heat Transfer

Some knowledge of heat transfer is essential to the understanding of fire behaviour. Heat transfer occurs by the three processes of *conduction*, *convection* and *radiation*, which can occur separately or together depending on the circumstances.

3.9.1 Conduction

Conduction is the mechanism for heat transfer in solid materials. In materials which are good conductors of heat, the heat is transferred by interactions involving free electrons, hence materials which are good electrical conductors are usually also good conductors of heat. In other materials which are poor conductors, heat is conducted by mechanical vibrations of the molecular lattice. Conduction of heat is an important factor in the ignition of solid surfaces, and in the fire resistance of barriers and structural members.

Several material properties are needed for heat transfer calculations in solid materials. These are the *density*, *specific heat* and *thermal conductivity*. Density ρ is the mass of the material per unit volume (in kg/m³). Specific heat c_p is the amount of heat required to heat a

Table 3.6 Thermal properties of some common materials^a

Material	Thermal conductivity, k (W/mK)	Specific heat, c_p (J/kgK)	Density, ρ (kg/m ³)	Thermal diffusivity, α (m ² /s)	Thermal inertia, $k\rho c_p$ (W ² s/m ⁴ K ²)
Copper	387	380	8940	1.14×10^{-4}	1.3×10^9
Steel (mild)	45.8	460	7850	1.26×10^{-5}	1.6×10^8
Brick (common)	0.69	840	1600	5.2×10^{-7}	9.3×10^5
Concrete	0.8–1.4	880	1900–2300	5.7×10^{-7}	2×10^6
Glass (plate)	0.76	840	2700	3.3×10^{-7}	1.7×10^6
Gypsum plaster	0.48	840	1440	4.1×10^{-7}	5.8×10^5
PMMA ^b	0.19	1420	1190	1.1×10^{-7}	3.2×10^5
Oak ^c	0.17	2380	800	8.9×10^{-8}	3.2×10^5
Yellow pine ^c	0.14	2850	640	8.3×10^{-8}	2.5×10^5
Asbestos	0.15	1050	577	2.5×10^{-7}	9.1×10^4
Fibre insulating board	0.041	2090	229	8.6×10^{-8}	2.0×10^4
Polyurethane foam ^d	0.034	1400	20	1.2×10^{-6}	9.5×10^2
Air	0.026	1040	1.1	2.2×10^{-5}	—

Source: Reproduced from Drysdale (2011) by permission of John Wiley & Sons, Ltd.

^a From Pitts and Sissom (1977) and others. Most values for 0 or 20 °C. Figures have been rounded off.

^b Poly(methyl methacrylate). Values of k , c_p and ρ for other plastics are given in Drysdale (2011), Table 1.2.

^c Properties measured perpendicular to the grain.

^d Typical values only.

unit mass of the material by one degree (with units of J/kgK). Thermal conductivity k represents the amount of heat transferred through a unit thickness of the material per unit temperature difference (with units of W/mK). There are two derived properties which are often needed. These are the *thermal diffusivity* given by $\alpha = k/\rho c_p$ (with units m²/s) and the *thermal inertia* $k\rho c_p$ (with units W²s/m⁴K²). For a given fire load, rooms lined with materials of low thermal inertia will experience higher temperatures than rooms lined with materials of higher thermal inertia. Thermal properties for common materials are given in Table 3.6. A more extensive list is given in Appendix A of the SFPE Handbook (SFPE, 2008), including temperature dependent thermal properties for metals.

In the steady-state situation, the transfer of heat by conduction is directly proportional to the temperature gradient between two points, with a constant of proportionality known as the thermal conductivity, k , so that

$$\dot{q}'' = kdT/dx \quad (3.32)$$

where \dot{q}'' is the heat flow per unit area (W/m²), k is the thermal conductivity (W/mK), T is temperature (°C or K) and x is distance in the direction of heat flow (m). The steady-state calculation does not require consideration of the heat required to change the temperature of the material that is being heated or cooled.

For transient heat flow when temperatures are changing with time, the amount of heat required to change the temperature of the material must be included. For one-dimensional heat transfer by conduction in a material with no internal heat being released, the governing equation is:

$$\frac{\delta^2 T}{\delta x^2} = \frac{1}{\alpha} \frac{\delta T}{\delta t} \quad (3.33)$$

where t is time (s) and α is thermal diffusivity (m^2/s). It can be seen that materials with low thermal diffusivity will conduct more heat than materials with high thermal diffusivity, when exposed to increasing surface temperatures in unsteady-state conductive heat transfer.

This type of analysis can be extended to two or three dimensions as necessary. There are many methods of solving the heat conduction equation, using analytical, graphical or numerical methods. Some methods are given by Drysdale (2011) and there are many standard textbooks on heat transfer. Calculation of conductive heat transfer can be by simple formulae, the use of design charts or by numerical analysis.

3.9.1.1 Simple Formulae

Standard textbooks on heat transfer contain simple formulae for conductive heat transfer in various materials and geometries. Some of these are available for common materials exposed to fire. A lumped heat capacity formula can be used for a protected or unprotected steel element on the assumption that the internal steel temperatures are constant. This type of formula is most accurate where it is used repeatedly with sequential time steps. Some formulae can take account of the heat required to heat up heavy insulating materials, or the time delay resulting from driving off moisture. Typical formulae are given by Pettersson *et al.* (1976), Eurocode 3 Part 1.2 (CEN, 2005b) and Milke (2008). A simple spreadsheet formulation is described by Gamble (1989). Examples of these methods are given in Chapter 6.

A semi-infinite slab analysis can be used in situations where the heat transfer is essentially one-dimensional, such as with large flat surfaces. This analysis assumes that the heat is absorbed before reaching the unexposed side, so the material has to be relatively thick. Schaffer (1977) has applied this type of analysis to wood slabs.

3.9.1.2 Numerical Analysis

The most powerful tools for calculating conductive heat transfer are computer-based numerical methods such as finite element or finite difference formulations. These techniques are well established, but there are not many user-friendly commercial computer packages customized for fire applications. Special characteristics needed for structural fire applications include internal voids and temperature dependent thermal properties. The most widely used finite element programs for thermal analysis of structural members include SAFIR

(Franssen *et al.*, 2000) and TASEF (Sterner and Wickström, 1990). A review of some of these programs and others that have now been discontinued is given by Sullivan *et al.* (1994). Many generic finite element stress analysis programs can calculate heat transfer by conduction. Some widely used commercial programs include ABAQUS (2010) and ANSYS (2009). These are versatile programs which can analyse any three-dimensional mesh which is input by the user. More information is given in Chapter 11.

Both two- and three-dimensional heat transfer analysis is possible, but two-dimensional analysis is adequate for almost all fire engineering applications. This is because structural elements are mostly planar or linear, and there will be no temperature gradient along an element if it can be assumed that temperatures are uniform within a post-flashover fire compartment. This assumption holds for fires in small rooms but is less accurate for fires in large spaces.

3.9.2 Convection

Convection is heat transfer by the movement of fluids; either gases or liquids. Convective heat transfer is an important factor in flame spread and in the upward transport of smoke and hot gases to the ceiling or out the window from a room fire. Convective heat transfer calculations usually involve heat transfer between the surface of a solid and a surrounding fluid which heats or cools the solid material. The rate of heating or cooling depends on several factors, especially the velocity of the fluid at the surface. For given conditions the heat transfer is usually taken to be directly proportional to the temperature difference between the two materials, so that the heat flow per unit area \dot{q}'' (W/m²) is given by:

$$\dot{q}'' = h_c \Delta T \quad (3.34)$$

where h_c is the convective heat transfer coefficient (W/m²K), and ΔT is the temperature difference between the surface of the solid and the fluid (°C or K). The value of the heat transfer coefficient h_c can vary depending on factors such as the geometry of the surface, the nature of the flow, and the thickness of the boundary layer. The Eurocode recommends a convective heat transfer coefficient of 25 W/m²K for exposure to the standard fire. For the hydrocarbon fire the recommended coefficient is 50 W/m²K while 35 W/m²K is recommended for exposure to a natural fire or the Eurocode parametric fire (CEN, 2002b). Other values are available in many heat transfer textbooks.

3.9.3 Radiation

Radiation is the transfer of energy by electromagnetic waves which can travel through a vacuum, or through a transparent solid or liquid. Radiation is extremely important in fires because it is the main mechanism for heat transfer from hot flames to fuel surfaces, from hot smoke to building objects and from a burning building to an adjacent building. The radiant heat flux \dot{q}'' (W/m²) at a point on a receiving surface is given by:

$$\dot{q}'' = \varphi \varepsilon_e \sigma T_e^4 \quad (3.35)$$

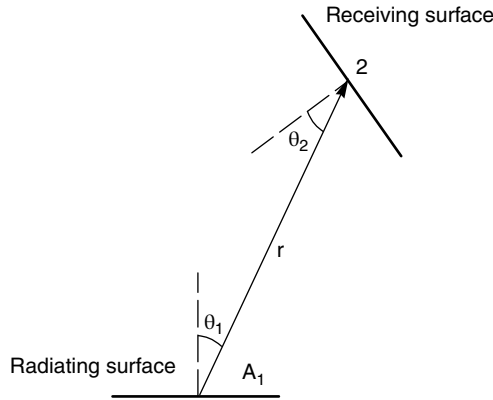


Figure 3.26 Radiation from one surface to another

where φ is the configuration factor, ε_e is the emissivity of the emitting surface, σ is the Stefan–Boltzmann constant ($5.67 \times 10^{-8} \text{ W/m}^2\text{K}^4$) and T_e is the absolute temperature of the emitting surface (K). The resulting heat flow \dot{q}'' (W/m^2) from the emitting surface to the receiving surface is given by:

$$\dot{q}'' = \varphi \varepsilon \sigma (T_e^4 - T_r^4) \tag{3.36}$$

where T_r is the absolute temperature of the receiving surface (K) and ε is the resultant emissivity of the two surfaces, given by:

$$\varepsilon = \frac{1}{1/\varepsilon_e + 1/\varepsilon_r - 1} \tag{3.37}$$

where ε_r is the emissivity of the receiving surface.

The emissivity ε indicates the efficiency of the emitting surface as a radiator, with a value in the range from zero to 1.0. A so-called ‘black-body’ radiator has an emissivity of 1.0. In fire situations, most hot surfaces, smoke particles or luminous flames have an emissivity between 0.7 and 1.0. The emissivity can change during a fire; for example, zinc-coated steel (galvanized steel) has a very low emissivity until the temperature reaches about 400 °C when the zinc melts and the bare steel is exposed to the fire.

The configuration factor φ (sometimes called the ‘view factor’) is a measure of how much of the emitter is ‘seen’ by the receiving surface. In the general situation shown in Figure 3.26 (Drysdale, 2011) the configuration factor for incident radiation at point 2, a distance r from a radiating surface of area A_1 , is:

$$\varphi = \int_{A_1} \frac{\cos \theta_1 \cos \theta_2}{\pi r^2} dA_1 \tag{3.38}$$

where the terms are shown in Figure 3.26.

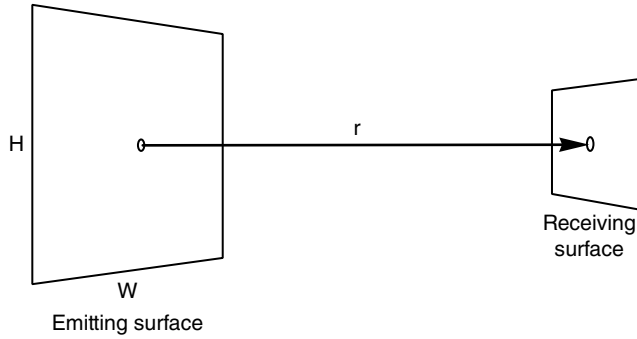


Figure 3.27 Emitting and receiving surfaces

For the particular case of two parallel surfaces as shown in Figure 3.27, the configuration factor φ at a point on the receiving surface at distance r from the centre of the rectangular radiator is:

$$\varphi = \frac{2}{\pi} \left[\frac{x}{\sqrt{1+x^2}} \tan^{-1} \left(\frac{y}{\sqrt{1+x^2}} \right) + \frac{y}{\sqrt{1+y^2}} \tan^{-1} \left(\frac{x}{\sqrt{1+y^2}} \right) \right] \quad (3.39)$$

where $x=H/2r$; $y=W/2r$; H is the height of the rectangular source, W is the width of the rectangular source, and \tan^{-1} is the inverse tangent (in radians). If the distance r is large relative to the size of the emitting surface, the configuration factor φ is given approximately by:

$$\varphi = A_1 / \pi r^2 \quad (3.40)$$

where A_1 is the area of the emitting surface ($A_1 = HW$ in Figure 3.27). Configuration factors for many other situations and values of emissivity are given by Drysdale (2011) and many heat transfer textbooks.

3.9.4 Design Charts for Fire Resistance Calculation

As a quick way of estimating the temperatures of structural elements exposed to fire, several design charts are available for structural materials exposed to the elevated temperatures of standard fires (described in Chapter 4). Available charts include those by Milke (2008) and Fleischmann *et al.* (2008) for standard fire exposure of steel and concrete elements, respectively. Lie (1972) provides design charts for walls or slabs exposed on one or two sides to the standard fire, which can be used for any inert material such as steel, concrete, or wood before charring occurs. Design charts for steel members exposed to realistic fires are provided by Pettersson *et al.* (1976).

3.10 Worked Examples

3.10.1 Worked Example 3.1

Calculate the average heat release rate when 200 kg of paraffin wax burns in half an hour. Assume the calorific value of paraffin wax is 46 MJ/kg.

Mass of fuel	$M = 200 \text{ kg}$
Calorific value	$\Delta H_c = 46 \text{ MJ/kg}$
Energy contained in the fuel	$E = M\Delta H_c = 200 \text{ kg} \times 46 \text{ MJ/kg} = 9200 \text{ MJ}$
Time of burning	$t_b = 1800 \text{ s}$
Heat release rate	$Q = \frac{E}{t} = \frac{9200 \text{ MJ}}{1800 \text{ s}} = 5.11 \text{ MW}$

Calculate the fuel load energy density in an office 5 m × 3 m containing 150 kg of dry wood and paper and 75 kg of plastic materials. Assume calorific values of 16 and 30 MJ/kg, respectively.

Mass of wood	$M_{\text{wood}} = 150 \text{ kg}$
Calorific value	$\Delta H_{c, \text{wood}} = 16 \text{ MJ/kg}$
Energy contained in the wood	$E_{\text{wood}} = M\Delta H_c = 150 \text{ kg} \times 16 \text{ MJ/kg} = 2400 \text{ MJ}$
Mass of plastic	$M_{\text{plastic}} = 75 \text{ kg}$
Calorific value	$\Delta H_{c, \text{plastic}} = 30 \text{ MJ/kg}$
Energy contained in plastic	$E_{\text{plastic}} = M\Delta H_c = 75 \text{ kg} \times 30 \text{ MJ/kg} = 2250 \text{ MJ}$
Total energy in fuel	$E_{\text{total}} = E_{\text{wood}} + E_{\text{plastic}} = 2400 + 2250 = 4650 \text{ MJ}$
Floor area	$A_f = 5 \text{ m} \times 3 \text{ m} = 15 \text{ m}^2$
Fuel load energy density	$e_f = E/A_f = 4650/15 = 310 \text{ MJ/m}^2$

3.10.2 Worked Example 3.2

A room in a storage building has 2000 kg of polyethylene covering the floor. Calculate the heat release rate and duration of burning after the roof collapses in a fire. The room is 6.0 m by 10.0 m. Use the open-air burning rates from Table 3.2. Take the calorific value of polyethylene as 43.8 MJ/kg.

Mass of polyethylene	$M = 2000 \text{ kg}$
Calorific value	$\Delta H_c = 43.8 \text{ MJ/kg}$
Energy content of fuel	$E = M\Delta H_c = 2000 \text{ kg} \times 43.8 \text{ MJ/kg} = 87600 \text{ MJ}$
Surface burning rate	$q = 0.031 \text{ kg/s/m}^2$
Floor area	$A_f = 6.0 \times 10.0 = 60.0 \text{ m}^2$
Specific heat release rate	$Q_s = q\Delta H_c = 0.031 \times 43.8 = 1.36 \text{ MW/m}^2$
Total heat release rate	$Q = Q_s A_f = 1.36 \times 60 = 81.6 \text{ MW}$
Duration of burning	$t = E/Q = 87600/81.6 = 1074 \text{ s} = 18 \text{ min}$

3.10.3 Worked Example 3.3

Calculate the heat release rate for 160kg of office furniture with an average calorific value of 20MJ/kg, if it burns as a 'fast' t -squared fire with a peak heat release rate of 9.0MW.

Mass of fuel	$M = 160 \text{ kg}$
Calorific value	$\Delta H_c = 20 \text{ MJ/kg}$
Energy contained in fuel	$E = M\Delta H_c = 160 \text{ kg} \times 20 \text{ MJ/kg} = 3200 \text{ MJ}$
Growth factor for fast fire	$k = 150 \text{ s}/\sqrt{\text{MW}}$
Peak heat release rate	$Q = 9.0 \text{ MW}$
Time to reach peak heat release t_1	$t_1 = k\sqrt{Q_p} = 150 \times \sqrt{9} = 450 \text{ s}$
Total energy released by time t_1 (area under the heat release rate vs time curve)	$E_1 = t_1 Q_p / 3 = 450 \times 9 / 3 = 1350 \text{ MJ}$

$E_1 < E$ so there is steady burning

Energy released in steady burning	$E_2 = E - E_1 = 3200 - 1350 = 1850 \text{ MJ}$
Duration of steady burning	$t_b = E_2 / Q_p = 1850 / 9 = 206 \text{ s}$

The heat release rate curve for this fire is shown as the 'fast' fire in Figure 3.6.

Repeat the calculation for a 'slow' t -squared fire growth rate.

Growth factor for slow fire	$k = 600 \text{ s}/\sqrt{\text{MW}}$
Time to reach peak heat release t_1	$t_1 = k\sqrt{Q_p} = 600 \times \sqrt{9} = 1800 \text{ s}$
Energy released in time t_1	$E_1 = t_1 Q_p / 3 = 1800 \times 9 / 3 = 5400 \text{ MJ}$

$E_1 > E$ so the fire does not reach steady-burning stage

$$\text{Time for all fuel to burn } t_m = (3Ek^2)^{1/3} = (3 \times 3200 \times 600^2)^{1/3} = 1512 \text{ s}$$

$$\text{Heat release at time } t_1 \quad Q_m = \left(\frac{t_m}{k} \right)^2 = \left(\frac{1512}{600} \right)^2 = 6.3 \text{ MW}$$

The heat release rate curve is shown as the 'slow' fire in Figure 3.6.

3.10.4 Worked Example 3.4

Using Thomas's flashover criterion, calculate the heat release rate necessary to cause flashover in a room 6.0m by 4.0m in floor area, and 3.0m high, with one window 2.0m high by 3.0m wide.

Length of room	$l_1 = 6.0 \text{ m}$
Width of room	$l_2 = 4.0 \text{ m}$
Height of room	$H_r = 3.0 \text{ m}$
Area of internal surfaces	$A_r = 2(l_1 l_2 + l_1 H_r + l_2 H_r)$ $= 2(6 \times 4 + 6 \times 3 + 4 \times 3) = 108 \text{ m}^2$
Height of window	$H_v = 2.0 \text{ m}$
Width of window	$B = 3.0 \text{ m}$

$$\begin{aligned}
 \text{Area of window} \quad A_v &= BH_v = 3.0 \times 2.0 = 6.0 \text{ m}^2 \\
 \text{Heat release for flashover} \quad Q_{fo} &= 0.0078A_t + 0.378A_v\sqrt{H_v} \\
 &= 0.0078 \times 108 + 0.378 \times 6.0\sqrt{2.0} \\
 &= 4.05 \text{ MW}
 \end{aligned}$$

3.10.5 Worked Example 3.5

Calculate the ventilation controlled heat release rate for a post-flashover fire in the room of Worked Example 3.4, if the burning wood has a heat of combustion of 16 MJ/kg.

$$\begin{aligned}
 \text{Rate of burning} \quad \dot{m} &= 0.092 A_v \sqrt{H_v} \\
 &= 0.092 \times 6.0 \times \sqrt{2.0} = 0.781 \text{ kg/s} \\
 \text{Heat of combustion} \quad \Delta H_c &= 16 \text{ MJ/kg} \\
 \text{Heat release rate} \quad Q_{vent} &= \dot{m} \Delta H_c = 0.781 \times 16 = 12.5 \text{ MW}
 \end{aligned}$$

Calculate the duration of burning if the available fuel load energy density is 800 MJ/m² floor area.

$$\begin{aligned}
 \text{Fuel load energy density} \quad e_f &= 800 \text{ MJ/m}^2 \\
 \text{Floor area} \quad A_f &= 6.0 \times 4.0 = 24 \text{ m}^2 \\
 \text{Total energy} \quad E &= e_f A_f = 800 \times 24 = 19200 \text{ MJ} \\
 \text{Duration of burning} \quad t_b &= E / Q_{vent} = 19200 / 12.5 = 1536 \text{ s (25.6 min)}
 \end{aligned}$$

3.10.6 Worked Example 3.6

Calculate the ventilation controlled heat release rate and duration of burning for the room of the previous examples, using Law's equation. Assume that the window is in the long side of the room.

$$\begin{aligned}
 \text{Opening factor} \quad \Omega &= (A_t - A_v) / A_v \sqrt{H_v} \\
 &= (108 - 6) / 6\sqrt{2} = 12.02 \text{ m}^{-1/2} \\
 \text{Room length} \quad W &= 6.0 \text{ m} \\
 \text{Room breadth} \quad D &= 4.0 \text{ m} \\
 \text{Rate of burning} \quad \dot{m} &= 0.18 A_v \sqrt{\frac{H_v W}{D}} (1 - e^{-0.036 \Omega}) \\
 &= 0.18 \times 6 \times \sqrt{\frac{2 \times 6}{4}} (1 - e^{-0.036 \times 12.02}) \\
 &= 0.657 \text{ kg/s} \\
 \text{Heat release rate} \quad \dot{Q}_{vent} &= \dot{m} \Delta H_c = 0.657 \times 16 = 10.5 \text{ MW} \\
 \text{Duration of burning} \quad t_b &= E / Q_{vent} = 19200 / 10.5 = 1829 \text{ s (30.5 min)}
 \end{aligned}$$

3.10.7 Worked Example 3.7

Recalculate the heat release rate from Example 3.5 with a ceiling opening of 3.0 m².

Area of ceiling opening	$A_h = 3.0 \text{ m}^2$
Height above window mid-height	$h = 1.5 \text{ m}$ (assume window is mid-way between floor and ceiling)
Window area	$A_v = 6.0 \text{ m}^2$
Window height	$H_v = 2.0 \text{ m}$
Modified opening parameter	$\begin{aligned} \left(A_v \sqrt{H_v}\right)_{\text{fict}} &= A_v \sqrt{H_v} + 2.3 A_h \sqrt{h} \\ &= 6.0 \sqrt{2.0} + 2.3 \times 3.0 \sqrt{1.5} \\ &= 8.49 + 8.45 = 16.9 \text{ m}^{3/2} \end{aligned}$
Rate of burning	$\begin{aligned} \dot{m} &= 0.092 \left(A_v \sqrt{H_v}\right)_{\text{fict}} \\ &= 0.092 \times 16.9 = 1.55 \text{ kg / s} \end{aligned}$
Heat of combustion	$\Delta H_c = 16 \text{ MJ / kg}$
Heat release rate	$Q_{\text{vent}} = \dot{m} \Delta H_c = 1.55 \times 16 = 24.8 \text{ MW}$

(Note that this ceiling opening almost doubles the rate of burning and the heat release rate, which will halve the duration of burning.)

3.10.8 Worked Example 3.8

Calculate the maximum temperature for the room of Example 3.5, using Law's equation.

Duration of burning	$t_b = 30.5 \text{ min}$
(from Example 3.6)	
Opening factor	$\Omega = 12.02 \text{ m}^{-1/2}$
Maximum temperature	$\begin{aligned} T_{\text{max}} &= 6000 \left(1 - e^{-0.1\Omega}\right) / \sqrt{\Omega} \\ &= 6000 \left(1 - e^{-0.1 \times 12.02}\right) / \sqrt{12.02} = 1210^\circ\text{C} \end{aligned}$

Check reduction factor for fuel load

Total fuel load	$E = 19200 \text{ MJ}$
Calorific value of wood	$\Delta H_c = 16 \text{ MJ/kg}$
Fuel load (wood equivalent)	$L = \frac{E}{\Delta H_c} = \frac{19200 \text{ MJ}}{16 \text{ MJ/kg}} = 1200 \text{ kg}$
Area of windows	$A_v = 6.0 \text{ m}^2$
Area of internal surfaces	$A_t = 108.0 \text{ m}^2$
Temperature parameter	$\psi = \frac{L}{\sqrt{A_v(A_t - A_v)}} = \frac{1200}{\sqrt{6.0 \times (108 - 6.0)}} = 48.5$
Reduced maximum temperature	$\begin{aligned} T &= T_{\text{max}} \left(1 - e^{-0.05\psi}\right) \\ &= 1210 \left(1 - e^{-0.05 \times 48.5}\right) = 1103^\circ\text{C} \end{aligned}$

3.10.9 Worked Example 3.9

Estimate a time–temperature curve for the previous room using the Swedish curves.

Area of window	$A_v = 6.0 \text{ m}^2$
Height of window	$H_v = 2.0 \text{ m}$
Area of internal surfaces	$A_t = 108.0 \text{ m}^2$
Floor area	$A_f = 24 \text{ m}^2$
Ventilation factor	$F_v = A_v \sqrt{H_v} / A_t = 6.0 \times \sqrt{2.0} / 108 = 0.079 \text{ m}^{-1/2}$
Fuel load (floor area)	$e_f = E / A_f = 19200 \text{ MJ} / 24 \text{ m}^2 = 800 \text{ MJ/m}^2$
Fuel load (total area)	$e_t = \frac{e_f A_f}{A_t} = \frac{800 \times 24}{108} = 178 \text{ MJ/m}^2$

The time–temperature curve can be roughly interpolated from the bottom right hand graph in Figure 3.13, giving a maximum temperature of about 950 °C after 20 min, dropping to 350 °C after 1 h.

3.10.10 Worked Example 3.10

Use the parametric fire equations to calculate the duration and the maximum temperature for a fire in a room 4.0 m × 6.0 m in area, 3.0 m high, with one window 3.0 m wide and 2.0 m high. The fire load is 800 MJ/m². The room is constructed from concrete with the following properties:

Thermal conductivity	$k = 1.6 \text{ W/mK}$
Density	$\rho = 2300 \text{ kg/m}^3$
Specific heat	$c_p = 980 \text{ J/kgK}$

Calculations:

Thermal inertia of concrete	$b = \sqrt{k\rho c_p} = 1900 \text{ W s}^{0.5} / \text{m}^2 \text{ K}$
Length of room	$l_1 = 6.0 \text{ m}$
Width of room	$l_2 = 4.0 \text{ m}$
Floor area	$A_f = 6.0 \times 4.0 = 24 \text{ m}^2$
Height of room	$H_r = 3.0 \text{ m}$
Area of internal surfaces	$A_t = 2(l_1 l_2 + l_1 H_r + l_2 H_r)$ $= 2(6 \times 4 + 6 \times 3 + 4 \times 3) = 108 \text{ m}^2$
Window height	$H_v = 2.0 \text{ m}$
Window width	$B = 3.0 \text{ m}$
Window area	$A_v = BH_v = 3.0 \times 2.0 = 6.0 \text{ m}^2$
Ventilation factor	$F_v = A_v \sqrt{H_v} / A_t = 6.0 \times \sqrt{2.0} / 108 = 0.079 \text{ m}^{-1/2}$
Fuel load energy density	$e_f = 800 \text{ MJ/m}^2$
Duration of parametric fire,	$t_{max} = \max \left[(0.2 \times 10^{-3} e_t / F_v); t_{lim} \right]$
for an office (from Table 3.5)	$t_{lim} = 20 \text{ min} = 0.33 \text{ h}$

$$e_t = \frac{e_f A_f}{A_t} = \frac{800 \times 24}{108} = 178 \text{ MJ/m}^2$$

$$t_{max} = 0.2 \times 10^{-3} e_t / F_v = 0.2 \times 10^{-3} \times 178 / 0.079 = 0.45 \text{ h} = 27 \text{ min}$$

Fictitious duration $t_{max}^* = \Gamma t_{max}$

$$\Gamma = \frac{(F_v / 0.04)^2}{(b / 1160)^2} = \frac{(0.079 / 0.04)^2}{(1900 / 1160)^2} = 1.454$$

$$t_{max}^* = \Gamma t_{max} = 1.454 \times 0.45 \text{ h} = 0.65 \text{ h} = 39 \text{ min}$$

$$\begin{aligned} \text{Maximum temperature } T &= 20 + 1325(1 - 0.324e^{-0.2t^*} - 0.204e^{-1.7t^*} - 0.472e^{-19t^*}) \\ &= 20 + 1325(1 - 0.284 - 0.068 - 0) \\ T_{max} &= 879^\circ\text{C} \end{aligned}$$

Because the fictitious heating duration is between 30 min and 2 h, the temperature decays according to Equation 3.30b:

$$T = T_{max} - 250(3 - t_{max}^*)(t^* - t_{max}^* x)$$

but $x = 1.0$ because $t_{max}^* > t_{lim}$

by using the equation above and the values of T_{max} and t_{max}^* , the total duration of the fire can be calculated by rearranging to solve for t^* . The total fictitious duration is found to be $t^* = 2.112 \text{ h}$, which is $t = 87 \text{ min}$ in real time. Hence the temperature in the office drops from 879 to 20°C in 60 min ($87 - 27 \text{ min}$). These curves can be easily calculated and plotted using a spreadsheet.

3.10.11 Worked Example 3.11

Repeat Worked Example 3.10 if the concrete walls and ceiling are covered with a 12 mm thick layer of gypsum plaster board.

The thermal properties of concrete have been calculated in Worked Example 3.10. Therefore, for gypsum board:

	Gypsum board
Thermal conductivity	0.20 W/mK
Density, ρ	800 kg/m ³
Specific heat, c_p	1700 J/kg K
$b = \sqrt{(k\rho c_p)}$	522 W s ^{0.5} /m ² K

Length of room	$l_1 = 6.0 \text{ m}$
Width of room	$l_2 = 4.0 \text{ m}$
Floor area	$A_f = 6.0 \times 4.0 = 24 \text{ m}^2$
Height of room	$H_r = 3.0 \text{ m}$
Area of internal surfaces	$A_i = 2(l_1 l_2 + l_1 H_r + l_2 H_r)$ $= 2(6 \times 4 + 6 \times 3 + 4 \times 3) = 108 \text{ m}^2$
Window height	$H_v = 2.0 \text{ m}$
Window width	$B = 3.0 \text{ m}$
Window area	$A_v = BH_v = 3.0 \times 2.0 = 6.0 \text{ m}^2$
Ventilation factor	$F_v = A_v \sqrt{H_v} / A_i = 6.0 \times \sqrt{2.0} / 108 = 0.079 \text{ m}^{-1/2}$
Fuel load energy density	$e_f = 800 \text{ MJ/m}^2$
Duration of parametric fire, from Worked Example 3.10	$t_{max} = \max \left[\left(0.2 \times 10^{-3} e_f / F_v \right); t_{lim} \right]$ $t_{max} = 0.45 \text{ h}$
The limiting thickness, $s_{lim, 1}$, of the fire-exposed material is calculated from	

$$\text{Since } b_1 < b_2, b = b_1$$

$$b = 522 \text{ W s}^{0.5} / \text{m}^2 \text{ K}$$

Fictitious duration $t_{max}^* = \Gamma t_{max}$

$$\Gamma = \frac{(F_v / 0.04)^2}{(b / 1160)^2} = \frac{(0.079 / 0.04)^2}{(522 / 1160)^2} = 19.26$$

$$t_{max}^* = \Gamma t_{max} = 19.26 \times 0.45 \text{ h} = 8.67 \text{ h}$$

$$\begin{aligned} \text{Maximum temperature } T &= 20 + 1325 \left(1 - 0.324 e^{-0.2t^*} - 0.204 e^{-1.7t^*} - 0.472 e^{-19t^*} \right) \\ &= 20 + 1325 (1 - 0.057 - 0 - 0) \end{aligned}$$

$$T_{max} = 1269^\circ \text{C}$$

Because the fictitious heating duration is more than 2 h, the temperature decays according to Equation 3.35c:

$$T = T_{max} - 250 \left(t^* - t_{max}^* x \right)$$

but $x = 1.0$ because $t_{max} > t_{lim}$

by using the equation above and the values of T_{max} and t_{max}^* , the total duration of the fire can be calculated by rearranging the equation to solve for t^* . The total fictitious duration is found to be 13.67 h, which is equivalent to 43 min (in real time). The temperature in the office drops from 1269 to 20°C in 16 min (43 – 27 min).

3.10.12 Worked Example 3.12

Calculate the steady-state heat transfer through a 150 mm thick concrete wall if the temperature on the fire side is 800 °C and the temperature on the cooler side is 200 °C.

Wall thickness	$x = 0.15 \text{ m}$
Temperature difference	$\Delta T = 800 - 200 = 600 \text{ °C} = 600 \text{ K}$
Temperature gradient	$dT/dx = 600 / 0.150 = 4000 \text{ K/m}$
Thermal conductivity	$k = 1.0 \text{ W/mK}$ (from Table 3.4)
Heat transfer	$\dot{q}'' = kdT/dx = 1.0 \times 4000 = 4000 \text{ W/m}^2$ $= 4 \text{ kW/m}^2$

Calculate the convective heat transfer coefficient on the cool side of the wall if the ambient temperature is 20 °C and all the heat passing through the wall is carried away by convection.

Temperature of wall	$T_w = 200 \text{ °C}$
Ambient temperature	$T_a = 20 \text{ °C}$
Temperature difference	$\Delta T = 200 - 20 = 180 \text{ °C} = 180 \text{ K}$
Heat transfer	$\dot{q}'' = 4000 \text{ W/m}^2$
Convective heat transfer coefficient	$h = \dot{q}''/\Delta T = 4000/180 = 22.2 \text{ W/m}^2\text{K}$

3.10.13 Worked Example 3.13

Calculate the radiant heat flux from a window in a burning building to the surface of an adjacent building 5.0 m away. The window is 2.0 m high by 3.0 m wide and the fire temperature is 800 °C. Assume an emissivity of 0.9.

Emitter height	$H = 2.0 \text{ m}$
Emitter width	$W = 3.0 \text{ m}$
Distance from emitter	$r = 5.0 \text{ m}$
Height ratio	$x = H/2r = 2/(2 \times 5) = 0.20$
Width ratio	$y = W/2r = 3/(2 \times 5) = 0.30$
Configuration factor φ	$\varphi = \frac{2}{\pi} \left[\frac{x}{\sqrt{1+x^2}} \tan^{-1} \left(\frac{y}{\sqrt{1+x^2}} \right) + \frac{y}{\sqrt{1+y^2}} \tan^{-1} \left(\frac{x}{\sqrt{1+y^2}} \right) \right]$ $\varphi = 0.0703$

Emitter temperature	$T = 800 \text{ °C} = 1073 \text{ K}$
Emissivity	$\varepsilon = 0.9$
Stefan–Boltzmann constant	$\sigma = 5.67 \times 10^{-8} \text{ W/m}^2\text{K}^4$
Radiant heat flux	$\dot{q}'' = \varphi \varepsilon \sigma (T_f^4 - T_s^4)$ $\dot{q}'' = 0.0703 \times 0.9 \times 5.67 \times 10^{-8} \times (1073^4 - 293^4) / 1000 = 4.73 \text{ kW/m}^2$

3.10.14 Worked Example 3.14

Calculate the radiant heat flux at floor level in a room with a hot upper layer at 600°C. Assume that the smoke in the upper layer has an emissivity of 0.7. Assume that the area of the ceiling is large relative to the room height, so that the configuration factor is 1.0.

Emitter temperature $T = 600^\circ\text{C} = 873\text{K}$

Configuration factor $\varphi = 1.0$

Emissivity $\varepsilon = 0.7$

Stefan–Boltzmann constant $\sigma = 5.67 \times 10^{-8} \text{ W/m}^2\text{K}^4$

Radiant heat flux $\dot{q}'' = \varphi \varepsilon \sigma (T_f^4 - T_s^4)$

$$\dot{q}'' = 1.0 \times 0.7 \times 5.67 \times 10^{-8} \times (873^4 - 293^4) / 1000 = 22.5 \text{ kW/m}^2$$

4

Fire Severity and Fire Resistance

Chapter 3 described fire development from ignition through growth to full-room involvement and decay. It provided alternative models to represent fires in rooms and to estimate the temperatures at the surface of structural elements as a result of exposure to these fires. Subsequent chapters describe structural behaviour and suggest ways to design building elements.

This chapter outlines methods of assessing the adequacy of building components in fire conditions. It quantifies the requirements for design and provides alternative means of achieving these. It also describes methods of quantifying the severity of post-flashover fires, for comparison with the provided fire resistance, including the concept of equivalent fire severity, which is used for comparing real fires with the standard time–temperature curve. This chapter further describes the standard fire resistance test and ways for calculating the fire resistance of structural members and discusses the importance of fire resistance of components and assemblies in real buildings.

4.1 Providing Fire Resistance

4.1.1 Background

The fundamental step in designing structures for fire safety is to verify that the fire resistance of the structure (or each part of the structure) is greater than the severity of the fire to which the structure is exposed. This verification requires that the following design equation be satisfied:

$$\text{fire resistance} \geq \text{fire severity} \quad (4.1)$$

Table 4.1 Three methods for comparing fire severity with fire resistance

Domain	Units	Fire resistance	≥	Fire severity
Time	min or h	Time to failure	≥	Fire duration as calculated or specified by code
Temperature	°C	Temperature to cause failure	≥	Maximum temperature reached during the fire
Strength	kN or kNm	Load capacity at elevated temperature	≥	Applied load during the fire

where *fire resistance* is a measure of the ability of the structure to resist collapse, and to prevent spread of fire during exposure to a fire of specified severity, and *fire severity* is a measure of the destructive impact of a fire, or a measure of the forces or temperatures which could cause collapse or other failure as a result of the fire. There are several different definitions of fire severity and fire resistance, leading to different ways of comparing them using different units. These comparisons can be confusing if not made correctly, so it is important for designers to understand the alternatives clearly.

As shown in Table 4.1, there are three alternative methods of comparing fire severity with fire resistance. The verification may be in the *time* domain, the *temperature* domain or the *strength* domain, as discussed below.

4.1.1.1 Time domain

By far the most common procedure is for fire severity and fire resistance to be compared in the *time domain* such that:

$$t_{fail} \geq t_s \quad (4.2)$$

where t_{fail} is the fire resistance, or time to failure of the element when exposed to the standard fire, and t_s is the fire severity, which is the design duration of the standard fire for the building under consideration, as specified by a code or calculated. All of these times have units of minutes or hours.

The time to failure of a building element is usually given as a *fire resistance rating*, which may be obtained from a published listing of ratings or by calculation, as described later. The fire duration, or fire severity, is usually a time of standard fire exposure specified by a building code, or the equivalent time of standard fire exposure calculated for a real fire in the building.

4.1.1.2 Temperature domain

It is sometimes necessary to verify design in the *temperature domain* by ensuring that the maximum temperature (°C) in a part of the structure is no greater than the temperature (°C) which would cause failure. Failure in this context could be failure of a separating element by

excessive temperature rise, or structural collapse of a load-bearing member. Verification in the temperature domain requires that:

$$T_{fail} \geq T_{max} \quad (4.3)$$

where T_{fail} is the temperature which would cause failure of the element and T_{max} is the maximum temperature reached in the element during the expected fire, or the temperature after a certain time of standard fire exposure, specified by the building code.

The temperature reached in the element can be calculated by a thermal analysis of the structural assembly exposed to the design fire. For a separating element, the failure temperature is the temperature on the unexposed face which would allow fire to spread into the next compartment, by local ignition or radiation to other items. For a structural element, the temperature which would cause collapse can be calculated from the knowledge of the loads on the element, the load capacity at normal temperatures, and the effect of elevated temperatures on the structural materials, as described in Chapter 5.

The temperature domain is typically used for an element which serves an insulating or containing function, although it cannot be used to predict integrity failures. The temperature domain is less suitable for structural elements because it does not adequately consider internal thermal gradients or structural behaviour. However, some simple elements (e.g. in steel structures) may be designed in this domain (CEN, 2005b).

4.1.1.3 Strength domain

Verification in the *strength domain* is a comparison of the applied load at the time of the fire with the load capacity of structural members throughout the fire, such that

$$R_f \geq U_f \quad (4.4)$$

where R_f is the minimum load capacity reached during the fire, or the load capacity at a certain time specified by the code, and U_f is the applied load at the time of the fire.

These values may be expressed in units of force and resistance for the whole building, or as internal member actions such as axial force or bending moment in individual members of the structure. The load capacity during the fire can be calculated from a thermal analysis and a structural analysis at elevated temperatures. The loads at the time of the fire can be calculated using load combinations from national loadings codes.

4.1.1.4 Example

The comparison of fire severity with fire resistance described above can be rather confusing, so the three alternative domains of verification are illustrated with a simple example. Figure 4.1(a) shows the temperature of a steel beam during fire exposure. Calculations show that the beam will fail when the steel temperature reaches T_{fail} at time t_{fail} . The building code requires that the beam should have a fire resistance of t_{code} or in other words the required fire severity is t_{code} . Verification in the time domain requires checking that the beam does not fail

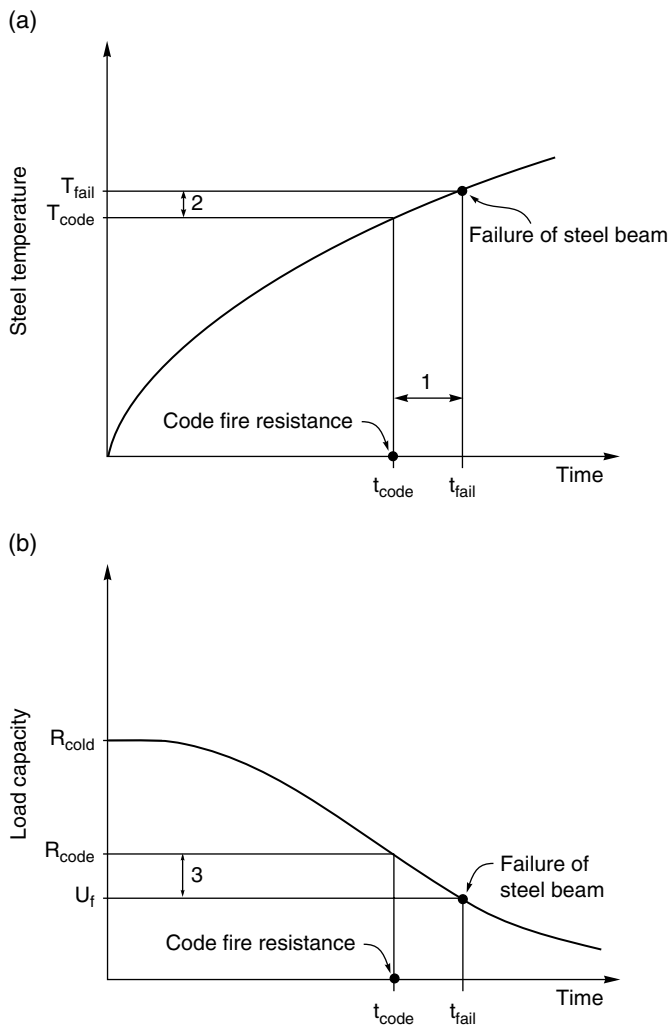


Figure 4.1 Behaviour of a steel beam in fire: (a) temperature increase; (b) loss of strength

prematurely, so that the time to failure t_{fail} is greater than the fire severity specified by the code t_{code} [check 1 in Figure 4.1(a)]. Verification in the temperature domain requires checking that the steel temperature which would cause failure T_{fail} is greater than T_{code} which is the temperature reached in the beam at time t_{code} [check 2 in Figure 4.1(a)]. These two checks will give identical results because they are both based on the same process.

Figure 4.1(b) shows the load capacity of the same steel beam during the fire. The imposed load at the time of the fire is U_f . The load capacity before the fire is R_{cold} and the graph shows how this decreases during the fire. At the time t_{code} the load capacity of the beam has reduced to R_{code} . Verification in the strength domain simply requires checking that the reduced load capacity is greater than the applied load [check 3 in Figure 4.1(b)]. All three of these verification checks give identical results.

4.1.2 Fire Exposure Models

Figure 4.2 illustrates a range of alternative design situations. The left-hand column shows three different ways in which a design fire can be specified. Fire exposure H_1 represents exposure to a standard test fire for a specified period of time t_{code} as prescribed by a building code. This is the most common specification of fire exposure. Traditional prescriptive codes specify the required fire resistance directly, leaving little opportunity for fire engineers to calculate a specific fire severity for any particular building. Prescriptive codes usually require fire resistance to be somewhere between half an hour and 4h, in half hour or 1 h steps, with little or no reference to the severity of the expected fire.

Fire exposure H_2 represents a modified duration of exposure to the standard test fire. The equivalent time t_e is the time of exposure to the standard test fire considered to be equivalent to a complete burnout of a real fire in the same room. Methods of calculating equivalent fire severity are described in subsequent sections. Many performance-based codes allow the use of time equivalent formulae as an improvement on simple prescriptive fire resistance requirements.

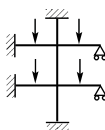
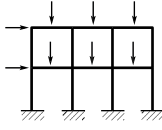
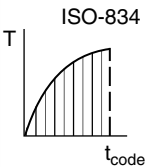
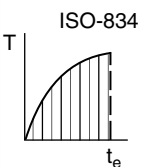
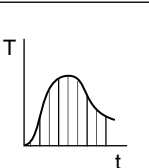
Structural response model		S ₁	S ₂	S ₃
		Elements	Sub-assemblies	Structures
Fire exposure model				
H_1		Test or calculation	Calculation occasional test	Difference in schematization becomes too large
H_2		Test or calculation	Calculation occasional test	Calculation unpractical
H_3		Calculation occasional	Calculation	Calculation occasional and for research

Figure 4.2 Fire models and structural response models. Reprinted from CIB (1986) with permission from Elsevier Science

Table 4.2 Design combinations for verifying fire resistance

Combination	Fire exposure model	Assessment of fire resistance	Verification domain
1	Prescriptive code (H_1)	Listed rating or calculation	Time
2	Time equivalent formula (H_2)	Listed rating or calculation	Time or strength
3	Predicted real fire (H_3)	Calculation	Temperature or strength

Fire exposure H_3 represents a realistic fire which would occur if there was a complete burnout of the room, with no intervention or fire suppression. This is the type of fire described by the time–temperature curves in Chapter 3.

The other columns of Figure 4.2 show that assessment of fire resistance may consider a single element, a sub-assembly or a whole structure. The words in the lower boxes show that test results are only likely to be used for single elements exposed to H_1 or H_2 fires, with calculations becoming necessary in most other cases. Verification that a member or structure has sufficient fire resistance will be by comparison of times, temperatures, or strength as described above. With reference to Figure 4.2, verification to fire exposures H_1 and H_2 is likely to be in the time domain, where an assigned fire resistance (in hours) is compared with the required fire resistance (also in hours). Verification using exposure to a complete burnout (H_3) is more likely to be a comparison of temperatures for insulating elements or a comparison of strength for structural elements.

4.1.3 Design Combinations

The above options illustrate that several alternative methods can be used for verifying fire resistance requirements. Because of the large number of possible combinations, it is essential for designers to specify clearly which combination of exposure and resistance is being used. Both the design and the assessment of the design can become very confusing if the selected combination is not clearly stated and used accordingly. Table 4.2 shows a list of the most common combinations, to help designers select a combination for a particular design. In very general terms, both the accuracy of the prediction and the amount of calculation effort increase downwards in the table.

4.2 Fire Severity

Fire severity is a measure of the destructive potential of a fire. Fire severity is most often defined in terms of a period of exposure to the standard test fire, but this is not appropriate for real fires which have very different characteristics. The fire severity used for design depends on the legislative environment and on the design philosophy. In a prescriptive code environment, the design fire severity is usually prescribed with little or no room for discussion. In a performance-based code environment, the design fire severity is usually a complete burnout fire or the equivalent time of a complete burnout fire. In some cases the design fire may be for a shorter time which only allows for escape, rescue or firefighting. The equivalent time of a complete burnout is the time of exposure to the standard test fire that would result in an equivalent impact on the element, as described later in this chapter.

Damage to a structure is largely dependent on the amount of heat absorbed by the structural elements. Heat transfer from post-flashover fires is mainly radiative which is proportional to the fourth power of the absolute temperature. Hence the severity of a fire is largely dependent on the temperatures reached and the duration of the high temperatures. Some damage such as phase changes or melting are temperature-dependent rather than heat-dependent, so the maximum temperature as well as the duration of the fire is also important.

4.3 Equivalent Fire Severity

The concept of *equivalent fire severity* is used to relate the severity of an expected real fire to the standard test fire. This is important when designers want to compare published fire-resistance ratings from standard tests with estimates of the severity of a real fire. The behaviour of post-flashover fires has been described in Chapter 3. This section describes methods of comparing real fires to the standard test fire.

4.3.1 Equal Area Concept

Early attempts at time equivalence compared the area under time–temperature curves. Figure 4.3 illustrates the concept, first proposed by Ingberg (1928), by which two fires are considered to have equivalent severity if the areas under each curve are equal, above a certain reference temperature. This has little theoretical significance because the units of area are not meaningful. Even though Ingberg was aware of its technical inadequacy he used the equal area concept as a crude but useful method of comparing fires. After carrying out furnace tests, he developed a relationship between fire load in a room and the required fire resistance of the surrounding elements. This approach, subsequently used by US code writers to specify fire resistance ratings, has been useful, but ignores the effects of ventilation and fuel geometry on fire severity.

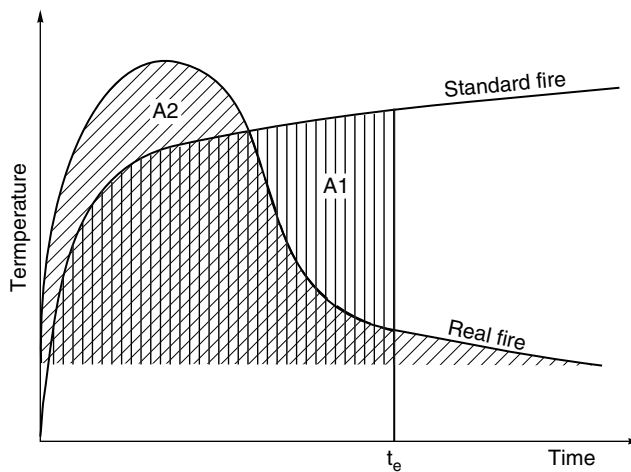


Figure 4.3 Equivalent fire severity on equal area basis

The equal area concept is used for correcting the results of standard fire resistance tests if the standard curve is not exactly followed within the tolerances specified in the standard (ASTM, 2012). The impact of a fire on a surrounding structure is a function of the heat transfer into the structure. A problem with the equal area concept is that it can give a very poor comparison of heat transfer for fires with different shaped time–temperature curves. Heat transfer from a fire to the surface of a structure is mostly by radiation, the balance by convection. Because radiative heat transfer is proportional to the fourth power of the absolute temperature, heat transfer to the surface in a short hot fire may be much greater than in a long cool fire, even if both have equal areas under their time–temperature curves.

Babrauskas and Williamson (1978a, 1978b) also point out that there could be a critical difference between a short, hot fire and a longer cool fire if the maximum temperature in the former is sufficient to cause melting or some other critical phase change in a material which would be much less affected in the cooler fire.

4.3.2 Maximum Temperature Concept

A more realistic concept, developed by Law (1971), Pettersson *et al.* (1976) and others, is to define the equivalent fire severity as the time of exposure to the standard fire that would result in the same maximum temperature in a protected steel member as would occur in a complete burnout of the fire compartment. This concept is shown in Figure 4.4, which compares the temperatures in a protected steel beam exposed to the standard fire with those when the same protected beam is exposed to a particular real fire.

In principle, this concept is applicable to insulating elements if the temperature on the unexposed face is used instead of the steel temperature, and is also applicable to materials which have a limiting temperature, such as the 300 °C temperature at which charring of wood generally begins. The maximum temperature concept is widely used, but it can give misleading results if the maximum temperatures used in the derivation of a time equivalent formula are much greater or lower than those which would cause failure in a particular building.

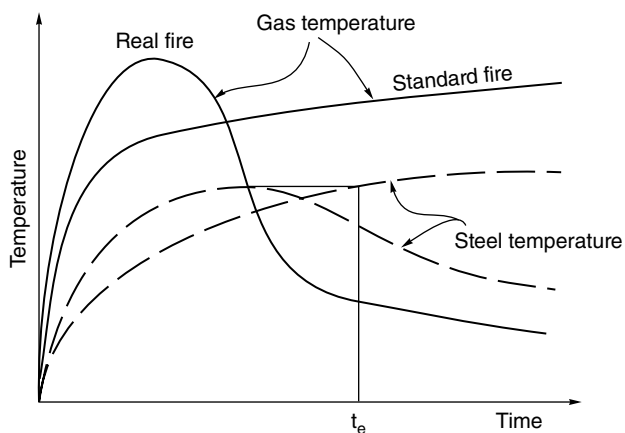


Figure 4.4 Equivalent fire severity on temperature basis

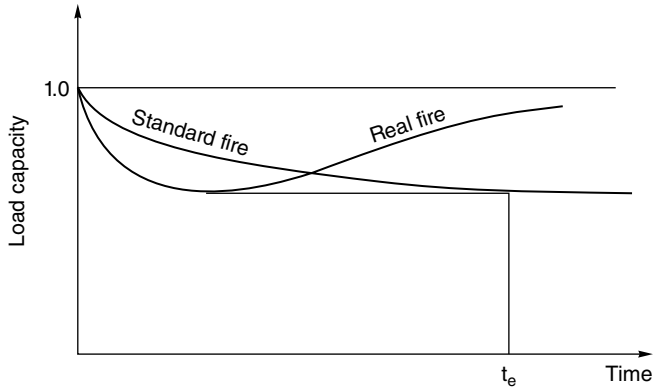


Figure 4.5 Equivalent fire severity on load-bearing capacity basis

4.3.3 Minimum Load Capacity Concept

In a similar concept based on load capacity, the equivalent fire severity is the time of exposure to the standard fire that would result in the same load-bearing capacity as the minimum which would occur in a complete burnout of the firecell. This concept is shown in Figure 4.5 where the load-bearing capacity of a structural member exposed to the standard fire decreases continuously, but the strength of the same member exposed to a real fire increases after the fire enters the decay period and the steel temperatures decrease. This approach is the most realistic time equivalent concept for design of load-bearing members. The minimum load concept is difficult to implement for a material which does not have a clearly defined minimum load capacity, for example with wood members where charring can continue after the fire temperatures start to decrease.

4.3.4 Time Equivalent Formulae

A number of time equivalent formulae have been developed by fitting empirical curves to the results of many calculations of the type shown conceptually in Figure 4.4. The resulting formulae are based on the maximum temperature of protected steel members exposed to realistic fires.

4.3.4.1 CIB Formula

The most widely used time equivalent formula is that published by the CIB W14 group (CIB, 1986), derived by Pettersson (1973) based on the ventilation parameters of the compartment and the fuel load. The equivalent time of exposure to an ISO 834 test t_e (in minutes) is given by:

$$t_e = k_c w e_f \quad (4.5)$$

where e_f is the fuel load (MJ/m² floor area), k_c is a parameter to account for different compartment linings and w is the ventilation factor (m^{-0.25}) given by:

$$w = \frac{A_f}{\sqrt{A_v A_t} \sqrt{H_v}} \quad (4.6)$$

where A_f is the floor area of the compartment (m²), A_v is the total area of openings in the walls (m²), A_t is the total area of the internal bounding surfaces of the compartment (m²) and H_v is the height of the windows (m).

4.3.4.2 Law Formula

A similar formula was developed by Margaret Law on the basis of tests in small-scale compartments (Thomas and Heselden, 1972) and larger scale compartments (Law, 1973). The formula is given by:

$$t_e = \frac{A_f e_f}{\Delta H_c \sqrt{A_v (A_t - A_v)}} \quad (4.7)$$

where ΔH_c is the calorific value of the fuel (MJ/kg).

The CIB formula and the Law formula are only valid for compartments with vertical openings in the walls. They cannot be used for rooms with openings in the roof. The Law formula gives similar results to the CIB formula, generally with slightly larger values of equivalent time.

4.3.4.3 Eurocode Formula

The above formulae were later modified and incorporated into the Eurocode 1 Part 1.2 (CEN, 2002b), referred to often as the 'Eurocode formula' giving t_e (in minutes) as:

$$t_e = k_b w e_f \quad (4.8)$$

where k_b replaces k_c and the ventilation factor w is altered to allow for horizontal roof openings. The ventilation factor is given by:

$$w = \left(\frac{6.0}{H_r} \right)^{0.3} \left[0.62 + \frac{90(0.4 - \alpha_v)^4}{1 + b_v \alpha_h} \right] \geq 0.5 \quad (4.9)$$

where H_r is the compartment height (m) and

$$\alpha_v = A_v / A_f \quad 0.025 \leq \alpha_v \leq 0.25 \quad (4.10)$$

$$\alpha_h = A_h/A_f \quad (4.11)$$

$$b_v = 12.5(1 + 10\alpha_v - \alpha_v^2) \geq 10.0 \quad (4.12)$$

A_f is the floor area of the compartment (m^2), A_v is the area of vertical openings in the walls (m^2) and A_h is the area of horizontal openings in the roof (m^2).

The derivation of the Eurocode formula is based on work by Schneider *et al.* (1990). It is understood to have come from an empirical analysis of calculated steel temperatures in a large number of fires simulated by a German computer program called Multi-Room-Fire-Code. An important difference from the CIB formula is that the Eurocode equivalent time is independent of opening height, but depends on the ceiling height of the compartment, so the two formulae can give different results for the same room geometry. The results are similar for small compartments with tall windows, but the Eurocode formula gives much lower fire severities for large compartments with tall ceilings and low window heights.

Values of the terms k_c and k_b are given in Table 4.3, where they are shown to depend on the compartment lining materials (roughly inversely proportional to the thermal inertia). The 'general' case is that recommended for compartments with unknown materials. Note that k_c and k_b have slightly different numerical values and units, because of the different ventilation factors in the respective formulae. The bottom line marked 'large compartments' is a modification to the Eurocode formula recommended by Kirby *et al.* (1999) for large spaces, after several experimental fires in a large compartment measuring 23×5.5 m by 2.7 m high. Using typical thermal properties of materials from Table 4.3, a building constructed with steel walls is in the 'high' category, normal and lightweight concrete are 'medium', and gypsum plaster and any materials with better insulating properties are in the 'low' category.

4.3.4.4 Validity

Time equivalent formulae are empirical. They have generally been derived by calculation, for a particular set of design fires for small rooms, using the maximum temperature concept for certain protected steel members with various thicknesses of insulation. As such the formulae may not be applicable to other shapes of time–temperature curve, to larger rooms, to other types of protection, or to other structural materials. None of the formulae described above have well documented derivations which describe their limitations. It is generally accepted

Table 4.3 Values of k_c or k_b in the time equivalent formulae

Formula	Term	Units	$b = \sqrt{(k\rho c_p)}$			General
			High >2500	Medium 720–2500	Low <720	
CIB W14	k_c	$\text{min m}^{2.25}/\text{MJ}$	0.05	0.07	0.09	0.10
Eurocode	k_b	$\text{min m}^2/\text{MJ}$	0.04	0.055	0.07	0.07
Large compartments	k_b	$\text{min m}^2/\text{MJ}$	0.05	0.07	0.09	0.09

k , thermal conductivity (W/mK); ρ , density (kg/m^3); c_p , specific heat (J/kgK).

that the time equivalent formulae can be applied to protected steelwork (for which they were derived) and reinforced concrete members (CEN, 2002b). The UK national application document restricts the use of the Eurocode time equivalent formula to steel structures (BSI, 2007). Law (1997) and Thomas *et al.* (1997) investigated the suitability of the different time equivalent formulae, and concluded that there are many situations where the formulae do not give a good prediction of actual behaviour, usually on the unsafe side.

In conclusion, these time equivalent formulae are a crude approximate method for introducing real fire behaviour into fire engineering calculations. It is much more accurate to make designs from first principles with the use of estimated post-flashover fire temperatures such as those described in Chapter 3.

4.4 Fire Resistance

4.4.1 Definition

Fire resistance is a measure of the ability of a building element to resist a fire. Fire resistance is most often quantified as the time for which the element can meet certain criteria during exposure to a standard fire resistance test. Structural fire resistance can also be quantified using temperature or load capacity of a structural element exposed to a fire. It is important to recognize that fire resistance cannot be assigned to materials. Fire resistance is a property assigned to building elements which are constructed from a single material or a mixture of materials. Some building elements may be simple elements such as a single steel column or a concrete floor slab. Other building elements may be complex assemblies of several layers of different materials such as a composite floor and suspended ceiling system.

A *fire resistance rating* is the fire resistance assigned to a building element on the basis of a test or some other approval system. Some countries use the terms *fire rating*, *fire endurance rating* or *fire resistance level*. These terms are usually interchangeable. Fire resistance ratings are most often assigned in whole numbers of hours or parts of hours, in order to allow easy comparison with the fire resistance requirements specified in building codes. For example, a wall that has been shown by test to have a fire resistance of 75 min will usually be assigned a fire resistance rating of 1 h.

4.4.2 Assessing Fire Resistance

Building elements need to be assigned fire resistance ratings for comparison with the fire severity specified by codes. The most common method of assessing fire resistance is to carry out a full-scale fire resistance test. It is becoming increasingly possible to assess fire resistance by calculation in lieu of full-scale tests, as permitted explicitly by codes such as the Uniform Building Code (ICC, 2015). Values of fire resistance obtained from tests, calculations or expert opinions are listed in various documents maintained by testing authorities, code authorities or manufacturers. These listings of fire resistance ratings are in three main categories: *generic ratings* which apply to typical materials; *proprietary ratings* which are linked to particular manufacturers; and approved *calculation methods*. Generic and proprietary ratings are obtained directly or indirectly from full-scale fire resistance tests. This chapter describes all these methods for assessing and listing fire resistance.

The fire resistance of any building element depends on many factors, including the severity of the fire test, the material, the geometry and support conditions of the element, restraint from the surrounding structure and the applied loads at the time of the fire. Many building codes and manufacturers' documents simply list fire resistance ratings of 1, 2 or 4 h with little or no reference to these factors which are discussed further in this book.

4.5 Fire Resistance Tests

All countries have building codes that specify required fire resistance ratings for building elements. Fire resistance ratings are most often specified in hours or minutes, with typical values ranging from half an hour to 4 h, in increments of 30 min. The time–temperature curves in standard fire tests have been described in Chapter 3. Fire resistance tests are not intended to simulate real fires. Their purpose is to allow a standard method of comparison between the fire performance of structural assemblies.

Many countries require that fire resistance be based on the results of *full-scale* fire resistance tests. The required sizes for full-scale tests are given below. Full-scale tests are expensive, but for many years it has been considered essential to test elements of building construction at a large scale because cheaper small-scale tests are not able to assess the effects of potential problems caused by connections, shrinkage, deflections, and gaps between panels of lining materials. Full-scale testing is the most common method of obtaining fire resistance ratings, but fire resistance tests are very expensive, so are only undertaken when considered necessary. The high expense of full-scale fire resistance testing is encouraging manufacturers to share test results within trade organizations, and is hastening the development of new calculation methods to predict fire resistance by calculation rather than by test. All calculations should be verified using the results of full-scale tests to avoid the potential problems described above.

Fire resistance tests are carried out on representative specimens of building elements. For example, if a representative sample of a flooring system has been exposed to the standard fire for at least 2 h while meeting the specified failure criteria, a similar assembly can be assigned a 2 h fire resistance rating for use in a real building. The implication is that the built assembly will behave at least as well in a real fire as the tested assembly did in the full-scale fire test. Obvious difficulties are that there are many differences between the tested and the built assemblies. The tested assemblies nearly always have different sizes and shapes, and different loads or boundary conditions than in real buildings, and the test fire may be very different from a real fire.

4.5.1 Standards

For fire resistance testing, many countries use the International Standard ISO 834 (ISO, 1999a) or have national standards based on ISO 834, for example AS 1530 Part 4 (SA, 2005). European countries follow EN 1363 (CEN, 2012). The standard used in the United States and some other countries is ASTM E119 (ASTM, 2012), first published in 1918. The Canadian standard (ULC, 2007) is based on ASTM E119. The relevant British Standards are BS 476 Parts 20–23 (BSI, 1987).

4.5.2 Test Equipment

A typical fire test furnace consists of a large steel box lined with fire bricks or ceramic fibre blanket. The furnace has a number of burners, most often fuelled by gas but sometimes by oil. There must be an exhaust chimney, several thermocouples for measuring hot gas temperatures and usually a small observation window. National and international standards for fire resistance testing do not specify the construction of the furnace in detail, which sometimes causes problems when making comparisons between tests from different furnaces. The standards are more concerned with the fire temperatures to be followed during the test and the failure criteria. As stated earlier, most national standards are based on either the ASTM E119 test or the ISO 834 test, which have some minor but important differences. Fortunately, despite minor differences, fire resistance test methods are very similar around the world, so that international comparisons are always possible. It is exceedingly difficult for any country to make a major change to standard test procedures because of the cost of re-testing and re-classifying the large number of assemblies which have been tested in the past.

In a typical test, a wall or floor assembly is constructed in a frame remote from the furnace, then brought to the furnace in its frame, and used to close off the furnace opening before the test begins. The burners are ignited at the start of the test and controlled to produce the time-temperature curve specified by the testing standard. Temperatures, deformations and applied loads are monitored during the test. The essential temperature measurements are those in the furnace itself and on the unexposed face of the specimen. In some tests, temperatures are measured at other locations within the test specimen or inside the furnace for research and development purposes. The most common apparatus for full-scale fire resistance testing is the vertical wall furnace (Figure 4.6). The minimum size specified by most testing standards is $3.0 \times 3.0 \text{ m}^2$ (ISO 834 or ASTM E119). Some wall furnaces are 4.0 m tall. Floors, roofs or beams are tested in a horizontal furnace (Figure 4.7 and Figure 4.8). ASTM E119 specifies a minimum size of 16 m^2 with a span at least 3.7 m. ISO 834 recommends a size of $3 \text{ m} \times 4 \text{ m}$. Some furnaces can be tipped from horizontal to vertical orientation to test both walls and floors. Special furnaces are available in some laboratories for testing individual columns or beams, or other non-standard items.

Test specimens are intended to represent actual construction as closely as possible. The moisture content of the test specimen is important because high moisture content can increase fire resistance considerably, especially delaying the temperature rise on the unexposed surface of floors or walls. Most testing standards specify conditions of relative humidity and temperature for conditioning of specimens and also methods of correcting test results for non-standard moisture content.

4.5.3 Failure Criteria

The three failure criteria for fire resistance testing are *stability*, *integrity* and *insulation*. To meet the *stability* criterion, a structural element must perform its load-bearing function and carry the applied loads for the duration of the test, without structural collapse. Many testing standards have a limitation on deflection or rate of deflection for load-bearing tests, so that a test can be stopped before actual failure of the test specimen which would damage the furnace. Commonly specified failure criteria are a deflection of $L/20$ of the span, or a limiting rate of

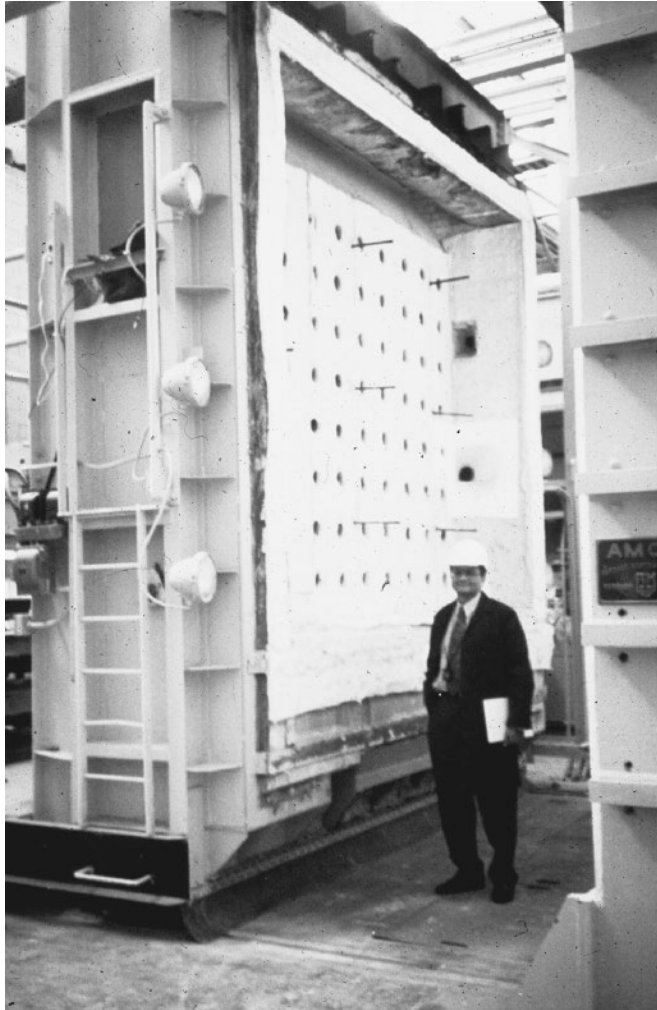


Figure 4.6 Typical furnace for full-scale fire resistance testing of walls

deflection of $L^2/9000d$ when the deflection is $L/30$ of the span. d is the thickness of the specimen (BSI, 1987; ISO, 1999a; SA, 2005). The European standard (CEN, 2012) specifies:

(a) For flexural elements

Limiting deflection $D = \frac{L^2}{400d}$ mm; or

Limiting rate of deflection $\frac{dD}{dt} = \frac{L^2}{9000d}$ mm/min

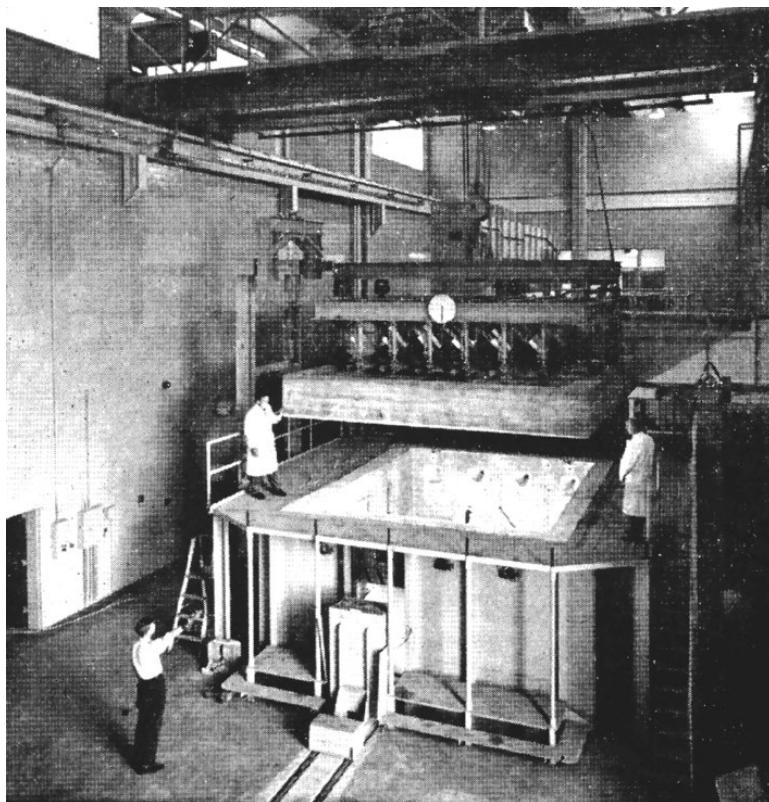


Figure 4.7 Floor furnace with a heavy surrounding beam for providing axial restraint to the test specimens. Reproduced from Lie (1992) with permission from ASCE

(b) For vertically loaded members

Limiting vertical contraction (negative elongation) $C = \frac{h}{100}$ mm; or

Limiting rate of vertical contraction (negative elongation) $\frac{dC}{dt} = \frac{3h}{1000}$ mm/min

where h is the initial height (in millimetres) of the test specimen once the load has been applied.

The integrity and insulation criteria are intended to test the ability of a barrier to contain a fire, to prevent fire spreading from the room of origin. To meet the *integrity* criterion, the test specimen must not develop any cracks or fissures which allow smoke or hot gases to pass through the assembly. The ASTM E119 specification requires that there be no passage of flame or hot gases sufficient to ignite cotton waste. To meet the *insulation* criterion the temperature of the cold side of the test specimen must not exceed a specified limit, usually an average increase of 140 °C and a maximum increase of 180 °C at a single point. These temperatures represent a conservative indication of the conditions under which fire might be initiated on the cool side of the barrier.

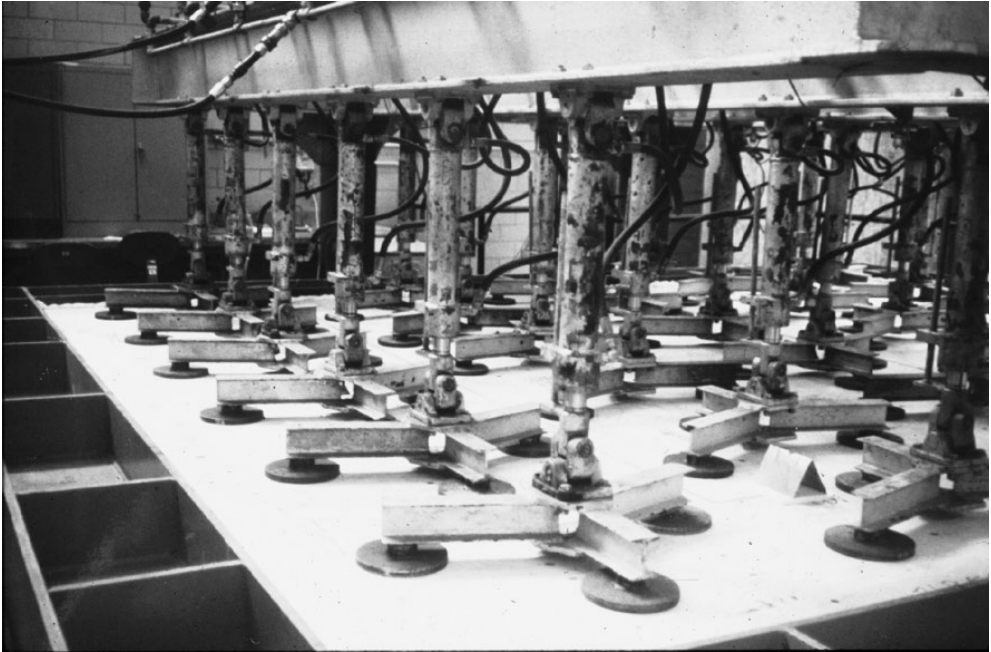


Figure 4.8 Detail of loading arrangement for fire testing of floors

Table 4.4 Failure criteria for construction elements

	Stability	Integrity	Insulation
Partition		X	X
Door		X	X
Load-bearing wall	X	X	X
Floor – ceiling	X	X	X
Beam	X		
Column	X		
Fire resistant glazing		X	

All fire rated construction elements must meet one or more of the three criteria as shown in Table 4.4, depending on their function. Note that fire resistant glazing need only meet the integrity criterion because it is not load bearing and it cannot meet the insulation criterion because glass has very little resistance to radiant transfer of heat. An increasing international trend is for fire codes to specify the required fire resistance separately for stability, integrity and insulation. For example, a typical load-bearing wall may have a specified fire resistance rating of 60/60/60, which means that a 1 h rating is required for stability, integrity and insulation. If the same wall was non-load bearing, the specified fire resistance rating would be –/60/60. A fire door with a glazed panel may have a specified rating of –/30/–, which means that this assembly has an integrity rating of 30 min, with no fire resistance for stability or insulation.

An additional integrity criterion for walls and partitions in some testing standards is the hose stream test. This test requires that no water should pass through the wall when it is subjected to water from a standard firefighting hose immediately after the fire test. The ASTM E119 standard allows a duplicate test specimen to be subjected to the hose stream test after fire exposure of half of the time of the fire resistance rating. The ISO 834 standard does not include a hose stream test.

4.5.4 *Standard of Construction*

The standard of construction of fire test specimens is sometimes of concern. Fire tests are supposed to be carried out on representative samples typical of normal construction, but some manufacturers may want to use their very best materials and workmanship for the fire test. Such problems can be overcome with accurate reporting by independent testing agencies, including good descriptions of the details of materials and fastenings. Many unsuccessful fire tests are never reported, so published test results may only represent the very best of the specimens actually tested.

4.5.5 *Furnace Pressure*

The pressure inside the test furnace is important. The furnace pressure affects the *integrity* criterion, because positive pressure will force flames or hot gases through any cracks. There are no requirements for pressure in the ASTM E119 test specification, hence many fire resistance tests in the United States are conducted at a low negative pressure to give the most favourable test result. The ISO 834 test method specifies a positive pressure of 10 Pa under a horizontal test specimen such as a floor system. For vertical test specimens such as walls the pressure gradient must be linear, with 10 Pa at the top and at least two-thirds of the specimen subjected to positive pressure. The British Standard BS 476 Part 20 (BSI, 1987) specifies a pressure gradient of 8.5 Pa per metre of height with the neutral axis 1 m above the floor level and a maximum pressure of 20 Pa. These pressures are sufficient to force hot gases through small openings near the top of a wall, but are too low to have a significant effect on load-bearing capacity.

Standard fire resistance tests do not assess resistance to blast forces. Special design is necessary for walls, partitions, or other barriers which may be subjected to impact loading or forces resulting from explosions or blast. This problem was highlighted in the Piper Alpha oil platform disaster, where walls with otherwise adequate fire resistance were blown out by explosions, leading to rapid and catastrophic spread of fire.

4.5.6 *Applied Loads*

All elements which are required to meet the *stability* criterion (see Table 4.4) should be tested under an applied load. As an exception, the ASTM E119 test method permits steel columns and beams to be tested without an applied load provided that the average temperature does not exceed 538 °C. At this temperature, a fire-exposed steel member would have approximately half of its normal temperature load capacity (see Chapter 6). Testing of unloaded specimens can produce unsafe results because the test does not assess the effect of deformations during

the fire which could affect the restraint from surrounding structure, the behaviour of connections or the 'stickability' of the applied fire protection materials.

The level of load on a structural element during a real fire can have a large effect on its structural performance, as discussed in Chapter 5. Similarly, the level of applied load during a fire test can have a significant effect on the level of fire resistance achieved. It is not easy to decide what level of load to apply to a test specimen during a fire resistance test, because low applied loads will give a high fire resistance rating but may limit the use of the product in other applications, whereas higher applied loads will lead to a lower fire resistance rating and may result in an additional test being required if the assembly just fails to achieve a particular rating. Such difficulties can be overcome with the use of calculations to predict fire resistance ratings based on a small number of full-scale tests.

Both ASTM E119 and ISO 834 recommend that the applied load in a fire test should be the maximum permitted load under nationally accepted design rules, but they also permit lower loads to be used provided that they are clearly identified. The definition of 'maximum permitted load' or 'maximum design load' will vary greatly from country to country depending on whether the relevant structural design code is in 'working stress' format or 'limit states' format. See Chapter 5 for more discussion of loads and loading standards. When deciding what level of loads to apply during a fire resistance test, it is best to apply those loads which produce stresses in the tested element similar to those expected in the actual building at the time of an unwanted fire. This may be possible if a specific prototype is being tested, but may be very difficult if a proprietary product is being tested for possible use in a multitude of different situations. The precise level of the loads and stresses is not important, but it is essential that the loads applied during the test be described accurately in the test report. Designers can then ensure that the corresponding stresses are not exceeded in the fire design. Loading devices and levels of structural restraint vary significantly from furnace to furnace, so it is important that these are also described in the test report.

The loads in some real members may be very low at the time of a fire, especially if the member was designed for deflection rather than strength, so it may be decided to use higher stresses in the fire test specimen, to allow subsequent use in a wider variety of applications. If the designed assembly has a larger span than that tested, the comparison with the test results should be on the basis of stresses rather than loads, but it is often difficult to keep shear stresses and flexural stresses in the same ratio.

4.5.7 *Restraint and Continuity*

Flexural continuity and axial restraint have a significant effect on fire resistance, as described in Chapter 5. For this reason, the support and restraint conditions are important in fire tests of structural elements. Most national testing standards require test specimens to be supported in a condition similar to that expected in actual buildings (Figure 4.7). Since 1970, ASTM E119 has had separate requirements for 'restrained ratings' and 'unrestrained ratings', but it does not clearly define these. For floors, ASTM E119 requires that restrained specimens shall be 'reasonably restrained in the furnace', whereas restrained beams are to be tested 'simulating the restraint in the construction represented'.

ISO 834 states that the test specimens should be installed in the furnace in such a way that the boundary conditions provide the degree and the type of restraint to which they will be

subjected in practice. Where details of the use are not available, ISO 834 specifies that the support conditions should be clearly pinned or be fully fixed against rotation, and be clearly free to expand or be fully restrained against axial movement, with the actual support conditions documented in the test report. See Chapter 5 for more discussion of restraint and continuity.

4.5.8 *Small-scale Furnaces*

Many laboratories have small-scale furnaces which are used for research and development. Intermediate-scale furnaces (1.0–2.5 m²) are used for standard testing of small items such as fire doors, using the same standard time–temperature curve as in a full-scale furnace. Even if the same time–temperature curve is followed, the fire severity may not be identical to a large furnace because the different geometry may result in different heat transfer coefficients from the walls and hot gases of the furnace to the test specimen. Tests in small- and intermediate-scale test furnaces may not pick up potential problems such as shrinkage, deflections or connection behaviour. Despite these difficulties, they can give useful information in many situations, particularly regarding thermal transmission.

4.6 Specifying Fire Resistance

4.6.1 *Approved Fire Resistance Ratings*

4.6.1.1 Listings

Most countries require that fire resistance tests be certified by a recognized testing laboratory or approval agency. In North America, independent testing organizations such as Underwriters Laboratories (UL, 2012) and Southwest Research Institute (SWRI, 2012) maintain registers of approved assemblies to which they have assigned fire resistance ratings. Most of these ratings are based on tests which they have carried out in accordance with recognized testing standards. Generic ratings based on these approvals are listed in national building codes (e.g. NBCC, 2010; ABCB, 2015; ICC, 2015). Some trade organizations (e.g. Gypsum Association, 2012; ASFP, 2014) maintain industry listings of approvals for products manufactured or used by their members.

Listings generally fall into three categories: *generic ratings*; *proprietary ratings*; or *calculation methods*.

4.6.1.2 Generic Ratings

Generic fire resistance ratings, or ‘tabulated ratings’ are listings which assign fire resistance to typical building elements with no reference to individual manufacturers or detailed specifications. For example, many national codes list tables of generic ratings for fire protection of structural steel members by encasement in a certain thickness of concrete, with no details of concrete quality or reinforcing. Generic ratings are derived from many full-scale fire resistance tests carried out over many years. Generic ratings are widely used because they can be applied to commonly available materials in any country. Generic ratings are usually very conservative, and they are often inadequate because they apply only to standard fire exposure, and make no allowance for the size and shape of the fire-exposed member or the level of load.

4.6.1.3 Proprietary Ratings

Proprietary fire resistance ratings apply to proprietary materials or structural products made by specific manufacturers. Proprietary ratings are based on the results of full-scale fire tests commissioned by the manufacturers. Proprietary ratings are usually accompanied by an approved specification detailing the materials and construction methods, and it is the assembly rather than the materials which has the approved rating. Unless they are covered by a suitable agreement, proprietary ratings cannot be applied to similar products from other manufacturers because there may be differences in materials or installation methods, and the fire resistance rating may legally be the property of the manufacturer.

Proprietary ratings may be less conservative than generic ratings because they relate to more closely defined products. Proprietary ratings are usually based on standard fire exposure and make no allowance for the level of applied load, but they sometimes include reference to the size and shape of the fire exposed member in a more accurate way than generic ratings.

4.6.1.4 Calculation Methods

As the art and science of fire engineering develops, it is becoming more feasible to assess fire resistance by calculation as well as by test. Many listing agencies and national design codes now include approved calculation methods for assessing fire resistance. Many of these methods are described in this book. Calculation methods should be verified by full-scale fire resistance test results of similar assemblies.

4.6.1.5 Expert Opinion

Most of the listings described in the above documents are based directly on the results of full-scale fire resistance tests. Such fire tests are very expensive, so testing and approving authorities are increasingly asked to give written expert opinions on assemblies which are similar but different to those which have passed a test. An increasing number of listed fire resistance ratings are based on such expert opinions. The opinion will state whether the assembly would be considered likely to pass a test, based on observations of similar successful tests and the considered experience of the testing and approving personnel.

As an indication of the factors to be considered in making an opinion, Figure 4.9 illustrates a useful set of empirical 'rules' for comparing fire resistance of similar assemblies (Harmathy, 1965). These 'rules' of fire endurance have stood the test of time and are applicable in almost all situations. These rules have been expanded and explained in more detail by Lie (1992).

4.6.2 *Fire Resistance by Calculation*

Figure 4.10 shows a flow chart for the process of calculating the strength of a structural assembly exposed to a complete burnout of a fire compartment. The resulting load capacity can be compared with the expected applied load at the time of a fire, to verify whether the design is satisfactory. This is design in the strength domain. The process of calculating structural fire behaviour has three essential component models: a fire model; a heat transfer model; and a structural model.

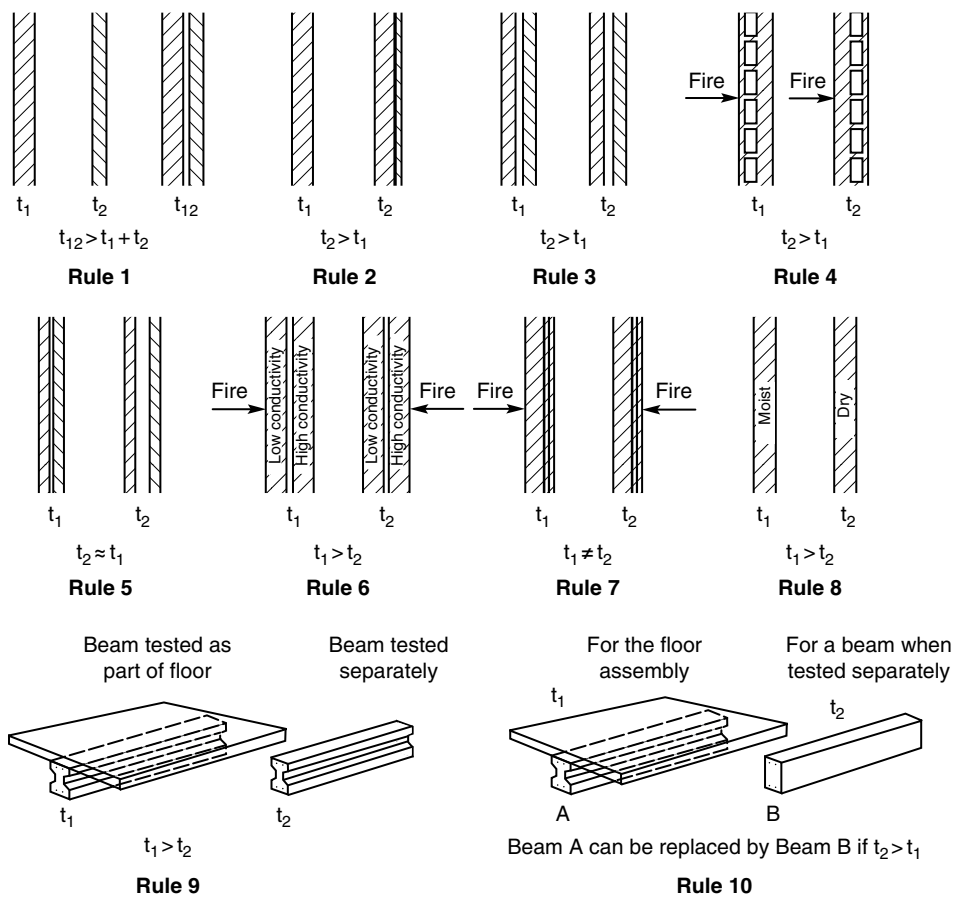


Figure 4.9 Harmathy's ten rules of fire endurance. Reprinted with permission from Harmathy (1965). © 1965 National Fire Protection Association, all rights reserved

4.6.2.1 Fire Model

Fire models have been discussed in Chapter 3. Input can be any selected time-temperature curve including the standard fire, a measured real fire or a parametric fire curve.

4.6.2.2 Heat Transfer Model

The heat transfer model is an essential component of calculating fire resistance because the load capacity or the containment ability of a fire exposed element or structure depends on the internal temperatures. The temperature of any material exposed to a fire increases as heat is conducted from the hot fire exposed surface to the cooler interior. The temperature gradients depend on the radiative and convective heat transfer coefficients at the surface, and the conduction of heat within the member. For non-load-bearing elements designed to contain

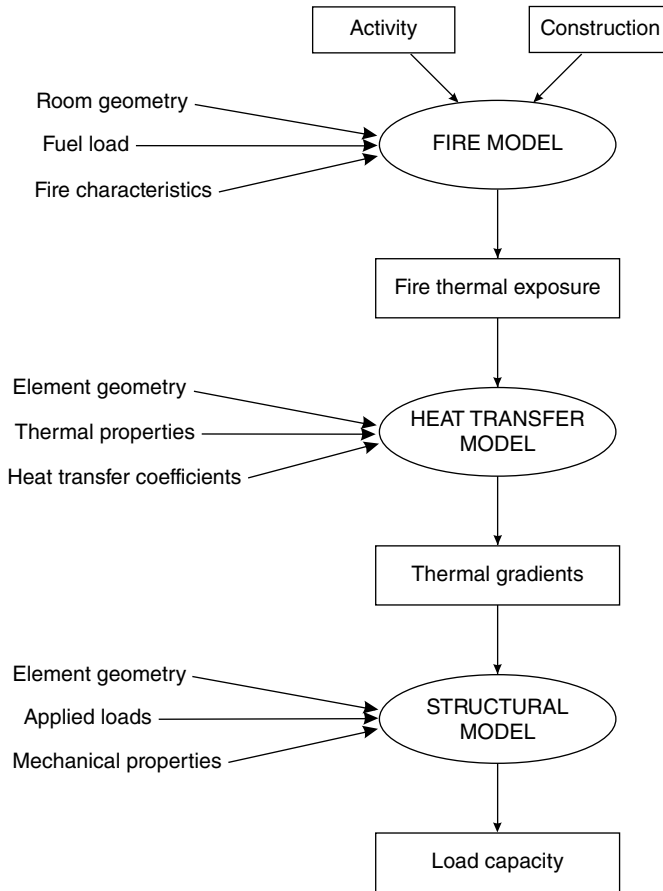


Figure 4.10 Flow chart for calculating strength of a structure exposed to fire

fires, the output from a heat transfer model can be used directly to assess whether the time to critical temperature rise on the unexposed face is acceptable. For simple structural elements with a single limiting temperature, the output from a heat transfer model can be used directly to assess whether the critical temperature is exceeded. These situations do not require the application of a structural model. They are examples of verification in the temperature domain.

For more complicated structural elements or assemblies, the output from the heat transfer model is essential input to a structural model for calculating load-bearing capacity. Temperature gradients within a member may or may not be significant. When a material such as steel with a high thermal conductivity is heated slowly, as in a protected assembly, it may be sufficiently accurate to disregard temperature gradients and assume that all the material is at the same temperature. For materials with low thermal conductivity like concrete, it becomes very important to know the thermal gradients during the fire because these affect the temperature of the reinforcing steel. Heat transfer calculations are less important for large timber members

because the rate of charring is more dependent on the thermal diffusivity of the wood than on the fire environment.

Calculation of heat transfer requires knowledge of the geometry of the element, thermal properties of the materials and heat transfer coefficients at the boundaries. Practical difficulties are that some thermal properties are very temperature-dependent, and heat transfer coefficients are not well established. Heat transfer to surfaces of the element is a combination of convection and radiation. Heat transfer through solid materials is by conduction. Heat transfer through voids is a combination of convection and radiation. Heat transfer calculations have been described briefly in Chapter 3, and specific examples are given in later chapters.

4.6.2.3 Structural Model

Models for calculating the performance of structural elements exposed to fire are described in Chapter 5. Hand calculation methods can be used for simple elements but sophisticated computer models are necessary for the analysis of frames or larger structures. Computer-based structural analysis models must be able to include the effects of thermal expansion, loading and unloading, large deformations and non-linear material properties which are temperature-dependent, all for a framework of interconnected members of different materials. Hand calculation methods for the main structural materials are given later in this book.

4.7 Fire Resistance of Assemblies

Most of the above discussion relates to fire resistance of individual elements of building construction. Real buildings are more than just a collection of elements, so the fire resistance of the whole building must be assessed by considering the fire resistance of its component parts and their location in the building. Many elements in a real building may be of different sizes, shapes and with different fixing details than those tested. Any assessment of fire resistance must consider the three failure criteria of stability, insulation and integrity. Fire resistance of a few representative assemblies are discussed in this section.

4.7.1 Walls

Most fire resistance furnaces are specifically designed for testing of walls, as briefly described earlier in this chapter. Non-load-bearing partitions are easier to test than load-bearing walls, because only the integrity and insulation criteria are important, and large movement at the edges of the walls is not expected. When testing load-bearing walls, it is necessary to have suitable loading devices such as hydraulic jacks at the top or bottom of the wall. These need to be protected from the furnace temperatures, and be installed in such a way that the loaded edge of the wall is free to move as the load is applied or as subsequent deflections occur. For framed systems such as stud walls, it is important to ensure that the applied load is not all carried by the end studs which are bolted to the edge of the furnace. When assessing fire test results for real buildings, it is important to find out whether the height, load or end fixity conditions are different from those in the fire test.

4.7.2 Floors

Floors are more difficult to test than walls because a larger furnace is necessary and the loading equipment is much more extensive. All floors are load bearing, so they all must be loaded during testing. Because of furnace size limitations, most floor systems are tested at spans less than commonly used in buildings. A tested floor system should have similar stresses and similar deformations to those expected in longer spans in a real building, to enable the test results to be extrapolated. Floors designed to span in only one direction must be free to behave in that way in the test furnace. Deformations are particularly important because the flexural curvature of a floor will affect the integrity of any fire resisting membrane or applied fire protection.

Many floor–ceiling assemblies rely on a ceiling membrane as an essential part of the fire resisting system, so these assemblies must be tested as a complete system. Flexural continuity and axial restraint can have a large influence on the results of fire resistance testing of floors, as described previously. Traditionally, floors have only been fire tested from below. This is because most fires tend to spread up, not down, and the most vulnerable part of the structure is usually on the underside. There has been some recent concern about the possibility of fires burning downwards through light timber floors clad on the top surface with particle board or plywood, but observations at real fires show that there is often a lot of debris on the floors, from collapsed ceilings, fittings and contents, which can provide some protection to the top surface of the floor system.

4.7.3 Beams

Beams are always tested for fire resistance as part of a floor or roof assembly, with fire exposure from below. The floor or roof may be structurally part of the beam, with composite action, or it may simply be a non-structural component to seal off the top of the furnace. When assessing fire resistance of beams it is essential to know whether there is composite action. A major difficulty in fire testing of beams is the limited span available in almost all furnaces. As with floors, a tested beam should have similar stresses and similar deformations to those expected in longer spans in a real building, but this can be very difficult to achieve over a small span. Flexural continuity and axial restraint can be difficult to provide because of the large forces involved, but these can have a very large influence on the results. Effects such as these may be better assessed by calculation.

4.7.4 Columns

Columns are usually tested in special furnaces which expose the column to fire from all sides (Figure 4.11). There are only a few column furnaces in the world, so fire resistance of columns is often achieved by calculation rather than by test, or by using conservative generic ratings. In real buildings, columns are often built into walls which protect one or more sides of the column from fire exposure. Partial fire protection of a column may reduce the load-bearing capacity during a fire because of temperature gradients through the cross section leading to thermal distortion and eccentricity.

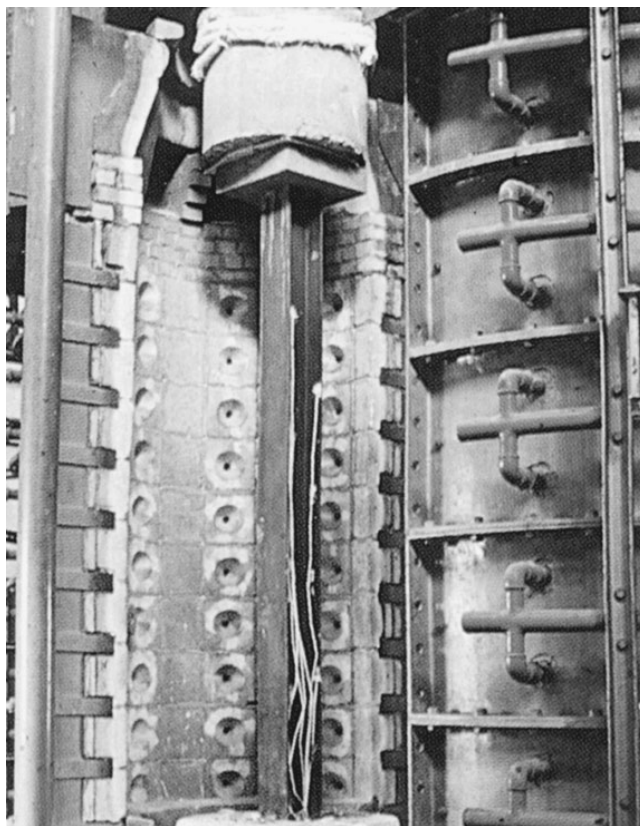


Figure 4.11 A special furnace for fire resistance testing of columns, with an unprotected steel column ready for testing. Reproduced by permission of Corus UK Ltd

4.7.5 Penetrations

Penetrations through walls and floors can severely reduce the ability of these barriers to contain a fire. If fire enters a cavity in a wall or floor assembly through a penetration, it can also severely reduce the load capacity. Walls and floors in typical buildings have numerous penetrations for electrical, plumbing and air handling services. The fire resistance of all of these must be considered as part of the fire safety design. There are standard methods of testing fire stops at penetrations through walls and floors (e.g. ASTM, 2012). Methods for protecting ‘poke-through’ penetrations are given by Gustaferrero and Martin (1988). Particular problems can occur if unprotected penetrations are not visible, such as hidden penetrations through walls above suspended ceilings, and penetrations made at a later date during alterations to the building. Many proprietary products are available for sealing gaps and openings in buildings, including fire resisting boards, paints, mastic sealants, intumescent strips and pillows. Products such as these can make the difference between success and failure of passive fire protection strategies.

Fire test performance of plastic pipe penetrations is described by England *et al.* (2000). The fire resistance of walls and floors can also be reduced if the barrier is penetrated by a heat-conducting member such as an unprotected steel beam. Fire on one side of the barrier can

cause the member to heat up, conducting heat to the unexposed side, where ignition can occur if combustible materials are in contact. Some codes prohibit this type of penetration. The danger of fire spread can be reduced by insulating the beam for a certain distance on either side of the wall. Deformations in steel beams passing through walls can also damage the wall unless the structure is specifically designed to prevent such damage.

4.7.6 *Junctions and Gaps*

Junctions between walls and floors are seldom fire tested. It is important for designers to assess the connecting details to ensure that the junctions do not give weaknesses in barriers that otherwise have excellent fire resistance. There are many proprietary products for providing fire resistance at junctions. Most common materials including concrete steel and wood can be used for preventing fire spread through junctions, provided that the materials have sufficient thickness and are well detailed. Aluminium and plastic materials are not suitable because they melt at low temperatures. Gaps between precast concrete panels can be fire rated using ceramic fibre blanket (Gustaferro and Martin, 1988; ICC, 2015).

4.7.7 *Seismic Gaps*

In seismic regions, buildings are provided with seismic gaps to allow differential movements to occur in the event of an earthquake. These seismic gaps can be within a building (to separate non-structural items and prevent damage when the structure moves) or between buildings (to allow separate parts of the building to move independently). Expected movement on one floor within a building can be 50mm or more, and expected movement between parts of multi-storey buildings can be up to half a metre. It is very difficult to provide details and flexible filling materials to accommodate these movements, and also provide fire resistance before, during and after an earthquake. A review of this problem is given by James and Buchanan (2000). Many proprietary products are available for filling seismic gaps, but their fire performance after large movements is often not proven.

4.7.8 *Fire Doors*

Doors are a very important part of the passive fire protection in many buildings. There are many proprietary fire resisting doors on the market, but they are usually expensive and have to meet different requirements in different countries. If a fire door is to match the fire resistance of the wall in which it is installed, the whole door assembly must be able to meet the integrity and insulation requirements for the specified fire resistance period. Solid core doors can easily be made with sufficient fire resistance, but weaknesses occur at the handle, hinges and all around the door edges. Many countries require that fire-rated doors be tested with exactly the same hardware as will be used in practice (Figure 4.12). The edge of the door or the frame is often fitted with a strip of intumescent material that swells into a foam when heated, to prevent flames penetrating the gap around the door.

Glazed doors are only required to meet integrity requirements because glazed panels cannot meet insulation requirements. Various codes have different limitations on the maximum size of the glass panel in fire doors. To meet the integrity requirements, the glass must be special fire resistant glass or be wired glass. There are an increasing number of proprietary fire resistant



Figure 4.12 Fire resistance test of two doors. The door on the left has had an integrity failure, as shown by penetration of flames and hot gases. Reproduced by permission of Building Research Association of New Zealand

glazing products on the market. Fire safety requirements for doors are very different in different countries. Some fire doors are required to prevent spread of smoke, in which case they must pass an air leakage test as well as a fire test. Many aspects of the performance of fire doors under test are described by England *et al.* (2000), who also propose an improved test method.

Real fire experience has shown that steel roller-shutter doors maintain excellent integrity in severe fires. No insulation rating is possible because the thin steel of the door heats up very rapidly, but a roller-shutter door can restrict the spread of fire provided that there are no combustible materials near the unexposed face of the door.

4.7.9 Ducts

Air handling ducts are potential paths for fire spread in buildings. Some authorities require ducts to be provided with fire resistance. Typical steel ducts can only provide an integrity rating, which can be improved to an insulation rating with insulating material such as ceramic fibre blanket placed internally or externally. More fire resistant ducts can be made from multiple layers of material such as gypsum board. There is no standard test method for ducts, but some systems have been tested successfully in non-standard tests.

An air-handling duct passing through a barrier can cause a serious reduction in the fire resistance of the barrier. This can be prevented by placing a 'fire damper' inside the duct where it passes through the barrier. Some fire dampers are also designed to control smoke movement. The dampers are designed to close automatically. Small dampers operate when a

spring-loaded blade or curtain inside the duct is released by melting of a heat-activated fusible link. Dampers in large ducts may have motorized closers which are activated by the fire detection system in the building. Another type of system has blades covered with intumescent material which swells up to close the duct at high temperatures. Testing requirements are described by England *et al.* (2000).

When there is a severe fire on one side of a wall penetrated by a duct, the collapsing duct on the hot side of the wall may cause damage to the wall itself, reducing the fire resistance. To prevent such damage, the fire damper should be firmly attached to the wall, and the duct should be constructed with joints which allow the duct to pull away from the damper, leaving the damper intact as part of the wall. This approach cannot be easily applied to fixed services such as cable trays.

4.7.10 Glass

Glass is a vitreous solid material with crystal structure similar to a liquid. On heating, it goes through a series of phases of decreasing viscosity. Most typical glass softens or melts at temperatures from 600 to 800 °C, but it will crack or break if exposed to thermal shock at much lower temperatures, due to differential temperatures within the glass or because of expansion of the surrounding frame. Normal window glass is assumed to break and fall out of the windows at the time of flashover (typically around temperatures of 500–600 °C), although tests have shown that this does not always occur. Toughened glass or heat strengthened glass may not shatter at high temperatures. Double glazing tends to remain in place much longer than single layers of glass.

Glass is sometimes used in fire resisting barriers, where it can only provide an integrity rating, because it has no structural capability at elevated temperatures and cannot provide an insulation rating unless it is coated with some sort of intumescent coating. If glazing is to be used in a fire resisting barrier, it must be assembled with special glass, either wired glass (reinforced with fine wires in both directions) or specially formulated fire resistant glass. Fire resisting glazing is usually installed in steel frames which clamp the glass and prevent it from deforming excessively when it gets hot. Aluminium frames cannot be used because of low melting temperatures. Glazed assemblies can be tested in full-scale fire resistance tests, but the assessment is only for the integrity criterion.

A number of proprietary insulated glazing systems have recently been developed, consisting of alternating layers of glass or sodium silicate with transparent intumescent materials. These products are transparent at room temperatures, but become opaque at high temperatures, achieving fire resistance of up to 2 h. Glass walls and windows can provide resistance to fire spread if they are sprayed continuously with water from a properly design sprinkler system (Kim *et al.*, 1998; England *et al.*, 2000).

4.7.11 Historical Buildings

Fire engineers are sometimes asked to report on the fire safety of historical buildings. This often requires information on fire resistance of old materials and obsolete building systems. This information can often be obtained from many current listings, and calculations can be made using the information in this book. A useful reference is Appendix L to NFPA 909 (NFPA, 2010b) which gives extensive lists of fire ratings of elements such as masonry walls, hollow clay tile floors, old-style doors and cast iron columns, which are no longer used in new construction.

4.8 Worked Examples

4.8.1 Worked Example 4.1

Calculate the equivalent fire severity using the Eurocode formula for a room 4.0 m × 6.0 m in area, 3.0 m high, with one window 3.0 m wide and 2.0 m high. The fire load is 800 MJ/m² floor area. The room is constructed from concrete.

Length of room	$l_1 = 6.0 \text{ m}$
Width of room	$l_2 = 4.0 \text{ m}$
Floor area	$A_f = l_1 l_2 = 6.0 \times 4.0 = 24.0 \text{ m}^2$
Height of room	$H_r = 3.0 \text{ m}$
Fuel load energy density	$e_f = 800 \text{ MJ/m}^2$

For concrete

Thermal conductivity	$k = 1.6 \text{ W/mK}$
Density	$\rho = 2300 \text{ kg/m}^3$
Specific heat	$c_p = 980 \text{ J/kgK}$
Thermal inertia	$\sqrt{(k\rho c_p)} = 1900 \text{ W s}^{0.5}/\text{m}_2\text{K}$ (medium)
Conversion factor	$k_b = 0.055$
Window height	$H_v = 2.0 \text{ m}$
Window width	$B = 3.0 \text{ m}$
Window area	$A_v = H_v B = 2.0 \times 3.0 = 6.0 \text{ m}^2$
Horizontal vent area A_h	$= 0$ (no ceiling opening)

$$\alpha_v = A_v / A_f = 6.0 / 24.0 = 0.25$$

$$\alpha_h = A_h / A_f = 0$$

$$b_v = 12.5(1 + 10\alpha_v - \alpha_v^2) = 43.0$$

$$\text{Ventilation factor } w = \left(\frac{6.0}{3.0}\right)^{0.3} \left[0.62 + \frac{90(0.4 - 0.25)^4}{1 + 43.0 \times 0}\right] = 0.820 \text{ m}^{-0.3}$$

$$\text{Equivalent fire severity } t_e = e_f k_b w = 800 \times 0.055 \times 0.820 = 36.1 \text{ min}$$

4.8.2 Worked Example 4.2

Repeat Worked Example 4.1 with an additional ceiling opening of 3.0 m².

Ceiling opening area $A_h = 3.0 \text{ m}^2$

$$\alpha_h = A_h / A_f = 3.0 / 24 = 0.125$$

$$\text{Ventilation factor } w = \left(\frac{6.0}{3.0}\right)^{0.3} \left[0.62 + \frac{90(0.4 - 0.25)^4}{1 + 43.0 \times 0.125} \right] = 0.772 \text{ m}^{-0.3}$$

$$\text{Equivalent fire severity } t_e = e_f k_b w = 800 \times 0.055 \times 0.772 = 34 \text{ min}$$

4.8.3 Worked Example 4.3

Repeat Worked Example 4.1 using the CIB formula and the Law formula.

CIB formula

Length of room	$l_1 = 6.0 \text{ m}$
Width of room	$l_2 = 4.0 \text{ m}$
Floor area	$A_f = l_1 l_2 = 6.0 \times 4.0 = 24.0 \text{ m}^2$
Height of room	$H_r = 3.0 \text{ m}$
Fuel load energy density	$e_f = 800 \text{ MJ/m}^2$
Total area of the internal surface	$A_t = 2(l_1 l_2 + l_1 H_r + l_2 H_r) = 2(6 \times 4 + 6 \times 3 + 4 \times 3) = 108 \text{ m}^2$

For concrete

Thermal inertia	$\sqrt{(k \rho c_p)} = 1900 \text{ W s}^{0.5} / \text{m}_2 \text{ K (medium)}$
Conversion factor	$k_c = 0.07 \text{ min m}^{2.25} / \text{MJ}$
Window height	$H_v = 2.0 \text{ m}$
Window width	$B = 3.0 \text{ m}$
Window area	$A_v = H_v B = 2.0 \times 3.0 = 6.0 \text{ m}^2$
Ventilation factor	$w = \frac{A_f}{\sqrt{A_v A_t} \sqrt{H_v}} = \frac{24.0}{\sqrt{6.0 \times 108.0} \times \sqrt{2.0}} = 0.793 \text{ m}^{-0.25}$
Equivalent fire severity	$t_e = e_f k_c w = 800 \times 0.07 \times 0.793 = 44.4 \text{ min}$

Law formula

Net calorific value of wood	$\Delta H_c = 16 \text{ MJ/kg}$
Equivalent fire severity	$t_e = \frac{A_f e_f}{\Delta H_c \sqrt{A_v (A_t - A_v)}} = \frac{24.0 \times 800}{16.0 \sqrt{6.0 (108.0 - 6.0)}} = 48.6 \text{ min}$

5

Design of Structures Exposed to Fire

This chapter describes the process of designing structures to resist fire exposure. It also describes some simple tools for making structural calculations, and explains the importance of loads and support conditions in estimating load capacity under fire conditions. These procedures can be used for verifying structural fire performance in the strength domain.

Building structures are made up of a number of elements such as walls, floors and roofs, often supported by structural members such as beams and columns. To avoid collapse of a building structure, the combination of elements and their supporting members must perform their load-bearing function for the duration of the fire.

In many simple structures, collapse of one member can result in total collapse of the structure. Hence in a fire, structural failure can occur if the applied load exceeds the load capacity of a critical member at any time during the fire. In more complex structures it may be possible for the structure to survive a fire even if one or more members loses its load-carrying capacity. This is more likely to occur in a redundant structure with a number of alternative load paths.

5.1 Structural Design at Normal Temperatures

Before describing the procedure for structural design under fire conditions, it is important to review design at normal temperatures, in order to define terms and maintain consistency. The basic steps in making a structural design are:

1. Establish the functional requirements for the building
2. Make a conceptual design of the structural system
3. Assume the sizes of the main structural members

4. Estimate the loads on the structure
5. Make a structural analysis to determine internal forces and stresses
6. Check whether the guessed initial sizes have sufficient strength and stiffness
7. Repeat steps as necessary

Steps 4–6 will be described in more detail. These steps apply equally to new or existing buildings.

5.2 Loads

5.2.1 *Types of Load*

Loads on structures are usually differentiated as ‘dead loads’ and ‘live loads’. These types of loads are referred to in some codes as ‘permanent actions’ and ‘imposed actions’, respectively. Dead loads are loads which are always present, being the self-weight of the building materials and any permanent fixtures. Live loads, or ‘occupancy loads’, are loads which may or may not occur at any time, from a wide variety of sources including the following:

- Human occupancy loads are from the weight of people. These may vary from zero to very high levels, especially where crowds can gather. Day-to-day loads are usually much less than the loads specified by structural design codes.
- Non-human occupancy loads come from equipment, goods, and other moveable objects. The weight of objects may be very low and variable in spaces like office buildings, or heavy and semi-permanent in warehouses and libraries.
- Snow loads are seasonal, with large geographic differences. Some areas may expect heavy snow to remain for several months every year, whereas others may expect no snow, or very infrequent snow loads.
- Wind loads are experienced by most buildings. The probability of extreme wind loads varying greatly, depending on location and topography. Critical wind loads are usually lateral loads on walls or uplift loads on roofs.
- Major earthquakes are extreme events which do not occur often. Some areas expect no earthquakes, others may have many small earthquakes and others have a low but significant probability of a rare major earthquake. Earthquake loads are inertial loads acting at the centre of mass, mostly in the horizontal plane.

5.2.2 *Load Combinations*

The above loads never all occur at the same time. Structural design at normal temperatures requires investigation of several alternative load combinations as specified by national building codes. At the time of a fire the most likely load is the dead load and a part of the occupancy load.

5.2.3 *Structural Analysis*

Structural analysis is the process of assessing the load paths in a building, to understand ways in which applied loads on the floors or roofs or walls of the building ‘flow’ through the beams,

columns and other structural members to the foundations. A building structure resists the applied loads by deforming slightly when the loads are applied. The flow of loads through the structure is accompanied by deformations and the development of internal forces in each structural member. These internal forces may be bending moments, axial forces, or shear forces.

Structural analysis is used to calculate the deformations of the structure under the applied loads and the internal forces in every member. Structural analysis of simple structures is performed by hand calculation from first principles of statics and mechanics, often with reference to standard formulae. Computer programs are widely used for structural analysis of more complex structures.

If member sizes are known, internal forces can be converted to stresses, usually expressed as a combination of normal stresses and shear stresses.

5.2.4 *Non-linear Analysis*

Most simple structural analysis assumes that the structure behaves in a linear and elastic manner. A linear elastic structure is one where deformations are directly proportional to the applied loads and the structure reverts to its original shape when all loads are removed. The linear elastic assumption is good for most structures at low levels of load.

There are two main sources of non-linearities in structural analysis. Geometrical non-linearities occur when deformations become so large that they induce additional internal actions, resulting in even larger deformations. Column buckling is the most common case of geometrical non-linearity. Material non-linearities occur when materials are stressed beyond the elastic range causing yielding or 'plastic' behaviour, in which case the structure will have permanent deformations after the loads are removed. Understanding of non-linear behaviour becomes important if the ultimate strength of the structure is to be well understood.

The simplest computer programs for structural analysis consider only linear elastic behaviour. More advanced programs can include both geometrical and material non-linear analysis. Non-linear behaviour can be very important under fire conditions because deformations are larger and material strength is less than in normal temperature conditions. Computer programs for structural analysis in fire conditions are discussed in Chapter 11.

5.2.5 *Design Format*

The specification of design loads and material strength depends on the format of the national building code, which varies from country to country.

The traditional design format, still used in many countries, is *working stress* design or *allowable stress* design where calculated member stresses under the actual loads expected in the building are compared with the allowable or permissible stresses which are considered safe for the material under long term loads. There is usually a large safety factor built into the safe working stresses.

Modern design codes use the *ultimate strength* design format in which internal forces resulting from the maximum likely values of load ('characteristic loads') are compared with the expected member strength using the short term strength of the likely materials ('characteristic strength'). This design format is known as *limit states design* in Europe and *load and resistance factor design* (LRFD) in North America. There are minor differences between these formats, but the principles are similar.

Limit states design clearly differentiates between the strength limit state (or ultimate limit state) and the serviceability limit state. The ‘strength’ or ‘ultimate’ limit state is concerned with preventing collapse or failure whereas the ‘serviceability’ limit state is concerned with controlling deflection or vibration which may affect the service of the building. The loads specified for the serviceability limit state are those load combinations which are expected to occur more frequently during the life of the building. Structural design for fire is mainly concerned with the ultimate limit state because it is strength and not deflection which is critical to prevent collapse of buildings exposed to fire.

Some national codes are in transition from working stress design to ultimate strength design. It is possible to make a rough comparison (or soft conversion) between the two formats. The use of either design format should result in similar member sizes, especially for simple structural members.

5.2.6 Working Stress Design Format

The loads in *working stress design* or *allowable stress design* are the typical loads expected in normal use of the building. The dead load is the self-weight of the structure estimated by the designer, and the live loads are specified by national design codes.

Considering dead loads and live loads, most codes specify only one load combination for the design load L_w given by:

$$L_w = G + Q \quad (5.1)$$

where G is the dead load and Q is the live load.

Other combinations are given for situations including snow, wind or earthquake loading. In the structural design process, the load L_w is used to calculate internal forces (bending moment, axial force and shear force) in each structural member, then the resulting stresses are calculated and these are compared with the allowable design strength for the material, which is considered to be the safe stress for long term loads.

For example, in the design of a tension member, the axial tensile force N_w (N) in the member is calculated from the above load combination. The resulting tensile stress f_t^* (MPa) is calculated from:

$$f_t^* = N_w / A \quad (5.2)$$

where A is the cross-sectional area of the member (mm^2).

The design equation which must be satisfied is:

$$f_t^* \leq f_a \quad (5.3)$$

where f_a is the allowable design stress in the code (MPa).

The actual level of safety is not clearly known in this format because the loads are not the worst loads that could occur, and the allowable stresses are known to be safe, but are not directly related to the failure stresses.

5.2.7 Ultimate Strength Design Format

In *ultimate strength design*, the characteristic dead load is the self-weight of the structure calculated by the designer, the same as in working stress design. Characteristic live loads are specified by national codes for various uses, usually being estimates of loads which have a 5% probability of being exceeded in a 50 year period.

Considering only dead loads and live loads for the strength limit state, most codes specify two load combinations, one for dead load only and the other for dead and live loads combined, where each load is increased by a 'load factor' or 'partial safety factor' (γ_G, γ_Q in the Eurocodes). Values from the Eurocode (CEN, 2002a), the US Standard (ASCE, 2010) and the Australia/New Zealand Standard (SA, 2002), are given in Equation 5.4a, Equation 5.4b and Equation 5.4c, respectively.

$$L_u = 1.35 G_k \quad \text{or} \quad L_u = 1.35 G_k + 1.5 Q_k \quad (5.4a)$$

$$L_u = 1.4 G_k \quad \text{or} \quad L_u = 1.2 G_k + 1.6 Q_k \quad (5.4b)$$

$$L_u = 1.35 G_k \quad \text{or} \quad L_u = 1.2 G_k + 1.5 Q_k \quad (5.4c)$$

where L_u is the factored load combination, G_k is the characteristic dead load and Q_k is the characteristic live load.

Of the two equations given in each row above, the first is the combination for dead load only and the second is the combination for dead load and live load combined. In the structural design process, the combination having maximum effect is used to calculate the internal forces (bending moment, axial force and shear force) in each structural member, to be compared with the load capacity of the proposed member. Additional combinations for use with wind, snow or earthquake loads can be found in the relevant national standards.

The load capacity is obtained from the short term characteristic strength specified in the material code. The characteristic stress is an estimate of the 5th percentile failure stress. The nominal load capacity is reduced by a *strength reduction factor* Φ which is intended to allow for uncertainty in the estimates of material strength and section size. The value of Φ is normally in the range 0.7–0.9. In the European system, the strength reduction factor Φ is replaced by $1/\gamma_M$ where γ_M is the partial safety factor, analogous to the inverse of the strength reduction factor Φ , for each material.

Hence, verification of the design for strength requires that

$$U^* \leq \Phi R \quad (5.5)$$

where U^* is the internal force resulting from the applied load, R is the nominal load capacity and Φ is the strength reduction factor ($1/\gamma_M$).

The internal force U^* may be axial force N^* , bending moment M^* or shear force V^* occurring singly or in combination. The load capacity R will be the axial strength, flexural strength or shear strength, in the same combination.

For example, in the design of a tensile member, the axial force N^* (N) obtained from the worst factored load combination in Equation 5.6 must not exceed the design capacity ΦN_n so the design equation is:

$$N^* \leq \Phi N_n \quad (5.6)$$

where N_n is the nominal axial load capacity (N) given by:

$$N_n = f_t A \quad (5.7)$$

where f_t is the characteristic tensile strength (MPa) and A is the cross-sectional area (mm²).

When comparing working stress design with ultimate strength design, note that the characteristic tensile strength f_t is larger than the long term allowable tensile strength f_{tw} with a corresponding difference between the loads N^* and N_w .

5.2.8 Material Properties

The derivation of material design values for strength depends on the format of the design system in use. In the traditional system of *working stress* design, the design strength (or permissible stress) represents the stress which can be sustained safely under long duration loads. In the more modern system of *limit states design* or *LRFD*, the characteristic strength (or design strength) represents the stress at which the material will fail under short duration loads. In most countries the characteristic strength is the 5th percentile short term failure stress (estimated with 75% confidence) for a typical population of material of the size and quality under consideration. For modulus of elasticity two values are needed; the 5th percentile value (or 'lower bound' value) for buckling strength calculations, and the mean value for deflection calculations.

The normal temperature properties of steel, concrete and timber are compared briefly as an introduction to elevated temperature design in subsequent chapters, using Figure 5.1 and Figure 5.2. Figure 5.1 shows a simply supported beam with two point loads. The bending moment at mid-span produces the internal strain distribution as shown with tensile strains at the bottom and compressive strains at the top. Figure 5.2 shows typical stress–strain relationships for the three materials. These are not drawn at the same scale because the yield strain for steel is much greater than the crushing strength of concrete or wood which are similar.

It can be seen that typical steel has the same properties in both compression and tension, with elastic behaviour to a well-defined yield point, followed by very ductile behaviour. Concrete has very little dependable tensile strength, but is strong in compression, with limited ductility. The ductility of reinforced concrete can be substantially increased by confining the compression zone with stirrups. Wood is ductile in compression but exhibits brittle failure in tension. In Figure 5.2 the solid line shows parallel to grain behaviour where the tensile strength is very high, and the dotted line shows perpendicular to grain behaviour where the tensile strength is very weak (splitting failure).

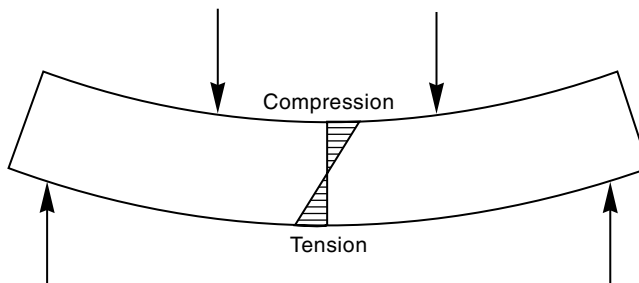


Figure 5.1 Internal strains in a simply supported beam

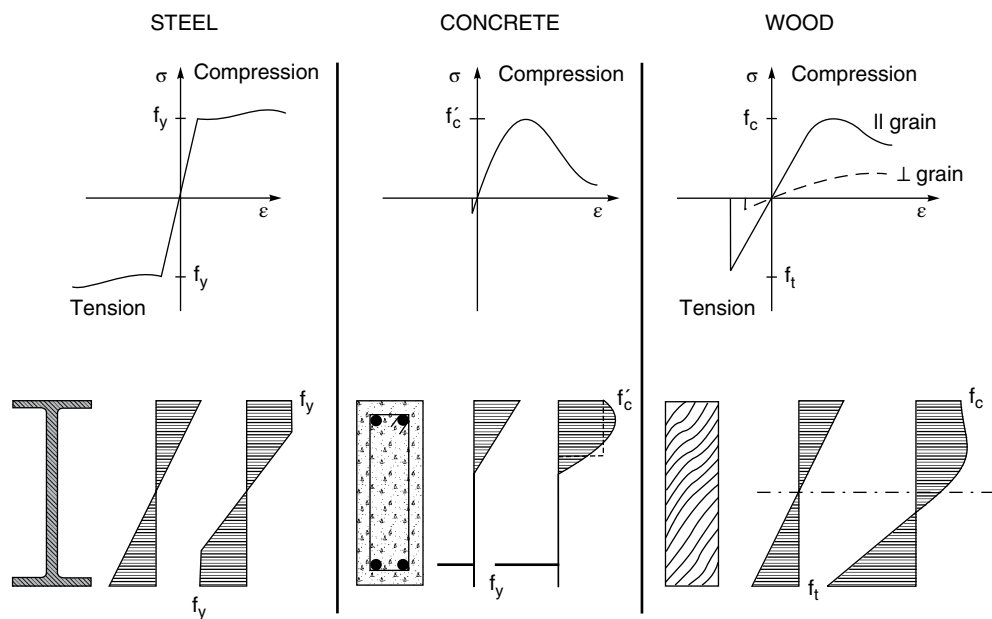


Figure 5.2 Stress–strain relationships and internal flexural stresses for steel, concrete and timber beams

All three materials show some non-linear material behaviour, especially in compression. This non-linear behaviour under increasing load is often termed ‘plasticity’.

The lower parts of Figure 5.2 show flexural stresses in beams of typical cross sections, based on the stress–strain relationships shown above. Internal stresses are shown twice: initially for beams lightly stressed in the elastic range; and secondly for beams stressed to near failure in the inelastic range. The steel beam develops plastic yielding over most of the cross section when approaching its ultimate flexural strength, depending on the amount of curvature. The reinforced concrete beam has a parabolic stress distribution in compression at ultimate strength, with the resulting compressive force equal to the yield force of the reinforcing bars which are yielding in tension. The parabolic compression block is approximated by the dotted rectangle for design purposes (Park and Paulay, 1975). The internal stress distribution for timber depends on the material properties. Commercial quality timber usually has low tensile strength due to defects, so it fails when the stress distribution is in the linear elastic range. For high quality timber with no defects in the tension zone, ductile yielding occurs in compression as shown, leading to lowering of the neutral axis and causing very high tensile stresses.

5.2.9 Probability of Failure

The objective of structural design is to provide buildings with an acceptably low probability of failure under extreme loading conditions. Probabilities of failure are not usually stated in design codes, but they have been used by the writers of ultimate strength design codes to establish the necessary strength reduction factors to give a target level of safety for all anticipated conditions, using characteristic values of load and resistance.

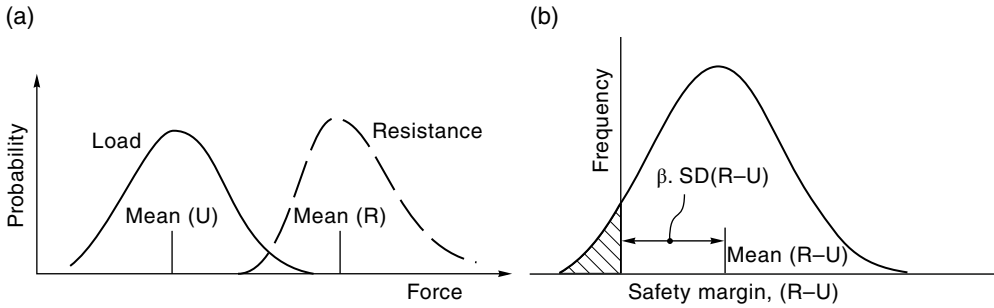


Figure 5.3 Probabilistic design concept

Figure 5.3(a) shows schematically that load U and resistance R are both probabilistic quantities, with a distribution of values about a mean. There is a small probability of failure which can be calculated from the area of overlap between the two curves if their distributions are known. The characteristic value of member resistance usually represents the lower 5th percentile tail of the strength distribution, and the design load represents a high percentile of likely loads for a given return period.

When considering Figure 5.3(a) for fire design, the load and resistance curves can be quantified in the time domain, the temperature domain or the strength domain (as shown in Chapter 4). If Figure 5.3(a) represents load and resistance at room temperatures, both the curves will shift to the left under fire conditions because the expected loads are less and the strength decreases due to elevated temperatures.

The ultimate limit state representing failure occurs if $R < U$, so the likelihood of failure is related to the difference $R - U$. Figure 5.3(b) shows the frequency distribution of $R - U$. The probability $R - U < 0$ is given by the shaded area under the distribution. Limit state design codes are usually calibrated to give a certain reliability index β , which is the number of standard deviations of the mean value of $R - U$ above zero, as shown in Figure 5.3(b). For given distributions, the strength reduction factor Φ is derived by code writers to give a target reliability index β , in the range between 2 and 3 (roughly equivalent to a probability of failure between 10^{-2} and 10^{-3}).

The above discussion shows that although there is a probabilistic framework behind the ultimate strength code formats, day-to-day design is a deterministic process.

Structural design for fire safety has far more uncertainty than structural design for normal temperature conditions. This book considers structural fire safety in a deterministic framework, rather than a probabilistic framework. The science of structural reliability is rapidly developing, but applications to structural fire safety are still in their infancy despite pioneering work many years ago by Magnusson (1972) and Schleich (1999).

5.3 Structural Design in Fire Conditions

Structural design for fire is conceptually similar to structural design for normal temperature conditions. Before making any design it is essential to establish clear objectives, and determine the severity of the design fire. The design can be carried out using either working stress or ultimate strength format, but only the ultimate strength design format will be illustrated

here. The main differences of fire design compared with normal temperature design are that, at the time of a fire:

- The fire limit state loads are less.
- Internal forces and deformations may be induced by differential thermal expansion.
- Interactions with the surrounding structure occur as members try to expand.
- The strength of materials may be reduced by elevated temperatures.
- Cross-sectional areas may be reduced by charring or spalling.
- Smaller safety factors can be used, because of the low likelihood of the event.
- Deflections are not important (unless they affect strength).
- Different failure mechanisms need to be considered.

The above factors may be different for different materials. For example, Figure 5.4(a) shows how failure of a simply supported steel beam occurs when the yield strength of the material drops so low that it is exceeded by the actual stress in the member at the time of the fire. The stress in the member does not change during the fire because the loads are constant and the section properties do not change. In contrast, Figure 5.4(b) shows a similar situation for a timber beam, where the stresses increase steadily (under constant load) due to loss of cross section by charring. The material strength only decreases very slightly due to elevated temperatures within the beam. As before, failure occurs when the stress in the member exceeds the material strength.

5.3.1 Design Equation

Verification of design for strength during fire requires that the applied loads are less than the load capacity of the structure, for the duration of the fire design time. This requires satisfying the design equation given by:

$$U_{fire}^* \leq \Phi_{fire} R_{fire} \quad (5.8)$$

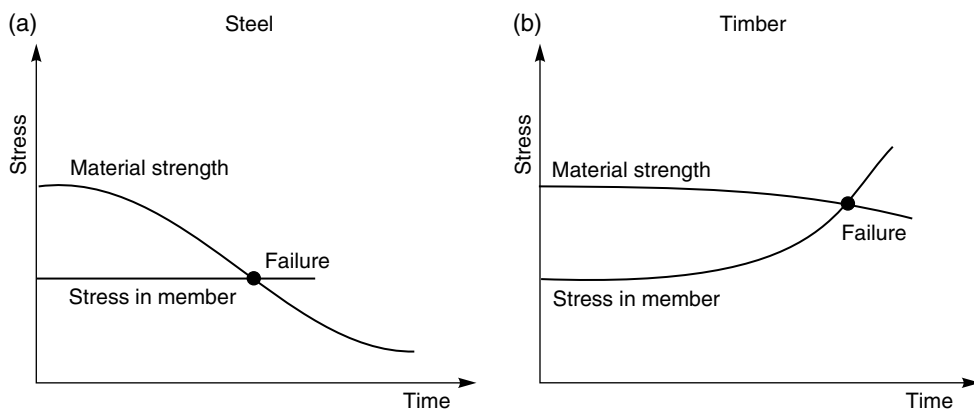


Figure 5.4 Member failure in fire, due to internal stresses exceeding material strength

where U_{fire}^* is the design action from the applied load at the time of the fire, R_{fire} is the nominal load capacity at the time of the fire and Φ_{fire} is the strength reduction factor for fire design.

The design force U_{fire}^* may be axial force N_{fire}^* , bending moment M_{fire}^* or shear force V_{fire}^* occurring singly or in combination, with the load capacity calculated accordingly.

The strength reduction factor Φ_{fire} accounts for uncertainty in the estimates of material strength and section size. Fire design is based on the most likely expected strength, so most national and international codes specify a strength reduction factor of $\Phi_{fire} = 1.0$. In the Eurocodes, the partial safety factor γ_M is also equal to 1.0 for fire design. In both the North American and European formats the design equation for fire conditions now becomes:

$$U_{fire}^* \leq R_{fire} \quad (5.9)$$

This is the equation that will be used in the following chapters for design of steel, concrete and timber structures.

5.3.2 Loads for Fire Design

5.3.2.1 Load Combinations

In the ‘accidental’ event of a fire, the most likely applied loads are much lower than the maximum design loads specified for normal temperature conditions. Most codes refer to an ‘arbitrary point-in-time load’ to be used for the fire design condition, often known as the fire limit state loads. Fire limit state load combinations from the Eurocode (CEN, 2002a), the US Standard (ASCE, 2010) and the Australia/New Zealand Standard (SA, 2002), are given in Equation 5.10a, Equation 5.10b and Equation 5.10c respectively.

$$L_f = G_k + 0.5Q_k \quad \text{or} \quad L_f = G_k + 0.9Q_k \quad (5.10a)$$

$$L_f = 1.2G_k + 0.5Q_k \quad (5.10b)$$

$$L_f = G_k + 0.4Q_k \quad \text{or} \quad L_f = G_k + 0.6Q_k \quad (5.10c)$$

where L_f is the factored load combination for fire, G_k is the characteristic dead load and Q_k is the characteristic live load.

Where two equations are given, the second is the combination for storage occupancies with semi-permanent live loads, and the first equation is for all other occupancies. It can be seen that the loads under fire conditions are much less than in normal temperature conditions. This is especially true for members which have been designed for load combinations including wind, snow or earthquake, or for members over-sized for deflection control or architectural reasons.

National standards should be consulted for more detail. For example, ASCE (2010) requires that $1.2G_k$ in Equation 5.10b should become $0.9G_k$ if the dead load has a stabilizing effect. Some codes including the Eurocode and US codes have additional load combinations to consider the possible effects of snow or wind occurring at the same time as a fire.

The fire itself may induce forces in a structure, and these must also be included in the design. These are most likely as a result of restraint from the surrounding structure preventing

thermal expansion, or from a flexural member becoming a tensile member after large deformations have occurred. Such loads are most likely to occur in steel structures because steel members tend to heat and deform more rapidly than other materials. Restraining forces are often significant in concrete structures, whereas fire-induced forces are less important in timber structures.

5.3.2.2 Load Ratio

Under normal day-to-day conditions, all buildings have an extremely low probability of failure. The 'load ratio', r_{load} , is the ratio of the expected loads on the structure during a fire to the loads that would cause collapse at normal temperatures, given by:

$$r_{load} = U_{fire}^* / R_{cold} \quad (5.11)$$

Most buildings have a load ratio of 0.5 or less, at most times, so that the strength of any member could drop by half or more before collapse would be expected. The load ratio is far less than 0.5 for buildings or parts of buildings designed to resist extreme events such as rare snowstorms, hurricanes or earthquakes. The lower the load ratio, the greater the fire resistance, because of the large loss in load-carrying capacity which can occur before failure would occur in a fire. This is a most important concept for structural fire design.

5.3.2.3 Working Stress Design

Most modern loading codes, which specify load combinations for fire design, are in limit states (LRF) format with loads similar to those described above. Loading codes which are in working stress format do not usually include load combinations for fire design, so designers have to use the normal temperature design load combination of $L_w = G + Q$ for fire design, which is very conservative because it does not recognize the likely reduction of loads at the time of an unexpected fire.

5.3.3 Structural Analysis for Fire Design

Structural analysis for fire design is essentially the same process as structural analysis for normal temperature design, but it is complicated by the effects of elevated temperatures on the internal forces and the properties of materials.

For many simple structural elements exposed to fire, load carrying capacity can be calculated with simple hand calculation methods, using the same techniques as for cold conditions. Examples for steel, concrete and timber structures are given in later chapters. The major changes from cold conditions are the use of lower fire limit state loads and temperature-reduced material properties. For some materials such as wood, an alternative approach is to use reduced section properties with no change in the material properties.

Hand calculations are most appropriate for single elements with simple supports, especially where internal temperatures are uniform or where the temperature of one part of the member is critical. Structural analysis must consider the possibility of instability failures as well as

strength failures. Many tools are available for calculating the structural fire performance of load-bearing construction, ranging from hand calculations and design charts to a variety of computer programs discussed in Chapter 11.

5.4 Material Properties in Fire

Material properties at normal temperatures have been briefly described with reference to Figure 5.2. The strength and modulus of elasticity of all materials change with elevated temperature. Methods of deriving material properties at elevated temperature are discussed below. Details for specific materials are given in following chapters.

5.4.1 Testing Regimes

When structural elements are exposed to fire, they experience temperature gradients and stress gradients, both of which vary with time. Mechanical properties of materials for fire design purposes must be determined and published in a way that is consistent with the anticipated fire exposure.

Constant temperature tests of materials can be carried out in four possible regimes:

1. The most common test procedure to determine stress–strain relationships is to measure the load and calculate the stress while using a testing machine to impose a constant rate of increase of strain (by controlling the rate of travel of the machine’s loading head).
2. A similar regime is to control the rate of increase of load (or stress) and measure the deformation (hence the strain).
3. A creep test is one in which the load is kept constant and the deformations over time are measured.
4. A relaxation test is one in which a constant initial deformation is imposed and the reduction in load over time is measured.

When the effects of changing temperatures are added, there are two more possible testing regimes:

5. In a transient creep test, the specimen is subjected to an initial load, then the temperature is increased at a constant rate while the load is maintained at a constant level and deformations are measured, or
6. The applied load is varied throughout the test in order to maintain a constant level of strain as the temperature is increased at a constant rate.

These six regimes are illustrated in Figure 5.5 derived from Anderberg (1988) and Schneider (1988). The most common of these are regimes 1 and 5. The results of tests in regime 1 depend on the rate of loading, because of the influence of creep. The results of tests in regime 5 depend on the rate of temperature increase. All these regimes present some difficulties because the effect of creep influences all of the test results, and a difficulty with transient tests on large specimens is that the rate of temperature increase may not be uniform over the cross section. Figure 5.5 does not consider the effect of changing moisture content which can be another important variable, especially for timber structures, making testing for material properties even more difficult.

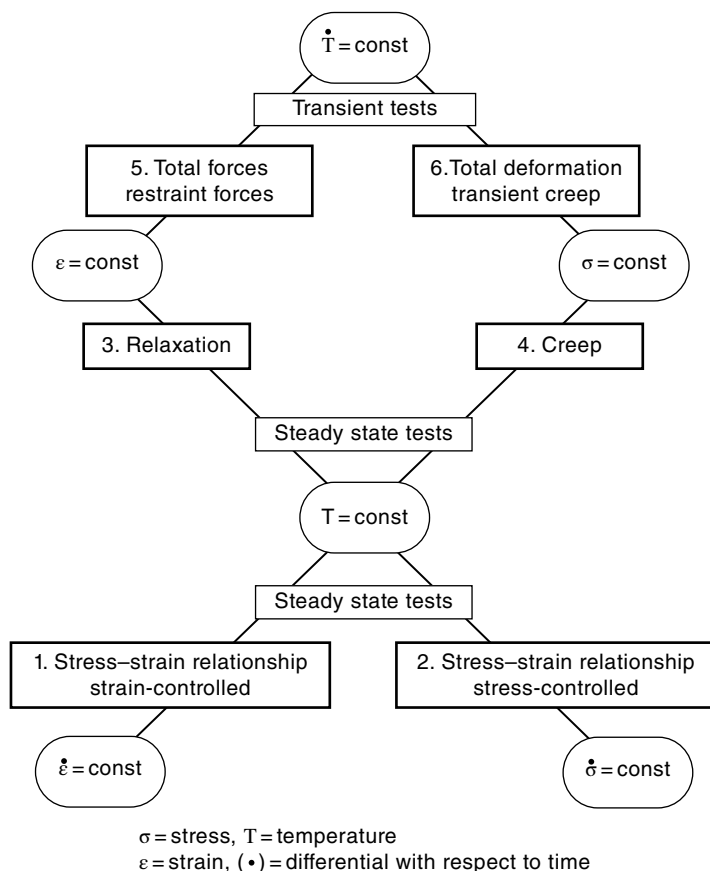


Figure 5.5 Testing regimes for determining mechanical properties of materials at elevated temperatures. Reproduced from Anderberg (1988) by permission of Elsevier Science

For most materials, stress–strain relationships at elevated temperatures can be obtained directly from steady-state tests at certain elevated temperatures (regime 1), or they can be derived from the results of transient tests. Anderberg (1988) compares stress–strain relationships obtained in both ways and points out that there are differences due to the effect of creep. For most materials, yield strength and modulus of elasticity both decrease with increasing temperature.

5.4.2 Components of Strain

Analysis of a structure exposed to fire requires consideration of the deformation of the structural under the fire limit state loads. The deformation of materials at elevated temperature is usually described by assuming that the change in strain $\Delta\epsilon$ consists of four components:

$$\Delta\epsilon = \epsilon - \epsilon_i = \epsilon_{\sigma}(T) + \epsilon_{th}(T) + \epsilon_{cr}(\sigma, T, t) + \epsilon_{tr}(\sigma, T) \tag{5.12}$$

where ε is the total strain at time t , ε_i is the initial strain at time $t=0$, $\varepsilon_\sigma(\sigma, T)$ is the mechanical, or stress-related strain, being a function of both the applied stress σ and the temperature T , $\varepsilon_{th}(T)$ is the thermal strain being a function only of temperature T , $\varepsilon_{cr}(\sigma, T, t)$ is the creep strain, being additionally a function of time t , and $\varepsilon_{tr}(\sigma, T)$ is the transient strain which only applies to concrete.

5.4.2.1 Stress-related Strain

The stress-related strain (or mechanical strain) refers to the strain which results in stresses in the structural members. These stresses are based on the stress–strain relationships shown in Figure 5.2, used for the structural design of all materials. For fire design of individual structural members such as simply supported beams which are free to expand on heating, the stress-related strain is the only component of strain that needs to be considered. If the reduction of strength with temperature is known, member strength can easily be calculated at elevated temperatures using simple formulae such as those given in this chapter.

The stress-related strains in fire-exposed structures may be well above yield levels, resulting in extensive plastification, especially in steel buildings with redundancy or restraint to thermal expansion. Computer modelling of fire-exposed structures requires knowledge of stress–strain relationships not only in loading, but also in unloading, as members deform and as structural members heat up and cool down in real fires (Franssen, 1990, El-Rimawi *et al.*, 1996).

5.4.2.2 Thermal Strain

Thermal strain is the well known thermal expansion that occurs when most materials are heated, with expansion being related to the increase in temperature. Thermal strain is not usually important for fire design of simply supported members, but must be considered for frames and complex structural systems, especially where members are restrained by other parts of the structure and the thermal strains can induce large internal forces.

5.4.2.3 Creep Strain

Creep is the term which describes long term deformation of materials under constant load. Under most conditions, creep is only a problem for members with very high permanent loads. If the load is removed there will be slow recovery of some of the creep deformations, as shown in Figure 5.6(a). Creep becomes more important at elevated temperatures because creep can accelerate as load capacity reduces, leading to secondary and tertiary creep as shown in Figure 5.6(b). ‘Relaxation’ is the complementary term which describes the reduction of stress in materials subjected to constant deformation over a long period of time.

Creep is relatively insignificant in structural steel at normal temperatures. However, it becomes very significant at temperatures over 400 or 500 °C and is highly dependent on stress level. At higher temperatures the creep deformations in steel can accelerate rapidly, leading to plastic behaviour and ‘runaway’ failure. Creep in wood is complicated by changes in moisture content such that creep deformations tend to be larger in environments where the moisture content of the wood fluctuates over time, hence creep can become a major concern in fire-exposed wood which is at temperatures around 100 °C.

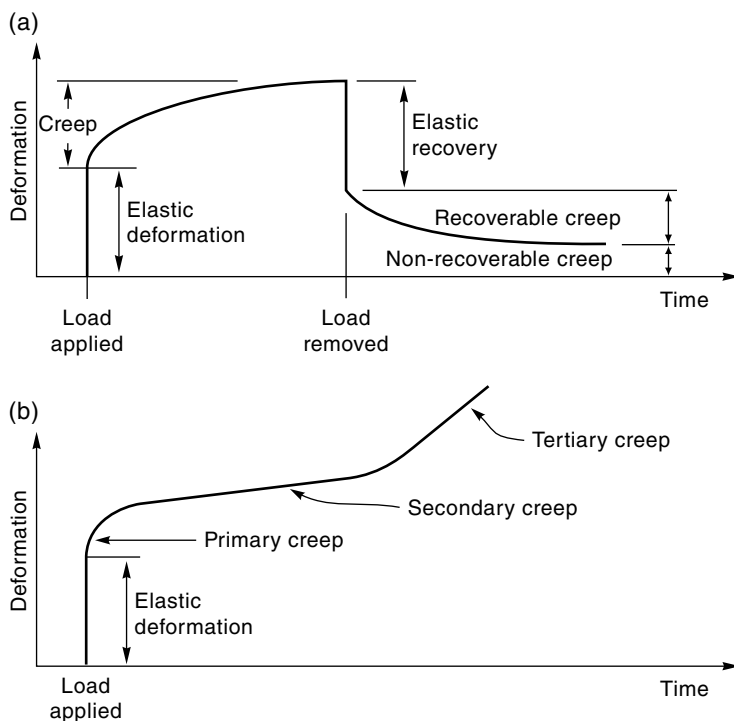


Figure 5.6 Creep in structural materials: (a) creep under normal conditions; (b) creep at elevated temperatures

Creep strain is not usually included explicitly in fire engineering calculations because of the added complexity and the lack of sufficient input data. This applies to both hand and computer methods. Any structural analysis computer program for elevated temperature is already very complex without have to explicitly include the effects of time-dependent behaviour. The effects of creep are usually allowed for implicitly by using stress–strain relationships which include an allowance for the amount of creep that might usually be expected in a fire-exposed member.

5.4.2.4 Transient Strain

Transient strain is caused by expansion of cement paste when it is heated for the first time under load. Transient strain is often included in analytical models for predicting the behaviour of reinforced concrete structures exposed to fire. See Chapter 7.

5.4.2.5 Effect of Strain Components

Equation 5.11 can be simplified, ignoring the last two terms to give

$$\epsilon_{total} = \epsilon_{\sigma} + \epsilon_{th} \tag{5.13}$$

where ε_σ is the stress-related strain and ε_{th} is the thermal strain resulting from thermal expansion. This is a key relationship for understanding the structural behaviour of fire-exposed structures, because structural engineers are interested in stresses and deformations in structures. The deformations in the structure depend on the total strain ε_{total} and the stresses in the structure depend on the stress-related strain ε_σ .

Rotter *et al.* (1999) explain this further by considering two contrasting types of structure. For a lightly loaded structure in which there is no resistance to thermal expansion, the total strain is dominated by the thermal strain and the mechanical strain is very low, and hence most deformations (bowing or elongation) result from the thermal strain which is only a function of temperature. In a very different type of structure where there is severe restraint to thermal expansion, there can be no elongation, so $\varepsilon_{total}=0$, hence the thermal and mechanical strains are approximately equal and opposite. Both may be very large, resulting in high levels of plastification and high stresses (with much yielding) because of the high mechanical strains.

These aspects of structural behaviour under fire conditions would not be intuitively expected by most structural engineers. The design of simple members exposed to fire is not difficult, as described in this book, but highly redundant structures must be analysed with sophisticated computer programs in order to quantify these effects.

5.5 Design of Individual Members Exposed to Fire

This section outlines the principles of structural design for individual members exposed to fire conditions. This is the ‘simplified’ design method as described in the Eurocodes. The following sections describe the different approach needed for members which form part of larger structural assemblies.

5.5.1 Tension Members

To continue the example of a simple tension member, the design process for fire is essentially the same as for normal temperature conditions. In the event of a fire, the factored axial force will reduce to N_{fire}^* (N) and the strength will reduce due to elevated temperatures or reduction of the cross section. To prevent failure, the expected loads must be compared with the expected strength N_f (N) at the time of the fire. The strength reduction factor Φ is taken as 1.0 for fire design, so that the design equation becomes:

$$N_{fire}^* \leq N_f \quad (5.14)$$

where $N_f = f_{t,f} A_{fi}$

and A_{fi} is the area of the cross section (possibly reduced by fire exposure) (mm²) and $f_{t,f}$ is the characteristic tensile strength of the material at elevated temperature (MPa).

5.5.2 Compression Members

Design for compression follows similar principles, except that the factored axial force N_{fire}^* is now compressive. The design equation is the same as for tension:

$$N_{fire}^* \leq N_f$$

Calculation of N_f requires understanding of the basic behaviour of compression members. A ‘short column’ will fail when the applied stress reaches the crushing strength of the column material. A ‘long column’ is a compression member whose load capacity is limited by lateral buckling, leading to an instability failure at an average stress less than the crushing strength of the material. Figure 5.7(a) shows the relationship between axial load capacity and length for a pin ended long column where the crushing strength N_c (N) of a short column is:

$$N_c = f_c A \quad (5.15)$$

where f_c is the crushing strength of the material (MPa) and A is the cross-sectional area of the column (mm²).

The theoretical axial load capacity of a perfectly straight long column is known as the critical buckling strength N_{crit} (N) given by the Euler buckling formula:

$$N_{crit} = \frac{\pi^2 EI}{L^2} \quad \text{or} \quad N_{crit} = \frac{\pi^2 EA}{(L/r)^2} \quad (5.16)$$

where E is the modulus of elasticity (MPa), A is the cross-sectional area of the column (mm²), I is the moment of inertia of the cross section in the direction of buckling (mm⁴), L is the length of the column (mm), r is the radius of gyration of the cross section $r = \sqrt{I/A}$ (mm) and L/r is the slenderness ratio.

The dashed line in Figure 5.7(a) shows the behaviour of real columns, as obtained from testing, with a gradual transition from short to long column behaviour. The deviation from the theoretical curve, which is allowed for in design codes, results from initial out-of-straightness, residual stresses and other factors. Column design can consider crushing and buckling behaviour separately, but most codes provide a ‘buckling factor’ which reduces the crushing strength to allow for the possible effects of buckling. The buckling factor is usually a function of the slenderness ratio (L/r), with a value of 1.0 for low slenderness, decreasing as the slenderness increases. A buckled column, under fire exposure, is shown in Figure 5.7(b).

When compression members are exposed to fire, strength decreases because of reductions in the crushing strength and the modulus of elasticity. For some materials such as timber, the cross section is reduced by charring, leading to smaller section properties and an increase in the slenderness ratio. Design of columns for fire is covered in the following chapters.

5.5.3 Beams

5.5.3.1 Flexural Design

The process shown above for tensile members can be applied to bending members. This section refers only to simply supported beams. Beams with continuous supports, axial restraint, or larger frames are described in a later section.

Figure 5.8 shows loads and bending moments for a simply supported roof beam designed to support both dead load and snow load. Note that in this book, bending moment diagrams are plotted on the tension side of flexural members, following the European convention which is opposite to that used in North America. A positive bending moment is one which causes

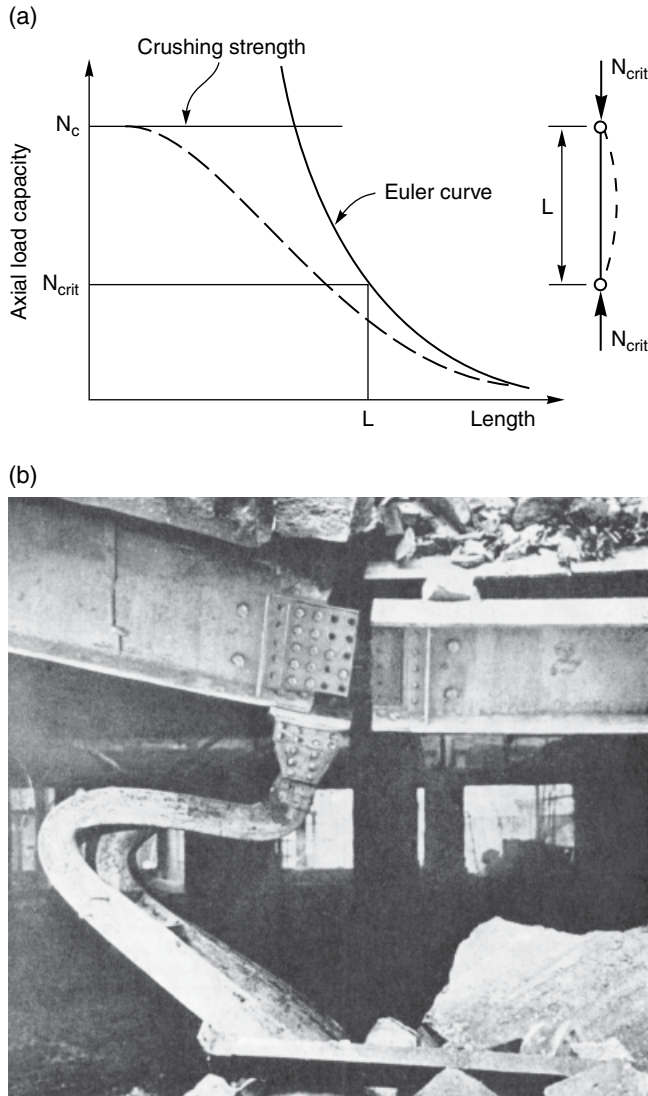


Figure 5.7 Column buckling. (a) Effect of member length on compressive load capacity. (b) Steel column which has buckled during fire exposure. Reproduced from HMSO (1961) by permission of Her Majesty's Stationery Office

tension on the underside of the beam (a 'sagging' moment). A negative bending moment is one which causes tension on the top of the beam (a 'hogging' moment).

Under factored design loads of self-weight and snow load, the bending moment diagram is shown by the solid curve, where the mid-span bending moment M_{cold}^* (kNm) is given by:

$$M_{cold}^* = w_c L^2 / 8 \quad (5.17)$$

where w_c is the uniformly distributed factored load (kN/m) and L is the span (m).

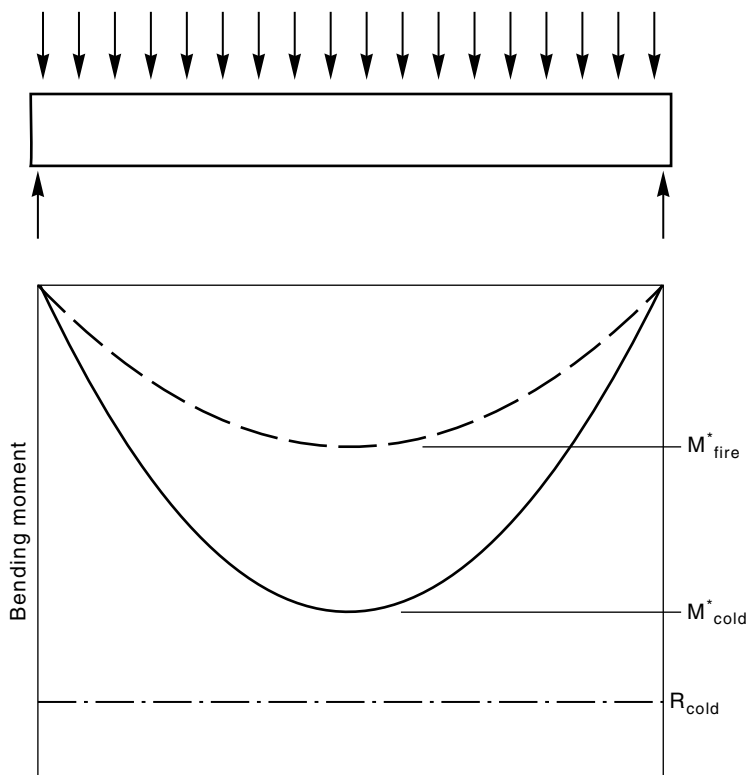


Figure 5.8 Bending moment diagrams for a simply supported beam

Under normal temperature conditions a member size must be selected with a sufficiently large section modulus Z to satisfy the design equation:

$$M_{cold}^* \leq M_n \tag{5.18}$$

where

$$M_n = \Phi f_b Z$$

and Φ is the strength reduction factor, f_b is the characteristic flexural strength at normal temperatures and Z is the section modulus of the cross section.

For materials such as wood, where design is based on elastic behaviour, Z is the elastic section modulus. For rectangular sections $Z = bd^2/6$. For ductile materials like steel, the plastic section modulus S may be used instead of Z , giving slightly higher design strengths. (Note that the symbols Z and S are used with reversed meanings in some countries.)

The resulting short term flexural capacity under cold conditions is $R_{cold} = f_b Z$, shown by the lower straight line in Figure 5.8. R_{cold} is greater than M_{cold}^* because of the following factors in the design process:

1. The strength reduction factor Φ is always less than 1.0 in normal temperature conditions.
2. The size of the selected member may be larger than exactly needed (because of steps in available sizes or because the size was chosen to control deflections, or for architectural reasons).

3. For some materials such as timber, the strength depends on the duration of the load, so there will be a difference between the short term capacity and long term load demand.

If a fire occurs when there is no snow on the roof, the bending moment at mid-span will be less, as shown by the dotted curve. The mid-span bending moment M_{fire}^* (kNm) is given by:

$$M_{fire}^* = w_f L^2 / 8 \quad (5.19)$$

where w_f is the uniformly distributed factored load for fire conditions (kN/m).

It can be seen that for failure to occur as a result of the fire, the flexural capacity would have to drop from R_{cold} to M_{fire}^* . In this case the design equation becomes:

$$M_{fire}^* \leq M_f \quad (5.20)$$

where $M_f = f_{b,f} Z_f$

and $f_{b,f}$ is the characteristic flexural strength of the material at elevated temperature and Z_f is the appropriate section modulus of the cross section (possibly reduced by fire exposure).

The ratio M_{fire}^* / R_{cold} is the 'load ratio'. This example demonstrates the important principle that if the load ratio is low, the necessary drop in strength for failure to occur is large, hence the greater the fire resistance.

5.5.3.2 Lateral Buckling of Beams

The above equations for bending assume that the beam will fail by flexural yielding. Slender beams with no lateral restraint may fail by lateral torsional buckling at a load less than the flexural load capacity. This can only happen if the compression edge of the beam is free to buckle sideways. Lateral buckling is more of a problem for slender beams of materials like steel than for compact materials like concrete. At normal temperatures the critical buckling load can be calculated by using formulae from structural design codes. Chapter 6 gives guidance for checking lateral buckling of steel beams under fire exposure.

Any members providing lateral bracing to beams or columns must have at least the same fire resistance as the main members. This can be difficult to calculate if the bracing members are not actually load bearing, but they only provide bracing. A common rule-of-thumb is that bracing members should be designed to resist 2½% of the axial force in the braced member, in addition to any applied loads and self-weight. This can also be used in fire design. The hierarchy of lateral support must be followed through carefully. For example, main roof beams may rely on secondary beams for lateral stability, the secondary beams may rely on purlins and the purlins may rely on the roofing material. If the main beams are to resist a design fire, then all of the related materials must remain in place for the duration of the fire exposure.

5.5.3.3 Shear Design

Design for shear can be handled in the same way if sufficient information is available on the shear resistance of materials and members at elevated temperatures.

5.6 Design of Structural Assemblies Exposed to Fire

All the discussion above has referred to individual members. This section describes how the structural behaviour of a member exposed to fire can be enhanced by consideration of the whole structural assembly.

5.6.1 Frames

The behaviour of moment resisting frames is more complex than the behaviour of individual members, because of continuity and axial restraint, and because fire-induced elongations and rotations affect other areas of the building which are not subjected to heating. For example, Figure 5.9 shows calculated deformations resulting from a fire in one bay of a multi-storey building. In general, the continuity of moment-resisting connections enhances fire resistance of members in frames, so that design of individual members using the methods described above is conservative. Special purpose computer programs should be used when assessing the expected fire performance of large or special structures including multi-bay frames. Design of unbraced frames is more difficult than braced frames because lateral deformations and the resulting $P-\Delta$ (P -Delta) effects must also be considered.

5.6.2 Redundancy

Many structures have very little structural redundancy, so that failure of a single element can cause failure of the whole structure. On the other hand, redundant structures have the capacity for considerable load sharing, so that when one element fails its load can be redistributed to other stiffer and stronger elements. This process is conceptually similar to moment redistribution. Many structures have many alternative load paths for load sharing between frames or trusses. In such structures a localized fire may cause local structural failure of one or more individual elements without resulting in collapse of the whole building.

The effects of redundancy are also related to the load ratio, because if the total loads on a structure at the time of a fire are much less than the full design loads, then fewer structural

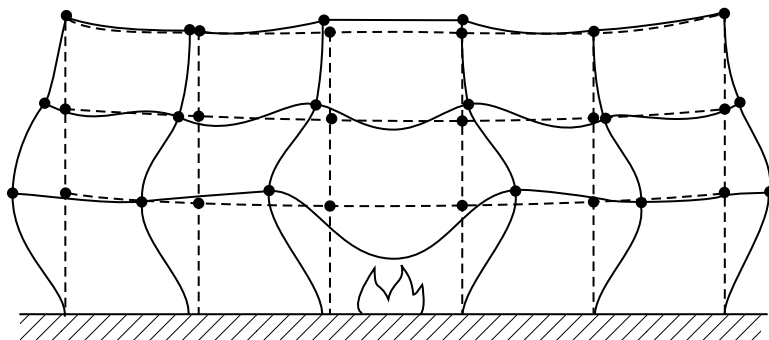


Figure 5.9 Frame deformations in the lower floors of a multi-storey frame resulting from a fire on the ground floor. Reproduced from Bresler and Iding (1982) by permission of Wiss, Janney Elstner Associates, Emeryville, California, USA

members may be necessary to support the structure, provided that there are sufficient load paths for the applied loads to get to the undamaged members. Redundancy is most often quoted as a benefit of steel construction, but it can apply to buildings of all materials, especially if the materials are ductile and there are a number of alternative load paths.

If a fire-exposed structure is very redundant with many alternative load paths, as in a modern multi-storey steel-framed building, Rotter *et al.* (1999) have shown how large deformations can develop without any significant loss in load-carrying capacity, provided that the structure has sufficient ductility to accommodate the large deflections. In such buildings, failure must not be defined as loss of load capacity of any single member because loads can be carried by other members.

5.6.3 *Disproportionate Collapse*

Disproportionate collapse is conceptually opposite to redundancy. Whereas a redundant structure can suffer the failure of some parts without structural collapse, disproportionate collapse refers to a situation where failure of one element causes a major collapse, with a magnitude disproportionate to the initial event. This is a major concern in the UK largely as a result of the Ronan Point disaster in 1968 (Figure 5.10) where an explosion in one room of a multi-storey building caused a whole section of the building to collapse with considerable loss of life (HMSO, 1968). Design against disproportionate collapse requires the provision of some structural toughness with redundant load paths.

Disproportionate collapse can also occur if elements providing lateral restraint to main beams or columns are destroyed in a fire, allowing subsequent collapse of the main member. As an example, Comeau (1999) describes the collapse of a timber truss roof during a fire, resulting in the deaths of three firefighters. In this case the collapse was not a result of fire damage, but was caused when the firefighters cut a hole in the roof which removed the lateral restraint to the compression chord of the main roof trusses, causing collapse by buckling. For this reason, members providing lateral restraint to fire rated members must also have appropriate fire resistance.

5.6.4 *Continuity*

5.6.4.1 **Continuous Beams**

Flexural continuity can improve the fire resistance of a bending member. A member with flexural continuity is a statically indeterminate member which would need to fail at more than one cross section to lose its load-carrying capability. A simply supported beam has no continuity, so failure at mid-span will cause collapse. Beams which are continuous over several supports or built into rigid frames have continuity which is beneficial in fire design, because collapse does not occur when the ultimate strength is reached at only one cross section.

In fire-exposed structures, the benefits of continuity allow load to be resisted in alternative ways through moment redistribution as heat-affected areas lose strength. The benefits are greatest in ductile concrete or steel members which can undergo large rotations at 'plastic hinges'. Additional benefits can occur in materials like reinforced concrete or composite structures where the flexural strength may be different in positive and negative bending.



Figure 5.10 Multi-storey apartment building after a gas explosion caused disproportionate collapse to upper floors. Reproduced from HMSO (1968) by permission of Building Research Establishment, UK

A plastic hinge is a segment of a beam where large rotations occur with no significant increase in bending moment. Figure 5.11 shows the moment–curvature relationship for a beam of a ductile material like steel, for which the stress–strain relationship is shown in Figure 5.2. At low levels of bending moment there is a linear relationship between moment and curvature, with the slope of the line given by the product EI . The elastic curvature k of a beam is given by:

$$k = M/EI \quad (5.21)$$

where M is the bending moment, E is the modulus of elasticity and I is the moment of inertia (second moment of area) of the cross section.

The relationship becomes non-linear after yielding begins to occur in the cross section at a bending moment M_y . The maximum bending moment which can be resisted by the cross section is the plastic moment M_p .

To assess the possible benefits of moment redistribution, the collapse mechanism causing failure must be considered. Figure 5.12 shows three different support conditions for a beam

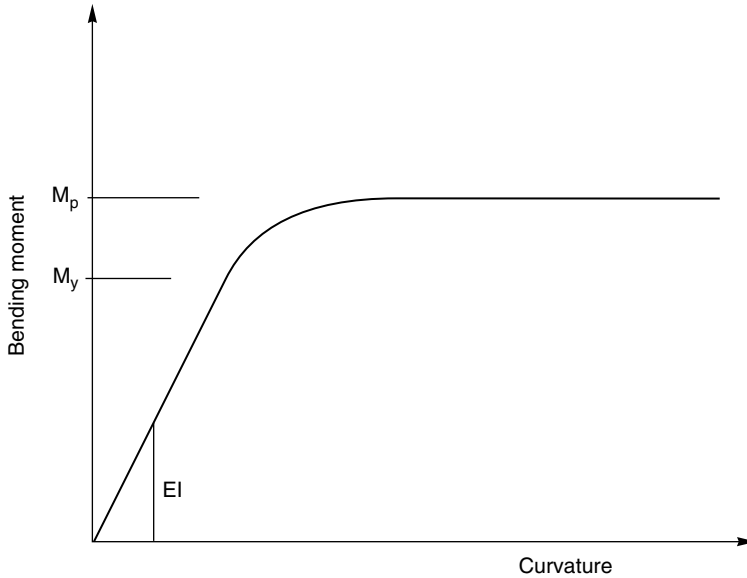


Figure 5.11 Moment–curvature relationship for a beam of ductile material

with a span L and uniformly distributed load w . The three support conditions are simply supported, continuous with built-in supports at both ends, and continuous at one end representing the end span of a continuous beam or a two-span beam. The bending moment diagrams and elastic deflected shapes for these and other combinations of load and support conditions can be obtained from structural engineering textbooks, or from structural analysis computer programs.

Figure 5.12 shows the elastic bending moment diagram and deflected shape for each of the three conditions under service loads. Figure 5.12 also shows the mechanisms that would occur if the loads were to increase towards the failure loads (or if the strength decreases due to fire exposure). Note that the deflections are sketched with similar magnitudes for the elastic deflection and the failure mechanism, although the actual deflections at failure will be much greater than the elastic deflections.

Observation of the failure mechanism in Figure 5.12(a) shows that the simply supported beam will fail when its strength is exceeded at mid-span and a plastic hinge occurs at that point. There is no benefit from flexural continuity for a simply supported beam.

In Figure 5.12(b) it can be seen that the continuous beam will not reach its maximum load capacity until plastic hinges form at three points. If the flexural capacity is the same along the full length of the beam, and the same in both positive and negative directions, the final bending moment at all three plastic hinges will be identical, and the bending moment diagram at failure will be different from the elastic bending moment diagram. This shift in the bending moments is known as ‘moment redistribution’.

The end span beam in Figure 5.12(c) is an intermediate case between the simply supported and continuous beams, requiring two hinges to cause a failure mechanism. Consider the behaviour as the load increases steadily from the elastic condition to the plastic condition.

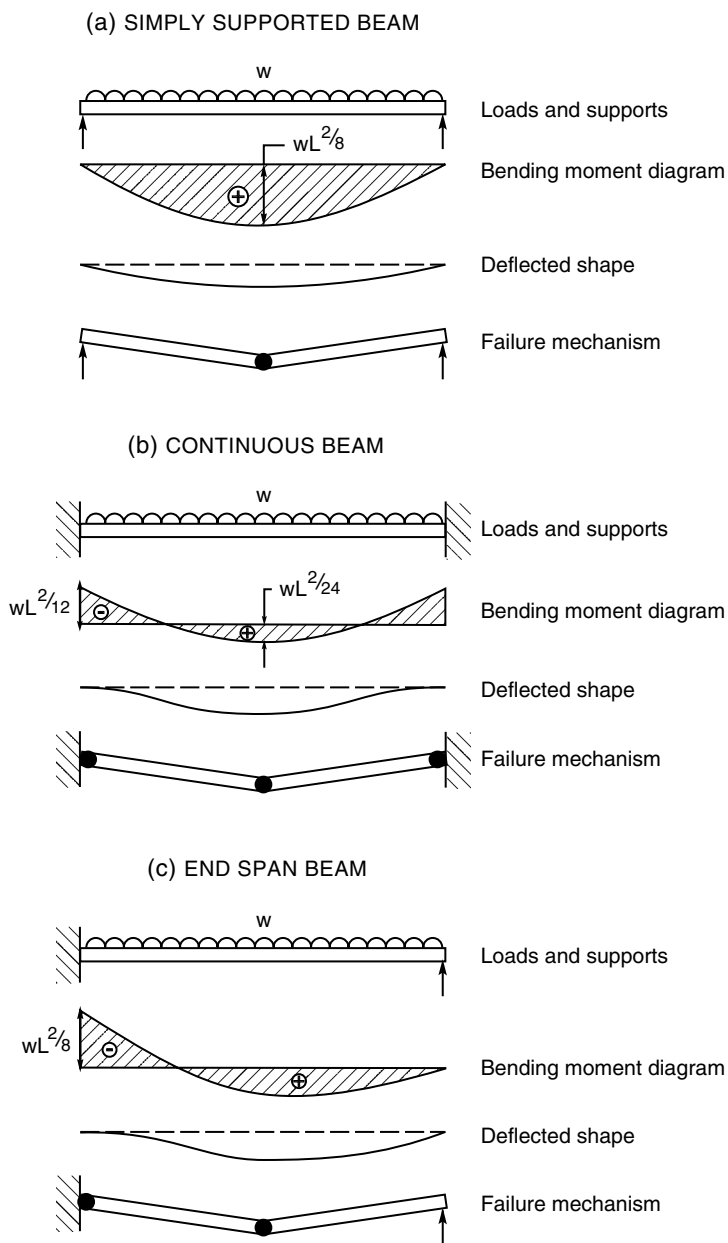


Figure 5.12 Behaviour of simply supported and continuous beams

Because the initial negative bending moment at the support is greater than the positive bending moment near mid-span, the plastic moment M_p will occur first at the support, then the bending moment near mid-span will increase as the load increases, accompanied by plastic rotation in the plastic hinge at the support. Eventually the plastic moment will be reached near mid-span

causing the failure mechanism shown. The final shape of the bending moment diagram will again have changed due to moment redistribution.

5.6.4.2 Moment Redistribution

Moment redistribution is discussed in more detail with reference to Figures 5.12 and 5.13 which show one span of a beam which is continuous over several supports. First consider Figure 5.13 which is the same situation as shown in Figure 5.12(b). Under cold conditions with full factored dead and live loads, the elastic bending moment diagram for a continuous beam is the solid line marked M_{cold}^* . This curve has exactly the same shape as the solid curve in Figure 5.8, but the continuity causes it to be re-positioned such that the end moment is double the mid-span moment. Any introductory book on structural mechanics will give the derivation of this elastic bending moment diagram.

With the reduced loads expected in fire conditions, the bending moments reduce to those shown by the curve M_{fire}^* . If this beam has a symmetrical cross section, such as a steel I-beam, the positive and negative flexural capacities at normal temperatures are equal, and the capacities are shown by the horizontal lines marked R_{cold} with a larger safety margin against failure in positive bending (mid-span) than in negative bending (at the supports). As the flexural capacity drops from R_{cold} under fire exposure, a plastic hinge will occur first at the support when the flexural capacity reaches M_{fire}^* . As the flexural capacity drops even further due to elevated temperatures, plastic rotation will occur at the support and the mid-span bending moment will increase due to moment redistribution. Failure will occur when a plastic hinge

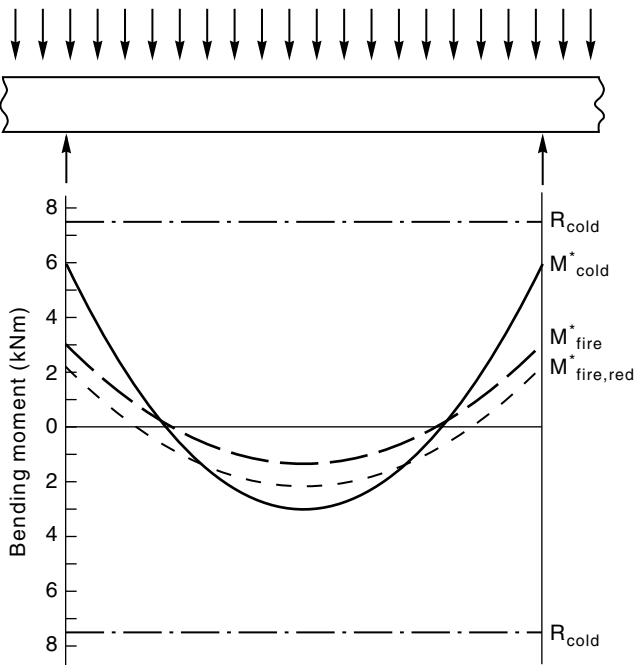


Figure 5.13 Moment redistribution to equal positive and negative moments

occurs at mid-span, and the bending moments are as shown by $M_{fire,red}^*$ with equal positive and negative moments, both equal to the plastic moment capacity M_p .

This situation will change if the beam has different flexural capacities in positive and negative bending, more common in reinforced concrete structures, or where the fire causes non-uniform heating in the cross section. In Figure 5.14 the solid line M_{cold}^* and the dotted line M_{fire}^* are exactly the same as in Figure 5.13. The lines marked R_{cold} have been shown with different values in positive and negative bending, assuming that this is a reinforced concrete beam where the number of reinforcing bars has been selected to match the M_{cold}^* bending moment diagram. If the fire exposure causes the positive flexural capacity of the beam to drop to zero at mid-span, the beam will not fail provided that the negative flexural capacity R_{cold}^- does not drop below the value of $M_{fire,red}^*$ at the supports. The beam now carries its entire load by cantilever action from the supports. The bending moment diagram $M_{fire,red}^*$ is the same as the diagram M_{fire}^* except that it has been lifted as moment redistribution has occurred. The value of $M_{fire,red}^*$ at the supports is now equal to the mid-span simply supported value of M_{fire}^* from Figure 5.8. A serious consequence of moment redistribution in reinforced concrete is the need to re-evaluate the locations where reinforcing bars are terminated within the span of the beam. Numerical values are put on these moment redistributions in the worked examples at the end of this chapter.

Redistribution of bending moments can give a significant advantage in fire design of continuous beams, in all materials. For a reinforced concrete beam, the final shape of the redistributed bending moment diagram depends on the relative amount of positive and negative reinforcing provided, and the expected influence of the fire on the flexural strength for both positive and negative bending moments. Depending on the strength of the beam when plastic

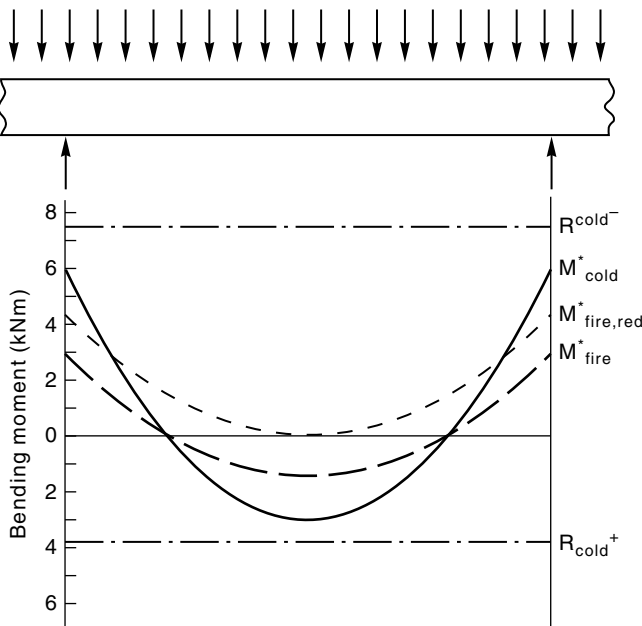


Figure 5.14 Moment redistribution to unequal positive and negative moments

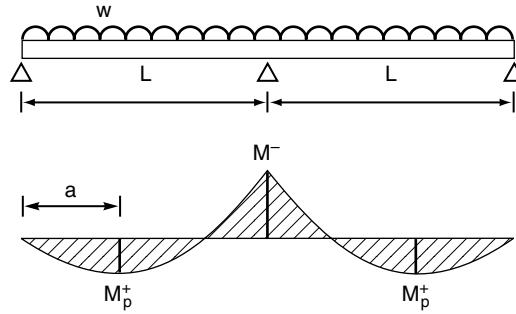


Figure 5.15 Bending moment diagram for a two-span continuous beam

hinges develop at its ends or in the centre the bending moment diagram M_{fire}^* may move up or down to any statically admissible position as the plastic hinges occur. This can be assessed visually with sketched bending moment diagrams, or it can be calculated.

It is useful to know the shape of the bending moment diagram for a propped cantilever or the end bay of a multi-span beam, such as shown in Figure 5.15. If the positive plastic moment capacity is known, the negative moment M^- (kNm) at the support is given by:

$$M^- = wL^2/2 - wL^2 \sqrt{2M_p^+/wL^2} \quad (5.22)$$

where w is the uniformly distributed load on the beam (kN/m), L is the span of the beam (m) and M_p^+ is the positive plastic moment capacity (kNm).

The distance a (m) of the maximum positive moment from the pinned support is given by:

$$a = \sqrt{2M_p^+/L} \quad (5.23)$$

Derivation of these equations can be found in structural mechanics textbooks.

5.6.5 Plastic Design

Some methods of calculating the benefits of moment redistribution in statically indeterminate beams have been described above. An alternative approach which is more versatile is to use plastic theory and the simple equations of 'virtual work'.

Figure 5.16 shows a fixed end beam of span L with a uniformly distributed load w in the undeformed state, and after large plastic deformations. In the plastic deformed state, the beam can be considered to be two rigid bars each with a rotation θ , which produce a mid-span deflection of $\delta = \theta L/2$. The virtual work equation is based on the principle that the external work done by vertical movement of the applied load is equal to the internal work done by plastic rotation at all the plastic hinges. In this case the total load on the beam is wL and the average vertical displacement is $\delta/2$. The two plastic hinges at the supports have a rotation θ with plastic moment M_p^- and the central plastic hinge has a rotation 2θ with plastic moment M_p^+ . The virtual work equation now gives:

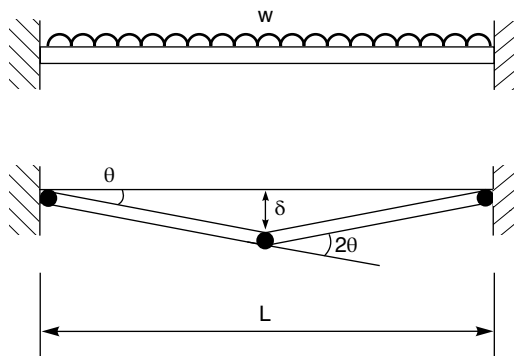


Figure 5.16 Plastic deformation of a fixed end beam

$$\begin{aligned} \text{external work} &= \text{internal work} \\ wL\delta/2 &= 2M_p^-\theta + 2\theta M_p^+ \end{aligned} \tag{5.24}$$

Substituting $\delta = \theta L/2$ gives:

$$wL^2/8 = M_p^- + M_p^+ \tag{5.25}$$

If the positive and negative plastic moments are equal, $M_p = M_p^- = M_p^+ = wL^2/16$. If they are different, either one can be determined if the other is known.

This approach can be used for any system of continuous beams, for any ductile material. If the plastic failure mechanism is not known exactly, several alternative mechanisms can be tried, and the one giving the least amount of internal work will be the correct answer. Calculus can be used to determine the exact solution if necessary, but it is usually sufficiently accurate to assume that all the positive plastic hinges are at mid-span, making the solution very easy. An exception is the end span of a continuous beam or propped cantilever where the positive plastic hinge may be nearer the pinned support [as shown in Figure 5.12(c)] in which case Equation 5.22 and Equation 5.23 can be used.

As an example of a more difficult structure, Figure 5.17 shows a beam with several different spans and supports. Two separate plastic mechanisms should be considered, as shown. This approach can be used for a wide variety of problems.

5.6.6 Axial Restraint

Another significant influence on fire performance of some structures is axial restraint, which refers to the effect of those axial forces which occur when a heated member is restrained from thermal expansion by a more rigid surrounding structure. Axial restraint is particularly important for reinforced or prestressed concrete slabs or beams, and for composite concrete-steel deck slabs, where the axial restraint force can partly or completely compensate for the loss in strength of steel reinforcing at elevated temperatures. The effects of axial restraint can be particularly beneficial when a fire occupies only part of a floor of a building, leaving a considerable area of surrounding structure at normal temperatures, able to resist the restraint forces.

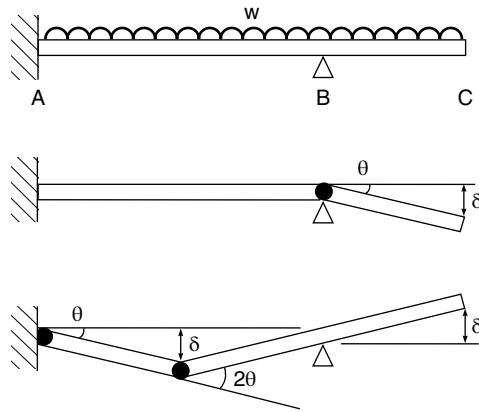


Figure 5.17 Plastic failure mechanisms for an indeterminate beam

Axial restraint can be of significant benefit in concrete and steel structures, but not in timber structures because wood has low thermal conductivity, and a low coefficient of thermal expansion. Note that flexural continuity is also sometimes called ‘restraint’, but the effects of these two phenomena are quite different, as explained previously, so the two should not be confused.

Some types of construction have two listed fire resistance ratings, one for ‘restrained’ conditions and another for ‘unrestrained’ conditions. The difference in behaviour is most easily described with an example, as given below, considering first the heated structural member then the surrounding structure.

5.6.6.1 Effect of Restraint on Heated Members

Figure 5.18 shows a simply supported concrete beam, located between rigid supports which permit rotation but no elongation at the ends. As the bottom of the beam heats up, it tries to expand, but is unable to do so because of the rigid supports. An axial thrust T develops in the beam, contributing to its strength. The thrust may be thought of as external prestressing. Figure 5.18 shows a situation where the elevated temperature moment capacity M_f^* can drop to less than the applied moment M_{fire}^* without collapse because the flexural resistance is enhanced by the moment Te , where e is the eccentricity between the line of action of the thermal thrust and the centroid of the compression block near the top of the beam. The total flexural resistance $R_{fire} = M_f + Te$ is then greater than the applied moment M_{fire}^* . The Te line is curved as shown because of the deflection of the beam.

In some situations, where the surrounding structure has sufficient stiffness, the moment capacity M_f at elevated temperature can drop to zero without failure, with all of the moment being resisted by the Te couple. This explains the large difference between the listed ‘restrained’ and ‘unrestrained’ ratings for some assemblies which have been tested under both conditions (e.g. UL, 2012).

Figure 5.19 shows a free body diagram of a reinforced concrete beam subjected to a compressive axial restraint force T . The compression stress block must now develop a force C equal to the sum of the axial restraint force T plus the tensile force in the reinforcing T_y .

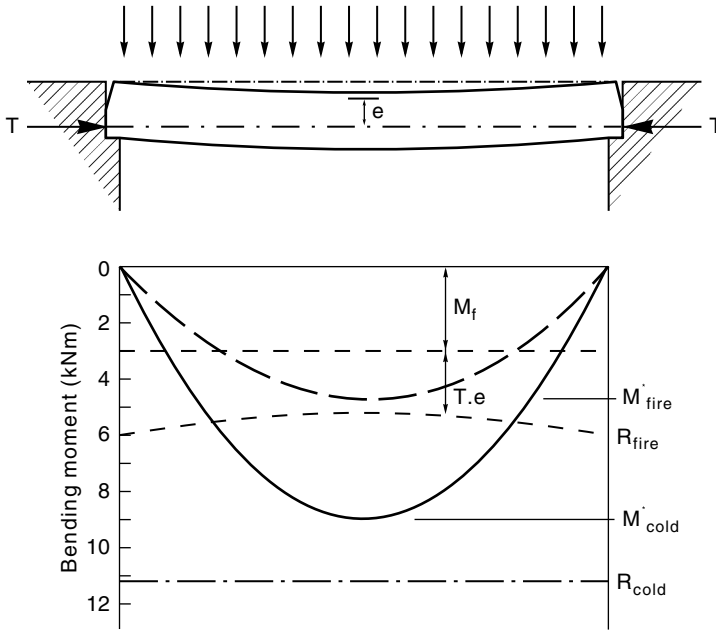


Figure 5.18 Effect of axial restraint force on bending moment diagram

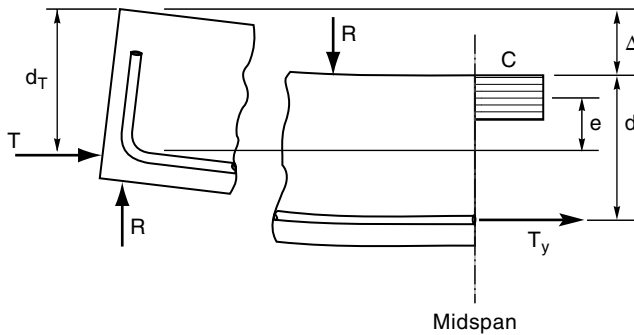


Figure 5.19 Free body diagram of reinforced concrete beam with axial restraint

Axial restraint does not always have a beneficial effect on fire resistance. Restraint can have a negative effect if mid-span deflections become excessive, or if the axial thrust develops near the top of the cross section. In order to utilize the beneficial effects of axial restraint, it is essential that the line of thermally induced thrust is below the centroid of the compression region of the beam or slab, so that the eccentricity e shown in Figure 5.17 and Figure 5.18 has a positive value. It can sometimes be difficult to calculate the axial restraint because the position of the axial thrust can change from being positive to negative and vice versa as deformations and rotations occur during fire exposure. Figure 5.20 (Carlson *et al.*, 1965) shows how the location of the axial restraint force depends on the support conditions of the beam or slab. An axial restraint force near the top of the beam as shown in Figure 5.20(a) would lead to

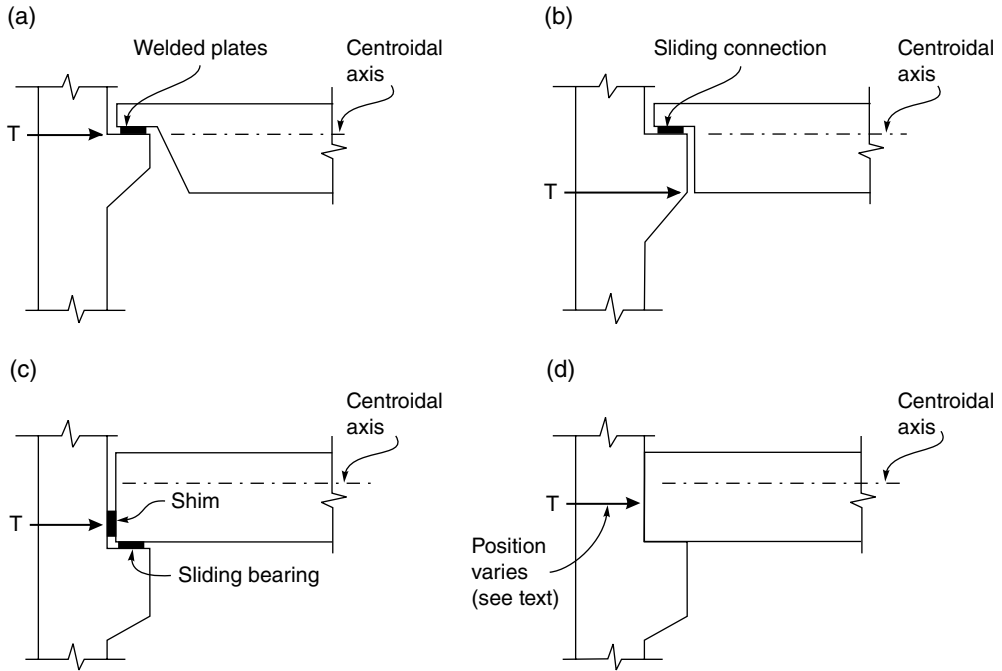


Figure 5.20 Location of axial thrust for several support conditions. Reproduced from Carlson *et al.* (1965) by permission of Portland Cement Association

premature failure of the floor system. This can be a problem with double-tee precast prestressed concrete floor panels if the webs are cut away at the ends and all the support is provided at the level of the top flange, as shown in Chapter 7. For the sliding connection in Figure 5.20(b), the axial thrust is below the centroidal axis, resulting in a positive value of eccentricity. Figure 5.20(c) also shows a positive eccentricity, due to the lower location of the axial thrust force. For built-in construction where the line of action of the restraint force is not known [Figure 5.20(d)] the thrust will usually be near the bottom where most of the heating and thermal expansion occurs.

This discussion has been based on the assumption that the restrained slab or beam does not buckle due to lateral instability under high axial loads, which is usually a good assumption for reinforced concrete structures. Rotter *et al.* (1999) have shown that fire-exposed steel beams with composite concrete slabs may buckle as a result of the large axial forces induced when they try to expand axially against a stiff and strong surrounding structure. This buckling results in large downwards deflections of the beam and slab which can be beneficial because the large deflections reduce the horizontal restraint forces on the surrounding structure. There is a complex interaction between the axial forces, downwards deflections and stiffness of the structure. Once buckling occurs, resulting in large deformations, the analysis presented above for single members does not apply. Later in the fire, the slab or slab-beam assembly may lose flexural strength and deform into a catenary. The slab will then develop internal tensile forces which pull inwards on the surrounding structure with tensile membrane action. This behaviour is described with reference to the Cardington tests in Chapter 6.

5.6.6.2 Effect of Restraint on the Surrounding Structure

A very stiff surrounding structure is necessary in order to develop the beneficial effects of axial restraint. Fire resistance tests can be used to assess the performance of an assembly in a restrained or unrestrained condition, but cannot be easily used to predict behaviour in a real building. A building structure will only be able to provide axial restraint if the part heated by the fire is surrounded by cooler structural members which have sufficient strength and stiffness to restrain the thermal elongation. This is most likely when a fire occurs in a restricted area of a large building, or where a fire-exposed concrete slab is surrounded by massive concrete beams. Rotter *et al.* (1999) have shown how tension ring restraint can occur in fire-protected composite edge beams, even when the fire occurs near the corner of a building. A structural engineering assessment is required on a case-by-case basis, considering the design of the actual building, but it may be difficult to assess how the surrounding structure can provide the necessary resistance to the axial restraint forces.

A negative effect of axial restraint may be serious damage to the surrounding structure, caused by large forces resulting from the thermal expansion. Such damage is more likely in concrete or masonry buildings rather than in ductile steel buildings, because of the inability of a stiff and brittle surrounding structure to absorb the imposed thermal forces or deformations.

5.6.6.3 Code Requirements for Restraint

This section has shown that consideration of axial restraint in fire resistance assessment is difficult because it requires information about the tested assembly and also about the structure in which the assembly is to be used. Codes do not handle axial restraint very well. Recognizing the difficulty of assessing a structure to resist axial restraint forces, an appendix to ASTM E119 gives ‘interim’ guidance for determining conditions of restraint for floor and roof assemblies and individual beams. The following clauses and Table 5.1 are extracted directly from ASTM E119 (ASTM, 2012):

X3.5 For the purposes of this appendix, restraint in buildings is defined as follows: ‘Floor and roof assemblies and individual beams in buildings are considered restrained when the surrounding or supporting structure is capable of resisting substantial thermal expansion and rotation throughout the range of anticipated elevated temperatures caused by a fire. Constructions not complying with this description are assumed to be free to rotate and expand and therefore are considered as unrestrained.’

X3.6 The description provided in X3.5 requires the exercise of engineering judgment to determine what constitutes restraint to ‘substantial thermal expansion and rotation’.

X3.7 In actual building structures, restraint capable of improving fire resistance may be provided by the stiffness of the contiguous construction. In order to develop sufficient restraint, thermally-induced forces must be adequately transferred through connections or by direct bearing on contiguous structural members. The rigidity of connections and contiguous structural members should be considered in assessing the capability of the fire-exposed construction to resist thermal expansion and rotation. Continuity, such as that occurring in beams acting continuously over more than two supports, will induce rotational restraint which will usually add to the fire resistance of structural members.

Table 5.1 ASTM E119 classification for restrained and unrestrained construction

TABLE X3.1 Guide for Determination of Restrained and Unrestrained conditions of Construction

I. Wall bearing:	
Single span and simply supported end spans of multiple bays: ^A	
(1) Open-web steel joists or steel beams, supporting concrete slab, precast units, or metal decking	unrestrained
(2) Concrete slabs, precast units, or metal decking	unrestrained
Interior spans of multiple bays:	
(1) Open-web steel joists, steel beams or metal decking, supporting continuous concrete slab ^B	restrained
(2) Open-web steel joists or steel beams, supporting precast units or metal decking	unrestrained
(3) Cast-in-place concrete slab construction ^B	restrained
(4) Precast concrete construction ^{B,C}	restrained
II. Steel framing: ^B	
(1) Steel beams welded, riveted, or bolted to the framing members	restrained
(2) All types of cast-in-place floor and roof construction (such as beam-and-slabs, flat slabs, pan joists, and waffle slabs) where the floor or roof construction is secured to the framing members	restrained
(3) All types of prefabricated floor or roof construction where the structural members are secured to the framing members ^C	restrained
III. Concrete framing: ^B	
(1) Beams fastened to the framing members	restrained
(2) All types of concrete cast-in-place floor or roof construction (such as beam-and-slabs, flat slabs, pan joists, and waffle slabs) where the floor or roof construction is cast with the framing members	restrained
(3) Interior and exterior spans of precast construction with cast-in-place joints resulting equivalent to that which would exist in condition III (1)	restrained
(4) All types of prefabricate floor or roof construction where the structural members are secured to such construction ^C	restrained
IV. Wood construction:	
All types	unrestrained

^A Floor and roof construction may be considered restrained where they are tied (with or without tie beams) into walls designed and detailed to resist thermally induced forces from the floor or roof construction exposed to fire.

^B To provide sufficient restraint, the framing members or contiguous floor or roof construction should be capable of resisting the potential thermal expansion resulting from a fire exposure as described in X3.5 and X3.6.

^C Resistance to potential thermal expansion resulting from fire exposure may be achieved when one of the following is provided:

- (1) Continuous structural concrete topping is used.
- (2) The space between the ends of precast units or between the ends of units and the vertical face of supports is filled with concrete or mortar, or
- (3) The space between the ends of precast units and the vertical faces of supports, or between the ends of solid or hollow core slab units does not exceed 0.25% of the length for normal weight concrete members or 0.1% of the length for structural lightweight concrete members.

Source: Reprinted from ASTM (2012). © ASTM International

These extracts from ASTM E119 are useful, but confusing because flexural continuity and axial restraint are mixed up, and the table mentions only the type of construction with no reference to the extent of the fire or the stiffness of the building. If structural calculations show that the effects of axial restraint are essential to ensure structural stability in fire conditions, then the stiffness of the structure must be calculated. Methods of calculating the effects of axial restraint and the required stiffness of the surrounding structure for reinforced and prestressed concrete buildings are described in Chapter 7. For wood structures, Table 5.1 recommends that all types of wood construction should be considered to be unrestrained, which ignores the beneficial effect of continuity in glulam beams or timber decking, for example.

The three issues of continuity, redundancy and restraint all require structural engineering assessment on a case-by-case basis because they cannot be tested in traditional fire resistance tests.

5.6.7 *After-fire Stability*

The above discussion describes the design process for structures during a fire, without addressing the performance of the structure after the fire. After a fire the structure may be partly damaged, with some members missing or having reduced strength.

For example, many single-storey industrial buildings have unprotected roof structures, so that the roof can collapse in a fire, leaving the boundary walls cantilevering from the foundations after a fire, in danger of falling in wind or earthquake. This situation can be designed for if the design requirements are explicitly stated. Unfortunately, this is a common problem which most codes do not address properly.

The verification method for the New Zealand Building Code (MBIE, 2014) requires that the residual structure be able to resist a face load of 0.5 kN/m^2 on the exposed surfaces after the fire. This is intended to allow for wind or earthquake loads on the residual fire-damaged structure after the fire has been extinguished or has burned itself out, especially for single-storey buildings where the roof could collapse in a fire leaving unsupported wall panels in place. This load also provides for some unspecified resistance to failure during the fire, possibly due to wind loads or catenary loads from collapse of a fire-damaged roof.

A common older form of construction for multi-storey buildings ('mill construction') consists of unreinforced masonry perimeter walls with timber floors supported on heavy timber beams and columns. The timber floors provide lateral stability to the walls. A severe fire can damage the timber floors and beams, hence removing lateral support, possibly leading to serious failure endangering the lives of firefighters and others. Such buildings must be provided with adequate fire resistance for the floors and good connections between the floor diaphragm and the exterior walls.

5.7 **Worked Examples**

5.7.1 *Worked Example 5.1*

Calculate the factored bending moment at the centre of a simply supported floor slab, for normal temperature design and for fire design. Use these bending moments to calculate the load ratio for fire design.

The slab has a span of 3.5 m. The characteristic dead load is 2.4 kN/m² and the characteristic live load is 2.0 kN/m². Make all calculations for a strip of slab 1 m wide. Refer to Figure 5.8.

Calculate load combinations:

$$\text{Characteristic dead load} \quad G_k = 2.40 \text{ kN/m}^2$$

$$\text{Characteristic live load} \quad Q_k = 2.00 \text{ kN/m}^2$$

$$\text{Factored load for cold design} \quad 1.35 G_k = 3.24 \text{ kN/m}^2$$

$$1.2 G_k + 1.5 Q_k = 5.88 \text{ kN/m}^2 \text{ (governs)}$$

$$\text{Factored load for fire design} \quad G_k + 0.4 Q_k = 3.20 \text{ kN/m}^2$$

Convert to uniformly distributed loads on a strip 1 m wide:

$$\text{Factored load for cold design} \quad w_c = 5.88 \times 1 = 5.88 \text{ kN/m}$$

$$\text{Factored load for fire design} \quad w_f = 3.20 \times 1 = 3.20 \text{ kN/m}$$

Calculate bending moments in centre of 3.5 m span:

$$\text{Design bending moment for cold design} \quad M_{cold}^* = w_c L^2 / 8 = 5.88 \times 3.5^2 / 8 = 9.00 \text{ kNm}$$

$$\text{Design bending moment for fire design} \quad M_{fire}^* = w_f L^2 / 8 = 3.20 \times 3.5^2 / 8 = 4.90 \text{ kNm}$$

Calculate the required flexural design capacity of the slab, using a strength reduction factor $\Phi = 0.8$, and the load ratio for fire design, assuming that the slab is provided with exactly the required strength.

$$\text{Flexural design capacity} \quad R_{cold} = M_{cold}^* / \Phi = 9.00 / 0.8 = 11.25 \text{ kNm}$$

$$\text{Load ratio for fire design} \quad r_{load} = M_{fire}^* / R_{cold} = 4.90 / 11.25 = 0.44$$

This shows that the slab would not be expected to fail in a fire until its strength drops to 44% of its strength at normal temperatures.

5.7.2 Worked Example 5.2

Recalculate the bending moments from Worked Example 5.1 for a slab which is continuous over several supports. Assuming that the slab has equal positive and negative flexural capacity, calculate the load ratio considering redistribution to equal positive and negative moments. Refer to Figure 5.13.

Calculate the design bending moments for cold conditions:

Design bending moment at support (negative moment)

$$M_{cold}^* = w_c L^2 / 12 = 5.88 \times 3.5^2 / 12 = 6.00 \text{ kNm}$$

Design bending moment at mid-span (positive moment)

$$M_{cold}^* = w_c L^2 / 24 = 5.88 \times 3.5^2 / 24 = 3.00 \text{ kNm}$$

These bending moments are shown by the solid curve in Figure 5.13. The sum of the negative and positive moments is $6.0 + 3.0 = 9.0 \text{ kNm}$, the same as M_{cold}^* in Worked Example 5.1. The minimum flexural capacity that must be provided to resist the negative moment is now $R_{cold} = M_{cold}^* / \Phi = 6.00 / 0.8 = 7.50 \text{ kNm}$, so a weaker slab can be used than in the simply supported case. The flexural capacity provided is shown in Figure 5.13 by the line $R_{cold} = 7.50 \text{ kNm}$ for equal positive and negative moments.

With the reduced loads for fire conditions, the negative and positive bending moments become 3.27 and 1.63 kNm , respectively, shown by the dashed curve M_{fire}^* . The sum of the negative and positive moments is $3.27 + 1.63 = 4.90 \text{ kNm}$, the same as M_{fire}^* in Worked Example 5.1.

Consider the effect of a fire which causes the flexural capacity R_{cold} to drop at the same rate for both positive and negative bending. If there is no redistribution of moments, the slab would fail at the supports when the flexural capacity drops to 3.27 kNm . The load ratio is $r_{load} = 3.27 / 7.50 = 0.44$. However, with redistribution, the bending moment diagram can take any position provided that the sum of positive and negative moments remains at $w_f L^2 / 8 = 4.90 \text{ kNm}$.

If positive and negative flexural strengths are equal, the optimum location of the bending moment diagram is the shape shown by the dotted curve, with positive and negative moments both $M_{fire,red}^* = 4.90 / 2 = 2.45 \text{ kNm}$ (which could also have been obtained from Equation 5.26). This gives a revised load ratio for fire design of:

$$\begin{aligned} r_{load} &= M_{fire,red}^* / R_{cold} \\ &= 2.45 / 7.50 = 0.33 \end{aligned}$$

Final failure of the slab will not be expected until its strength in fire conditions has reduced to 33% of its strength at normal temperatures.

5.7.3 Worked Example 5.3

Reconsider the slab from Worked Example 5.2, assuming that the slab can have different positive and negative flexural capacities. Calculate the revised load ratio assuming that the flexural capacity at mid-span (positive moment) drops to zero during fire exposure. Refer to Figure 5.14.

Before moment redistribution, the bending moments shown by the solid curve (M_{cold}^*) and the dashed curve (M_{fire}^*) are the same as in Worked Example 5.2. The maximum flexural capacities are shown by the two lines marked R_{cold} for unequal positive and negative values.

With moment redistribution, the bending moment diagram M_{fire}^* can again take any position, provided that it remains the same shape. The dotted line marked $M_{fire,red}^*$ in Figure 5.14 shows the bending moment diagram lifted to give a maximum value at the supports and a zero value at mid-span.

In this case the slab could survive a fire even though the positive flexural capacity at mid-span drops to zero during the fire. The slab must be able to resist a negative bending moment at the supports of $M_{fire,red}^* = 4.90$ kNm, which corresponds to:

$$\begin{aligned} \text{Load ratio for fire design } r_{load} &= M_{fire,red}^* / R_{cold} \\ &= 4.90 / 7.50 = 0.65 \end{aligned}$$

Failure of the slab will not be expected until its cantilever strength in fire conditions has reduced to 65% of its strength at normal temperatures and the mid-span strength has dropped to zero.

5.7.4 Worked Example 5.4

Consider the continuous beam shown in Figure 5.17. The span AB is 6 m and BC is 2 m. The uniformly distributed load during the fire conditions is $w = 22$ kN/m.

- Calculate the minimum flexural capacity of the positive and negative plastic hinges.
- Calculate the required flexural capacity of the negative plastic hinge if the strength of the positive plastic hinge decreases to 30 kNm under fire exposure.

(a) Span BC

By the principle of the conservation of energy, the magnitude of the external virtual work is equal to the internal virtual work.

external work = internal work

$$w L_{BC} \delta / 2 = M_p^- \theta$$

Substituting $\delta = \theta L_{BC}$

$$w L_{BC}^2 \theta / 2 = M_p^- \theta$$

Substituting $w = 22$ kN/m and $L_{BC} = 2$ m gives:

$$M_p^- \geq \frac{22 \times 2^2}{2} = 44 \text{ kNm} \quad (1)$$

Span AB

Assume that the positive hinge occurs in the centre of span AB.

external work = internal work

$$w L_{AB} \delta / 2 - w L_{BC} \delta / 2 = M_p^- \theta + 2 M_p^+ \theta$$

from geometry, $L_{AB} = 6$ m, $L_{BC} = 2$ m

$$\delta' = 2\delta/3$$

$$\delta = \theta L_{AB}/2$$

Making these substitutions with $w = 22$ kN/m gives:

$$M_p^- + 2M_p^+ \geq 154 \text{ kNm} \quad (2)$$

Combining (1) and (2) gives:

$$M_p^- \geq 44 \text{ kNm}$$

$$M_p^+ \geq 55 \text{ kNm}$$

(b) If M_p^+ is reduced to 30 kNm, substituting into (2) gives:

$$M_p^- \geq 94 \text{ kNm}$$

6

Steel Structures

This chapter provides the information needed for calculating the performance of steel buildings exposed to fires. Simple methods are described for designing individual steel members to resist fire exposure, including calculations of elevated temperatures, methods of fire protection, and information on thermal and mechanical properties of steel at elevated temperatures. Fire behaviour of large steel buildings is also discussed.

This chapter draws information from Eurocode 3 Part 1.2 (CEN, 2005b), which with the other structural Eurocodes, summarizes the results of a large international cooperative programme over recent decades.

6.1 Behaviour of Steel Structures in Fire

When a steel structure is exposed to a fire, the steel temperatures increase and the strength and stiffness of the steel are reduced, leading to possible deformation and failure, depending on the applied loads and the support conditions (Figure 6.1). The increase in steel temperatures depends on the severity of the fire, the area of steel exposed to the fire and the amount of applied fire protection. There are many methods of protecting steel members from the effects of fire, so that structural steel buildings with applied fire protection can be designed to have excellent fire resistance.

Unprotected steel structures tend to perform poorly in fires compared with reinforced concrete or heavy timber structures, because the steel members are usually much thinner [Figure 6.2(a)] and steel has a higher thermal conductivity than most other materials. Unprotected steel structures can survive some fires if the severity is low and the steel does not get too hot [Figure 6.2(b)]. Full-scale tests and some real fires in large steel buildings have shown that well-designed steel structures can resist severe fires without collapse, even if some of the main load-bearing members are unprotected. Thermal expansion of steel members can



Figure 6.1 Typical fire damage to unprotected steel frames in an industrial building

cause damage elsewhere in the building [Figure 6.2(c)]. A review of steel behaviour in many fire tests is given by Cooke (1996). The main factors affecting the behaviour of steel structures in fire, as discussed further in this chapter, are:

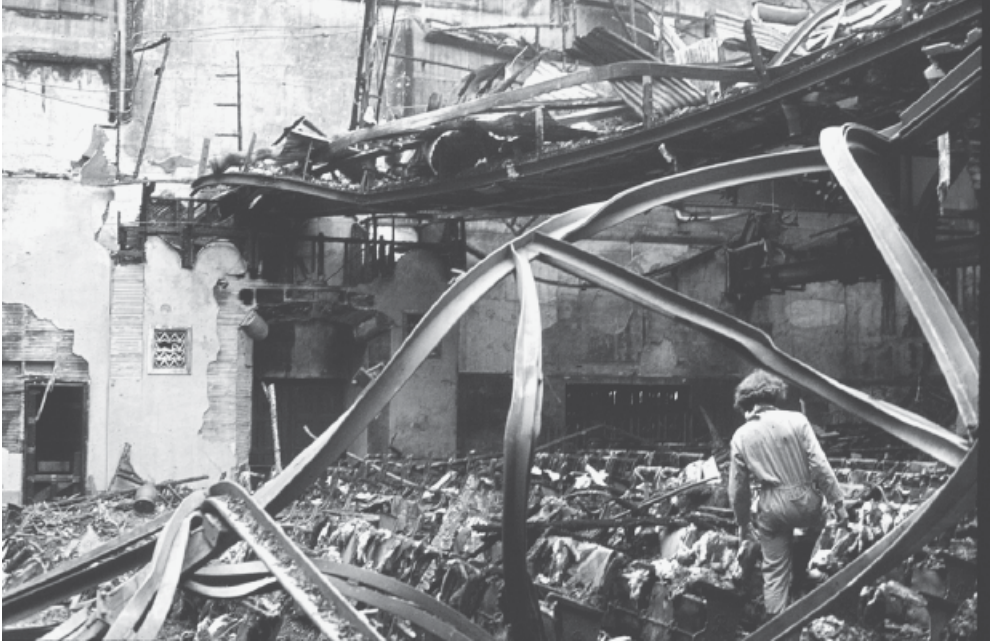
- the elevated temperatures in the steel members;
- the fire limit state loads on the structure;
- the mechanical properties of the steel;
- the geometry and design of the structure.

6.1.1 Structural Steel Design Process

The design process for fire resistance requires verification that the provided fire resistance exceeds the design fire severity. Using the terminology from Chapter 4, verification may be in the *time domain*, the *temperature domain* or the *strength domain*. All three domains are often used for assessing the fire resistance of steel structures. The traditional method of using fire resistance ratings in the time domain is described first.

In the time domain, the required fire resistance time may be prescribed by a code, or calculated from a time equivalent formula if the fire load and ventilation are known. The required fire resistance can then be compared with the fire resistance rating of the selected assembly. The fire resistance rating can be obtained from listings of generic ratings, proprietary ratings, or expert opinion ratings, or from calculations of the time to reach the limiting temperature.

(a)



(b)



(c)



Figure 6.2 (a) Severe fire in a theatre, showing collapsed steel roof trusses in the foreground; the gallery seating which did not collapse is visible in the upper background. (b) Buckling of a compression member in the heavy steel truss supporting the gallery seating; this truss is close to failure, but did not collapse. (c) Holes punched through a reinforced concrete wall by thermal expansion of the heavy steel truss supporting the gallery seating

In the temperature domain, the limiting steel temperature is compared with the maximum temperature reached in the design fire exposure. The limiting temperature is the steel temperature at which the load-bearing capacity of the member would just equal the design loads, this being the steel temperature above which the member would be expected to fail. Eurocode 3 Part 1.2 (CEN, 2005b) gives a limiting temperature option for fire design of single members. The limiting temperature calculation is most suitable when the whole steel cross section is assumed to be at a uniform temperature.

In the strength domain, the load-bearing capacity during the fire is compared with the expected loads on the member at the time of the fire (the fire limit state loads). This is the method recommended in this book. Calculations in the strength domain must be used if there are temperature gradients across the steel cross sections, and for assessing fire behaviour of whole structures.

Most steel structures require some form of fire protection in order to achieve fire resistance. Fire resistance of protected steel can be assessed by the use of generic ratings, proprietary ratings or by calculation. *Generic ratings* or ‘tabulated ratings’ are those which assign a time of fire resistance to materials with no reference to individual manufacturers or to detailed specifications. Many national codes and some trade organizations provide lists of generic ratings for fire protection of structural steel members. The most common ratings are for encasement in concrete or some other generic material, with a table of the minimum thickness of material needed to provide certain ratings. Many manufacturers of passive fire protection products provide *proprietary* listings of approved ratings. These are similar to generic ratings in that they generally provide ratings for exposure to the standard fire, but they may be less conservative because they relate to more closely defined products. Proprietary ratings usually make no allowance for the level of load, but they often include reference to the size and shape of the member using the section factor. A list of proprietary ratings is given by the Association of Specialist Fire Protection in the UK (ASFP, 2014). This document gives the required thickness of particular proprietary spray-on or board protection to provide fire resistance to steel beams or columns depending on their *section factor* F/V , where F is the exposed surface area per unit length of the beam and V is the volume per unit length of the beam.

This chapter describes calculation methods for steel structures exposed to fires. Most calculations will compare loads with load capacity in the strength domain. Using the terminology of the Eurocodes, there are two main types of calculation: namely, simple calculation methods; and advanced calculation methods. Simple methods are used for single members in uncomplicated structures, often using hand calculations with the equations presented below. Advanced calculation methods require the use of computer programs for analysis of complex structures using the material properties from this chapter, and as described in Eurocode 3 Part 1.2 (CEN, 2005b).

6.2 Steel Temperature Prediction

6.2.1 Fire Exposure

In any design of steel structures to resist fires, it is essential to know the temperature of the steel, which depends on the fire exposure. The fire exposure may be the standard time–temperature curve or a more realistic fire curve, such as the Eurocode parametric curve (CEN, 2002b), depending on the design philosophy. Generic and proprietary protection methods are all based on standard fire exposure, but calculations are often based on simulated real fires.

6.2.2 Calculation Methods

The simplest hand calculation method is to use a best-fit empirical formula (ECCS, 1985) to obtain the temperature of steel members exposed to the standard fire, assuming that the steel temperature is uniform over the cross section. A more accurate ‘lumped mass’ design method employs the step-by-step calculation technique in Eurocode 3 Part 1.2 (CEN, 2005b). This method assumes a lumped mass of steel at uniform temperature over the cross section, and can be used with any design fire curve as input.

More sophisticated computer-based methods can calculate temperatures within the cross section, for any combination of materials or shapes, for exposure to any desired fire. A two-dimensional calculation is suitable for most situations, based on an assumption of the same temperatures at each point along the member, which is reasonable if the fire temperature is assumed to be the same throughout the fire compartment. Three-dimensional heat transfer calculations may be useful at member junctions or other special situations. Figure 6.3 shows the temperature contours in an unprotected heavy steel section (Universal Column 356×406×634 kg/m) after exposure for 30 min to the standard fire curve, calculated by the SAFIR program (Franssen *et al.*, 2000). It can be seen that there are temperature differences of over 100 °C within the cross section, the largest difference being between the high temperatures in the thin web and the lower temperatures in the much thicker flanges.

6.2.3 Section Factor

The rate of temperature rise of a protected or unprotected structural steel member exposed to fire depends on the *section factor*, or *massivity factor*, which is a measure of the ratio of the heated perimeter to the area or mass of the cross section. The section factor is important because the rate of heat input is directly proportional to the area exposed to the fire environment, and the subsequent rate of temperature increase is inversely proportional to the heat capacity of the member (equal to the product of the specific heat, the density and the volume of the steel segment).

The section factor can be expressed in one of four alternative ways:

- ratio of heated surface area to volume, both per unit length, F/V (m^{-1});
- ratio of heated perimeter to cross-sectional area, H_p/A (m^{-1});
- ratio of heated surface area to mass, both per unit length, F/M (m^2/t);
- effective thickness, V/F or A/H_p (m or mm).

Here F is the surface area of unit length of the member (m^2), V is the volume of steel in unit length of the member (m^3), H_p is the heated perimeter of the cross section (m), A is the cross-sectional area of the section (m^2), and M is the mass per unit length of the member (t).

The first two ratios are identical and can be easily converted to the third using the density of steel (7850 kg/m^3 or 7.85 t/m^3). The heated surface is the actual surface area of unprotected members or members with sprayed-on fire protection, and the area of the equivalent rectangle for box protection, with allowance for any unexposed surfaces, as shown in Figure 6.4. The fourth ratio listed above is V/F or A/H_p with units in metres (or millimetres). This ratio gives much better physical understanding because it is an effective thickness of the cross section.

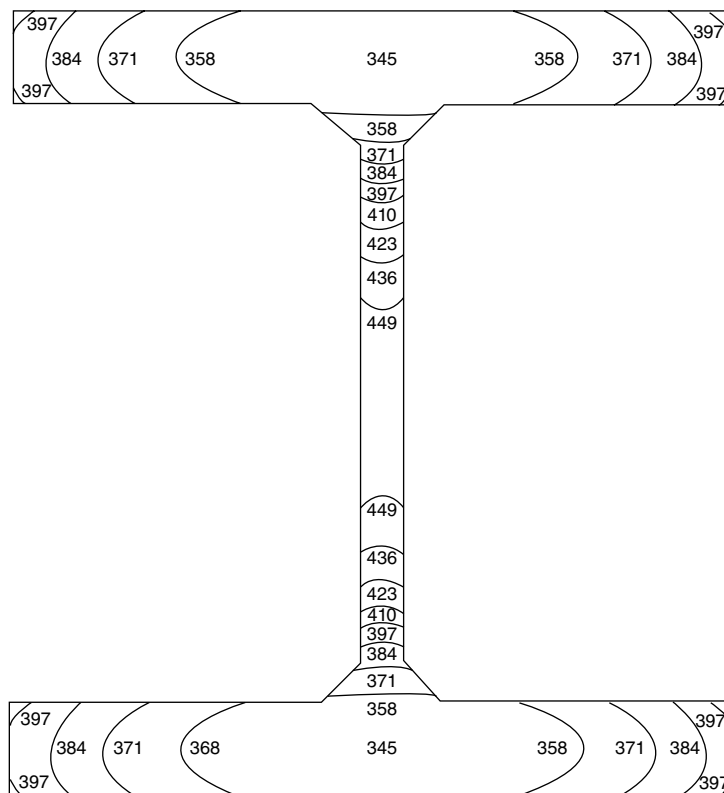


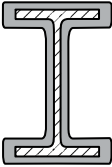
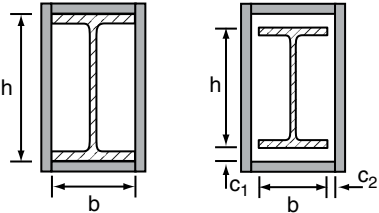
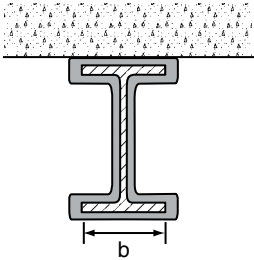
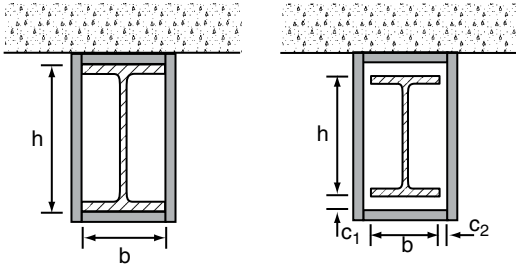
Figure 6.3 Temperature contours in a heavy steel section exposed to fire. Reproduced from Franssen *et al.* (2000) with permission of Franssen

Calculated in this way, the section factor for a steel plate exposed to a fire on both sides is $V/F = t/2$ where t is the thickness of the plate. For a hollow tube of thickness t , the section factor becomes $V/F = t$. For an I-beam, the section factor V/F is one half of the average thickness of the different parts. Mistakes in the calculation of the section factor are much less likely when it is defined in this way.

Tables of section factors for common structural steel shapes are available from distributors of steel products. Section factors for steel members are listed by ICC (2015), ASFP (2014) and HERA (1996) for American, British and New Zealand steel sections, respectively. Some of these section factors are listed in Appendix B.

6.2.4 Thermal Properties

In order to make calculations of temperatures in fire-exposed structures, it is necessary to know the thermal properties of the materials. The density of steel is 7850 kg/m^3 , remaining essentially constant with temperature. The specific heat of steel varies according to

Sketch	Description	Section factor (F/V)
	<p>Contour encasement of uniform thickness</p>	$\frac{\text{Steel perimeter}}{\text{Steel cross-sectional area}}$
	<p>Hollow encasement⁽¹⁾ of uniform thickness</p>	$\frac{2(b+h)}{\text{Steel cross-sectional area}}$
	<p>Contour encasement of uniform thickness, exposed to fire on three sides</p>	$\frac{\text{Steel perimeter} - b}{\text{Steel cross-sectional area}}$
	<p>Hollow encasement⁽¹⁾ of uniform thickness, exposed to fire on three sides</p>	$\frac{2h+b}{\text{Steel cross-sectional area}}$

(1) The clearance dimensions c_1 and c_2 should not normally exceed $h/4$

Figure 6.4 Definition of section factor in the Eurocode. Reproduced from CEN (2005b). © CEN, reproduced with permission

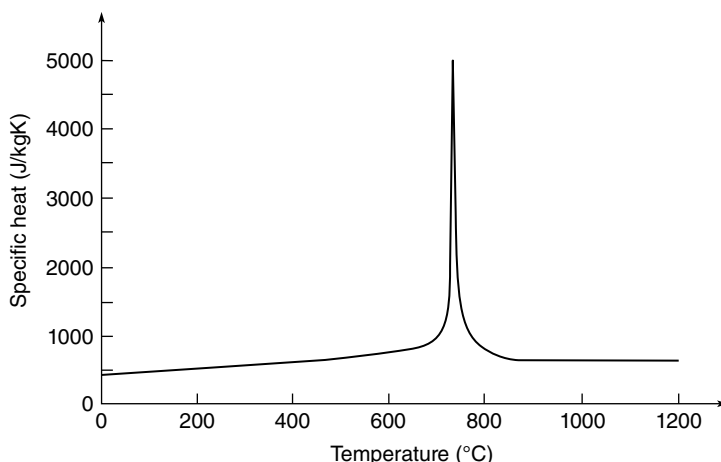


Figure 6.5 Specific heat of steel as a function of temperature. Reproduced from CEN (2005b). © CEN, reproduced with permission

temperature as shown in Figure 6.5 (CEN, 2005b) where the spike results from a metallurgical change at about 735 °C. For simple calculations the specific heat c_p (J/kgK) can be taken as 600 J/kgK, but it is more accurate to use the following:

$$\begin{aligned}
 c_p &= 425 + 0.773T - 1.69 \times 10^{-3}T^2 + 2.22 \times 10^{-6}T^3 & 20^\circ\text{C} \leq T < 600^\circ\text{C} \\
 &= 666 + 13002/(738 - T) & 600^\circ\text{C} \leq T < 735^\circ\text{C} \\
 &= 545 + 17820/(T - 731) & 735^\circ\text{C} \leq T < 900^\circ\text{C} \\
 &= 650 & 900^\circ\text{C} \leq T \leq 1200^\circ\text{C}
 \end{aligned} \tag{6.1}$$

where T is the steel temperature (°C).

The thermal conductivity of steel varies according to temperature as shown in Figure 6.6, reducing linearly from 54 W/mK at 0°C to 27.3 W/mK at 800°C (CEN, 2005b). For simple calculations the thermal conductivity k (W/mK) can be taken as 45 W/mK but it is more accurate to use the following:

$$\begin{aligned}
 k &= 54 - 0.0333T & 20^\circ\text{C} \leq T < 800^\circ\text{C} \\
 &= 27.3 & 800^\circ\text{C} \leq T \leq 1200^\circ\text{C}
 \end{aligned} \tag{6.2}$$

6.2.5 Temperature Calculation for Unprotected Steelwork

Unprotected steel members can heat up quickly in fires, especially if they are thin and have a large surface area exposed to the fire. The Eurocode method of calculating temperature is given below; it treats the entire steel cross section as a lumped mass. In situations where parts of the steel cross section are insulated, there will be temperature gradients within the cross section, and these temperatures cannot be calculated with a lumped mass approach, so a finite

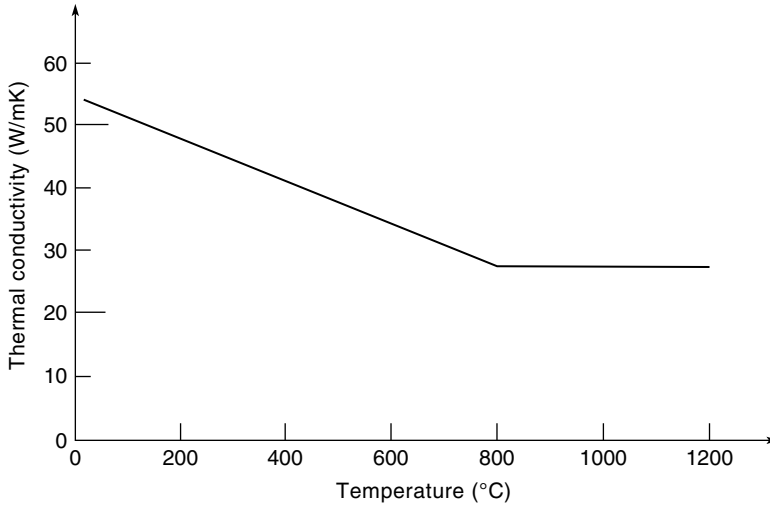


Figure 6.6 Thermal conductivity of steel as a function of temperature. Reproduced from CEN (2005b). © CEN, reproduced with permission

element method is necessary (see Chapter 3). There are some limited cases where the lumped mass temperature calculation can be performed for different parts of the cross section, as demonstrated in Chapter 8 with a steel-concrete composite beam.

6.2.5.1 Eurocode Method

The step-by-step calculation method for unprotected steelwork is based on the principle that the heat entering the steel over the exposed surface area in a small time step is equal to the heat required to raise the temperature of the steel, assuming that the steel section is a lumped mass at uniform temperature. The temperature increase over a given time step Δt in an unprotected steel member is calculated by:

$$\Delta T_s = k_{sh} \frac{(F/V)}{\rho_s c_s} \left[h_c (T_f - T_s) + \sigma \varepsilon (T_f^4 - T_s^4) \right] \Delta t \quad (6.3)$$

where ρ_s is the density of steel (kg/m^3), c_s is the specific heat of steel (J/kgK), ΔT_s is the change in steel temperature in the time step ($^{\circ}\text{C}$ or K), h_c is the convective heat transfer coefficient ($\text{W/m}^2\text{K}$), σ is the Stefan–Boltzmann constant ($56.7 \times 10^{-12} \text{ kW/m}^2\text{K}^4$), ε is the resultant emissivity, T_f is the temperature in the fire environment (K), T_s is the temperature of the steel (K) and k_{sh} is a correction factor for shadow effects. For I-sections, k_{sh} is calculated as $0.9 (F/V)_b / (F/V)$, and it is $(F/V)_b / (F/V)$ for all other cross sections. (F/V) is the section factor for contour protection, while $(F/V)_b$ is the section factor for board protection, called the box value of the section factor.

Eurocode 1 Part 1.2 (CEN, 2002b) recommends a convective heat transfer coefficient of $25 \text{ W/m}^2\text{K}$ for the standard fire, $50 \text{ W/m}^2\text{K}$ for the hydrocarbon fire and $35 \text{ W/m}^2\text{K}$ for

Table 6.1 Spreadsheet calculation for temperatures of unprotected steel sections

Time	Steel temperature, T_s	Fire temperature, T_f	Difference in temperature	Change in steel temperature, ΔT_s
$t_1 = \Delta t$	Initial steel temperature T_{s0}	Fire temperature at time t_1	$T_f - T_{s0}$	Calculate from Equation 6.3 with values of T_f and T_{s0} from this row
$t_2 = t_1 + \Delta t$	T_s from previous time step + ΔT_s from previous row	Fire temperature at time t_2	$T_f - T_s$	Calculate from Equation 6.3 with values of T_f and T_s from this row
etc.				

all parametric fires. Heat transfer in typical fires is not very sensitive to this value because radiative heat transfer dominates at typical fire temperatures (Thomas, 1997). The resultant emissivity ϵ is calculated as the product of the emissivity of the fire ϵ_f and the emissivity of the material ϵ_m ($\epsilon = \epsilon_f \epsilon_m$). The Eurocodes specify values of $\epsilon_f = 1.0$ (CEN, 2002b) and $\epsilon_m = 0.7$ for steel (CEN, 2005b).

A spreadsheet for calculating steel temperatures using this method is shown in Table 6.1. Eurocode 3 Part 1.2 (CEN, 2005b) suggests a time step of no more than 5 s for unprotected steel, and a minimum section factor (F/V) value of 10 m^{-1} (maximum effective thickness V/F of 100 mm).

6.2.6 Temperature Calculation for Protected Steelwork

Protected steel members heat up much more slowly than unprotected members because of the applied thermal insulation which protects the steel from rapid absorption of heat. The Eurocode method is described below. When using these methods with thick insulation, the section factor F/V should strictly be calculated using the fire-exposed perimeter rather than the inside face of the insulating material, but the inside perimeter is more often used because it is published in tables such as those in Appendix B. For steel members protected with heavy insulating materials or those with temperature-dependant thermal properties, a finite element computer program is recommended for calculating the temperatures due to the complexities involved in the calculation, even though a spreadsheet may be used.

6.2.6.1 Eurocode Method

The calculation method for protected steelwork is similar to that for unprotected steel. The equation is slightly different and does not require heat transfer coefficients because it is assumed that the external surface of the insulation is at the same temperature as the fire gases. It is also assumed that the internal surface of the insulation is at the same temperature as the steel. The equation is:

$$\Delta T_s = \frac{k_i (F/V)}{d_i \rho_s c_s} \frac{(T_f - T_s)}{(1 + \phi/3)} \Delta t - (e^{\phi/10} - 1) \Delta T_f \quad (\text{but } \Delta T_s \geq 0, \text{ if } \Delta T_f > 0) \quad (6.4)$$

Table 6.2 Thermal properties of insulation materials

Material	Density, ρ_i (kg/m ³)	Thermal conductivity, k_i (W/mK)	Specific heat, c_i (J/kgK)	Equilibrium moisture content (%)
Sprays				
Sprayed mineral fibre	300	0.12	1200	1
Perlite or vermiculite plaster	350	0.12	1200	15
High density perlite or vermiculite plaster	550	0.12	1200	15
Boards				
Fibre-silicate or fibre-calcium silicate	600	0.15	1200	3
Gypsum plaster	800	0.20	1700	20
Compressed fibre boards: Mineral wool, fibre silicate	150	0.20	1200	2

Source: ECCS (1995).

with

$$\phi = \frac{\rho_i c_i}{\rho_s c_s} d_i (F/V)$$

where c_i is the specific heat of the insulation (J/kg K), ρ_i is the density of the insulation (kg/m³), k_i is the thermal conductivity of the insulation (W/mK) and d_i is the thickness of the insulation (m).

The spreadsheet calculation is similar to that shown in Table 6.1 except that Equation 6.4 is used instead of Equation 6.3. Eurocode 3 suggests a maximum time step of 30 s. If the insulation is of low mass and specific heat such that the heat capacity of the insulation will not significantly slow the temperature increase of the steel, then Equation 6.4 can be simplified by making the ϕ term zero.

The effect of the time delay for moist materials can be incorporated into the Eurocode calculation method by modifying the specific heat of the insulating material to include a local increase of specific heat at 100 °C. Typical values of thermal properties of insulating materials are given in Table 6.2 (ECCS, 1995).

6.2.7 Typical Steel Temperatures

Figure 6.7(a) shows steel temperatures for a 360UB45 beam, with $F/V=210\text{ m}^{-1}$ and $(F/V)_b=153\text{ m}^{-1}$, exposed to the ISO 834 standard fire. The top curve is the fire temperature and the second curve is the temperature of an unprotected steel beam. The lower two curves are for the same beam protected with insulating material, using thicknesses of 15 and 30 mm. Figure 6.7(b) shows steel temperatures for the same beam exposed to a parametric fire, also calculated using the spreadsheet. The top curve is the fire temperature and the second curve, following the fire closely, is the temperature of the steel beam with no protection. The lower

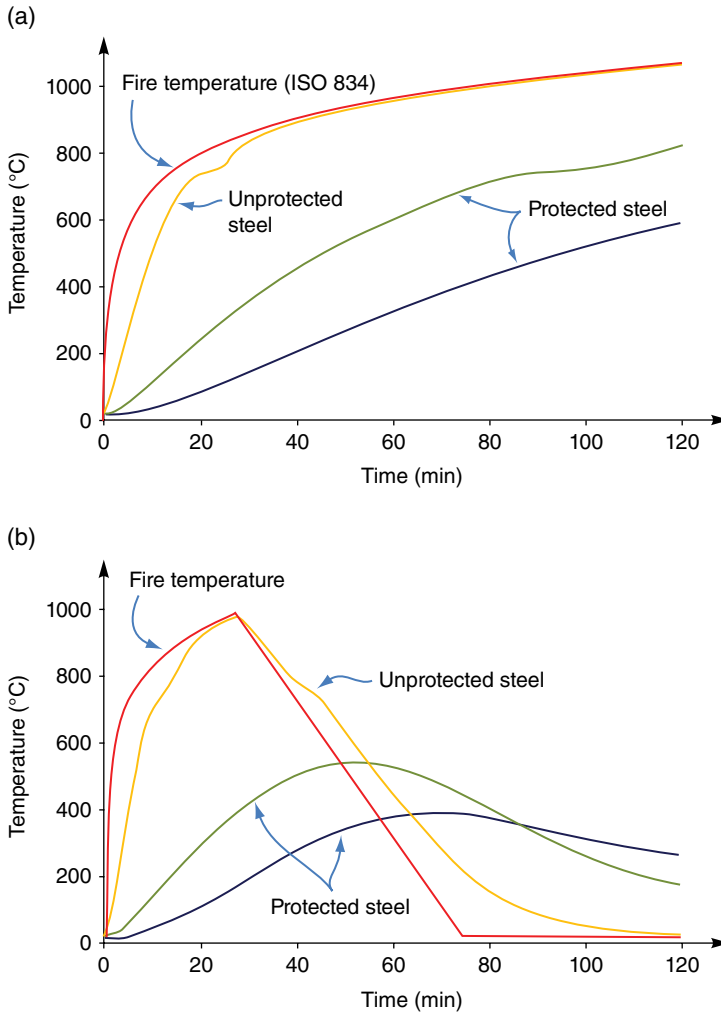


Figure 6.7 Typical steel temperatures for unprotected and protected steel beams exposed to: (a) the standard fire; (b) a parametric fire

two curves are the temperatures of steel beam protected with insulating material, using thicknesses of 15 and 30 mm as before. The kink that is observed in the steel temperature at about 750°C is as a result of changes in specific heat capacity due to the rearrangement of its crystal structure at that temperature.

6.2.8 Temperature Calculation for External Steelwork

Steel beams and columns outside a fire compartment may be subjected to elevated temperatures as a result of radiation from the window opening, radiation from flames, or engulfment in flames. Methods for estimating the temperature of such exposed steel members have been

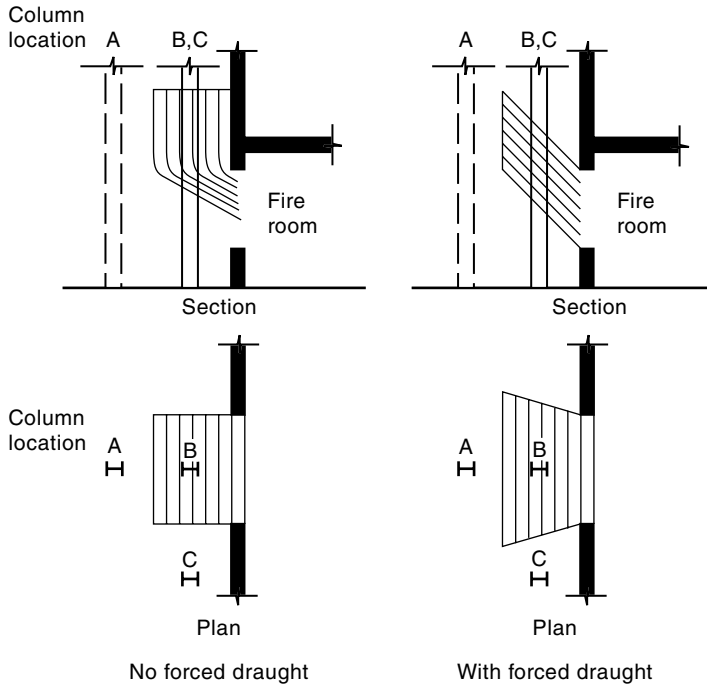


Figure 6.8 Fire exposure of external steel columns. Reproduced from CEN (2005b). © CEN, reproduced with permission

developed by Law and O'Brien (1989) and are incorporated into the Eurocodes. Flame sizes, temperatures and heat transfer coefficients are given in Eurocode 1 Part 1.2 (CEN, 2002b) and methods for calculating the steel temperatures are given in Eurocode 3 Part 1.2 (CEN, 2005b). The design method allows for conditions with or without wind creating a forced draught to influence the shape of the idealized flame.

Typical flame shapes and radiation geometries are shown in Figure 6.8 for two conditions of forced draught and no forced draught, which produce different flame shapes. The design documents show many additional shapes for conditions with cross winds, flame deflectors and other variations. Figure 6.8 shows three possible column locations which require different designs. Columns at locations A and C are exposed to radiation from the flame itself and also from the window opening behind the flame, but column C has less severe exposure. The column at location B is engulfed in the flame. The design documents mentioned above give equations for all of these situations.

6.3 Protection Systems

There are many alternative passive fire protection systems to reduce the rate of temperature increase in steel structures exposed to fire. Even if the fire resistance is assessed by calculation, each type of fire protection system should have at least one fire resistance rating obtained from full-scale load-bearing testing, to demonstrate that the insulating material has sufficient

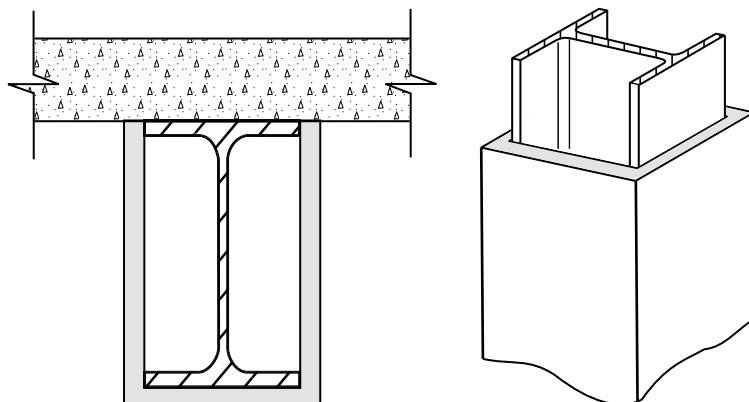


Figure 6.9 Steel beam and column protected with board materials

‘stickability’ to remain in place for the duration of the expected fire, with realistic deflections of the steel member. The toughness of passive fire protection often depends on the quality of the building materials and workmanship.

6.3.1 Concrete Encasement

A traditional method for fire protection of steelwork is encasement in poured concrete. An advantage of this system is excellent durability in corrosive environments. The required thickness of concrete to achieve standard fire resistance ratings is given in prescriptive building codes. The reinforcing in the concrete may be nominal reinforcing simply to hold the concrete in place in the event of a fire, or it may be substantial in which case the member will be designed for composite behaviour of all three materials. This form of construction is very common in Japan where it is called *steel-reinforced-concrete*. Elsewhere, concrete encasement is not widely used because it is expensive, bulky, and time-consuming, requiring the combined cost of a steel frame plus boxing for all of the concrete.

6.3.2 Board Systems

There are many proprietary board systems for protecting structural steelwork, such as shown in Figure 6.9, Figure 6.10 and Figure 6.11. Most fire protective boards are manufactured from calcium silicate or gypsum plaster. Calcium silicate board is more expensive than gypsum board in many places because it is imported from manufacturers in only a few countries. Calcium silicate boards are made of an inert material that is designed to remain in place with little damage for the duration of the fire, protecting the steel by its insulating properties. Gypsum board also has good insulating properties, and its behaviour is enhanced by the water of crystallization which is driven off as the board is heated. This dehydration process gives an additional time delay at about 100 °C, but it reduces the strength of the residual board after fire exposure, as described in Chapter 10.

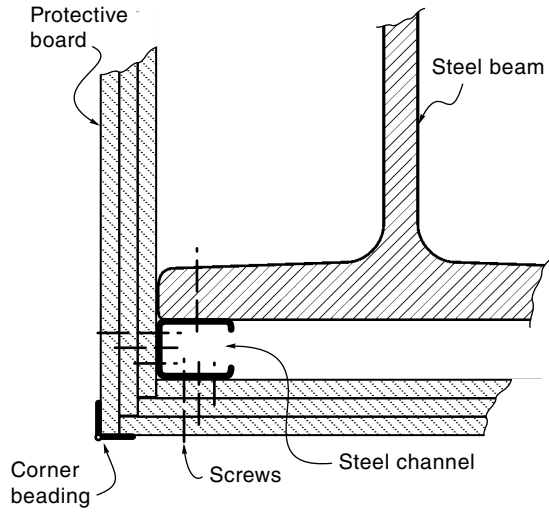


Figure 6.10 Detail of steel beam protected with board materials. Reproduced from Milke (2008) by permission of Society of Fire Protection Engineers



Figure 6.11 Box protection being placed on a steel column using sheet material

Board systems have the advantages that they are easy to install in a dry process, and easy to finish with decorative materials, but they are slower and more expensive than spray-on materials. Board systems are more often used for columns than for beams because columns are more often visible in the finished building. The boards are usually glued or screwed to metal or wood framing which has been fastened to the steel member. The number and thickness of layers can be easily adapted to the particular application. Possible fixing arrangements are shown in Figure 6.10 and Figure 6.11. Calcium silicate boards can be fixed to additional pieces of board wedged between the flanges of steel I-beams. Empirical formulae for calculating the required thickness of gypsum board to achieve standard fire resistance ratings are given by Milke (2008) and the International Building Code (ICC, 2015).

6.3.3 *Spray-on Systems*

Spray-on proprietary protection is usually the cheapest form of passive fire protection for steel members. Spray-on materials are usually cement based with some form of glass or cellulosic fibrous reinforcing to hold the material together. Earlier spray-on materials used asbestos fibres which are no longer used for health reasons. Disadvantages of spray-on protection are that the process is wet and messy, and the resulting finish is not suitable for decorative finishes. The spray-on material is often rather soft, so that it has to be protected from damage if it is in a vulnerable location. For these reasons, spray-on materials are more often used for beams than for columns (Figure 6.12). Spray-on protection is easy to apply to complicated details such as bolted connections or steel brackets.

Approved spray-on systems must have proof that they have sufficient ‘stickability’ to remain in place during fire exposure. Test methods are available for testing the cohesion and adhesion of spray-on fire protection (ICC, 2015). The required thickness of proprietary spray-on fire protection to achieve fire resistance ratings can be found in individual manufacturers’ literature or trade publications (e.g. ASFP, 2014). Some generic ratings are available for spray-on systems (e.g. NBCC, 2010) but proprietary ratings from individual manufacturers are more likely to be used.

6.3.4 *Intumescent Paint*

Intumescent paint is a special paint material that swells up into a thick charred mass when it is heated. The intumescent material provides insulation to the steel member beneath. Several coats of intumescent paint may have to be applied to obtain the necessary thickness. Intumescent paints have the advantages that they do not take up much space, they can be applied quickly, and they allow the structural steel members to be seen directly, without any covering other than the paint. A disadvantage is the high cost compared with-board and spray-on materials, especially for longer duration fire resistance ratings. Many intumescent paints are not suitable for external use because of unknown durability. All intumescent paints are proprietary products, and many are under continual development. A minor disadvantage of intumescent coatings is that the protection is not obvious to casual observers, and it can be difficult to verify at a later date. Some specialist intumescent products incorporating multiple layers of fibre-glass reinforcing have been developed for high level protection of structural steel in the offshore oil industry. Structural elements coated with intumescent paints should be given enough clearance to expand on heating, especially when they abut other construction materials.



Figure 6.12 Sprayed-on fire protection to steel beams supporting precast concrete floor slabs

6.3.5 Protection with Timber

It is possible to provide fire protection to steel beams and columns with timber boards. Twilt and Witteveen (1974) describe fire tests and fixing details for fire-exposed steel columns. Using a conservative critical steel temperature of 200°C they show that 35 mm thick softwood boards can provide fire resistance for 60 min to a steel column with F/V 100 m^{-1} . It is essential that the timber completely encloses the steel member, and be firmly fixed in place with a thermosetting adhesive such as resorcinol. The wood must be well seasoned to prevent shrinkage cracks.

6.3.6 Concrete Filling

Hollow steel sections can be filled with concrete to improve the fire performance. A major advantage is the lack of bulky external protection, and the steel can be finished with normal paint. There are several structural possibilities. The filling concrete can either be considered simply as a heat sink to reduce the temperature increase, or as a structural material which can carry an increasing proportion of the load as the steel temperatures increase. The filling concrete can be plain concrete, or it can be reinforced with conventional bars or with steel fibres. The steel tube can provide excellent structural confinement to the concrete under non-fire conditions, for example during seismic loading. It is essential to provide vent holes to prevent

excessive steam pressure from exploding the hollow member during heating. A variation on this theme is to fill the two spaces between the flanges of a steel I-beam with concrete, with reinforcing to hold the concrete in place. The reinforcing must be welded to the web and not be welded between the flanges. Structural design of concrete filled columns exposed to fire is covered in Chapter 8.

6.3.7 Water Filling

A less common but effective way of preventing rapid heating of hollow steel sections is to fill them with water. A plumbing system is necessary to ensure that the water can flow by convection from member to member and to avoid excessive pressures when the water is heated. This will require imaginative detailing of the connections between individual elements. Additives may be necessary to prevent corrosion, and to prevent freezing in cold climates. This method of protection is expensive and is only used for special structures. Design information is given by Bond (1975).

6.3.8 Flame Shields

In some situations, it is possible to use flame shields to protect external structural steelwork from radiation or direct impingement by flames coming out of window openings. In these cases, the temperatures of the steel exposed to flame contact or radiation can be calculated using the methods referred to above for external steelwork. An example of a flame shield protecting the flanges of a deep steel beam in a 54-storey building in New York is shown in Figure 6.13 (Seigel, 1970).

6.4 Mechanical Properties of Steel at Elevated Temperature

This section reviews the effects of the mechanical properties of steel on the behaviour of steel structures in fire.

6.4.1 Components of Strain

The deformation of steel at elevated temperature is usually described by assuming that the change in strain $\Delta\varepsilon$ consists of three components, as described in Chapter 5:

$$\Delta\varepsilon = \varepsilon - \varepsilon_i = \varepsilon_{th}(T) + \varepsilon_{\sigma}(\sigma, T) + \varepsilon_{cr}(\sigma, T, t) \quad (6.5)$$

where ε is the total strain at time t , ε_i is the initial strain at time $t=0$, $\varepsilon_{th}(T)$ is the thermal strain being a function only of temperature, T , $\varepsilon_{\sigma}(\sigma, T)$ is the stress-related strain, being a function of both the applied stress σ and the temperature T and $\varepsilon_{cr}(\sigma, T, t)$ is the creep strain, being a function of stress, temperature and time.

These three components of strain are discussed in more detail below. For simple structural members such as simply supported beams, only the stress-related strain needs to be

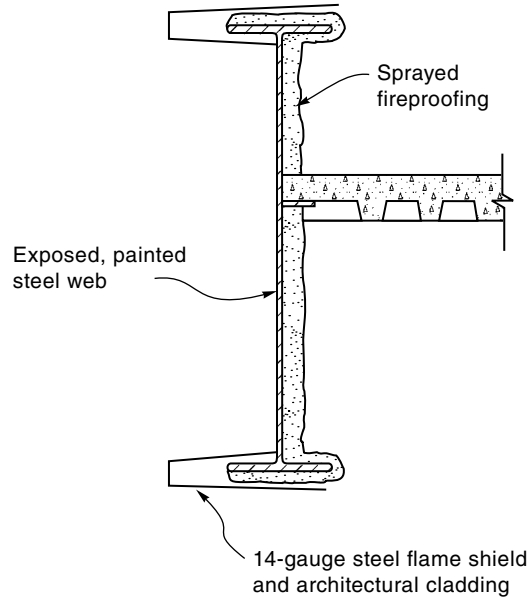


Figure 6.13 Flame protection of exterior steel beam. Reproduced with permission from Seigel (1970). © 1970 National Fire Protection Association, all rights reserved

considered, allowing the reduced strength at elevated temperatures to be calculated without reference to the deformations. For more complex structural systems, especially where members are restrained by other parts of the structure, the thermal strain and the creep strain must also be considered, using a computer model for the structural analysis.

6.4.2 Thermal Strain

The thermal strain is the well-known thermal expansion that occurs when most materials are heated. Anderberg (1988) reports four studies which obtained very similar linear relationships for the thermal expansion of steel. At room temperatures, the coefficient of thermal expansion is usually taken to be $11.7 \times 10^{-6}/^{\circ}\text{C}$. At higher temperatures such as those experienced in fires, the coefficient increases, and a discontinuity occurs between 700°C and 800°C . On the basis of extensive testing, Poh (1996) has proposed an equation which includes all of these effects. For normal design purposes, Eurocode 3 Part 1.2 (CEN, 2005b) recommends a linear coefficient of $14.0 \times 10^{-6}/^{\circ}\text{C}$; hence the thermal elongation of steel $\Delta L/L$ can be approximated by a linear function of temperature T ($^{\circ}\text{C}$) given by:

$$\Delta L/L = 14 \times 10^{-6} (T - 20) \quad (6.6)$$

For design of simple members such as single beams and columns it is not usually necessary to calculate and include the effects of thermal strains. For continuous systems, the development of thermal restraint forces in beams may be beneficial or detrimental, depending on the

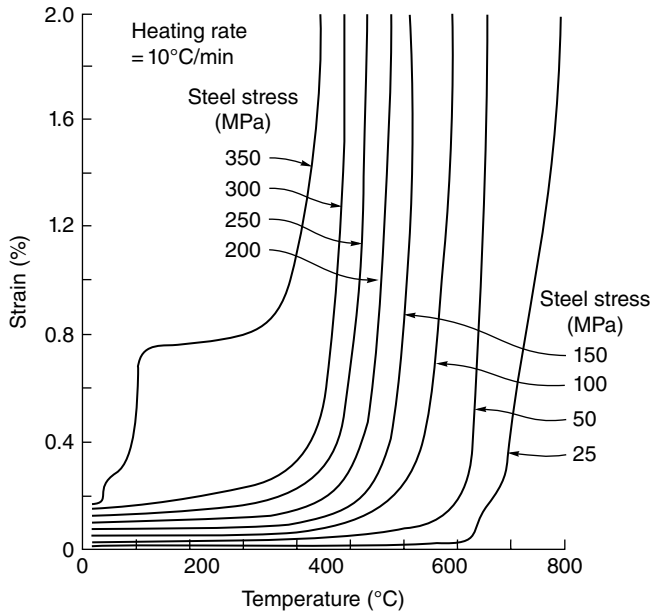


Figure 6.14 Creep of steel tested in tension. Reproduced from Kirby and Preston (1988) with permission from Elsevier Science

scenario. For beams with a thermal gradient through the section, the restraint forces may cause local buckling of the bottom flange, which could help the beam-slab system to sag for enhanced fire resistance. However, for uniformly heated beams the restraint forces may cause global buckling of the beams. Columns, on the other hand, experience increases in load levels when restraint forces are present.

6.4.3 Creep Strain

Creep is relatively insignificant in structural steel at normal temperatures. However, it becomes very significant at temperatures over 400 or 500 °C. Poh (1996) has carried out many experiments on the creep behaviour of steel at elevated temperatures. Figure 6.14 shows the results of transient tests (regime 6 in Figure 5.5) by Kirby and Preston (1988) where it can be seen that the creep is highly dependent on temperature and stress level. The creep deformations accelerate rapidly where the creep strain curve becomes nearly vertical.

Despite the great importance of creep deformations in fire-exposed steel structures which are approaching their collapse loads, creep is not usually included explicitly in the computer-based fire design process because of lack of data and the difficulty of the calculations. The usual assumption is that the stress–strain relationships used for design are ‘effective’ relationships which implicitly include the likely deformations due to creep during the time of fire exposure (CEN, 2005b). On the other hand, Anderberg (1986), Srpčić (1995) and Poh and Bennetts (1995) have shown how creep deformations can be explicitly included in computer models, finding that the effects of creep and the nature of the strain hardening of the material can have a significant influence on predicted behaviour.

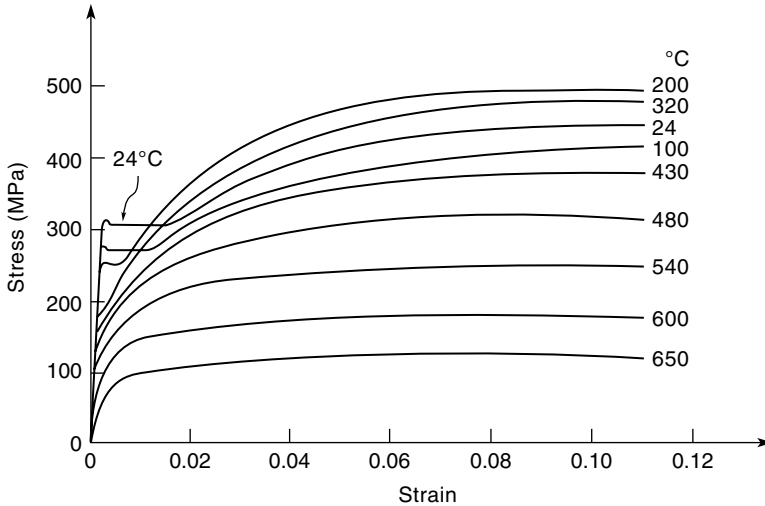


Figure 6.15 Stress–strain curves for typical hot rolled steel at elevated temperature. Adapted from Harmathy (1993)

6.4.4 Stress-related Strain

Stress–strain relationships at elevated temperatures can be obtained directly from steady-state tests at certain elevated temperatures or they can be derived from the results of transient tests such as those shown in Figure 6.14. Typical stress–strain relationships for structural steel at elevated temperatures are shown in Figure 6.15, where it can be seen that yield strength and modulus of elasticity both decrease with increasing temperature, but the ultimate tensile strength increases slightly at moderate temperatures before decreasing at higher temperatures. Similar curves for cold-drawn prestressing steel are shown in Figure 6.16, where there is a less well-defined yield point and slightly different behaviour at elevated temperatures.

6.4.5 Proof Strength and Yield Strength

Design of structural steel members at normal temperatures requires knowledge of the yield strength of the steel. Most normal construction steels have a very well-defined yield strength at normal temperatures, but this disappears at elevated temperatures, as shown in Figure 6.15. Figure 6.17 is a sketch of stress–strain relationships for a typical steel, showing a well-defined yield strength at normal temperatures and a much softer curve at elevated temperatures. A value of yield strength is required for design at elevated temperatures. Kirby and Preston (1988) recommend using the 1% proof strength as the effective yield strength in fire engineering calculations. In Figure 6.17 the line AB has been constructed so that it passes through 1% strain on the x-axis and is parallel to the linear elastic portion of the 400 °C curve. The vertical value of point B is defined as the 1% proof strain. This could be done for any level of proof strain at any steel temperature.

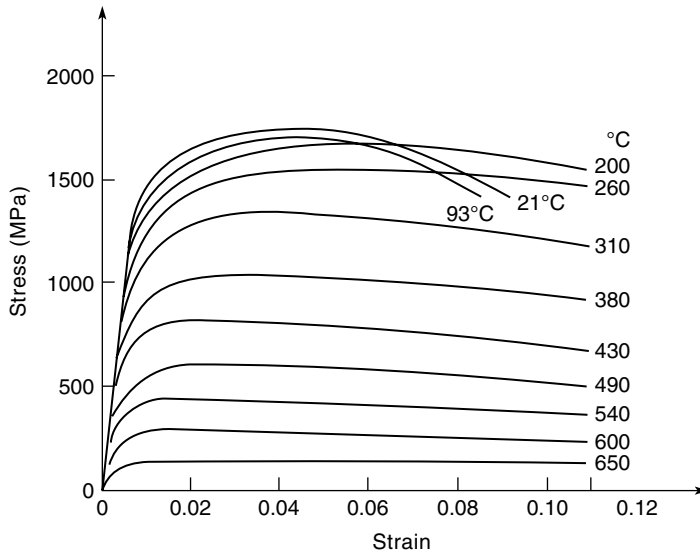


Figure 6.16 Stress–strain curves for prestressing steel at elevated temperature. Adapted from Harmathy (1993)

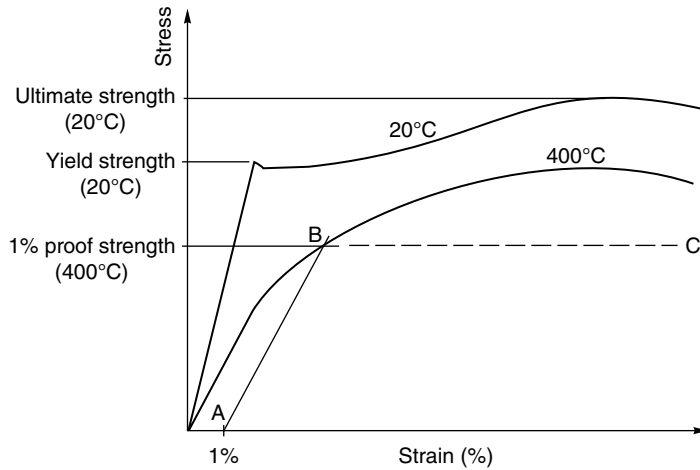


Figure 6.17 Stress–strain curves for steel illustrating yield strength and proof strength

6.4.6 Design Values

Test reports of steel properties at elevated temperatures show considerable scatter. Harmathy (1993) reviewed a large amount of literature, resulting in Figure 6.18 and Figure 6.19 which show the scatter in published data for hot-rolled steel and cold-worked steel, respectively. Some of this scatter may be due to lack of a clear definition of yield strength, as discussed above. The dotted straight lines in these figures show suggested values for design (IStructE, 1978).

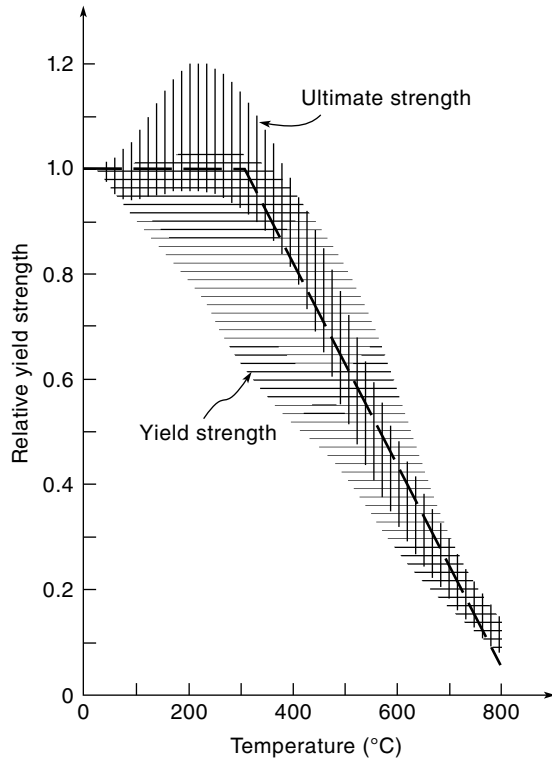


Figure 6.18 Scatter in published results of hot-rolled steel. Adapted from Harmathy (1993)

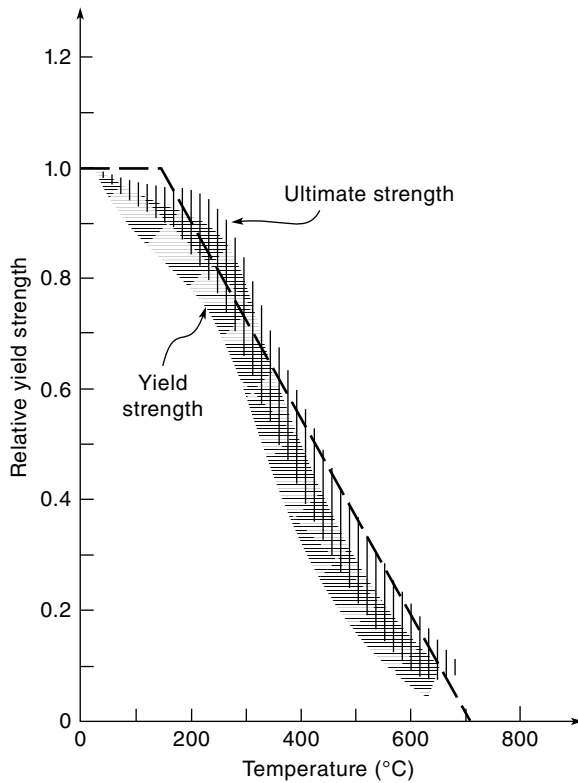


Figure 6.19 Scatter in published results of cold-worked steel. Adapted from Harmathy (1993)

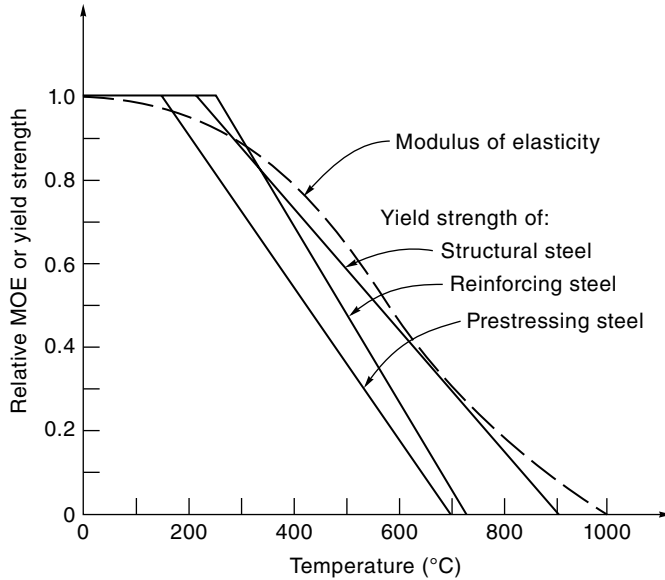


Figure 6.20 Design curves for reduction in yield strength and modulus of elasticity of with temperature

For design purposes, many national codes have proposed slightly different approximations to the published test data. Typical relationships are shown in Figure 6.20, where the line for structural steel is from AS 4100 and NZS 3404, and the lines for reinforcing steel and prestressing steel are from BS 8110, AS 3600 and NZS 3101. The equations of the lines (below $k_{y,T}=1.0$) are:

$$\begin{aligned}
 k_{y,T} &= (905 - T)/690 && \text{structural steel} \\
 k_{y,T} &= (720 - T)/470 && \text{reinforcing steel} \\
 k_{y,T} &= (700 - T)/550 && \text{prestressing steel}
 \end{aligned}
 \tag{6.7}$$

where $k_{y,T}$ is the ratio of $f_{y,T}$ (the yield strength at elevated temperature) to f_y (the yield strength at 20°C).

The relationships in Equation 6.7 can be reversed to give the limiting temperature for a given load ratio r_{load} . The limiting temperature is that at which an individual steel member is expected to fail, assuming no load sharing or redundant behaviour. The limiting temperatures are given by:

$$\begin{aligned}
 T_{lim} &= 905 - 690r_{load} && \text{structural steel} \\
 T_{lim} &= 720 - 470r_{load} && \text{reinforcing steel} \\
 T_{lim} &= 700 - 550r_{load} && \text{prestressing steel}
 \end{aligned}
 \tag{6.8}$$

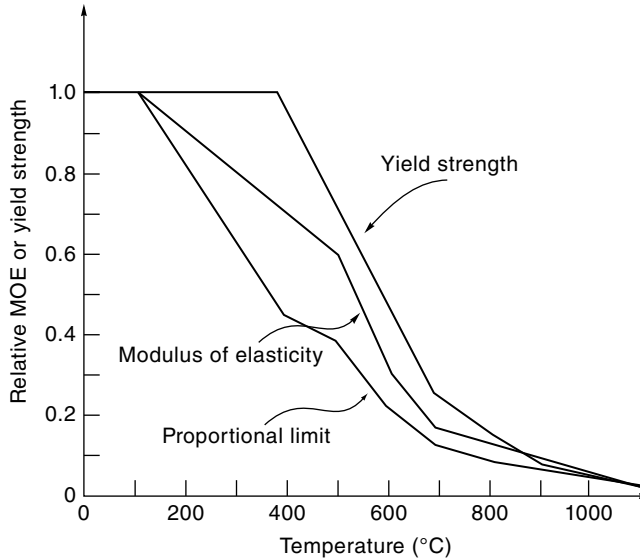


Figure 6.21 Reduction in yield strength and modulus of elasticity with temperature. Reproduced from CEN (2005b). © CEN, reproduced with permission

Similar curves from Eurocode 3 are shown in Figure 6.21. The reduction in modulus of elasticity is defined by a number of points. Eurocode 3 gives an expression for critical temperature, from which an approximate curve for the reduction in yield strength is:

$$k_{y,T} = \left(0.9674 \left\{ 1 + \exp \left[\frac{T - 482}{39.19} \right] \right\} \right)^{-1/3.833} \quad (6.9)$$

The structural Eurocodes for steel (CEN, 2005b) and concrete (CEN, 2004a) have more detailed expressions, with equations for the stress–strain relationship of various steels, both with and without strain hardening included. These have not been quoted here in the interests of providing a consistent document but they can be consulted as necessary. It is interesting to note that the curves used for reduction in yield strength in various countries are quite different, as seen by a comparison of Figure 6.20 and Figure 6.21, even though the materials are very similar. This may be more to do with different definitions of yield strength than differences in materials.

6.4.7 Modulus of Elasticity

The modulus of elasticity is needed for buckling calculations. The modulus of elasticity is also required for elastic deflection calculations, but these are rarely attempted under fire conditions because elevated temperatures lead rapidly to plastic deformations. The reduction in modulus of elasticity shows the same trend as the reduction in yield strength. There can be obvious numerical difficulties if both properties do not reach zero at the same temperature (as shown in Figure 6.20). The Eurocode 3 reduction in modulus of elasticity with temperature is

shown in Figure 6.21, with some nominal strength and stiffness up to 1200 °C. In AS 4100 and NZS 3404 the relationship for modulus of elasticity is given by the curve shown in Figure 6.20, with the equation given by:

$$\begin{aligned} k_{E,T} &= 1.0 + T / [2000 \ln(T/1100)] & 0 < T \leq 600^\circ\text{C} \\ &= 690(1 - T/1000) / (T - 53.5) & 600 < T \leq 1000^\circ\text{C} \end{aligned} \quad (6.10)$$

where $k_{E,T}$ is the ratio of E_T (the modulus of elasticity at elevated temperature) to E (the modulus of elasticity at 20 °C).

6.4.8 Residual Stresses

Residual stresses are internal stresses which exist in unloaded steel members, resulting from the hot rolling manufacturing process. Residual stresses do not usually have a significant effect on the ultimate load capacity of steel structures at normal temperatures, and even less during fire exposure. Sophisticated computer-based structural analysis models used for fire design of large structures can include the effects of residual stresses, and can accurately assess their effects on structural performance if necessary.

6.5 Design of Steel Members Exposed to Fire

6.5.1 Design Methods

There are two main techniques for structural design of steel structures exposed to fire: the *simplified method* for single elements; and *advanced calculation methods* for restrained members, more complex assemblies, or large frames (CEN, 2005b). The simplified method is described in this section, and advanced calculation methods are described in Chapter 11.

6.5.1.1 Verification

As for members of any material, verification in the strength domain requires that

$$U_{fire}^* \leq R_{fire} \quad (6.11)$$

where U_{fire}^* is the design force resulting from the applied load at the time of the fire and R_{fire} is the load-bearing capacity in the fire situation.

Fire limit state loads have been described in Chapter 5. Design forces are obtained from the applied loads by conventional structural analysis. Calculations of the load capacity are described below, based on the mechanical properties of steel at elevated temperatures. The design force U_{fire}^* may be axial force N_{fire}^* , bending moment M_{fire}^* or shear force V_{fire}^* occurring singly or in combination, with the load capacity calculated accordingly as axial force N_f , bending moment M_f or shear force V_f in the same combination.

Note that that Equation 6.11 does not include a partial safety factor for mechanical properties γ_M (or a strength reduction factor Φ) because both have a value of 1.0 in fire conditions,

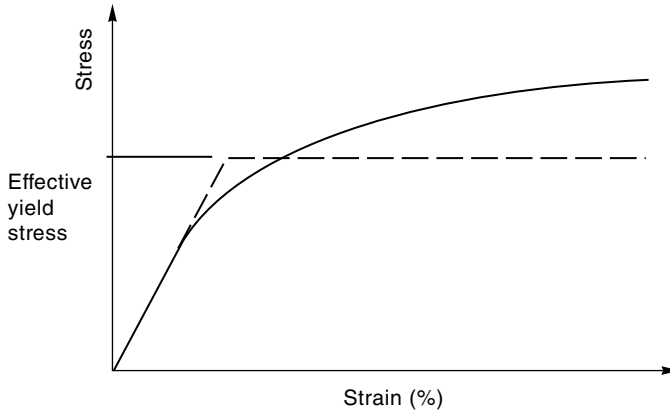


Figure 6.22 Stress–strain curve with elasto-plastic approximation

as described in Chapter 5. The recommendations for member design presented below are based on the simplified method of Eurocode 3 Part 1.2 (CEN, 2005b) presented in a form which allows adaptation to national steel design codes in any country. The simplified method follows the ultimate strength design method as for normal temperatures, except that there are reduced loads for the fire condition and reduced values of modulus of elasticity and yield strength of steel at elevated temperatures. The effects of restraint caused by thermal deformations are not included.

Flexural continuity can be included by ensuring that the collapse mechanism, formed after plastic hinges occur, has sufficient strength to resist the fire limit state loads. Design of steel structures is based on the assumption that steel is ductile, with a long flat yield plateau, so that under fire conditions the stress–strain relationship follows the dashed line in Figure 6.22, rather than the actual solid curve. Such design will be conservative if the actual curve rises much above the assumed straight line, depending on the criteria for deriving the ‘effective yield strength’ from the actual stress–strain relationship (Figure 6.17).

Structural design at normal temperatures requires prevention of collapse (the ultimate limit state) and preventing excessive deformations (the serviceability limit state). Much of the effort in the normal temperature design process is to ensure that excessive deformations do not occur. Design for fire resistance is mainly concerned with preventing collapse. Large deformations are expected under severe fire exposure, so they are not normally calculated unless they are going to affect the structural performance.

6.5.2 Design of Steel Tensile Members

Single tensile members are relatively simple elements to design because there is no possibility of buckling and the stresses are often uniform over the cross section. The design equation is given by:

$$N_{fire}^* \leq N_f \quad (6.12)$$

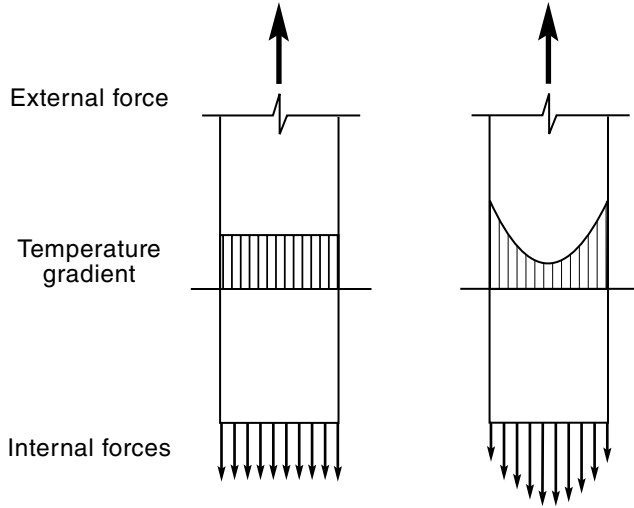


Figure 6.23 Internal forces in a steel tensile member

Design for fire depends on whether the temperature is uniform over the cross section. If the temperature is uniform, the tensile load-bearing capacity is obtained from:

$$N_f = Ak_{y,T}f_y \tag{6.13}$$

where A is the cross-sectional area (mm^2), $k_{y,T}$ is the reduction factor for yield strength of the steel at temperature T and f_y is the yield strength of the steel at $20\text{ }^\circ\text{C}$ (MPa).

In the unlikely event that there is a temperature gradient over the cross section, the strength of the member can be obtained by summing the contributions of the respective parts, considering the temperature-reduced yield strength of each part. This equation, and others to follow, is based on the assumption that steel is a ductile material, so that sufficient elongation can occur for each elemental area to develop its yield strength. The equation is:

$$N_f = \sum_{i=1,n} A_i k_{y,T_i} f_y \tag{6.14}$$

where A_i is an elemental area of the cross section with a temperature T_i and k_{y,T_i} is the reduction factor for yield strength of the steel at temperature T_i .

If there is a temperature gradient over the cross section, it is conservative to assume that the whole of the cross section is at the maximum temperature. Figure 6.23 shows the distribution of internal forces at ultimate load for an idealised rectangular steel tension member with a uniform and non-uniform temperature gradient.

6.5.3 Design of Simply Supported Steel Beams

The design equation for flexure is given by:

$$M_{fire}^* \leq M_f \tag{6.15}$$

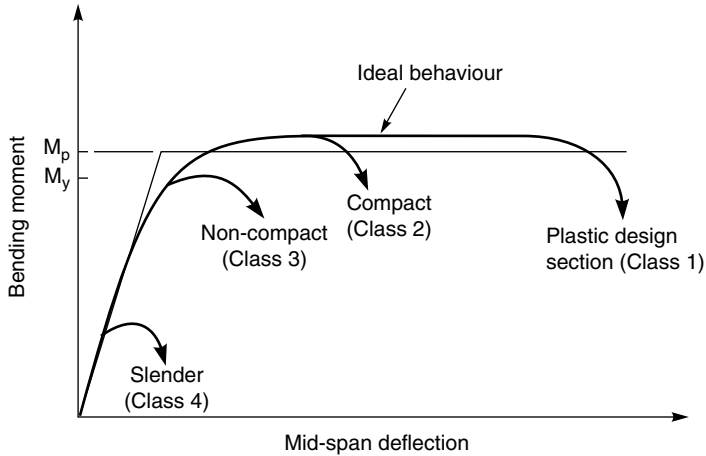


Figure 6.24 Moment–deflection relationship for a steel beam

As with tension members, the strength of bending members in fire depends on whether the temperature is uniform over the cross section. An additional consideration for beams is the susceptibility of the cross section to local buckling. If the temperature is uniform, the design load-bearing capacity is obtained from:

$$\begin{aligned} M_f &= Sk_{y,T}f_y \quad (\text{plastic design}) \\ M_f &= Zk_{y,T}f_y \quad (\text{elastic design}) \end{aligned} \quad (6.16)$$

where S is the plastic section modulus (mm^3), Z is the elastic section modulus (mm^3), $k_{y,T}$ is the reduction factor for yield strength of the steel at temperature T and f_y is the yield strength of the steel at 20°C (MPa).

The decision whether to use the elastic or plastic design equation depends on the compactness of the selected cross section. Figure 6.24 shows a plot of mid-span moment versus deflection for a simply supported steel beam (Kulak *et al.*, 1995), showing how excellent plastic behaviour can be achieved for compact sections, but not for others.

The equation for plastic design applies if the shape of the steel section allows full plastic moment to be achieved without local buckling occurring (Class 1 or Class 2 section in Canada or Eurocodes, or ‘compact’ section in Australian codes). The equation for elastic design should be used for steel sections where only the elastic moment can be achieved without local buckling occurring (Class 3 or ‘non-compact’ section). For light cold-rolled sections vulnerable to local buckling (Class 4), a simple design approach is to ensure that the steel temperature does not exceed 350 or 400°C as described in Chapter 10.

If there is a temperature gradient over the cross section, there are several options for design. The most accurate method is to calculate the temperature of each part, so that the strength of the member can be obtained by summing the contributions of the respective parts, considering the temperature-reduced yield strength of each part, to give:

$$M_f = \sum_{i=1,n} A_i z_i k_{y,T,i} f_y \quad (6.17)$$

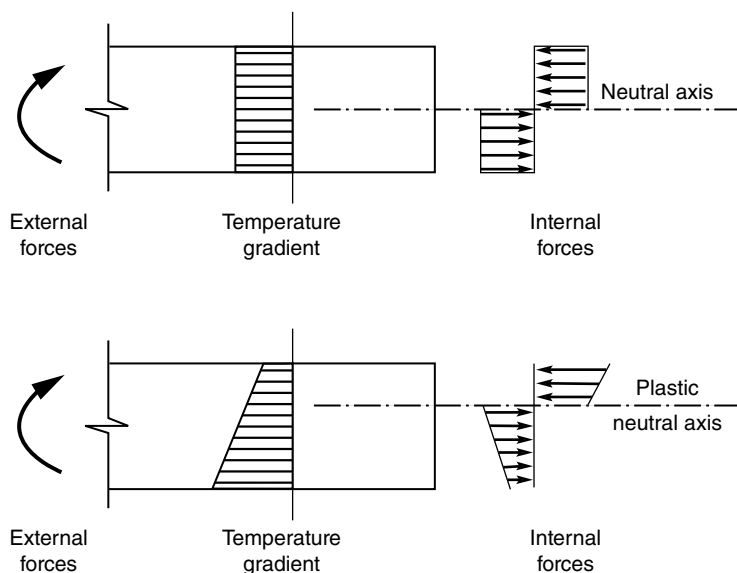


Figure 6.25 Internal forces in a steel flexural member

where z_i is the distance from the plastic neutral axis to the centroid of the elemental area A_i and the other terms are as defined above.

The plastic neutral axis of a flexural section with a non-uniform temperature distribution is the axis perpendicular to the plane of bending such that the elemental areas yielding in tension and compression on either side of the axis are in equilibrium. The axis is then located such that

$$\sum_{i=1,n} A_i k_{y,Ti} f_y = 0 \quad (6.18)$$

Figure 6.25 shows the distribution of internal forces for plastic design of a simple rectangular flexural member with a uniform and non-uniform temperature gradient.

If the temperature gradient over the cross section is known, it is conservative to assume that the whole of the cross section is at the maximum temperature. If the top surface of the beam is protected from fire by a concrete slab, Eurocode 3 Part 1.2 (CEN, 2005b) allows the strength calculated using the maximum temperature to be increased by a factor 1/0.7. This increase does not apply if the temperature of the steel is calculated using a lumped mass method.

If the beam is statically indeterminate, with continuity at the supports, Eurocode 3 Part 1.2 (CEN, 2005b) allows the calculated strength to be increased by another empirical factor to allow for the steel temperature being lower in the support region than in the span of the beam, resulting from heat conduction into the columns or other supports. The factor is 1/0.85 for four-sided exposure or 1/0.60 if the top surface of the beam is protected from fire by a concrete slab.

6.5.4 Lateral-torsional Buckling

Lateral-torsional buckling must be considered for beams. Slender beams with no lateral restraint to the compression flange can fail by buckling before the flexural capacity of the cross section is reached. Lateral-torsional buckling does not occur if the compression edge is restrained against lateral movement, or if the cross section is reasonably compact and the slenderness is not too large. In typical design of steel beams, buckling is allowed for with a strength reduction factor, or buckling factor, which reduces the design strength by an amount depending on the unrestrained length of the beam and the compactness of the cross section.

The Eurocode provisions (CEN, 2005b) permit buckling to be ignored for well restrained fire-exposed beams of Class 1 or Class 2 cross sections. For beams with larger distances between locations of lateral restraint, the flexural capacity, allowing for buckling, is calculated by:

$$M_f = \chi_{LT,fi} S k_{y,T.com} f_y \quad (6.19)$$

where

$$\chi_{LT,fi} = \frac{1}{\phi_{LT,T.com} + \sqrt{[\phi_{LT,T.com}]^2 - [\bar{\lambda}_{LT,T.com}]^2}}$$

with

$$\phi_{LT,T.com} = \frac{1}{2} \left[1 + \alpha \bar{\lambda}_{LT,T.com} + (\bar{\lambda}_{LT,T.com})^2 \right]$$

and $\alpha = 0.65 \sqrt{235/f_y}$

$$\bar{\lambda}_{LT,T.com} = \bar{\lambda}_{LT} \left[k_{y,T.com} / k_{E,T.com} \right]^{0.5}$$

In the above equations, $k_{y,T.com}$ is the yield stress reduction factor for the compression flange of the beam, $k_{E,T.com}$ is the elastic modulus reduction factor for the compression flange and $\bar{\lambda}_{LT}$ is the non-dimensional slenderness at room temperature.

For laterally unrestrained beams, British Standard 5950 (BSI, 2003b) gives a method of calculating the limiting temperature which is about 65 °C lower than for restrained beams. Bailey *et al.* (1996b) used a finite element model to predict that theoretical failure would occur at an even lower temperature than the limiting temperatures from BS 5950 or Eurocode 3, but they also point out that real beams will often have support conditions which provide considerably more continuity and restraint than assumed in the computer model.

6.5.5 Design for Shear

The design equation to resist a shear force V_{fire}^* during fire is:

$$V_{fire}^* \leq V_f \quad (6.20)$$

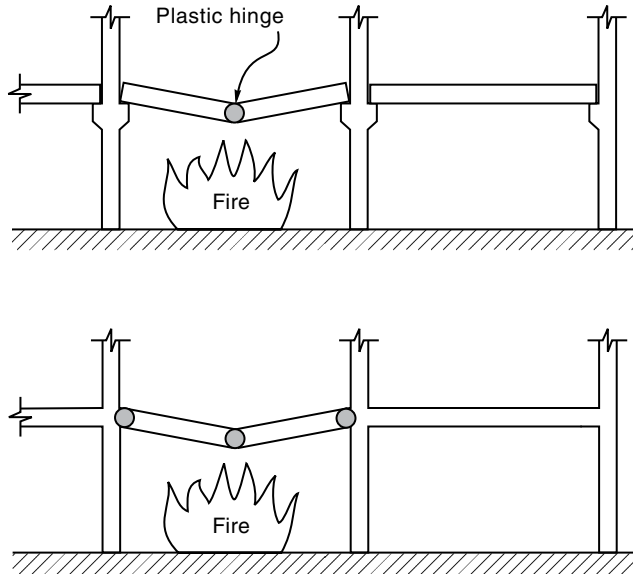


Figure 6.26 Failure mechanisms for simply supported and continuous beams

The design shear resistance V_f under fire conditions is calculated from

$$V_f = k_{y,T} V_s \quad (6.21)$$

where V_s is the design shear resistance of the cross section for normal temperature design. If there is a temperature gradient over the cross section, Equation 6.20 should be based on the maximum temperature in the cross section. As for bending, Eurocode 3 allows the shear strength calculated in this way to be increased by a factor 1/0.7 if the top surface of the beam is protected from fire by a concrete slab.

6.5.6 Continuous Steel Beams

Beams which are continuous over several supports or form part of a moment resisting frame are different from simply supported beams in several ways. The main advantage of continuity in fire design is the possibility for considerable moment redistribution during the fire, which can lead to a considerable increase in fire resistance as described in Chapter 5. A possible negative aspect of flexural continuity for steel beams is the lack of lateral restraint to the lower flange of the beam where it is in compression in the negative moment regions near the supports.

With reference to Figure 6.26, a simply supported beam will fail as soon as one plastic hinge forms at the centre, when the flexural strength becomes equal to the applied bending moment. A continuous beam will not fail until three plastic hinges form, which can give greatly increased fire resistance in many cases. The end span of a continuous beam is

intermediate between these two cases, as shown in Figure 5.12. Design of continuous beams is essentially the same as for simply supported beams, but including the redistribution of moments using plastic analysis as described in Chapter 5.

6.5.7 Steel Columns

The design of columns is often more difficult than the design of beams because lateral buckling must usually be considered and the prediction of behaviour is less reliable. If there is a temperature gradient over the cross section, it is not possible to accurately consider the variation of strength segment by segment without a computer program because thermal bowing and instability considerations dominate the behaviour. Following Eurocode 3 Part 1.2 (CEN, 2005b), an approximate design method is based on the assumption that the whole cross section is at the maximum temperature T_{max} . It is important to note that the steel temperature for the calculation must be the maximum temperature, not the average temperature obtained from a lumped mass calculation. This approximate method is not always conservative if the thermal gradient causes significant bowing. Columns with thermal gradients across the section should preferably be analysed with a specialist computer program. The design equation for a column subjected to an axial load N_{fire}^* is:

$$N_{fire}^* \leq N_f \quad (6.22)$$

In the approximate method, the compressive load-bearing capacity is obtained from:

$$N_f = \chi_{fi} A k_{y,Tmax} f_y \quad (6.23)$$

where χ_{fi} is the normal temperature buckling factor, calculated using the effective length for the fire design situation, A is the cross-sectional area (mm^2), $k_{y,Tmax}$ is the reduction factor for yield strength of steel which is at the maximum temperature T_{max} and f_y is the yield strength of the steel at 20 °C (MPa).

The χ_{fi} term is the lesser of the buckling factors with respect to the axis of bending, calculated by:

$$\chi_{fi} = \frac{1}{\phi_T + \sqrt{\phi_T^2 - \bar{\lambda}_T^2}}$$

with

$$\phi_T = \frac{1}{2} \left[1 + \alpha \bar{\lambda}_T + \bar{\lambda}_T^2 \right]$$

and $\alpha = 0.65 \sqrt{235/f_y}$

$$\bar{\lambda}_T = \bar{\lambda} \left[k_{y,T} / k_{E,T} \right]^{0.5}$$

In the above equations $k_{y,T}$ is the yield stress reduction factor for the steel, $k_{E,T}$ is the elastic modulus reduction factor for the steel, and $\bar{\lambda}$ is the non-dimensional slenderness at room temperature.

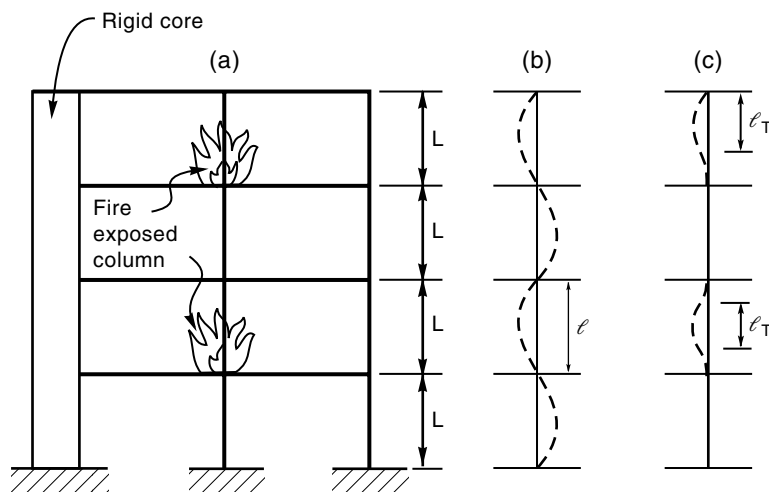


Figure 6.27 Effective lengths of fire exposed columns in a multi-storey frame: (a) section through the building; (b) deformation mode at room temperature; and (c) deformation mode at elevated temperature. Reproduced from CEN (2005b). © CEN, reproduced with permission

The buckling length of a column should usually be calculated in the same way as for normal temperature design. However, in a braced frame, the buckling length may be determined by considering it to have fixity to the columns above and below, as shown in Figure 6.27, provided that the building design is such that the fire is not able to spread to an upper floor.

6.6 Bolted and Welded Connections

Connections must perform as well or better than the members they are connected to, in fire conditions. Bolted connections generally behave well despite the drop in bolt strength with elevated temperatures because connections are often at much lower temperatures than the members they help to support. There has been significant research into connection behaviour at elevated temperatures. Lawson (1990) tested eight beam-to-column connections, with some of the beams supporting composite concrete slabs. All of the connections were exposed to the ISO 834 standard time-temperature curve. Bolt temperatures were found to be lower than those of the exposed flange and the grade 8.8 bolts behaved very well. There were no failures of bolts or welds and the rotations at the connections resulted from local flexural deformation of the end-plates welded to the ends of the beams.

In composite beams, the mesh reinforcing in the slab was found to provide a significant contribution to flexural capacity. Al-Jabri *et al.* (1998) tested a series of bolted connections, also finding that typical connections which are considered to be pinned at normal temperature are capable of resisting considerable bending moments at elevated temperatures. In all tests the deformation was small up to about 400 °C, beyond which there was a progressive increase in rotation. Failure modes were similar to those observed at normal temperatures, generally localized bending or fracture of the end-plates. In composite slabs there was some failure of the reinforcing mesh and the shear studs connecting the slab to the beam. Finite element modelling

of bolted connections in steel, and steel composite construction, is described by Liu (1999). More recent research has focused on optimizing the contribution of connections to the resistance of structural frames. These include tests and the development of the 'component method', which treats a connection as an assembly of uncoupled springs having the characteristics of the various parts of the connection (Block, 2006; Yu *et al.*, 2008, 2009; Wang *et al.*, 2012).

In support of the above observations, Annex D of Eurocode 3 has a simple calculation procedure for the resistance of connections in fire conditions, based on a simple estimation of component temperatures and strength reduction factors for the degradation of bolts and welds at elevated temperatures (CEN, 2005b).

For certain structures, a key component of connection design is to design the connections with sufficient ductility to accommodate large local displacements without significant loss of strength. This can prevent the need to oversize connections for the very high tensile forces which can occur during the decay stage of a fire, especially in buildings with unprotected steel beams acting compositely with concrete floor slabs (Wang *et al.*, 2012).

6.7 Cast-iron Members

Cast-iron was manufactured and used widely in buildings throughout the 19th century, being replaced by rolled steel sections in the early years of the 20th century. Fire engineering assessment of historical buildings sometimes requires calculation of the fire resistance of cast-iron columns or beams. Barnfield and Porter (1984) have confirmed earlier reports that the behaviour of cast-iron under fire conditions is difficult to predict accurately because brittle fracture can occur in some circumstances, usually associated with distortion resulting from applied loads, casting defects, thermal movements of adjacent elements or sudden cooling of the cast iron element. They state that cast-iron elements are unlikely to fail as long as the cast-iron temperature remains below a limiting temperature. The suggested limiting temperature is 300 °C for cast-iron members attached to iron or steel elements, and 550 °C for members attached to timber elements which are likely to impose much lower thermal deformations in a fire. Cast-iron has similar thermal properties to structural steel, so the same methods of thermal analysis can be used. Intumescent paint is the best method of protecting cast-iron members which are intended to remain visible in the finished building.

6.8 Design of Steel Buildings Exposed to Fire

Because most real buildings consist of a combination of materials, guidance on the structural design of steel buildings exposed to fire is covered in Chapter 8, where separate sections are provided for multi-storey steel framed buildings, car-parking buildings and single-storey portal frame buildings.

6.9 Worked Examples

6.9.1 Worked Example 6.1

Calculate the section factor for a steel H-section column, of dimensions 300×300 mm². The column is exposed to fire on all four sides.

Make calculations for (a) box-type protection and (b) spray-on protection.

Given:

Height of section	h	=	300 mm
Width of section	b	=	300 mm
Flange thickness	T	=	20 mm
Web thickness	t	=	8 mm

Calculation:

(a) Box-type protection

Area of cross section	$A = 2(b \times T) + t(h - 2T)$ $= 14080 \text{ mm}^2 = 0.01408 \text{ m}^2$
Volume of 1 m length	$V = A \times 1.0 \text{ m} = 0.01408 \text{ m}^3$
Perimeter of section	$H_p = 2(b + h) = 1200 \text{ mm} = 1.2 \text{ m}$
Surface area of 1 m length	$F = H_p \times 1.0 \text{ m} = 1.2 \text{ m}^2$
Section factor	$H_p/A = H_p/A = 1.2/0.01408 = 85.2 \text{ m}^{-1}$
Section factor	$F/V = F/V = 1.2/0.01408 = 85.2 \text{ m}^{-1}$
Effective thickness	$V/F = 1000/(F/V) = 11.7 \text{ mm}$

(b) Spray-on protection

Perimeter of section	$H_p = 2(b + h + (b - t)) = 1784 \text{ mm} = 1.784 \text{ m}$
Surface area of 1 m length	$F = H_p \times 1.0 \text{ m} = 1.784 \text{ m}^2$
Section factor	$H_p/A = H_p/A = 1.784/0.01408 = 126 \text{ m}^{-1}$
Section factor	$F/V = F/V = 1.784/0.01408 = 126 \text{ m}^{-1}$
Effective thickness	$V/F = 1000/(F/V) = 7.9 \text{ mm}$

6.9.2 Worked Example 6.2

Use the Eurocode method shown in Table 6.1 to calculate the steel temperature of an unprotected beam exposed to the ISO 834 standard fire.

The beam section factors are $F/V = 210 \text{ m}^{-1}$ and $(F/V)_b = 153 \text{ m}^{-1}$. Use a convective heat transfer coefficient h_c of $25 \text{ W/m}^2\text{K}$ and resultant emissivity 0.8. The density of steel is 7850 kg/m^3 and the specific heat varies as given in Equation 6.1.

The first six steps of the solution are shown in the following table. Note that successive time increments for thermal analysis of unprotected steel should not exceed 5 s. The results are plotted in Figure 6.7(a).

Time (s)	Steel temperature, T_s (°C)	Fire temperature, T_f (°C)	Difference in temperature	Change in steel temperature, ΔT_s
0.0	20.0	20.0	0.0	0.0
5	20.0	96.5	76.5	0.5
10	20.5	147.0	126.5	0.8
15	21.3	14.6	163.3	1.1
20	22.4	214.7	192.3	1.4
25	23.8	239.7	215.9	1.6
30	25.4	261.1	235.7	1.8

6.9.3 Worked Example 6.3

Use the Eurocode method shown in Table 6.1 to calculate the steel temperature of a protected beam exposed to the ISO 834 standard fire. The beam is the same as in Worked Example 6.2. The beam is protected with 15 mm of gypsum plaster board, which has thermal conductivity of 0.2 W/mK.

The first six steps of the solution are shown in the following table. Note that successive time increments for thermal analysis of protected steel should not exceed 30 s. The results are plotted in Figure 6.7(a), with another curve for 30 mm of insulation.

Time (s)	Steel temperature, T_s (°C)	Fire temperature, T_f (°C)	Difference in temperature	Change in steel temperature, ΔT_s
0.0	20.0	20.0	0.0	0.0
30.0	20.0	261.1	241.1	0.0
60.0	20.0	349.2	329.2	0.0
90.0	20.0	404.3	384.3	0.2
120.0	20.2	444.5	424.3	1.9
150.0	21.9	476.2	454.3	3.0
180.0	24.9	502.3	477.4	3.8

6.9.4 Worked Example 6.4

Use the spreadsheet method shown in Table 6.1 to calculate the steel temperature of an unprotected beam exposed to a parametric fire. The beam is the same as in Worked Example 6.2. The fire compartment is made from normal weight concrete with density 2300 kg/m³, specific heat 980 J/kgK and thermal conductivity 0.8 W/mK. The room is 6 m by 4 m and 3 m high with one window 3.0 m wide and 2.0 m high. The fuel load is 800 MJ/m² floor area.

Length of room	$l_1 = 6.0 \text{ m}$
Width of room	$l_2 = 4.0 \text{ m}$
Height of room	$H_r = 3.0 \text{ m}$
Area of internal surfaces	$A_i = 2(l_1 l_2 + l_1 H_r + l_2 H_r)$ $= 2(6 \times 4 + 6 \times 3 + 4 \times 3) = 108 \text{ m}^2$
Height of window	$H_v = 2.0 \text{ m}$
Width of window	$B = 3.0 \text{ m}$
Area of window	$A_v = BH_v = 3.0 \times 2.0 = 6.0 \text{ m}^2$
Ventilation factor	$F_v = A_v \sqrt{H_v} / A_i = 6.0 \times \sqrt{2.0} / 108 = 0.08 \text{ m}^{-1/2}$
Fuel load (floor area)	$e_f = 800 \text{ MJ/m}^2$
Fuel load (total area)	$e_t = e_f A_f / A_i = 800 \times 24 / 108 = 178 \text{ MJ/m}^2$
Thermal conductivity	$k = 0.8 \text{ W/mK}$
Density	$\rho = 2300 \text{ kg/m}^3$
Specific heat	$c_p = 980 \text{ J/kgK}$
Thermal inertia	$b = \sqrt{k \rho c_p} = 1343 \text{ W s}^{0.5} / \text{m}^2 \text{K (medium)}$

$$\text{Gamma factor} \quad \Gamma = \frac{(F_v/0.04)^2}{(b/1160)^2} = \frac{(0.08/0.04)^2}{(1343/1160)^2} = 2.879$$

The parametric fire can be calculated using this value of gamma.

The first six steps of the solution are shown in the following table. Note that successive time increments for thermal analysis of unprotected steel should not exceed 5 s. The results are plotted in Figure 6.7(b).

Time (s)	Steel temperature, T_s (°C)	Fire temperature, T_f (°C)	Difference in temperature	Change in steel temperature, ΔT_s
0.0	20.0	20.0	0.0	0.0
5	20.0	67.9	47.9	0.3
10	20.3	112.5	92.2	0.6
15	20.9	153.9	133.0	0.9
20	21.8	192.5	170.7	1.2
25	23.0	228.4	205.4	1.5
30	24.5	261.8	237.3	1.8

6.9.5 Worked Example 6.5

Repeat Worked Example 6.4 with the beam protected with 15 mm of insulation, as in Worked Example 6.3.

The first six steps of the solution are shown in the following table. Note that successive time increments for thermal analysis of protected steel should not exceed 30 s. The results are plotted in Figure 6.7(b), with another curve for 30 mm of insulation.

Time (s)	Steel temperature, T_s (°C)	Fire temperature, T_f (°C)	Difference in temperature	Change in steel temperature, ΔT_s
0.0	20.0	20.0	0.0	0.0
30.0	20.0	261.8	241.8	0.0
60.0	20.0	419.4	399.4	0.0
90.0	20.0	523.4	503.4	0.0
120.0	20.0	593.3	573.3	0.4
150.0	20.4	641.4	621.4	4.2
180.0	24.6	675.7	655.7	5.3

6.9.6 Worked Example 6.6

Fire calculation in strength domain

For a simply supported steel beam of known span, load, yield strength, and section properties, calculate the flexural strength after exposure for 15 min to the standard fire. The beam has no applied fire protection.

Given:

Dead load	$G_k = 8.0 \text{ kN/m}$ (including self-weight)
Live load	$Q_k = 15.0 \text{ kN/m}$
Beam span	$L = 8.0 \text{ m}$
Beam size	410 UB 54 (410 mm deep Universal Beam, 54 kg/m)
<i>This is a 'compact' section (type 1)</i>	
Plastic section modulus	$S = 1060 \times 10^3 \text{ mm}^3$
Section factors:	
Area to volume ratio	$F/V = 192 \text{ m}^{-1}$, $(F/V)_b = 143 \text{ m}^{-1}$

Cold calculations:

Strength reduction factor	$\Phi = 0.9$
Yield strength	$f_y = 300 \text{ MPa}$
Design load (cold)	$w_c = 1.2 G_k + 1.5 Q_k = 32.1 \text{ kN/m}$
Bending moment	$M_{cold}^* = w_c L^2 / 8 = 257 \text{ kNm}$
Bending strength	$M = S f_y = 318 \text{ kNm}$ (assume adequate lateral restraint)
Design flexural strength	$\Phi M = 286 \text{ kNm}$
Design is OK ($M_{cold}^* < \Phi M$).	

Fire calculations:

Strength reduction factor	$\Phi = 1.0$ (hence not used in the calculations)
Design load (fire)	$w_f = G_k + 0.4 Q_k = 14.0 \text{ kN/m}$
Bending moment	$M_{fire}^* = w_c L^2 / 8 = 112 \text{ kNm}$
Using the Eurocode method, the temperature of the beam at 15 min, $T = 640^\circ \text{C}$	
Yield strength reduction	$k_{y,T} = (905 - T) / 690 = 0.38$
Flexural capacity	$M_f = S k_{y,T} f_y$ (assume adequate lateral restraint)
	$= 1060 \times 10^3 \times 0.38 \times 300 / 10^6 = 121 \text{ kNm}$

Design is OK ($M_{fire}^* < M_f$).

6.9.7 Worked Example 6.7

Fire calculation in time domain

For a simply supported steel beam of known span, load, yield strength, and section properties, calculate the time to failure when exposed on three sides to the standard fire.

(a) Unprotected and (b) protected with insulation of known thickness and properties.

Given:

Dead load	$G_k = 6.0 \text{ kN/m}$ (including self-weight)
Live load	$Q_k = 12.5 \text{ kN/m}$
Beam span	$L = 15.0 \text{ m}$
Beam size	610UB125 (610 mm deep Universal Beam, 125 kg/m)
<i>This is a 'compact' section (type 1)</i>	
Plastic section modulus	$S = 3680 \times 10^3 \text{ mm}^3$

Section factors:

$$\begin{aligned} \text{Area to volume ratio} \quad F/V &= 118 \text{ m}^{-1} \\ (F/V)_b &= 91 \text{ m}^{-1} \end{aligned}$$

Cold calculations:

$$\begin{aligned} \text{Strength reduction factor} \quad \Phi &= 0.9 \\ \text{Yield strength} \quad f_y &= 300 \text{ MPa} \\ \text{Design load (cold)} \quad w_c &= 1.2 G_k + 1.5 Q_k = 26 \text{ kN/m} \\ \text{Bending moment} \quad M_{cold}^* &= w_c L^2 / 8 = 731 \text{ kNm} \\ \text{Bending strength} \quad M &= S f_y = 1104 \text{ kNm} (= R_{cold}) \end{aligned}$$

(assume adequate lateral restraint)

$$\text{Design flexural strength} \quad \Phi M = 994 \text{ kNm}$$

Design is OK ($M_{cold}^* < \Phi M$).

Fire calculations:

$$\begin{aligned} \text{Design load (fire)} \quad w_f &= G_k + 0.4 Q_k = 11 \text{ kN/m} \\ \text{Bending moment} \quad M_{fire}^* &= w_c L^2 / 8 = 309 \text{ kNm} \\ \text{Load ratio} \quad r_{load} &= M_{fire}^* / R_{cold} = 309 / 1104 = 0.28 \\ \text{Limiting steel temperature} \quad T_{lim} &= 905 - 690 r_{load} = 712^\circ\text{C} \end{aligned}$$

(a) Unprotected steel (three-sided exposure)

Using the Eurocode method, the time for the beam to reach the limiting temperature

$$t = 23.4 \text{ min}$$

Design is OK if the equivalent fire severity is no more than 23 min.

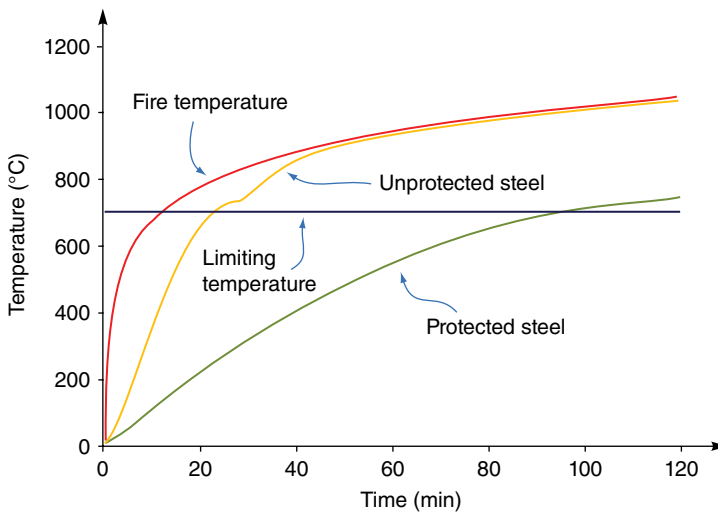


Figure 6.28 Temperature–time relationship of protected and unprotected steel in the standard fire

(b) Protected steel

Using the Eurocode method with sprayed mineral fibre protection ($\rho=300 \text{ kg/m}^3$, $k_i=0.12 \text{ W/mK}$ and $c_p=1200 \text{ J/kgK}$)

Thickness of insulation	$d_i=0.010 \text{ m}$ (10 mm)
The time for the protected beam to reach the limiting temperature	$t=96 \text{ min}$
Moisture content of insulation	$m=1\%$
Time delay for insulation	$t_v = m\rho_i d_i^2 / 5k_i$ $t_v = 1 \times 300 \times 0.01^2 / 5 \times 0.12 = 0.05 \text{ min} < 1.0 \text{ min}$
Total time	total = $t + t_v = 96 \text{ min}$

Design is OK if the equivalent fire severity is no more than 96 min. Refer to Figure 6.28 for the temperature–time relationship for the unprotected and protected steel heating profiles.

(Note: The flexural calculation method would be identical.)

7

Concrete Structures

This chapter describes simple methods of designing reinforced concrete structures to resist fires, including information on thermal and mechanical properties of concrete at elevated temperatures. Prestressed concrete structures are also covered briefly.

7.1 Behaviour of Concrete Structures in Fire

Concrete structures have a reputation for good behaviour in fires. A very large number of reinforced concrete buildings which have experienced severe fires have been repaired and put back into use as shown in Figure 7.1. Concrete is non-combustible and has a low thermal conductivity. The cement paste in concrete undergoes an endothermic reaction when heated, which assists in reducing the temperature rise in fire-exposed concrete. Concrete tends to remain in place during a fire, with the cover concrete protecting the reinforcing steel, with the cooler inner core continuing to carry load (Figure 7.2).

Calculation of the behaviour of concrete structures in fire depends on many factors, the most important being the fire limit state loads on the structure, the elevated temperatures in the concrete and reinforcing steel and the mechanical properties of the steel and concrete at those elevated temperatures. When a reinforced concrete structure is exposed to a fire, the temperatures of both steel and concrete increase, leading to increased deformation and possible failure, depending on the applied loads and the support conditions. Most types of concrete behave similarly in fires. This chapter refers to slightly different performance of concrete made with different types of aggregate, lightweight concrete and high strength concrete.

Catastrophic failures of reinforced concrete structures in fire are rare, but some occasionally occur as shown in Figure 7.3 (e.g. Papaioannou, 1986; Berto and Tomina, 1988). Observations have shown that when concrete buildings fail in fires, it is seldom because of the loss of strength



Figure 7.1 Non-structural fire damage to a typical reinforced concrete office building

of the materials, but nearly always because of the inability of other parts of the structure to absorb the large imposed thermal deformations which can cause shear or buckling failures of columns or walls (Van Acker, 2010).

7.2 Concrete Materials in Fire

7.2.1 Normal Weight Concrete

Most of this chapter refers to normal weight concrete which is made from gravel and sand aggregate and cement paste. Compressive strength is usually in the range from 20 to 50 MPa, and the density is about 2300 kg/m³. Normal weight concrete is generally cast in place, or it may be poured in a precasting yard and transported to the construction site after curing.

7.2.2 High Strength Concrete

There is considerable interest in high strength concrete as a high performance construction material. High strength concrete contains additives such as silica fume and water-reducing admixtures which result in compressive strength in the range from 50 to 120 MPa. An extensive survey of high strength concrete properties at elevated temperatures by Phan (1996) shows that they tend to have a higher rate of strength loss than normal concrete properties at temperatures up to 400 °C, and explosive spalling is a problem in some cases. Fire tests on high strength columns are reported by Aldea *et al.* (1997) and Kodur (1997). In some studies,

(a)



(b)



Figure 7.2 (a) A multi-storey office building engulfed in flames. The reinforced concrete structure did not collapse in the fire (Sao Paolo, Brazil, 1972). (b) Severe spalling of a reinforced concrete wall in the fire



Figure 7.3 Major structural damage to a multi-storey reinforced concrete department store (Athens, Greece, 1980). Reproduced from Papaioannou (1986) by permission of John Wiley & Sons, Ltd

the compressive strength at elevated temperatures is found to be higher when the concrete is heated under stress, rather than when loaded after heating. Design recommendations are given by Tomasson (1998) who recommends the simplified method of Eurocode 2 Part 1.2 (CEN, 2004a), ignoring the strength contribution of concrete which is hotter than 500 °C. For high strength concrete columns, he suggests changing the limiting temperature to 400 °C.

7.2.3 *Lightweight Concrete*

Lightweight concrete is usually made with normal cement and some form of lightweight aggregate such as pumice or expanded clay or shale. Other possible materials to use include perlite and vermiculite. Lightweight concrete has been shown to have excellent fire resistance,

due to its low thermal conductivity compared with normal weight concrete. Many listings of generic fire resistance ratings have separate tables for lightweight concrete. Many lightweight aggregates have been manufactured at high temperatures, so they remain very stable during fire exposure.

7.2.4 *Steel-fibre Reinforced Concrete*

Steel-fibre reinforced concrete uses small steel fibres added to the concrete mix, to improve concrete toughness and strength. The fibres are typically 0.5 mm diameter, and 25–40 mm long with crimped or hooked ends to improve the bond. Thermal and mechanical properties of steel-fibre reinforced concrete at elevated temperatures are given by Lie and Kodur (1996). They show that the presence of steel fibres increases the ultimate strain and improves the ductility of the concrete.

7.2.5 *Masonry*

Concrete masonry usually consists of hollow concrete blocks mortared together, most often used in walls. In many areas, especially seismic regions, reinforcing bars are placed in the hollow cores which are then filled with concrete to create solid reinforced concrete masonry which has essentially the same fire behaviour as reinforced concrete. Concrete masonry blocks are often manufactured from lightweight concrete, giving enhanced fire resistant properties.

Fire resistance ratings of many different types of concrete masonry are given by Allen (1970). Unfilled unreinforced hollow masonry has less thermal mass and potential lines of integrity failure at the mortar joints, but has demonstrated excellent fire resistance, provided that the foundations and supporting structure can keep the wall in place during the anticipated fire. Hollow core concrete masonry walls can be considered to have equivalent thickness to a solid wall of the same volume of concrete, and to have the same generic fire resistance rating (NBCC, 2010). All joints between blocks and shrinkage control joints must be able to provide the same fire rating as the rest of the wall. Some construction details are given in the Uniform Building Code (ICC, 2015). Some methods for fire design of concrete masonry are given in Eurocode 6 (CEN, 2005d).

Brick masonry also behaves well in fires. Ceramic bricks are made by firing clay at high temperatures, producing bricks which remain stable when exposed to fires. Brick masonry can be reinforced if it is made from hollow bricks, but most brick masonry consists of solid bricks joined only with lime or cement mortar. Thermal bowing of very tall unreinforced cantilever masonry walls can lead to collapse during a severe fire on one side of the wall (Cooke, 1988) as shown in Figure 8.17.

7.2.6 *Prestressed Concrete*

The term *prestressed concrete* refers to concrete structures which are stressed prior to the application of any external loads. There are two main types of prestressed concrete: *pre-tensioned* concrete; and *post-tensioned* concrete. For pre-tensioned prestressed concrete, the steel tendons are stressed in tension against a reaction frame or mould before the concrete is cast,

so that the prestressing force is resisted by bond stresses between the concrete and the tendon when the tendons are cut, after the concrete has cured. Post-tensioned prestressed concrete is cast with ducts for the steel tendons which are stressed with hydraulic jacks after the concrete has cured. The prestressing force is resisted by permanent anchorage points.

Pre-tensioning is most often used for precast components for flooring, including flat panels, hollow core panels, double-tee floors or precast concrete planks. Post-tensioning is used in larger components such as beams, slabs or bridges, or for connecting several precast concrete elements together. Prestressing tendons are made of high strength steel, often manufactured by pulling steel wires through a die, or otherwise cold-working the steel. Cold-worked steel suffers permanent loss of strength when subjected to elevated temperatures.

Most of this chapter refers to reinforced concrete, but the same principles apply to prestressed concrete which is often more vulnerable in fires for three reasons: prestressing steel tendons are much more sensitive to elevated temperatures than mild steel reinforcing bars; prestressed concrete is often manufactured in slender components with thin cover concrete and little or no shear reinforcing; and some failure modes such as debonding, shear and spalling are more critical in prestressed concrete (Gustaferro and Martin, 1988).

Full-scale fire tests have shown that bond failures of pre-tensioned tendons have caused premature failures long before the calculated fire resistance time. A series of tests on double-tee and hollow core slabs, simply supported without axial restraint over a span of 6 m, showed that the ends of the tendons were pulled into the concrete due to loss of bond near the ends of the specimens (Andersen and Lauridsen, 1999). In these tests, collapse resulted from shear failure in the webs after the compressive stresses had been reduced near the ends of the slabs. Similar results for hollow core slabs have been observed elsewhere (Fontana and Borgogno, 1995). Pre-tensioned hollow core slabs have often performed poorly in fires because the only steel reinforcing is the longitudinal prestressing tendons, with no transverse reinforcing in the flanges or shear reinforcing in the webs (Fellinger, 2004; Bailey and Lennon, 2008). More recent research on hollow core slabs has looked at shear and anchorage failure (Fellinger, 2004) and the different ways these slabs may be modelled. The models have looked at grillage models for simulating two-way behaviour (Chang, 2007) to the connections between hollow core slabs and their supporting structure (Min, 2012).

7.2.7 *External Reinforcing*

Various forms of external reinforcing are used in special structures. The most common is steel decking used as permanent formwork in composite construction (Figure 8.10). Design of composite steel decking exposed to fires is described in Chapter 8.

The use of external fibre-epoxy coatings is another form of external reinforcing. This is new technology, increasingly being used to improve the strength of existing reinforced concrete structures. The fibre-epoxy coatings consist of mats of glass, carbon or Teflon fibres surrounded by epoxy resin. These fibre-epoxy coatings can be wrapped around columns to improve the confinement to the concrete or can be glued to the surface of beams to increase the flexural strength. External fibre-epoxy coatings provide no additional fire resistance because the epoxy will melt and burn away at low temperatures. However, the residual reinforced concrete structure will usually have sufficient strength to carry the fire limit state loads, and the coating can be re-applied after a fire.

7.3 Spalling of Cover Concrete

7.3.1 Cover

‘Cover concrete’ refers to the concrete outside the main reinforcing cage, protecting the reinforcing steel from moisture, corrosion and fire. Reinforced concrete structures rely on the cover concrete to protect the reinforcing steel from elevated temperatures during fires. The ‘cover’ is the distance from the surface of the concrete to the reinforcing steel. For durability considerations, the cover is usually measured from the concrete surface to the closest face of the main bars, but most fire engineering calculations use the ‘axis distance’ measured from the concrete surface to the centre of the main bars. Care must be taken to avoid confusing these two definitions.

7.3.2 Spalling

The design recommendations in this book, for calculating thermal gradients and structural behaviour in concrete members, are based on the assumption that all the concrete remains intact for the duration of the fire. This assumption is not valid if the cover concrete spalls off during a fire, exposing some or all of the reinforcing steel to the fire. Experiments and real fire experience have shown that most normal weight concrete members can withstand severe fires without serious spalling, but minor spalling often occurs (Figure 7.4).



Figure 7.4 Local spalling at the corner of a concrete beam

The phenomenon of spalling is not well understood because it is a function of several different factors, often leading to unpredictable behaviour. In some cases, spalling is related to the type of aggregate or to thermal stresses near corners, but it is more often linked to the behaviour of the cement paste. It is generally agreed that spalling most often occurs when water vapour is driven off from the cement paste during heating, with high pore pressures creating effective tensile stresses in excess of the tensile strength of the concrete. Experiments have shown that increased susceptibility to spalling results from high moisture content, rapid rates of heating, slender members, and high concrete stresses at the time of the fire. Malhotra (1984), Phan (1996), and Purkiss and Li (2013) review studies of spalling. Recent research suggests that spalling is initiated by high compressive stresses, and further enhanced by high pore water pressures (Jansson, 2013). High strength concrete tends to be more susceptible to spalling than normal concrete since it has higher compressive stresses and smaller free pore volume (higher paste density), so that the pores become filled with high pressure water vapour more quickly than in normal weight concrete, and the low porosity results in slower diffusion of water vapour through the concrete.

Even though serious spalling of normal concrete is unlikely, the probability of occurrence requires consideration for critical structures. The addition of an additional reinforcing cage to prevent spalling is impractical and expensive. The best economical method of preventing spalling is the addition of microfilament polypropylene fibres to the concrete mix (0.15–0.3%). These fibres, which are often up to 32 μm diameter and 20 mm long, reduce the likelihood of spalling possibly because the polypropylene melts during fire exposure, increasing the porosity by leaving cavities through which the water vapour can escape, as described by Kodur (1997) and Jansson and Boström (2008). Steel fibres added to the concrete mix will reduce the probability of spalling by increasing the fracture toughness of the concrete, but this is much more expensive than adding polypropylene fibres.

7.4 Concrete and Steel Reinforcing Temperatures

7.4.1 Fire Exposure

In any specific design of a concrete structure exposed to fires, it is essential to know the temperatures of the concrete and the reinforcing steel. The design fire exposure may be the standard time–temperature curve or a more realistic fire curve, depending on the design philosophy. Many design charts are available giving thermal gradients in beams, columns and slabs exposed to the standard fire, but not for realistic design fires.

There is good published information available on temperatures within concrete members exposed to the standard fire (e.g. Gustaferro and Martin, 1988; Wade 1991; CEN, 2004a; ACI, 2007; Fleischmann *et al.*, 2008). Most of these data have been derived from the work of Abrams and Gustaferro (1968). The availability of this information makes it much easier to design for standard fire exposure than for realistic fire temperatures, especially for simple hand calculations. Computer-based thermal calculations can be used to provide accurate temperature gradients in concrete members exposed to realistic fires, as described in Chapter 11.

7.4.2 Calculation Methods

When making thermal calculations in reinforced or prestressed concrete members, it is usual to assume that the heat transfer is a function of the thermal properties of the concrete

alone, and the temperature of the reinforcing is the same as the temperature of the surrounding concrete. Steel has a much higher thermal conductivity than concrete, but most reinforcing steel is parallel to the fire-exposed surfaces, so it does not have a significant influence on heat transfer perpendicular to the surfaces. Some authorities have suggested that the much higher specific heat of steel than concrete, and possible moisture condensation, may result in the reinforcing steel being cooler than the surrounding concrete, but this concept is not used in design.

Unlike steel members, the only accurate way to calculate temperatures is to use a two-dimensional finite element computer program which gives the temperature distribution with time over the cross section. The advantage of such a program is that any combination of materials, shapes and voids can be included, for exposure to any desired fire. Most programs do not consider the mass transport of water or water vapour in fire-exposed concrete, although this has been studied by Ahmed and Hurst (1995) and Huang *et al.* (1996).

For simple members of normal weight concrete, empirical hand calculation methods are available, derived from computer-based thermal analysis (Hertz, 1981; Wickström, 1986). The simple lumped mass approach used for steel members is not appropriate for concrete because of the much lower thermal conductivity. Wickström's method of calculating the temperatures in a normal weight concrete slab in the standard fire is based on the fire-exposed surface temperature T_w being:

$$T_w = \eta_w T_f \quad (7.1)$$

where

$$\eta_w = 1 - 0.0616 t_h^{-0.88} \quad (7.2)$$

T_f is the fire temperature and t_h is the time (in hours).

At any depth x (m) into the slab, at time t_h , the concrete temperature T_c is a factor η_x of the surface temperature T_w with η_x given by:

$$\eta_x = 0.18 \ln(t_h/x^2) - 0.81 \quad (7.3)$$

Hence the concrete temperature T_c is given by:

$$T_c = \eta_x \eta_w T_f \quad (7.4)$$

This formula generally gives similar results to those shown in Figure 7.5.

The method can be used for corners of beams where there is heat conduction in two directions, using η_y calculated in the same way as η_x so that the concrete temperature T_c is now given by:

$$T_c = \left[\eta_w (\eta_x + \eta_y - 2\eta_x \eta_y) + \eta_x \eta_y \right] T_f \quad (7.5)$$

This approximate equation gives temperatures roughly similar to those shown in Figure 7.6 for 160 mm wide beams, but does not make any allowance for the different rates of temperature increase in wider or narrower beams. Wickström (1986) shows how these equations can be modified for other types of concrete, and also gives approximate methods

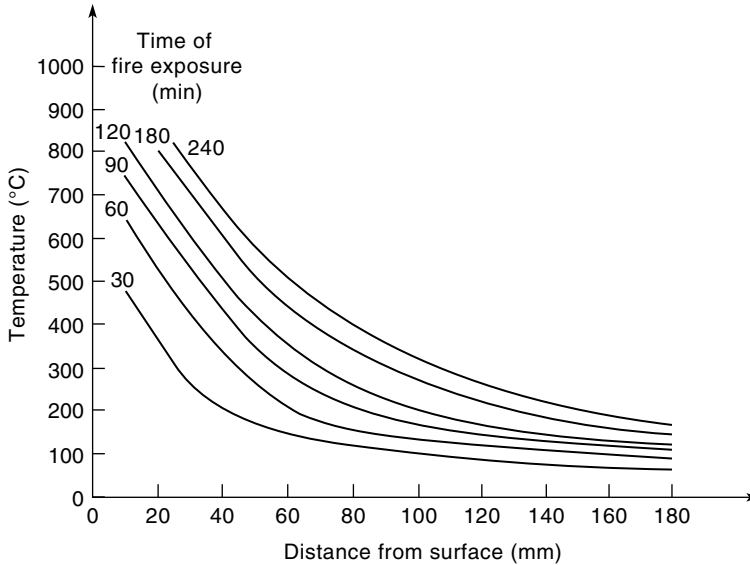


Figure 7.5 Temperatures in concrete slabs exposed to the standard fire. Reproduced from Wade (1991) by permission of Building Research Association of New Zealand

of calculating temperatures in concrete members exposed to realistic fires with a decay period. Empirical calculations in the decay period are less accurate because the maximum concrete temperatures occur a considerable time after the fire temperature passes its peak value, as shown in Figure 7.7(a).

For exposure to typical real fires, very little published information is available on thermal gradients. Figure 7.7(b) shows typical peak temperatures reached at various depths in a concrete slab, calculated by Wade (1994) using the design fires proposed by Lie (1995) for a range of opening factors and a fuel load of 600 MJ/m^2 floor area. Figure 7.7(a) shows the progression of temperature versus time at various depths within the slab, for one of those real fires. It can be seen that temperatures within the slab continue to increase well beyond the time of 35 min when the fire reached its peak temperature. The greater the cover, the greater the delay in reaching the peak temperature. An advanced finite element calculation is recommended for thermal analysis of concrete structures exposed to realistic fires.

7.4.3 Thermal Properties

In order to calculate temperatures within structural concrete assemblies it is necessary to know the thermal properties of the concrete materials. These are discussed briefly below. For more detail see Schneider (1986), Bazant and Kaplan (1996), Neville (1997) or Harmathy (1993).

The density of concrete depends on the aggregate and the mix design. Typical 'dense' concrete has a density of about 2300 kg/m^3 . There are many 'lightweight' concretes which use porous aggregates or air entrainment to reduce the density to less than half of this value. When heated to 100°C the density of most concretes will be reduced by up to 100 kg/m^3 due to the evaporation of free water, which has a minor effect on thermal response. Other than moisture

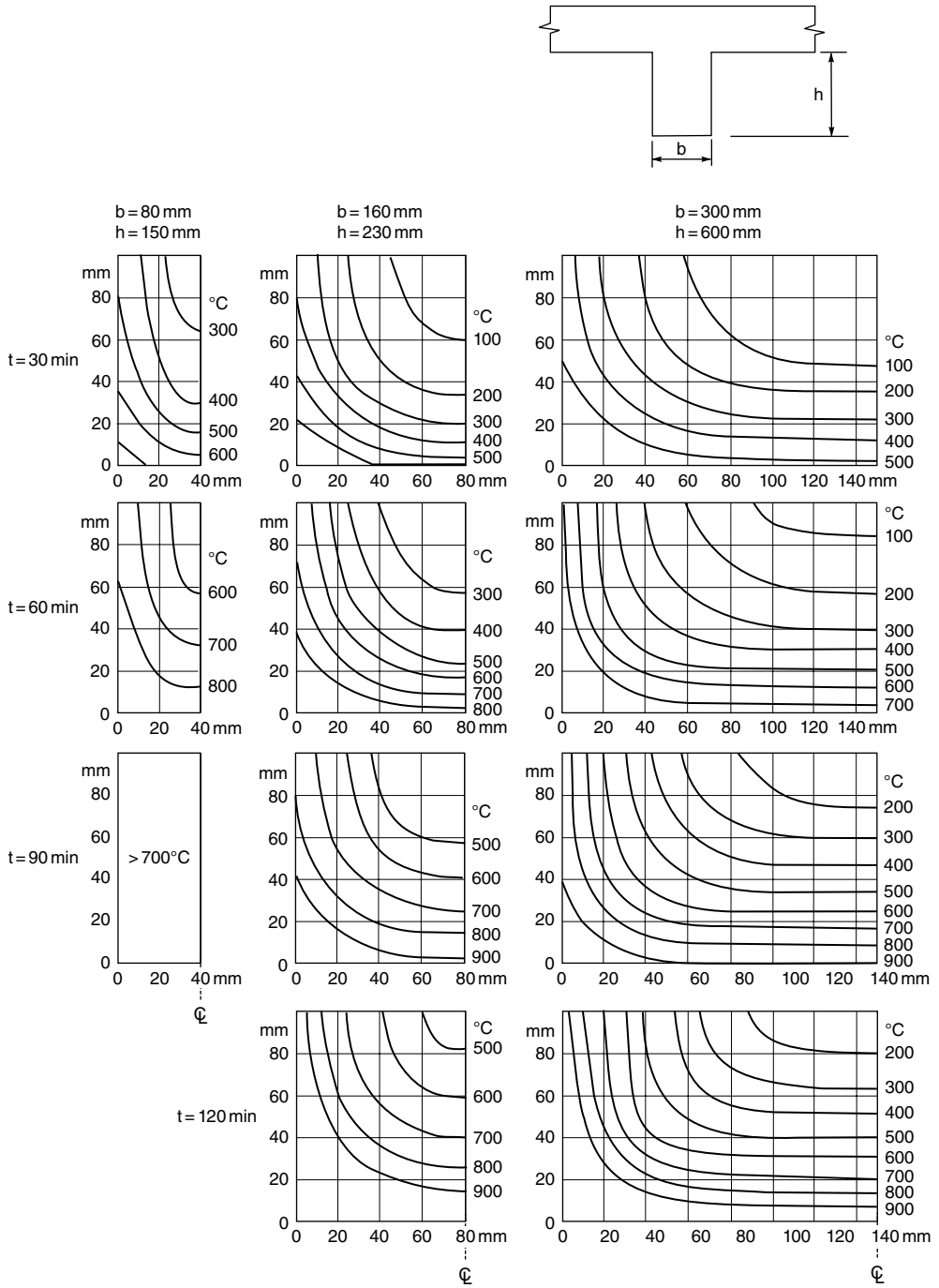


Figure 7.6 Temperature contours in concrete beams exposed to the standard fire. Reproduced from CEN (2004a). © CEN, reproduced with permission

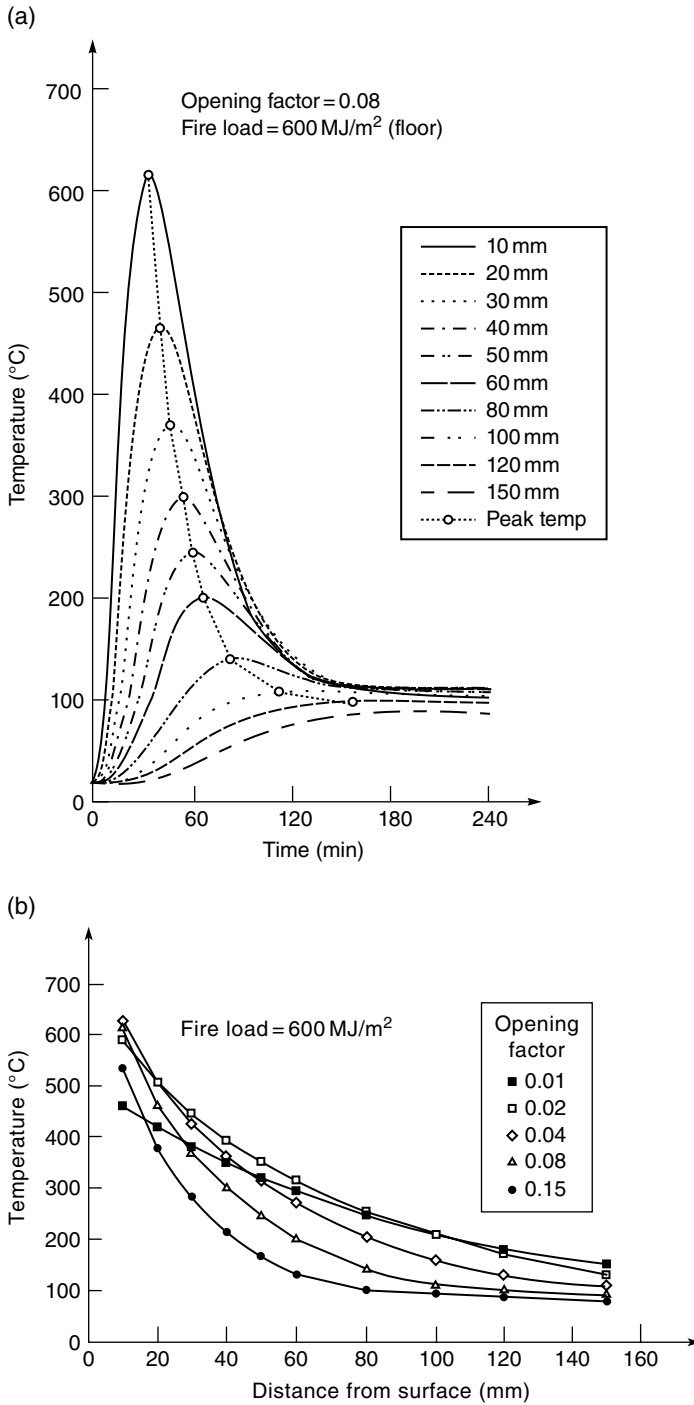


Figure 7.7 Temperatures inside concrete slabs exposed to design fires: (a) time-temperature curves; (b) peak temperatures. Reproduced from Wade (1994) by permission of Society of Fire Protection Engineers

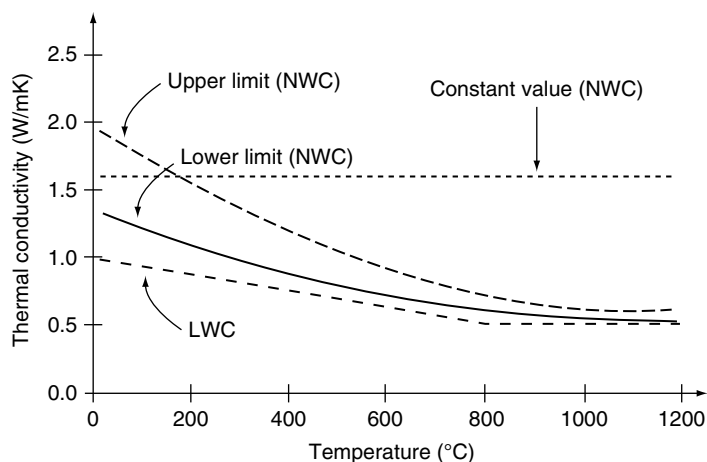


Figure 7.8 Thermal conductivity of concrete. LWC, lightweight concrete; NWC, normal weight concrete. Reproduced from Eurocodes 2 and 4 (CEN, 2004a, 2005c). © CEN, reproduced with permission

changes, the density of concrete does not change much at elevated temperature, except for limestone (calcareous) aggregate concrete which decomposes above 800 °C with a corresponding decrease in density.

The thermal conductivity of concrete is temperature dependent, and varies in a broad range, depending on the type of aggregate. Values from Eurocode 2 Part 1.2 (CEN, 2004a) are shown in Figure 7.8. An approximate value for design purposes is 1.6 W/mK for normal weight concrete and 0.8 W/mK for lightweight concrete (CEN, 2005c). Data for other types of concrete are given by Schneider (1988).

The specific heat of concrete also varies in a broad range, depending on the moisture content, with design values from Eurocode 2 Part 1.2 (CEN, 2004a) shown in Figure 7.9. The peak between 100 °C and 200 °C allows for water being driven off during the heating process. Approximate design values are 1000 J/kgK for normal weight concrete and 840 J/kgK for lightweight concrete.

7.5 Mechanical Properties of Concrete at Elevated Temperatures

7.5.1 Test Methods

The same test methods as described earlier for steel are generally applicable to concrete. Mechanical properties of concrete at elevated temperatures are described by Schneider (1986), Harmathy (1993), Bazant and Kaplan (1996) and Bailey and Khoury (2011).

7.5.2 Components of Strain

The deformation of concrete at elevated temperatures is slightly more complicated than that of steel, because of an additional component of strain called ‘transient strain’.

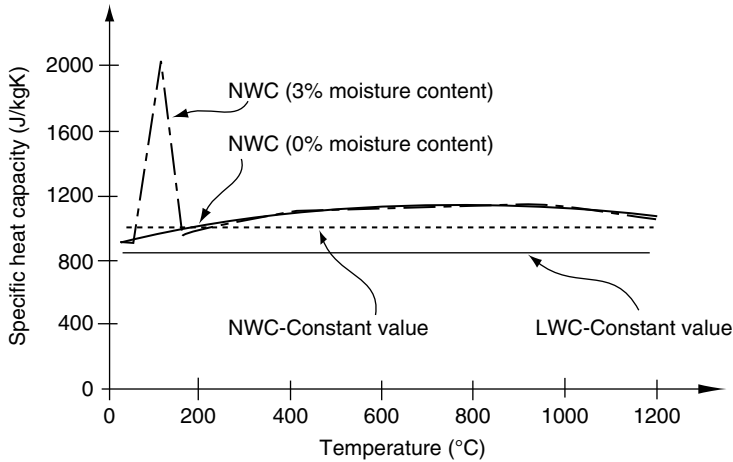


Figure 7.9 Specific heat of concrete. LWC, lightweight concrete; NWC, normal weight concrete. Reproduced from Eurocodes 2 and 4 (CEN, 2004a, 2005c). © CEN, reproduced with permission

The deformation of concrete is usually described by assuming that the total strain ε consists of four components:

$$\varepsilon = \varepsilon_{th}(T) + \varepsilon_{\sigma}(\sigma, T) + \varepsilon_{cr}(\sigma, T, t) + \varepsilon_{tr}(\sigma, T) \quad (7.6)$$

where $\varepsilon_{th}(T)$ is the thermal strain being a function only of temperature, T , $\varepsilon_{\sigma}(\sigma, T)$ is the stress related strain, being a function of both the applied stress σ and the temperature, $\varepsilon_{cr}(\sigma, T, t)$ is the creep strain, being also a function of time, t , and $\varepsilon_{tr}(\sigma, T)$ is the transient strain, being a function of both the applied stress and the temperature.

These components of strain are described in slightly different ways by different researchers (Anderberg, 1976; Khoury *et al.*, 1985a; Schneider, 1988). Some details are given below. A slightly different strain model is given by Schneider *et al.* (1994). For simple structures such as simply supported beams, only the stress related strain needs to be considered, allowing the reduced strength at elevated temperatures to be calculated without reference to the deformations. For more complex structural systems, especially where members are restrained by other parts of the structure, the thermal strain and the creep strain must also be considered, by using a computer model for the structural analysis.

7.5.3 Thermal Strain

Expressions for thermal strain $\varepsilon_{th}(T) = \Delta L/L$ of concrete are given by:

Siliceous aggregates

$$\begin{aligned} \varepsilon_{th}(T) &= -1.8 \times 10^{-4} + 9 \times 10^{-6} T + 2.3 \times 10^{-11} T^3 & \text{for } 20^{\circ}\text{C} \leq T \leq 700^{\circ}\text{C} \\ \varepsilon_{th}(T) &= 14 \times 10^{-3} & \text{for } 700^{\circ}\text{C} < T \leq 1200^{\circ}\text{C} \end{aligned} \quad (7.7)$$

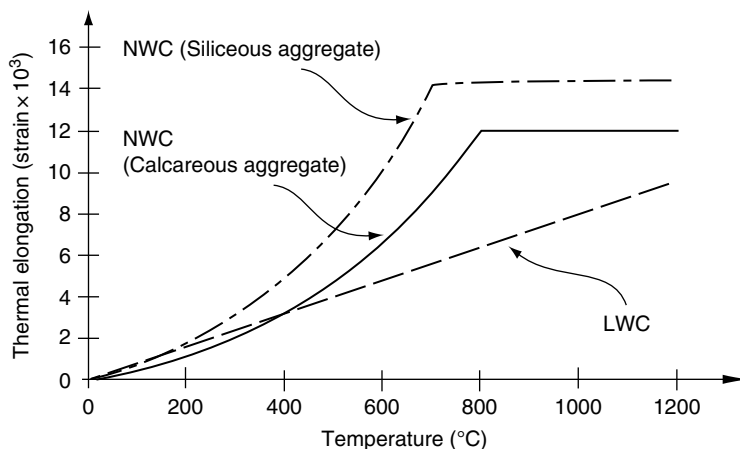


Figure 7.10 Variation of thermal elongation with temperature. LWC, lightweight concrete; NWC, normal weight concrete. Reproduced from Eurocodes 2 and 4 (CEN, 2004a, 2005c). © CEN, reproduced with permission

Calcareous aggregates

$$\begin{aligned} \varepsilon_{th}(T) &= -1.2 \times 10^{-4} + 6 \times 10^{-6} T + 1.4 \times 10^{-11} T^3 & \text{for } 20^\circ\text{C} \leq T \leq 805^\circ\text{C} \\ \varepsilon_{th}(T) &= 12 \times 10^{-3} & \text{for } 805^\circ\text{C} < T \leq 1200^\circ\text{C} \end{aligned} \quad (7.8)$$

where T is the concrete temperature. The variation of thermal elongation with temperature is shown in Figure 7.10. It is difficult to separate thermal strain and shrinkage in tests, so the above expressions also include effects of shrinkage.

7.5.4 Creep Strain and Transient Strain

Creep strain and transient strain are closely linked. If a concrete specimen is heated up under load (regime 5, Figure 5.5), all of the strain components described above combine to produce deformations as shown in Figure 7.11 (Schneider, 1988).

Khoury *et al.* (1985a) have measured creep strains during testing under constant temperature and stress (regime 3, Figure 5.5) producing results such as those shown in Figure 7.12. They also describe transient thermal strain, which occurs during the first time heating of concrete to 600°C under load, but not on subsequent heating. During all these processes there are complex changes in the moisture content and chemical composition of the cement paste, interacting with the aggregate which remains relatively inert (Schneider, 1988).

7.5.5 Stress Related Strain

The stress related strain includes the elastic and plastic components of strain resulting from applied stresses. Typical stress–strain relationships for normal concrete at elevated

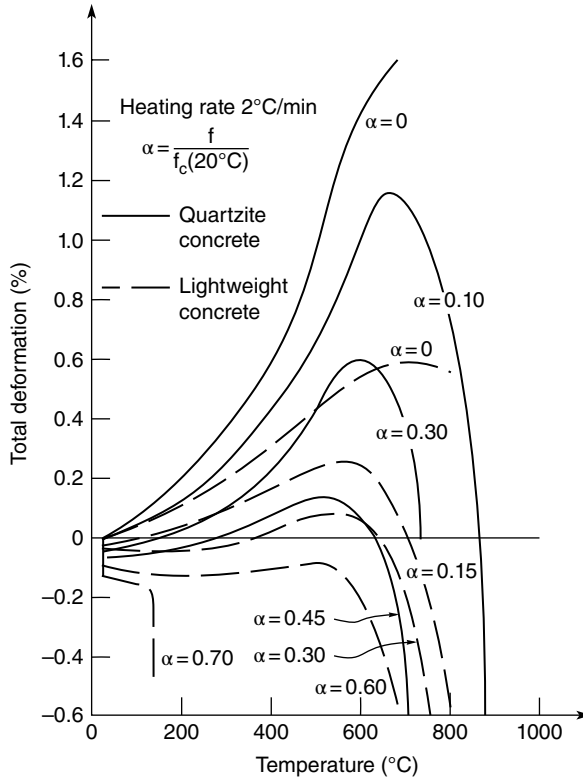


Figure 7.11 Total deformation in different types of concrete during heating. Reproduced from Schneider (1988) with permission from Elsevier Science

temperatures are shown in Figure 7.13. It can be seen that the ultimate compressive strength drops, and the strain at peak stress increases with increasing temperature. Similar curves and corresponding equations are given by Eurocode 2 Part 1.2 (CEN, 2004a).

The reduction in ultimate compressive strength with temperature for typical structural concrete is shown in Figure 7.14 (Schneider, 1988), derived from several studies.

7.5.5.1 Confinement of Concrete

It is well established that confinement of concrete by reinforcing such as hoops or ties gives a significant increase in ductility at normal temperatures. Such confinement is often used in seismic design of concrete structures. No specific studies of confined concrete under elevated temperature are known of, although Schneider (1988) reports studies showing that the ratio of biaxial compressive strength to uniaxial strength increases at elevated temperatures. It follows that confined concrete members designed for seismic loads probably have enhanced fire resistance. Franssen and Bruls (1997) describe how the flexural performance of a fire-exposed prestressed concrete tee-beam can be enhanced with confining reinforcing around the tendons.

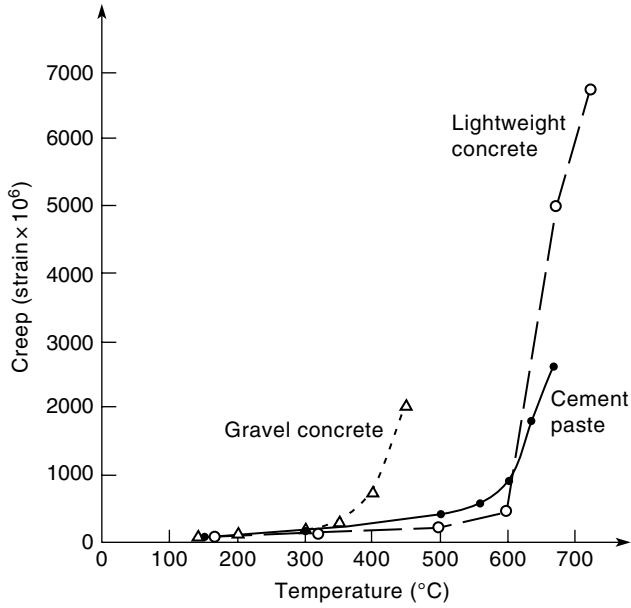


Figure 7.12 Creep in concrete 1 day after loading at 10% of the initial cold strength. Reproduced from Khoury and Sullivan (1988) with permission from Elsevier Science)

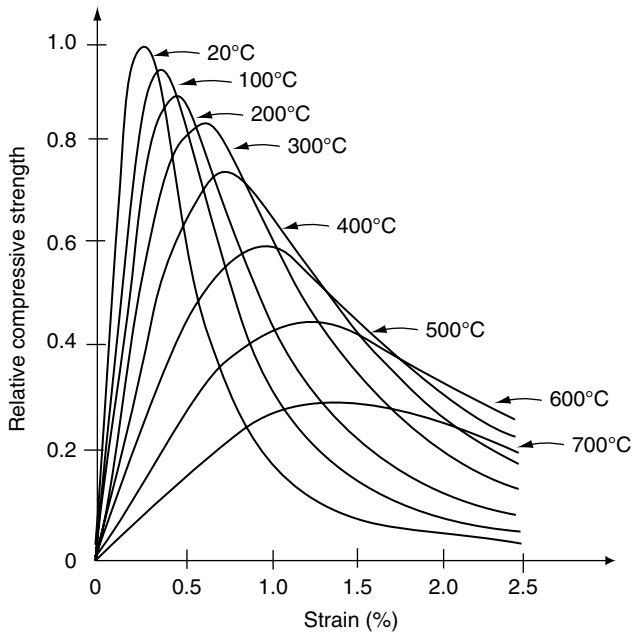


Figure 7.13 Stress–strain relationships for concrete at elevated temperatures. Reproduced from Eurocode 2 Part 1.2 (CEN, 2004a) by permission of CEN

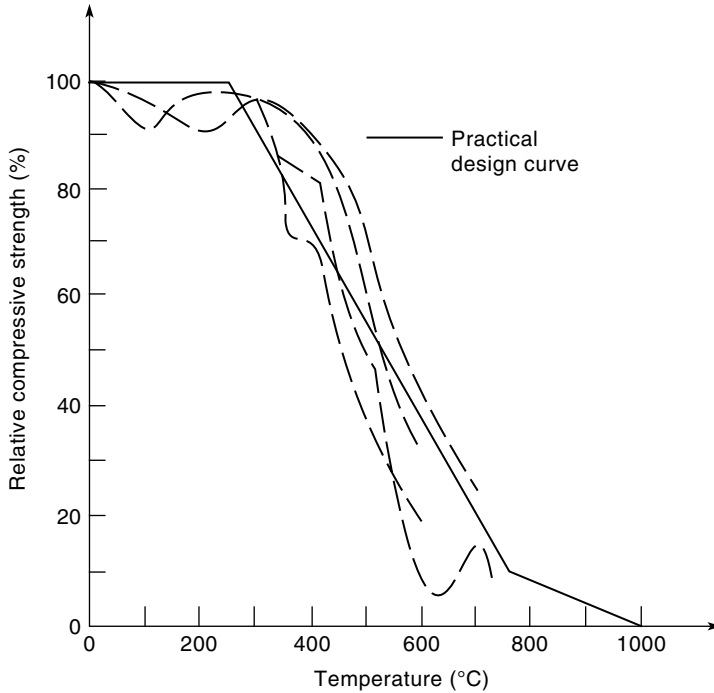


Figure 7.14 Reduction in compressive strength with temperature. Reproduced from Schneider (1988) with permission from Elsevier Science

7.5.5.2 Design Values

Typical stress–strain curves for concrete at elevated temperatures are shown in Figure 7.13. The tensile strength of concrete is usually assumed to be zero at elevated temperatures. In similarity with steel properties, the reduction of ultimate strength with temperature is variable and a simple expression is necessary for design purposes, giving $k_{c,T}$ which is the proportion of the strength at ambient temperature. Figure 7.15 shows the lines used in BS 8110 (BSI, 1985), SA (2009) and SNZ (2006) for normal and lightweight concrete, with detailed expressions from Eurocodes 2 and 4 (CEN, 2004a, 2005c). The line for normal weight concrete in Figure 7.15 is given by:

$$\begin{aligned} k_{c,T} &= 1.0 && \text{for } T < 350^\circ\text{C} \\ k_{c,T} &= (910 - T)/560 && \text{for } T > 350^\circ\text{C} \end{aligned} \quad (7.9)$$

The line for lightweight concrete in Figure 7.15 is given by:

$$\begin{aligned} k_{c,T} &= 1.0 && \text{for } T < 500^\circ\text{C} \\ k_{c,T} &= (1000 - T)/500 && \text{for } T > 500^\circ\text{C} \end{aligned} \quad (7.10)$$

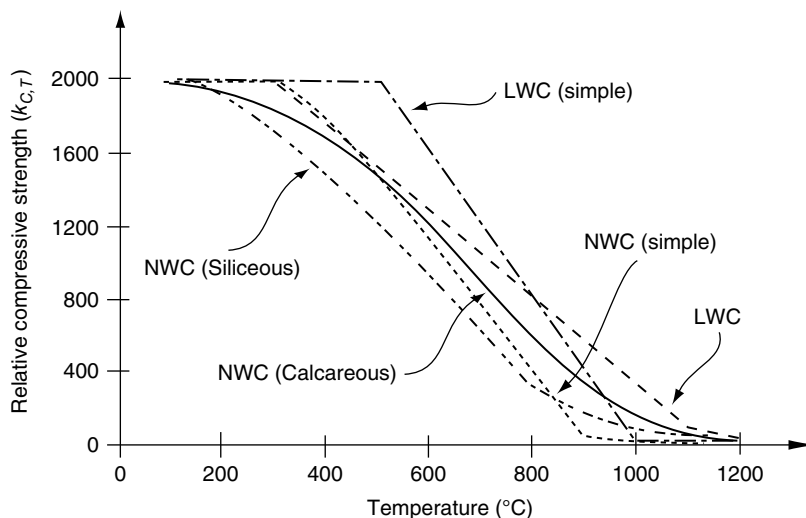


Figure 7.15 Design values for the reduction of compressive strength with temperature. LWC, lightweight concrete; NWC, normal weight concrete. Reproduced from Eurocodes 2 and 4 (CEN, 2004a, 2005c) by permission of CEN

7.5.5.3 Modulus of Elasticity

The modulus of elasticity of concrete also drops with increasing temperature. Figure 7.16 shows the line used in BS 8110 (BSI, 1985) to give $k_{E,T}$ which is the proportion of the modulus of elasticity at ambient temperature. More detailed expressions are given in Eurocode 2 Part 1.2 (CEN, 2004a). Lightweight and high strength concretes behave similarly to normal weight concrete. The solid line in Figure 7.16 is given by:

$$\begin{aligned}
 k_{E,T} &= 1.0 && \text{for } T < 150^\circ\text{C} \\
 k_{E,T} &= (700 - T)/550 && \text{for } T > 150^\circ\text{C}
 \end{aligned}
 \quad (7.11)$$

A problem occurs with the use of Figure 7.14 and Figure 7.16 at high temperatures, because the compressive strength and the modulus of elasticity can be seen to reach zero at different temperatures. Because this is physically impossible, Inwood (1999) has proposed a minor alteration shown by the dashed line in Figure 7.16, in order to increase the temperature at which the modulus of elasticity reaches zero.

7.6 Design of Concrete Members Exposed to Fire

The overall strategy for structural design of concrete structures exposed to fire is the same as for design at normal temperature, but taking into account the effect of elevated temperatures on the material properties. In all cases, design of concrete members should follow ‘ultimate strength design’ or ‘limit states design’ as used in all modern concrete design codes.

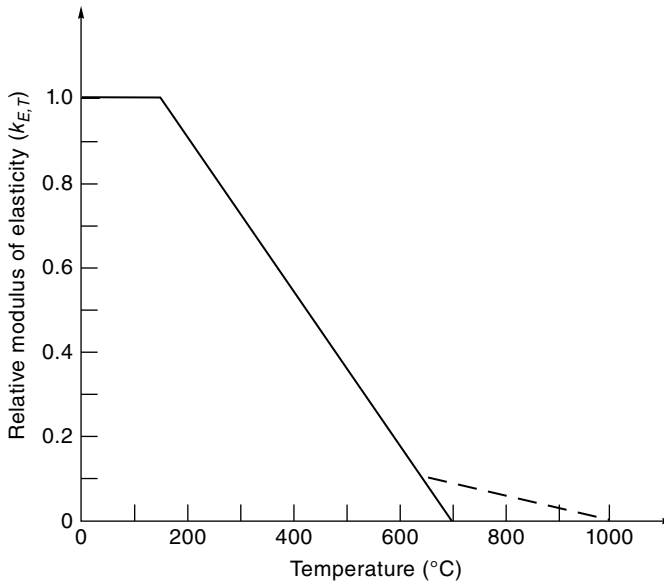


Figure 7.16 Design values ($k_{E,T}$) for reduction of modulus of elasticity with temperature

A hierarchy of design methods is as follows:

1. For simply supported slabs or tee-beams exposed to fire from below, concrete in the compression zone remains at normal temperatures, so structural design need only consider the effect of elevated temperatures on the yield strength of the bottom reinforcing steel. Simple hand calculations are possible.
2. For continuous slabs or beams, some of the fire-exposed surfaces are in compression, so the simple hand calculation methods must consider the effects of elevated temperature on the compression strength of the concrete.
3. Similar methods can be applied to fire-exposed concrete walls and columns, but these methods are less accurate because of deformations caused by non-uniform heating and the possibility of instability failures.
4. For moment-resisting frames, or structural members affected by axial restraint or non-uniform heating, it is recommended to use a special-purpose computer program for advanced structural analysis under fire conditions.

Eurocode 2 Part 1.2 (CEN, 2004a) describes three methods of design: the generic ‘tabulated’ method; a ‘simplified’ calculation method; and an ‘advanced’ calculation method. Advanced calculation methods include those which provide a realistic analysis of concrete structures exposed to fire, based on fundamental physical behaviour (design method 4 in the above list). Complex structures must be designed using advanced calculation methods, using a computer program for analysing the structure at elevated temperatures, including all the components of strain described above. Thermal gradients are also calculated by computer, so any type of fire exposure can be used.

The simplified method is useful for single members, using the hand calculations which are used for design at normal temperatures (design methods 1–3 in the above list). It is essential to know the temperatures inside the members. For standard fire exposure, these can be obtained from design charts, from Wickstrom's method or by computer calculation. Computer calculation is essential for real fire exposure. For simply supported slabs or beams, only the reduction of steel strength needs to be considered because the heated concrete is all in the tension zone. The effect of temperature on concrete strength becomes important if heated concrete is loaded in compression, in columns or continuous beams or slabs, for example. The simplified calculation method ignores any concrete over a certain limiting temperature and may include a reduction in strength of the remaining cooler concrete core. The Eurocode recommends assigning full strength to concrete below 500 °C and zero strength to concrete above 500 °C. This simplified method is excellent for large members, but may become inaccurate for thin concrete members where all the temperatures are over 500 °C and the concrete has some residual strength.

7.6.1 Member Design

As for steel members, verification in the strength domain requires that

$$U_{fire}^* \leq R_{fire} \quad (7.12)$$

where U_{fire}^* is the design force resulting from the fire limit state load at the time of the fire and R_{fire} is the load-bearing capacity in the fire situation.

Fire limit state loads have been described in Chapter 5. Design forces are obtained from conventional structural analysis. The design force U_{fire}^* may be axial force N_{fire}^* , bending moment M_{fire}^* or shear force V_{fire}^* occurring singly or in combination, with the load capacity calculated accordingly as axial force N_f , bending moment M_f or shear force V_f in the same combination. Calculations of the load capacity are described below, based on the mechanical properties of concrete and reinforcing steel at elevated temperatures. Note that Equation 7.10 does not include a partial safety factor for mechanical properties γ_M (or a strength reduction factor Φ) because both have a value of 1.0 in fire conditions, as described in Chapter 5.

This section describes the design of individual components, using the simplified calculation method with zero strength for concrete above 500 °C. This design method uses the normal assumptions for reinforced concrete design, assuming that concrete has no tensile strength, and the parabolic compressive stress block in the concrete can be approximated by an equivalent rectangle. For the examples in this book, the equivalent rectangle is calculated assuming that the characteristic strength is 85% of the crushing strength of the concrete (Park and Paulay, 1975). For beams and slabs it is conservative to ignore any compression reinforcing, which simplifies the calculations.

7.6.2 Simply Supported Concrete Slabs and Beams

The simplest reinforced concrete members to design are simply supported slabs, such as shown in Figure 7.17. None of the compression region is exposed to elevated temperatures, so the strength under fire conditions is solely a function of the temperature of the reinforcing steel.

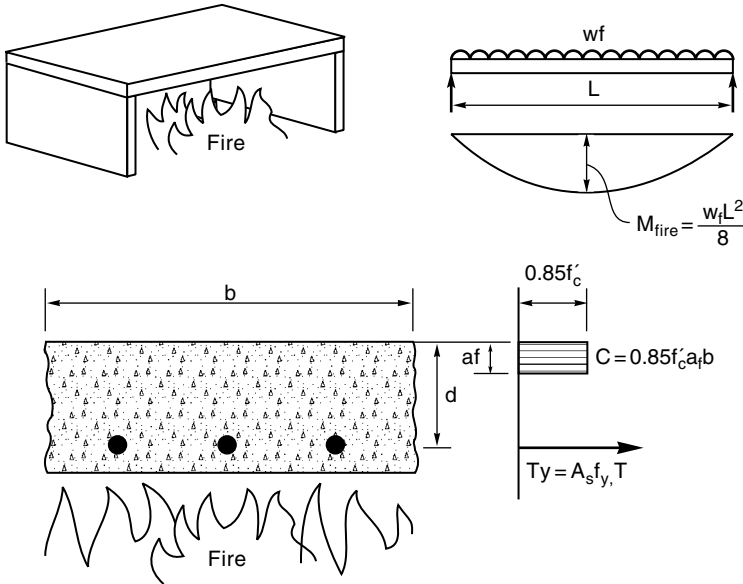


Figure 7.17 Simply supported reinforced concrete slab exposed to fire

There is no possibility of moment redistribution in simply supported slabs or beams. The design equation for a member submitted to a bending moment M_{fire}^* is:

$$M_{fire}^* \leq M_f \quad (7.13)$$

The flexural capacity under fire conditions M_f is given by:

$$M_f = A_s f_{y,T} (d - a_f / 2) \quad (7.14)$$

where A_s is the area of the reinforcing steel, $f_{y,T}$ is the yield stress of the reinforcing steel, reduced for temperature ($f_{y,T} = k_{y,T} f_y$), d is the effective depth of the cross section (distance from the extreme compression fibre to the centroid of the reinforcing steel) and a_f is the depth of the rectangular stress block, given by:

$$a_f = A_s f_{y,T} / 0.85 f'_c b \quad (7.15)$$

where f'_c is the compressive strength of the concrete and b is the width of the beam or slab.

These calculations assume that the concrete in the compression zone is not hot enough to cause any reduction in strength. A simply supported tee-beam (Figure 7.18) has the same conditions, hence the same simple design procedure and equations. A simply supported beam with a non-composite slab (Figure 7.19) is slightly more affected by fire because the two sides of the compression zone of the beam are affected by elevated temperatures, so that the depth of the rectangular stress block now becomes

$$a_f = A_s f_{y,T} / 0.85 f'_c b_f \quad (7.16)$$

where b_f is the fire-reduced effective width of the beam.

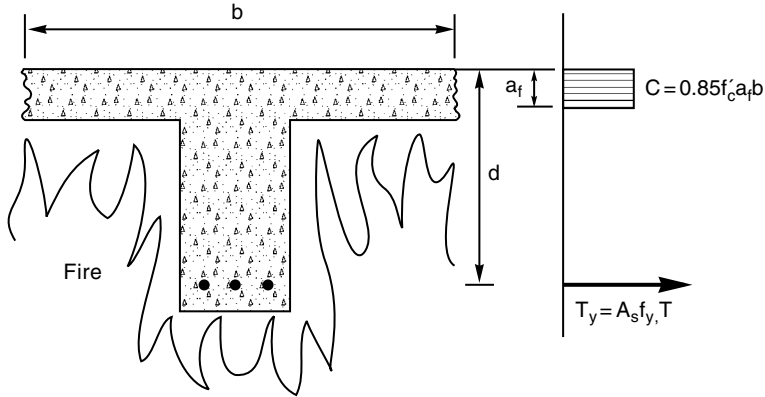


Figure 7.18 Simply supported reinforced concrete tee-beam exposed to fire

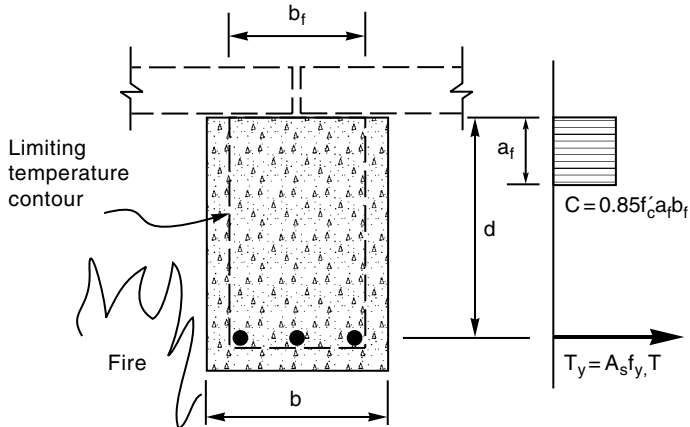


Figure 7.19 Simply supported non-composite beam exposed to fire

7.6.3 Shear Strength

Shear is not usually a problem in fire-exposed concrete structures, with the exception of some precast pre-tensioned slabs. For shear design, Eurocode 2 Part 1.2 (CEN, 2004a) recommends using normal temperature design methods with the mechanical properties reduced for temperature and the cross section reduced to the 500°C contour. Franssen and Bruls (1997) have shown that the concrete contribution to shear strength reduces much more slowly than the contribution from the stirrup reinforcing, and any contribution from the prestressing force to shear strength drops rapidly to zero as the concrete temperature increases. Shear failures have been observed in precast pre-tensioned hollow core and double-tee slabs after loss of prestress due to bond failure near the ends of the slabs (Andersen and Lauridsen, 1999; Fellinger, 2004; de Feijter and Breunese, 2007).

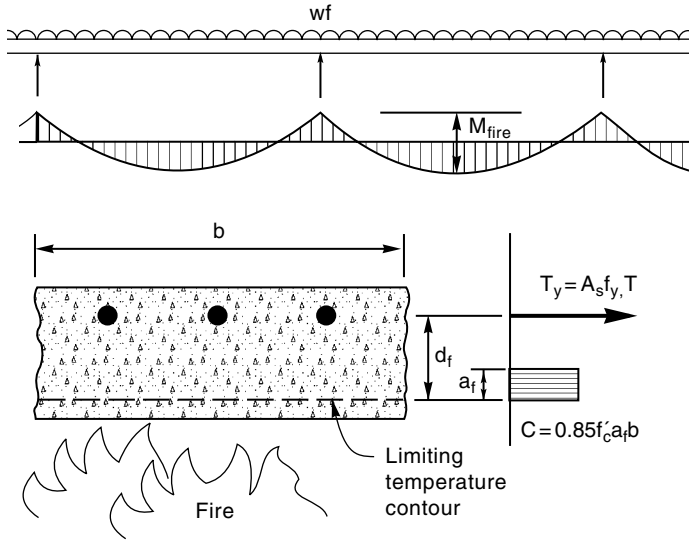


Figure 7.20 Support region of continuous concrete slab exposed to fire

7.6.4 Continuous Slabs and Beams

Slabs or beams which are built into one or more supports usually have enhanced fire resistance because of the moment redistribution which must occur before a collapse mechanism can develop, as described in Chapter 5. If calculations show that the slab or beam can resist the fire as a simply supported member, no additional calculations for continuity are necessary.

7.6.4.1 Plastic Design

Reinforced concrete is very different from steel because the strength of a beam of a given size can have many possible values depending on the amount of reinforcing steel inside the concrete. Positive and negative flexural capacities may be very different for the same reason. The methods of moment redistribution and plastic design methods described in Chapter 5 can be used for analysis or design of reinforced concrete structures.

7.6.4.2 Negative Flexural Capacity

To allow for the effects of flexural continuity it is necessary to calculate the negative moment capacity at the supports during fire exposure. Part of the compression region is now exposed to fire temperatures, which must be accounted for in the design process. For a slab of uniform thickness, the negative flexural capacity M_f^- at the supports is given by the following equation, where the terms are illustrated in Figure 7.20.

$$M_f^- = A_s f_{y,T} (d_f - a_f / 2) \quad (7.17)$$

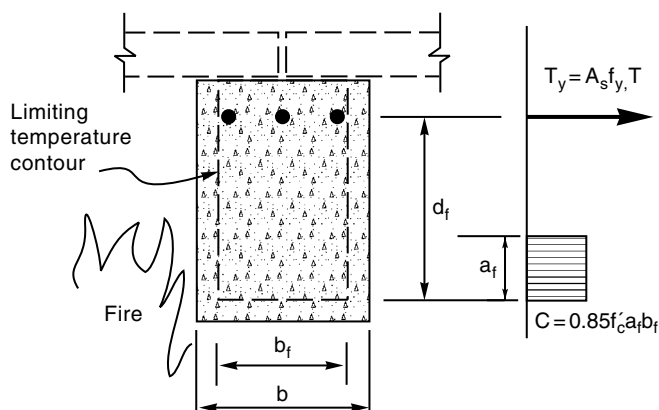


Figure 7.21 Support region of continuous concrete beam exposed to fire

where d_f is the effective depth of the slab, reduced to allow for the hot layer of concrete on the bottom surface, and a_f is the depth of the rectangular stress block, given by:

$$a_f = A_s f_{y,T} / 0.85 f'_c b \quad (7.18)$$

For a beam with its compression edge exposed to fire, the beam width b must be replaced by the effective width b_f of concrete above the critical temperature. The reduced cross section and reduced rectangular stress block are shown in Figure 7.21. When the compression region of a slab or beam is exposed to fire, it becomes important to ensure that the compression capacity is not reduced so low as to cause a sudden compression failure. This can be ensured by checking that

$$A_s f_{y,T} / b d_f f'_{cT} < 0.30 \quad (7.19)$$

It can be shown that Equation 7.17 checks that the depth of the compression zone a_f is not more than 35% (0.3/0.85) of the effective depth of the cross section d_f . This check is not necessary if there is significant longitudinal reinforcing in the compression zone.

7.6.4.3 Curtailment of Reinforcing Bars

For continuous beams and slabs in reinforced concrete structures, major benefits can often be obtained by redistributing bending moments to achieve optimum behaviour, as described in Chapter 5. Redistribution of moments under fire conditions may change the location of the points of inflection, so the curtailment locations for reinforcing must allow the sections to develop the required flexural strength, with allowance for anchorage as required by national codes. Any redistribution of bending moments must be followed by a calculation check of the curtailment locations of the reinforcing bars, to avoid the possibility of structural failure due to top bars being terminated in regions of high tensile stress. Several sources recommend that the lengths of negative moment reinforcing bars should be increased by 15% of the span to

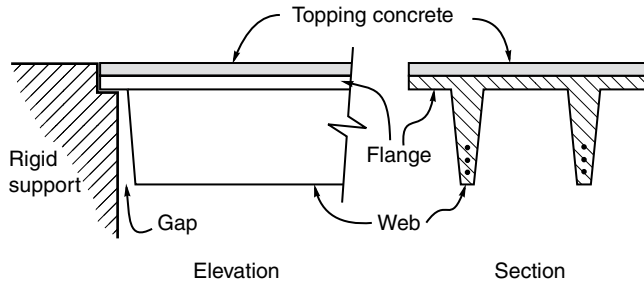


Figure 7.22 Unsatisfactory axial restraint in flange-supported double-tee floor slab

avoid this problem. If adjacent spans are of different lengths, the bars on both sides of the support should be increased in length by 15% of the length of the longer of the two spans. It is also widely recommended that at least 20% of the negative moment reinforcing should be extended throughout the span of all beams.

Another related issue is the bond strength of deformed reinforcing bars in fire conditions, which has been investigated by Hertz (1982) and Schneider (1986) who show that bond strength drops by about half at 500 °C, which can be a problem in some cases.

7.6.5 Axial Restraint

Axial restraint can have a significant influence on the fire resistance of reinforced concrete slabs and beams, as described in Chapter 5. Axial restraint has a more profound influence on concrete structures than on steel structures because the more rapid heating and more ductile behaviour of steel structures can result in large vertical deflections which reduce the horizontal axial restraint forces. Compared with steel structures, concrete members tend to heat up more slowly, but when they become hot they tend to undergo larger horizontal displacements with lower vertical deflections, resulting in larger horizontal restraint forces if the building offers sufficient resistance to the thermal expansion.

Axial restraint is beneficial for reinforced or prestressed concrete slabs or beams, and for composite concrete and metal deck slabs, where the axial restraint force can partly or completely compensate for the loss in strength of steel reinforcing at elevated temperatures. As pointed out in Chapter 5, it is essential for the line of thrust to be below the compressive stress block if the beneficial effects of axial restraint are to be utilized. Figure 7.22 shows a double-tee concrete floor unit with cut-away webs, supported on the flange, where the line of action of the axial thrust is so high that premature failure could occur during fire exposure.

7.6.5.1 PCA Method for Calculating Restraint

A semi-empirical method of calculating the required strength and stiffness of the surrounding structure is given by Gustaferro and Martin (1988) based on a large series of tests by the Portland Cement Association which showed that the thermal thrust for a given expansion varied directly with the heated perimeter of the member and the modulus of elasticity of the concrete. The applicability of this approach to slabs and beams other than those tested has not

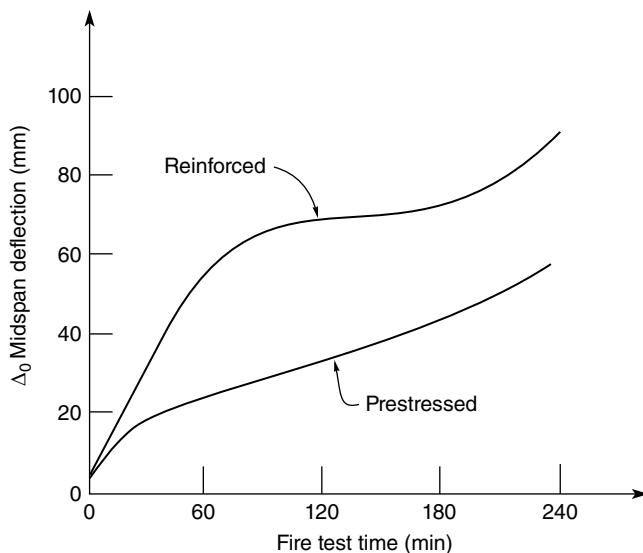


Figure 7.23 Mid-span deflection of reference specimens. Reproduced from Gustaferro and Martin (1988) by permission of Precast/Prestressed Concrete Institute

been demonstrated. Anderberg and Forsen (1982) have shown that this method does not give accurate results in many cases because it over-predicts the thermal strains. The PCA method is included here because it is the only method of assessing restraint without a comprehensive computer-based analysis package.

A step-by-step guide to the PCA procedure is as follows:

1. Calculate the bending moment at mid-span under fire limit state loads M_{fire}^* (kNm) assuming simply supported behaviour.
2. Calculate the flexural capacity at mid-span during the fire M_f^+ . If $M_f^+ > M_{fire}^*$ no continuity or restraint is necessary.
3. Calculate the flexural capacity at the supports during the fire M_f^- . If $M_f^+ + M_f^- > M_{fire}^*$ continuity is sufficient and no restraint is necessary. If the member is not symmetrical, the flexural capacity M_f^- should be the average of the two ends.
4. Estimate the mid-span deflection Δ using

$$\Delta = L^2 \Delta_0 / 89000 y_b \quad (7.20)$$

where Δ_0 is the mid-span deflection of the reference specimen, from Figure 7.23 (mm), L is the heated length of the member (mm) and y_b is the distance from the neutral axis of the member to the extreme bottom fibre (mm).

5. Estimate the distance of the line of thrust from the top of the member d_r (mm) at the supports. For built-in construction assume that the line of thrust is $0.1h$ above the bottom of the member where h is the overall depth of the member. For other support conditions an independent estimate may be necessary.

6. Calculate the magnitude of the required axial thrust T (kN) to prevent collapse, using

$$T = 1000 \frac{M_{fire}^* - (M_f^+ + M_f^-)}{d_r - a_f/2 - \Delta} \tag{7.21}$$

where a_f (mm) is the height of the internal rectangular compression stress block in the member, approximated by $a_f \approx aM_{fire}^*/M_f^+$ where a is a_f from Equation 7.15.

7. Calculate a_f more accurately, using

$$a_f = \frac{T + A_s^+ f_{y,T}^+}{0.85 f_{c,T}' b_f} \tag{7.22}$$

where $A_s^+ f_{y,T}^+$ is the tensile strength of the bottom steel at mid-span.

Repeat steps 6 and 7 if necessary to get convergence

8. Calculate the non-dimensional thrust parameter T/AE and the parameter $z = A/s$ (mm) where A is the cross-sectional area of the member (mm^2), E is the modulus of elasticity of concrete (usually about 25 GPa) and s is the heated perimeter of the member (mm).
9. Determine the strain parameter Δ_L/L from Figure 7.24 using T/AE and z .
10. Calculate the maximum permitted displacement Δ_L (mm) by multiplying the strain parameter Δ_L/L by the heated length L (mm).
11. Determine independently whether the surrounding structure can withstand the thrust T with a displacement no greater than Δ_L . If so, the structure can withstand the fire.

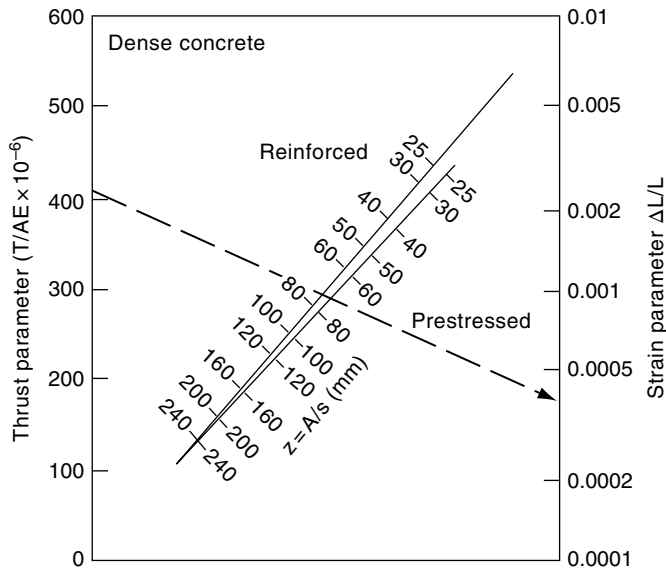


Figure 7.24 Nomogram for thrust in concrete members. Reproduced from Gustafarro and Martin (1988) by permission of Precast/Prestressed Concrete Institute

7.6.6 Reinforced Concrete Columns

Columns can be more difficult to design than flexural members because of possible instability problems. There are a range of design methods in the literature which will be described briefly. At a simple level, minimum dimensions such as those shown in Table 7.1 can be used. Table 7.1 gives minimum dimensions and axis distance as a function of load level, for columns fully or partially exposed to fire. The fire resistances defined in Table 7.1 can only be achieved if the following limits are observed:

1. Effective length under fire conditions $l_e \leq 3\text{m}$.
2. First order eccentricity under fire conditions, $e \leq e_{max} = 0.15h$.
3. Amount of reinforcing $A_s \leq 0.04 A_c$.

Width is the minimum dimension of the column and axis distance is the location of the centre line of the reinforcing relative to the outside of the column. Cover required for durability may control in some cases.

Some codes such as the Canadian Code (NBCC, 2010) have empirical formulae (from Harmathy, 1993) which are based on the results of fire tests, but give no insight into the fire performance of the column. The recommended conservative design approach is to use the simplified method assuming zero strength for all concrete above 500 °C (or 400 °C for high strength concrete) and normal temperature design formulae.

7.6.7 Reinforced Concrete Walls

Concrete walls or partitions which are not part of the main load-bearing structure do not require structural design, so fire resistance requirements can be met by providing a minimum thickness to meet the insulation criterion. This thickness is often the same as required for slabs, but minimum cover requirements may be different. Load-bearing walls with vertical axial loads should be designed in the same way as slender columns, using the tables or

Table 7.1 Generic fire resistance ratings for concrete columns

Load ratio	Column exposed on more than one side				Exposed on one side			
	0.2		0.5		0.7		0.7	
	Width (mm)	Axis distance (mm)	Width (mm)	Axis distance (mm)	Width (mm)	Axis distance (mm)	Width (mm)	Axis distance (mm)
30 min	200	25	200	25	200	32	155	25
60 min	200	25	200	36	250	46	155	25
90 min	200	31	300	45	350	53	155	25
120 min	250	40	350	45	350	57	175	35
180 min	350	45	350	63	450	70	230	55
240 min	350	61	450	75	—	—	295	70

Source: Eurocode 2 Part 1.2 (CEN, 2004a).

calculation methods given for columns. A difference is that columns are most often designed for fire exposure on all sides, but most walls are exposed to fire on only one side. In rare cases they may be exposed to fire on both sides.

O'Meagher and Bennetts (1991) showed that the load-bearing capacity of reinforced concrete walls exposed to fire is very sensitive to the top and bottom end conditions. Computer analysis shows that load-bearing walls with pinned connections at the top and the bottom have low fire resistance, but walls built into the structure with some continuity at top and bottom have far greater fire resistance because the deflections of the walls are greatly reduced.

For industrial buildings, Lim (2000) has shown how the SAFIR program can be used to model cantilever walls, either as free-standing walls, or with the top of the wall connected to a steel roof structure. Free-standing cantilever walls with a single layer of central reinforcing have considerable fire resistance because they tend to deflect outwards, away from the fire, resulting in the compressive face of the wall being on the cool side, with the reinforcing protected by a thick layer of cover concrete.

7.6.8 Reinforced Concrete Frames

There are no simple hand methods available for structural design of reinforced concrete frame structures exposed to fires, especially if frame action, continuity and restraint are to be properly considered. Individual members can be designed by the methods described above, but a computer program is necessary for detailed analysis and design of significant structures. Available programs include CONFIRE (Forsen, 1982), FIRES-RC-II (Iding *et al.*, 1977), TCD (Anderberg, 1989) and SAFIR (Franssen, 2000), as described in Chapter 11. The detailing requirements described above for slabs and beams also apply to reinforced concrete frame structures.

7.7 Worked Examples

7.7.1 Worked Example 7.1

Simply supported reinforced concrete slab (refer to Figure 7.17)

For a simply supported reinforced concrete slab with known span, load, geometry and reinforcing, check the flexural capacity after exposure for 60 min to the standard fire. Use Wickstrom's formula to calculate the reinforcing temperature. Ignore the self-weight of the reinforcing bars.

Given:

Slab span	$L = 7.0 \text{ m}$	Dead load	$G_1 = 0.5 \text{ kN/m}$
Slab thickness	$h = 200 \text{ mm}$		(Excluding self-weight)
Concrete density	$\rho = 24 \text{ kN/m}^3$	Live load	$Q = 2.5 \text{ kN/m}$
Concrete strength	$f'_c = 30 \text{ MPa}$		
Yield stress	$f_y = 300 \text{ MPa}$		
Bar diameter	$D_b = 16 \text{ mm}$	Bar spacing	$s = 125 \text{ mm}$
Bottom cover	$c_v = 15 \text{ mm}$		

Design a 1 m wide strip	$b = 1000 \text{ mm}$
Self-weight	$G_2 = \rho hb = 4.8 \text{ kN/m}$
Total dead load	$G = G_1 + G_2 = 0.5 + 4.8 = 5.3 \text{ kN/m}$
Steel area	$A_s = n\pi r^2 b/s = 1608 \text{ mm}^2$
Effective depth	$d = h - c_v - D_b/2 = 177 \text{ mm}$
Effective cover	$c_e = c_v + D_b/2 = 23 \text{ mm} = 0.023 \text{ m}$

Cold calculations (for a 1 m wide strip):

Strength reduction factor	$\Phi = 0.85$
Stress block depth	$a = A_s f_y / 0.85 f'_c b = 1608 \times 300 / 0.85 \times 30 \times 1000 = 18.9 \text{ mm}$
Internal lever arm	$jd = d - a/2 = 177 - 18.9/2 = 168 \text{ mm}$
Design load (cold)	$w_c = 1.2G + 1.5Q = 10.1 \text{ kN/m}$
Bending moment	$M_c^* = w_c L^2 / 8 = 10.1 \times 7.0^2 / 8 = 62 \text{ kNm}$
Bending strength	$M_n = A_s f_y jd = 1608 \times 300 \times 168 / 10^6 = 81 \text{ kNm}$ $\Phi M_n = 69 \text{ kNm}$ $\Phi M_n > M_c$ so design is OK.

Fire calculations:

Revised strength reduction factor	$\Phi = 1.00$
Design load (fire)	$w_f = G + 0.4Q = 6.3 \text{ kN/m}$
Bending moment	$M_f^* = w_f L^2 / 8 = 6.3 \times 7.0^2 / 8 = 38.6 \text{ kNm}$
After 60 min of standard fire exposure	$t = 60 \text{ min}$ ($t_h = 1.0 \text{ hr}$)
Fire temperature	$T_f = 20 + 345 \log(8t + 1) = 945^\circ \text{C}$
Surface temperature	$T_w = \left[1 - 0.0616 t_h^{-0.88} \right] T_f$ $= \left[1 - 0.0616 t_h^{-0.88} \right] \times 945^\circ \text{C} = 887^\circ \text{C}$
Concrete temperature	$T_c = \left[0.18 \ln(t_h / c_e^2) - 0.81 \right] T_w$ $= \left[0.18 \ln(1.0 / 0.023^2) - 0.81 \right] \times 887^\circ \text{C} = 486^\circ \text{C}$
Steel temperature	$T_s = T_c = 486^\circ \text{C}$
Reduced yield stress	$f_{y,T} = (1.53 - T_s / 470) f_y = (1.53 - 486 / 470) \times 300 = 149 \text{ MPa}$
Stress block depth	$a_f = A_s f_{y,T} / 0.85 f'_c b = 1608 \times 149 / 0.85 \times 30 \times 1000 = 9.4 \text{ mm}$
Internal level arm	$jd_f = d - a_f / 2 = 177 - 9.4 / 2 = 172 \text{ mm}$
Bending strength	$M_{nf} = A_s f_{y,T} jd_f = 1608 \times 149 \times 172 / 10^6 = 41.2 \text{ kNm}$ $\Phi M_n = 1.0 \times 41.2 = 41.2 \text{ kNm}$ $\Phi M_{nf} > M_f$ so design is OK.

7.7.2 Worked Example 7.2

Reinforced concrete beam (refer to Figure 7.19 and Figure 7.25)

For a simply supported reinforced concrete beam with known span, load, geometry and reinforcing, check the positive flexural capacity after exposure for 90 min to the standard fire. Ignore the self-weight of the reinforcing bars.

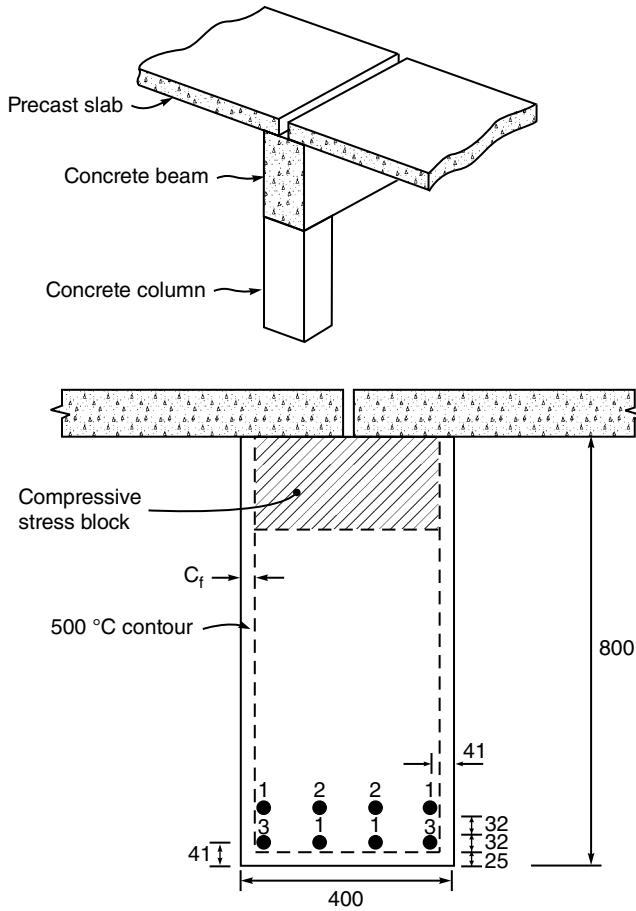


Figure 7.25 Beam for Worked Example 7.2

Given:

Beam span	$L = 15.0 \text{ m}$	Dead load	$G_1 = 6.0 \text{ kN/m}$
Beam width	$b = 400 \text{ mm}$	(Excluding self-weight)	
Beam depth	$h = 800 \text{ mm}$	Live load	$Q = 12.5 \text{ kN/m}$
Bottom cover	$c_v = 25 \text{ mm}$	Concrete density	$\rho = 24 \text{ kN/m}^3$
Bar diameter	$D_b = 32 \text{ mm}$	Concrete compressive strength	$f'_c = 30 \text{ MPa}$
Number of bars	$n = 8$ (2 rows of four bars)	Steel yield stress	$f_y = 300 \text{ MPa}$
Area of one bar	$A_{s1} = \pi r^2 = 804 \text{ mm}^2$		
Total steel area	$A_s = n\pi r^2 = 6434 \text{ mm}^2$		
Effective depth	$d = h - c_v - D_b / 2 = 800 - 25 - 48 = 727 \text{ mm}$		
Self-weight	$G_2 = \rho hb = 24 \times 0.4 \times 0.8 = 7.7 \text{ kN/m}$		
Total dead load	$G = G_1 + G_2 = 6.0 + 7.7 = 13.7 \text{ kN/m}$		

Cold calculations:

Strength reduction factor	$\Phi = 0.85$
Stress block depth	$a = A_s f_y / 0.85 f'_c b = 6434 \times 300 / 0.85 \times 30 \times 400 = 189 \text{ mm}$
Internal lever arm	$jd = d - a/2 = 727 - 189/2 = 632 \text{ mm}$
Design load	$w_c = 1.2G + 1.5Q = 35.2 \text{ kN/m}$
Bending moment	$M_c^* = w_c L^2 / 8 = 35.2 \times 15.0^2 / 8 = 990 \text{ kNm}$
Bending strength	$M_n = A_s f_y jd = 6434 \times 300 \times 632 / 10^6 = 1219 \text{ kNm}$ $\Phi M_n = 0.85 \times 1219 \text{ kNm} = 1036 \text{ kNm}$ $\Phi M_n > M_c$ so design is OK.

Fire calculations:

Design load (fire)	$w_f = G + 0.4Q = 13.7 + 0.4 \times 12.5 = 18.7 \text{ kN/m}$
Bending moment	$M_f^* = w_f L^2 / 8 = 18.7 \times 15.0^2 / 8 = 526 \text{ kNm}$
Fire duration	$t = 90 \text{ min}$
Depth of 500 °C isotherm (From Figure 7.6 assuming one-dimensional heat transfer at side of beam.)	$c_f = 33 \text{ mm}$
Reduced width	$b_f = b - 2c_f = 400 - 2 \times 33 = 334 \text{ mm}$

We assume that the concrete with temperature above 500 °C has no compressive strength and concrete below 500 °C has full compressive strength.

Steel temperatures from the isotherms in Figure 9.6:

- Bar group (1): 450 °C
- Bar group (2): < 200 °C
- Bar group (3): 580 °C

Reduced yield strength of reinforcing bars at elevated temperatures (from Equation 8.13):

$$f_{y,T1} = (1.53 - T_s/470)f_y = (1.53 - 450/470) \times 300 = 172 \text{ MPa}$$

$$f_{y,T2} = 300 \text{ MPa}$$

$$f_{y,T3} = (1.53 - 580/470) \times 300 = 89 \text{ MPa}$$

$$\begin{aligned} A_s f_{y,T} &= (4 \times A_{s1} \times f_{y,T1} + 2 \times A_{s1} \times f_{y,T2} + 2 \times A_{s1} \times f_{y,T3}) \\ &= 804 \times (4 \times 172 + 2 \times 300 + 2 \times 89) / 1000 = 1179 \text{ kN} \end{aligned}$$

Stress block depth	$a_f = A_s f_{y,T} / 0.85 f'_c b_f = 1179 \times 1000 / 0.85 \times 30 \times 334 = 138 \text{ mm}$
Internal lever arm	$jd_f = d - a_f/2 = 727 - 138/2 = 658 \text{ mm}$
Bending strength	$M_{nf} = A_s f_{y,T} jd_f = 1179 \times 1000 \times 658 / 10^6 = 776 \text{ kNm}$ $\Phi M_n = 1.0 \times 776 = 776 \text{ kNm}$ $\Phi M_{nf} > M_f$ so design is OK.

7.7.3 Worked Example 7.3

Reinforced concrete tee-beam

A reinforced concrete tee-beam is continuous over three supports (two spans). Check the structural adequacy of the beam before and after exposure to 2 h of the standard fire. Ignore the contribution of compressive reinforcing. The beam is one of a series of beams 400 mm wide by 800 mm deep, at 4.0 m centres, supporting a 150 mm thick concrete slab, as shown in Figure 7.26. Assume the structure is a storage building.

Given:

Beam span	$L = 13.0 \text{ m}$	Live load = 3.0 kN/m ² (storage)
Beam depth	$h = 800 \text{ mm}$	Concrete density 24 kN/m ³
Web width	$b_w = 400 \text{ mm}$	Concrete strength $f'_c = 30 \text{ MPa}$
Tributary width (for load)	$b_t = 4.0 \text{ m}$	Steel strength $f_y = 300 \text{ MPa}$
Effective flange width (for positive moment)	$b_e = 2.0 \text{ m}$	

Reinforcing	Bottom	Top
Number of bars	$n_b = 5$	$n_t = 18$
Bar diameter	$D_b = 28 \text{ mm}$	$D_t = 20 \text{ mm}$
Area of one bar	$A_{sb1} = \pi (D_b/2)^2 = 616 \text{ mm}^2$	$A_{st1} = \pi (D_t/2)^2 = 314 \text{ mm}^2$
Total steel area	$A_{sb} = n_b \pi A_{sb1} = 3079 \text{ mm}^2$	$A_{st} = n_t \pi A_{st1} = 5655 \text{ mm}^2$
Cover	$c_v = 25 \text{ mm}$	$c_v = 25 \text{ mm}$
Effective depth	$d_b = h - c_v - D_b/2 = 761 \text{ mm}$	$d_t = h - c_v - D_b/2 = 765 \text{ mm}$

Loads

Dead load (self-weight)	$G = (0.15 \times 4.0 + 0.65 \times 0.4) \times 24 = 20.6 \text{ kN/m}$
Live load	$Q = 3.0 \text{ kN/m}^2 \times 4.0 \text{ m} = 12.0 \text{ kN/m}$
Load combination for cold conditions	$w_c = 1.2G + 1.5Q = 42.7 \text{ kN/m}$
Load combination for fire conditions	$w_f = G + 0.6Q = 27.8 \text{ kN/m}$
(Load combination for fire, storage occupancy, from Chapter 5.)	

Check cold capacity:

Strength reduction factor	$\Phi = 0.85$
---------------------------	---------------

	Near mid-span (positive moment)	At support (negative moment)
Elastic bending moment	$M_m^* = 9w_c L^2/128 = 507 \text{ kNm}$	$M_s^* = w_c L^2/8 = 902 \text{ kNm}$
Stress block depth	$a_m = A_{sb} f_y / 0.85 f'_c b_e$ $= 3079 \times 300 / 0.85 \times 30 \times 2000$ $= 18.1 \text{ mm}$	$a_s = A_{st} f_y / 0.85 f'_c b_w$ $= 5655 \times 300 / 0.85 \times 30 \times 400$ $= 166 \text{ mm}$
Internal lever arm	$jd_b = d_b - a_m/2$ $= 761 - 9 = 752 \text{ mm}$	$jd_t = d_t - a_s/2$ $= 765 - 166/2 = 682 \text{ mm}$
Flexural strength	$M_m = A_{sb} f_y jd_b$ $= 3079 \times 300 \times 752 / 10^6$ $= 695 \text{ kNm}$	$M_s = A_{st} f_y jd_t$ $= 5655 \times 300 \times 682 / 10^6$ $= 1157 \text{ kNm}$
Design strength	$\Phi M_m = 591 \text{ kNm}$	$\Phi M_s = 983 \text{ kNm}$

$\Phi M_m > M_m^*$ and $\Phi M_s > M_s^*$ so design is OK.

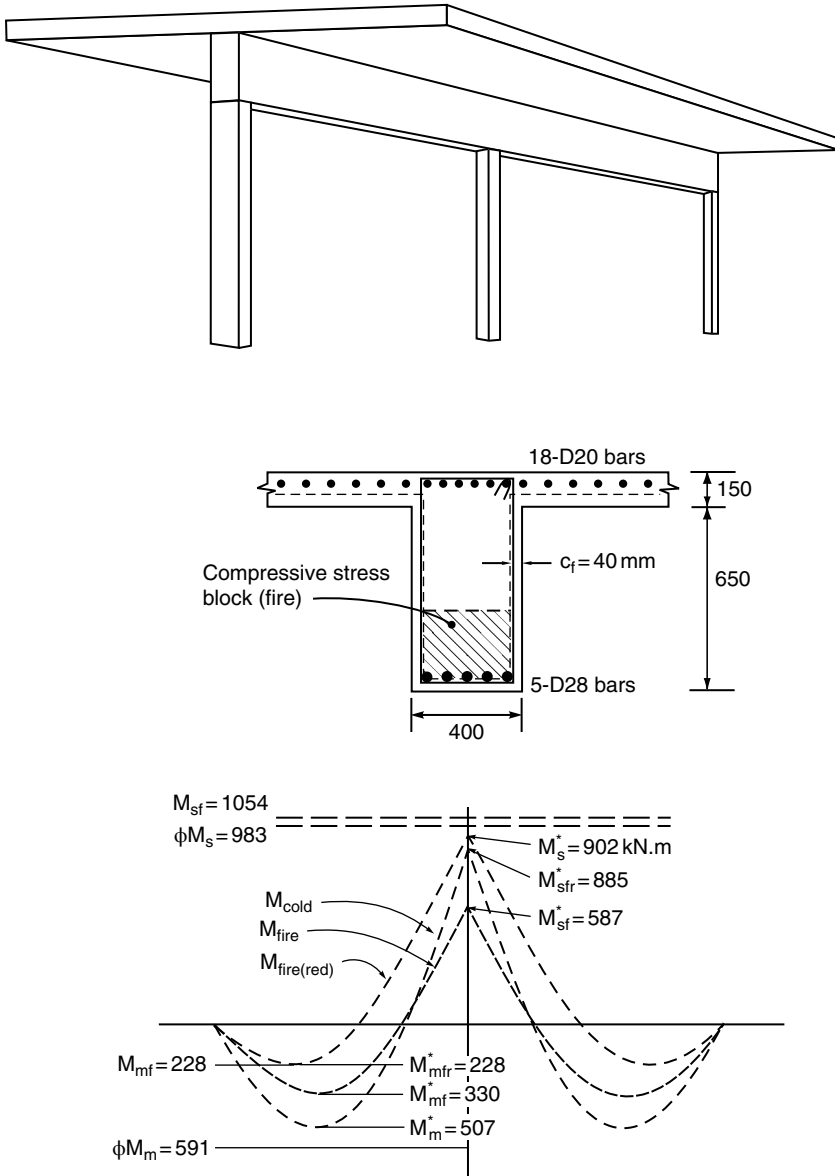


Figure 7.26 Beam for Worked Example 7.3

Design for fire:

Fire duration $t = 120$ min

Near mid-span:

Elastic bending moment

$$M_{mf}^* = 9 w_f L^2 / 128 = 330 \text{ kNm}$$

Effective cover to bottom bars

$$c_e = c_v + D_b / 2 = 25 + 28 / 2 = 39 \text{ mm}$$

Steel bar temperature from the isotherm of Figure 7.6:

Bar Group (1): 650 °C

Bar Group (2): 510 °C

$$\begin{aligned} \text{Reduced yield strength} \quad f_{y,T1} &= (1.53 - 650/470) \times 300 = 44.1 \text{ MPa} \\ f_{y,T2} &= (1.53 - 510/470) \times 300 = 134 \text{ MPa} \\ A_{sb} f_{y,T} &= (2 \times A_{sb1} \times f_{y,T1} + 2 \times A_{sb1} \times f_{y,T2}) \\ &= 616 \times (2 \times 44 + 2 \times 134) / 1000 = 301 \text{ kN} \end{aligned}$$

$$\begin{aligned} \text{Stress block depth} \quad a_{mf} &= A_{sb} f_{y,T} / 0.85 f'_c b_e \\ &= 301 \times 1000 / (0.85 \times 30 \times 2000) = 5.9 \text{ mm} \end{aligned}$$

Check concrete temperature:

From Figure 7.6 concrete at depth of 150 mm is less than 200 °C, so no reduction in f'_c

$$\begin{aligned} \text{Internal lever arm} \quad jd_{bf} &= d_b - a_{mf} / 2 \\ &= 761 - 3 = 758 \text{ mm} \end{aligned}$$

$$\begin{aligned} \text{Bending strength} \quad M_{mf} &= A_{sb} f_{y,T} jd_{bf} \\ &= 301 \times 1000 \times 758 / 10^6 \\ &= 228 \text{ kNm} \\ M_{nf} &< M_{mf}^* \text{ so the cross section fails.} \end{aligned}$$

At support:

$$\text{Elastic bending moment} \quad M_{sf}^* = 9w_f L^2 / 8 = 587 \text{ kNm}$$

Top bars are less than 250 °C so no reduction in strength.

Check concrete temperature:

We assume that the concrete with temperature above 500 °C has no compressive strength and concrete below 500 °C has full compressive strength.

$$\begin{aligned} \text{Depth of 500 °C isotherm} \quad c_f &= 40 \text{ mm} \\ \text{(From Figure 7.6 assuming one-dimensional heat transfer near surface.)} \end{aligned}$$

$$\begin{aligned} \text{Reduced width of stress block} \quad b_{wf} &= b_w - 2c_f = 400 - 2 \times 40 = 320 \text{ mm} \\ \text{Reduced effective depth} \quad d_t &= d_t - c_f = 765 - 40 = 725 \text{ mm} \\ \text{Stress block depth} \quad a_{sf} &= A_{st} f_y / 0.85 f'_{c,T} b_{wf} a_{sf} \\ &= 5655 \times 300 / 0.85 \times 30 \times 320 = 208 \text{ mm} \\ \text{Internal lever arm} \quad jd_{if} &= d_{if} - a_{sf} / 2 = 765 - 208 / 2 = 621 \text{ mm} \\ \text{Bending strength} \quad M_{sf} &= A_{st} f_y jd_{if} = 5655 \times 300 \times 621 / 10^6 = 1054 \text{ kNm} \end{aligned}$$

These calculations show that the fire has caused the mid-span flexural capacity to drop below the elastic bending moment which would cause failure if this was a simple supported beam. However, the flexural capacity over the support has increased (due to the change in Φ in fire conditions) so it is necessary to establish whether the beam can survive with the help of moment redistribution.

Moment redistribution:

For an end span of a continuous beam of length L , with uniformly distributed load w , and known positive moment M^+ , it can be shown (Gustaferro and Martin, 1988) that the negative bending moment at the support M^- is given by Equation 5.22:

$$M^- = wL^2 / 2 - wL^2 \sqrt{2M^+ / wL^2}$$

This can be used to calculate the redistributed bending moment at the support when the mid-span moment is just equal to the fire-reduced flexural capacity.

$$\begin{aligned} M^+ &= M_{mf} = 228 \text{ kNm}, w_f = 27.8 \text{ kN / m and } L = 13\text{m} \\ M_{sfr}^* &= w_f L^2 / 2 - w_f L^2 \sqrt{2M_{mf} / w_f L^2} \\ M_{sfr}^* &= 27.8 \times 13^2 / 2 - 27.8 \times 13^2 \sqrt{2 \times 228 / 27.8 \times 13^2} = 885 \text{ kNm} \\ M_{sfr}^* &< M_{sf} \end{aligned}$$

This shows that the design is OK, because the bending moments can be redistributed to the line shown by $M_{fire(red)}$ in Figure 7.26 where the maximum negative moment is now 885 kNm, less than the flexural capacity of 1054 kNm.

The location of the maximum mid-span moment is give by Equation 5.23:

$$\begin{aligned} a &= \sqrt{2M^+ / L} \\ a &= \sqrt{2 \times 228 / 13} = 5.9\text{m} \end{aligned}$$

The termination of the bottom reinforcing bars must be checked to determine if it is possible to develop full flexural strength at this location.

7.7.4 Worked Example 7.4

Axial restraint

Consider a reinforced concrete floor constructed from precast concrete tee-beams as shown in Figure 7.27. The slabs are simply supported over a span of 6.0m, carrying a live load of 3.0kPa. The dead load is 4.8kPa (including the self-weight). Calculate the restraint condition necessary to give a fire resistance rating of 90 min.

Given:

Slab span	L	=	6.0 m	Concrete strength	$f'_c = 25 \text{ MPa}$
Overall depth	h	=	300 mm	Steel strength	$f_y = 350 \text{ MPa}$
Web width	b_w	=	200 mm	Concrete modulus of elasticity	$E = 25 \text{ GPa}$
Overall width	b_f	=	1200 mm		
Cross-sectional area	A	=	85 000 mm ²		
Heated perimeter	s	=	1550 mm		

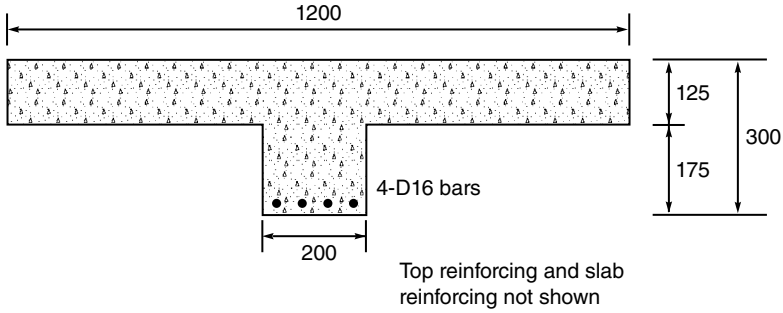


Figure 7.27 Beam for Worked Example 7.4

Load combinations:

Dead load per metre $G = 1.2 \times 4.8 = 5.76 \text{ kN/m}$

Live load per metre $Q = 1.5 \times 3.0 = 3.60 \text{ kN/m}$

Load combination for cold conditions: $w_c = 1.2G + 1.5Q = 12.3 \text{ kN/m}$

Load combination for fire conditions: $w_f = G + 0.4Q = 7.20 \text{ kN/m}$

Reinforcing:

Number of bars $n = 4$

Bar diameter $D_b = 16 \text{ mm}$

Bar area $A_s = \pi (D_b/2)^2 = 804 \text{ mm}^2$

Cover $c_v = 20 \text{ mm}$

Effective depth $d = h - c_v - D_b/2 = 272 \text{ mm}$

Effective cover $c_e = c_v + D_b/2 = 28 \text{ mm}$

Cold calculations:

Strength reduction factor $\Phi = 0.85$

Mid-span bending moment $M_c^* = w_c L^2/8 = 12.3 \times 6.0^2/8 = 55.4 \text{ kNm}$

Stress block depth $a = A_s f_y / 0.85 f'_c b_f = 804 \times 350 / 0.85 \times 25 \times 1200 = 11.0 \text{ mm}$

Internal lever arm $jd = d - a/2 = 272 - 11/2 = 266 \text{ mm}$

Flexural strength $M_c = A_s f_y jd = 804 \times 350 \times 266 / 10^6 = 75.0 \text{ kNm}$

$\Phi M_c = 0.85 \times 75.0 = 63.8 \text{ kNm}$

$\Phi M_c > M_c^*$ so cold design is OK.

Fire calculations:

Strength reduction factor $\Phi = 1.00$

Mid-span bending moment $M_f^* = w_f L^2/8 = 7.2 \times 6.0^2/8 = 32.4 \text{ kNm}$

Steel bar temperature from the isotherms on Figure 7.6:

Bar group (1) (corner bars) $T_{s1} = 750^\circ\text{C}$

Bar group (2) (inner bars) $T_{s2} = 660^\circ\text{C}$

Reduced yield strength $f_{y,T1} = (1.53 - 750/470) \times 350 = 0 \text{ MPa}$
 $f_{y,T2} = (1.53 - 660/470) \times 350 = 44.7 \text{ MPa}$
 $A_s f_{y,T} = (2 \times A_{s1} \times f_{y,T1} + 2 \times A_{s1} \times f_{y,T2})$
 $A_s f_{y,T} = (2 \times 201 \times 0 + 2 \times 201 \times 4.7) / 1000 = 18 \text{ kN}$

Stress block depth $a_f = A_s f_{y,T} / 0.85 f'_c b_f$
 $= 18 \times 1000 / (0.85 \times 25 \times 1200) = 0.71 \text{ mm}$

Internal lever arm $jd_f = d - a_f / 2 = 272 - 0.71 / 2 = 271.6 \text{ mm}$

Flexural strength $\Phi M_f = A_s f_{y,T} jd_f = 18 \times 1000 \times 271.6 / 10^6 = 14.9 \text{ kNm}$
 $\Phi M_f < M_f^*$ so slab will fail unless we provide restraint or continuity.

Provide axial restraint (numbers in brackets are steps from text)

(4) Estimate the mid-span deflection

Mid-span deflection of the reference specimen $\Delta_o = 65 \text{ mm}$ (from Figure 7.19)

Heated length $L = 6000 \text{ mm}$

Distance from neutral axis to extreme bottom fibre $y_b = 290 \text{ mm}$

(Assume that neutral axis is 10 mm from top of slab.)

Mid-span deflection $\Delta = L^2 \Delta_o / 89000 y_b$
 $= 6000^2 \times 65 / 89000 \times 290 = 90.7 \text{ mm}$

Height of line of thrust above the support $d_T = 0.9h = 270 \text{ mm}$

(Assume that the slab is built-in to the surrounding construction, thrust 0.1 h from bottom.)

(6) Calculate the required thrust to prevent collapse $T = 1000(M_{fire}^* - M_f) / (d_T - a_f / 2 - \Delta)$
 $= 1000[32.4 - 4.9] / (270 - 0.71 / 2 - 90.7)$
 $= 153.7 \text{ kN}$

(7) Recalculate a_f $a_f = (T + A_s f_{y,T}) / 0.85 f'_c b_f$
 $= (153700 + 18000) / 0.85 \times 25 \times 1200$
 $= 6.7 \text{ mm}$

Recalculate T $T = 1000[32.4 - 4.9] / (270 - 6.7 / 2 - 90.7)$
 $= 156.3 \text{ kN}$

(8) Non-dimensional thrust parameter $T/AE = 156300 / (185000 \times 25000) = 33.8 \times 10^{-6}$
 Shape parameter $z = A/s = 185000 / 1550 = 119 \text{ mm}$
 Strain parameter $\Delta/l/l = 0.006$ (from Figure 7.24)
 Maximum permitted displacement $\Delta l = 0.006 \times 6000 = 36 \text{ mm}$

So, this slab will have a fire resistance of 90 min if the surrounding structure at each end is capable of resisting an axial thrust of 156 kN with an axial elongation of less than 36 mm.

8

Composite Structures

This chapter describes simple methods of designing composite steel-concrete structures to resist fires. Composite construction refers to combined structural systems of steel and concrete, where both materials contribute to the load-bearing capacity. In many composite structures the steel member is partly or fully protected from direct fire exposure by concrete.

This chapter describes some common examples of composite construction and provides simple calculation methods of design for fire exposure. This chapter also gives design guidance for the structural fire design of single-storey and multi-storey steel frame buildings, with varying levels of composite action.

8.1 Fire Resistance of Composite Elements

Structural elements provide fire resistance by satisfying their intensity, insulation and load-bearing criteria, as specified in the standard fire test. As described in Chapter 4, different building elements would meet one or more of these criteria. Slabs perform a load-bearing function and separating function. As such they are required to meet all three criteria, while beams and columns are only required to satisfy the load-bearing criterion. The most common example of composite construction is a concrete slab with a steel deck or a supporting steel beam as shown in Figure 8.1. The steel beam in Figure 8.1 is called a ‘downstand beam’. Sometimes the steel beam is partly or completely buried in the concrete as shown in Figure 8.2. The system with the beam completely buried in the concrete floor slab is often called ‘slim-floor’. The simple calculation methods outlined in this chapter follow guidance in Eurocode 4 Part 1.2 (CEN, 2005c). They provide means of meeting the load-bearing criterion, and are based on standard fire testing.

The commonest examples of composite slabs are trapezoidal and re-entrant decking systems as shown in Figure 8.3. Composite steel beams can be completely exposed, partially exposed

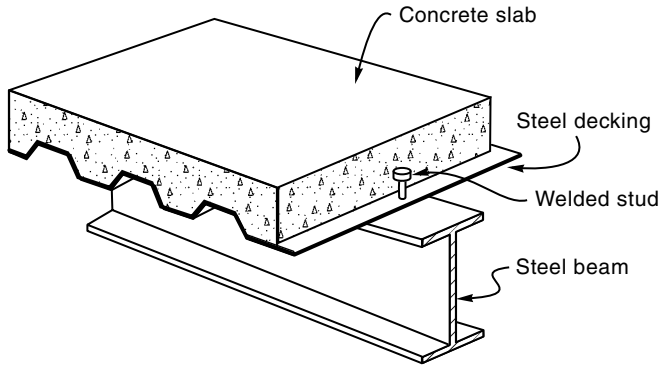


Figure 8.1 Composite construction with concrete slab on steel deck and steel beam

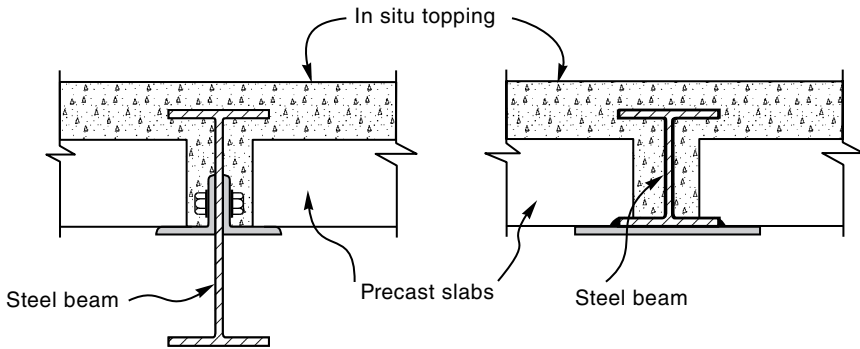


Figure 8.2 Composite construction with steel members protected by concrete

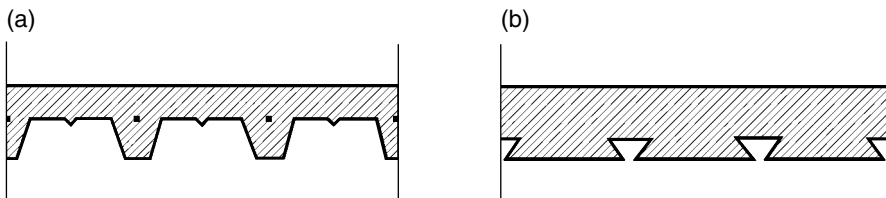


Figure 8.3 Typical examples of composite flooring systems: (a) trapezoidal decking system; (b) re-entrant decking system

or completely buried in concrete, as shown in Figure 8.1 and Figure 8.2. Completely buried beams allow reductions in the total floor depth, which maximize the use of the floor.

Figure 8.4 and Figure 8.5 show a concrete-encased steel column and a partially encased steel column while a rectangular tubular steel section filled with concrete is shown in Figure 8.6. In certain cases, concrete may be considered to act only as a heat sink for the steel structure, or, it may be designed with suitable reinforcing as a load-bearing material as part of the composite structure. In all cases the concrete increases the thermal mass of the

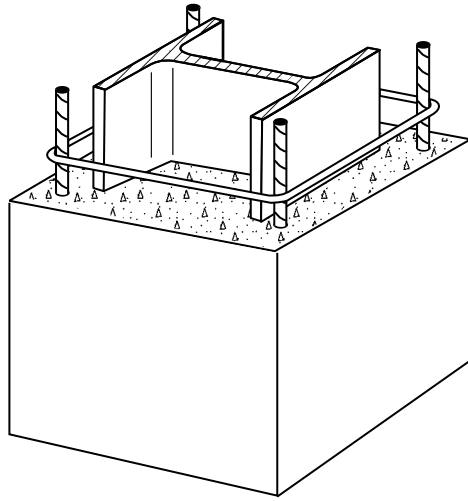


Figure 8.4 Steel column protected with concrete encasement

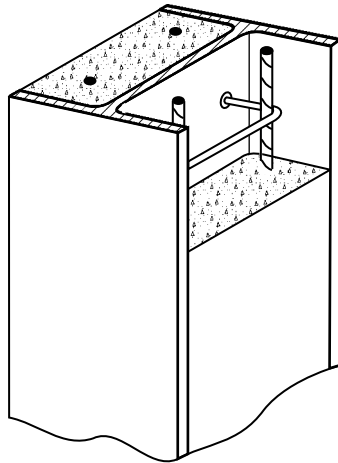


Figure 8.5 Steel column protected with concrete between the flanges

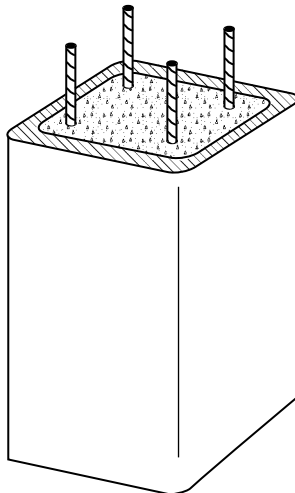


Figure 8.6 Concrete filled tubular steel column

assembly, which reduces the rate of increase of steel temperatures. In the first two column examples, the concrete is fully or partially reducing the area of steel surface exposed to the fire environment.

8.2 Assessing Fire Resistance

As composite structures are made up of both steel and concrete materials their assessment for fire resistance follows fundamental combinations of the strength contributions of the two materials, once appropriate cross-section temperature distributions have been calculated. Accurate temperatures are best calculated by two-dimensional finite element analyses, as provided by SAFIR, ABAQUS, ANSYS, and other specialized computer programs (Wang, 2002). Thermal analyses of this nature are ideal for advanced calculation methods but are unsuitable for routine design, due to the cost of analysis setup times and run times. They are therefore primarily used for research purposes. Details of processes involved in advanced thermal analyses are provided in Chapter 11.

Simple calculation methods exist for thermal and structural analyses of a limited range of composite members. The use of tabulated data for the design of composite structures is very common. The tabulated data cover thermal and structural behaviour at standard times. This chapter expands on the different design approaches for the design of composite structures. The primary source for the information presented here is Eurocode 4 Part 1.2 (CEN, 2005c).

8.2.1 *Tabulated Data for Beams and Columns*

Tabulated data are very helpful for simple design of beams and columns of composite structures, because simple calculation methods only exist for certain limited types of construction, and advanced calculation methods are costly to setup, run and post-process for routine design. Eurocode 4 Part 1.2 (CEN, 2005c) limits the use of tabulated data to very special cases, under standard fire exposure and only in braced frames. It is also assumed that the applied loads and boundary conditions do not change during the fire, although the thermal gradients may change. Fire resistance is assessed as a function of the load level, the cross-sectional properties and reinforcing ratio. The Eurocode tabulated data are applicable to the following types of systems:

Beams

- Composite steel beams with partial concrete encasement
- Fully encased steel beams

Columns

- Fully encased steel columns
- Partially encased composite steel columns
- Concrete filled tubular (CFT) steel columns

8.2.2 *Simple Calculation Methods*

Simple calculation methods are suitable for isolated structural members, in which the contributions of each part of the cross section can be easily assessed. As they have been developed from extensive testing of these members, they are limited to standard fire exposure along the

entire length of the structural element. Simplified calculation methods inherently account for load ratio and thermal gradients. They do not account for restraints from adjacent structures, and they may not be used beyond the limits to which they have been tested. The limited structural systems that can be analysed with these methods are (CEN, 2005c):

Slabs

- Unprotected composite slabs
- Protected composite slabs

Beams

- Composite steel beams with no concrete encasement
- Composite steel beams with partial concrete encasement
- Steel beams with partial concrete encasement (non-composite)

Subsequent sections of this chapter provide guidance on some of these simple calculation approaches. Advanced hand calculation methods for composite steel-concrete floor slabs are given in Chapter 11.

8.2.3 *Advanced Calculation Methods*

Advanced calculation methods provide realistic predictions of structural behaviour under fire conditions. This is achieved by using computer models to consider the relevant combinations of fundamental fire dynamics, thermal analysis and mechanical response of structures under high temperatures. To accurately model physical behaviour the mechanical models must adequately incorporate geometric and material nonlinearities. They must also consider the effects of adjacent structures on heated members, which range from additional restraints to load redistributions, which may or may not be detrimental to the fire resistance of the heated zones.

It must be borne in mind that even though these computer-based methods produce good predictions, they are also approximate, so care needs to be taken to ensure that the right types of analyses are performed with the right tools. For design, the capabilities of the tools need to be discussed with the client, the designer and the approving authority. Chapter 11 addresses advanced calculation methods in more detail.

8.3 Behaviour and Design of Individual Composite Members in Fire

8.3.1 *Composite Slabs*

Composite steel-concrete slabs shown in Figure 8.1 and Figure 8.3 are popular because they eliminate the need for re-useable formwork and they are light enough to be installed over large areas without heavy lifting equipment. The thin steel decking material acts as permanent formwork and as external reinforcing. There are a number of different profiles available, all of which have deformations in the steel to ensure bond between the steel and the concrete to carry shear forces and to resist delamination. Fire behaviour is discussed under the three categories of integrity, insulation and stability.

8.3.1.1 Integrity

Composite steel-concrete slabs generally have excellent integrity because even if cracks occur in the concrete slab, the continuous steel decking will prevent any passage of flames or hot gases through the floor system.

8.3.1.2 Insulation

To meet the insulation criterion, it is simply necessary to provide sufficient thickness of concrete. A solid slab of uniform thickness would require the same thickness as a normal reinforced concrete slab. For trapezoidal or dovetail profiles it is necessary to evaluate an effective thickness. Generic listings are given in some codes including Eurocode 4 (CEN, 2005c). All manufacturers of steel decking provide proprietary ratings for their products which give this information. It is possible to spray the underside of the steel sheeting with spray-on insulation, but this is rarely economical. Calculation of temperatures in the concrete slab can be made as suggested in Chapter 7, ignoring the presence of the steel deck which heats up rapidly during fire exposure.

8.3.1.3 Stability

The strength of composite steel-concrete slabs is severely influenced by fire because the steel sheeting acting as external reinforcing loses strength rapidly when it is exposed to the fire. However, composite slabs have been shown to have good fire resistance because of three contributing factors: axial restraint; moment redistribution; and fire emergency reinforcing.

Composite slabs often have different fire resistance ratings for restrained and unrestrained conditions (e.g. UL, 2012). During a fire test, if a composite slab is built into a rigid testing frame which allows almost no axial expansion (Figure 4.7), the slab can achieve a fire resistance rating with no reinforcing other than the external steel sheeting, because of the thermal thrust developed at the supports (see Chapter 5). Some buildings are sufficiently stiff and strong to provide such restraint to a fire-exposed floor system, but this is difficult to assess accurately, so it is usual to rely on some reinforcing within the slab.

Composite steel-concrete slabs usually have nominal reinforcing consisting of welded wire mesh or normal reinforcing bars, to control any cracking caused by shrinkage or overloading. If this is placed near the top of the concrete and if the slab is continuous over several supports, the slab can develop significant negative moment capacity over the supports (hogging moment) through moment redistribution, and hence retain sufficient load capacity during the fire.

If a slab is simply supported, or if moment redistribution is insufficient to resist the applied loads, it is common practice to place 'fire emergency reinforcing' in the slab, consisting of steel reinforcing bars in the troughs of the sheeting, with sufficient cover (25–50 mm) from the bottom surface to control temperature rise in the bars. If the temperature of the bars is known, the flexural strength of the composite slab can be calculated as for a conventional reinforced concrete slab. Design recommendations are given by ECCS (1983), Lawson (1985) and Eurocode 4 Part 1.2 (CEN, 2005c). As described in subsequent sections of this chapter, composite steel-concrete slabs have been observed to behave well in fires when they are part of a large composite structure. After long periods of fire exposure, such slabs can develop

tensile membrane action as described by Wang (2002). Further discussion of composite slabs is given in Chapter 11.

8.3.2 Composite Beams

Composite steel-concrete beams generally consist of reinforced concrete slabs supported by hot-rolled structural steel beams, connected together to provide composite structural action. The most common system is for the composite steel-concrete slab to run over the top of the steel beams as shown in Figure 8.1, but the beams are sometimes partially embedded in the slab as shown in Figure 8.2 with precast concrete slabs. The required shear connection between the steel beam and the concrete slab is usually provided by shear studs welded to the top of the beam (Figure 8.1). Composite beams act as tee-beams, with the slab in compression under positive (sagging) moments and the slab in tension under negative (hogging) moments.

Several alternative methods of thermal analysis are available, as described in Chapter 6. Equation 6.3 and Equation 6.4 can be used to determine the temperatures of the steel section in Figure 8.1. If a large part is buried in concrete (as shown in Figure 8.2), then there will be large temperature gradients and the only accurate way to calculate the steel and concrete temperatures is to use a heat transfer computer program (such as TASEF, ABAQUS, ANSYS, or SAFIR). A rough calculation of the steel temperature profile can be made using the Eurocode method in Sections 6.2.5 and 6.2.6, where the section factor should be obtained using the fire-exposed perimeter of that portion of the steel section not buried in concrete. Note that the cross-sectional area in the section factor calculation is the entire cross-sectional area of the steel section.

If the slab consists of a composite steel-concrete slab spanning between the beams, there will be intermittent voids between the underside of the slab and the top of the beam, so the beam will be exposed on all four sides in these regions, which must be considered in the thermal calculations (Newman and Lawson, 1991). The structural calculation during fire exposure is essentially the same procedure as in normal temperature conditions. Detailed design methods are given by BS 5950 Part 8 (BSI, 2003b) and Eurocode 4 Part 1.2 (CEN, 2005c), but an approximate design is often sufficient. Two methods for estimating the structural resistance are given by Eurocode 4 Part 1.2, and are detailed below.

8.3.2.1 Critical Temperature Method

This is a simplified method, which can be used for the positive moment (sagging) resistance of simply supported composite steel downstand beams with steel I-section depths up to 500 mm and concrete slab thickness of at least 120 mm. The principal advantage of this method is that the bending moment capacity in fire does not need to be calculated. As the compressive strength of concrete does not significantly influence the sagging moment capacity at elevated temperatures the method predicts the beam's critical temperature based on steel yield stress and the utilization of the composite beam at room temperature.

The critical temperature is calculated from:

$$r_{load} = \frac{f_{y,T_f}}{f_{y,20^\circ C}} \quad (8.1)$$

where r_{load} is the load ratio at the fire limit state and f_{y,T_i} and $f_{y,20^\circ\text{C}}$ are the yield stresses of steel at the critical temperature and at 20°C , respectively. The load ratio can be derived in terms of the applied moment at room temperature M^* and the beam capacity M_n :

$$r_{load} = \frac{f_{y,T_i}}{f_{y,20^\circ\text{C}}} = \frac{M_{nf}}{M_n} = \frac{M_{fire}^*}{M_n} = \frac{U_{load} M^*}{M_n} \quad (8.2)$$

$$U_{load} = \frac{G_k + \psi_{fi} Q_k}{\gamma_G G_k + \psi_Q Q_k} \quad (8.3)$$

where M_{nf} is the failure capacity of the composite beam in fire conditions, M_{fire}^* is the applied moment in the fire and U_{load} is the ratio of the applied actions at the fire limit state to the applied actions at room temperature

8.3.2.2 Bending Moment Capacity Method

This approach, from Eurocode 4 is general in nature, so that all downstand composite beams can be designed using this method. However, this is the only option in Eurocode 4 for the simplified assessment of beams with either a steel section depth greater than 500mm or a concrete slab thickness less than 120mm. In addition, the method can handle asymmetric beams – beams with different dimensions of the top and bottom flanges (as shown in Figure 8.7).

For sagging moment capacity of the beam, the cross section is broken into four components for thermal and structural analysis as shown in Figure 8.7. These are the concrete slab, the top flange, the web and the bottom flange of the steel section. The concrete flange in compression is treated as being at 20°C throughout the fire exposure. The three steel components are assigned the following section factors, where the terms are all defined in Figure 8.7:

Top flange

$$F_i/V_i \text{ or } F_{p,i}/V_i = (b_2 + 2t_{f2})/b_2 t_{f2}, \text{ if 85\% of the flange is in contact with the concrete slab} \quad (8.4a)$$

$$F_i/V_i \text{ or } F_{p,i}/V_i = 2(b_2 + t_{f2})/b_2 t_{f2}, \text{ if contact with the concrete slab is less than 85\%} \quad (8.4b)$$

Web

$$F_i/V_i \text{ or } F_{p,i}/V_i = (2d_w)/d_w t_w \quad (8.5)$$

Bottom flange

$$F_i/V_i \text{ or } F_{p,i}/V_i = 2(b_1 + t_{f1})/b_1 t_{f1} \quad (8.6)$$

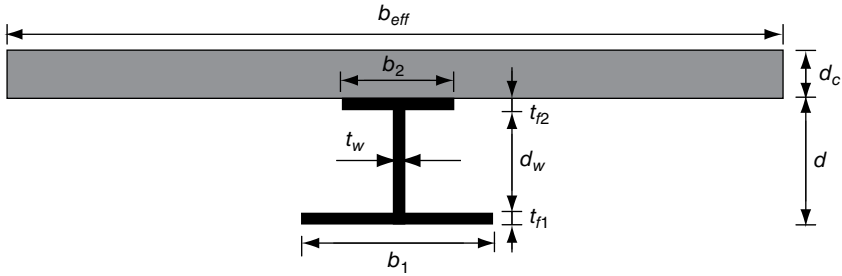


Figure 8.7 Generalized composite beam for the bending moment capacity method. Reproduced from CEN (2005c). © CEN, reproduced with permission

If the beam depth is not greater than 500 mm the web temperature may be taken to be the same as the bottom flange temperature. The percentage of the top flange of the steel section in contact with the slab considers filled or unfilled voids that may be present between the steel deck and the steel beam due to the corrugations on the shape of the deck.

Once section factors have been calculated, the individual temperatures in the web and flanges of the beam can be estimated with the incremental approach outlined in Sections 6.2.5 and 6.2.6. The shadow effect may be calculated from Equation 8.7 (with the dimensions as defined in Figure 8.7). The moment capacity can then be calculated with Equation 8.8, after the neutral axis has been obtained with Equation 8.9.

$$k_{shadow} = 0.9 \left(\frac{t_{f1} + t_{f2} + 1/2 \cdot b_1 + \sqrt{d_w^2 + 1/4 \cdot (b_1 - b_2)^2}}{d_w + b_1 + 1/2 \cdot b_2 + t_{f1} + t_{f2} - t_w} \right) \quad (8.7)$$

$$M_{mf} = \sum_{i=1}^n A_i z_i k_{y,T_i} f_{y,i} + 0.85 \sum_{j=1}^m A_j z_j k_{c,T_j} f_{c,j} \quad (8.8)$$

$$\sum_{i=1}^n A_i k_{y,T_i} f_{y,i} + 0.85 a_f \sum_{j=1}^m A_j k_{c,T_j} f_{c,j} = 0 \quad (8.9)$$

where $f_{y,i}$ is the yield strength of a particular part of the cross section, $f_{c,j}$ is the concrete compressive strength, A_i and A_j are the algebraic areas of the various sections with respect to the neutral axis, a_f is the depth of the concrete compression block, k_{y,T_i} and k_{c,T_j} are the reduced properties of steel and concrete, respectively, and z_i and z_j are the distances from the centroids of areas A_i and A_j , respectively, to the plastic neutral axis.

For negative moment (hogging) near the supports, the situation described above is reversed such that the slab is in tension and the bottom flange is in compression, so it can now be considered to be a compressive member. The bottom flange is restrained vertically by the web, but lateral buckling must be considered by using calculation methods for a column or an unrestrained beam, depending on the distance between any lateral restraints. The reinforcing in the slab should be checked for axial tensile capacity, which can be assisted by the top flange of the

beam if necessary. If the slab has steel tray decking, that can enhance the flexural capacity of the cross section, but only if it is running parallel to the beam.

The capacity of the shear studs between the beam and the slab is unlikely to be seriously affected by fire exposure. BS 5950 Part 8 (BSI, 2003b) does not require any check on the studs, but Eurocode 4 Part 1.2 (CEN, 2005c) gives a formula based on normal temperature behaviour with the temperature at the base of the stud being 80% of the top flange temperature, and the concrete temperature being half of that at the base of the stud.

8.3.2.3 Slim-floor Beams and Fully Encased Beams

Using a similar approach, the moment capacity of partially encased, fully encased and slim-floor beams can be determined by estimating temperatures of parts of the individual components of the cross section (I-sections or asymmetrical sections, and the layers of reinforcing and concrete). For sagging moment capacity only parts of the concrete which are not affected by temperature are included. For hogging moment capacity, the tension and compression components are evaluated by dividing the cross section into strips of uniform temperature. The moment capacity (for both sagging and hogging moments) is evaluated with Equation 8.7 after the neutral axis has been determined from Equation 8.8. The calculation ignores any tension contribution from concrete.

8.3.2.4 Light Steel Joists

Another common system of composite construction uses open web steel joists or light gauge cold-rolled steel joists combined with concrete, as shown in Figure 8.8. These systems often include a special formwork system that allows the light steel joists to support the boxing (formwork) with no additional propping (shoring). These low cost systems are mainly designed as simply supported spans because the negative flexural capacity is very low. The fire resistance of this type of composite construction is very poor without additional protection to the steel joists, because of the very high section factor (low effective thickness) of the steel, which will heat up and lose strength rapidly when exposed to a post flashover fire. Additional fire resistance can be provided with a fire resisting ceiling membrane or with fire protection material sprayed on to the steel elements.

8.3.3 Composite Columns

Examples of composite columns have been shown in Figure 8.4, Figure 8.5 and Figure 8.6: fully encased steel columns; partially encased steel columns; and CFT columns, respectively. Columns fail by one of three criteria: local buckling; global buckling; or compressive crushing of the column cross section. In most observed cases of fire tests on steel columns, failure has been either due to local buckling or global buckling, as typical column cross sections have high slenderness in the standard fire test (Wang, 2002). For composite construction, the presence of the concrete tends to prevent the occurrence of local buckling. As a result of these observations the simplified design guidance in Eurocode 4 Part 1.2 (CEN, 2005c) is primarily

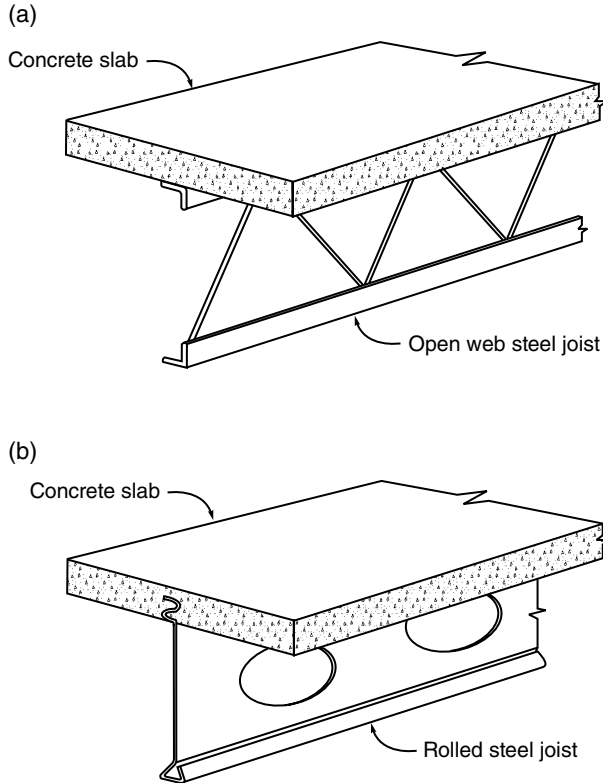


Figure 8.8 Composite construction with light steel joists: (a) open web steel joist; (b) rolled steel joist

to determine the global buckling resistance of these columns in braced frames. The simplified design method is restricted to braced frames so that the columns are not part of the lateral load resisting system.

These calculations assume that the fire is only on one storey, at any given time, and that the heated columns are restrained at their ends by cold columns at the upper and lower storeys. It is also assumed that the heated-column-ends are rotationally restrained.

The buckling resistance N_{bf} of a composite column in fire conditions is given by:

$$N_{bf} = \chi N_{cf} \quad (8.10)$$

where χ is the buckling reduction coefficient, depending on the relative slenderness $\bar{\lambda}_r$ and N_{cf} is the axial compression capacity of the column in fire conditions, given by Equation 8.11.

$$N_{cf} = \sum_j (A_{s,T} f_{sy,T}) + \sum_k (A_{r,T} f_{ry,T}) + \sum_m (A_{c,T} f_{c,T}) \quad (8.11)$$

where $A_{i,T}$ is the area of material i , at any given temperature T (i is steel reinforcing or concrete), $f_{iy,T}$ is the yield stress of material i , at any given temperature T [i is either steel (s) or reinforcing (r)] and $f_{c,T}$ is concrete compressive stress, at a temperature T .

For most composite column types the determination of buckling reduction coefficient χ is by the use of buckling curve 'c' (shown in Figure 8.9), following the rules of Eurocode 3 Part 1.1 (CEN, 2005a), which requires the relative slenderness λ_T to be calculated as:

$$\bar{\lambda}_T = \sqrt{N_{cf} / N_{f,crit}} \quad (8.12)$$

with the Euler buckling load or elastic critical load in fire conditions ($N_{f,crit}$) calculated as:

$$N_{f,crit} = \pi^2 (EI)_f / l_T^2$$

in which l_T is the buckling length of the column in fire conditions. The effective flexural stiffness at elevated temperatures is calculated as:

$$(EI)_f = \sum_j (\varphi_{s,T} E_{s,T} I_{s,T}) + \sum_k (\varphi_{r,T} E_{r,T} I_{r,T}) + \sum_m (\varphi_{c,T} E_{c,sec,T} I_{c,T}) \quad (8.13)$$

where $I_{i,T}$ is the second moment of area, of part i of the cross section for bending around the relevant axis, $\varphi_{i,T}$ is the bending stiffness reduction coefficient depending on the effect of thermal stresses, $E_{c,sec,T}$ is the characteristic value for the secant modulus of concrete in fire conditions and $E_{i,T}$ is the modulus of elasticity of the steel reinforcing in fire conditions.

The secant modulus of concrete at any temperature is calculated as the concrete strength at that temperature ($f_{c,T}$) divided by the strain at ultimate stress ($\epsilon_{cu,T}$). The reduction coefficients for the effects of thermal stress on the column cross section are to account for equilibrating stresses induced as a result of non-uniform expansions of steel and concrete. The Eurocode specifies these coefficients for partially encased steel columns in Annex G of Eurocode 4 Part 1.2 (CEN, 2005c), but does not specify what they should be for CFT sections. As a result, a common design practice is to set these equal to unity, which may inherently make these columns unsafe. As part of developing simplified rules for the design of these columns (Espinosa *et al.*, 2013) recent studies have proposed an approach to calculate these coefficients based on the size of the columns and their buckling length (Espinosa *et al.*, 2012). For bar-reinforced CFT columns additional bending stiffness reduction coefficients need to be calculated for the rebars as well.

In addition to the above, test result comparisons and numerical simulations have shown that buckling curve 'a' in Figure 8.9 is better for the design of unreinforced CFT sections, while buckling curve 'b' is found suitable for reinforced CFT sections (Espinosa *et al.*, 2012, 2013).

Buckling lengths of columns can be obtained from Figure 6.27. Buckling lengths of intermediate storey columns are $0.5l$ while those of top storey columns are $0.7l$. Bottom storey columns may have buckling lengths between $0.5l$ and $0.7l$ depending on the rotational fixity of the base of the column.

Considerable research has been carried out on CFT columns exposed to fires (Figure 8.6). In addition to preventing local buckling, the concrete filling has two beneficial effects: it acts as a heat sink to slow the rise in temperature of the steel column; and it can carry some or all of the axial load when the strength of the steel reduces. In some cases of low fire exposure, a thermal analysis may show that the steel column can carry the entire axial load, relying on the concrete only to slow the increase in steel temperature. For more severe fire exposure, it is more likely that the heated concrete filling carries the applied loads without any

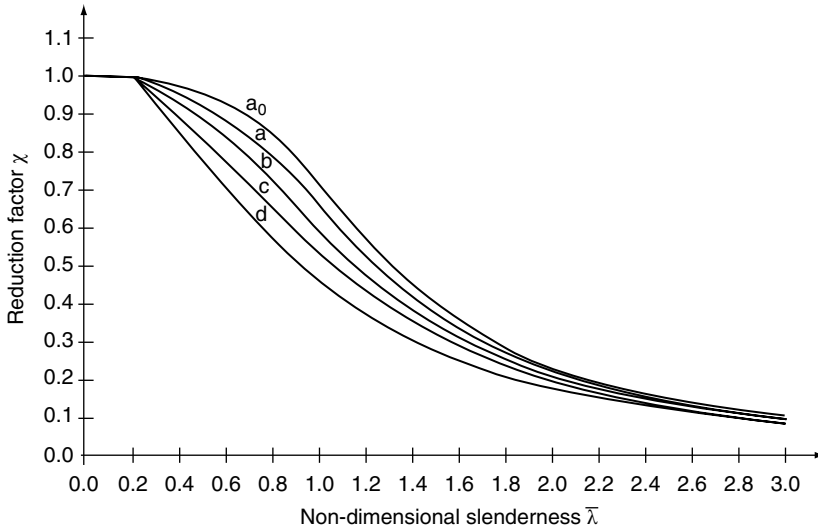


Figure 8.9 Buckling curves for the design of composite compression members. Reproduced from CEN (2005a). © CEN, reproduced with permission

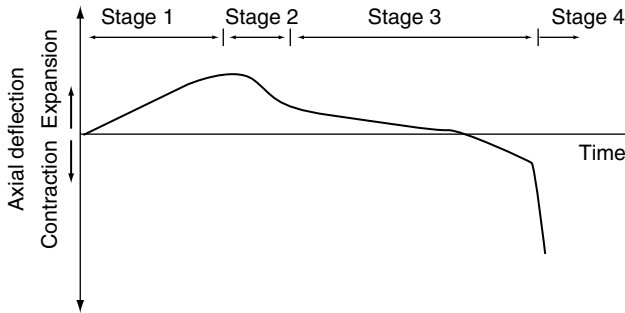


Figure 8.10 Typical axial deformation of CFT column exposed to a standard fire. Reproduced from Wang (2002) by permission of Taylor and Francis Books UK

contribution from the hot steel member. This behaviour is evidenced in Figure 8.10 which shows the behaviour of these columns exposed to the standard fire.

The CFT column goes through four stages in a fire. As steel expands faster than concrete the first stage shows the load resistance being provided by the steel casing alone. This continues until temperatures become high enough to initiate buckling of the steel tube. At this point the load is transferred to the concrete core in stage 2. In stage 3 the concrete core resists the load until it deteriorates to an extent where it can no longer support the applied loading. The column subsequently fails in stage 4. The confinement provided by the steel tube prevents direct exposure of the concrete to the fire and spalling, thereby prolonging the resistance of the column. To avoid the build-up of water pressure due to evaporation of free water and

Table 8.1 Value of factor f for fire resistance of concrete filled steel columns (Kodur, 1999)

Filling concrete	Square columns	Circular columns
Plain concrete	0.06	0.07
Bar reinforced concrete	0.065	0.075
Fibre reinforced concrete	0.065	0.075

Note that tabulated values of f may be increased cumulatively as follows:

- Tabulated values are for siliceous aggregate concrete. For carbonate aggregate concrete, add 0.01.
- Bar reinforced concrete values are for cover <25 mm. For cover \geq 25 mm, add 0.005.
- Bar reinforced concrete values are for reinforcing <3%. For reinforcing \geq 3%, add 0.005.

decomposition of chemically bound water, CFT columns drain holes of at least 20 mm diameter must be provided at every floor level to allow the water to escape.

Design equations for concrete filled steel columns are available from several sources (e.g. ECCS, 1988; BSI, 2003b) and tables of fire resistance ratings are given in Eurocode 4 (CEN, 2005c). Lie and Kodur (1996) tested many columns, leading to a design formula in the National Building Code of Canada (NBCC, 2010) and the American standards for the design of concrete filled columns (ASCE, 2005; ACI, 2007), for 1 and 2 h fire resistance ratings. Kodur (1999) extended the applicability of the equation, showing that fibre reinforced concrete is similar to conventional reinforced concrete, both having greater fire resistance than plain concrete filling. The Canadian empirical design equation gives the fire resistance t_r (in minutes) of a circular or square steel column completely filled with concrete, as:

$$t_r = \frac{f(f'_c + 20)d^{2.5}}{(KL - 1000)\sqrt{N}} \quad (8.14)$$

where f is a factor from Table 8.1, f'_c is the strength of the filling concrete (MPa), d is the outside diameter or width of the column (mm), L is the unsupported length of the column (mm), KL is the effective length of the column, considering the end support conditions (mm) and N is the applied load on the column (kN).

Equation 8.14 is valid for fire resistance times up to 2 h for plain concrete, and 3 h for reinforced concrete, for column sizes from about 140 to 410 mm, except that bar reinforcing cannot be used in columns smaller than about 200 mm. Square columns with fibre reinforced concrete can be as small as 100 mm. The width to thickness ratio should not exceed 'class 3' according to the Canadian steel design code (Canadian Standards Association, 2009). Recent research has developed simple calculation models for standard fire exposure (Espinosa *et al.*, 2012, 2013), which considerably improves upon simplified methods suggested in Eurocode 4 Part 1.2 (CEN, 2005c). The approach calculates representative temperatures for the concrete core and the steel tube at any time in the standard fire, and uses the approach described in Section 8.2.3 to design the column.

The design methods described above are for standard fire exposure. Design methods for exposure to real fire time–temperature curves are not well established, but an approximate calculation can be made by carrying out a thermal analysis, then summing the load-resisting contribution of the steel and the filling concrete calculated separately.

8.4 Design of Steel and Composite Buildings Exposed to Fire

8.4.1 Multi-storey Steel Frame Buildings

In recent years, a number of large fires in steel and composite buildings have demonstrated that the fire performance of large frame structures is often much better than can be predicted by consideration of the fire resistance of the individual structural elements (Moore and Lennon, 1997). This excellent behaviour results from the ductility of steel, allowing large rotations and deflections without significant loss of strength. These observations have been supported by extensive computer analyses, including Franssen *et al.* (1995) who showed that when axial restraint from thermal expansion of the members is included in the analysis of a portal frame building, the behaviour is completely different from that of the column and beam analysed separately.

An often quoted example is the severe fire at the Broadgate complex in London in 1990 (SCI, 1991). The fire occurred in a contractor's hut on the second storey of a 14-storey building nearing completion, before most of the columns had been protected with fire resisting materials. It is estimated that many of the structural members in the fire area reached temperatures of 650 °C. The fire caused severe distortion of trusses and beams supporting the floor slabs, and axial shortening of five columns, but there was no structural collapse and no loss of integrity of the floor slabs (Figure 8.11). The building was repaired with no serious difficulties.

A large series of full-scale fire tests was carried out between 1994 and 1996 in the Cardington Laboratory of the Building Research Establishment in England (Figure 8.12). A full size eight-storey steel building was constructed with composite reinforced concrete slabs on exposed metal decking, supported on steel beams with no applied fire protection other than a suspended ceiling in some tests. The steel columns were fire-protected. A number of fire tests were carried out on parts of one floor of the building, resulting in steel beam temperatures up to 1000 °C, leading to deflections up to 600 mm, but no collapse and generally no integrity failures (Armer and O'Dell, 1996; Martin and Moore, 1997).

The good performance of the floor/beam systems in such buildings has been attributed to a complex inter-related sequence of events, described in the following simple steps:

1. The fire causes heating of the beams and the underside of the slab.
2. The slab and beams deform downwards as a result of thermal bowing.
3. Thermal expansion causes compressive axial restraint forces to develop in the beams.
4. The reaction from the stiff surrounding structure causes the axial restraint forces to become large.
5. The yield strength and modulus of elasticity of the steel reduce steadily.
6. The downward deflections increase rapidly due to the combined effects of the applied loads, thermal bowing and the high axial compressive forces.
7. The axial restraint forces reduce due to the increased deflections and the reduced modulus of elasticity, limiting the horizontal forces on the surrounding structure.



Figure 8.11 Local buckling of an unprotected steel column during a fire in a building under construction (Broadgate, London, 1990) (SCI, 1991)

8. Higher temperatures lead to a further reduction of flexural and axial strength and stiffness.
9. The slab beam system deforms into a tensile membrane, with tensile forces in the middle of the slab and a ring of compressive forces on its periphery.
10. As the fire decays, the structural members cool down and attempt to shorten in length.
11. High tensile axial forces are induced in the slab, the beam and the beam connections.

These actions can take place in two dimensions or three dimensions, depending on the geometry of the building and the layout of the structure. The large deformations are often accompanied by local buckling of the steel members. The high axial tensile forces can result in fractures of buckled beams after the fire (Tide, 1998).

Modern computing power makes it possible to model the structural response of steel frame buildings exposed to fires. Computer modelling has been used to help interpret the behaviour of the Cardington building (e.g. Wang *et al.*, 1995; O'Connor and Martin, 1998; Rose *et al.*, 1998; Rotter *et al.*, 1999). Some of the studies have found that the building can be modelled using two-dimensional sub-frames rather than the complete three-dimensional frame, but others have emphasized the three-dimensional behaviour. Other studies have found that column yielding causes beams to behave as if they are on pinned supports, and beam behaviour is significantly influenced by web buckling. The development of tensile membrane action in composite steel-concrete floors is described in Chapter 11.

(a)



(b)



(c)



Figure 8.12 (a) Flames coming from the window during a post-flashover fire in the Cardington fire test building. Reproduced from Kirby (1999) by permission of Corus UK Ltd). (b) Large vertical deflection of unprotected steel beams supporting a composite steel-concrete floor slab; the column was protected during the fire. (c) Cracking in the top surface of the composite slab around the column; integrity was maintained. Reproduced from Kirby (1999) by permission of Corus UK Ltd

8.4.2 Car Parking Buildings

Fires in car parking buildings are less severe than fires in many other occupancies. Many studies have shown that the fire load is low, and fires do not often spread from car to car because each car body acts like a form of enclosure. Schleich *et al.* (1999) suggest that the fire should be considered to spread from car to car every 12 min in an unsprinklered building. Even if there is no structural problem, burning cars can produce large volumes of toxic smoke which is a major hazard to life.

The required level of fire protection depends on whether the car parking building is open to the outside air, or enclosed. A burning car in an enclosed car parking building can result in high temperatures in the structural members, so that installation of sprinklers or applied fire protection is necessary to ensure no collapse of steel members. Maximum temperatures in structural members may be much more localized in car parking buildings than in other occupancies, so local temperatures should be checked if flashover does not occur.

Tests in Australia (Bennetts *et al.*, 1999) have shown that fires are much less severe in car parking buildings which are open to the air on at least two opposite sides. Much of the heat and smoke from burning cars in open car parking buildings is carried directly to the outside, so that hot gas temperatures remain low. Maximum temperatures measured in exposed unprotected steel beams do not exceed 260 °C, so that unprotected steel can be used for the beams and columns of such buildings, provided that the steel members are not too light. Bennetts *et al.* (1999) recommend a maximum section factor F/V of 230 m⁻¹ (minimum effective thickness 4.3 mm) provided that the beam is in continuous contact with a reinforced concrete slab designed for composite action. The same recommendations apply to closed car parking buildings which have sprinklers installed. Schleich *et al.* (1999) also recommend the use of unprotected steel for columns and composite beams in closed car parking buildings which are protected with sprinklers.

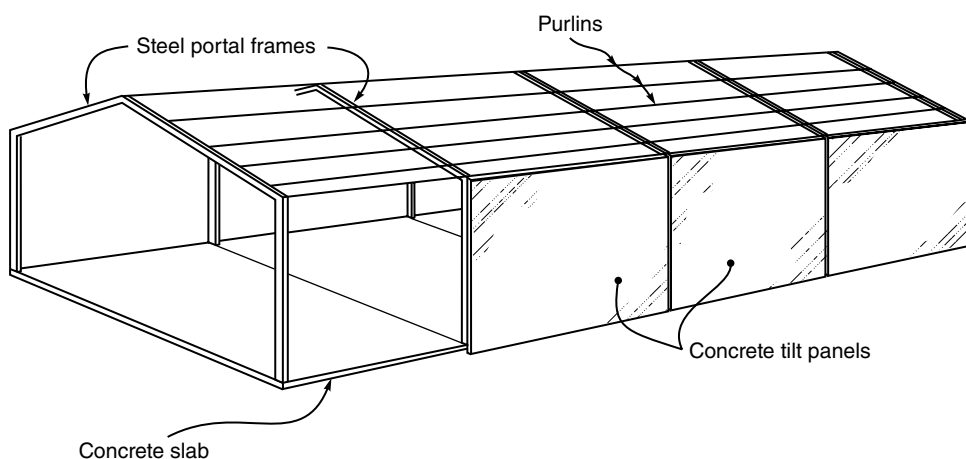


Figure 8.13 Single-storey portal frame industrial building

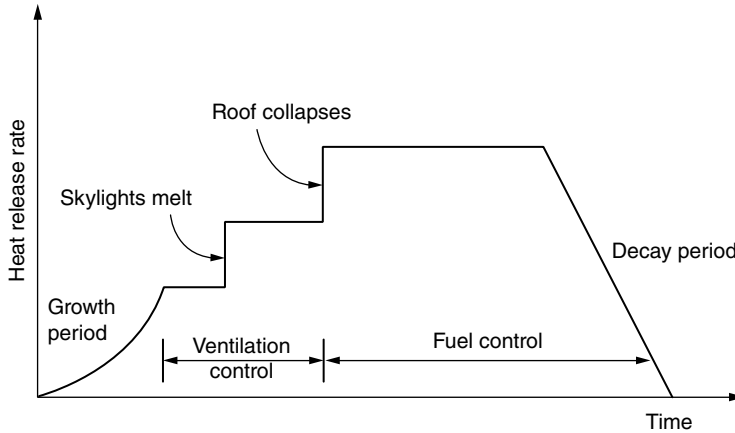


Figure 8.14 Heat release rate for fire in an industrial building

8.4.3 Single-storey Portal Frame Buildings

A very common form of steel construction is single-storey portal frames for industrial buildings as shown in Figure 8.13. There is considerable debate about the objectives and strategies for fire resisting design of such buildings. Typical buildings have steel portal frames 5–10 m apart, spanning from 20 to 50 m, or more with internal columns. The roof usually has a slope between 2° and 15° , consisting of thin steel sheeting and translucent plastic sheeting supported on timber or steel purlins up to 1 m apart, spanning between the portal frames. Other types of roofing include deep trough steel sheeting or sandwich panels, which can span much larger distances. Walls of single-storey portal frame buildings are often brick, concrete masonry or concrete ‘tilt-panels’. Concrete tilt-panels are precast concrete panels, cast on the floor slab on the site before lifting into place. In some buildings the side walls are load bearing, such that there is no steel column and the concrete wall panel provides vertical and flexural support to the steel rafters.

For an uncontrolled fire in a single-storey industrial building, the possible heat release rate is shown in Figure 8.14 (Cosgrove, 1996), where the fire is initially limited by available ventilation, but becomes fuel controlled after the skylights melt and the roof eventually collapses. The steel roof structure is seldom fire-rated, so it will usually collapse in a fully developed fire. The area of fully developed fire and hence the area of collapsing roof will move around the building as the fire grows and spreads. If the purlins supporting the roofing are of timber, the roofing will probably fall into the fire before the main beams collapse. Steel purlins will tend to deform into a tensile catenary shape, holding the steel roofing in place between the main beams until they collapse. Large amounts of roof venting, caused by melting of large plastic skylights or aluminium roof cladding, result in lower temperatures because much of the heat from the fire is released directly to the atmosphere without heating the steel structure.

Portal frame buildings are often constructed near property boundaries, so one of the main fire safety objectives may be prevention of fire spread to neighbouring properties. Fire spread

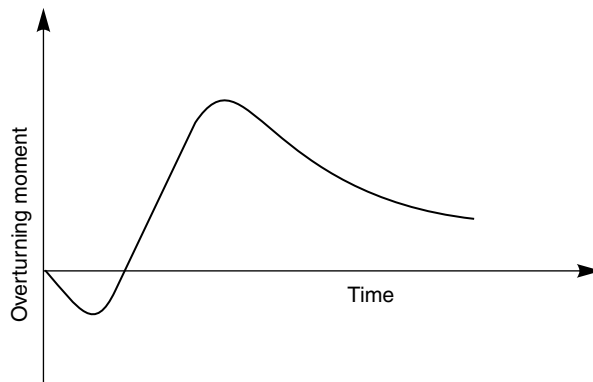


Figure 8.15 Axial thrust in rafter of portal frame during fire. Reproduced from Newman (1990) by permission of the Director, The Steel Construction Institute



Figure 8.16 Failure of an unreinforced brick masonry wall of an industrial building; the wall was pushed outwards by thermal expansion of the steel portal frames, which later collapsed inwards. Reproduced by permission of the Cement and Concrete Association of Australia

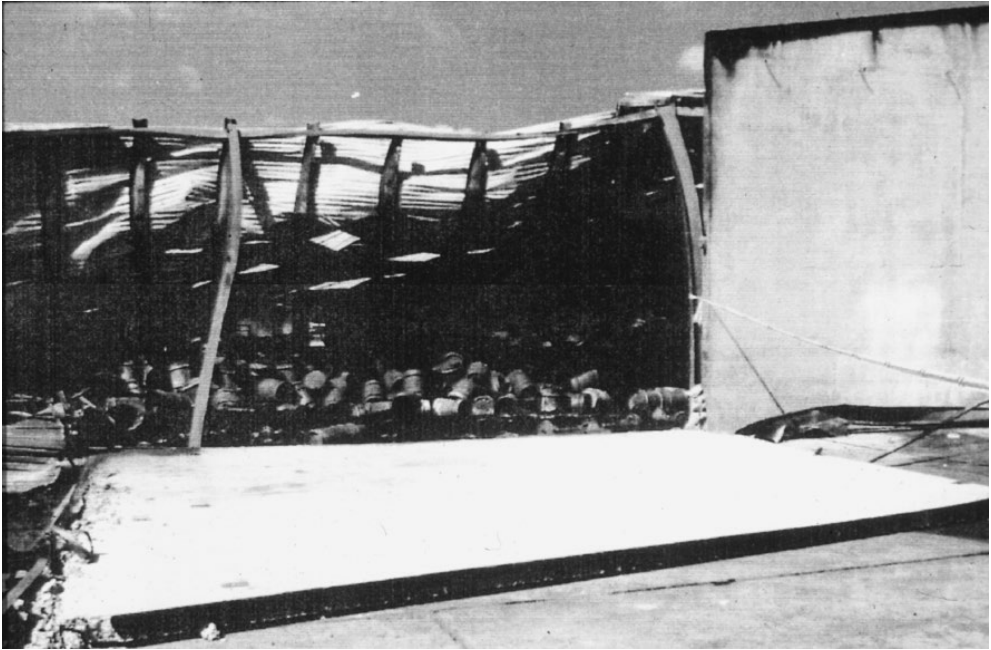


Figure 8.17 Outward collapse of a precast concrete wall panel during a fire in an industrial building; such a collapse would endanger firefighters and allow fire spread. Reproduced by permission of the Cement and Concrete Association of Australia

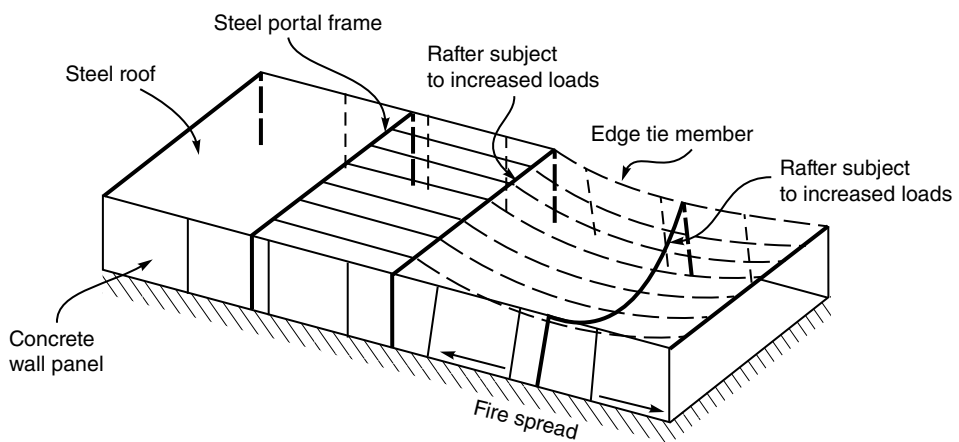


Figure 8.18 Failure mechanism for single-storey industrial building in fire. Reproduced from O'Meagher *et al.* (1992) by permission of Australian Institute of Steel Construction

is controlled with the use of fire resisting boundary walls. Special design for the fire situation is necessary because under normal temperature conditions the wall panels are supported by non-fire-rated steel frames. There are two alternative strategies for preventing fire spread: cantilever construction to ensure that the exterior walls remain in place for the duration of the fire; or pinned column bases which allow the wall panels to fall inwards towards the fire.

The traditional approach is to provide the steel portal frames with a fixed (or partially fixed) base, and to apply passive fire protection to the steel columns of the portal frame. In this case the fire resisting walls are supported before the fire by portal frame action, then during and after the fire by the cantilevered steel columns with moment-resisting base connections. With fixed or partially fixed column bases, Newman (1990) has shown how a fire initially causes an outward thrust on the columns as the rafters expand and deflect, followed by an inwards tensile force as the rafters droop into a catenary (Figure 8.15). The initial outwards movement can cause masonry or precast concrete walls to collapse outwards as shown in Figure 8.16 and Figure 8.17. Newman also describes how to calculate the overturning moment at the column base, and shows that design for full fixity is not required.

A common variation is to rely on reinforced concrete columns instead of steel columns for the portal frames, in which case the after-fire condition is of less concern. Yet another approach is to provide the concrete wall panels with a cantilever base connection to a strong foundation, on the assumption that the panels will remain free-standing after the steel roof structure collapses, depending on the connection between the panels and the steel roof framing. A fire inside the building will cause cantilevered walls to deform outwards due to the temperature gradient through the wall (Cooke, 1988; Lim, 2000) possibly leading to undesirable outwards collapse if the separate panels are not tied together.

An alternative approach, promoted in Australia by O'Meagher *et al.* (1992) is to design the portal frames with pinned bases and no applied fire protection, so that the frames provide lateral support to concrete wall panels which have pinned connections at the foundation level. O'Meagher *et al.* (1992) have used computer-based structural analysis to demonstrate that the walls of such a building will collapse inwards, not outwards, and there will be good protection of adjacent properties if the walls remain tied together as they collapse or partially collapse inwards, as shown in Figure 8.18. To achieve this behaviour, it is essential that the concrete wall panels are tied together at their tops, the roofing has some diaphragm stiffness, and the connections of the panels to the steel frames have adequate fire resistance.

8.5 Worked Example

8.5.1 Worked Example 8.1

Calculate the fire resistance of a circular steel column filled with concrete (Kodur, 1999).

Given:

Column length	$L = 4800$ mm
Effective length factor	$K = 0.67$ (fixed-fixed end conditions)
Axial load	$N = 1344$ kN
Concrete strength	$f'_c = 30$ MPa (carbonate aggregate concrete)
Column size	Circular hollow section (CHS) 324×6.4 ($d = 324$ mm)
Bar reinforcing	3%
Cover	25 mm

From Table 8.1, $f=0.095$. From Equation 8.14 the fire resistance is given by:

$$t_r = \frac{f(f'_c + 20)d^{2.5}}{(KL - 1000)\sqrt{N}}$$

$$t_r = \frac{0.095(30 + 20)324^{2.5}}{(0.67 \times 4800 - 1000)\sqrt{1344}} = 110 \text{ min}$$

9

Timber Structures

This chapter describes the fire behaviour of timber structures, and gives design methods for heavy timber structural members exposed to fire. The fire behaviours of connections in timber structures are also discussed.

9.1 Description of Timber Construction

Timber structures tend to fall into two distinct categories: ‘heavy timber’; and ‘light timber frame’ (‘light wood frame’ in North America). Heavy timber structures are those where the principal structural elements are beams, columns, decks, or truss members made from glue laminated timber (glulam), laminated veneer lumber (LVL), cross laminated timber (CLT), or large dimension sawn timber. Many innovative structures using heavy timber structural members are described by Kolb (2008) and Mayo (2015). Fire safety in modern timber buildings has been covered in many recent studies, including those by Gerard *et al.* (2013) and Buchanan *et al.* (2014).

Light timber frame construction uses smaller sizes of wood framing, as studs in walls, and as joists in floors. Walls and floors are covered with panels of lining materials to provide resistance to impact, sound transmission, and fire spread. Fire resistance of light timber frame construction is covered in Chapter 10.

9.1.1 Heavy Timber Construction

‘Heavy timber’ or ‘massive wood’ construction describes all uses of large dimension timber framing in buildings. Many historic commercial and industrial buildings consist of external load-bearing masonry walls, with internal timber columns and beams supporting thick timber

floor decking. The term ‘heavy timber construction’ or ‘mill construction’ has a specific meaning in North American fire codes where it applies to beams and columns with a minimum nominal dimension of 150 mm and decks with a minimum nominal thickness of 50 mm. In this book, the term ‘heavy timber’ generally refers to timber members whose smallest dimension is no less than 80 mm.

9.1.2 *Laminated Timber*

There is a wide range of laminated timber products on the market. The major products are described briefly below.

9.1.2.1 **Glulam**

Glue laminated timber (glulam) describes timber members which are manufactured from several solid timber laminations glued together. The laminations are normally boards of sawn timber which have been planed to give a smooth surface before gluing. The length of individual laminations is often the full length of the member, joined end-to-end with finger-joints. Glulam members can be manufactured in any size or shape, the major limitation being transportation. The individual laminations must be thin for curved members (10–25 mm thickness, depending on the radius of curvature) but can be thicker in straight members (usually 35–45 mm thickness).

The most common adhesives for glulam are thermosetting resins with different combinations of phenol, resorcinol, formaldehyde, melamine and urea (PRF, RF, MUF, UF), one-component polyurethane adhesives (1C-PUR), and emulsion polymerized isocyanate adhesives (EPI). Many fire tests have shown that glulam members exposed to fire behave in the same way as solid sawn timber members of the same cross section, provided that approved structural adhesives for load-bearing wood members are used and finger joints are spaced well apart (Klippel, 2014). Two-component epoxy resin adhesives have less predictable fire performance than the adhesives listed above, so they should only be used when the results of relevant fire resistance tests are available. Elastomeric adhesives, such as polyvinyl acetate (PVA) should not be used.

In some countries, especially in North America, the laminations at the top and bottom edges of glulam members are made from specially selected higher strength wood, in order to increase the flexural strength and stiffness. This practice must be considered in fire design when the outer laminations may be burned away, placing more reliance on the inner laminations which are of lower strength.

9.1.2.2 **Laminated Veneer Lumber**

LVL is made by peeling logs into thin wood veneers (each about 3 mm thick), then gluing these veneers into a solid wood panel. Other common names for LVL include Microlam (in USA) and Kerto (in Europe). Typical LVL panel production is a width of 1.2 m or more, with specified thickness between 25 mm and 120 mm, manufactured in a continuous process giving very long lengths. Many LVL panels are re-manufactured into structural timber beams or other engineered wood products such as I-joists or box-beams. LVL is similar to thick plywood, except that most LVL panels have all the grain running in the longitudinal direction. Some cross-banded LVL panels, more like thick plywood, are made with two or more veneers rotated 90°, which provides more stability under fluctuating moisture conditions. LVL

generally has the same fire properties as solid timber or glulam members of the same size provided that approved thermosetting adhesives are used.

9.1.2.3 Cross Laminated Timber

CLT is made from sawn timber boards glued together in layers at 90° to each other as shown in Figure 9.1, rather like thick plywood. CLT is manufactured in large panels several metres in each direction. The individual board thickness is usually between 10 mm and 40 mm, sometimes with different thicknesses in one panel. The most common layups are three-ply, five-ply, or seven-ply, so the finished thickness of typical panels is from about 40 mm (three thin layers) to 300 mm (seven thicker layers) or more. Some manufacturers glue the edges of the boards together, whereas others leave the edges with no adhesive. Most CLT is used for prefabricated building systems, with pre-assembled panels for walls or floors. Most CLT panels are glued with one-component polyurethane adhesive, although some manufacturers offer other adhesives or even non-glued panels where the boards held together with nails or hardwood dowels. If no delamination of layers occurs, CLT has roughly similar fire properties to solid timber or glulam, but the effect of gluelines and the influence of layers in the weak direction must both be allowed for, as discussed further in Section 9.5.10.

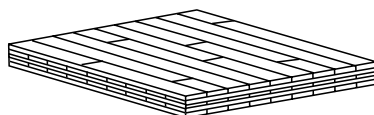


Figure 9.1 Typical cross laminated timber panel

9.1.3 Behaviour of Timber Structures in Fire

Heavy timber construction is recognized as having very good fire resistance. There are many well documented examples of structures surviving severe fire exposure without collapse, and many of these have been repaired for re-use (Figure 9.2 and Figure 9.3). A summary of fire performance of timber structures is given by White (2008), and an extensive overview of fire safety in timber buildings is given by Östman *et al.* (2010).

When large timber members are exposed to a severe fire, the surface of the wood initially ignites and burns rapidly. The burned wood becomes a layer of char which insulates the solid wood below. The initial rapid burning rate decreases to a slower steady rate which continues throughout the fire exposure, but the charring rate will increase again if the residual cross section becomes very small. As burning progresses, the increasing layer of residual char becomes thinner than its original wood thickness because of shrinkage. This shrinkage also causes fissures which facilitate the passage of combustible gases to the surface (Drysdale, 2011). The char layer does not usually burn because there is insufficient oxygen in the flames near the surface for oxidation of the char to occur.

When the wood below the char layer is heated above 100°C , the moisture in the wood evaporates. Some of this moisture travels out to the burning face, and some travels into the wood, resulting in an increase in moisture content in the heated wood a few centimetres below the char front (White and Schaffer, 1980; Fredlund, 1993). The boundary between the char layer and the remaining wood is quite distinct, corresponding to a temperature of about 300°C . There is a layer of heated wood about 35 mm thick below the char layer, and the inner core

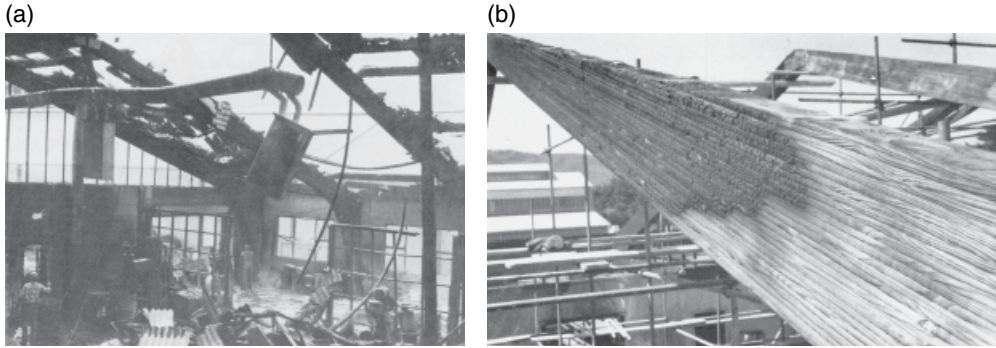


Figure 9.2 (a) Severe fire damage to an industrial building with curved glulam portal frames. (b) One of the beams repaired for re-use by sandblasting. Reproduced from (TRADA, 1976) by permission of the New Zealand Timber Industry Federation



Figure 9.3 Curved glulam roof beams after repair following a severe fire. Reproduced by permission of Timberlab

remains at ambient temperatures. The residual cross section is capable of supporting loads, providing a level of fire resistance which depends on the load ratio (see Chapter 5). Failure occurs when the residual cross section is stressed beyond its ultimate strength.

Any large area of exposed wood will contribute to the fuel in the room where flashover occurs, so it must be included in the assessment of fuel load. This applies to both structural and non-structural wood surfaces. However, the slow and predictable charring rate of heavy timber means that only a thin layer of wood need be added to the fuel load, depending on the expected fire duration, because the fire may be out before much of the potential wood fuel becomes available. If the only exposed wood surfaces are typical timber beams and columns, the resulting increase in fuel load from the timber structure will be modest, so that no special calculations of fuel load are required.

9.1.4 Fire Resistance Ratings

Fire resistance of timber structures can be assessed using the same general principles as for other materials. The design process for fire resistance requires verification that the provided fire resistance exceeds the design fire severity. Using the terminology from Chapter 2, the

temperature domain is not used for timber structures because there is no critical temperature for fire-exposed timber. In most countries, fire design of heavy timber structures is by calculation using the methods outlined in this chapter, which are verified in the *time domain* by comparing the time of structural collapse with a specified fire resistance time, or in the *strength domain* by comparing the residual strength with the fire limit state loads after a certain period of fire exposure.

Some countries have *generic* fire resistance ratings for heavy timber construction. For example, some US codes allow heavy timber construction to be used in certain classes of buildings, with no calculations required (e.g. UBC, 1997; ICC, 2015). There are very few *proprietary* ratings for heavy timber, in contrast to light timber construction where there are many proprietary ratings based directly on test results, as described in Chapter 10.

9.1.5 Fire Retardant Treatments

A large number of different fire retardant chemicals are available for treating wood to reduce its combustibility (Schaffer, 1992; Wood Handbook, 2010). The main purpose of such chemical treatments is to retard the rate of flame spread over the surface of the wood, to improve fire safety in rooms lined with wood or wood-based panel products. Pressure impregnation of chemicals is considered to be more effective than surface painting, and the pressure impregnation process is similar to that used for applying decay resistant chemicals. Impregnation by fire retardant chemicals can have some negative effects including loss of wood strength and corrosion of fasteners, exacerbated by the hygroscopic nature of many of the chemicals (LeVan and Winandy, 1990; Winandy, 1995).

Fire retardant chemicals do not significantly improve fire resistance of timber members, because even though treated wood will not support combustion, it will continue to char if exposed to the temperatures and heat flux of a fully developed fire. Some proprietary intumescent paints have been developed with properties which claim to increase fire resistance of timber members, but insufficient test results have been published to recommend such products for general use. A discussion is given by White (1984), and some fibre-glass reinforced coatings are described by del Senno *et al.* (1998). The long term reaction to fire performance of fire retardant treated wood products in interior and exterior applications is being developed in Europe (CEN, 2015).

9.2 Wood Temperatures

When heavy timber members are exposed to severe fires, the outer layer of wood burns and is converted to a layer of char. The temperature of the outer surface of the char layer is close to the fire temperature, with a steep thermal gradient through the char. The boundary between the char layer and the remaining wood is quite distinct, corresponding to a temperature of about 300 °C. The commonly accepted charring temperature in North America is 288 °C (550 °F), but the precise temperature is not important because of the steepness of the temperature gradient. Below the char layer there is a layer of heated wood, normally about 35 mm thick. The part of this layer above about 200 °C is known as the pyrolysis zone, because this wood is undergoing thermal decomposition into gaseous pyrolysis products, accompanied by loss of weight and discoloration. Moisture evaporates from the wood above 100 °C. The inner core of

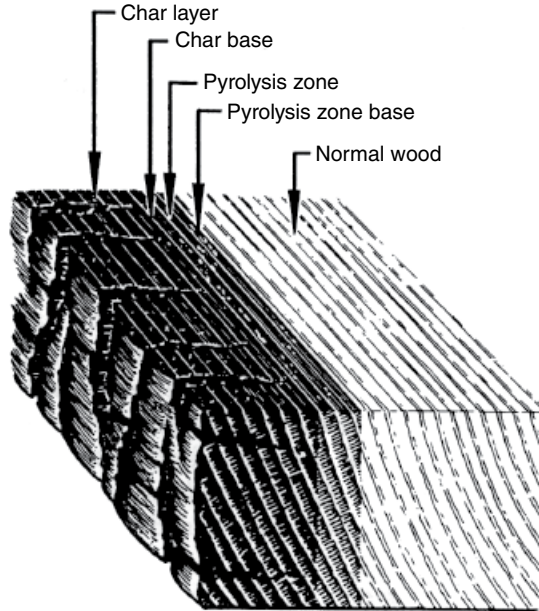


Figure 9.4 Char layer and pyrolysis zone in a timber beam. From Schaffer, 1967

the member remains at its initial temperature for a considerable time. These layers are shown in Figure 9.4 (Schaffer, 1967).

Structural design of heavy timber members is based on the rate of charring of the wood surface, so it is not usually necessary for designers to calculate temperatures within the fire-exposed wood.

9.2.1 *Temperatures Below the Char*

Temperatures in the wood below the char layer have been measured in many tests. For wood thick enough to be considered as a semi-infinite solid, Janssens and White (1994) give the temperature T (°C) below the char layer as:

$$T = T_i + (T_p - T_i)(1 - x/a)^2 \quad (9.1)$$

where T_i is the initial temperature of the wood (°C), T_p is the temperature at which charring starts (300°C), x is the distance below the char layer (mm) and a is the thickness of the heat-affected layer (35 mm).

9.2.2 *Thermal Properties of Wood*

The temperatures inside fire-exposed timber members can be calculated using finite element numerical methods. The thermal properties are not well defined, and vary considerably with

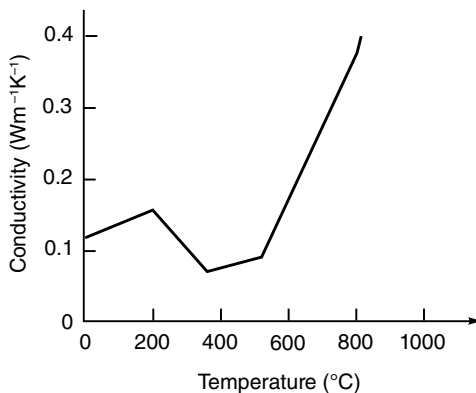


Figure 9.5 Variation of thermal conductivity of wood and char layer with temperature

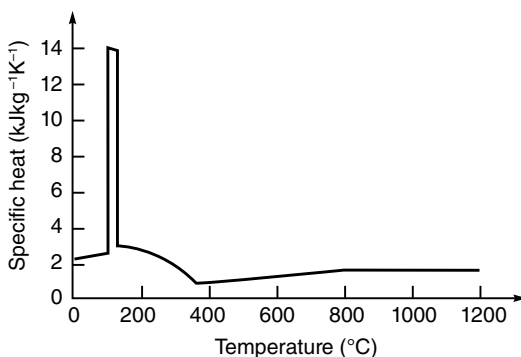


Figure 9.6 Variation of specific heat of wood and the char layer with temperature

temperature as moisture is driven off at 100 °C and as wood turns to char over 300 °C (Janssens, 1994). The values given below are typical average values from the literature (Thomas, 1997; König and Walleij, 1999; Östman *et al.*, 2010).

The density of wood varies significantly between species. It also varies between trees of the same species and within individual trees. The density drops to about 90% of its original value when the temperature exceeds 100 °C, and to about 20% of its original value when the wood is converted to char above 300 °C.

The published values of thermal conductivity vary greatly between different authors. Figure 9.5 shows the dependence of thermal conductivity on temperature from Eurocode 5 Part 1-2 (CEN, 2004b), obtained by König and Walleij (1999) who had to increase the thermal conductivity presented earlier by Knudson and Schniewind (1975) and others, to much higher values at temperatures over 500 °C in order to give good predictions of measured behaviour. Figure 9.6 shows the variation of specific heat with temperature from Eurocode 5, obtained by König and Walleij (1999). The large spike at 100 °C represents the heat required to evaporate the moisture in the wood, which can cause problems in numerical computations. An alternative formulation for specific heat is to use a temperature–enthalpy curve as proposed by Werther *et al.* (2012) and described further in Chapter 11.

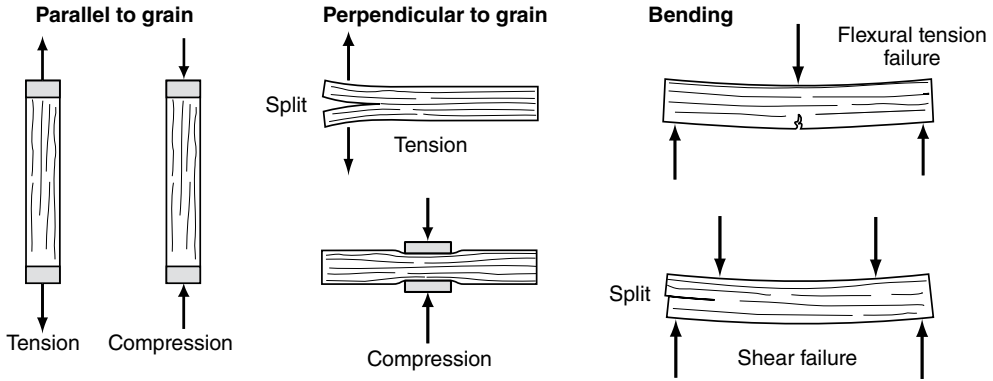


Figure 9.7 Loading of wood in different directions

9.3 Mechanical Properties of Wood

Wood has several significant differences from other common materials such as steel and concrete. For example:

- Wood strength can be very variable, both within boards and between boards.
- Mechanical properties are different in different directions (parallel and perpendicular to the grain).
- Strength and ductility are very different in tension and compression.
- Failure stresses may vary with the size of the test specimens.
- The strength reduces under long duration loads.

Figure 9.7 shows different ways in which wood can be loaded, each producing a different failure mode. This chapter briefly reviews wood behaviour at normal temperature before describing properties at elevated temperatures.

9.3.1 Mechanical Properties of Wood at Normal Temperatures

9.3.1.1 Tension and Compression Behaviour

Figure 9.8 shows typical stress–strain relationships for small clear specimens of wood with no defects. Considering behaviour parallel to the grain, the straight line in tension indicates linear elastic behaviour until a brittle failure occurs at a tensile stress f_t . Wood is brittle in tension because there is no load sharing within the wood material, so that a crack can lead to sudden failure as soon as it reaches a certain critical size.

In compression the stress–strain relationship is linear in the elastic region, with the same modulus of elasticity as in tension. The line then curves, indicating yielding (or crushing), it reaches a peak and eventually drops as the wood is crushed further. With larger strains the specimen will continue to deform in a ductile manner. Compression yielding is accompanied by visible wrinkles on the surface of the wood. The compression curves in Figure 9.8

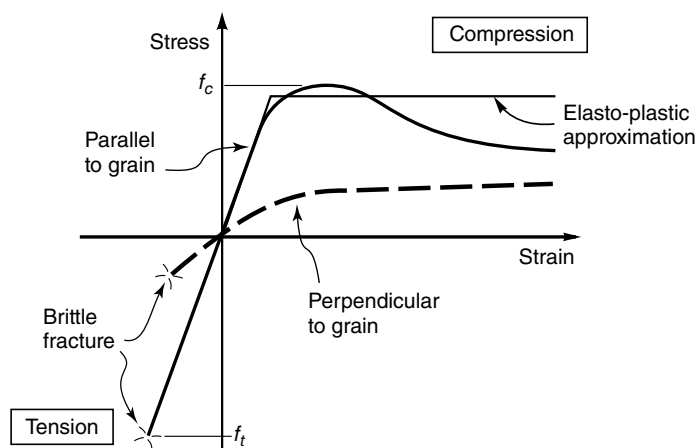


Figure 9.8 Stress–strain relationships for clear wood

indicate crushing of wood in short columns. Long slender columns have lower load capacity because they will fail by buckling at loads well below the crushing strength, as described in Chapter 5.

In clear wood, the tension strength f_t is usually much greater than the compression strength f_c . In commercial quality timber, the relative strengths are often reversed because growth characteristics such as knots have a severe effect on tensile strength but only a small effect on compressive strength (Bodig and Jayne, 1982).

The dashed line in Figure 9.8 shows the stress–strain relationship for wood loaded perpendicular to the grain. The slope indicates a lower modulus of elasticity than for loading parallel to grain. The wood is ductile in compression, with the load slowly increasing as strains increase. In tension perpendicular to the grain, the strength is very low and unpredictable, with splitting causing brittle fractures. This weakness can lead to structural failure if it is not properly allowed for in design.

9.3.1.2 Bending Behaviour

Bending behaviour is a combination of tension and compression behaviour (Buchanan, 1990). Internal compressive and tensile stresses in a timber beam are shown in Figure 5.2. Commercial quality timber beams tend to fail suddenly due to poor tensile strength at knots in the tension zone. Some ductility is available in timber beams when the material is stronger in tension than in compression, and this ductility can increase during fire exposure because of softening of the wood in the compression zone.

9.3.1.3 Design Values

Structural design calculations require the design strength of the wood. For *limit states design* (LRFD) the design stress, or ‘characteristic stress’, is the 5th percentile failure stress under short-duration loading, for a typical population of timber boards. Because the strength of

timber is much more variable than that of steel or concrete, characteristic stresses are usually obtained from *in-grade* tests of large numbers of representative samples of full size timber members, selected from typical production. This allows the effects of size, grade, defects, and variability to be determined directly. To accommodate a very large number of species and grades, most codes specify characteristic values of strength and stiffness for a number of defined strength classes. The 5th percentile value for design in normal temperature conditions may be modified to the 20th percentile strength value for fire design, as described later in this chapter.

Failure stresses in timber depend on many factors, including the size of the test specimen. Large timber members tend to fail at lower stresses than similar small members, because a large member has a larger number of potential defects than a small member (Madsen and Buchanan, 1986). Such size effects are recognized in many design codes.

The design strength of timber also depends on the duration of the applied load, so that most timber design codes include a duration-of-load factor. In *limit states design* (LRFD) codes, the duration-of-load factor is usually 1.0 for short-duration loads, decreasing to 0.8 or 0.6 for medium- and long-duration loads. In *working stress design* codes, allowable stresses are for long-duration loading, obtained from test results of small clear specimens of wood. In this case the duration-of-load factor is usually 1.0 for long-duration loads, increasing to 1.25 or 1.6 for medium- and short-duration loads, respectively. The duration-of-load factor for fire design should be the appropriate value for short-duration loads, because the duration of the load during the fire is likely to be less than 1 h.

9.3.2 Mechanical Properties of Wood at Elevated Temperatures

9.3.2.1 Sources

A comprehensive review on the effect of moisture content and temperature on the mechanical properties of wood is given by Gerhards (1982) who reported the results of many previous studies. Much of this information is summarized by the Wood Handbook (2010). Wood properties are affected by steam at 100 °C, wood begins to pyrolyse at about 200 °C and it turns into char by 300 °C. The range of interest for fire engineering is therefore from room temperature up to 300 °C.

9.3.2.2 Effect of Moisture Content

The strength of wood at elevated temperatures is not well understood. In addition to temperature, the interaction with moisture content is very important, making the range of testing options even more difficult than shown in Figure 5.5. When testing timber at elevated temperatures, the moisture content is sensitive to the test method and the size of the test specimen. Some test specimens are maintained at constant moisture content throughout the test with a climate-controlled testing facility or an oil bath (Östman, 1985). In other tests the wood specimen is at a certain moisture content before the test and allowed to dry out when heated, either before or during the test, in which case some moisture may migrate into the interior of the specimen and the moisture gradients will depend on the size of the specimen. If wood is heated to a temperature above 100 °C, all free moisture will evaporate after some time, depending on the permeability of the particular species.

9.3.2.3 Plasticity

When the temperature of wood increases, the wood may become more ‘plastic’ exhibiting more non-linear material behaviour under increasing load, both in compression and in tension. This increase in wood plasticity is very important, especially for tension members and bending members. When a timber beam is tested in bending at normal temperatures, it usually fails suddenly, with fracture at a weak point on the tension edge when a small crack reaches a critical size. If heated wood were to lose strength with no increase in plasticity, any cracks in the heated tension zone of the beam would lead to premature failure in fire, but the excellent performance of large timber beams in fire results from plastic behaviour in the heated wood, allowing for redistribution of stresses into the cooler wood further from the char layer.

9.3.2.4 Steam Softening

It is well known from the furniture and boat building industries that hot moist wood can be bent into curved shapes using steam bending. Steam softening occurs because wood becomes plastic under certain combinations of temperature and moisture content (Stevens and Turner, 1970). The Wood Handbook (2010) explains that the thermoplastic lignin polymer in the cell walls softens and can undergo thermoplastic flow when heated above the glass transition temperature which is approximately 170°C. This plasticizing process allows compressive deformation of wood which has been steamed or boiled for some time.

When wood is heated in a fire, the conditions which produce softening of the wood may occur for a short period of time. If the moisture content subsequently decreases, the wood will harden, even if temperatures continue to increase. The effect of wood softening will be very different for large and small members. In a large member, conditions to produce softening may occur in a thin layer which progresses into the wood at about the same velocity as the rate of charring, having little effect on the overall strength or stiffness of the member. Small members may experience these conditions over a large proportion of the cross section, in which case the member may deform plastically in compression or bending, leading to premature failure (Young and Clancy, 1998). These conditions may only occur for a short time period, so if the assembly can resist the fire limit state loads during this short period, with the help of other load paths or cladding materials, the wood may regain strength after it dries and be able to survive a much longer time of fire exposure.

9.3.2.5 Parallel to Grain Properties

Modulus of Elasticity

Figure 9.9 shows the modulus of elasticity of wood at elevated temperatures from Eurocode 5, similar to the values obtained by König and Walleij (2000) from tests of 145 × 45 mm timber studs in insulated wall assemblies, exposed to the ISO 834 standard furnace fire while loaded in bending. Similar results were obtained by Young (2000) who used even lower values of modulus of elasticity to model the results of full-scale fire resistance tests of timber stud walls. Earlier test results, including Preusser (1968), Schaffer (1973), Nyman (1980), Gerhards (1982), Östman (1985) and the Wood Handbook (2010) all show a smaller reduction of modulus of elasticity with temperature, especially for dry wood. The values in Figure 9.9 are recommended for design purposes.

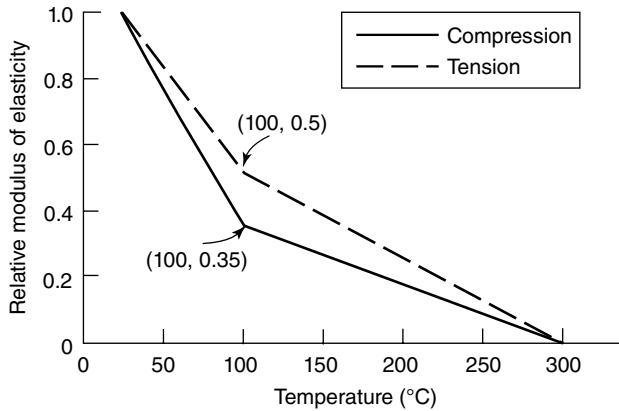


Figure 9.9 Effect of temperature on modulus of elasticity parallel to grain (Eurocode 5). Reproduced from CEN (2004b). © CEN, reproduced with permission

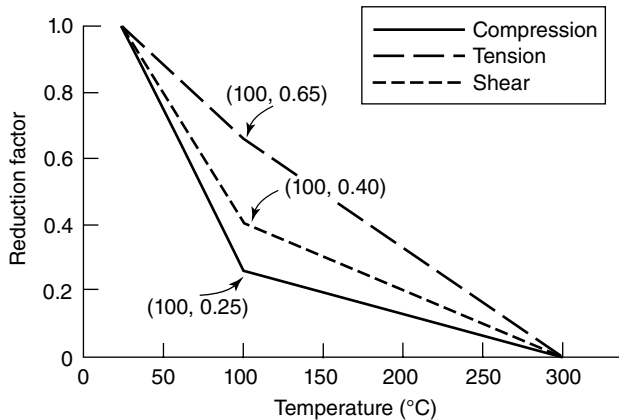


Figure 9.10 Effect of temperature on strength in tension and compression parallel to grain, and in shear (Eurocode 5). Reproduced from CEN (2004b) by permission of CEN

Tensile Strength

The top dashed line in Figure 9.10 shows the tensile strength of wood at elevated temperatures from Eurocode 5. These values are similar to those described by König and Walleij (2000). Östman (1985) tested samples of spruce (1×10 mm cross section) at a range of temperatures and moisture contents, and found that the failure stress at 90°C and 30% moisture content is about 60% of that of dry wood at ambient temperature, with a small amount of plastic behaviour before failure.

The only reported 'in-grade testing' at elevated temperatures is by Lau and Barrett (1997) who tested a large number of 90×35 mm boards in tension, 25 min after heating the surfaces to temperatures up to 250°C . They showed that the tension behaviour remains brittle, and failure is governed by the weakest link in the test specimen, generally a knot. A comparison with other test data shows similar results to Schaffer (1973), Knudsen and Schniewind (1975), Nyman (1980) and Östman (1985). Lau and Barrett (1997) used a damage accumulation

model to predict the tensile strength under constant temperature, finding that the strength reduction over 150 °C is slightly greater for long-duration loading.

Compressive Strength

The effect of temperature on compressive strength parallel to grain is also shown in Figure 9.10. This reduction of strength with temperature is again based on the results of König and Walleij (2000) for testing of wood with typical indoor moisture content. Similar results were obtained by Young and Clancy (1998). For initially dry wood, several authors including Gerhards (1982) have shown a straight line reduction in compressive strength from 20 to 300 °C. The question as to whether the strength of initially moist wood increases again after the moisture is driven off at temperatures over 100 °C requires further research, because this information is required for finite element modelling of timber structures exposed to fires.

Bending Strength

Bending behaviour in wood can be best described from an understanding of the tension and compression behaviour (Buchanan, 1990). The effect of elevated temperatures on bending behaviour is, in theory, predictable from the behaviour in tension and compression, but this may be complicated for moist wood, because plastic behaviour with large strains in the compression zone will result in large flexural deformations due to a relocation of the neutral axis as shown in Figure 5.2.

There are limited bending test results available, including those reported by Gerhards (1982), and the results obtained by Glos and Henrici (1991) for bending strength of 70 × 150 mm beams at temperatures of 100 and 150 °C with moisture content in the range of 7–10% for the 100 °C beams and 3–6% for the 150 °C beams. Earlier German design values were described by Kordina and Meyer-Ottens (1983) from tests by Kollman and Schulz (1944).

König (1995) performed fire resistance tests on single joists with the narrow edge unprotected and the wide sides protected by rock wool insulation. The joists were tested in bending with the fire-exposed side in tension or compression. Extreme plastic behaviour was observed, with a very large shift in the neutral axis location, especially for those members with the fire-exposed edge in compression. Fire tests of unprotected timber joist floors by Woeste and Schaffer (1979) and tests of studs by Norén (1988) showed less variability between boards and an increase in load sharing during fire, resulting from increased ductility. Tests of glulam beams by Bolonius Olesen and König (1992) showed continued softening of the wood during the cooling period, even after charring had stopped.

Thermal Expansion

The effect of thermal expansion of fire-exposed wood is usually negligible compared with other materials such as steel and concrete, especially for large size timber members. This is because the coefficient of thermal expansion is very low, the area of heat affected wood is usually very small due to low thermal conductivity, and the thin surface layer of heat-affected wood has reduced mechanical properties.

9.3.2.6 Perpendicular to Grain Properties

Modulus of Elasticity

For modulus of elasticity perpendicular to the grain, Gerhards (1982) reports eight studies which all lie in the range shown in Figure 9.11, for temperatures up to 100 °C. The dependence on temperature tends to be greater for moisture content above 20%, but there is a lot of overlap

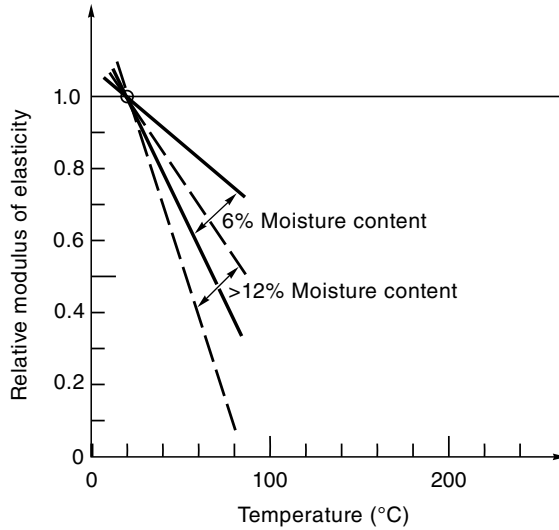


Figure 9.11 Effect of temperature on modulus of elasticity perpendicular to grain. Adapted from Gerhards (1982) with permission of Society of Wood Science and Technology

between the studies. Many of the data show negligible stiffness for moist wood as the temperature approaches 100°C, indicating plastic behaviour as reported for parallel to grain behaviour.

Tensile Strength

Gerhards (1982) describes some tests on the effect of temperature on tensile strength perpendicular to grain, showing a wide range of results with much overlap for different moisture contents similar to the results for modulus of elasticity shown in Figure 9.11. There is little reduction in tensile strength for very dry wood, and a strong trend of more strength reduction as the moisture content increases. Tensile strength perpendicular to grain is an indication of resistance to splitting, which is a very unpredictable wood property, even in the best conditions.

Compressive Strength

Gerhards (1982) also reports on the effect of temperature on strength in compression perpendicular to grain. Again the results are similar to those for modulus of elasticity shown in Figure 9.11. The measured strength in such tests is the proportional limit which is very difficult to define when the stress–strain relationship may be curved from very low loads as shown in Figure 9.8. The ultimate crushing strength is more useful, but is also difficult to measure because it requires very large strains, and there may be no maximum value, also shown in Figure 9.8.

9.3.2.7 Shear

Shear in Beams

Figure 9.12(a) shows a beam with applied loads. The elemental volume near the left-hand support is enlarged in Figure 9.12(b). In a homogeneous isotropic material, the stresses shown here would usually produce a diagonal tension failure along the dashed diagonal line A–A. However, in timber, which has a well-defined longitudinal grain structure, a shear failure will

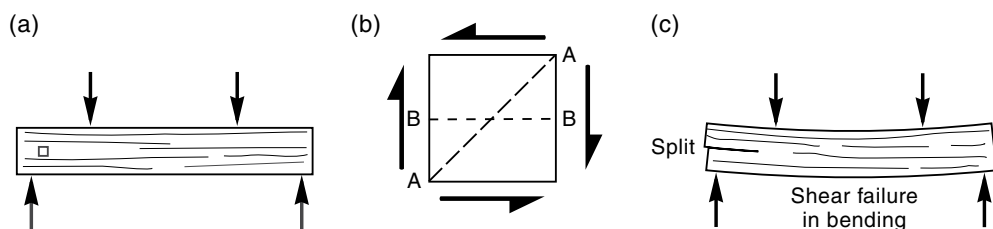


Figure 9.12 Shear stresses and shear failure in a timber beam

usually be a horizontal split along the grain as shown by the dashed line B–B, producing the split shown in Figure 9.12(c). Standard tests are available to measure the shear strength and shear modulus (shear stiffness) of wood. Shear failures rarely occur in rectangular timber beams, and shear only becomes critical if there are pre-existing splits at the ends of the beam or if very high shear stresses are developed near connections. Shear may be more critical for timber I-beams or box-beams with thin webs.

Gerhards (1982) reports two studies on shear strength of wood at elevated temperatures, by Ohsawa and Yoneda (1978) and Sano (1961a, 1961b, 1961c), giving results similar to those in Figure 9.10 which is recommended for design purposes. For shear modulus (or modulus of rigidity) he reports only one study, by Okuyama *et al.* (1977) who observed the shear modulus dropping to 20–50% of the 20 °C values at 80 °C.

Shear stresses are not normally a critical design consideration in rectangular beams, but may become important for I-beams, box beams, or beams with large holes for services. Design can be made using the fire-reduced cross section with allowance for reduced strength of the residual cross section. Eurocode 5 Part 1.2 (CEN, 2004b) states that shear may be disregarded in solid cross sections, and for notched beams it should be verified that the residual cross section in the vicinity of the notch is at least 60% of that required for normal temperature design. Kordina and Meyer-Ottens (1995) describe fire tests of glulam beams with rectangular openings reinforced with extra wood glued around the opening.

9.3.2.8 Variability in Wood Properties

A significant difference between wood and other materials is the often higher variability of wood strength between pieces from the same production run. This can have an effect on structural design in fire conditions, depending on how the design strength is obtained from test results. For normal temperature design, the characteristic design strength of a population of timber boards is taken as the 5th percentile value. In most limit states design (LRFD) formats, the 5th percentile value of strength obtained from in-grade testing $f_{0.05}$ is listed in the code and used directly in the design calculations. For fire design, some codes (e.g. SNZ, 1993; SA, 2006) use the 5th percentile value of strength $f_{0.05}$ so that the strength f_b to be used in the fire calculation is given by:

$$f_b = f_{0.05} \quad (9.2)$$

where $f_{0.05}$ is the characteristic design strength (5th percentile value) in the code for normal temperature design.

Some other codes (e.g. Eurocode 5, CEN, 2004b) modify the 5th percentile strength for normal temperature design to the 20th percentile strength for fire design, justified by the low

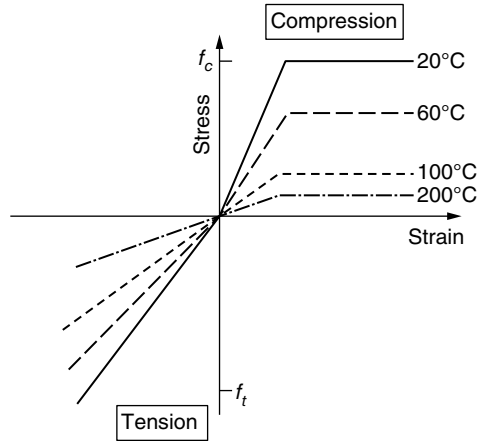


Figure 9.13 Stress–strain relationships for wood at elevated temperatures

probability of occurrence of serious fires. The design strength f_b for fire conditions is then increased by the k_{20} factor according to:

$$f_b = k_{20} f_{0.05} \quad (9.3)$$

The value of k_{20} given in Eurocode 5 is 1.25 for solid timber, 1.15 for glulam or wood-based panels, and 1.1 for LVL.

The USA method (AWC, 2012) uses the mean value of wood strength for fire design. This method is based on working stress design, so the allowable stress in the code is multiplied by a factor (2.85 for tension and bending, 2.58 for compression, and 2.03 for buckling failures) to give a design stress for fire calculations. Using the mean strength rather than a lower percentile implies that there is little or no safety factor in this method. However, the ‘working stress’ design methods in North American codes require fire design for full dead and live load without the reduction in live load which would be found in limit states design methods (see Chapter 5) so the end results may actually be more conservative than codes in other countries.

9.3.2.9 Derived Stress–Strain Relationships

Most of the properties listed earlier in this chapter have been obtained from test results, with a lot of scatter. These values do not always give good results when used in finite element computer modelling, because not all parameters are included in the models, such as mass transfer of moisture and time-dependent mechanical properties. For this reason, notional values can be chosen and modified to give more accurate overall results in computer models.

Figure 9.13 shows stress–strain relationships derived by König and Walleij (2000) from computer modelling of bending tests carried out by König (1995). These relationships are consistent with Figure 9.8, but idealized in a simple way to allow prediction of overall behaviour. It can be seen that in the tension region, linear elastic behaviour has been assumed until failure. There may be some plasticity in tension (Östman, 1985) which may need to be modelled to

avoid premature tensile fracture. In the compression region, idealized elasto-plastic behaviour has been assumed, as shown, which has been shown by Buchanan (1990) to give good results when modelling flexural behaviour. Similar relationships were derived by Thomas *et al.* (1995) who investigated the structural performance of light timber frame walls and floors exposed to fire using finite element models for both thermal and structural analysis.

The derived curves shown in Figure 9.13 include some indirect allowance for the creep that takes place in the duration of typical fire resistance testing. The different moduli of elasticity in tension and compression at elevated temperatures are a result of greater creep in compression than in tension (Thomas, 1997). Similar results are reported by Young (2000) who included an increase in compressive strength as the heated wood dried out over 100 °C.

9.4 Charring Rate

9.4.1 Overview of Charring

Investigations in many fire resistance tests have shown that the rate of charring of timber is roughly uniform and very predictable in the standard test fire, depending on the density and moisture content of the wood. Many national codes specify a constant charring rate in the range 0.60–0.75 mm/min for softwoods and about 0.5 mm/min for hardwoods (e.g. CEN, 2004b). Glulam and solid wood are usually considered to char at the same rate. The charring rate may reduce after prolonged fire exposure due to the increasing thickness of the insulating layer of char, but this is not usually recognized in design codes.

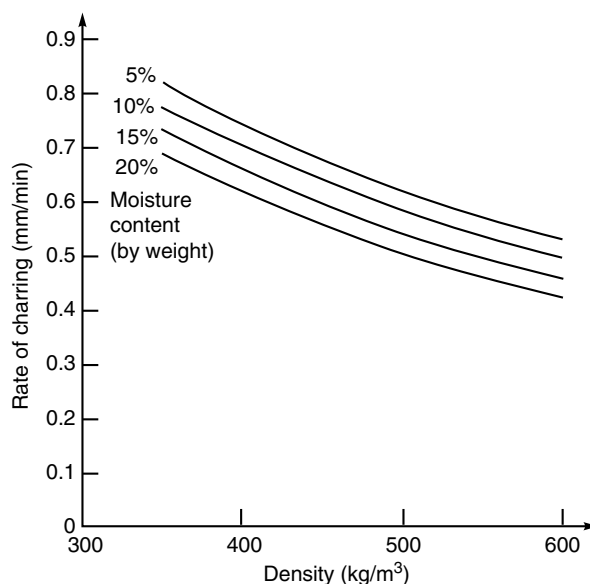


Figure 9.14 Charring rate as affected by density and moisture content. Reproduced from Lie (1992) by permission of ASCE

Table 9.1 Charring rates from Eurocode 5

Material	Minimum	Charring rate	
	density (kg/m ³)	β_0 (mm/min)	β_n (mm/min)
<i>Softwood</i>			
Glued laminated timber	290	0.65	0.7
Solid softwood timber	290	0.65	0.8
<i>Hardwood</i>			
Solid or glued laminated timber	290	0.65	0.7
Solid or glued laminated timber	450	0.50	0.55
<i>LVL</i>			
LVL panels	480	0.65	0.7
<i>Panels</i> (minimum thickness 20 mm)			
Plywood	450	1.0	—
Other wood panel products	450	0.9	—

The effect of density and moisture content on charring rate is shown in Figure 9.14 (from Lie, 1992, after Schaffer, 1967). The Australian code (SA, 2006) gives the following equation for charring rate β (mm/min) as a function of wood density, which gives similar values to those shown in Figure 9.14 for moisture content between 10% and 15%:

$$\beta = 0.4 + (280/\rho)^2 \quad (9.4)$$

where ρ is the wood density at a moisture content of 12% (kg/m³). For dense hardwoods, Equation 9.4 will give much lower charring rates than shown in Table 9.1, especially for hardwoods with density greater than 800 kg/m³.

Many charring studies have been carried out, including Schaffer (1977), Hadvig (1981), Mikkola (1990), White and Nordheim (1992) and Lau *et al.* (1999). König and Walleij (1999) experimentally studied the charring rates of glulam in the standard fire and in parametric fires. Lane *et al.* (2004) investigated the charring rate of LVL.

For solid timber, the current New Zealand code (SNZ, 1993) specifies a charring rate of $\beta=0.65$ mm/minute, obtained from Collier (1992) who carried out charring tests on radiata pine glulam beams, and used the equations of White and Nordheim (1992) to relate charring rate to density for typical radiata pine which has a density of 550 kg/m³ at 12% moisture content, as described by Buchanan (1994). Correlations with density must be made with care, because wood density varies considerably both within and between trees and sites, and there are several different definitions of wood density depending on how the moisture is included in the calculation (Collins, 1983).

Table 9.1 shows the recommended charring rates from Eurocode 5, which also gives modification factors for other densities and panel thicknesses. Many other national codes specify similar charring rates. Of the two charring rates shown in Table 9.1, β_0 is the one-dimensional charring rate intended to be used for large flat surfaces and β_n is the 'notional' charring rate to be used for rectangular beams or columns, when any loss of cross section due to rounding of the exposed corners is ignored. The one-dimensional charring rate β_0 can be used for design of beams or columns, but only if the cross section is reduced to allow for rounded corners, which is not normally done.

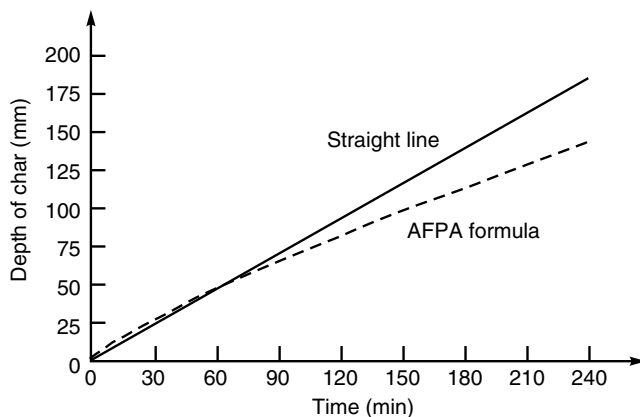


Figure 9.15 Depth of char from North American recommendations

In the USA, recommendations for the charring rate are given by AWC (2015), based on the non-linear model of White (1988). The proposed charring rate β is the average charring rate (mm/min) over the period to time t (min), given by:

$$\beta = 2.58 \beta_n / t^{0.187} \tag{9.5}$$

where β_n is the nominal charring rate obtained from the char depth measured after 1 h of fire exposure ($\beta_n = 0.635$ mm/per min) and t is the time (min).

The resulting char layer thickness c (mm) at time t (minutes) is then given by:

$$c = \beta t = 2.58 \beta_n t^{0.813} \tag{9.6}$$

Equation 9.6 includes a 20% increase in charring rate over measured rates to allow for rounding at the corners and the reduction of strength of the heated layer below the char front. It has been converted from imperial units in the original publication, based on $\beta_n = 1.5$ in/h. The dashed curve in Figure 9.15 shows the resulting depth of char during 4 hours of standard fire exposure, compared with the solid straight line which is the depth of char for a uniform charring rate of 0.762 mm/min (1.2×0.635). It can be seen that there is little difference up to 1 hour where the curve crosses the line, but the AWC non-linear equation gives less depth of char than the uniform charring rate for exposure times over 2 hours.

9.4.2 Corner Rounding

All fire tests of large rectangular timber sections show some rounding of the corners, because the corners are subjected to heat transfer from two surfaces. Figure 9.16 shows the shape of a typical charred cross section, from BS 5268 (BSI, 1978). Most design codes, including Eurocode 5 (CEN, 2004b), use the simple relationship whereby the radius of the rounding is equal to the depth of the charred layer.

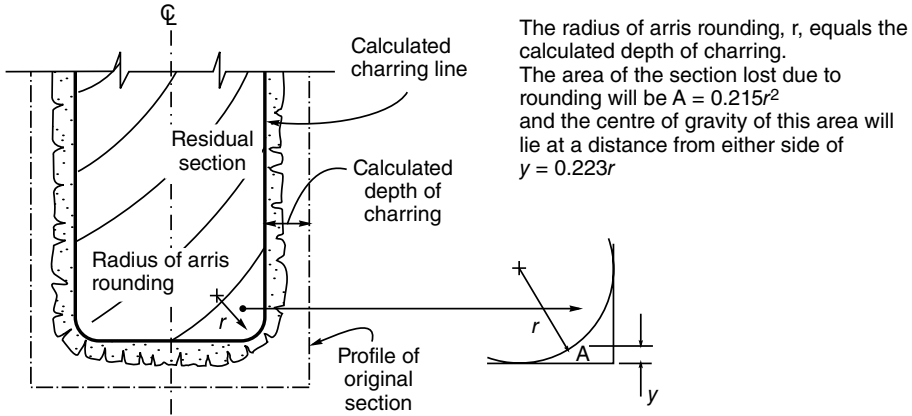


Figure 9.16 Residual cross section of timber beam exposed to fire. Reproduced from BSI (1978). Permission to reproduce extract from BS 5268 is granted by BSI

If corner rounding is taken into account, the section properties will be affected slightly, depending on the size of the member. For a beam exposed to fire on three sides, the section modulus $Z_{f,r}$ of the reduced cross section is given approximately by:

$$Z_f = b_f d_f^2 / 6 - 0.215 r^2 d_f \tag{9.7}$$

where b_f is the residual width of the beam, d_f is the residual depth of the beam and r is the radius of the charred corner.

9.4.3 Charring Rate of Protected Timber

Applying a protective layer to wood surfaces can delay the onset of charring, and can reduce the rate of charring below the layer. However, even if no charring occurs below the protective layer, the protected wood may be heated up, leading to a more rapid rate of charring after the layer falls off. König and Walleij (1999) experimentally studied the charring rates of glulam in the standard fire and in parametric fires, and investigated the effect of protective materials before and after they fell off the surface of the wood. For glulam beams and columns, White (2009) has proposed an increase in fire resistance of 30 or 60 min when using one or two layers, respectively, of 16 mm Type X gypsum board.

The benefit of protective layers is covered more explicitly in Eurocode 5 and by Östman *et al.* (2010), where it is assumed that the charring rate under a protective layer is half of the charring rate of unprotected wood, but that increases (fourfold) to double the rate of unprotected wood after the protection falls off, until a char depth of 25 mm has been reached. This is described with reference to Figure 9.17. Figure 9.17a) shows the charring depth versus time for unprotected wood (line 1), compared with wood with a protective layer that falls off at time t_f . The initial charring rate of the heated wood after time t_f (line 2a) is double that of the unprotected wood until time t_a when the char reaches a depth of 25 mm, after which the charring rate reverts to the rate for unprotected wood (line 2b). It can be seen that the longer the time t_f the greater the benefit of the protective layer.

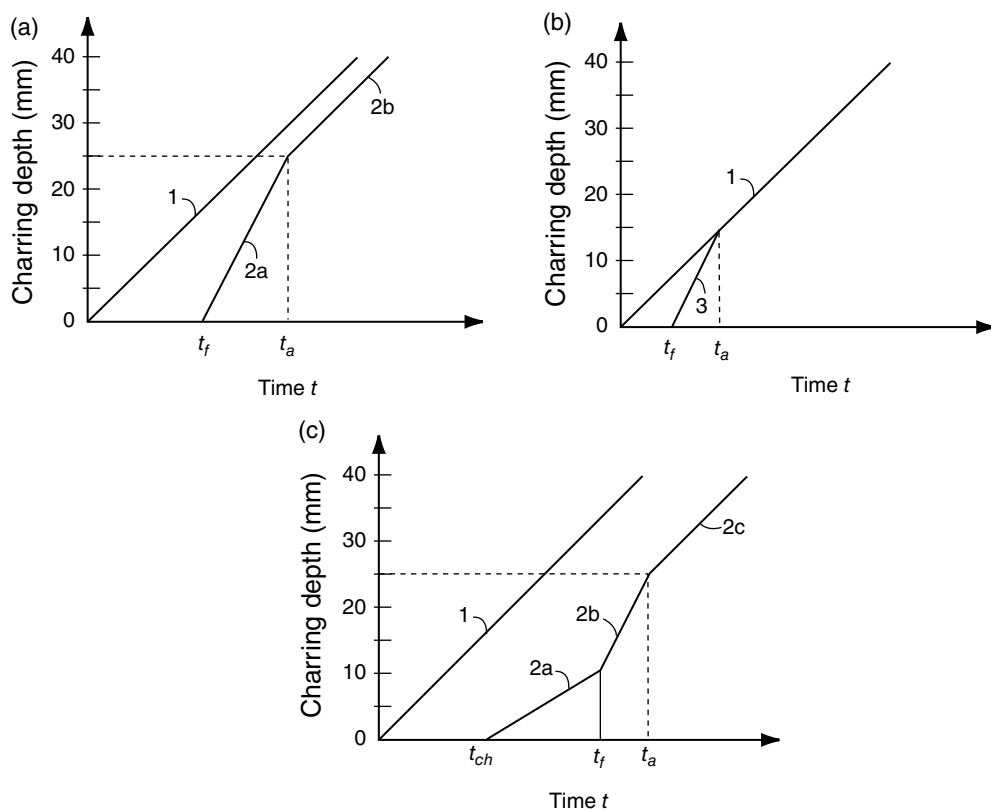


Figure 9.17 Charring depth versus time for wood with a protective layer. (a) Charring starts after the protective layer falls off. (b) The protective layer falls off too soon to be of any use. (c) Charring starts behind the protective layer before it falls off. Adapted from CEN (2004b). © CEN, reproduced with permission

The protective layer provides no benefit at all if falls off too soon, as shown in Figure 9.17(b) where the charring rate after the fall-off time t_f (line 3) is double that of the charring rate in the unprotected wood until time t_a when the depth of char becomes equal to that in the initially unprotected wood (line 1). In other words, the protection can be ignored if the charring at the double rate (after fall-off) never reaches a depth of 25 mm.

Figure 9.17(c) shows what happens if the wood starts to char under the protective layer at time t_{ch} before the layer falls off. In this case the initial charring rate (line 2a) is only half of the unprotected rate because of the protection, then it increases fourfold (line 2b) after the layer falls off at time t_f (line 2b) and finally drops back to the unprotected charring rate (line 2c) after the char reaches a depth of 25 mm.

9.4.4 Effect of Heated Wood Below the Char Line

There are several alternative design methods to allow for heated wood below the char line. Some codes (BSI, 1978; SNZ, 1993) ignore any reduction of wood strength below the char, which leads to unsafe results for small cross sections (especially those less than 100 mm thick).

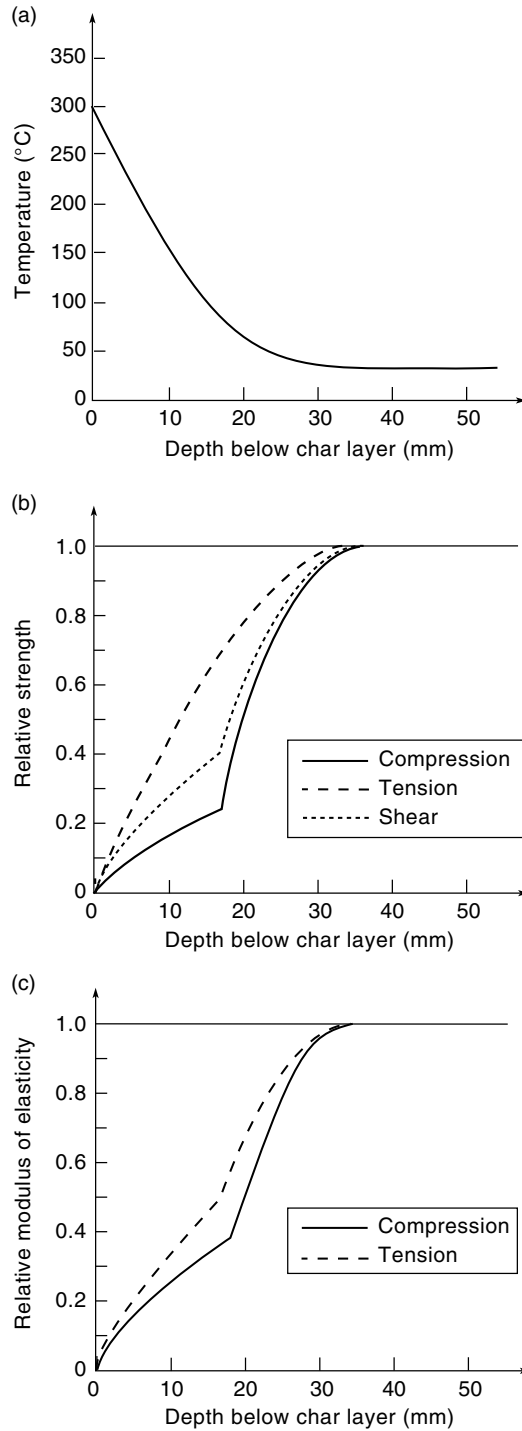


Figure 9.18 (a) Temperature profile below the char layer. (b) Reduction in strength of wood below the char layer. (c) Reduction in modulus of elasticity below the char layer

The temperature and moisture gradients in heated wood below the char layer affect the strength and stiffness of a fire-exposed member. An approximate estimate of the reduced strength and stiffness can be made by combining the predicted temperatures of the wood beneath the char with the effects of temperature on strength. Figure 9.18(a) shows the temperature profile from Equation 9.1. Figure 9.18(b) shows the resulting drop in strength of the wood below the char layer, obtained by combining these temperatures with the strength reduction factor from Figure 9.10. Figure 9.18(c) shows the reduction in modulus of elasticity by combining the temperatures in Figure 9.18(a) with the reduction factors from Figure 9.9. All three properties are significantly reduced in the 25 mm of wood below the char layer, the greatest reduction being in the compression strength and stiffness over the first 18 mm of depth, with a plateau at 17 mm depth which corresponds with wood temperatures at or above 100 °C.

For calculations in accordance with Eurocode 5, the thickness of the zero strength wood layer is $z = 7$ mm for fire exposure greater than 20 minutes. For exposure less than 20 minutes, the 7 mm thickness is reduced proportionately to zero. The Australian code (SA 2006) specifies a thickness $z = 7.5$ mm for the zero strength layer. A justification for the 7 mm thickness is given by Schaffer et al (1986) who considered the reduction in modulus of elasticity of the heated wood below the char layer.

The American design method in the National Design Specification (NDS) for Wood Construction (AWC, 2012) increases the nominal charring rate by 20% to allow for the heated wood below the char layer. This implies a zero strength layer of wood with increasing thickness during the fire exposure, the thickness being about 8 mm for each hour of exposure which becomes increasingly significant for long periods of fire resistance.

9.4.5 Design for Realistic Fires

All the design methods in this chapter are based on investigations of timber exposed to the standard test fire. For more realistic fires, a design method is given in Annex A of Eurocode 5 (CEN, 2004b) with charring rates and strength reduction factors for the ‘parametric fires’ which were described in Chapter 4.

According to Eurocode 5, the charring rate for realistic fires depends on the amount of ventilation in the fire compartment, so that for a compartment with an opening factor of $F_v = 0.04$, the expected charring rate is the same value used for standard fires, as described earlier in this chapter. This charring rate decreases roughly in proportion to the opening factor for compartments with smaller openings and increases, by up to 50%, for compartments with larger openings. This is based on the work of Hadvig (1981) who published the predicted depth of char for timber members exposed to parametric fires, confirmed by Bolonius Olesen and Toft Hansen (1992) who carried out full-scale tests on glulam beams exposed to such fires, and König and Walleij (1999) who tested 95 mm thick blocks of glulam exposed to fire on one side. Friquin *et al.* (2010) tested CLT panels exposed to parametric fires. The Eurocode 5 design method for realistic fires is not described in detail in this chapter [and is not included in Östman *et al.* (2010)] because it has not been verified sufficiently to become an accepted design method.

The time equivalent formula is not accurate for timber structures because it was only derived for protected steel structures. However, it is sometimes used for timber because there is no better approach available.

One major problem with design of heavy timber structures for realistic fires is that no guarantee can be given that the timber members will stop charring after a complete burnout of a fire compartment, even if the calculated char depth at the end of the burning period provides

sufficient residual strength. Observations from full-scale fire tests show that charring often continues and timber beams continue to lose cross section after the burning phase of the fire is over. Saito *et al.* (2007) showed that the charring stops if the air supply is sufficiently restricted. Hevia (2014) observed a temperature rise during the decay phase when parts of charred lamellae detached from inner layers, exposing fresh wood and leading to a second flashover. Even if the charring stops, temperatures will increase in the centre of the timber member leading to further loss of strength. Kinjo *et al.* (2014) subjected glulam beams to one hour of fire exposure followed by three additional hours of cooling. The charring was minimal during the cooling period, but the temperatures in the centre of the beams steadily increased to reach 100 °C after 2 h, with a corresponding reduction in beam strength and stiffness.

This section has shown that heavy timber members can be designed for long periods of fire resistance, but they may not be able to resist a complete burnout unless firefighters arrive to cool the timber structure with water at the end of the fire, in order to terminate the charring and slow down the temperature increase inside the timber members. More full-scale experimental research on this topic is required before design of heavy timber structures for complete burnout can be carried out with confidence (Buchanan, 2015).

9.5 Design for Fire Resistance of Heavy Timber Members

This section describes the structural design of large timber structural elements exposed to fire.

9.5.1 Design Concepts

Large timber members exposed to fire have excellent fire resistance. Figure 9.19 shows large glulam beams in a fire resistance test, and Figure 9.20 shows the surviving beam from a similar test.

The fire resistance is easily calculated because of the predictable rate of charring on surfaces exposed to the standard fire. Figure 9.21 shows the common cases of three- and four-sided fire exposure of a rectangular member. The original cross section $b \times d$ is reduced to the *residual cross section* $b_f \times d_f$ as a result of charring. The depth to the char front is shown as the dimension c (mm) which is equal on all exposed surfaces, given by:

$$c = \beta t \quad (9.8)$$

where β is the rate of charring (mm/min) and t is the time of fire exposure (min).

The dimensions of the residual cross section are given by:

$$\begin{aligned} b_f &= b - 2c \\ d_f &= d - c \quad (\text{three-sided exposure}) \\ d_f &= d - 2c \quad (\text{four-sided exposure}) \end{aligned} \quad (9.9)$$

9.5.2 Timber Beams

Large timber beams exposed to fire have demonstrated excellent and predictable behaviour. Beams can be designed using the same design equations as for normal temperature conditions, with modifications for reductions in strength or cross section.



Figure 9.19 Fire resistance test of glulam beams; the beams span a 4 m long furnace with loads applied using concrete blocks



Figure 9.20 Residual cross section of a large glulam beam after a fire test. Reproduced by permission of American Institute of Timber Construction

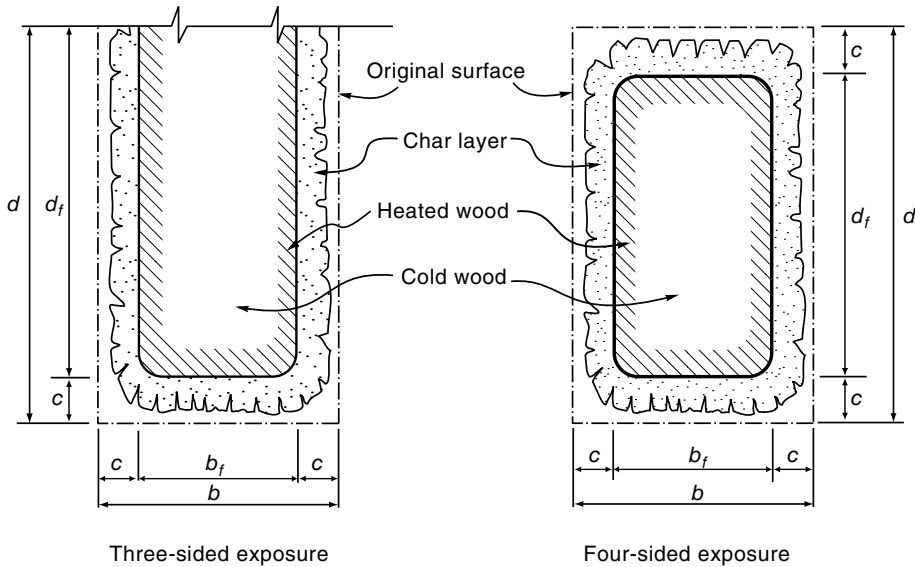


Figure 9.21 Design concepts for large timber members

The design of a beam is verified by satisfying the following design equation:

$$M_{fire}^* \leq M_f \quad (9.10)$$

where M_{fire}^* is the bending moment at the time of the fire and M_f is the design flexural capacity under fire conditions, given by:

$$M_f = Z_f f_b \quad (9.11)$$

where f_b is the design strength of wood in fire conditions (MPa) and Z_f is the elastic section modulus (mm^3) reduced for fire exposure.

Note that Equation 9.11 does not include a partial safety factor for mechanical properties γ_M or a strength reduction factor Φ because both have a value of 1.0 in fire conditions, as described in Chapter 5.

The recommended *effective cross section method* from Eurocode 5 uses a rectangular cross section, slightly smaller than the residual cross section to allow for corner rounding, and a layer of zero strength wood below the char line, with the material properties in the inner part of the member unaffected by temperature.

The design flexural capacity M_f should be calculated using Equation 9.10, where (assuming no corner rounding), the section modulus $Z_{f,z}$ for three-sided fire exposure is given by:

$$Z_{f,z} = (b_f - 2z)(d_f - z)^2 / 6 \quad (9.12)$$

where z is the thickness of the zero strength layer (mm).

Eurocode 5 gives an alternative *reduced properties method* which uses the residual cross section dimensions with an average reduction in the material properties over the whole residual

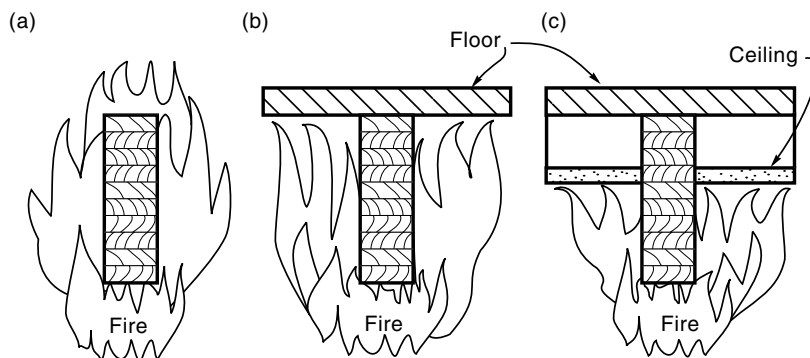


Figure 9.22 Three- and four-sided fire exposure of beams

cross section. The reduced properties method is not described further because the effective cross section method is preferred (Östman *et al.*, 2010).

It is important to determine which surfaces of the beam are exposed to fire. Beams, such as truss members, are exposed on four sides, as shown in Figure 9.22(a). Most beams have the top edge protected by the floor or roof, as shown in Figure 9.22(b). In some cases, more of the beam may be protected from fire, as shown in Figure 9.22(c).

In addition to the calculations of flexural strength, beams must be checked to ensure that they are not likely to fail by lateral torsional buckling. No buckling check is necessary if the compression edge of the beam is provided with continuous lateral restraint. If lateral restraint is missing or intermittent, normal calculations from timber design codes should be used, based on the residual charred cross section of the beam. Buckling resistance depends on the torsional rigidity of the cross section, which can drop to low levels as charring proceeds, especially for slender rectangular beams (Fredlund, 1979).

9.5.3 Timber Tensile Members

Tensile members are not affected by buckling. The tensile load capacity of a fire-reduced cross section can be calculated in the same way as for a flexural member. There are no reported fire test results of large timber tensile members, but there is no reason why a tensile member will not behave in the same way as the tension edge of a deep beam, many of which have been tested.

9.5.4 Timber Columns

The compressive strength of a short column depends on the crushing strength of the material. Under fire exposure this can be calculated from the reduction of the cross section and the reduced strength of the wood. Long columns are susceptible to buckling failures, so the failure load depends on the moment of inertia and modulus of elasticity of the residual cross section. The likelihood of buckling will increase as the fire progresses because the reduced cross section increases the slenderness of the column, especially for free-standing columns with no lateral support over the full height. For columns with intermediate restraint, the supporting members must have fire resistance for the full duration of the fire.

A series of 16 full-scale column fire tests is described by Malhotra and Rogowski (1970). The columns achieved fire resistance ratings between 30 min and 90 min, depending on load and slenderness ratio. In all cases the fire resistance was greater than predicted by simple analysis of the charring rate. Precise analysis is difficult because of the partial fixity at the column ends, and unknown ultimate strength of the wood. A report by AWC (2015) analyses these and other tests to verify the North American design equations. Schaffer (1984) describes several studies of large timber columns exposed to fire, considering buckling of the fire-reduced cross section, reporting that the German design equation gives results 'in reasonably good accordance with the results of fire resistance tests' (Meyer-Ottens, 1983).

9.5.5 Empirical Equations

Most North American building codes include a set of simple equations for calculating fire resistance of large timber beams and columns, based on the work of Lie (1977). In the United States the design method applies to glulam and sawn timber (e.g. ICC, 2015) but in Canada it only applies to glulam (NBCC, 2010). Lie assumed a uniform charring rate of 0.6 mm/min, and allowed for the reduced strength of the hot wood layer under the char by assuming that the section remains rectangular and the entire residual core has 80% of its initial strength. The derivation assumes that the ultimate strength of the wood is three times the allowable design stress. The resulting equations are non-linear and must be solved in an iterative manner to determine the fire resistance time, so Lie approximated them by a set of simple equations that allow a straightforward calculation of fire resistance time as a function of member size and load ratio.

The derivation is based on a beam loaded with the maximum allowable load, so that failure in fire occurs when the ultimate flexural strength of the residual section is equal to the allowable design strength of the original section. Comparing the section moduli of the two cross sections gives the failure condition as:

$$\alpha b_f d_f^2 = k_a b d^2 \quad (9.13)$$

where α is the ratio of hot wood strength to cold wood strength (=0.8) and k_a is the ratio of allowable strength to ultimate strength (=0.33).

The fire resistance time can be calculated by eliminating b_f , d_f and c from Equation 9.8, Equation 9.9 and Equation 9.6 and solving for t . Lie solved these equations for a realistic range of member sizes, also introducing a load factor z which to allow for the ratio of actual to allowable load on the member. For dimensions in millimetres, the approximate solution to these equations for beams gives the time to failure t_f (min) as:

$$\begin{aligned} t_f &= 0.1 z b (4 - b/d) \quad (\text{three-sided exposure}) \\ t_f &= 0.1 z b (4 - 2b/d) \quad (\text{four-sided exposure}) \end{aligned} \quad (9.14)$$

with

$$z = 0.7 + 0.3/R_a \quad (9.15)$$

where R_a is the ratio of actual to allowable load at normal temperature.

For columns, the failure mode depends on the slenderness. Short columns fail when the ultimate compressive stress is exceeded, so comparing the cross-sectional area of the two sections gives the failure condition as:

$$\alpha b_f d_f = k_a b d \quad (9.16)$$

Long columns fail by buckling. Assuming that d is the smaller dimension and buckling occurs in that direction, comparing the moment of inertia of the two sections gives the failure condition as:

$$\alpha b_f d_f^3 = k_a b d^3 \quad (9.17)$$

The fire resistance time can be calculated by eliminating b_f , d_f and c and solving for t . For columns, Lie obtained:

$$\begin{aligned} t_f &= 0.1 z b (3 - d/2b) \quad (\text{three-sided exposure}) \\ t_f &= 0.1 z b (3 - d/b) \quad (\text{four-sided exposure}) \end{aligned} \quad (9.18)$$

For long columns, z is calculated from Equation 9.15. For short columns the value of z is increased to give better agreement with experimental results for columns of low slenderness ratio, using:

$$z = 0.9 + 0.3/R_a \quad (9.19)$$

In the current version of the North American codes, these equations can only be used for values of R_a greater than or equal to 0.5, which ignores the increase in fire resistance for loading less than 50% of the allowable load. These equations have been derived for use in working stress design format. They can be used in limit states design (LRFD) format if R_a is taken as the ratio of the applied moment to the design flexural resistance at normal temperatures.

9.5.6 Timber Beam-columns

A 'beam-column' is a member subjected to combined bending and axial loading. This may be a beam with some axial load, or more often a column with some bending moment.

Some equations for design of beam-columns use the 'secant formula' which gives an exact expression for maximum stress in an elastic column. These formulae are difficult to use in fire situations because neither the location nor the strength of the extreme fibre are readily identified. It is more appropriate to follow the normal temperature design approach of codes (e.g. SA, 2006) which give a general interaction formula including both flexural strength and axial load capacity, such as:

$$\left(N/N_u\right)^2 + M/M_u \leq 1 \quad (9.20)$$

where N is the applied axial load (kN), N_u is the axial load capacity, including the effects of buckling (kN), M is the applied bending moment, including a moment magnifier for slender members (kNm) and M_u is the flexural capacity including the effects of lateral buckling (kNm).

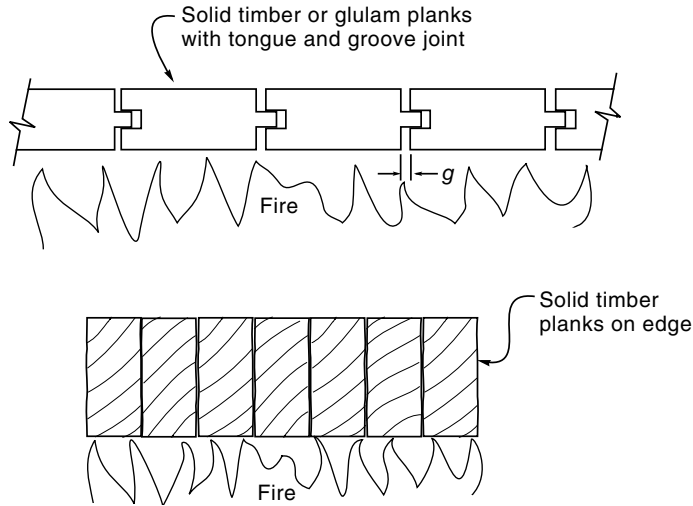


Figure 9.23 Tongue and groove decking and solid plank decking exposed to fire

9.5.7 Timber Decking

Fire resistance of timber decking must consider all three possible failure criteria of stability, integrity and insulation. Solid wood decking in this chapter includes solid timber or glulam timber planks laid flat and butted together with tongue and groove edges, and timber planks set on edge and nailed together, as shown in Figure 9.23.

This discussion is for fire exposure to the underside of timber decking. Fire exposure to the top surface of floors is not generally considered a serious problem because room temperatures are lower near the floor, convective flows are always up, not down, and the top surface of floors are often protected with furniture, floor coverings, and debris from the fire.

9.5.7.1 Strength

The strength of timber decking can be assessed in the same way as for beams. If the planks are fitted tightly together, the fire exposure will cause charring only on the lower surface, with gradually decreasing thickness as the charring proceeds. Strength can be calculated from the reduced thickness of the remaining wood. For decking continuous over several spans, moment redistribution can be included as described in Chapter 5. To avoid such calculations, Janssens (1997) has proposed an empirical design formula for structural performance of solid wood decks.

9.5.7.2 Integrity

The integrity criterion must prevent the spread of flames or hot gases through the floor, leading to ignition of items on the upper surface. Junctions between planks can increase in width due

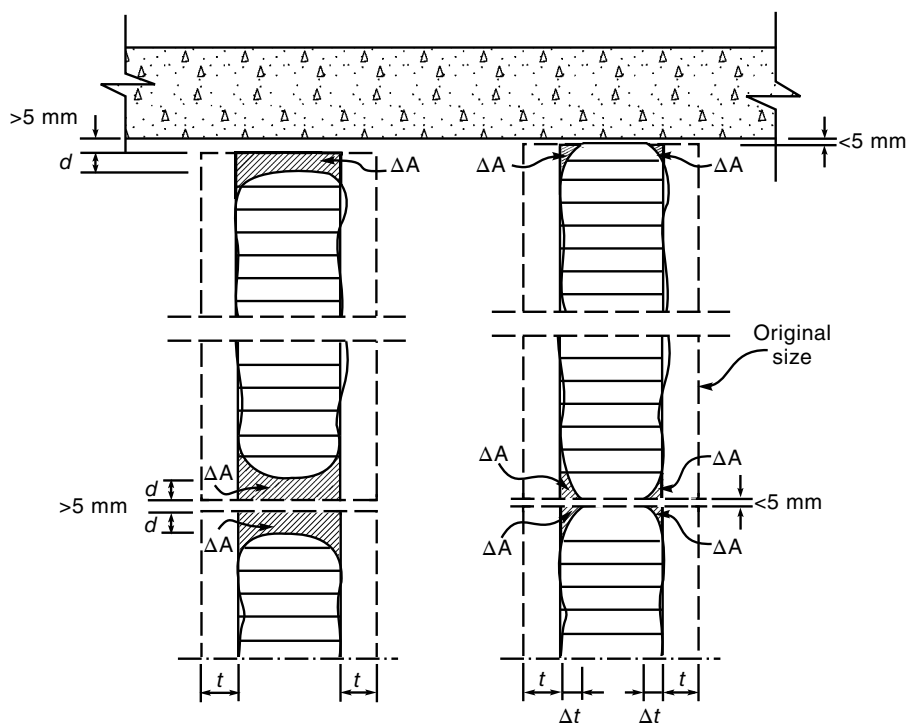


Figure 9.24 Effect of gap width on charring. Reproduced from Carling (1989) by permission of Building Research Association of New Zealand

to shrinkage of wood, so convective flows of hot gases through the deck must be prevented. This can be done with intumescent paint, fire resistant caulking, tongue and groove joints between the planks, or a sheet of plywood on the top surface.

If the gap between the planks (dimension g in Figure 9.23) is small enough, and air flow through the gap is prevented, the wood inside the gap will not be exposed to fire temperatures. Carling (1989) reports studies by Aarnio (1979) and Aarnio and Kallioniemi (1983) who studied gaps between glulam beams, as shown in Figure 9.24. These showed that temperatures within the gap remained low enough to prevent charring if the gap was less than 5 mm wide. A maximum gap of 3 mm is recommended for design purposes (Kordina and Meyer-Ottens, 1995).

9.5.7.3 Insulation

If the integrity and stability criteria are satisfied, there will be no problem meeting the insulation criterion, because the thickness of remaining wood required to carry fire limit state loads will be greater than that required to prevent excessive temperature rise on the top surface. Annex E of Eurocode 5 gives additional information on the separating function of wall and floor assemblies including timber decking. To satisfy the insulation criterion for non load-bearing elements, it is recommended that 25mm of uncharred wood should remain below the char layer.

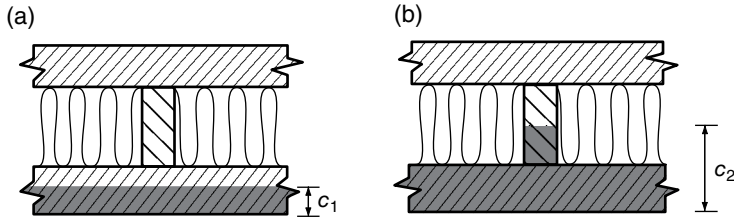


Figure 9.25 Charring model for hollow core timber floors: (a) charring phase 1; (b) charring phase 2. Based on Östman *et al.* (2010)

9.5.8 Hollow Core Timber Floors

Prefabricated hollow core timber flooring panels are manufactured from solid sawn timber, LVL or CLT. Hollow core timber floors are often referred to as ‘stressed skin’ panels, because the flexural stresses are resisted by the top and bottom skins, and the shear stresses are resisted by the internal timber webs. Östman *et al.* (2010) summarize a fire design method from Frangi *et al.* (2009c). The charring model is shown in Figure 9.25. The charring rate of the bottom skin is the same as for any flat solid timber element (charring depth c_1 in phase 1), but after the bottom skin has gone the webs may char at a faster rate depending on their thickness and protection. If the bottom skin of the floor cannot provide sufficient fire resistance, it is essential that the cavities be completely filled with mineral wool batts which are fixed to remain in place at temperatures over 1000°C so that only the bottom edges of the residual webs (now acting as joists) are exposed to fire (charring depth c_2 in phase 2).

9.5.9 Timber-concrete Composite Floors

Timber-concrete composite floors have a structural concrete topping over timber planks or timber joists, and a shear connection between the concrete and the wood. A variety of shear connections are available including notches cut into the timber joists, or steel bolts, screws, or steel plates fastened to the timber. Timber-concrete composite floors are used to strengthen historical buildings by casting a new concrete topping on existing timber floors, with suitable shear connectors. The fire resistance of timber-concrete composite floors can be predicted by calculating the charring of the timber components and by taking into account the temperature-dependent reduction of the connection strength and stiffness, as described by Fontana and Frangi (1999), Frangi *et al.* (2010) and O’Neill *et al.* (2011).

9.5.10 Cross Laminated Timber

Large CLT panels are becoming popular for construction of timber walls and floors as described in Section 9.1.2. Typical CLT panels glued with approved structural adhesives for load-bearing wood members have shown sufficient performance in fire tests to match the requirements of most building codes. Advice should be sought from CLT manufacturers about the fire performance of their particular adhesives. Panels with nail or dowel fasteners are not covered here. A summary of many recent fire tests is given by Klippel *et al.* (2014).

A design method is provided by Östman *et al.* (2010), following the work of Schmid and König (2010) and Schmid *et al.* (2010). A similar Canadian design method is given by Gagnon and Pirvu (2011) who suggest that the normal charring rate for solid wood should be used for the first layer, but double that charring rate should be used for successive layers due to pre-heating of the next layer. This design method is recommended, but if any of the inner layers are more than 25 mm thick, a reasonable approximation is for the charring rate to drop back to the normal charring rate after the first 25 mm has charred (Klippel *et al.*, 2014), in the same way as described for protected wood in Section 9.4.3. In all cases, a zero-strength heat-affected layer 7 mm thick should be assumed below the char front. Following this procedure, it is clear that CLT panels with the best fire performance will be those with thick layers of wood, especially the layer on the fire-exposed face.

Charred layers have been observed to fall off the bottom of CLT floors in some full-scale fire tests, but falling off is less common for CLT walls. Nevertheless, the same charring rate is recommended for both floors and walls, based on many test results. Despite the possibility of some charred layers falling off, the design of CLT floors is not normally governed by fire resistance, because the floor thickness required to limit deflections and to control vibrations under normal gravity loading will usually provide a sufficiently high level of fire resistance (Frangi *et al.*, 2009b).

The strength and stiffness of CLT walls and floors is mainly provided by the layers parallel to the load direction, because the intermediate layers of boards, rotated 90°, do not contribute to the strength. This can be taken into account in the fire design of CLT floors or walls, using the reduced cross-section method, in a simple step-by step procedure which considers all the layers, and the charring rates recommended above.

9.5.11 Reinforced Glulam Timber

There are several methods of reinforcing glulam beams to increase the bending strength and stiffness. One method is to glue steel reinforcing bars into grooves in the outer tensile laminations. Another method of reinforcing is to glue a high-strength fibre reinforced polymer (FRP) laminate to the bottom outside edge of a beam, or between the outer laminate and the rest of the beam. Martin and Tingley (2000) show that such reinforcing can double the bending strength of glulam beams under normal temperatures. FRP has poor fire performance without adequate protection, so the fire resistance of an FRP reinforced glulam beam is likely to be similar to that of an unreinforced glulam beam.

9.5.12 Post-tensioned Timber Structures

Prestressed timber is increasingly being used for innovative large timber structures, using unbonded high strength steel tendons or bars, which are post-tensioned during construction of the building (Buchanan *et al.*, 2011). Such structures are known as Pres-Lam (pre-stressed laminated) timber structures. Because the post-tensioning is usually provided to reduce deflections or to resist seismic loads, the structure may be able to perform satisfactorily in fire conditions even if the post-tensioning loses its strength. If the post-tensioning is required during fire exposure, the tendons can be protected to ensure that excessive temperatures do not occur. Protection of the post-tensioned anchorages may also be important. Full-scale fire resistance testing of post-tensioned hollow timber beams is described by Costello *et al.* (2014).

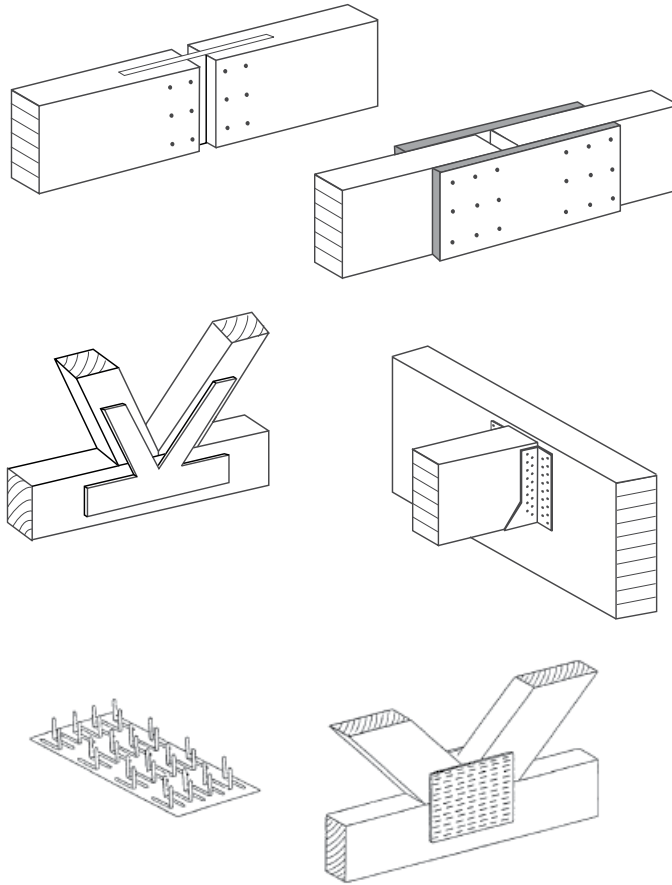


Figure 9.26 Typical connections in timber structures

9.6 Timber Connections in Fire

The ability of any structure to carry loads and perform its function depends on the strength and stiffness of the structural members and the connections between those members. In a fire resistant structure, both the members and their connections must perform throughout the fire exposure.

Some connections are not vulnerable to fire exposure. For example, a simple bearing support of a beam on a wall or a column on a foundation is unlikely to fail before the beam or column itself fails. Many other connections are much more vulnerable than the members themselves. The design philosophy should be to ensure that the connections have better fire resistance than the main members. Figure 9.26 shows a selection of typical connections in timber structures. The connections with side members of wood have much better fire resistance than connections with exposed steel plates. Typical connections after fire exposure are shown in Figure 9.27 and Figure 9.28.



Figure 9.27 Bolted connection between timber members, after fire exposure



Figure 9.28 Truss plate connection between timber members, after fire exposure

9.6.1 *Geometry of Timber Connections*

Referring to Figure 9.26, and following the principles from steel structures (Chapter 6), a steel fastener with a high ratio of heated perimeter to cross-sectional area will heat up much more rapidly than one with a low ratio. The high steel temperatures will conduct heat into the wood, causing softening or charring which will reduce the load-carrying capacity.

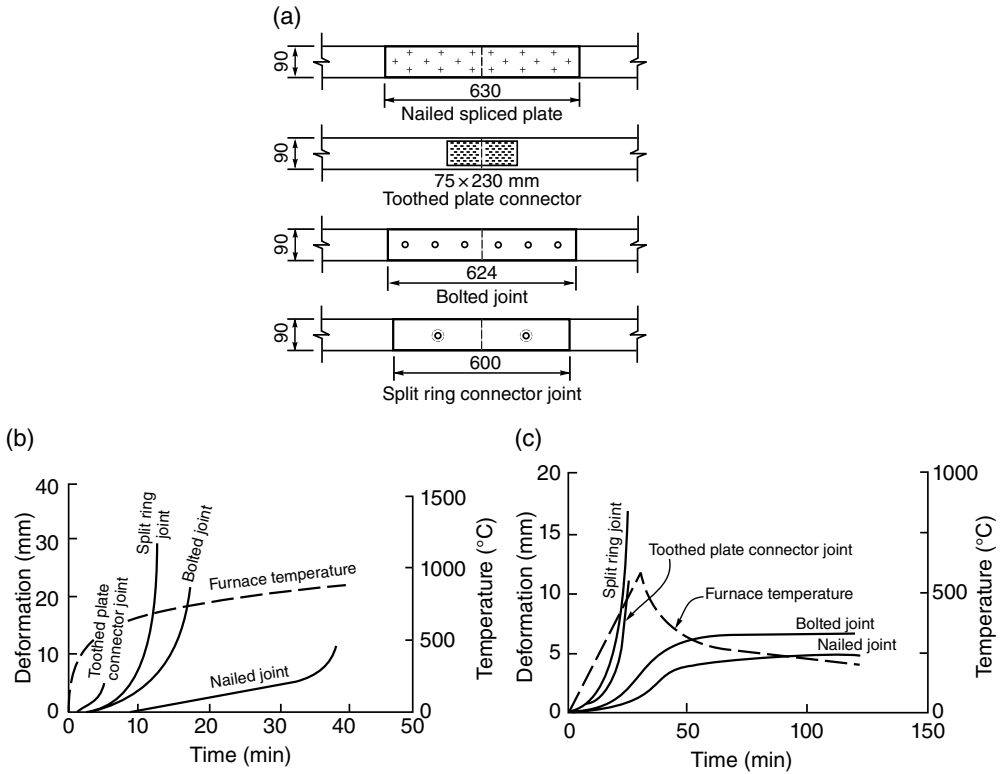


Figure 9.29 Tension tests of nailed and bolted joints. Reproduced from Leicester *et al.* (1979) by permission of CSIRO Australia

This principle is illustrated in a series of tests by Leicester *et al.* (1979). Figure 9.29(a) shows four tension splice connections which were subjected to two fire exposures. Figure 9.29(b) shows the load–deflection results for the standard fire exposure, where it can be seen that the toothed truss plate connector failed after only 5 min, as a result of rapid heating of the steel and conduction of heat into the wood around the teeth of the plate. The bolted joint resisted the load for almost 20 min, and the nailed joint for 40 min. When subjected to a less severe fire shown in Figure 9.29(c) both the bolted and nailed joints were able to carry the load for 2 h, but the truss plate failed after 20 min. The area of steel exposed to the fire is much less for bolts than for truss plates, and even less again for nails. Connections using steel plates will have much better fire resistance if the plates are slotted into the timber members exposing only one edge, rather than being on the outside where a large surface of steel is exposed to the fire.

9.6.2 Steel Dowel-type Fasteners

The behaviour of steel dowel-type fasteners such as nails, screws, bolts, or dowels depends on the temperature of the steel during the fire, because that affects the strength of the fastener itself, and high temperatures lead to charring or loss of strength of wood in contact with the fastener.

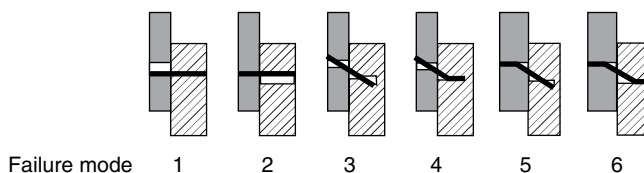


Figure 9.30 Possible failure modes of fasteners. Based on Johansen (1949)

All metals are much better conductors of heat than wood, so metal fasteners will conduct heat from the surface into the interior of any connection. Most international codes allow the design of fasteners under ambient conditions using the European Yield Model developed by Johansen (1949), with simple equations for each of the possible failure modes shown in Figure 9.30. The same principles can be applied to fire design of fasteners.

An early review of the fire performance of timber connections is by Carling (1989). Much new experimental and analytical research has been done since then. Recent test results and calculation models include those by Cachim and Franssen (2009), Frangi *et al.* (2009a), Erchinger *et al.* (2010), Moss *et al.* (2010), Peng *et al.* (2010) and Racher *et al.* (2010), with an excellent summary given by Östman *et al.* (2010).

9.6.3 Connections with Side Members of Wood

This section refers to the fire resistance of connections where the main external material exposed to fire is timber. This applies to all timber-to-timber connections, and timber-to-steel connections where the steel plate is protected from fire exposure by external timber.

9.6.3.1 Unprotected Connections

Nails and Screws

Nails make excellent connections in timber structures because they penetrate the wood much better than surface adhesives, they do not weaken the wood with drilled holes and they can distribute forces over a larger part of the surface than bolts. Temperatures in nailed connections exposed to fire can be calculated using a finite element model, as described by Fuller *et al.* (1992). Norén (1996) has tested nailed timber-to-timber splice joints in tension exposed to the ISO 834 standard test fire, showing that the load capacity can be calculated using Johansens's yield theory which is the basis for design of fasteners at normal temperatures.

Screws have many of the advantages of nails. In addition, they have much better gripping capacity than nails because of the threaded shaft, but some screws have poorer ductility under cyclic loading. The fire performance of screwed connections in wood has not been studied extensively, but it will generally be better than for nails.

Bolts and Dowels

Bolts and dowels are widely used in timber connections with excellent results. Dowel connections are similar to bolted connections, except that the dowels have no axial capacity. Connections with many small bolts or dowels are generally stronger than connections with a few large fasteners. Fire behaviour of bolt and dowel connections depends on the

Table 9.2 Fire resistance of unprotected connections with side members of wood

	Fire resistance (min)	Provisions ^a
Nails	15	$d \geq 2.8$ mm
Screws	15	$d \geq 3.5$ mm
Bolts	15	$t_1 \geq 45$ mm
Dowels	20	$t_1 \geq 45$ mm

^a d is the diameter of the fastener and t_1 is the thickness of the side member.

temperature of the fastener, so dowels can perform better than bolts because there is less surface area of steel exposed to the fire.

The theory of Norén (1996) developed for nails can also be applied to dowelled and bolted connections. Moss *et al.* (2010) calculated the connection strength at elevated temperatures using the temperature-based embedding strength determined from tests. Peng (2010) extended Norén's approach to calculate the temperature profile of bolted connections using finite element modelling, obtaining good agreement with experiments. Erchinger *et al.* (2010) further extended Norén's approach to multiple slotted steel-to-timber connections with dowels. A summary is provided by Östman *et al.* (2010). High fire resistance ratings can be achieved because the slotted-in steel plates are protected by the timber side members. Increasing the thickness of the timber side members improves fire performance.

Simplified calculation methods for the fire resistance of unprotected wood to wood double-shear connections, and double-shear connections using internal or external steel plates with either dowels or bolts as fasteners are proposed by Peng *et al.* (2010). These calculation methods are based on correlations using experimental results, accounting for the effects of wood side member thickness, fastener diameter and load ratio.

9.6.3.2 Eurocode 5

Eurocode 5 (CEN, 2004b) gives a simple table for fire resistance of unprotected connections with side members of wood, summarized in Table 9.2.

Eurocode 5 allows the fire resistances in Table 9.2 to be increased to 30 min by increasing the thickness or width of the wood side members, or by increasing the end and edge distances to the fasteners. Eurocode 5 also gives simplified rules for the load capacity of axially loaded screws in fire conditions.

9.6.3.3 Protected Connections

Steel fasteners can provide excellent fire resistance if they are sufficiently well protected from the fire. Protection can either be achieved by burying the metal fastener within the wood section, or by applying a layer of sheet material such as solid wood or gypsum plasterboard. For protected connections, Eurocode 5 provides a number of methods for calculating the fire resistance of connections with various types of fasteners and internal steel plates, for different types of protection.

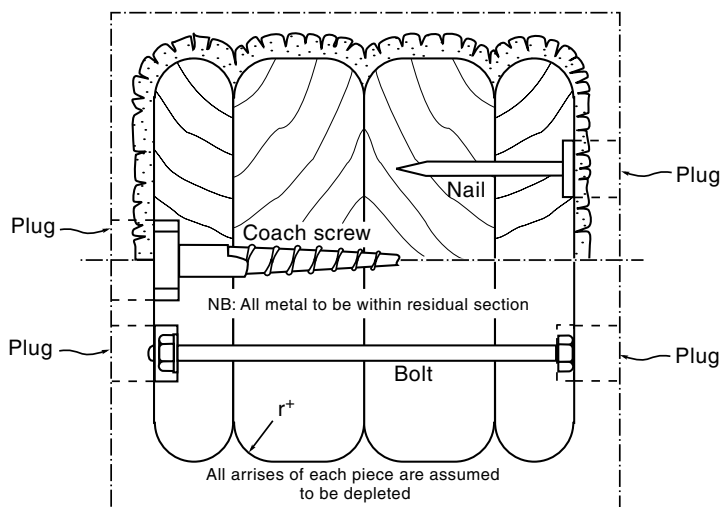


Figure 9.31 Protection of metal fasteners in BS 5268. Reproduced from BSI (1978). Permission to reproduce extract from BS 5268 is granted by BSI

A component additive method to calculate the fire resistance of timber connections loaded in tension, protected with protective membranes is given by Peng (2010). The additional fire resistance provided by membranes are 30 min for a single layer of 15.9 mm type X gypsum board, and 15 min for a double layer of 12.7 mm plywood. The results are close to the values for solid wood beams in tension reported by White (2009).

The British Standard and some American codes conservatively require that any metal connection be protected with sufficient wood for it to be within the residual uncharred section as shown in Figure 9.31 (BSI, 1978).

9.6.4 Connections with External Steel Plates

Eurocode 5 (CEN, 2004b) allows for the fire resistance of unprotected and protected external steel plates to be assessed in accordance with the requirements of Eurocode 3 for steel structures (CEN, 2005b), assuming that the steel surfaces in contact with wood are not exposed to fire.

9.6.4.1 Gusset Plates

Large nailed gusset connections have many nails passing through perforated steel or plywood plates, providing excellent structural behaviour but poor fire resistance because of the large surface area exposed to the fire. Buchanan and King (1991) showed that a layer of fire resistant gypsum plaster board can be used to increase the fire resistance of steel gusset connections beyond that of the connected members. Intumescent paint applied to the steel gusset plate provided only a small increase in fire resistance. Carling (1989) reports similar tests by Aarnio and Kallioniemi (1983) who achieved good fire resistance of steel gusset joints by protecting them with boxes made with glulam timber or particle board and mineral wool.

9.6.4.2 Truss Plates

Punched steel truss plates have a poor reputation for fire resistance because they have been associated with some premature failures of fire-exposed timber truss roof structures (Dunn, 1988). Figure 9.29 confirms this poor behaviour of unprotected truss plate connections. White and Cramer (1994) have investigated the fire performance of toothed truss plates, testing 38×89 mm timber members connected by a range of different plates, using the ASTM E-119 standard fire exposure, constant elevated temperatures of up to 300°C and also simulated plenum temperatures. In the E-119 tests, unprotected plates failed in less than 6 min, compared with almost 13 min for solid timber with no connection. Various combinations of protection increased the fire resistance by different amounts, the best being over 30 min when all four sides of the member were protected with 13 mm Type X gypsum plaster with taped edges.

In the tests simulating temperatures within the plenum space of a truss assembly protected by a fire resisting ceiling (reaching 327°C after 60 min) unprotected truss plates had a fire resistance rating just under 60 min, and various forms of protection increased this to over 100 min. Shrestha *et al.* (1995) have developed a model for predicting the stiffness of truss plates at elevated temperatures.

9.6.5 Glued Timber Connections

Many timber structures and timber members are connected with adhesives. When exposed to fire, glued wood members generally behave in the same way as solid wood provided that approved structural adhesives for load-bearing wood members are used, such as PRF, RF, MUF, UF, 1C-PUR, and EPI. Craft *et al.* (2008) conducted small-scale elevated temperature tests on polyurethane adhesives and found varying levels of performance at elevated temperatures, reinforcing the need for product standards to include elevated temperature performance requirements. All adhesives certified according to current EN standards and used for glulam beams show adequate fire performance (Klippel, 2014). Adhesives sensitive to elevated temperatures, such as elastomeric adhesives, should not be relied on in fire conditions.

9.6.5.1 Finger Joints

Nielsen and Olesen (1982) tested sawn timber in axial tension at four different temperatures, with and without finger joints. Their results, shown in Figure 9.32, indicate very similar strength for the two groups of material, except at 90°C where the finger-jointed material is significantly weaker than the unjointed material. Finger joints are used in most glulam members, so the strength of glulam beams and tension members depends on the strength of the finger joints, especially in the outer laminations.

Klippel (2014) describes experimental and analytical studies of fire-exposed glulam beams which show that the reduced cross-section method can be used safely for design, and the effects of fire on the finger joints can be ignored, provided that structural adhesives approved according to current EN standards are used and the finger joints are spaced well apart.

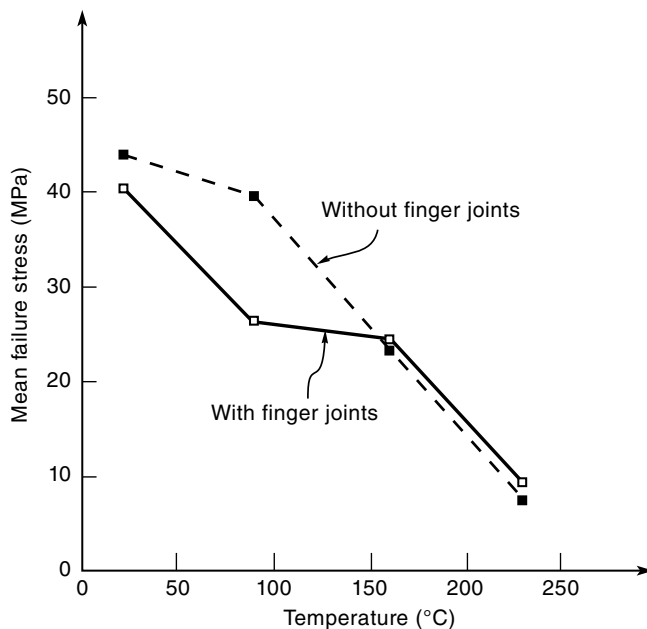


Figure 9.32 Effect of elevated temperature on strength of finger joints. Reproduced from Nielsen and Olesen (1982) by permission of Aalborg University

9.6.5.2 Epoxied Connections

Epoxied connections with glued-in steel rods have excellent performance under ambient temperature conditions. These can have poor fire resistance because of the rapid loss of strength of some epoxy adhesives at elevated temperatures. Buchanan and Barber (1994), Harris *et al.* (2004) and Gerard *et al.* (2010) carried out fire-exposed tension tests on steel rods epoxied into the end grain of glulam and LVL timber members. The fire resistance was limited because the epoxy adhesives started losing strength at 50 °C, and had very little strength at temperatures over 70 °C. Epoxied connections can only achieve good fire resistance if the epoxy itself is protected from elevated temperatures. This can be assisted by providing a large thickness of wood cover to the glued-in rods and ensuring that steel connecting brackets are not exposed directly to fire.

9.7 Worked Examples

9.7.1 Worked Example 9.1

Consider a softwood glulam beam, 130 mm wide by 720 mm deep, spanning 7.5 m with a dead load $G=4.0$ kN/m (including self-weight) and live load $Q=7.0$ kN/m. The beam is laterally restrained with timber decking nailed to the top edge. Check the design for normal conditions and for 60 min fire resistance rating, exposed to fire on three sides. Use the Eurocode 5 effective cross-section method with the charring rates from Table 9.1 and the factor $k_{20} = 1.15$.

The characteristic flexural strength is $f_b = 17.7$ MPa. The strength reduction factor is $\Phi = 0.8$ for normal design and $\Phi_f = 1.0$ for fire design. The duration-of-load factor is $k_d = 0.8$ for cold design and $k_d = 1.0$ for fire design.

Check design for normal conditions

Design load	$w_c = 1.2G + 1.5Q = 1.2 \times 4.0 + 1.5 \times 7.0 = 15.3$ kN/m
Bending moment	$M^* = w_c L^2 / 8 = 15.3 \times 7.5^2 / 8 = 108$ kNm
Section modulus	$Z = bd^2 / 6 = 130 \times 720^2 / 6 = 11.2 \times 10^6$ mm ³ $Z = bd^2 / 6$
Nominal strength	$M_n = k_d f_{0.05} Z = 0.8 \times 17.7 \times 11.2 \times 10^6 = 159$ kNm
Design strength	$\Phi M_n = 0.8 \times 159 = 127$ kNm
	$M^* \leq \Phi M_n$ so design is OK.

Loads for fire conditions

Design load	$w_f = 1.0G + 0.4Q = 1.0 \times 4.0 + 0.4 \times 7.0 = 6.8$ kN/m
Bending moment	$M_{fire}^* = w_f L^2 / 8 = 6.8 \times 7.5^2 / 8 = 47.8$ kNm

Method I (effective cross section, no corner rounding)

Rate of charring	$\beta_1 = 0.7$ mm/min
Depth of char	$c = \beta_1 t = 0.7 \times 60 = 42$ mm
Reduced breadth	$b_f = b - 2c = 130 - 2 \times 42 = 46$ mm
Reduced depth	$d_f = d - c = 720 - 42 = 678$ mm
Thickness of zero strength layer	$z = 7$ mm
Effective breadth	$b_e = b_f - 2z = 46 - 2 \times 7 = 32$ mm
Effective depth	$d_e = d_f - z = 678 - 7 = 671$ mm
Section modulus	$Z_f = b_e d_e^2 / 6 = 32 \times 671^2 / 6 = 2.40 \times 10^6$ mm ³
Flexural strength	$M_f = k_d f_f Z_f = k_d k_{20} f_{0.05} Z_f = 1.0 \times 1.15 \times 17.7 \times 2.4 \times 10^6 = 48.9$ km
	$M_{fire}^* \leq M_f$ so design is OK.

9.7.2 Worked Example 9.2

Repeat Worked Example 9.1 using the North American charring rate in the working stress design format.

The allowable stress under long duration loading in flexure is $f_a = 9.5$ MPa. The factor to convert allowable stress to mean failure stress is $k_{mean} = 2.85$.

Check design for normal conditions

Design load	$w = G + Q = 4.0 + 7.0 = 11.0$ kN/m
Bending moment	$M_w^* = wL^2 / 8 = 11.0 \times 7.5^2 / 8 = 77.3$ kNm
Section modulus	$Z = bd^2 / 6 = 130 \times 720^2 / 6 = 11.2 \times 10^6$ mm ³
Flexural stress	$f_b^* = M_w^* / Z = 77.3 \times 10^6 / 11.2 \times 10^6 = 6.91$ MPa
	$f_b^* \leq f_a$ so design is OK.

Fire design (North American char rate, no corner rounding)

Time of calculation	$t = 60$ min
Char rate	$\beta_n = 0.635$ mm/min

Depth of char	$c = 2.58\beta_n t^{0.813} = 2.58 \times 0.635 \times 60^{0.813} = 45.7 \text{ mm}$
Reduced breadth	$b_f = b - 2c = 130 - 2 \times 45.7 = 38.6 \text{ mm}$
Reduced depth	$d_f = d - c = 720 - 45.7 = 674 \text{ mm}$
Section modulus	$Z_f = b_f d_f^2 / 6 = 38.6 \times 674^2 / 6 = 2.92 \times 10^6 \text{ mm}^3$
Flexural stress	$f_{b,f}^* = M_w^* / Z_f = 77.3 \times 10^6 / 2.92 \times 10^6 = 26.4 \text{ MPa}$
Allowable stress	$f_{a,f} = k_{mean} f_a = 2.85 \times 9.5 = 27.1 \text{ MPa}$
	$f_{b,f}^* \leq f_{a,f}$ so the beam has 60 min fire resistance.

9.7.3 Worked Example 9.3

Calculate the time to failure for the beam in Worked Example 9.2 using the North American empirical design equation.

Design bending moment	$M^* = 77.3 \text{ kNm}$
Design strength	$M_n = f_b Z = 9.5 \times 11.2 \times 10^6 = 106 \text{ kNm}$
Load ratio	$Ra = M^* / M_n = 77.3 / 106 = 0.73$
z factor	$z = 0.7 + 0.3/Ra = 0.7 + 0.3/0.73 = 1.11$
Time to failure	$t_f = 0.1zb(4 - b/d) = 0.1 \times 1.11 \times 130(4 - 130/720) = 55.1 \text{ min}$

Time to failure is less than 60 min, so the beam does not have 60 min fire resistance.

9.7.4 Worked Example 9.4

A solid timber deck consists of 150 mm thick tongue-and-groove planks as shown in Figure 9.23. The tongues are 50 mm thick. The deck spans 5 m with a superimposed dead load of 1.25 kN/m² and live load $Q = 5.0 \text{ kN/m}^2$.

Use the Eurocode 5 effective cross-section method to calculate if the deck has a 90 min fire resistance rating. Check for integrity failure.

The characteristic flexural strength of the decking timber is $f_b = 25.0 \text{ MPa}$. The density of the wood is 5.0 kN/m^3 . The strength reduction factor is $\Phi = 0.8$ for normal design and $\Phi_f = 1.0$ for fire design. The duration of load factor is $k_d = 0.8$ for cold design and $k_d = 1.0$ for fire design. The factor k_j is 1.15 for fire design.

Check for normal conditions

Thickness of deck	$d = 150 \text{ mm}$
Self-weight of deck	$w_s = \rho d / 1000 = 5 \times 150 / 1000 = 0.75 \text{ kN/m}^2$
Total dead load	$G = 0.75 + 1.25 = 2.0 \text{ kN/m}^2$
Design load	$w_c = 1.2G + 1.5Q = 1.2 \times 2.0 + 1.5 \times 5.0 = 9.9 \text{ kN/m}^2$
Design a strip 1 m wide.	$w_c = 9.9 \times 1.0 = 9.9 \text{ kN/m}$
Uniformly distributed load	
Bending moment	$M^* = w_c L^2 / 8 = 9.9 \times 5^2 / 8 = 31 \text{ kNm}$
Section modulus	$Z = bd^2 / 6 = 1000 \times 150^2 / 6 = 3.75 \times 10^6 \text{ mm}^3$
Design strength	$M_n = \Phi k_1 f_b Z = 0.8 \times 0.8 \times 25 \times 3.75 \times 10^6 = 60 \text{ kNm}$
	$M^* \leq \Phi M_n$ so design is OK.

Eurocode 5 effective cross-section method

Design load	$w_f = 1.0G + 0.4Q = 1.0 \times 2.0 + 0.4 \times 5.0 = 4 \text{ kN/m}^2$
Design a strip 1 m wide.	
Breadth	$b = 1000 \text{ mm}$
Uniformly distributed load	$w_f = 4 \times 1.0 = 4 \text{ kN/m}$
Bending moment	$M_{fire}^* = w_f L^2 / 8 = 4 \times 5^2 / 8 = 12.5 \text{ kNm}$
Rate of charring	$\beta = 0.65 \text{ mm/min}$
Depth of char	$c = \beta t = 0.65 \times 90 = 58.5 \text{ mm}$
Reduced depth	$d_f = d - c = 150 - 58.5 = 91.5 \text{ mm}$
Effective depth	$d_e = d_f - z = 91.5 - 7 = 84.5 \text{ mm}$
Section modulus	$Z_f = b d_e^2 / 6 = 1000 \times 84.5^2 / 6 = 1.19 \times 10^6 \text{ mm}^3$
Flexural strength	$M_f = k_d f_f Z_f = k_d k_{20} f_{0.05} Z_f = 1.0 \times 1.15 \times 25.0 \times 1.19 \times 10^6$ $= 34.2 \text{ kNm}$
	$M_{fire}^* \leq M_f$ so design is OK.

Check for integrity failure

One-dimensional charring rate	$\beta_0 = 0.65 \text{ mm/min}$
Time to char through solid deck	$t_s = d / \beta_0 = 150 / 0.65 = 230 \text{ min}$
Time to char through 50 mm tongue	$t_s = 50 / 0.65 = 77 \text{ min}$
Some extra protection required in joints because	$77 \text{ min} < 90 \text{ min}$

10

Light Frame Construction

The objective of this chapter is to describe the fire behaviour of light frame construction using timber and steel components, and to review available design methods.

This chapter also describes fire performance of lightweight sandwich panel construction.

10.1 Summary of Light Frame Construction

Light timber frame construction ('wood frame construction' in North America) is widely used in low-rise buildings, up to four storeys or more, most often for residential occupancies. Walls and partitions are usually constructed with sawn timber studs. Floors consist of plywood or particle board sheathing nailed or screwed to joists which may be sawn timber or engineered products such as glulam, LVL, wood I-joists or parallel chord trusses. Figure 10.1 shows a perspective view of a single-storey timber framed house. Multi-storey construction uses similar components as shown in Figure 10.2. Typical timber floor construction is shown in Figure 10.3.

Light frame construction in this chapter also includes light steel framing, such as cold-rolled steel channel sections and light steel joists.

Because of the small size of timber and steel members used in this style of construction, fire resistance must be based on protective materials, by far the most common being gypsum board (often called 'drywall' or 'sheetrock' in North America). The gypsum board is used as wall and ceiling linings, where it provides a wearing surface, contributing to the acoustic, thermal and fire separation of the barrier. Other lining materials, used less often, include a variety of wood-based panel products, fibre cement panels, magnesium oxide and calcium silicate board. Gypsum board has superior fire resisting properties to most other similar

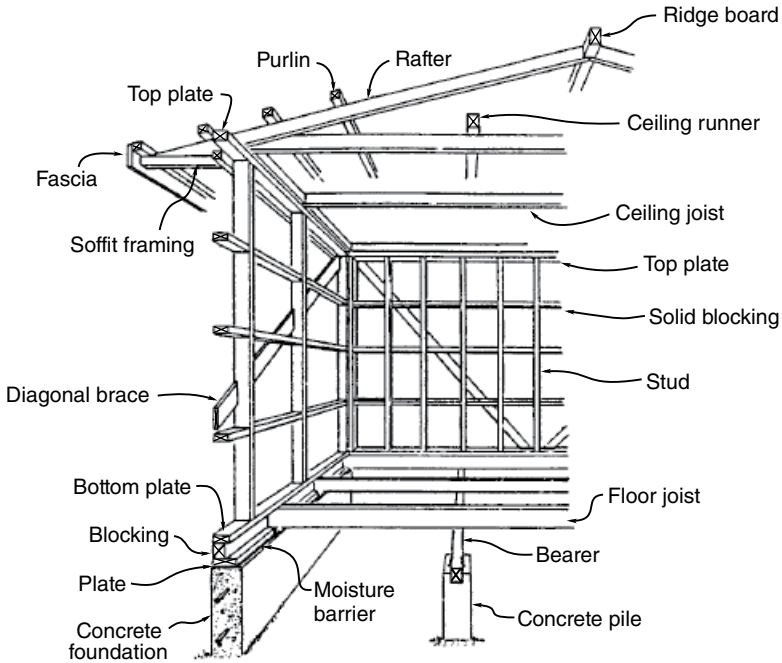


Figure 10.1 Typical light timber house framing

materials, because of the moisture in the gypsum crystals, described below. This chapter assumes the use of gypsum board as the lining material, but the same principles apply to other similar materials.

In most wall construction, the gypsum board is fixed directly to the studs using nails or screws. Elastomeric adhesives are used in some situations, but these should be ignored under fire conditions. Some wall and floor systems have the gypsum board lining spaced off the studs or joists with a thin steel resilient channel to improve acoustic performance. Insulating batts are often placed in the cavities to improve thermal and acoustic insulation. Other methods of improving acoustic performance are to use double stud walls or staggered stud walls where the wall lining material is only fixed to one side of each stud, to eliminate a direct path for transmission of sound.

Ceiling linings may be connected directly to the underside of the joists, but they are more often attached to timber ceiling battens or steel channels in order to give more tolerance for erection and better acoustic performance. Ceilings are sometimes suspended on a steel framing system, forming a ceiling cavity.

Light steel frame construction uses thin steel wall studs or floor joists manufactured by cold rolling a thin steel strip, 0.5–1.5 mm thick. Light steel frame construction is similar to light timber frame construction in that the lining is an essential part of the fire resistive construction, and the quality of the gypsum board and its fixings are most important. In addition to the typical stud wall construction shown in Figure 10.4, there are many other light steel frame systems for walls and floors. Wall designs include office partitions, elevator shafts, and exterior walls, some with multiple layers, insulated cavities and solid gypsum walls with no

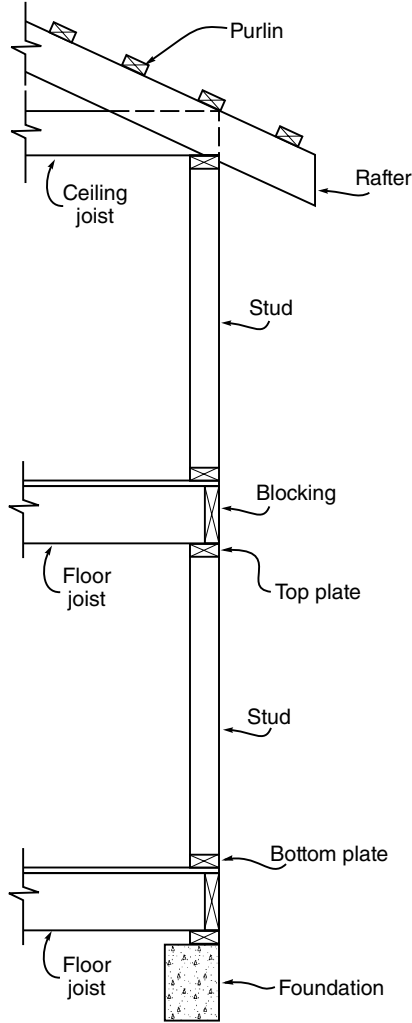


Figure 10.2 Multi-storey light timber frame construction

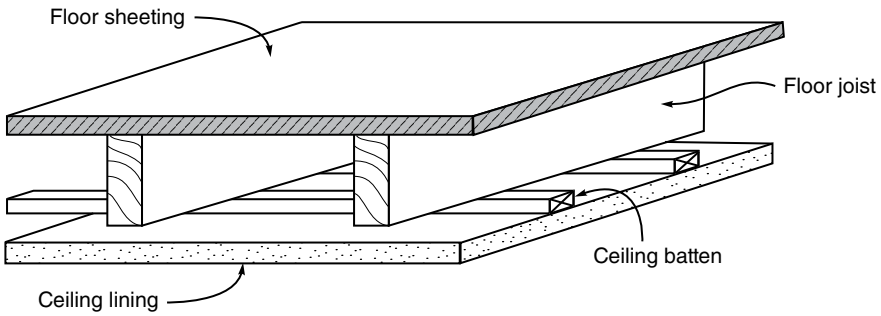


Figure 10.3 Light timber frame floor construction

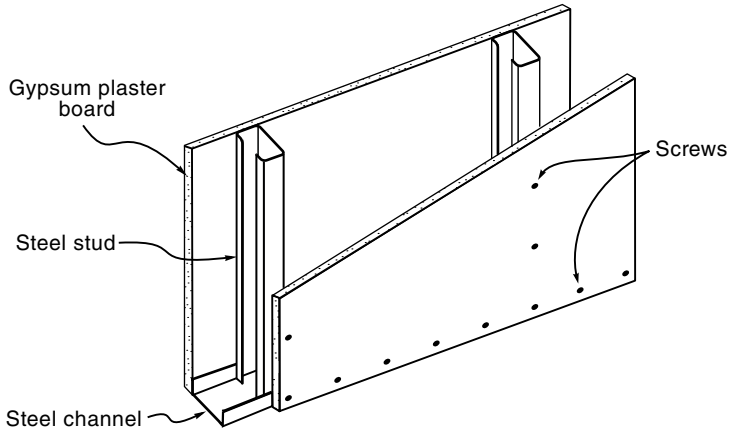


Figure 10.4 Light steel framed wall construction

cavities (Gypsum Association, 2012). A common type of floor construction in North America consists of a concrete slab on open-web steel joists, fire protected by a ceiling membrane of gypsum board or similar material. Open web steel joists are light trusses made from steel angles and rods as shown in Figure 10.8.

10.2 Gypsum Plaster Board

Gypsum plaster has been used as a construction material for many centuries. *Gypsum plaster-board* or *gypsum board* refers to rigid sheets made from gypsum plaster and other materials. Gypsum board is widely used for interior linings in domestic housing and commercial office buildings, and is the most common lining material used to provide light frame structures with fire resistance. In North America this is called *drywall* construction. Gypsum plaster can also be applied in a wet condition, trowelled over light wood or metal laths to make a smooth interior finish. Gypsum plaster often contains additives such as sand, perlite or vermiculite.

One of the most critical factors affecting fire performance of an assembly lined with gypsum board is the quality of the board itself. This aspect is often overlooked by designers who mistakenly assume that all gypsum boards are the same.

10.2.1 Manufacture

Gypsum is a crystalline mineral found in sedimentary rock formations in many parts of the world. Dehydrated gypsum is well known as ‘Plaster of Paris’, a white powder which sets hard after being mixed into a paste with water. The manufacturing process involves mining of the raw mineral, crushing and grinding it into a fine powder and heating to about 175 °C, driving off three-quarters of the chemically bound water in a process called calcining. To produce gypsum plaster, the calcined gypsum powder is mixed with water, some additives and an air-entraining agent, and the plaster sets hard in about 10 min. Typical gypsum board has a density between 550 kg/m³ and 800 kg/m³.

Most gypsum plaster boards consist of a sandwich of a gypsum core between two layers of paper, chemically and mechanically bonded to the core. Most gypsum boards are made with a thickness between 10 mm and 20 mm. The external paper provides tensile reinforcing to the board. Some boards, known as *fibrous plaster*, have no paper facing, relying on glass fibre or sisal reinforcing within the plaster to provide tensile strength.

Many countries have national standards for manufacture of gypsum board. In the United States, gypsum board is manufactured in accordance with ASTM C-36 (ASTM, 2005) which specifies dimensional tolerances, minimum flexural strength, hardness and nail-pull resistance under normal temperature conditions, as well as minimum fire resistance for Type X board. In New Zealand and Australia minimum manufacturing requirements are given in AS/NZS 2588:1998 Gypsum Plasterboard. It must be noted that these are minimum requirements and that most plasterboard in New Zealand and Australia is manufactured to higher standards in order to meet consumer expectations.

10.2.2 Types of Gypsum Board

Production and marketing of gypsum boards is different in various countries, but generally follows a similar pattern. There are three broad types of gypsum board, usually known as *Regular* board, *Type X* board, and *Special purpose* boards. All three categories are available in North America. Some parts of Europe and Asia have only the first two categories, and smaller market areas such as New Zealand and Australia only have regular board and special purpose boards.

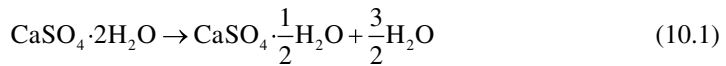
Regular gypsum board is a generic product sold very competitively for residential construction. Regular board is not required to have any fire resistance rating, so it usually has a low density gypsum core with no reinforcing (except the external paper faces). The low density results from air entrainment during manufacture. Regular gypsum board has poor performance in fire resistance tests compared with Type X or special purpose boards, because the board tends to crack and fall off the wall or ceiling when the face paper has burned away and the gypsum becomes dehydrated. Regular board has approved fire resistance ratings for certain assemblies, but the required thicknesses are greater than for the equivalent assemblies with improved boards.

The term *Type X* is used in North America for generic fire resistant gypsum board (similar to Type GF in Europe). Type X board is defined by performance rather than by a manufacturing specification. The definition of it is that Type X board is that it will give a 60 min load-bearing fire resistance rating when one layer of 15.9 mm board is fixed to each side of a wood or steel stud wall assembly (or a 45 min rating for 12.7 mm board). All type X boards contain some glass fibre reinforcing and may have other additives to improve fire performance.

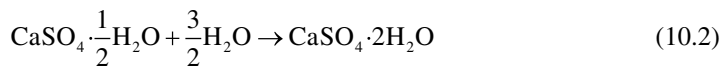
Special purpose boards are proprietary products made by many manufacturers, to obtain enhanced fire or structural performance over regular or Type X boards. Some are marketed as *Type C* in North America. Special purpose boards are often manufactured in non-standard thicknesses and formulations to meet special market needs for fire resistance or other performance. Special purpose boards usually have more glass fibres and more core additives than Type X boards. Industry listings (Gypsum Association, 2012) indicate that special purpose boards in the USA do not give significantly better fire ratings than generic Type X board, but some special purpose boards manufactured in other countries have better fire performance.

10.2.3 Chemistry

The chemistry of gypsum at its simplest level is described below. Solid gypsum plaster and gypsum rock is calcium sulphate dihydrate $\text{CaSO}_4 \cdot 2\text{H}_2\text{O}$ with two water molecules for each calcium sulphate molecule. The manufacturing process first involves driving the moisture out of the gypsum rock to create the powdery white material of calcium sulphate hemihydrate $\text{CaSO}_4 \cdot \frac{1}{2}\text{H}_2\text{O}$. The dehydration reaction (calcining) is an endothermic decomposition reaction which occurs between 100 °C and 120 °C:



When the powder is mixed with water and formed into flat sheets of gypsum plaster, the reaction is reversed to become a hydration reaction:



The resulting gypsum is 21% water by weight. Moisture in gypsum plaster is very important because it contributes to the excellent fire resisting behaviour. Gypsum plaster also contains about 3% free water, depending on the ambient temperature and relative humidity. When gypsum plaster is heated in a fire, the dehydration follows the reaction in Equation 10.1 as solid gypsum is converted back to a powdery form. Significant energy is required to evaporate the free water and make the chemical change which releases the water in the crystal structure. Complete dehydration occurs at temperatures between 200 °C and 300 °C, requiring additional energy input.

Gypsum plaster can be recycled relatively easily compared with other building materials, because the reactions in Equation 10.1 and Equation 10.2 can be repeated indefinitely.

10.2.4 Thermal Properties

Thermal properties of gypsum plaster are required if finite element thermal calculations are to be made. There is some scatter in published values, but most are similar to those shown below, based on tests of Canadian Type X gypsum board by Sultan (1996). Specific heat of gypsum plaster as a function of temperature is shown in Figure 10.5. The two peaks indicate chemical changes as moisture is driven off during heating, the first being the main reaction at about 100 °C described in Equation 10.1, which results in a delay in the temperature rise of protected wood or steel framing members.

Figure 10.6 shows the thermal conductivity of gypsum plaster as a function of temperature, with a drop at 100 °C and a steady rise after temperatures reach 400 °C. The value of thermal conductivity above about 400 °C will be affected by the presence of shrinkage cracks in the gypsum board, which will depend on the formulation of the individual board.

10.2.5 Fire Resistance

Because of the moisture related reactions described above, all gypsum board products exhibit similar behaviour in fires. When a board is heated from one side, temperatures on the exposed face will increase continuously until about 100 °C is reached, at which time there will be a

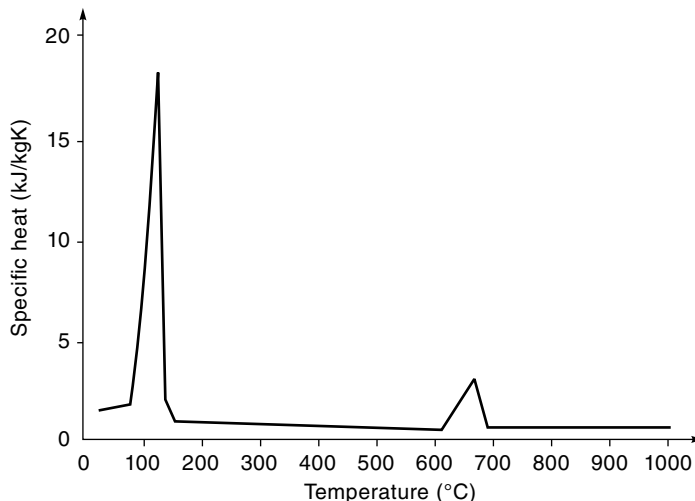


Figure 10.5 Specific heat of gypsum plaster (Sultan, 1996). Data obtained with permission from *Fire Technology*. © 1996 National Fire Protection Association, all rights reserved

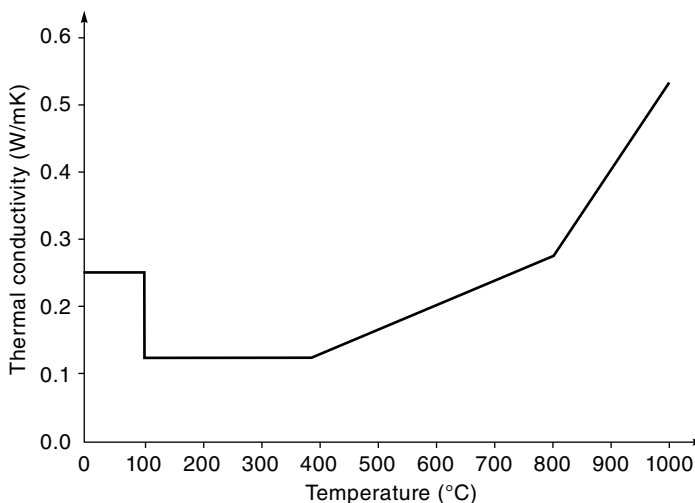


Figure 10.6 Thermal conductivity of gypsum plaster (Sultan, 1996). Data obtained with permission from *Fire Technology*. © 1996 National Fire Protection Association, all rights reserved

delay while the water of crystallization is driven off. As the heating continues, the 100°C temperature plateau will progress slowly through the board, until the entire board has been dehydrated. After dehydration the gypsum has almost no strength because it has been converted to a powdery form. Any residual strength depends on glass fibre reinforcing to hold the board together.

The fire resistance of assemblies made with gypsum based panel products depends on several important inter-related properties:

- The insulating capacity of the board, which protects internal structural members and delays temperature rise on unexposed surfaces.
- The ability of the board to remain in place and not disintegrate or fall off during or after dehydration.
- Resistance to excessive shrinkage which can cause cracking within the board or separation at joints between sheets.

Increased density will generally improve the fire performance of gypsum board, because it is a measure of the greater quantity of gypsum, resulting in fewer air voids. Increased density provides more heat absorbing capacity and requires more water of crystallization to be driven off during dehydration. Richardson and McPhee (1996) refer to tests where a 6% increase in density produced an 8% increase in fire resistance for otherwise identical construction.

Fire resisting gypsum boards contain glass fibres which control shrinkage, causing a maze of fine cracks rather than a single large crack which can initiate premature failure of regular board. One of the most critical aspects of fire resisting gypsum board is the extent to which the glass fibre reinforcing can hold the board together after the gypsum has dehydrated, to prevent the board pulling away from nailed or screwed connections when the board shrinks. Shrinkage can be reduced with various additives such as vermiculite.

Regular gypsum board can fall off a wall or ceiling as soon as the gypsum plaster has dehydrated, at about the same time as charring of the timber studs begins. The falling off of regular gypsum board is unpredictable because single large cracks can cause large sections to fall prematurely. Boards with glass fibre reinforcing and closely spaced fixings will not fall off until the glass fibres melt, when the entire board reaches a temperature of about 700 °C. König and Walleij (2000) report that the critical falling-off temperatures are 600 °C for ceiling linings and 800 °C for wall linings.

10.2.6 Ablation

In severe fires, it has been observed that the thickness of the gypsum board reduces slowly after dehydration has occurred. This is due to sloughing or ablation of the gypsum plaster after the glass fibres in the board melt at about 700 °C. Ablation is a minor effect, but should be included in finite element modelling, by increasing the thermal conductivity at high temperatures (Thomas, 1997) or allowing the geometry of the finite element grid to change at the fire-exposed face during the fire (Clancy, 1999).

10.2.7 Cavity Insulation

Light frame construction often contains cavity insulation, to improve thermal, acoustic and fire performance. Insulating batts have a mixed impact on fire performance, depending on the material. Loose fill insulation generally has poorer performance than batts.

The most common insulating materials are low density batts made from glass fibre or stone wool fibre. Less common materials include foam plastic sheets or batts made from cellulose

fibre or natural sheep's wool. Glass fibre (or glass wool) batts are made from thin glass fibres bonded into a mat with an organic binder. Stone wool (or rockwool or rock fibre) batts are made from mineral or ceramic fibres which do not melt at fire temperatures. The terminology is different in different countries; the European guidelines (Östman *et al.*, 2010) use 'mineral wool' to describe both glass wool and stone wool.

The major negative effect of all batts is that the gypsum board on the fire-exposed side heats up much faster than for an empty cavity, leading to earlier dehydration and possible falling off of the board. Richardson *et al.* (2000) observed that ceiling linings fell off timber joist floor assemblies 15 min earlier when the cavity was insulated.

If the fire-exposed board falls off any assembly containing glass fibre batts, the batts will rapidly melt leaving the studs or joists directly exposed to the fire. On the other hand, well-fitting mineral wool batts which remain in place will protect the studs, joists and unexposed lining from the fire. The batts must fit well and be tied in place because it has been observed by Sultan and Lougheed (1997) and König (1998) that loose fitting batts produce a worse result than no batts at all.

Insulation material that melts at relatively low temperature can have a small but often negligible negative effect on the fire resistance of light frame construction. Insulation material that retains its integrity at high temperature such as stone wool, rockwool or ceramic fibre, can have a significant beneficial effect provided that it is tightly fitted and remains in place.

10.3 Fire Behaviour

Light frame construction can have excellent fire behaviour, provided that it is well constructed from the correct materials. Experience in many fires has shown that gypsum board linings can prevent fire spread and protect the load-bearing light steel frame or light timber frame for the duration of a severe fire.

Fire resistance is assigned to complete assemblies of light frame construction, not to the individual components. The performance of the lining material exposed directly to the fire is most important because fire penetration into the cavity can result in premature fire spread or structural collapse of the barrier. Assemblies with no fire protection can fail in a few minutes (White *et al.*, 1984).

When gypsum board lining is heated during a fire, temperatures on the cavity side of the exposed face will increase steadily until about 100 °C is reached, at which time there will be a delay while the water of crystallization is driven off. As the heating continues, the 100 °C temperature plateau will progress slowly through the board, until the entire board has been dehydrated. Temperatures within the board will rise steadily after dehydration is completed, leading to increased temperatures in the cavity and in the framing members. The length of the 100 °C temperature plateau is a function of gypsum plasterboard thickness, density and quality.

Gypsum plaster has very low strength after dehydration because it is converted to a powdery form. Any residual strength depends on glass fibre reinforcing and other additives which hold the board together and prevent it from falling off the wall or ceiling. There is a wide range in performance between different types of gypsum boards. Fire resistance also depends on how much heat is transferred across the cavity and through the lining on the unexposed side.

As a fire progresses, timber framing will begin to char and steel framing will lose strength due to increased temperatures, but long periods of fire resistance can be achieved if the lining on the fire side remains in place. Critical factors are the thickness of the gypsum board, the quality of the board material and the details of the construction and the fixings.

10.3.1 Walls

In timber stud walls, the load capacity depends on the residual size, temperature and moisture content of the studs as charring occurs. Charring of studs will be greatest on the edge which is in contact with the fire-exposed lining, with lesser charring on the wide faces of the studs, depending on any insulation in the cavity. There is usually no charring on the edge fixed to the unexposed gypsum board. The strength of steel stud walls depends on the temperature of the studs and the level of lateral stability provided to the studs by the lining materials.

10.3.2 Floors

Timber joist floors exposed to fire behave similarly to walls. The critical factors are the thickness and integrity of the ceiling lining exposed to the fire. Fixings are very important because horizontal sheets of ceiling lining are more prone to falling off during a fire than vertical sheets of wall lining material. To achieve good fire performance, it is necessary to limit the rate of charring of the floor joists with good protection from the ceiling lining. Manufactured timber I-joists are more efficient than solid sawn timber joists under normal temperatures, but may not perform well in fire because of rapid strength loss due to charring of the thin webs. Steel joist floors behave similarly, except that strength loss is from elevated temperatures in the steel rather than loss of cross section.

Floors with parallel chord timber trusses behave similarly to floors with timber or steel joists, provided that the fire resisting ceiling remains in place. The strength and stiffness of the assembly also depends on the behaviour of the truss plate connections, which has been described in Chapter 9. Unprotected light wood trusses have very little fire resistance because of the vulnerability of truss plates exposed to fire conditions. Even if the truss plates are protected with sheets of gypsum board or similar, the small cross section timber members may fail after a short time of fire exposure.

10.3.3 Buildings

Several full-scale fire tests in real buildings have shown that light timber frame construction can be designed to provide excellent fire resistance. The most important factors in preventing fire spread are the use of high quality gypsum board and maintaining the integrity of all junctions, doors and penetrations. A full-scale six-storey building at the Cardington test facility in the UK was subjected to a post-flashover fire in one apartment (Lennon *et al.*, 2000). The fire was extinguished after 1 h of intense burning, and the building behaved as expected, with no fire spread or loss of load-carrying capacity. Important findings were that the standard of workmanship is of crucial importance in providing the necessary fire resistance, especially nailing of the gypsum board and correct installation of cavity barriers and fire-stopping.



Figure 10.7 Full-scale fire resistance test of a light timber frame wall

10.4 Fire Resistance Ratings

Fire resistance of light frame structures can be assessed using the same general principles as for other materials. A full-scale fire resistance test of a light timber frame wall is shown in Figure 10.7.

10.4.1 Failure Criteria

Fire resistance ratings are assigned to completed assemblies of light frame construction, and not to the individual components. For an assembly to be given a fire resistance rating, the relevant failure criteria must be met. All walls and floors are barriers which must meet the integrity and insulation criteria in order to provide a separating function, as described in Chapter 6. Floors and load-bearing walls must also meet the structural adequacy criterion for load-bearing capacity.

Assessment of integrity can only be done in full-scale tests because small-scale tests cannot assess factors such as shrinkage in large sheets of gypsum board or cracking due to structural deformations. Large-scale testing is also necessary to assess the resistance of the gypsum board to falling off walls or ceilings during fire.

10.4.2 Listings

Fire design of light frame assemblies is usually by direct reference to results of standard fire resistance tests or listed approvals based on such tests. Many full-scale fire resistance tests have been carried out on wall and floor assemblies. Listings of approved fire resistance ratings are produced and maintained by approval organizations (SNZ, 1991; NBCC, 2010), trade organizations (Gypsum Association, 2012), manufacturers (Winstone Wallboards, 2012) or testing and approval agencies (UL, 2012). Other countries and companies have similar listings. The listed fire resistance ratings are derived either directly from tests or from expert opinions based on successful tests. Manufacturers of gypsum board and other proprietary products may make their test results available on request.

10.4.3 Generic Ratings

Generic ratings, or ‘tabulated ratings’ are those which assign a time of fire resistance to materials with no reference to individual manufacturers or to detailed specifications. Many listed ratings in North America are generic ratings for non-proprietary products, such as regular gypsum board or Type X gypsum board manufactured by many companies.

10.4.4 Proprietary Ratings

Most manufacturers of gypsum board have proprietary fire resistance ratings for timber and steel framed assemblies containing their products. These fire resistance ratings usually include a specification of framing members, lining material and fixing methods, all of which must be followed if the assembly is to meet the intended rating. A typical specification for a proprietary rating is shown in Figure 10.8 (Winstone Wallboards, 2012).

Most designs will simply be a selection of an assembly from a list of proprietary ratings, comparing the listed rating with the prescribed fire resistance or an equivalent time of fire exposure. Calculations of thermal and structural behaviour in real fires are possible, but difficult, so they are only recommended for research and development purposes. Interpolation between listed ratings is possible, with an expert opinion required for significant changes from the listed assembly.

10.4.5 Typical Fire Resistance Ratings

Gypsum board on its own does not have a fire resistance rating. A fire resistance rating is assigned to a building system such as a wall or a floor which is an assembly of products including the protective board.

A summary of typical ratings for light frame walls and floors is shown in Table 10.1, giving the minimum thickness of gypsum board required to achieve various fire resistance ratings for assemblies with uninsulated cavities. This applies to symmetrical walls with gypsum board fixed to each face of the studs, and wood-panel floors with gypsum board ceiling fixed to the underside of the joists.

As expected, Table 10.1 shows increasing fire resistance with increasing thickness of gypsum board lining, and thicker lining required for load-bearing ratings. Thicknesses of

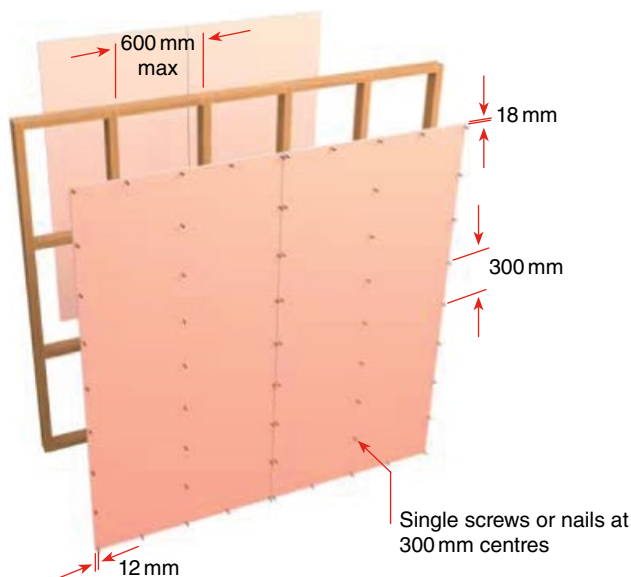


Figure 10.8 Specification for light timber frame proprietary rating. Reproduced from Winstone Wallboards (2012) by permission of Winstone Wallboards Ltd

19 mm or less are in a single layer of board, and larger thicknesses are the sum of two or more layers, with staggered joints between the layers.

This indicative table is not intended for design. Each listing has specific requirements for stud spacing, blocking between studs, type of board and fixings, none of which are shown in the table. The complete listing and specifications must be consulted for design purposes.

Some anomalies in Table 10.1 require discussion. The New Zealand figures are similar to those in Australia. The North American ratings are similar in parts of Europe. It can be seen that thinner boards can generally be used in New Zealand rather than in North America, which results from several factors. All of the New Zealand listings are proprietary ratings using special purpose GIB Fyrelite® board. All the North American listings are generic listings for Type X board, except for the 180 and 240 min ratings which are for special purpose Type C boards. For timber stud walls, fire tests in New Zealand were conducted with solid blocking between the studs to provide lateral stability and to protect the joints between the sheets, but such blocking is not required in North America. There are also some important differences between the standard fire resistance tests in the two regions, as described in Chapter 4.

10.4.6 Fire Severity

Because the fire resistance of most light frame structures is based on generic or proprietary ratings, the fire severity must be assessed in terms of standard fire exposure. This will either be the required fire resistance rating from a code or the equivalent fire severity for realistic fire burnout of the compartment, calculated as described in Chapter 4. Time equivalent formulae were not developed explicitly for light frame construction, but they can be used for this purpose.

Table 10.1 Minimum gypsum board thickness (mm) to give fire resistance ratings for cavity walls and floors

Fire resistance rating (min)	New Zealand				North America				
	Wood		Steel		Wood		Steel		
	Non-load bearing	Load bearing							
Walls	30	10.0	10.0	13.0	16.0				
	45					(12.7)	(12.7)		
	60	13.0	13.0	13.0	19.0	15.9	15.9	15.9	
	90	16.0	16.0	16.0	29.0	(25.4)	(25.4)	(25.4)	
	120	19.0	32.0	19.0		31.8	31.8	25.4	31.8
	180	32.0						38.1	
Floors	240			76.0				50.8	
	30		13.0						
	60		16.0				12.7		25.4
	90		32.0				31.8		
	120		38.0		38.0				

North American listings are from Gypsum Association (2012) except (12.7) from UL (2012) and (25.4) from NBCC (2010). The New Zealand listings are for GIB Fyrelite® board, from Winstone Wallboards (2012).

For timber structures, design to resist a complete burnout of a compartment is not as simple as with non-combustible materials, because charring of the wood may continue even after the fire is out (König, 1998) unless the timber is specially protected to prevent charring. To prevent collapse if charring occurs, the Fire Service or the owners must intervene to remove damaged linings and extinguish any charring after the fire has burned itself out. This is a requirement in some countries, including Norway, where regulations require that multi-storey timber buildings be designed for a complete burnout with no intervention from the Fire Service.

10.5 Design for Separating Function

For an assembly to be given a fire resistance rating, the relevant failure criteria must be met. All walls and floors are barriers which must meet the integrity and insulation criteria in order to provide a separating function, as described in Chapter 6.

10.5.1 Temperatures Within Light Frame Assemblies

Typical temperature profiles in an uninsulated wall during an ISO 834 standard fire resistance test are shown in Figure 10.9. The temperature on the cavity side of the fire-exposed gypsum board has a long plateau at 100 °C as the free water and water of crystallization are driven off and heat is conducted through the board. During this time, the temperature on the cavity side

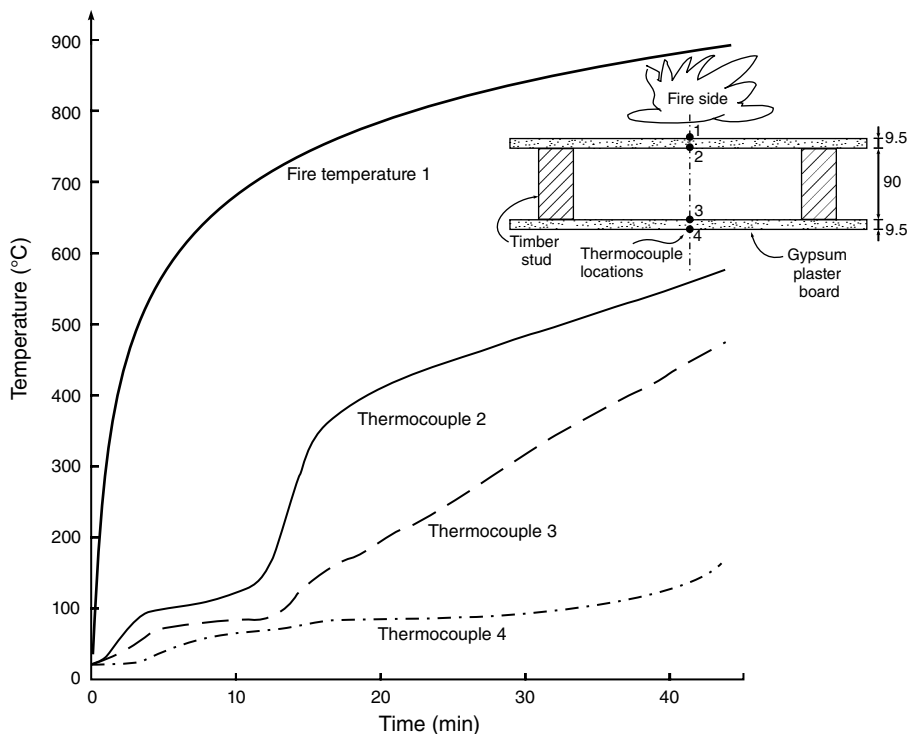


Figure 10.9 Temperature profiles within a cavity wall during a standard fire resistance test (Thomas, 1997)

of the unexposed gypsum board has a plateau at a slightly lower temperature, and the temperature on the unexposed face lags much further behind. For a steel stud wall, the gypsum temperatures would be identical, with the temperature of the steel stud being between the temperatures shown for points 2 and 3.

10.5.2 Insulation

The insulation criterion for fire resistance requires that the temperature on the unexposed face remains below a certain critical temperature, so there is no danger of ignition on the unexposed surface and subsequent fire growth. Using the ISO 834 criteria, the assembly is considered to have failed the test when the average temperature rise on the unexposed surface exceeds 140 °C, or the maximum temperature rise at any point exceeds 180 °C.

The insulating properties of an assembly depend on the geometrical arrangement and the component materials. For assemblies without insulating batts, the highest temperatures on the unexposed face occur remote from the studs or joists. Heat transfer in this region is essentially one-dimensional, with heat from the fire passing through the exposed sheet, across the cavity and through the unexposed sheet. The stud material (steel or timber) has no influence on these temperatures, and the distance across the empty cavity (the depth of the studs) is not very

significant. Heat transfer across the cavity is by both convection and radiation, with the radiative component increasing as the temperatures increases. Moisture movement may also contribute to heat transfer through the assembly, because moisture continually evaporates in hot regions and condenses on cool surfaces.

For assemblies with insulating batts in the cavities, the overall thickness of the wall becomes more important, and the highest temperatures may occur near the studs, especially if they are steel.

10.5.3 Component Additive Methods

Although fire resistance ratings are assigned to completed assemblies of light frame construction, and not to the individual components, some organizations permit fire resistance ratings for the separating function (insulation and integrity) to be estimated by adding up a contribution from each of the main components. These are crude methods which must be used with caution. The Canadian code (NBCC, 2010) gives an additive method which has been adopted by some US codes. Typical values shown in Table 10.2 where a time of fire resistance has been assigned separately to the lining material on the fire side, the studs and the insulation in the cavity. The lining on the unexposed face is not included in the calculation.

As an example using Table 10.2, an assembly with 15.9 mm Type X gypsum board on each face of wood studs at 400 mm centres with rock fibre (stone wool) batts would be assigned a fire resistance rating of $40 + 20 + 15 = 75$ min.

Other additive methods include the Swedish method described by Östman *et al.* (1994) and the UK method described in BS 5268, Section 4.2 (BSI, 1990). Annex E of Eurocode 5 Part 1.2 (CEN, 2004b) provides an additive method for assessing the separating function of wall and floor assemblies with one or two layers of lining materials, considering all the possible paths for heat transfer, as shown in Figure 10.10. The fire resistance is assessed by considering the effect of each layer separately using a position coefficient and a joint coefficient for different lining materials, insulating materials and joints between panels.

Table 10.2 Component additive method in the Canadian code

Description	Assigned time (min)
Gypsum board	
12.7 mm Type X gypsum board	25
15.9 mm Type X gypsum board	40
Wood frame	
Wood studs at 400 mm centres	20
Wood studs at 600 mm centres	15
Wood joists at 400 mm centres	10
Wood trusses at 600 mm centres	5
Insulation	
Rock fibre batts	15
Glass fibre batts	5

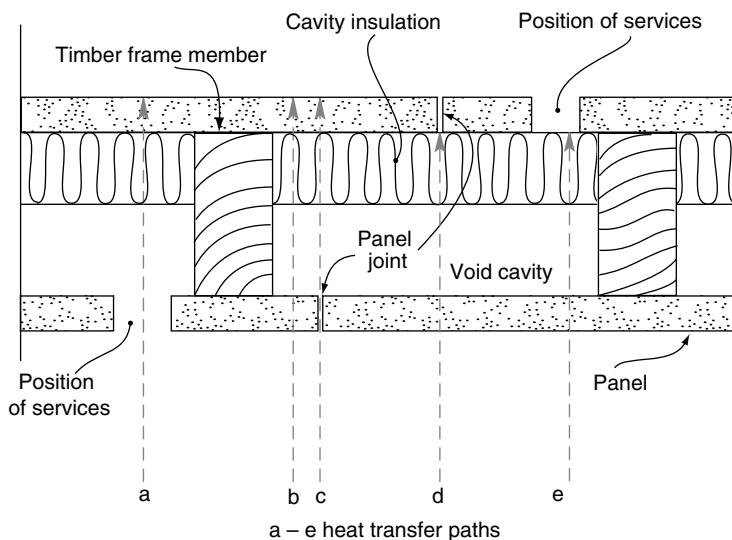


Figure 10.10 Heat transfer paths through separating multiple-layered construction. Reproduced from CEN (2004b). © CEN, reproduced with permission

More recently an improved Swiss method has been summarized by Östman *et al.* (2010) with worked examples. The new method considers timber framed assemblies with an unlimited number of lining layers made of gypsum plasterboard or wood panels, with or without cavity insulation, based on extensive finite element calculations backed up by experimental testing. It is an extension of the Eurocode 5 method with position coefficients and joint coefficients for different layups of various lining materials.

10.5.4 Finite Element Calculations

Calculations of thermal behaviour can provide an assessment as to whether an assembly would meet the insulation criterion when exposed to a standard fire resistance test or a simulated real fire. Thermal calculations are not simple because the thermal properties of gypsum and wood are highly temperature dependent, and because assumptions have to be made about heat transfer coefficients on the exterior surfaces and within the cavity.

A two-dimensional finite element model is appropriate in most cases, using the thermal properties of gypsum plaster given above, and the thermal properties of wood from Chapter 9. Thermal properties of mineral wool insulation are given by König and Walleij (2000) with thermal conductivity of 0.03 W/mK at 20 °C, rising to 0.12 W/mK at 400 °C and 0.45 W/mK at 800 °C, and the specific heat has a constant value of 1.0 kJ/kgK.

For timber members, the transition from wood to char at 300 °C not only effects changes in thermal properties, but also results in a shrinkage gap between the timber framing and the lining on the fire side of the assembly. It is necessary to include this gap in any finite element modelling to get good results. Another significant influence is moisture which evaporates at about 100 °C, travels through the wood, the gypsum and the cavity, and condenses on cooler

surfaces. Most finite element modelling does not allow for this explicitly, but the effects are considered to be included implicitly in the thermal properties.

Thomas (1997) used the TASEF finite element package to get excellent agreement with New Zealand test results for light timber frame walls. König and Walleij (2000) obtained similar results using TEMPCALC. Other computer models for predicting thermal behaviour are those by Collier (1996), Takeda and Mehaffey (1998) and Clancy (1999). Sultan (1996) and Cooper (1997) have developed heat transfer models for light steel framed walls.

10.6 Design for Load-bearing Capacity

This section describes structural design of light frame construction in fire conditions, with particular reference to the standard fire resistance test. The stability criterion, applied to all load-bearing elements, requires that load capacity be maintained throughout the duration of the design fire.

The strength of light frame assemblies is mainly in the timber or steel members themselves and not the lining materials. Lining materials are essential for providing lateral stability to the structural members, but their contribution to overall strength and stiffness is small. For load-bearing timber stud walls, Young (2000) has shown that the lining material on the cold side of the wall increases the flexural stiffness of the wall, hence increasing the resistance to buckling failure during a fire test.

10.6.1 Verification Methods

The design process for fire resistance requires verification that the provided fire resistance exceeds the design fire severity. Using the terminology from Chapter 4, verification may be in the *time domain*, the *temperature domain* or the *strength domain*.

The temperature domain is not used for timber structures because there is no critical temperature for fire-exposed timber, but it could be used for light steel framing members. Most often, verification of fire resistance of light frame structures is in the time domain, where proprietary ratings are compared with the code-specified fire resistance, or with the calculated equivalent time of a complete burnout.

10.6.2 Calculation Methods

Most designs will simply be a selection of an assembly from a list of proprietary ratings, comparing the listed rating with the prescribed fire resistance or an equivalent time of fire exposure. Calculations of structural behaviour are possible, but difficult as described below, so they are only recommended for research and development purposes.

10.6.3 Onset of Char Method

As an alternative conservative approach, some approval organizations permit protected timber assemblies to be assigned a fire resistance rating if it can be shown that the protected wood will not begin to char during the entire time of fire exposure (SNZ, 1991). Some listings

published by UL (2012) include a ‘finish rating’ for sheet materials fixed to timber studs, defined as the time at which the wood surface closest to the fire reaches an average temperature rise of 121 °C or an individual temperature rise of 163 °C. These temperatures are lower than the usually accepted charring temperature of 250–300 °C, so the ‘finish ratings’ are very conservative estimates of initiation of damage to protected wood members. Most Type X gypsum boards have finish ratings of 15 min for 12.7 mm board and 20 min for 15.9 mm board (UL, 2012).

Design to prevent the onset of char in protected timber members is a conservative approach which may have several applications if used with a realistic assessment of the expected fire severity. No charring during a complete burnout of the fire compartment will ensure that the timber structure will remain standing. It will also allow repair of the timber structure after a severe fire without having to replace charred wood. This may be appropriate for buildings containing very valuable items or essential services.

10.6.4 Fire Test Performance

Much can be learned about the fire behaviour of light timber and steel stud walls from observations in standard fire resistance tests. Behaviour in real fires will always be different from behaviour in standard tests because of different conditions including fire exposure, support conditions and loading arrangements. In standard furnace tests, load-bearing light timber framed walls almost always deform away from the furnace as shown in Figure 10.11 and fail

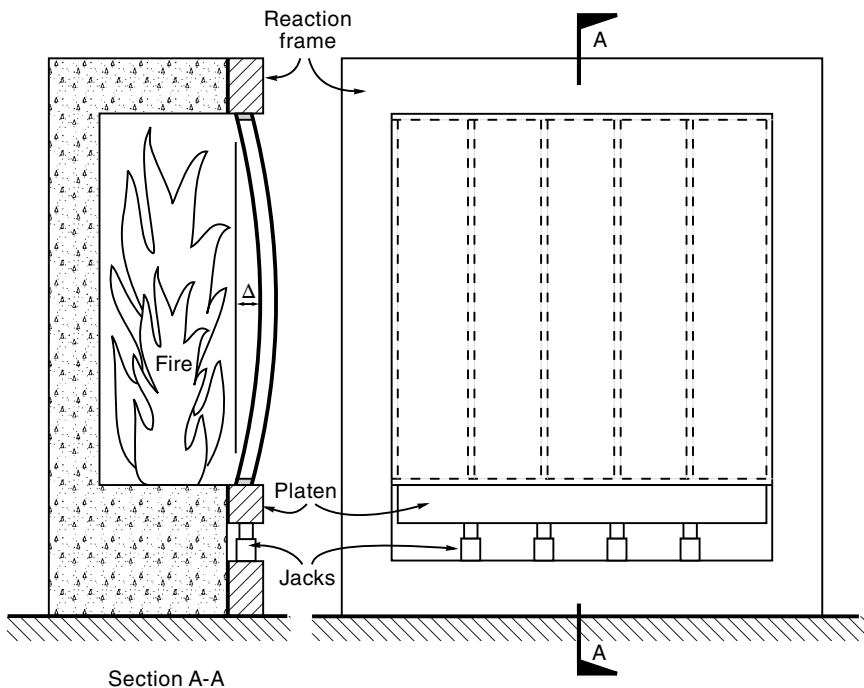


Figure 10.11 Fire resistance test of a light timber frame wall

by buckling in that direction. There may be a small movement towards the furnace in the early stages of the test caused by thermal expansion of the gypsum board on the furnace side, but this will be reversed as shrinkage occurs. After the stud starts to char, the centre of resistance moves towards the cool side of the wall, resulting in an eccentricity which causes the wall to deflect away from the fire. Any deflection results in an additional bending moment due to $P-\Delta$ effects. On the other hand, light steel frame walls bow in towards the furnace due to differential thermal expansion of the steel studs.

In a standard fire resistance test, it is essential to ensure that all the typical studs or joists have similar loads, and that the studs or joists at the sides of the furnace do not carry any load, because they are partially protected from the furnace temperatures. A difficulty of comparing fire resistance tests from different furnaces is that the exact method of applying load is not specified and it is seldom reported.

Because full-scale fire resistance tests are very expensive, it is often necessary to extrapolate from a listed rating to achieve a fire resistance rating for a wall with different height or different load from that tested. A few furnaces can test walls 4 m high, but most full-scale fire resistance wall furnaces are only 3 m high, which limits the height of a test specimen. Calculation methods are necessary to extrapolate to taller walls. Collier (1991a) provides a method based on New Zealand test results, applying the secant formula for column buckling to the residual studs.

10.6.5 Timber Stud Walls

The load capacity of the wall depends on the size, temperature and moisture content of the residual cross section of the timber studs. As described by Östman *et al.* (2010), there is a hierarchy of the contribution of various components to the fire resistance, with the greatest contribution coming from the layer closest to the fire, supported by well-fitting cavity insulation which can protect the sides of the studs after lining layers fall off.

In load-bearing timber walls it is essential to retain sufficient area of residual stud to carry the applied loads (Figure 10.12). In non-load-bearing walls, the studs only need to hold the lining material in place for the duration of the fire, so they may be almost completely burned away by the end of a fire test. It is not possible to re-use a wall after a severe fire if significant charring has occurred, even though the wall may have provided the fire resistance as expected.

10.6.6 Calculation of Structural Performance

For light timber frame walls, calculation of structural fire performance requires an assessment of the strength of the residual studs after a period of fire exposure.

Charring of the wood begins when its temperature reaches about 300 °C. Typical shapes of the charred profile are shown in Figure 10.13 for timber studs in walls with and without cavity insulation. For uninsulated walls, the charring rate on the wide surface facing into the cavity is about half of that on the edge on the fire-exposed side. There is no charring on the edge of the stud fixed to the unexposed gypsum board.

A simple design method for timber studs in various types of wall, with and without insulation, is given by Östman *et al.* (2010) with detailed calculation methods and worked examples,



Figure 10.12 Residual charred studs of a light timber frame wall after a full-scale fire resistance test

based on the extensive experimental and analytical research of König and Walleij (2000). The method is conceptually simple, with the following steps:

1. Estimate the time to onset of char of the timber studs.
2. Estimate the rate of char.
3. Calculate the char depth, hence the size of the fire-reduced cross section after a particular time of fire exposure.
4. Estimate the strength and stiffness of the heated wood in the residual cross section.
5. Calculate the load capacity.

The time to onset of char in the stud is estimated from the thickness and density of the gypsum board on the fire side of the wall. The rate of charring on the face of the stud in contact with the gypsum board is calculated as described above. The residual stud can be approximated as a rectangular cross section as shown in Figure 10.14, for walls with or without insulation in the cavity. In walls with glass fibre insulation, the timber studs will have a charred shape intermediate between the two shapes in Figure 10.14 (Östman *et al.*, 2010). Mechanical properties of the residual cross section are calculated from a simple empirical expression.

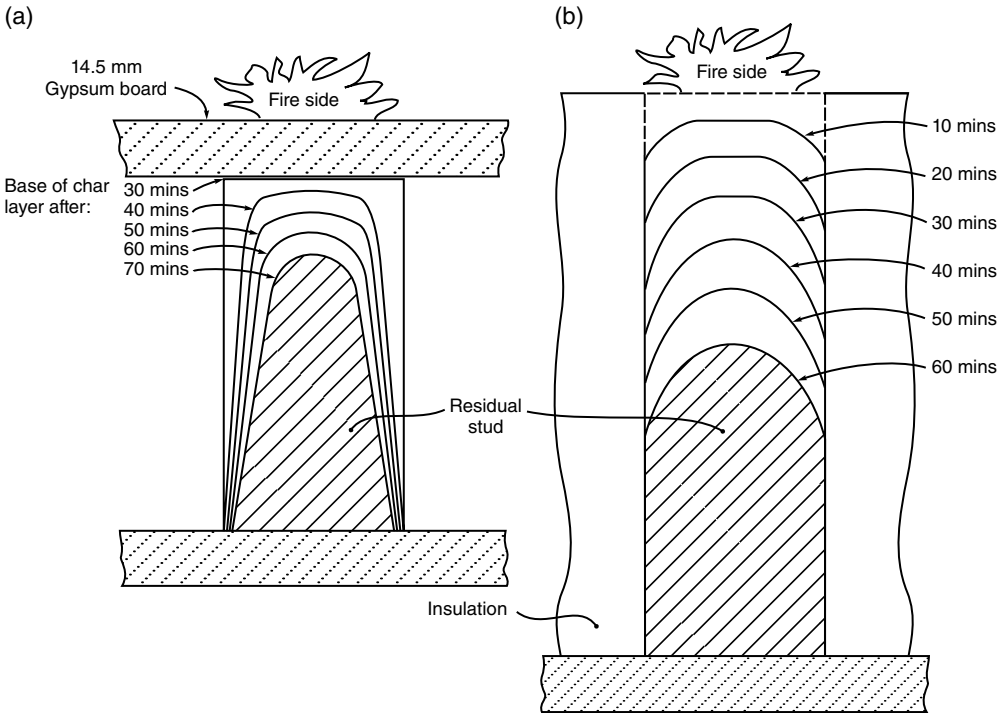


Figure 10.13 Measured char profiles on timber studs. (a) Stud in empty cavity, protected with 14.5 mm gypsum board. Reproduced from Collier (1991b) by permission of Building Research Association of New Zealand. (b) Stud in insulated cavity with no protection on the fire-exposed face. Reproduced from König and Walleij (2000) by permission of AB Trätek

The structural calculation uses the residual cross section with a conventional formula for timber column design, assuming that the stud is restrained against weak axis buckling by the gypsum board on the cooler face of the wall.

10.6.7 Buckling of Studs

When timber stud walls experience a structural failure in a fire resistance test, the failure is caused by buckling of the studs about the strong axis, usually outwards from the furnace. Buckling about the weak axis is prevented by the gypsum board on the cool unexposed face of the wall. The gypsum board on the hot exposed face provides very little lateral restraint after it has dehydrated. The cooler gypsum board providing lateral restraint is on the tension edge of the studs, which requires the residual stud to have some torsional rigidity, which will reduce as charring occurs. The provision of torsional restraint to studs becomes more important as the depth to width ratio of the stud cross section increases. Torsional restraint of the studs can be enhanced by the use of solid timber blocking between the studs. In New Zealand, all of the approvals listed by Winstone Wallboards (2012) have

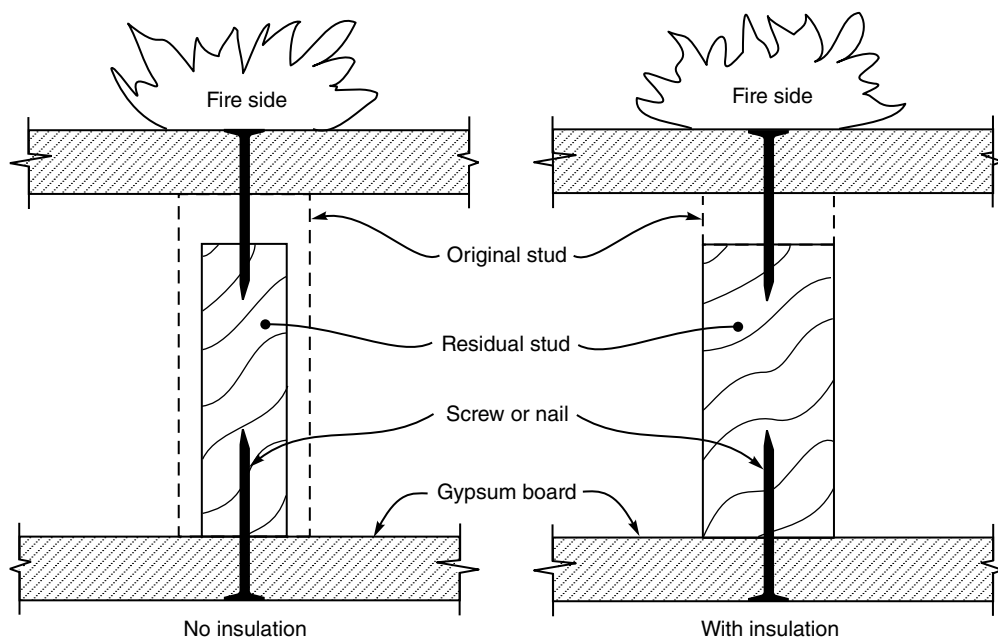


Figure 10.14 Notional residual stud in a light timber wall after fire exposure

solid timber blocking (also known as dwangs or noggins) at 1200 mm spacing between all the studs. Collier (1991b) demonstrated the effectiveness of such blocking by testing walls with and without blocking.

Blocking between the studs is not normally used in North America, which may partly explain the poorer fire performance of some North American assemblies compared with those in New Zealand. Thin steel resilient channel fixed to the exposed edge of the studs to improve acoustic performance may provide some torsional rigidity. Blocking between studs and provision of lateral restraint is more difficult for walls where the studs are staggered for acoustic performance.

Because failures occur by buckling under axial loads, the load capacity depends more on the modulus of elasticity of the stud parallel to the grain than on the compression strength of the wood.

10.6.8 End Restraint

The top and bottom end restraint of the studs can have a significant effect on the fire resistance. Most computer models assume a pinned connection top and bottom, but this is not always realistic. Figure 10.15 shows the top plate connection before and during a fire test. As the test proceeds, the stud chars and the ends of the stud rotate, causing deformations in the top and bottom plates and causing the line of application of the load to shift away from the fire. The bending moment in the stud increases due to $P-\Delta$ effects.

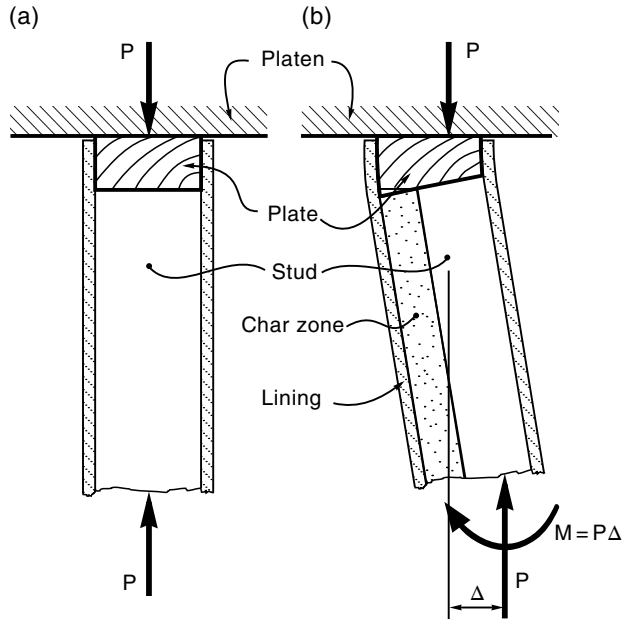


Figure 10.15 Detail of top end of timber stud (a) before and (b) during a fire test

10.6.9 Steam Softening

Structural failure of timber stud walls in fire is usually a result of reduced stud size and stiffness due to charring. In some cases, failure may occur before charring begins. For example, Young and Clancy (1996) tested load-bearing wall assemblies in which the ends of the studs were fitted with pinned connections allowing free rotation. The studs buckled and the wall failed to carry the applied load after only 35 min in two identical tests. When dismantled, the studs were found to have only minor charring, but they were permanently bent as a result of steam softening of the wood. The same wall design with the ends of the studs cut square and butted to the top and bottom plates achieved a fire resistance of almost 60 min. The difference is that the rotational stability of the square-end studs provides enough time for the wood in the studs to pass through the plastic stage without buckling, at which time the wood properties increased due to drying, and eventual failure was a result of charring.

10.6.10 Finite Element Calculation Methods

Several finite element calculation methods for assessing the fire resistance of light timber frame construction have been developed in recent years, but these are for research rather than for design purposes because they are much more complicated than simple selection of a proprietary system from a listing of fire ratings. Calculation of structural behaviour is more difficult than calculation of thermal behaviour because of the poor knowledge of mechanical properties of wood at elevated temperatures and changing moisture content. Computational models for walls must include three-dimensional second-order effects in order to predict buckling.

Thomas (1997) used the ABAQUS finite element package to get good agreement with test results for timber stud walls, assuming that all the load was carried by the studs without composite action. Clancy (1999) used the structural model of Young (2000) to do a probabilistic study of timber stud walls exposed to fires, finding that the time to failure of typical walls has a coefficient of variation of about 12%. Young's model includes the effect of composite action between the studs and the gypsum board, allowing for partial slippage in the connectors, but he recommends that full fixity be assumed for design.

10.7 Steel Stud Walls

Steel stud walls have similar fire performance to timber stud walls in many ways, but there are some important differences. In standard fire resistance tests, timber frame walls bow outwards from the furnace due to loss of charred cross section, but light steel frame walls bow in towards the furnace due to differential thermal expansion of the steel studs (Figure 10.16). Bowing inwards helps to improve the load-bearing capacity of steel studs during fire because the compression edge of the stud (rather than the tension edge) is laterally restrained by the plasterboard on the cold side of the wall. Canadian tests of load-bearing steel stud walls (Kodur *et al.*, 1999) showed bowing towards the furnace as expected, but the final sudden failure was away from the furnace after local buckling of the flange on the hot side of the stud. This buckling occurred near the top or bottom of the wall where the compression force in the hot flange was greater than at mid-height, due to the deflected shape of the wall.

Some steel stud walls have horizontal blocking between the studs, which will improve fire resistance by providing lateral stability. This is important because thin steel channel section studs have no torsional rigidity. Essential lateral restraint is provided by the gypsum board on the cold side of the wall so the lateral restraint will decrease after this board loses strength due to dehydration and melting of the glass fibres. Gerlich *et al.* (1996) suggest that at least 3 mm of the board should remain below 100 °C for this reason.

A review of the fire resistance of load-bearing steel stud walls protected with gypsum board has been published by Alfawakhiri and Sultan (1999) and a large experimental programme on such walls is described by Klippstein (1980).

10.7.1 Design of Steel Stud Walls

Once again, most designs will simply be a selection of an assembly from a list of proprietary ratings, comparing the listed rating with the prescribed fire resistance or an equivalent time of fire exposure.

Detailed calculation of structural behaviour is more difficult than calculation of thermal behaviour. Computational models for walls must include second-order effects in order to predict overall buckling, and models for steel stud walls must additionally be able to predict local buckling of thin steel sections restrained by degrading lining materials.

Gerlich *et al.* (1996) describe test results and simple calculation methods, showing how the normal temperature design equations can be modified to calculate the axial load capacity under fire conditions if the temperature of the steel studs is known. They used the TASEF program for calculating the temperatures in the steel, and modified the design equations of



Figure 10.16 Full-scale fire resistance test of a light steel frame wall. The wall has deflected inwards towards the furnace due to thermal bowing

AISI (1991) for calculating load capacity at elevated temperatures. This method can be used for standard or realistic fire exposure.

For load-bearing steel structures, a simple design approach is to make a thermal calculation and ensure that the maximum temperature of the steel does not exceed a limiting temperature of 350 or 400°C. In this case the normal temperature design methods can be used for fire

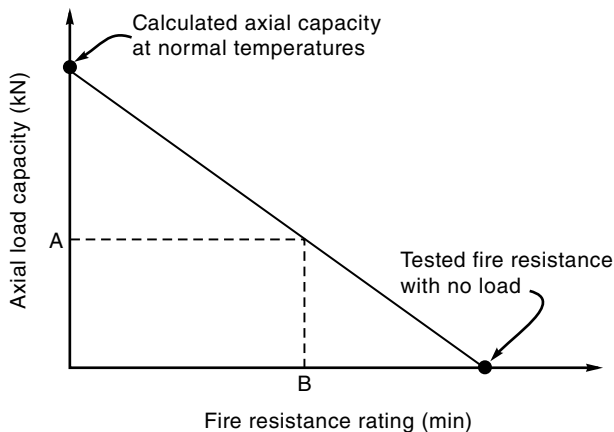


Figure 10.17 Linear interpolation for fire resistance of load-bearing steel stud walls

design. Gerlich *et al.* (1996) justified a temperature of 400°C, showing that a steel strength of 60% of the normal temperature strength gives sufficient safety margin in calculated fire resistance compared with the results of full-scale wall tests.

For steel stud walls, Gerlich *et al.* (1996) have proposed a conservative linear interpolation method for estimating the reduction in fire resistance rating as the applied load increases. This assumes a linear interaction diagram between the fire resistance of a non-load-bearing wall and the load capacity of the wall at normal temperatures as shown in Figure 10.17. If a fire test result is available for a non-load-bearing wall, the time resistance of a load-bearing wall can be estimated. For example, a wall with axial load 'A' (one-third of the normal temperature load capacity) would have a load-bearing fire resistance rating of 'B' (two-thirds of the non-load-bearing rating). This approach may also be applied to timber walls, but has not been extensively verified.

10.8 Timber Joist Floors

Timber joist floors behave similarly to timber stud walls, in that structural failure occurs when charring of the timber joists causes significant loss of load capacity. Wall strength is governed by modulus of elasticity, but floor strength is governed by flexural strength. Buckling of joists about the weak axis is prevented by the floor diaphragm on the cooler side of the assembly, fixed to the compression edge of the joist. This applies to simply supported floor assemblies exposed to fire from below, which covers almost all design situations.

Failure stresses within timber floor joists during fire exposure are shown in Figure 10.18 (König and Walleij, 2000). These stresses have been calculated from temperature profiles during charring as shown in Figure 10.13(b) for an insulated cavity, and mechanical properties of wood at elevated temperature as described in Chapter 9.

Figure 10.18(a, b) shows identical failure stresses in positive and negative bending for a joist at normal temperatures, assuming a bilinear stress–strain relationship. It can be seen that yielding of the wood has occurred near the compression face, producing a stress distribution

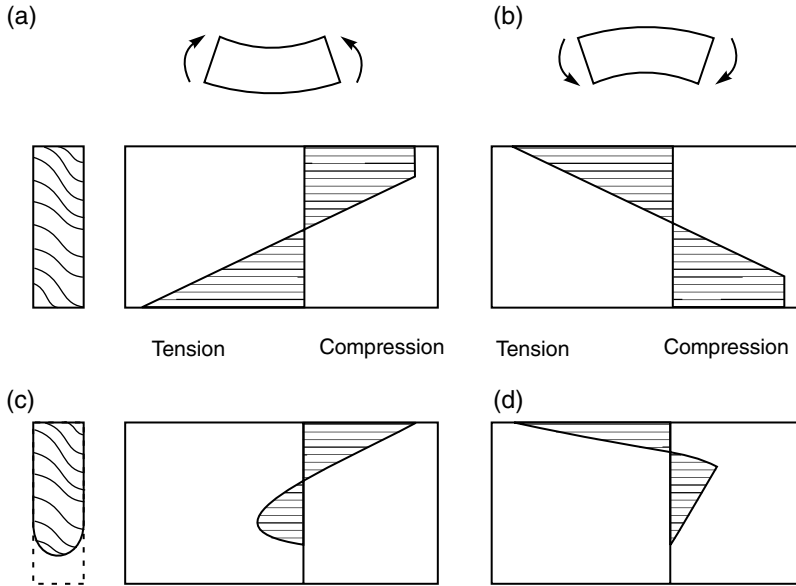


Figure 10.18 Failure stresses in timber floor joists at normal temperatures (a and b) and exposed to fire from below (c and d). Adapted from König and Walleij (2000) by permission of AB Träteck

similar to that shown in Figure 5.2. If the joist had any defects in the tensile region, it would fail in tension before yielding occurs (Buchanan, 1990).

Figure 10.18(c, d) shows failure stresses after the loss of 15% of the cross section due to charring, causing the flexural strength to drop by about two-thirds. When the fire side is in tension, Figure 10.18(c) shows a parabolic distribution of tensile stresses, with the maximum stress well up into the residual joist. When the fire side is in compression, Figure 10.18(d) shows low compressive stresses over most of the residual cross section, with high tensile stresses in the cold wood at the top edge. These calculations confirm those by Thomas (1997), based on the experimental results of König (1995). Similar stress diagrams for studs in walls show much more of the cross section in compression due to the applied compressive loads.

In some countries it is common to cast a thin concrete topping over light timber floors, in order to reduce sound transmission to the room below. Concrete toppings are usually 35–50 mm thick, not designed for composite action. Richardson *et al.* (2000) give an opinion that such concrete toppings will not reduce the fire resistance rating of a timber floor assembly if the cavity has no insulation, or contain mineral wool insulation.

10.9 Timber Trusses

Light timber trusses exposed directly to post-flashover fires have negligible fire resistance. Trusses protected by a fire resisting ceiling can have good fire resistance. Temperatures measured in a ceiling plenums are much less than furnace exposure, typically reaching 327 °C after exposure for 60 min to an ASTM E119 furnace test (Shrestha *et al.*, 1995). The weakest

link is usually the truss plate connectors rather than the wood members. Shrestha *et al.* (1994, 1995) have developed models for predicting the temperatures within truss members and the mechanical properties of the wood and the connectors at elevated temperatures. Deformations in the wood and in the connections affect the stresses in the members. Cramer *et al.* (1993) describe a truss analysis model (SAWTEF) which gives good agreement with full-scale test results for both trusses and truss plate connected joists (Cramer, 1995). This model can allow for non-uniform temperatures within the ceiling plenum and for load sharing between trusses or joists of different stiffnesses.

10.10 Construction Details

Construction details can have a significant influence on the fire resistance of light frame construction. Several important details are discussed below.

10.10.1 Number of Layers

Multiple layers of thin gypsum boards may be cheaper and lighter to fix than one thick board, but multiple layers do not usually provide the same fire resistance as a single layer of the same total thickness, because the outer layers can fall off sequentially, leading to much greater thermal exposure to the inner board. This is a particular problem for regular gypsum board which contains no glass fibres, because it will tend to fall off as soon as large cracks occur or the gypsum becomes dehydrated.

An advantage of multiple boards is that the joints between the sheets can be staggered, reducing the likelihood of early flame penetration into the cavity, especially if sheet joints are not on studs. If more than one layer is used, the inner layer is not usually taped or stopped at the joints.

Some light timber frame walls have additional layers of wood-based sheet material such as plywood or oriented strand board nailed to the studs to improve lateral load resistance. Kodur and Sultan (2000) investigated the fire performance of these 'shear walls' finding that the addition of such materials under the gypsum board increased the fire resistance. This result would be expected from the principles illustrated in Figure 4.9.

10.10.2 Fixing of Sheets

Gypsum board sheets must be fixed to the studs or joists such that the board remains in place for the intended period and gaps or cracks do not appear at joints. Most boards are attached to the studs or joists with screws, although nails are sometimes used on timber framing. The screws at the board edges must be close enough together and far enough from the edge to prevent the board pulling away from the joints during a fire. The strength of a cut edge is less than that of a machine-finished edge. Butt joints between boards are usually finished with plaster or jointing compound which falls off during a fire test and does not contribute to fire resistance.

The use of slender framing members reduces the edge distance between the nail or screw and the edge of the board. Figure 10.19 shows how little edge distance is available for nailing two sheets of board to a stud 38 mm wide. The edge distance of 10 mm meets

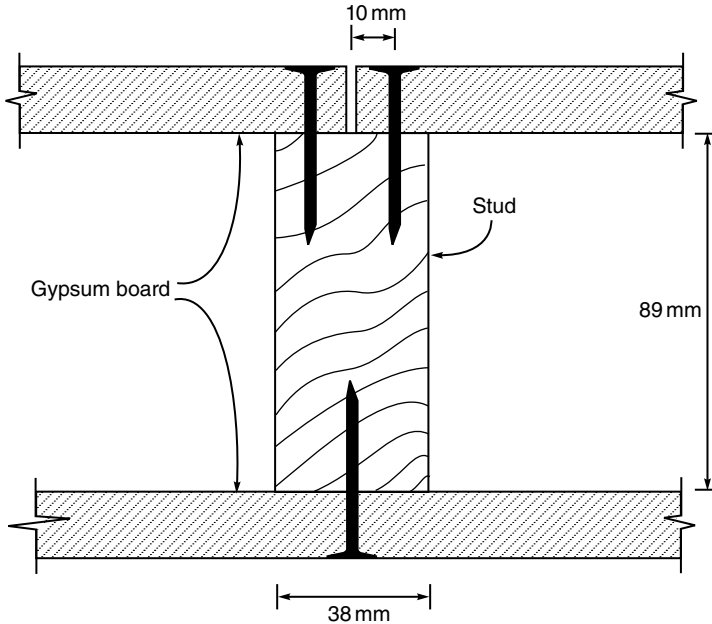


Figure 10.19 Nailing of gypsum board to 38 mm wide timber stud

current Canadian code requirements, but recent tests show a significant increase in fire resistance if the screws are located at least 35 mm from the edge of the gypsum board (Richardson *et al.*, 2000). For assemblies with double layers of gypsum board good performance can be obtained by screwing the outer sheet to the inner sheet using screws which have a very coarse thread (Type G screws). The more fasteners in a sheet, the better the resistance to falling off of the sheet, hence the better the fire performance, especially for ceiling panels.

Joints between sheets are usually made on main framing members (studs or joists) or on blocking members between them. All approvals in New Zealand are for sheet joints over framing members (Winstone Wallboards, 2012) which improves the fire resistance (Collier, 1991b). If the studs are not blocked and the 1.2 m wide sheets of gypsum board are fixed in a horizontal pattern to the vertical studs, the horizontal sheet joints will have no backing. The same applies if sheets of gypsum board are fixed in a vertical pattern to horizontal resilient channels. The Canadian code (NBCC, 2010) permits joints to have no backing provided that the studs or resilient channels are no more than 400 mm apart, but such joints are weak points for fire resistance. For timber frame construction, König and Walleij (2000) found that the time to onset of char in a stud decreased by 8 min if there was a joint between the sheets of gypsum board over the stud. For double layers a similar decrease occurred, but only if the joint was in the outer layer of gypsum board.

To prevent sheets of lining material from falling off timber framing during fires, it is essential that the fasteners are long enough to remain anchored in sound wood after significant charring has occurred. König and Walleij (2000) suggest a minimum length of

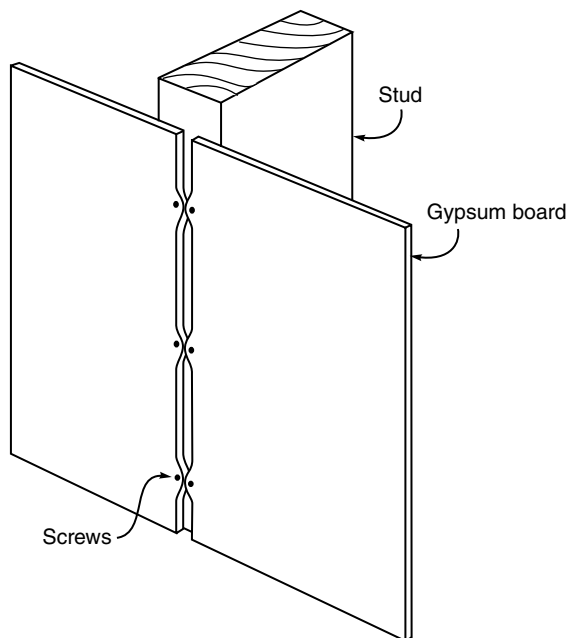


Figure 10.20 Gap between gypsum boards caused by shrinkage of gypsum plaster

10 mm. Figure 10.14 shows how little anchorage length may be left after charring of the stud occurs.

Figure 10.20 shows the type of gap that can occur at the joint between sheets, due to shrinkage in the gypsum board. This can only be prevented by using good quality fire resisting board with sufficient fasteners, preferably kept away from the edges of the sheet.

10.10.3 Resilient Channels

Acoustic performance of gypsum board assemblies can be improved by spacing one or both layers of board off the studs or joists using a pressed steel resilient channel (or resilient rail) as shown in Figure 10.21. From a fire point of view, this results in improved insulation, but less secure fixing of the gypsum board. Some tests have shown a 12% reduction in fire resistance resulting from the use of resilient channels on the fire side of the wall (Kodur and Sultan, 2000) but others have found no effect (König and Walleij, 2000). A weakness can occur in walls where one layer of gypsum board is fixed to resilient channels on the fire-exposed face. Once fire has penetrated the gap between two sheets of gypsum board, the gap between the board and the stud shown in Figure 10.21 allows hot gases to move throughout the assembly, causing premature charring of the studs and failure of the wall (Richardson and McPhee, 1996). This situation can be worse if the sheets are fixed in a vertical pattern where the joints have no backing.

Resilient channels can also be used to increase the distance between fixing screws and the edge of the sheets of gypsum board, as shown in Figure 10.22 (Richardson *et al.*, 2000).

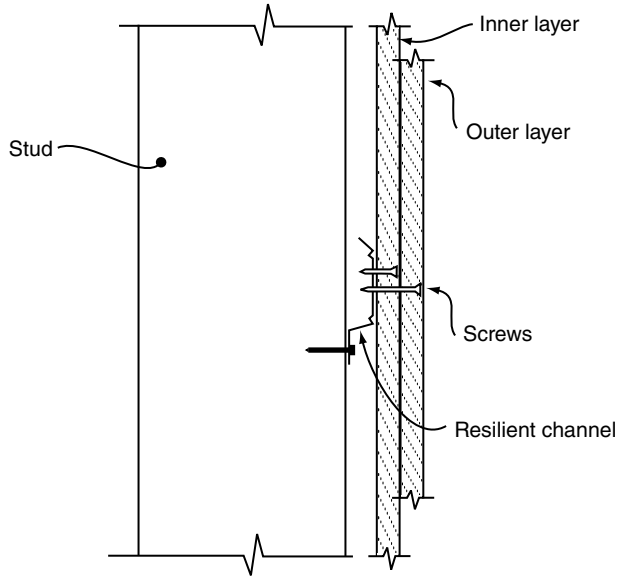


Figure 10.21 Gap between gypsum board and stud using a resilient rail

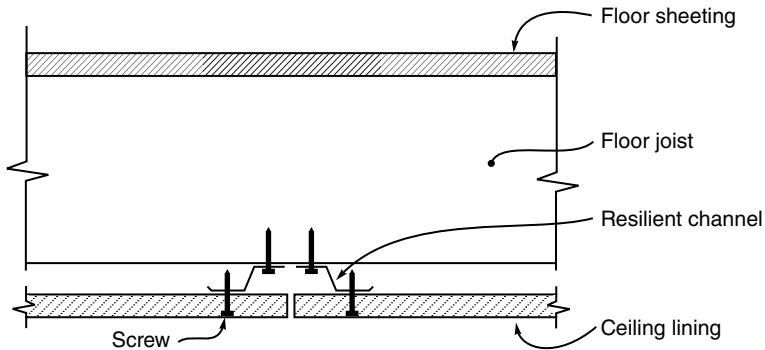


Figure 10.22 Distance between screws and edge of gypsum board increased with the use of resilient rails. Reproduced from Richardson *et al.* (2000) by permission of John Wiley & Sons, Ltd

10.10.4 Penetrations

A major concern about fire resistance of light frame assemblies is the effect of penetrations for services or fixtures. This problem is reduced if the cavity is completely filled with mineral wool insulation. Solid timber blocking or extra layers of gypsum board can be provided behind electrical outlets as shown in Figure 10.23. An alternative protection is to house the electrical fitting in a pressed-steel box containing intumescent material which will expand when subjected to fire temperatures. Electrical outlets should not be located back-to-back at the same location in a wall. Plastic pipe penetrations can be protected with a proprietary collar

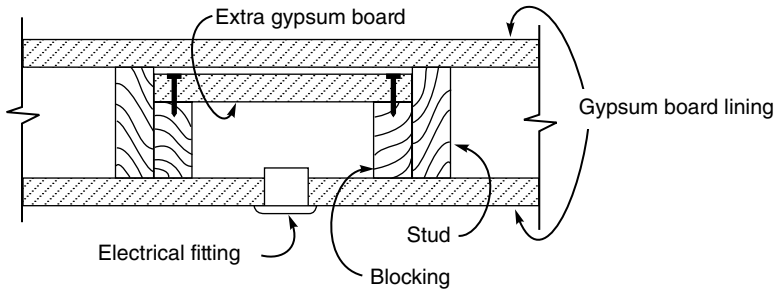


Figure 10.23 Protection of electrical fitting in cavity wall

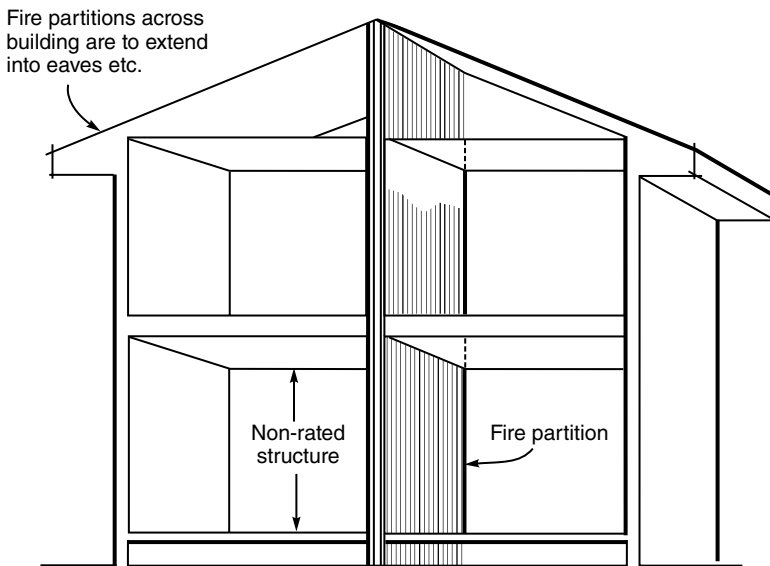


Figure 10.24 Party wall between apartments. Reproduced from SNZ (1986) by permission of Standards New Zealand

containing intumescent products that will expand to fill any gap produced by melting or burning of the pipe. Several alternative products are available. Fire tests are reported by Parker *et al.* (1975).

10.10.5 Party Walls

Figure 10.24 shows the situation that often occurs in light frame construction, where a fire resisting wall is required between two occupancies that are not otherwise required to have fire resistance. The party wall between the two apartments must remain in place and prevent fire spreading from one apartment to the other. If the construction burns down on one side of the wall, the remaining structure must provide lateral support to the party wall.

Non-load-bearing party walls can be attached to the construction on both sides with aluminium clips, so that a fire on one side will melt the clips and allow the structure to collapse without pulling down the wall (Gypsum Association 2012).

10.10.6 Fire Stopping, Junctions

Hollow cavity construction should be provided with fire stopping to ensure that any flames or hot gases entering the wall or floor cavity cannot spread into other storeys or other parts of the building. This is particularly important in multi-storey construction where the studs are continuous over more than one storey (balloon framing).

There are many alternative details for fire stopping. For junctions between floors and a fire rated wall, Figure 10.25(a) shows solid timber blocking in the floor cavity, to prevent fire from spreading through the separating wall, and Figure 10.25(b) shows a method of connecting timber floors to the fire resisting wall without reducing the fire resistance of the wall.

A fire resisting barrier is only as good as its weakest link. Junctions between walls, ceilings and floors must be constructed such that the fire resistance of the barrier is not reduced locally, and so that fire in one cavity cannot spread into an adjacent cavity. Junctions between fire rated and non fire rated construction must be constructed so that failure of the non fire rated element does not allow fire to enter the fire rated assembly.

Fire stopping in light timber framed buildings can be achieved with solid timber blocking between the studs and within the junctions between floors and walls. Typical details are given by manufacturers (e.g. Winstone Wallboards, 2012). Light gauge steel angles behind the gypsum board can be used to enhance the integrity of fire stopping at junctions (Collins, 1998).

In light steel framing, fire stopping can be achieved with blocking between the studs and the use of steel angles to close off paths for fire spread between separate cavities. Long walls are sometimes provided with control joints to allow for longitudinal thermal movements. Tested details of control joints are provided by the Gypsum Association (2012).

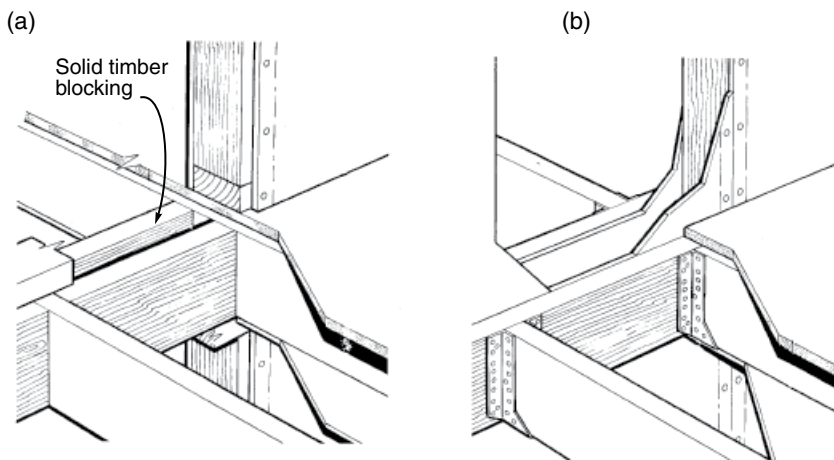


Figure 10.25 Fire stopping details. Reproduced from SNZ (1986) by permission of Standards New Zealand

Double stud walls are often used to meet acoustic requirements, but there is concern about possible fire spread into the cavity between the two leaves of the wall. In a series of fire tests, Sultan (2000) found that small openings from fire rated floors into wall cavities could be sealed with layers of various materials, including semi-rigid sheets of glass fibre or mineral wool, 0.4 mm steel sheet, or 13 mm oriented strand board.

10.10.7 Conflicting Requirements

Difficulties often arise when detailing light frame construction because of conflicting requirements for fire, structural, and acoustic performance. In general terms, the structural requirement is usually for all floors and walls to be continuous diaphragms, which also provides good fire safety by eliminating extended cavities where fire could spread. Acoustic requirements are for as much separation as possible, with floors and walls being non-continuous through junctions, and with gaps provided within walls to eliminate transfer of sound through structural elements. Careful consideration is often needed to meet these conflicting requirements without compromising fire safety.

10.11 Lightweight Sandwich Panels

Lightweight sandwich panels are becoming a very common building material, especially in buildings such as food processing facilities where hygiene and thermal insulation are very important. An increasing number of severe fires have recently occurred in sandwich panel buildings. This section is a brief overview of the fire performance of sandwich panels.

10.11.1 Description

Lightweight sandwich panels take many forms, but those referred to here are lightweight panels consisting of outer sheets of thin steel with a core of plastic foam. Cores may be made from a wide variety of foamed plastics, but the most common are polystyrene or polyurethane. Most sandwich panels have no structural connection between the two outer sheets other than adhesion to the lightweight core. Some manufacturers use combustion-modified foams which are more difficult to ignite than normal foams, but these will still burn in post-flashover fires. Some panels have cores made from non-combustible mineral wool fibres which perform much better in fire than panels with foamed plastic cores.

Sandwich panels are manufactured in a wide range of sizes and thicknesses, and are often used as structural materials for wall, roof or ceiling construction. The external surfaces of the steel sheets are coated with plastic film or high performance paint, and some may have a facing of gypsum board which will improve fire resistance.

10.11.2 Structural Behaviour

Under normal temperature conditions, sandwich panels have very good structural properties because of their light weight and high stiffness. The structural stiffness comes from the rigidity of the core material which holds the skins apart and prevents shear deformations. Figure 10.26 shows flexural behaviour of panels under normal temperature conditions.

10.11.3 Fire Behaviour

Lightweight sandwich panels can be a serious problem in fire because of their potential huge contribution to the fire load in the building, hidden fire spread within the panels, and rapid loss of strength when exposed to fire. Fire behaviour depends greatly on the type of foam and its behaviour when exposed to heat. Some plastic foam materials such as polystyrene will melt and shrink away from the heated facing, leading to rapid debonding and poor structural performance. Some other foams will remain in place for a longer period of time, although most of the adhesive bonds between the core and the facing will fail at temperatures below 150 °C. All plastic foams will burn fiercely when exposed to post-flashover fire temperatures.

Standard fire resistance tests or standard reaction to fire tests are not suitable for assessing the real fire performance of lightweight sandwich panels, because the size of specimens cannot accommodate the range and scale of joints between panels in real buildings.

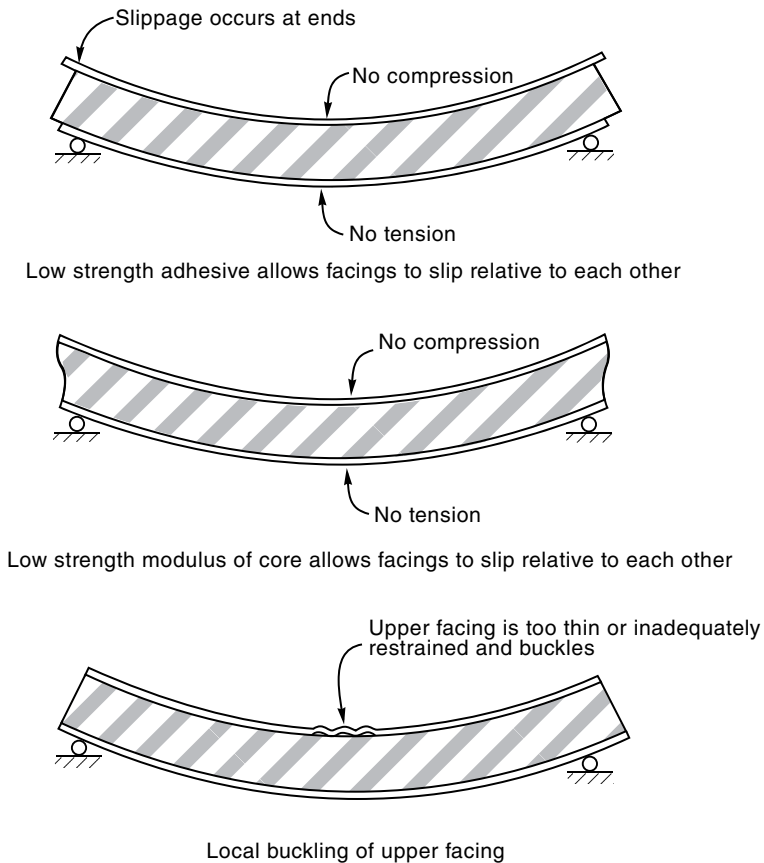


Figure 10.26 Flexural behaviour of sandwich panels. Reproduced from Cooke (1997) with permission from G.M.E. Cooke

The increased contribution to the fire load of the building from the foam plastic is a serious concern. The heated foam may melt and flow out of the panels, or will be converted to a flammable gas within the heated panel, depending on the temperatures, the type of plastic, and how well the panels are held together. Some foam will melt and produce flaming droplets which can spread fire to other locations. Burning foam plastic produces large volumes of toxic smoke.

10.11.4 Fire Resistance

It may be difficult to see how any fire resistance ratings can be achieved with such highly combustible material as foamed plastic. However, some manufacturers have obtained non-load-bearing fire resistance ratings of up to 4 h for sandwich panels containing polystyrene foam, but only meeting the *integrity* criterion. Observations show that the plastic foam melts and escapes in the first few minutes of the fire resistance test, leaving two skins of thin sheet steel supported by the frame of the furnace. The steel becomes very hot, rapidly exceeding the insulation criterion, but the integrity criterion can be met if the vertical joints between the steel sheets are well connected with an overlapping joint filled with an intumescent strip and fixed with steel (not aluminium) screws to prevent any penetration of flames or hot gases.

This type of fire resistance rating is only useful where the sandwich panels are supported on all sides by a fully fire rated structure, and where only an integrity rating is required, such as in a boundary wall situation. Most sandwich panel structures rely on the other sandwich panels or unprotected steel members for structural support, in which case the integrity rating described above is of limited use.

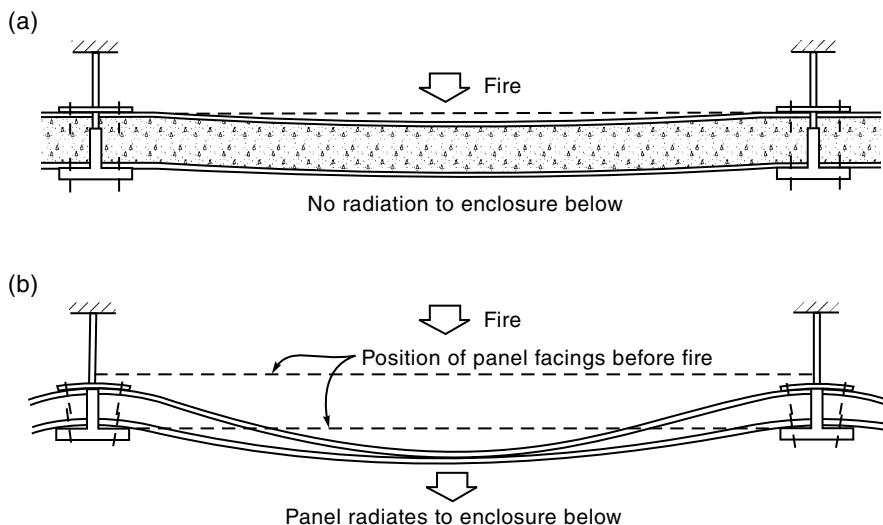


Figure 10.27 Support of sandwich panel wall (a) during initial fire exposure and (b) after the foam insulation has melted. Reproduced from Cooke (1997) with permission from G.M.E. Cooke

(a)



(b)



Figure 10.28 (a) Fire damage to foamed plastic sandwich panels in a factory fire. The building to the right of the photo was completely destroyed by the fire. (b) Steel skins of sandwich panel roofing, draped over the supporting structure after the fire

10.11.5 Design

Design of foam plastic sandwich panels for fire resistance is not possible, other than for an integrity rating as described above. Sandwich panels are often used as structural elements, but these will have negligible structural fire resistance. Design for integrity should ensure that there are fire resisting mechanical fastenings between the facing panels and the supporting structure, so that panels do not fall apart as soon as the bonding becomes delaminated in a fire, as shown in Figure 10.27 (Cooke, 1997). Junctions need to be carefully detailed. Many suitable details and a more complete discussion of fire behaviour of sandwich panels is given by Cooke (1997). The use of sandwich panels for fire resisting walls can only be recommended if they are manufactured with mineral wool cores rather than plastic foam cores. Figure 10.28 shows damage to sandwich panels after a factory fire.

11

Advanced Calculation Methods

As shown in previous chapters there are generally three methods to assess structural fire resistance: the use of tabulated data; simplified calculation methods; and advanced calculation methods. Tabulated data and simplified calculations are only suitable for analysis of isolated structural members. Although advanced calculations may also be used for isolated members, they are the only option for structural assemblies of two or more members. Advanced calculation methods allow the effect of structural interactions with the surrounding structure to be incorporated into the structural analyses, and they are also able to account for structural restraints and their associated forces, redundancies in structural behaviour and alternative failure mechanisms.

Advanced calculation methods can also be used to test the effects of varying different components on the fire behaviour of a structure, and they provide the most realistic predictions of structural behaviour, other than full-scale fire resistance tests which are more difficult and far more expensive. Most, but not all, advanced calculation methods require the use of finite element software. This chapter introduces advanced calculation methods, and highlights their advantages and disadvantages. It also discusses the required components of software for advanced calculations.

11.1 Types of Advanced Calculation Methods

Advanced calculation methods range from fire models that describe how compartment fire temperatures develop over time to models that predict temperatures in fire-exposed members and then models that predict structural performance. For appropriate designs of structures under fire conditions, the design process must incorporate reasonable models of the fire exposure, the thermal response and the structural response, as shown in Figure 4.10. The appropriateness of each model depends on the fire scenario and the conditions that are

judged to be the most onerous in terms of structural response. A general structural fire design proceeds by:

1. Setting objectives.
2. Defining the required structural performance during fire exposure.
3. Determining design acceptance criteria.
4. Selecting appropriate design fires.
5. Estimating member temperatures.
6. Assessing structural response.
7. Verifying member sizes, and repeating parts of the above process as necessary.

The three steps numbered 4, 5 and 6 each require the use of a calculation method. These calculation methods can be 'simple', 'intermediate' or 'advanced'. The choice of each depends on the complexity of the design problem. The fire response of a simply supported steel beam in a small compartment may be determined by the use of the standard fire as the fire model, followed by an assessment of its thermal response using the simple lumped mass approach and then a verification of its strength loss in comparison with the applied loading, as described in Chapter 6. On the other hand, the assessment of the failure of a structural connection in a composite structure under large deflections in fire conditions may require sophisticated use of an advanced fire model, an advanced thermal model and an advanced structural model. These two options demonstrate two extremes in the choice between simple and advanced calculation methods. However, an advanced structural analysis can also employ a simple fire model or a simple thermal model as appropriate for the problem being considered.

To aid in the selection of the most appropriate analysis methods, the following sections describe and give examples of different types of fire, thermal and structural models. The chapter later focuses on structural analysis methods by describing existing advanced calculation methods, available software for these calculations (highlighting the merits and demerits of each), and describing the conditions under which advanced calculation methods are either the only option or where their use gives significant advantages for designers. The fire, thermal and structural response models described in this chapter are generally classified as shown in Table 11.1.

11.2 Fire Models

Fires are classified into pre-flashover and post-flashover fires as shown in Chapter 3. For structural design the concern is usually with post-flashover fires, where structural members experience considerable temperature increments that significantly reduce their capacity. However, there are scenarios where structures are subjected to realistic fires which are better represented by pre-flashover fires, for example isolated fires in large open-plan compartments, such as the circulation areas of shopping malls or car parks. Pre-flashover fires can be represented by plume models, zone models or computational fluid dynamic (CFD) models, in increasing order of complexity.

Post-flashover fires can be represented by standard test fires, natural fire models, zone models or CFD models, in increasing order of complexity. Time equivalent formulae can be used to represent a natural fire as an equivalent period of exposure to a standard fire curve.

Table 11.1 Available approaches for the three components of structural fire design

Fire behaviour
Localized fire
Plume models
Zone models
CFD models
Fully developed fire
Standard test fires
Natural fire models
Zone models
CFD models
Thermal response
Test data
Simple heat transfer models
Advanced heat transfer models
Structural behaviour
Member behaviour
Frame behaviour
Whole building behaviour

CFD, computational fluid dynamic.

Source: Adapted from IStructE (2007).

The application of standard test fires, time equivalence and natural fire (parametric fire) models have been described in preceding chapters. All of these fire models assume that the temperature in the fire compartment is uniform, while the use of plume models, zone models and CFD models inherently consider variations of temperature in different parts of the fire compartment. For typical structural fire design these variations are ignored, so a discussion of these fire models can provide more realistic structural assessment options for certain buildings in fire conditions.

11.2.1 Plume Models

Plume models are simple empirical correlations that describe an axisymmetric fire with a flame which may or may not be touching the ceiling of a given compartment (Figure 11.1). The location of a structural member with respect to the fire is used to estimate the temperature in the member at any given time. Annex C of Eurocode 1 Part 1.2 (CEN, 2002b) provides a method to determine the net heat flux at the surface of a structural member exposed to such a fire. The UK National Application Document to Eurocode 1 Part 1.2 (BSI, 2007) ignores these provisions and suggests a more fundamental approach in PD7974-1 (BSI, 2003a) that calculates temperatures of a growing fire in a compartment before flashover occurs.

11.2.2 Zone Models

Zone models are simple computer models that divide a compartment of interest into ‘zones’ of uniform properties, but allow interactions between the zones that make up the compartment. The temperatures of the various zones are calculated by conservation of mass and energy

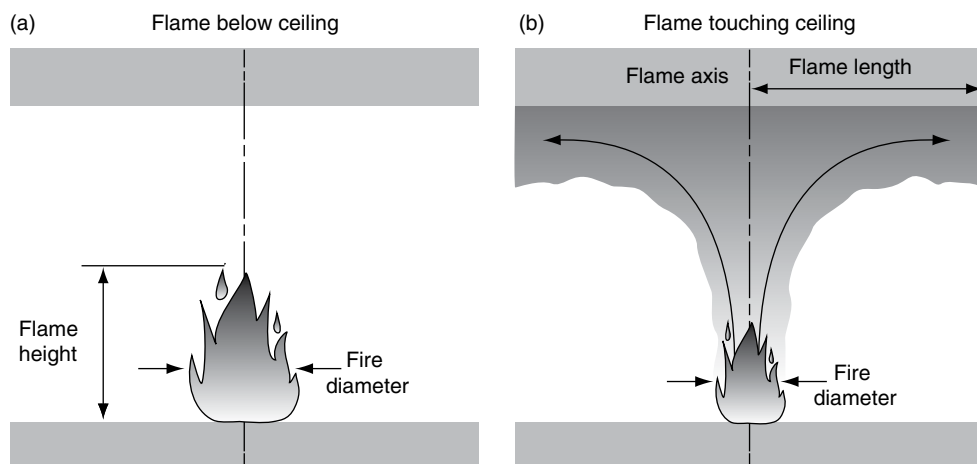


Figure 11.1 Localized fires (IStructE, 2007). Reproduced with permission from The University of Manchester

in each zone, as well as in the total system. There are two common types of zone models: two-zone models and one-zone models. Two-zone models are primarily used to estimate temperatures in pre-flashover fires. The separation of a hot upper layer from a cooler layer below allows the estimation of species [e.g. carbon monoxide (CO), carbon dioxide (CO₂)] concentrations over time and also estimates when tenability conditions are exceeded. When flashover conditions are attained, two-zone models may switch to a one-zone model to estimate post-flashover temperatures in a compartment. Popular two-zone models for fire engineering design, which can switch from two-zone to one-zone calculation methods are B-Risk (Wade *et al.*, 2013) and Ozone (Cadorin *et al.*, 2001).

11.2.3 CFD Models

CFD models assess temperatures in compartments by solving the fundamental equation of fluid flow. Unlike zone models, CFD models divide the compartment of concern into many tiny grids and solve the fluid flow equations for each grid. The effective use of these models requires expertise in the definition of input variables and interpretation of the results, which include temperature, fluid velocity, species concentration and visibility. For fire engineering, the commonest CFD model is the Fire Dynamics Simulator developed by the National Institute of Science and Technology, USA (McGrattan *et al.*, 2015a, 2015b).

11.2.4 Post-flashover Fire Models

Most structural fire engineering is concerned with post-flashover fires because fully developed fires have the greatest impact on structural members, as described in Chapter 3. Post-flashover fires can be represented by standard test fires, time equivalent formulae, natural fire models, zone models or CFD models, in increasing order of complexity. Standard test fires, time equivalent methods and natural fire models are all special examples of one-zone models, as they assume uniform temperatures in the compartment throughout the period of fire exposure.

Standard test fires and time equivalent methods are based on the standard test fire, which is useful if a simple fire resistance rating needs to be predicted, but these fire models do not include a decay phase when realistic fires need to be modelled. A decay phase at the end of the burning period can be included in natural fire models, zone models or CFD models.

A common zone model for post-flashover fires is the Ozone model (Cadorin *et al.*, 2001) which has been used to verify the Eurocode parametric fire curves for natural fires. CFD models can provide excellent predictions of fire temperatures in pre-flashover fires, but they are not yet well developed for post-flashover fires.

11.3 Thermal Response Models

The second stage in analysing a structure for fire resistance is an estimation of the realistic temperatures that the structural member is exposed to over the duration of the design fire. This process can be achieved in three ways:

- Test data
- Simple calculation methods
- Advanced calculation methods

11.3.1 Test Data and Simple Calculation Methods

Test data are mainly compiled from standard fire resistance tests. For exposure to non-standard fires, there are limited sources of reliable information for design. Any test data are limited by the shape of the cross section and the types of construction materials used in the fire test. Simple calculation methods developed over the years and based on the standard fire resistance test, are specific to isolated structural members of particular cross sections and materials. For instance, Eurocode 3 Part 1.2 (CEN, 2005b) provides simple equations to estimate the temperatures of steel members at any time in any fire. Although this approach is simple enough for hand calculations, it is more suited to a spreadsheet solution, as the temperature is obtained through an iterative process. For composite structures, where significant portions of the cross section are made up of two or more materials, the best option is to use an advanced calculation approach.

Advanced calculations require the use of finite difference methods or finite element methods. Finite difference methods predict temperatures at discrete points by simple approximations of derivatives between successive points in the same domain, whereas the finite element method discretizes the domain into small elements and solves for temperatures at the nodes of these elements. This chapter focuses on the finite element method. Both finite difference and finite element methods require definitions of thermophysical properties of materials, the most important properties being density, thermal conductivity and specific heat capacity. For the main construction materials – steel, concrete and timber – these values are provided in Chapters 6, 7 and 9, respectively.

11.3.2 Thermal Modelling with Advanced Calculation Methods

The Eurocodes allow ‘advanced calculation methods’ which make use of the finite element method in numerical computer models to determine the thermal response of structural

sections exposed to fire. The accurate application of such methods requires well educated and experienced practitioners who have a detailed understanding of the boundary conditions for heat transfer, the thermal and physical properties of materials and the different ways in which these thermal analyses can be carried out (Franssen, 2003). Instead of estimating the temperature at a particular time in a structure, it is preferable to track the development of temperatures as the fire progresses, as this allows continual monitoring of thermally induced loading, deformations, and load paths through the structure. An outline of the process of conducting thermal analysis and the associated pitfalls is given below.

Advanced thermal analysis begins by the definition of the geometry of the cross section to be analysed, which is then discretized into smaller segments. The segments make up the finite elements used in the analysis. Temperatures are calculated at the corners of these elements, which are called nodes. Depending on the sophistication of the software package, the definition of nodes and finite elements can be done automatically through a graphical user interface or by generating an input text file. Examples of software packages that use a graphical user interface are ABAQUS (2010), ANSYS (2009) and SAFIR (Franssen, 2011). The temperature of one finite element is an average of the temperatures at its nodes. Thus better approximations of the temperature at any location in a structural member are obtained with finer meshes. However, if a mesh is too fine, the analysis time increases significantly with little improvement in accuracy, so a balance is needed between high accuracy and analysis runtime.

A deficiency of all the above programs is their inability to model mass transfer such as the transport of water or water vapour through permeable materials. Moisture movement has an influence on fire performance of materials such as gypsum plaster and wood as described by Fredlund (1993). Most programs do not easily model shrinkage of the material or ablation of material from fire-exposed surfaces, but effects such as these can usually be simulated by varying the temperature-dependent thermal properties.

11.3.2.1 Calculations

For most structures under fire conditions, the input design fire is a time–temperature curve for a post-flashover fire, which could be the standard fire, the hydrocarbon fire, a Eurocode parametric fire, or a more realistic natural fire. For thermal modelling, the time–temperature relationship is converted to a heat flux–time relationship and is applied to the exposed surface of the structural member, as input to the model. The net heat flux (h_{net}) (Equation 11.1) is composed of the convective heat flux (Equation 11.2) and radiative heat flux (Equation 11.3).

$$h_{net} = h_{net,c} + h_{net,r} \quad (11.1)$$

$$h_{net,c} = h_c (T_f - T_s) \quad (11.2)$$

$$h_{net,r} = \phi \varepsilon_m \varepsilon_f \sigma (T_f^4 - T_s^4) \quad (11.3)$$

where h_c is the convective heat flux coefficient, T_f is the temperature of the fire, T_s is the temperature of the surface of the structural member, ϕ is the configuration factor, ε_m is the emissivity of the material, ε_f is the emissivity of the fire and σ is the Stefan–Boltzmann constant ($5.67 \times 10^{-8} \text{ W/m}^2\text{K}^4$).

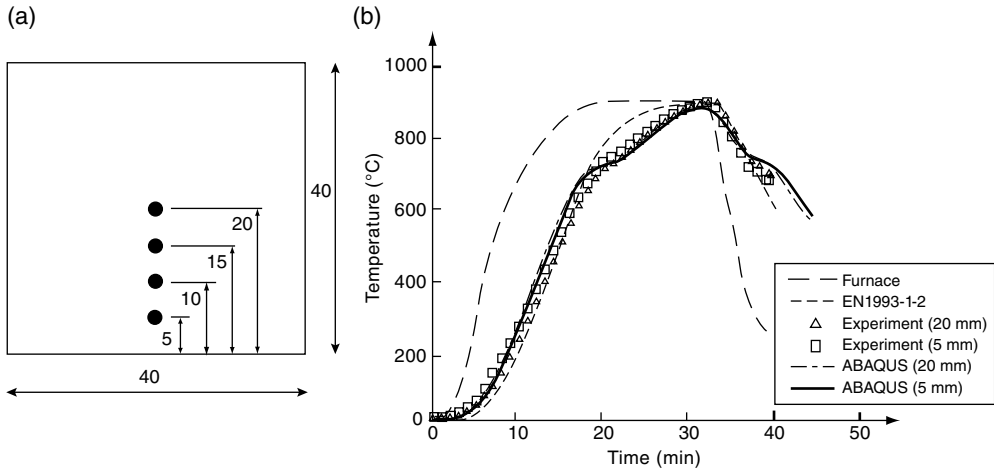


Figure 11.2 Comparison of simplified calculation method and advanced thermal analysis for a solid steel bar. (a) Heated cross section with locations of temperature readings (distances in millimetres). (b) Comparison of test results and thermal analysis

The Eurocodes (CEN, 2004a, 2004b, 2005b) list material emissivity factors as 0.7 for concrete, 0.8 for steel and 0.8 for timber, respectively. For radiative heat transfer from the fire gases, a conservative emissivity value of 1.0 is used for design. Configuration factors (or view factors) are dependent on the orientations of the exposed surfaces of the structural member to the fire. Surfaces that are parallel or perpendicular to the heat source are typically assigned configuration factors of 1.0 and 0.5, respectively, while inclined surfaces (as observed with composite steel decking) are assigned either 0.83 or 0.67 (CEN, 2005c). For standard fire exposure Eurocode 1 (CEN, 2002b) recommends a value of $25 \text{ W/m}^2\text{K}$ as the convective heat flux coefficient at the exposed surface. This value changes to $35 \text{ W/m}^2\text{K}$ for a parametric fire and $50 \text{ W/m}^2\text{K}$ for a hydrocarbon fire. The convective heat flux coefficient at the unexposed face is taken as $4 \text{ W/m}^2\text{K}$ when only convective losses are considered, or $9 \text{ W/m}^2\text{K}$ when radiative losses are included.

11.3.2.2 Typical Results

The level of accuracy which can be obtained with numerical thermal modelling is shown in Figure 11.2(b) which shows a comparison of experimental results with the Eurocode 3 simplified calculation method and numerical analysis using ABAQUS, for fire exposure of a $40 \text{ mm} \times 40 \text{ mm}$ square steel bar heated uniformly on all sides, with thermocouples at four locations as shown in Figure 11.2(a). The thermocouple readings are shown in Figure 11.2(b) as dark data points with additional plots for the fire, Eurocode 3 Part 1.2 calculation results and ABAQUS results at 5 mm and 20 mm. The coefficient of convective heat transfer used in the analyses was $25 \text{ W/m}^2\text{K}$. It is evident that the numerical simulation tracks the experimental result better than the Eurocode 3 simplified approach.

The thermophysical properties for the three common construction materials (steel, concrete and timber) are provided in earlier chapters. The variations of these properties with temperature are described in the Eurocodes, derived through extensive testing and validation.

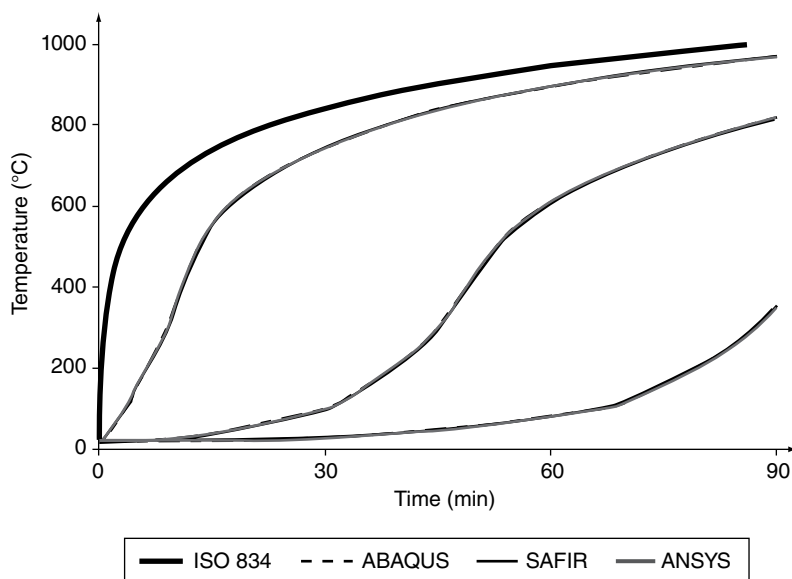


Figure 11.3 Numerical simulation results of one-dimensional heating through timber, using the latent heat of vaporization (enthalpy) approach for a 6 mm × 6 mm mesh size (Werther *et al.*, 2012)

For materials that lose their free water content on heating there are two options for their implementation in thermal analyses. The moisture content can be incorporated in the model as a spike in the specific heat capacity curve (as shown by the dotted curve in Figure 7.9) or included as latent heat of vaporization (enthalpy) on top of a flat specific heat capacity curve (0% moisture content in Figure 7.9). The latter approach ensures better accuracy even with larger time steps while the more common approach of specifying a specific heat capacity curve with peaks requires very small time steps to be used in the computer analysis in the initial phase of the fire, when temperature changes are steep.

Figure 11.3 and Figure 11.4 demonstrate the effects of the two approaches described above. Werther *et al.* (2012) conducted a comparative study on the temperature rise in timber members using ABAQUS, ANSYS and SAFIR to identify the differences in modelling techniques employed by the different software packages. The study investigated the two approaches to modelling moisture content in addition to mesh sensitivity effects during one-dimensional and two-dimensional exposure to the standard fire. Figure 11.3 shows numerical simulation results for one-dimensional heating of a 24 mm × 96 mm timber cross section using a mesh size of 6 mm × 6 mm, at three depths in the cross section, using the enthalpy approach. Although the simulations match test results from König and Walleij (1999), see Werther *et al.* (2012), the test data are not shown here to highlight the similarities and differences in the simulations. The analysis in Figure 11.3 uses a time step of 120 s. Almost identical results are obtained with a time step of 1 s, and even with a mesh size as small as 1 mm × 1 mm. The results show consistent accuracy among the three software packages. Additional analysis using the specific heat capacity approach showed that it is necessary to use much smaller time steps (<1 s) to achieve the same level of accuracy.

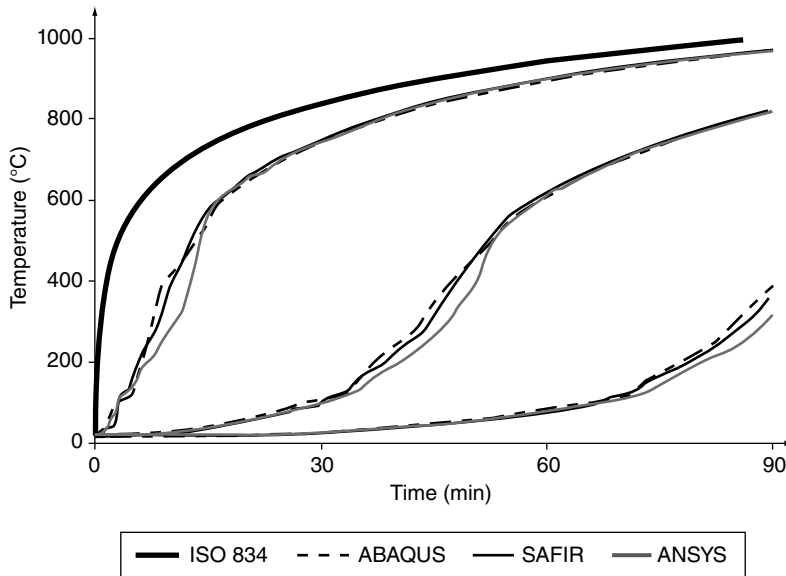


Figure 11.4 Numerical simulation results of one-dimensional heating through timber, using a $6\text{ mm} \times 6\text{ mm}$ mesh size, and the specific heat capacity approach for the ANSYS and ABAQUS models (Werther *et al.*, 2012)

Figure 11.4 shows the same analysis with a mesh size of $6\text{ mm} \times 6\text{ mm}$, and using the specific heat capacity approach. It is observed that the ABAQUS, ANSYS and SAFIR simulations converge for most of the analysis, except between temperatures of 200°C and 500°C . The differences reduce with smaller mesh sizes and converge to Figure 11.3 at a mesh size of $1\text{ mm} \times 1\text{ mm}$. In the simulations reported here, automatic time steps were employed, ensuring small time steps ($<1\text{ s}$) were only used where necessary with large time steps (1 min) for the rest of the simulation. It can be seen that the SAFIR results are unchanged from Figure 11.3, which is because SAFIR only allows the latent heat of vaporization approach (Franssen, 2003). The ABAQUS and ANSYS simulations permit the user to choose either approach, with results from the specific heat capacity approach shown in Figure 11.4.

11.4 Advanced Structural Models

There are a number of advanced models available for structural analysis and design. In most cases these advanced methods of structural analysis are used for assessment of structural performance of alternative structural systems which have been sized from the designer's experience. The selected structural system and the member sizes are then modified through a trial and error process to obtain a structure with the desired performance, using advanced structural analysis at each step. It should be noted that these tools only aid the analysis of the structural system, and engineering judgement must be exercised in 'designing' the structure.

In some areas of structural fire engineering, advanced hand calculation methods have been developed which are recommended in preference to advanced computer methods because they give the designer a better understanding of the actual structural behaviour. One area

where advanced hand calculation methods are widely used is in the structural analysis and design of steel-concrete composite floor slab systems exposed to fire, as summarized below.

11.5 Advanced Hand Calculation Methods

11.5.1 Steel-concrete Composite Floors

The 1990 Broadgate fire (described in Section 8.3.1) showed that unprotected steel-concrete composite floors possess high inherent fire resistance, as they did not fail when allowed to experience large deflections and two-way bending. Similar conclusions can be drawn from a fire in 1991 at Churchill Plaza – a 12-storey steel-framed composite building with a 90 min rated fire protection (Newman *et al.*, 2006), where due to access concerns the fire brigade left the fire to burn from the 8th floor to the 10th floor, where sprinklers eventually extinguished the fire. A key observation after the fire was that the protected composite floor could carry up to 1.5 times its original design load during a severe fire.

Accidental fires such as these led to the large-scale testing of steel-concrete composite buildings at Cardington in the 1990s. The conclusions of the Cardington tests were that although most steel floor beams lose strength and stiffness, flexural bridging of the beams at relatively small deflections and membrane action of the composite slabs at large deflections can provide structural stability and alternative load paths. Catenary action of beams and slabs bending in single curvature contribute to their enhanced capacity at large deflections. The ability of the composite slabs to perform well and carry large loads due to large deflections and biaxial bending is attributed to tensile membrane action (Martin and Moore, 1999; Huang *et al.*, 2002; Foster *et al.*, 2007).

11.5.2 Tensile Membrane Action

‘Tensile membrane action’ is a mechanism which provides thin slabs with large load-bearing capacity, resulting from large vertical displacements, where induced radial tension in the centre of the slab (due to the large deflection) is resisted by a peripheral compression ring. A diagrammatic representation of this mechanism is shown in Figure 11.5. A vertical deflection of at least the thickness of the slab marks the beginning of the mechanism. The conditions

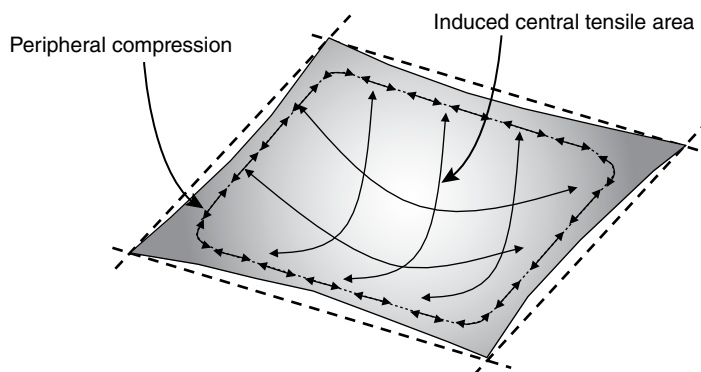


Figure 11.5 Tensile membrane action (Abu, 2009)

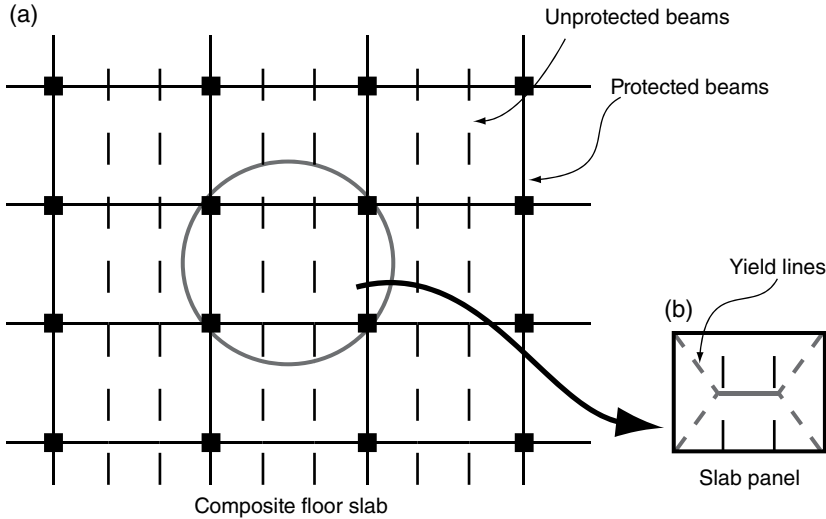


Figure 11.6 Schematic diagram of the Bailey-BRE method (Abu, 2009): (a) composite floor slab; (b) slab panel

necessary for effective tensile membrane action are two-way bending and vertical support along all of the slab's four edges. The self-sustaining nature implies that the process occurs with or without horizontal restraint once the basic requirement of biaxial bending and vertical edge support are satisfied. Tensile membrane action works for all thin two-way concrete slabs, whether they are conventional reinforced flat slabs or composite steel-concrete slabs. This mechanism works best for square slabs, or where the aspect ratio is no more than 2:1. Tensile membrane action applies to ambient temperature conditions (Park, 1964), but it is particularly useful for structural fire design, where large deflections more often occur (Lim, 2003).

For the fire designer of a composite floor to take advantage of this mechanism, the floor is divided into rectangular zones known as 'slab panels'. The slab panels are made up of unprotected composite beams in the interior of each panel and protected composite beams along their edges, on the column grid, to provide the necessary vertical support (Figure 11.6). The slab panels do not need any horizontal restraint at their edges. When the underside of the composite slab is exposed to fire, the unprotected beams rapidly lose strength and stiffness, and their loads are then carried by the composite slab in tensile membrane action. The slab undergoes two-way bending and increases its load capacity as deflections increase. The effective utilization of tensile membrane action in structural fire engineering of steel-concrete composite structures provides sufficient safety with economy in fire protection, by allowing a significant number of secondary steel floor beams to be left unprotected.

11.5.3 The Membrane Action Method

One method of analysis is the 'membrane action method', sometimes referred to as the 'Bailey-BRE method'. This approach devised by Bailey and Moore (2000a, 2000b) was the first simplified design approach for composite slabs at high temperatures that incorporated the benefits

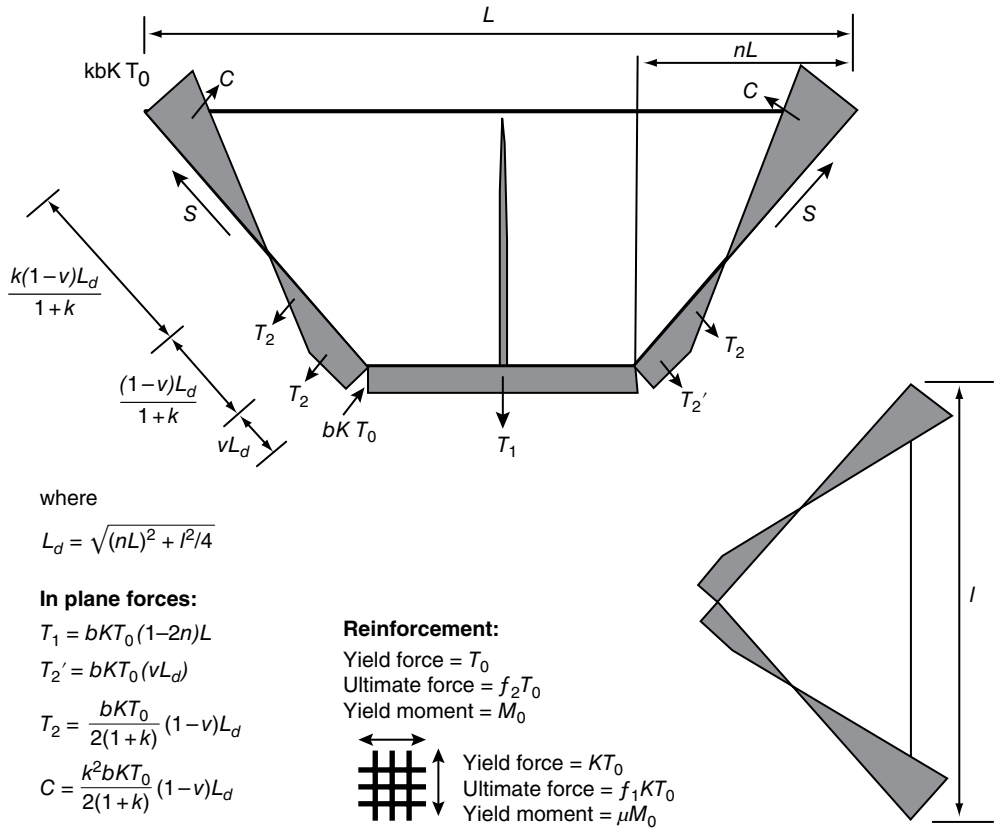


Figure 11.7 In-plane stress distribution for the Bailey-BRE method. Reproduced from Bailey and Toh (2007) with permission from Elsevier Science

of tensile membrane action. It assesses the structural capacity of composite slab in fire by calculating the tensile membrane enhancement to the traditional flexural capacity of the slab.

The method proceeds by dividing a composite floor into several slab panels, as described above, shown in Figure 11.6. With increasing exposure to elevated temperatures, the formation of plastic hinges in the unprotected beams redistributes the applied loads to the slab in two-way bending, resulting in large vertical deflections. Based on rigid-plastic theory with large changes of geometry, and following a similar procedure to one derived by Hayes (1968) for room temperature tensile membrane action, the additional slab capacity provided by the induced in-plane stresses is calculated as an enhancement to the traditional small-deflection yield-line capacity (Bailey and Moore, 2000a, 2000b). Figure 11.7 shows the distribution of tensile and compressive stresses along the yield lines when a slab panel such as that in Figure 11.7(b) approaches failure. See Bailey and Toh (2007) for derivation and explanation of the terms in Figure 11.7.

Failure of the slab panel is defined as the tensile fracture of reinforcing bars across the shorter span of the slab or the compressive crushing of concrete at its corners (Bailey and Toh, 2007). The method conservatively ignores any contribution of the tensile strength of

concrete to the capacity of the slab. It assumes that fire protected steel beams on the gridlines will provide the necessary vertical support along the slab panel boundaries. As an important part of the design, the protected secondary beams must be checked for their load capacity at elevated temperatures, while carrying increased loads from the deformed floor area.

To predict failure at the fire limit state, a vertical displacement limit v (derived from a combination of thermal bowing of the slab and the mechanical strain in the reinforcing) is defined as shown in Equation 11.4, which has been calibrated against the Cardington fire tests. The deflection due to mechanical strain of the reinforcing bars is limited to $l/30$, where l is the length of the shorter span of the slab panel. A full derivation of the method, and its recent modifications, for both isotropic and orthotropic reinforcing bar layouts can be found in the literature (Bailey, 2000, 2001, 2003, 2004; Bailey and Toh, 2007).

$$v = \frac{\alpha (T_2 - T_1) l^2}{19.2h} + \sqrt{\left(\frac{0.5f_{y,\theta}}{E_\theta} \right) \times \frac{3L^2}{8}} \quad (11.4)$$

where α is the coefficient of thermal expansion of the concrete slab, T_2 and T_1 are the bottom and top surface temperatures of the slab, respectively, L and l are the longer and shorter spans of the slab panel, respectively, h is the effective thickness of the slab and $f_{y,\theta}$ and E_θ are strength and Young's modulus of the reinforcing at a given time.

The composite slab capacity at any given time in fire is calculated as:

$$w_{p\theta} = e \left(\frac{\text{Internal work done by the composite slab in bending}}{\text{External work done by the applied load per unit load}} \right) + \frac{\text{Internal work done by the beams in bending}}{\text{External work done by the applied load per unit load}} \quad (11.5)$$

where $w_{p\theta}$ is the slab panel capacity at a given time and e is the enhancement of the slab capacity, calculated as in Bailey and Toh (2007).

A primary advantage of the membrane action method is its simplicity, as it is suitable for implementation in spreadsheet software. The Steel Construction Institute in collaboration with CTICM of France has further developed the method, and has implemented it in spreadsheet VB.NET software MACS+, which is available from the ArcelorMittal website. This software extends the basic Bailey-BRE method by performing thermal analyses on the unprotected intermediate beams and the composite slab for standard or non-standard fires. Then, using the temperatures of the individual components and the allowable vertical deflection criterion (Equation 11.4), it calculates the total capacity of the simply supported slab panel (by summation of the residual unprotected beam capacity and the enhanced slab capacity). This capacity is then checked against the applied load in the fire limit state. If the capacity of the panel cannot support the applied load, then either the resistance of the internal beams or the size of the reinforcing mesh must be increased.

Since the initial development of the Bailey-BRE method, attempts have been made by various researchers to enhance design methodologies employing tensile membrane action through experimental, analytical and numerical approaches.

11.5.4 The Slab Panel Method

Clifton (2001) expanded the initial Bailey-BRE method to include the effects of continuity and additional reinforcing bars that may be present in the ribs of slabs. The method, generally known as the Slab Panel Method (SPM) has some considerable differences from the Bailey-BRE method. In addition to the consideration of slab continuity, the SPM includes the contribution of the unprotected secondary beams in its yield-line load-carrying capacity. It performs a shear check of the panel and allows for some deflection of the protected secondary beams.

The method proceeds with the calculation of the fire limit state loading on the slab, following the loading standard of the particular jurisdiction. The yield-line capacity of the slab is calculated by aggregating the contributions of the reinforcing mesh, any reinforcing bars that may be present in the ribs of the composite slab and the residual capacity of the unprotected beams at the design time of the fire. The negative moments along continuous edges are also calculated. Two slab yield-line capacities are determined:

- one is calculated to include all pinned and fixed boundaries, as suggested by Park (1964);
- the other is calculated as the yield-line load capacity of a simply supported slab. It is to this capacity that the membrane enhancement is applied.

A deflection limit is calculated based on the desired fire design time, and this is used to determine the potential enhancement, similar to the process in the Bailey-BRE method. Once the enhancement has been calculated the load-carrying capacity of the slab panel W_u is determined as:

$$W_u = (w_{y1\theta} - w_{y1\theta,ss}) + w_{y1\theta,ss} e \quad (11.6)$$

where $w_{y1\theta}$ is the yield-line load-carrying capacity in fire, $w_{y1\theta,ss}$ is the simply supported yield-line load-carrying capacity in fire and e is the tensile membrane enhancement factor.

Structural safety is confirmed if W_u (from Equation 11.6) is greater than the fire limit state loading. The shear capacity of the slab is checked near the supporting beams. The slab thickness is the minimum slab thickness (using just the thickness of concrete above the ribs, for a ribbed slab), with further reductions in thickness due to the loss of strength of concrete at elevated temperatures. The SPM recognizes that protected secondary beams can deflect under load and heat, and so it includes an edge beam deflection of span/100 in the calculation of its slab panel deflection limit. Details of the method can be found in the literature (Clifton, 2006; Clifton *et al.*, 2010; Zhang *et al.*, 2014).

11.5.5 Failure Mechanisms of Composite Slabs

The Bailey-BRE method and the SPM both assume that full vertical support is available at all the slab panel boundaries. In practice, this is achieved by protecting the slab panel's edge beams, which must lie on the column grid of the building. When the unprotected secondary beams lose most of their strength at very high temperatures there is a redistribution of the loads carried by these protected edge beams; the primary beams lose load because of the loss

of load capacity of the unprotected beams whose ends they support, whereas the protected secondary beams gain load by tending to support the floor area with which they would be associated in a non-composite two-way-spanning slab.

The Bailey-BRE method therefore requires that the protected secondary beams are designed for increased load ratios at the fire limit state. As the protected beams lose strength with time, and the load redistribution causes increased deflections at the panel boundaries, the assumption of continuous vertical support along the panel edges becomes progressively less valid. The use of yield-line theory as the baseline for the strength enhancement also dictates that a slab panel's capacity increases with increased reinforcement area unless the increase is arrested by a compressive failure criterion, as identified by Bailey and Toh (2007). However, since the primary requirements for tensile membrane action to be mobilized are double-curvature bending, large deflections and vertical edge support, excessive deflections of the protected edge beams can result in the double-curvature bending being converted into single-curvature bending. As a consequence the panel may fail structurally, so that the reinforcement's tensile strength is not usefully employed.

Slab panels are usually continuous over at least two supports. Continuity provides higher slab panel resistance in fire. However, depending on the extent of the fire in a building and the lightness of the reinforcing bars used in composite floor construction, the continuity may be lost, or significantly higher loads may be imposed on the protected perimeter beam between two adjacent slab panels. Coupled with thermal degradations, these beams can experience large deflections, and may collapse. Therefore, Abu *et al.* (2011) and Duchow and Abu (2014) have proposed alternative collapse mechanisms for these slab panels, to ensure that designs following the simple approaches can dependably generate full tensile membrane capacity and not fail by the loss of support from the protected beams. An examination of all possible scenarios, including those in Figure 11.8, offers the possibility of selecting the mechanism which requires the least plastic energy.

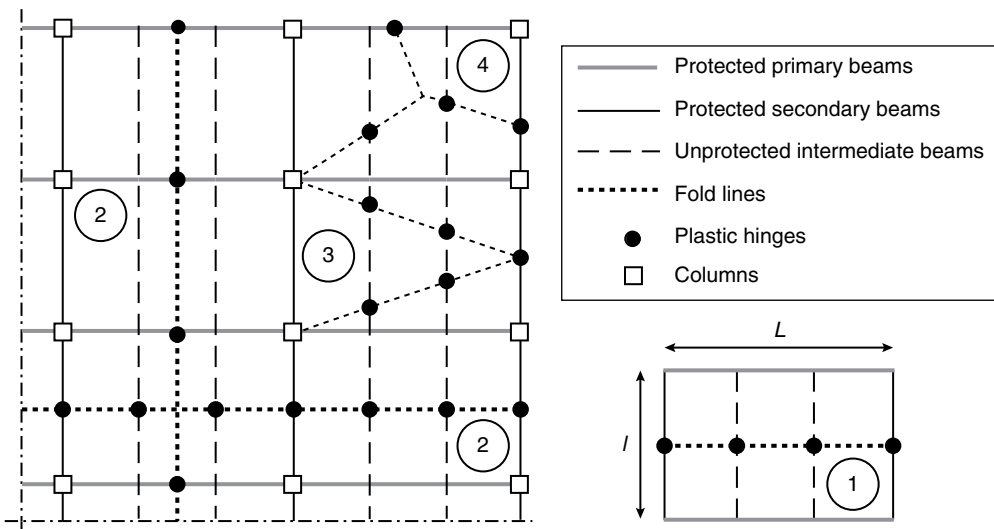


Figure 11.8 Collapse mechanisms of composite slab panels, including failure of protected beams (Duchow and Abu, 2014)

The collapse mechanism which actually occurs in a fire will depend on the aspect ratio of the slab, relative beam sizes, location of the slab panel within the building and the extent of the fire. With reference to Figure 11.8, as the simplified design approaches are based on failure of an isolated slab panel, Collapse Mechanism 1 examines the failure of isolated slab panels. Collapse Mechanism 2 addresses large compartments, such as open-plan offices where a large number of slab panels could be involved in the fire. Collapse Mechanism 3 is for slab panels located at the edge of a building, with Collapse Mechanism 4 developed for slab panels located at the corner of a building. The details of the calculation process can be found in the literature (Abu *et al.*, 2011; Duchow and Abu, 2014).

11.6 Finite Element Methods for Advanced Structural Calculations

As observed in earlier chapters of this book, the strength and stiffness of individual structural members degrade during fire exposure. When considering a whole structure, it must be recognized that the performance of any structural member depends on its interactions with the surrounding structure. The loss of strength and stiffness of one member results in the redistribution of loads to other members, which may in turn either degrade or have enhanced performance due to their thermal exposure and the deformations they experience. For a thorough understanding of the behaviour of any structural member exposed to fire conditions, it is prudent to examine the fire behaviour of the whole structure. Numerical analysis of the whole structure allows an investigation of local degradation of any heated structural member including its interaction with adjacent members and the surrounding structure.

In particular, finite element analysis is the best tool to account for varying capacities of the entire structure, as individual members lose strength or are subjected to increased loading. The finite element method allows the definition of thermal and mechanical actions on structural members or frames while accounting for the change in material properties with temperature. The finite elements are specified over small segments of the structural member, and may have varying properties through the cross section. As different structural and material properties can be assigned to different parts of different members, finite element analysis aids the simulation of progressive deformations of complex structures when exposed to fire. Finite element analysis helps to track realistic behaviour of structures under different fire exposure scenarios, and is very useful in optimizing fire resistant design as well as predicting collapse mechanisms of structures.

This section outlines the differences in isolated and global behaviour of structures under fire conditions. It describes the components necessary for global analysis of fire-exposed structures and discusses some of the available software packages. For a full understanding of the finite element method, interested readers should consult specialized books, such as Cook (1995), Bathe (1996) and Zienkiewicz and Taylor (1991).

11.6.1 Structural Behaviour Under Fire Conditions

11.6.1.1 Beams and Columns

In the earlier chapters of this book, simple expressions were provided to assess the axial, flexural and shear capacities of isolated structural beams and columns under fire conditions, including approximate expressions for lateral instability. However, the fire behaviour of

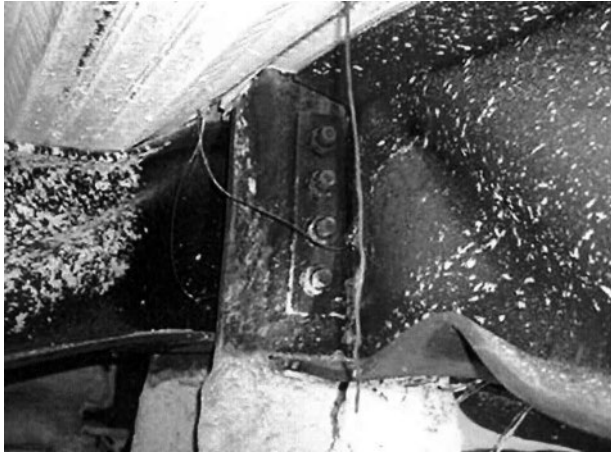


Figure 11.9 Local buckling of beam bottom flange in Cardington Test 7. Reproduced from Wald *et al.* (2006) with permission from Elsevier Science

structural members is much more complex than described by these simple expressions, and this realistic behaviour can only be assessed accurately by finite element analysis.

For example, when a steel beam in a structural frame is exposed to fire it experiences local buckling of its lower flanges in the initial stages of the fire, and it may later experience tensile catenary action under very high temperatures. The local buckling occurs as a result of thermal expansion which is restrained by the colder structure at the ends of the beam. This restraint induces axial compressive stresses in the bottom flanges, which in turn cause buckling. Figure 11.9 shows local buckling of a beam in Cardington Test 7 (Wald *et al.*, 2006). Catenary action occurs later in the fire when steel temperatures are much higher and the beam hangs like a tension cable from its supports. Advanced finite element modelling is necessary to predict behaviour such as local buckling and catenary action, as well as predicting the forces in connections which must be able to carry the imposed tensile forces if catenary action is allowed to develop, during both the heating and cooling stages of the fire.

Figure 11.10 shows the axial force variation in a restrained beam (Wang *et al.*, 2012). The beam is of composite construction; it is in tension at room temperature, supporting a concrete slab which also acts as its compression flange. When exposed to the fire, the beam heats up and tries to expand against colder adjacent structure, which induces an axial compressive force, which continues until local buckling of its bottom flange occurs. The beam continues to deflect downwards as a result of its loss of strength and the induced thermal gradients (due to differential heating through its depth). The axial force changes from a compressive force to a tensile force as the beam eventually hangs from its supports in catenary action. The axial force in the beam can be compared with its tensile strength. Upon cooling the beam contracts against its supports, increasingly generating higher tensile forces, which may cause failure of the connections.

Figure 11.11 shows a steel connection which has fractured during the cooling phase of one of the Cardington fire tests, as a result of thermal contraction. The internal forces and stresses associated with this type of behaviour can only be assessed by frame analysis, using the finite element method, with realistic fire curves which include the decay phase of the fire.

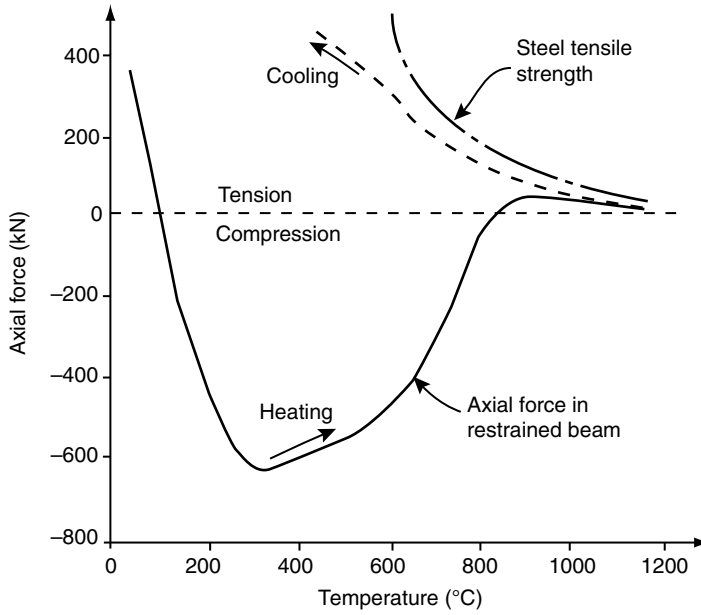


Figure 11.10 Axial force in a restrained composite beam. Reproduced from Wang *et al.*, (2012) with permission from CRC Press



Figure 11.11 Connection failure, during cooling, in Cardington tests. Courtesy of B.R. Kirby, Corus Fire Engineering

11.6.1.2 Slabs

Analysis of slabs in the earlier chapters of the book examined their fire resistance as either simply supported members or continuous members. Depending on the location of their supports with respect to the depth of the slab it was observed that their capacities could sometimes be enhanced by restrained thermal expansion, through compressive membrane action (or arch action). Section 11.5 has also shown how tensile membrane action can help to increase the fire resistance. However, tensile membrane action and compressive arch action are only effective if there are no large deformations of the supporting edges (i.e. beams), which is often unrealistic. Finite element methods provide the only accurate way of assessing realistic behaviour of the enhanced capacity of slabs at large deflections.

11.6.1.3 Connections

The material design chapters do not specifically include design of connections, because the emphasis is on behaviour and design of structural members. Connections are components that join different structural members, but for composite structures, connections are also needed to join the two materials together (e.g. shear connectors, studs, etc.). At room temperatures most member-to-member connection behaviour is represented by shear strength or by moment–rotation relationships.

The earlier parts of this chapter have shown that connections in fire conditions may be subjected to axial forces, bending moments and shear forces due to the structural deformations that occur. The failure sequence may thus be very different to what occurs at room temperature. Cardington Test 7 (Wald *et al.*, 2006) showed that different steel connection components can fail in fires. Figure 11.9 shows shear failure in the web, in addition to buckling of the beam lower flange, while Figure 11.12 shows column flange buckling. Other observed failures in that test included fracture of end plates and bolt failures, none of which can be modelled without finite element analysis, as an advanced calculation method.

The discussion so far has focused on the differences between behaviour of isolated structural members in fire conditions as compared with those that form part of a larger structure. The necessity to use finite element analysis has also been established. As the fire progresses and as loads are redistributed to other members in a fire, numerical analysis helps to identify alternative load paths and the progressive failure of building components. To model this successfully the finite element package should have an adequate library of finite elements, with adequate definitions of mechanical behaviour. The subsequent sections identify these and show how they may be applied.

11.6.2 *Finite Element Analysis Under Fire Conditions*

The previous section described some differences between the fire behaviour of isolated members and the fire behaviour of integrated members that form part of a larger structure. It was observed that tracking the complete behaviour of full-frame structures gives an understanding of the different load paths that can occur and how the use of finite element analysis can aid this process. The finite element method requires the definition of material and structural properties to allow the simulation of structural behaviour in fire conditions.

It is important to note that most of the previous chapters on the design of single members took the simple approach of reducing material strengths with increasing temperature, and comparing



Figure 11.12 Column flange buckling in Cardington Test 7. Reproduced from Wald *et al.*, 2006 with permission from Elsevier Science

the reduced capacities to the applied loads. Timber is the only exception, where physically reduced cross sections are considered instead. The preceding discussion on the effects of adjacent structure on the behaviour of structural members in fire suggest that a structure under fire exposure experiences a combination of thermally induced effects (i.e. thermal bowing, or restrained thermal expansion), reduced material strengths and reduced effective cross-sectional area.

It is only in very simple scenarios that the simplified calculation methods mimic real behaviour, as the changes in material properties and section properties need to be considered. Thus accurate predictions of structural behaviour under fire conditions require the consideration of second-order effects in mechanical behaviour. The presence of thermally induced effects and the loss of material strength also result in large deflections. The combination of restrained thermal expansion and large deflections cause variations in stresses in different parts of the structure, throughout the fire exposure, making it difficult to choose particular times or temperatures as being critical for the design (Wang *et al.*, 2012).

To adequately track stress and deformations of structural members exposed to fire it is essential to employ full non-linear material models and geometric non-linear elemental definitions in the analysis of the whole structure. Descriptions of the various material and structural properties that should be considered in numerical analysis, and some examples, are provided in this section.

11.6.3 Material Properties

Material properties for steel, concrete and timber have already been described in Chapters 6, 7 and 9, respectively, so they will not be covered thoroughly here, except to point out that suitable software for finite element analysis must incorporate full non-linear stress–strain characteristics of all materials, accounting for creep where necessary.

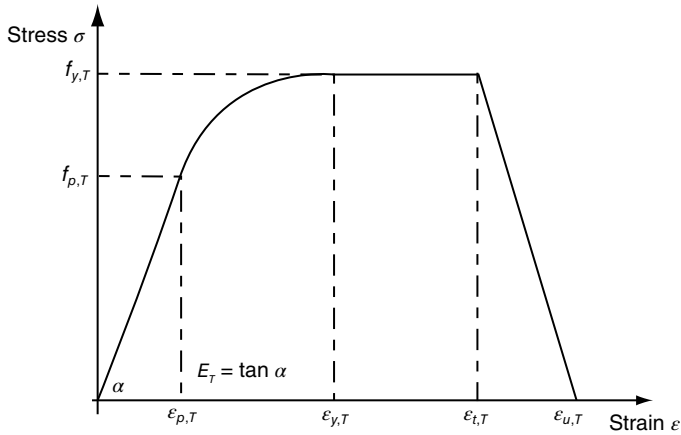


Figure 11.13 Stress–strain relationship for structural steel in fire from Eurocode 3 Part 1.2. Reproduced from CEN (2005b). © CEN, reproduced with permission

11.6.3.1 Steel

For steel, Eurocode 3 Part 1.2 (CEN, 2005b) provides a stress–strain model which adequately considers creep (Franssen *et al.*, 2009), see Figure 11.13. The model has a linear stress–strain relationship until the limit of proportionality ($f_{p,T}$) is reached. The transition from the proportionality limit to the yield stress ($f_{y,T}$) is described by an ellipse up to 2% strain. This is followed by a yield plateau until a strain of 15%, after which the stress in the steel decreases to zero at 20% strain.

A plot of stress–strain characteristics for S275 steel ($f_y = 275$ MPa) at temperatures from 20 to 1000 °C is shown in Figure 11.14. Details of the functions that aid the construction of the stress–strain curves can be found in Eurocode 3 part 1.2. Although the model is widely used, its rate of change of the gradient at the points of proportionality and yield are not continuous, and so the Ramberg–Osgood stress–strain model is preferred for numerical analysis (Wang *et al.*, 2012). The Ramberg–Osgood model has its stress–strain curves defined as continuous functions that vary with increasing temperature, as shown in Figure 11.15 (El-Rimawi, 1989).

11.6.3.2 Concrete

For concrete, Eurocode 2 Part 1.2 (CEN, 2004a) and Eurocode 4 Part 1.2 (CEN, 2005c) provide a stress–strain model for different types of concrete at high temperatures. The model, which only accounts for compressive strength, is shown in Figure 11.16. It is characterized by the compressive stress, its corresponding strain at elevated temperatures and the strain at which the stress drops to zero. A curve is used to describe the initial portion (region I) while the descending branch is described by a straight line approximation (region II). A plot of stress–strain characteristics for concrete of compressive strength 40 MPa at temperatures from 20 to 1000 °C is shown in Figure 11.17, derived from the Eurocode formulae. It should be noted that concrete does not regain its strength after cooling to room temperature, and Annex C

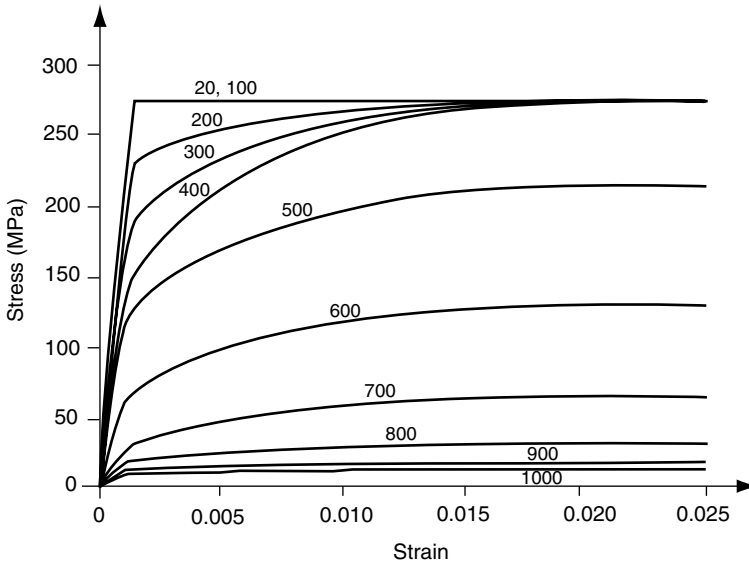


Figure 11.14 Stress–strain relationships for S275 structural steel at high temperatures (based on Eurocode 3 Part 1.2 model). Reproduced from CEN (2005b). © CEN, reproduced with permission

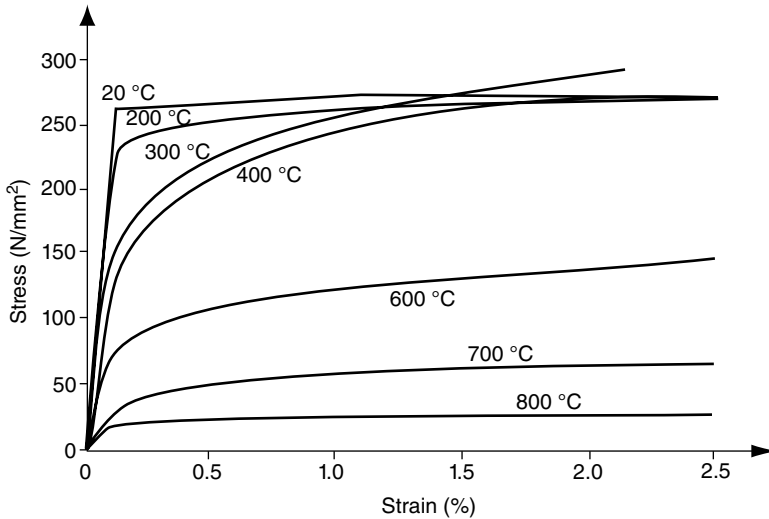


Figure 11.15 Ramberg–Osgood stress–strain relationship for S250 structural steel in fire. Reproduced from Wang *et al.* (2012) with permission from CRC Press

of Eurocode 4 Part 1.2 (CEN, 2005c) provides information on how to consider this loss of strength in advanced calculations.

Although the tensile strength of concrete is normally ignored at room temperature, there are scenarios where it becomes important in structural fire analysis. For example, the tensile strength

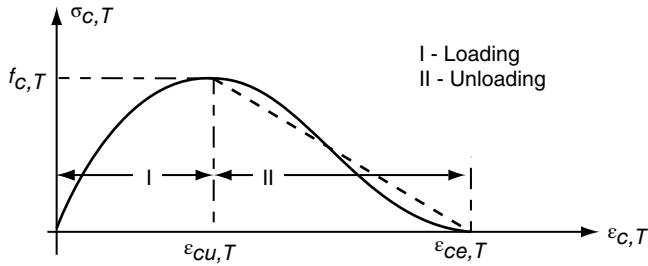


Figure 11.16 Stress–strain relationship for concrete in fire from Eurocode 4 Part 1.2. Reproduced from CEN (2005c). © CEN, reproduced with permission

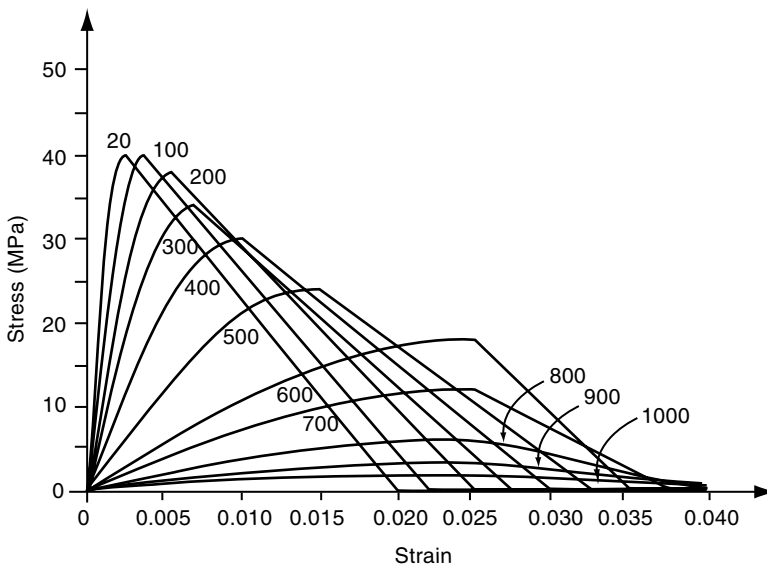


Figure 11.17 Stress–strain relationships for concrete of compressive strength 40 MPa at high temperatures (based on Eurocode 4 Part 1.2). Reproduced from CEN (2005c). © CEN, reproduced with permission

of concrete is critical in tracking the behaviour of slab panel systems in tensile membrane action at large deflections (Lim *et al.*, 2004). Figure 11.18 shows comparisons of numerical models with varying tensile strengths at elevated temperature with test results of a 4.3 m by 3.3 m 100 mm thick flat slab exposed to the ISO 834 fire for 3 h. The deflection profile of a quarter section of the slab is shown on the left-hand side with results of the numerical modelling, with three initial tensile strengths of concrete (0.0, 1.5 and 3.0 MPa) shown on the right-hand side. The large deflection of the slab produced deflections greater than 250 mm. The finite element simulations show that the inclusion of the tensile strength of concrete provides better predictions of slab behaviour at large deflections. Annex E of Eurocode 2 Part 1.2 provides a simple reduction expression to predict tensile strength of concrete at elevated temperatures, up to 600 °C. Other criteria that should be considered for concrete materials at high temperatures include biaxial failure surfaces for slabs and models for load-induced transient strains.

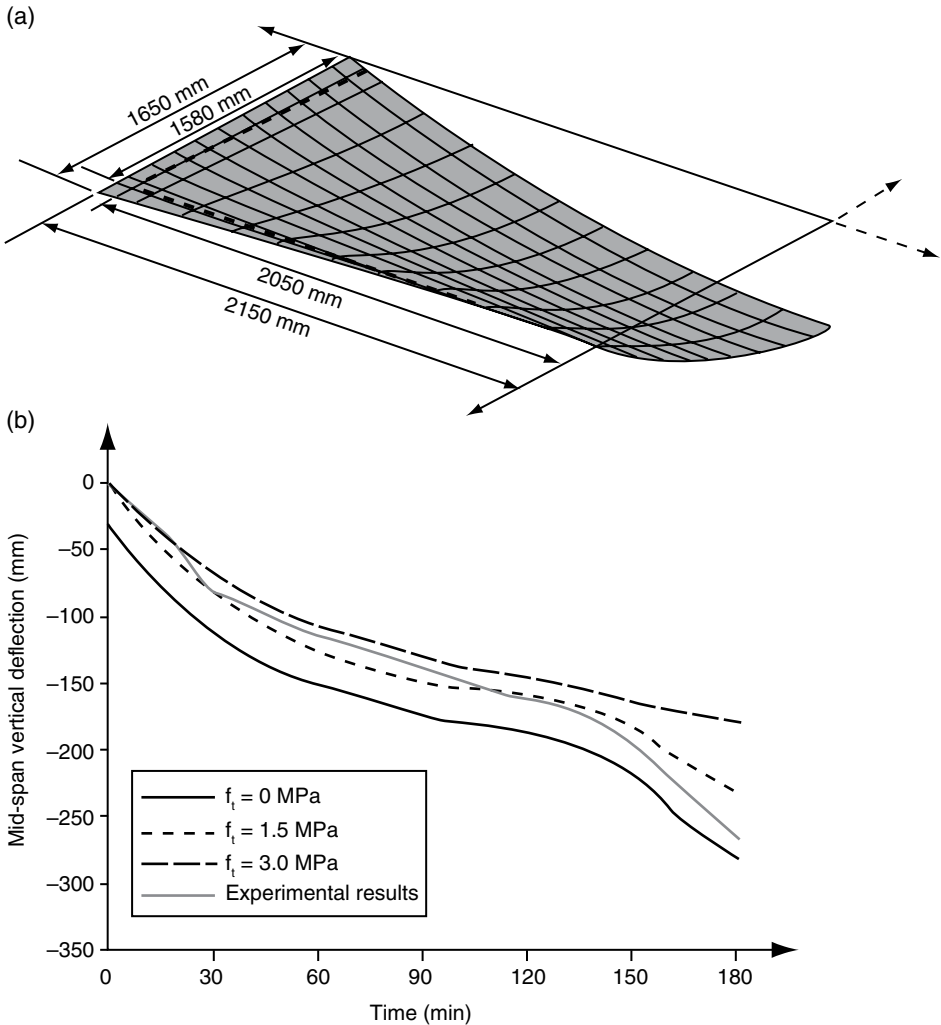


Figure 11.18 Importance of the tensile strength of concrete in numerical models of slabs at large deflections (Lim *et al.*, 2004). (a) Deflection profile of 100 mm thick slab. (b) Numerical modelling results comparison

For the analysis of slabs at large deflections, modelling of the failure surfaces of concrete at large deflections is desirable. As tests for biaxial failure surfaces are limited there is considerable debate about which formulation is appropriate at elevated temperatures. A discussion by Wang *et al.* (2012) expands on the best options currently available.

Load-induced transient strain occurs in concrete members subjected to compressive loading and heated for the first time. The compressive resistance to heating induces additional loading in the member. The resulting 'preload' tends to compress the concrete, thereby reducing the amount of thermal strain that would have otherwise occurred if there had been no 'preload'. The difference in strains between a preloaded specimen and an unloaded specimen can be of

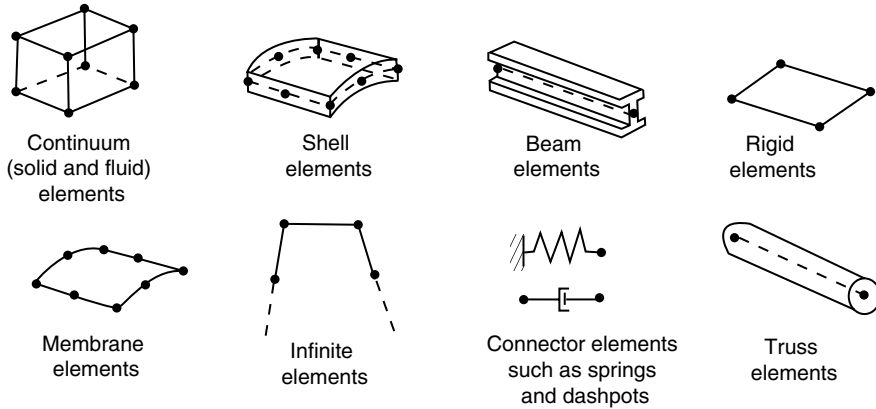


Figure 11.19 Examples of finite elements used in structural analysis. Based on ABAQUS 6.10 Manual

the order of the free thermal expansion of the original unloaded specimen. For analyses where concrete members under significant compressive loads are critical, the finite element software must include a consideration of this phenomenon (Anderberg and Thelandersson, 1976; Khoury *et al.*, 1985b; Khoury, 2000; Schneider and Horvath, 2003).

11.6.4 Structural Properties

11.6.4.1 Types of Finite Elements

The basic description of finite elements for structural members in fire conditions is the same as at room temperature. The major difference between the two analyses is to allow temperature variations through the depth of the cross section and to give the finite element the capacity to undergo large deflections, with an appropriate account of geometric non-linear behaviour. Geometric non-linear behaviour is appropriate under certain scenarios at room temperature but is especially needed in fire conditions, as large deflections and second-order effects are the norm.

Examples of finite elements used at room temperature include: line elements (e.g. beam elements, truss elements), brick elements (or continuum elements), shell elements, membrane elements and spring elements. Figure 11.19 shows some of these examples. Subsequent parts of this section explain how beams, columns, slabs and connections may be modelled for their analysis under fire conditions, using these elements.

11.6.4.2 Beams and Columns

Beams and columns can be modelled as one-dimensional (1D), two-dimensional (2D) or three-dimensional (3D) elements depending on the particular behaviour being investigated. As mentioned earlier, the complete behaviour of a fire-exposed steel beam involves thermal bowing, thermal expansion, restrained thermal expansion, local buckling, large deflections, catenary action and member contraction during cooling. The majority of these actions may be modelled with a 1D beam element. These analyses treat the beam as a line element with the

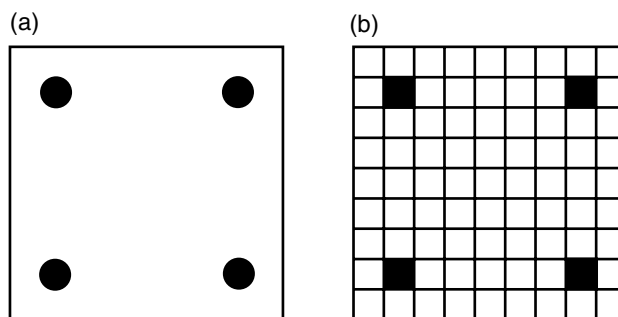


Figure 11.20 Discretized cross section of a reinforced concrete beam, showing positions of reinforcing bars. (a) Original beam cross section. (b) Discretized beam cross section

same cross-sectional properties as the original beam. As line elements can be characterized by finite cross sections, different temperatures can be defined through their depths.

A typical reinforced concrete beam cross section may be discretized as shown in Figure 11.20, where Figure 11.20(a) shows the cross section of the beam and rebar locations. The discretized cross section of the 1D element for structural analysis in fire is shown in Figure 11.20(b) where the different materials in the cross section are represented by square segments. The diameters of the rebar cross sections are represented by the shaded equivalent square sections. Different structural properties may be assigned to the individual materials, with each segment having a different temperature as well. The temperature variation through the depth may cause thermal bowing towards the fire, and is critical to the estimation of the reduced capacity of the cross section at any time in the fire. The section capacity is calculated by aggregating the residual capacities of each segment in the cross section once their individual temperatures are known. The disadvantage of line elements is that local buckling or shear failures of the beam cannot be suitably modelled (Wang, 2002; Franssen *et al.*, 2009). These require 3D modelling of the beam with brick or shell elements.

11.6.4.3 Slabs

Slabs are structural members with two dimensions much larger than the third dimension. They are normally modelled with shell or plate finite elements, as these model 2D planar behaviour. However, slabs can be modelled with brick elements as well, as shown in Figure 11.21 which shows a finite element model of a composite connection with the concrete slab made up of brick elements and the frame elements (beam and column) made up of shell elements. The column shown here is a rectangular concrete-filled tubular section, with only a quarter section shown, due to the symmetry of the problem (Franssen *et al.*, 2009).

The general cross section of a steel-concrete composite slab is shown in Figure 11.22(a). Shell elements treat slabs as being flat. With fire exposure only at the bottom, slabs are normally discretized as horizontal layers of thin strips of concrete and reinforcing, as shown in Figure 11.22(b). Reinforcing bars are modelled as thin steel layers that have the same cross-sectional area per unit length of the slab. These layers can also be modified to act only in one direction. Different stress–strain relationships can be specified for each layer, based on their

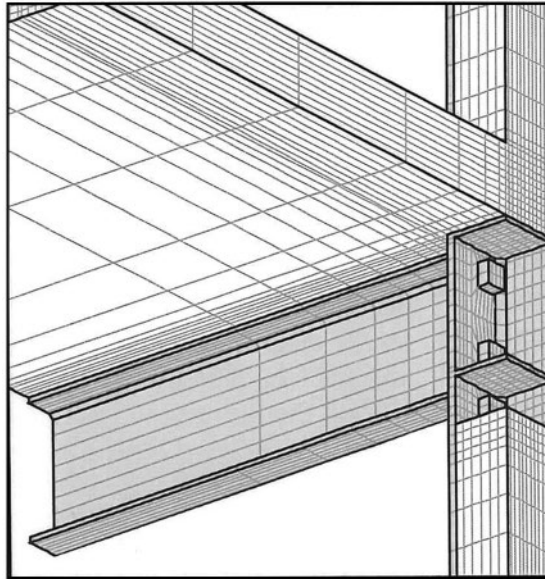


Figure 11.21 Three-dimensional model of a composite connection. Reproduced from Franssen *et al.* (2009) with permission from CRC Press

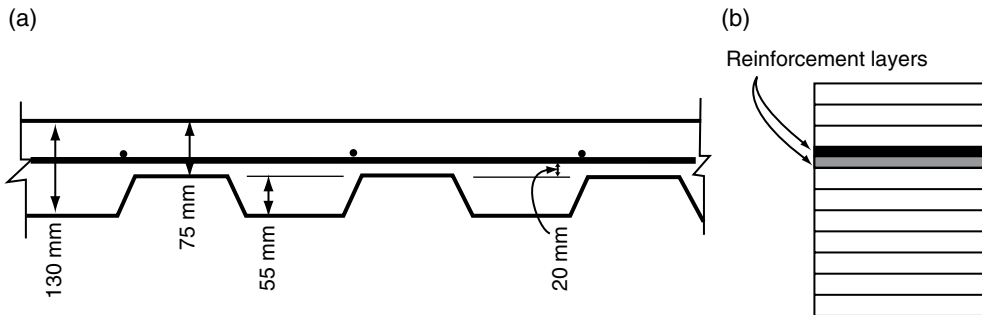


Figure 11.22 Modelling composite slabs with shell elements. (a) Profile of a Hibond composite slab. (b) Layered shell element

unique temperatures. Cracking of concrete is typically distributed over the surface of the element rather than being concentrated at specific points – this approach is known as the smeared cracking approach.

There are three different ways to transform the original slab cross section in Figure 11.22(a) into the discretized flat form in Figure 11.22(b). This can be achieved by:

1. Modelling the full depth of the slab.
2. Modelling the average (or effective) depth of the slab.
3. Modelling the thin continuous depth of the slab (above the trough).

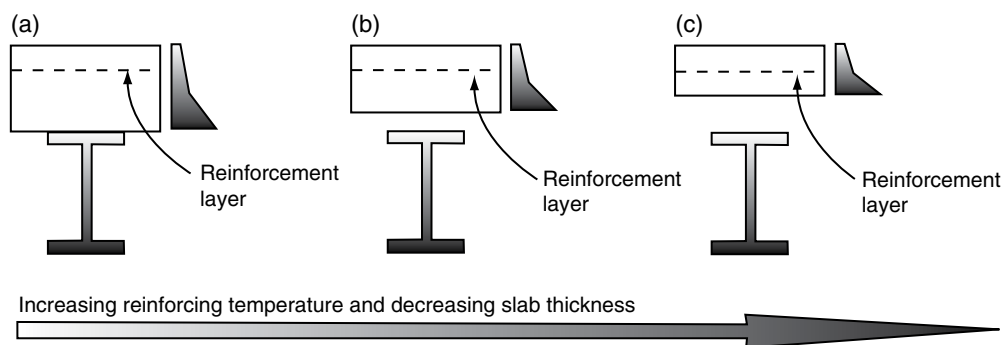


Figure 11.23 Options for modelling composite slabs in fire conditions: (a) full depth; (b) average depth; and (c) thin continuous depth

The three approaches are schematically explained in Figure 11.23. A full depth flat slab is stiffer in bending than the profiled slab in Figure 11.22(a). Hence modelling with option 1 requires a reduction of bending stiffness in the direction parallel to the ribs. That is achieved by using what is known as an effective stiffness approach (Huang *et al.*, 2000) which assigns relative stiffnesses to both directions to effectively mimic the different bending stiffnesses. Option 2 generates an equivalent flat slab that has the same overall bending stiffness as the full composite cross section, the same in both directions. Annex D of Eurocode 4 Part 1.2 (CEN, 2005c) provides a calculation method to determine the effective depth, based on the original slab profile (either trapezoidal or re-entrant). Option 3 is the most conservative. It requires that only the top continuous concrete (above the trough) is discretized as a flat slab. This option has the highest reinforcing temperatures and the lowest bending stiffness, ensuring that the design would be appropriate since the real stiffness will be greater and the actual reinforcing temperatures (in the parts above the ribs) will be lower.

11.6.4.4 Connections

The contribution of connections to the global behaviour of structures at elevated temperatures can be accounted for in two ways: using 1D spring elements; or by using detailed 3D analysis with shell or brick elements. When the finite element model is required to represent a large part of the structure with several beam-to-beam and column-to-column connections, the use of spring elements is ideal. They have zero length, are placed between two connecting structural members, and can have axial and/or rotational stiffness. Default spring connections are either classified as pinned or rigid connections. Semi-rigid connections, whose behaviour is between those of pinned and rigid connections, may be given specific stiffnesses based on their physical configuration. The use of the component method (CEN, 2005c) allows spring element characteristics to be defined based on an assemblage of springs that represent the components of the joint.

Figure 11.24 shows a schematic diagram for an endplate connection. This approach allows the incorporation of realistic connection features into the structural analysis, without excessive computational demands, making it effective in tracking the changes in internal forces that occur throughout the fire (Block *et al.*, 2007).

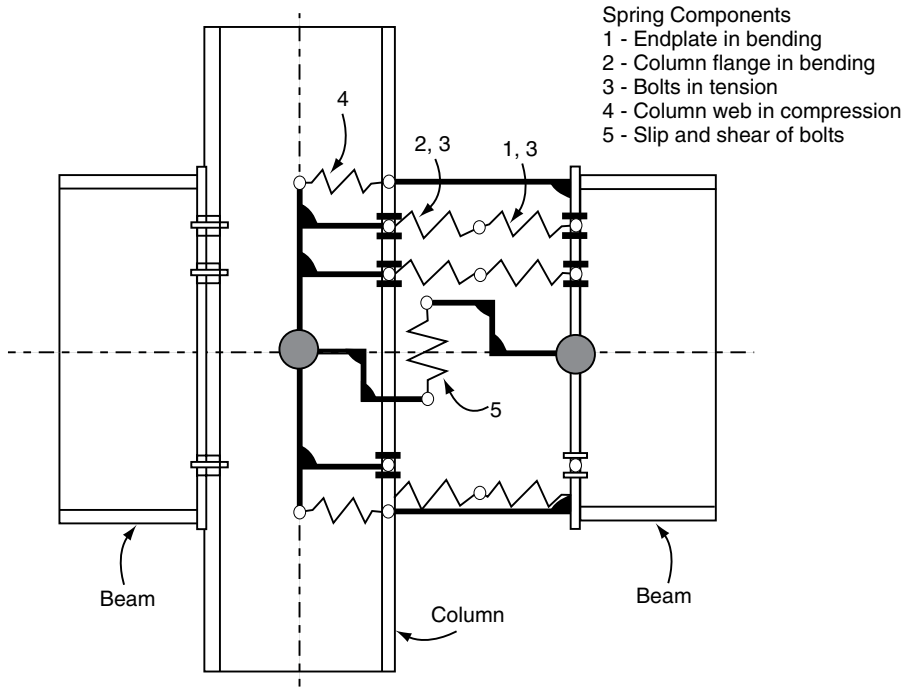


Figure 11.24 Component modelling of spring connections. 1, Endplate in bending; 2, column flange in bending; 3, bolts in tension; 4, column web in compression; and 5, slip and shear of bolts. Reproduced from Block *et al.* (2007) with permission from Elsevier Science

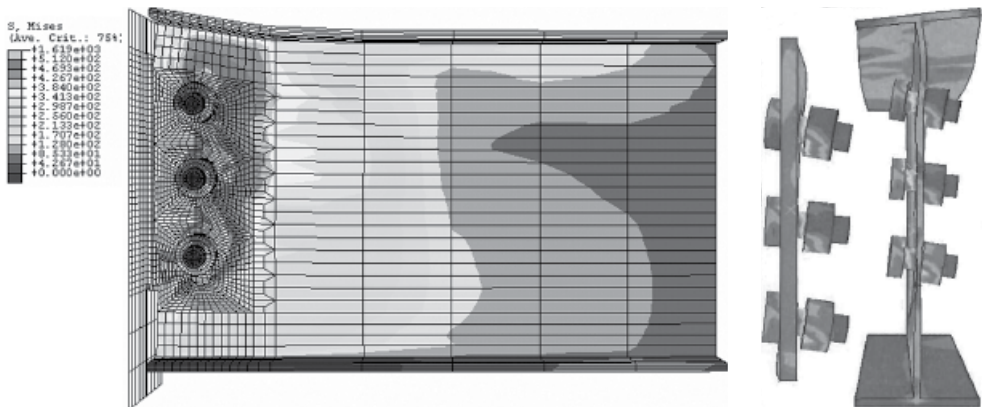


Figure 11.25 Three-dimensional model of a fin plate connection. Reproduced from Sarraj (2007 with permission from M. Sarraj

On the other hand, when a more detailed failure sequence of the connection is required then a 3D model of the connection allows the investigation of the build-up of stresses and deformations at various locations. Figure 11.25 shows a 3D analysis of a fin-plate connection in fire. The figure shows the full 3D model of the connection on the left-hand side, highlighting the stresses

around the fin plate. The deformations of the beam, fin plate and bolts are shown on the right-hand side. This type of analysis gives much more accurate local stresses than the simple analysis shown in Figure 11.24, with much more preparation time and computer run time, but this level of detail is not necessary for predicting the overall fire behaviour of the whole structure.

11.7 Software Packages for Structural and Thermal Fire Analysis

The preceding section identified the material and structural components needed for finite element modelling at elevated temperatures. A number of software packages available for structural fire analysis are described in the section. There are two main types:

1. Generic software packages
2. Specific structural fire engineering software packages

The generic software packages are designed for use by many other disciplines (e.g. mechanical engineering, computational fluid dynamics, etc.), and they are sophisticated enough to allow structural fire analysis. The specific packages on the other hand have been progressively developed by universities or other research institutions that investigate the specific behaviour of structures under fire conditions.

An important consideration in the selection of any software for structural fire analysis is that it should be validated for the type of analysis which the user intends investigating. One advantage of the specific software packages over the generic ones is that they have been extensively validated through their development for fire engineering, while there may not be specific validation information for the generic packages. On the other hand, the generic packages have vast libraries of elements, solution procedures and alternative analyses for various scenarios. The choice of the type of package may be determined by the specific use, and available resources.

11.7.1 Generic Software Packages

The most common generic software packages are ABAQUS, ANSYS and DIANA. These have not been specifically developed for structural fire analysis, but they allow the definition of various material properties to aid structural fire design. They can perform both thermal and structural analysis. Although some have the capability of performing coupled thermal and mechanical analysis, these have not been extensively explored and compared with known experimental data. Their rich element libraries mean that they can perform several different levels of analysis, from simple (1D elements) to complex (3D elements) structures. Their versatility also allows them to be used for many different materials.

Although they may not have specific validation information for structural fire analysis, these generic packages have been used to investigate a number of structures under fire conditions. For example, ABAQUS was used to study the steel and composite frames in the Cardington tests (Gillie, 1999), and is well suited to modelling reinforced concrete behaviour (Law, 2010) and timber structures in fire conditions (O'Neill, 2013). ANSYS has been used to model timber behaviour under fire conditions (Werther *et al.*, 2012) while DIANA has also been used to model the Cardington tests (Both *et al.*, 1996) and hollow core slabs in fire (Fellinger, 2004; Van Overbeek *et al.*, 2010).

The main disadvantages of the generic software packages are the cost of owning a licence, which includes the initial purchase cost, on-going licence fees, and upskilling of staff to use the software. For these reasons most designers prefer using specific structural fire engineering software packages.

11.7.2 *Specific Structural Fire Engineering Software*

A number of specialist software packages exist for structural fire engineering. A history of their development is given by Wang (2002). Some have ceased development, and are not discussed here. The three most popular software packages currently in circulation are ADAPTIC, SAFIR and VULCAN. Brief descriptions of their capabilities are given below.

11.7.2.1 ADAPTIC

The ADAPTIC software was developed at Imperial College, London (Izzuddin, 1991) to study non-linear dynamic behaviour of framed structures at room temperature. It was later extended to include fire effects on steel-framed structures and reinforced concrete slabs. A key feature of the software is its ability to model progressive collapse – the dynamic capability is able to track the behaviour of the structure after instability occurs. Recent additions to the software include slab elements that can handle orthotropy and large deflections under elevated temperature (Izzuddin and Elghazouli, 2004a, 2004b).

11.7.2.2 SAFIR

SAFIR has been developed at the University of Liege, Belgium by Franssen (2011). It can handle both thermal and mechanical analysis at elevated temperatures. For thermal analysis it performs 1D, 2D and 3D analysis. For structural analysis it has truss elements, 1D line elements, 2D shell elements and 3D brick elements. Its thermal analysis covers steel, timber and concrete materials, but it only has material constitutive laws for steel and concrete. Users can however define their own material model laws. It has pre- and post-processors for ease of use, and can handle thermal analyses of cross sections with voids (e.g. hollow core slabs and timber box beams). Its shell elements are capable of modelling large-deflection behaviour. Recent studies have used the software to model connections of precast prestressed concrete slabs (Min, 2012) and steel connections (Hanus, 2010).

11.7.2.3 VULCAN

VULCAN has been developed at the University of Sheffield, UK by successive researchers since 1985. It was initially developed to investigate 2D steel frames at room temperature. This was extended to 3D, with the capability to model concrete slabs added later (Bailey, 1995). Further development of the software included the capacity for semi-rigid connections (Bailey, 1995), and a layered slab approach (Huang *et al.*, 1999). It is limited in its element library, which only has 1D beam-column elements, spring elements and shell elements. More recent developments have included brick elements (Yu *et al.*, 2010) and progressive collapse (Song, 2009; Sun *et al.*, 2012). The software can only perform limited thermal analysis.

12

Design Recommendations

This chapter gives a brief summary of the recommendations outlined in this book for structural design of fire-exposed buildings constructed from structural steel, concrete or timber.

12.1 Summary of Main Points

The overall design approach is to compare the estimated *fire severity* with the *fire resistance* of the selected structural assembly. The comparison can be made in the *time domain* by comparing fire resistance times, in the *temperature domain* by comparing the maximum temperature with a critical value, or in the *strength domain* by comparing the actual load on the structure during the fire with the minimum load capacity at any point in the fire exposure.

12.1.1 Fire Exposure

There are four recommended levels for estimating the fire exposure:

1. The traditional level of fire exposure is simply the fire resistance time specified in a prescriptive code, based on the *standard fire* test. This can be compared with a generic or proprietary fire resistance rating.
2. The next level of fire exposure is to estimate the severity of the expected real fire based on fuel load, ventilation and construction materials, and use the *equivalent fire severity*, to give the equivalent time of exposure to the standard fire that would produce the same effect on the structural members.

3. The preferred method is to use the actual time temperature curve for a *realistic fire* in the compartment, using the Eurocode parametric fire. Any estimation of real fire temperatures involves some uncertainties, but calculations using a time–temperature curve will be more accurate than the equivalent fire severity method.
4. For special cases it may be appropriate to use a more advanced fire exposure model such as a CFD model for the fire compartment, or a plume model for local fire exposure.

12.1.2 Fire Resistance

There are three recommended levels at which fire resistance can be estimated:

1. The simplest method is to select from a list of *generic* or *proprietary* fire resistance ratings for the structural element or assembly. Sometimes it is appropriate to modify or extrapolate the listed rating for different loads or support conditions.
2. A more sophisticated method is to carry out simple structural calculations of load-bearing capacity, or critical temperature, to compare with conditions expected during the fire.
3. The most comprehensive method is to use advanced calculation methods for both thermal response and load-bearing capacity throughout the duration of the expected fire, as described in Chapter 11.

Selection from these options will depend on many factors, including the importance of the structure and the materials being used. Increasing levels of complexity are needed when moving from simple to advanced methods of calculating internal temperatures and structural capacity, most often providing benefits of increased accuracy. Recommended design methods for each material are discussed separately below.

12.2 Summary for Main Materials

Table 12.1 lists a hierarchy of design methods for the main materials, depending on which level of fire exposure is selected, or required by the local building code. It is recommended that a realistic fire be considered wherever possible, using a parametric time–temperature curve.

12.2.1 Structural Steel

For structural steel, the easiest design method is to compare a proprietary listing for protected steelwork with the fire severity prescribed by the code. The next level of accuracy is to use the time equivalent formula rather than the code-prescribed severity. Most proprietary listings for steel assume that the member is always loaded to its full design capacity, so considerable savings can be made by calculating the residual strength during standard fire exposure and comparing that with the actual design load in fire conditions, especially if the member has been over-designed for gravity loads.

Table 12.1 Summary of fire design methods for the main structural materials

Material	Prescribed fire resistance	Time equivalent formula	Realistic fire exposure
Structural steel	Compare with proprietary listing	Compare with proprietary listing Calculate residual strength in standard fire	Calculate residual strength in real fire
Steel-concrete composite slabs	Compare with proprietary or generic listing	Compare with proprietary listing Calculate residual strength in standard fire Use the slab panel method	Calculate residual strength in real fire Use the slab panel method with advanced analysis
Reinforced concrete	Compare with generic listing	Compare with generic listing Calculate residual strength in standard fire	Calculate residual strength in real fire
Heavy timber	Calculate strength of residual cross section	Calculate strength of residual cross section	Calculate strength of residual cross section
Light frame construction	Compare with proprietary listing	Compare with proprietary listing	No simple design methods

For single steel members, the residual strength can be easily calculated if the maximum steel temperature during the fire is known, as described in Chapter 6. Calculations of fire resistance can be made either in the strength domain or the temperature domain, with a simple transformation between the two. The strength domain, comparing applied loads with the load capacity, is recommended because it is more familiar to structural engineers.

For any steel structures which are more complex than simple beams, advanced calculation methods are necessary to assess the effects of thermal expansion and contraction, large deformations, and high thermal gradients in the structure during the fire.

12.2.2 Reinforced Concrete

For reinforced concrete structures, most typical building designs will have sufficient fire resistance to meet prescriptive code requirements, or time equivalent fire severity, with no special treatment. The design can be assessed by comparing the required fire resistance with listed generic ratings, or the residual strength under exposure to the standard fire can be calculated as described in Chapter 7. In special cases it will be appropriate to carry out advanced fire engineering calculations for exposure to realistic fires.

Considering the structural response, a hierarchy of calculation methods is as follows:

1. For simply supported slabs or tee-beams exposed to fire from below, concrete in the compression zone remains at normal temperatures, so structural design need only consider the effect of elevated temperatures on the yield strength of the reinforcing steel. Simple hand calculations are possible.
2. For continuous slabs or beams, some of the fire-exposed surfaces are in compression, so the simple hand calculation methods must consider the effects of elevated temperature on the compression strength of the concrete.
3. Similar methods can be applied to fire-exposed concrete walls and columns, but these methods are less accurate because of deformations caused by non-uniform heating and the possibility of instability failures.
4. For moment-resisting frames, or structural members affected by axial restraint and non-uniform heating, it is recommended to use advanced calculation methods.

12.2.3 Steel-concrete Composite Construction

For composite structures made up of steel and concrete materials, the easiest design approach is to use proprietary listings for fire resistance of protected steelwork and provide minimum concrete cover for insulation and integrity. This proprietary fire resistance can then be compared with the prescribed fire severity. The composite behaviour of the structural member ensures that this is the most conservative design method. This simple design approach can also be achieved by using tabulated data.

The next level of design is to use the time equivalent formula to calculate a fire severity and determine the residual strength of the structural member during exposure to the standard fire. For downstand composite beams with a steel beam depth less than 500 mm and a concrete flange thickness greater than 120 mm, Eurocode 4 allows the critical temperature method to be used to estimate the residual capacity. For all other composite members, design should be done in the strength domain. Parametric fire scenarios have not been verified for any composite systems other than downstand beams.

The slab panel design approach may be used for the design of composite floors in structures where tensile membrane action can be activated. Advanced calculation methods are recommended for all other fire exposure scenarios that are not specifically covered by simple calculation approaches. These range from simple composite columns exposed to parametric fires to full-frame analyses of composite structures.

12.2.4 Heavy Timber

For heavy timber construction exposed to the standard fire, strength can be calculated using the residual cross section after charring as described in Chapter 9. Fire resistance under more realistic fires can be assessed using the time equivalent formula or the Eurocode parametric fire with the charring rates from Annex A of Eurocode 5, but neither of these methods has been extensively verified, so they must be used with caution.

12.2.5 Light Frame Construction

For light frame construction, the recommended design method consists of selecting a listed proprietary assembly with a fire resistance rating greater than the design fire resistance, which is the fire resistance prescribed by the code, or an equivalent time of fire exposure calculated for a burnout of the fire compartment. Advanced calculations of thermal and structural behaviour in real fires are possible, but difficult, so they are only recommended for research and development purposes.

Table 12.2 Summary of thermal calculation methods for the main structural materials

Material	Calculation method	Notes
Structural steel	Charts for standard fire exposure (no thermal gradient in the steel)	
	Step-by-step method (no thermal gradient in the steel)	Easy to use
	Advanced calculation methods (to calculate thermal gradients)	Easy to write a spreadsheet program Requires access to suitable software
Reinforced concrete	Published temperature contours for standard fire exposure	Widely available, easy to use
	Wickström's formula for standard fire exposure	Easy to use
	Advanced calculation methods	Requires access to suitable software
Steel concrete composite	Charts for standard fire exposure (thermal gradient in the steel)	Easy to use
	Moment capacity method:	
	1. No thermal gradient in the steel	Easy to write a spreadsheet program
	2. Thermal gradients in the steel	Requires access to suitable software
	Advanced calculation methods	
Heavy timber	Thermal analysis not required	
Light frame construction	Thermal analysis not required	

12.3 Thermal Analysis

Most calculation methods require estimation of member temperatures. Table 12.2 summarizes the available tools for calculating internal temperatures in structural assemblies. The recommended design methods are limited by the availability of suitable heat transfer tools. Simple step-by-step methods can be easily used for calculating temperatures of protected or unprotected steel members in situations where thermal gradients are not important. Advanced calculation methods must be used for steel structures with non-uniform temperature gradients and for reinforced concrete structures exposed to real fires, where almost no published temperatures are available and hand calculations may not be accurate.

Thermal analysis calculations are not generally necessary for heavy timber construction or light frame structures.

12.4 Conclusions

Severe fires in large buildings are rare and unpredictable events, but when they occur they can cause great damage and loss of life. Structural fire design is a small but very important part of the overall process of providing fire safety in buildings. Safer buildings can help to reduce the risk of loss of life and property in the event of unwanted fires.

This book provides simple methods of designing building structures to resist fires, based on understanding of fire severity, fire resistance, and the behaviour of materials and structures at elevated temperatures, and it also describes the main considerations for performing advanced thermal and structural analyses of fire-exposed structures.

Appendix A

Units and Conversion Factors

This book uses metric units throughout. These are generally SI (Système International) units. The SI unit for length is the *metre* (m), for time the *second* (s), and for mass the *kilogram* (kg). Weight is expressed using the *newton* (N) where one newton is the force that gives a mass of one kilogram an acceleration of one metre per second per second. On the surface of the earth, one kilogram weighs approximately 9.81 newtons because the acceleration due to gravity is 9.81 m/s².

The SI unit of stress or pressure is the *pascal* (Pa) which is one newton per square metre (N/m²). It is more common to express stress using the megapascal (MPa) which is one meganewton per square metre (MN/m²) or identically one newton per square millimetre (N/mm²).

The SI unit of heat or energy or work is the *joule* (J) defined as the work done when the point of application of one newton is displaced one metre. Heat or energy is more often expressed in thousands of joules [kilojoules (kJ)] or millions of joules [megajoules (MJ)]. The basic unit for rate of power or heat release rate is the *watt* (W). One watt is one joule per second, hence a kilowatt (kW) is a thousand joules per second and a megawatt (MW) is a megajoule per second.

The SI prefixes for multiples and submultiples of units are:

Factor	Prefix	Symbol
10 ¹²	tera	T
10 ⁹	giga	G
10 ⁶	mega	M
10 ³	kilo	k
10 ²	hecto	h

(Continued)

Factor	Prefix	Symbol
10	deka	da
10 ⁻¹	deci	d
10 ⁻²	centi	c
10 ⁻³	milli	m
10 ⁻⁶	micro	μ
10 ⁻⁹	nano	n

Commonly used conversion factors are given in the following table (Lie, 1972). A much more extensive list of units and conversion factors can be found in the SFPE Handbook (SFPE, 2008). Units that are in accordance with Système International d'Unités are marked (SI).

Quantity	Multiply	By	To obtain
Activation energy	J/kg (SI)	4.302×10^{-4}	Btu/lb
Area	m ² (SI)	10.8	ft ²
	cm ² (SI)	0.155	in ²
Coefficient of expansion (linear)	m/m K (SI)	0.556	in/in °F
	m/m °C	0.556	in/in °F
Coefficient of expansion (cubic)	m ³ /m ³ K (SI)	0.556	in ³ /in ³ °F
	m ³ /m ³ °C	0.556	in ³ /in ³ °F
Coefficient of heat transfer	W/m ² K (SI)	0.176	Btu/ft ² h °F
	kcal/m ² h °C	0.205	Btu/ft ² h °F
	kcal/m ² h °C	1.166	W/m ² K (SI)
	kcal/m ² h °C	2.78×10^{-5}	cal/cm ² s °C
	cal/cm ² s °C	7.364×10^3	Btu/ft ² h °F
Density	cal/cm ² s °C	4.184×10^4	W/m ² K (SI)
	kg/m ³ (SI)	6.24×10^{-2}	lb/ft ³
	g/cm ³ (SI)	62.4	lb/ft ³
Energy	g/cm ³ (SI)	1×10^3	kg/m ³ (SI)
	J (SI)	9.48×10^{-4}	Btu
	kcal	3.966	Btu
	kcal	4.184×10^3	J (SI)
	cal	1.000	cal
	cal	3.966×10^{-3}	Btu
Fire load	cal	4.184	J (SI)
	kg (SI)	2.205	lb
Fire load density	kg/m ² (SI)	0.205	lb/ft ²
Flux (heat)	W (SI)	0.948	Btu/s
	kcal/h	3.966	Btu/h
	kcal/h	1.166	W (SI)
	kcal/h	0.278	cal/s
	cal/s	3.966×10^{-3}	Btu/s
	cal/s	14.278	Btu/h
	cal/s	4.184	W (SI)

Quantity	Multiply	By	To obtain
Flow rate	m ³ /s (SI)	35.3	ft ³ /s
Frequency	Hz (SI)	1	c/s
Force	N (SI)	0.225	lbf
	N (SI)	0.102	kgf
	kgf	2.205	lbf
Heat	see Energy		
Heat of combustion	J/kg (SI)	4.302×10^{-4}	Btu/lb
	kcal/kg	1.8	Btu/lb
	kcal/kg	4.184×10^3	J/kg (SI)
Intensity (heat)	W/m ² (SI)	0.317	Btu/ft ² h
	cal/cm ² s	1.326×10^4	Btu/ft ² h
	cal/cm ² s	4.184×10^4	W/m ² (SI)
Latent heat	J/kg (SI)	4.3×10^{-4}	Btu/lb
	kcal/kg	1.8	Btu/lb
	kcal/kg	4.184×10^3	J/kg (SI)
Length	m (SI)	3.281	ft
	cm (SI)	0.394	in
Mass	kg (SI)	2.205	lb
Modulus of elasticity	see Stress		
Opening factor	m ^{1/2} (SI)	1.811	ft ^{1/2}
Power	W (SI)	3.41	Btu/h
	W (SI)	9.48×10^{-4}	Btu/s
Pressure	see Stress		
Proportional limit	see Stress		
Rate of burning	kg/s (SI)	7.938×10^3	lb/h
	kg/h	2.205	lb/h
Rate of heating	see Flux (heat)		
Rate of heating per unit area	see Intensity (heat)		
Specific heat	J/kg K (SI)	2.39×10^{-4}	Btu/lb °F
	kcal/kg °C	1	Btu/lb °F
	cal/g °C	4.184×10^3	J/kg K (SI)
Specific heat (volumetric)	J/m ³ K (SI)	1.49×10^{-5}	Btu/ft ³ °F
	kcal/m ³ °C	6.234×10^{-2}	Btu/ft ³ °F
Stress	N/m ² (SI)	2.09×10^{-2}	lbf/ft ²
	N/m ² (SI)	1.45×10^{-4}	lbf/in ² (psi)
	MPa	145	lbf/in ² (psi)
	kgf/m ²	0.205	lbf/ft ²
	kgf/m ²	1.422×10^{-3}	lbf/in ²
	kgf/m ²	9.807	N/m ² (SI)
	kgf/cm ²	14.22	lbf/in ²
	kgf/cm ²	9.807×10^{-4}	N/m ² (SI)
Temperature	K (SI)	°C = K - 273.15	°C
	K (SI)	°F = 1.8 K - 459.67	°F
	K (SI)	°R = 1.8 K	°R
	°C	°F = 1.8 °C + 32	°F
	°C		

(Continued)

(Continued)

Quantity	Multiply	By	To obtain
Temperature interval	K (SI)	1.8	°F
	°C	1.8	°F
Thermal capacity	J/K (SI)	5.267×10^{-4}	Btu/°F
	kcal/°C	2.203	Btu/°F
	cal/°C	4.184	J/K (SI)
Thermal conductivity	W/m K (SI)	0.578	Btu/ft h °F
	kcal/m h °C	0.673	Btu/ft h °F
	kcal/m h °C	1.162	W/m K (SI)
	kcal/m h °C	2.78×10^{-3}	cal/cm s °C
	cal/cm s °C	241.8	Btu/ft h °F
	cal/cm s °C	418.4	W/m K (SI)
Thermal diffusivity	m ² /s (SI)	3.875×10^4	ft ² /h
	m ² /h	10.765	ft ² /h
	cm ² /s (SI)	0.36	m ² /h
	cm ² /s (SI)	1×10^{-4}	m ² /s (SI)
Velocity	m/s (SI)	3.281	ft/s
	km/h	0.278	m/s (SI)
	cm/min	0.394	in/min
Viscosity (dynamic)	N s/m ² (SI)	2.09×10^{-2}	lbf s/ft ²
	kg/ms	0.672	lb/ft s
Viscosity (kinematic)	m ² /s (SI)	10.8	ft ² /s
Volume	m ³ (SI)	35.32	ft ³
	cm ³ (SI)	6.1×10^{-2}	in ³
Wavelength	m (SI)	10 ¹⁰	Å
	μm (SI)	10 ⁴	Å
Weight	N (SI)	0.225	lbf
	N (SI)	0.102	kgf
	kgf	2.205	lbf

Appendix B

Section Factors for Steel Beams

This appendix provides section factors for standard hot rolled I-beams. The sections have been selected from published data for:

- North American Wide Flange Beams
- Australian Universal Beams
- UK Universal Beams
- Japanese H Sections
- IPE Narrow Flange Beams

The following tables give the dimensions and weight of each beam, but not the structural section properties which must be obtained from standard section property tables. The section factors have been calculated assuming that all sections are made from rectangular components, with no allowance for tapered flanges and root radii, and assuming that the protective insulation is in contact with the steel.

The tables do not include column sections, box sections, angles and channels. Section factors for these, and other sizes and shapes, can be calculated or can be obtained from manufacturer's literature.

The numbers in these tables have been obtained from The Heavy Engineering Research Association of New Zealand (HERA, 1996). Neither HERA nor the authors guarantee the accuracy of the tabulated data which can be calculated from standard section property tables. The geometrical data were obtained from the following sources. The North American Wide Flange Beam data are from the structural sections catalogue 'British Steel SPCS 4237/99' from British Steel. The Australian Universal Beam data are from the 'BHP Hot Rolled and Structural Steel Products' catalogue from BHP Steel (1998). The UK Universal Beam data are from the

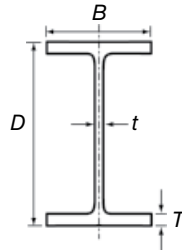


Figure B.1 Geometry of hot rolled section

‘Structural Sections Catalogue’ from British Steel (1996). The values for the Japanese H Sections are from the structural sections catalogue ‘Wide Flange Shapes Cat. No. EXE 210, Dec.1980’ from the Nippon Steel Corporation.

The basic geometry for a hot rolled I-beam is shown in Figure B.1.

North American Wide Flange Beams

Section factor

Contour

Hollow

3 Sides

4 Sides

3 Sides

4 Sides

4 Sides

3 Sides

4 Sides

3 Sides

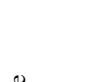
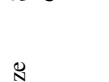
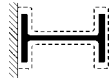
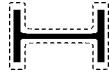
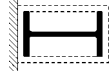
4 Sides

3 Sides

4 Sides

3 Sides

4 Sides



Size	Metric size	Section depth	Section width	Thickness Flange	Web	Contour				Hollow							
						D	B	T	t	F/N	V/F	F/N	V/F	F/N	V/F	F/N	V/F
in x lb/ft	mm x kg/m	mm	mm	mm	mm	mm	mm	mm	mm	mm	mm	mm	mm	mm	mm	mm	mm
W24 x 94	W610 x 140	618	230	22.2	13.1	9.4	106	119	8.4	82	12.2	95	10.5				
W24 x 84	W610 x 125	612	229	19.6	11.9	8.4	118	133	7.5	91	11.0	106	9.5				
W24 x 76	W610 x 113	608	228	17.3	11.2	7.7	130	146	6.9	100	10.0	116	8.6				
W24 x 68	W610 x 101	603	228	14.9	10.5	6.9	144	162	6.2	111	9.0	128	7.8				
W24 x 62	W610 x 92	603	179	15.0	10.9	6.8	146	162	6.2	118	8.5	133	7.5				
W24 x 55	W610 x 82	599	178	12.8	10.0	6.1	164	181	5.5	132	7.6	149	6.7				
W20 x 82	W530 x 123	544	212	21.2	13.1	9.2	108	122	8.2	83	12.1	96	10.4				
W20 x 73	W530 x 109	540	211	18.8	11.6	8.2	122	137	7.3	93	10.8	108	9.3				
W20 x 68	W530 x 101	537	210	17.4	10.9	7.7	130	146	6.8	99	10.1	116	8.7				
W20 x 62	W530 x 92	533	209	15.6	10.2	7.0	142	160	6.3	108	9.2	126	7.9				
W20 x 57	W530 x 85	535	167	16.5	10.3	7.0	143	159	6.3	114	8.7	130	7.7				
W20 x 50	W530 x 74	529	166	13.6	9.7	6.2	161	179	5.6	129	7.8	146	6.8				
W20 x 44	W530 x 66	525	165	11.4	8.9	5.5	182	202	4.9	145	6.9	165	6.1				
W18 x 71	W460 x 106	469	194	20.6	12.6	9.0	111	125	8.0	84	11.9	98	10.2				
W18 x 65	W460 x 97	466	193	19.0	11.4	8.3	121	137	7.3	92	10.9	107	9.3				
W18 x 60	W460 x 89	463	192	17.7	10.5	7.7	147	147	6.8	98	10.2	115	8.7				
W18 x 55	W460 x 82	460	191	16.0	9.9	7.1	159	159	6.3	106	9.4	125	8.0				
W18 x 50	W460 x 74	457	190	14.5	9.0	6.4	175	175	5.7	117	8.6	137	7.3				
W18 x 46	W460 x 68	459	154	15.4	9.1	6.4	174	174	5.8	123	8.1	141	7.1				
W18 x 40	W460 x 60	455	153	13.3	8.0	5.6	198	198	5.0	140	7.1	160	6.2				
W18 x 35	W460 x 52	450	152	10.8	7.6	4.9	202	225	4.4	159	6.3	182	5.5				

(Continued)

North American Wide Flange Beams

Section factor

Size	Metric size	Section depth	Section width	Thickness Flange	Web	Contour				Hollow			
						3 Sides		4 Sides		3 Sides		4 Sides	
						F/V	V/F	F/V	V/F	F/V	V/F	F/V	V/F
W16 × 57	W410 × 85	417	181	18.2	10.9	125	8.0	142	7.0	94	10.7	111	9.0
W16 × 50	W410 × 75	413	180	16.0	9.7	141	7.1	160	6.2	106	9.5	124	8.0
W16 × 45	W410 × 67	410	179	14.4	8.8	156	6.4	177	5.7	116	8.6	137	7.3
W16 × 40	W410 × 60	407	178	12.8	7.7	176	5.7	199	5.0	131	7.6	154	6.5
W16 × 36	W410 × 53	403	177	10.9	7.5	194	5.1	220	4.5	144	6.9	170	5.9
W16 × 31	W410 × 46	403	140	11.1	7.0	207	4.8	231	4.3	161	6.2	185	5.4
W16 × 26	W410 × 39	399	140	8.8	6.4	241	4.1	269	3.7	188	5.3	216	4.6
W14 × 38	W360 × 57	358	172	13.1	7.9	169	5.9	192	5.2	123	8.1	147	6.8
W14 × 34	W360 × 51	355	171	11.6	7.2	188	5.3	214	4.7	137	7.3	163	6.1
W14 × 30	W360 × 45	352	171	9.8	6.9	210	4.8	240	4.2	153	6.6	182	5.5
W14 × 26	W360 × 39	353	128	10.7	6.5	216	4.6	242	4.1	168	6.0	193	5.2
W14 × 22	W360 × 33	349	127	8.5	5.8	256	3.9	286	3.5	198	5.1	228	4.4
W12 × 22	W310 × 33	313	102	10.8	6.6	220	4.5	244	4.1	174	5.7	199	5.0
W12 × 19	W310 × 28	309	102	8.9	6.0	252	4.0	280	3.6	199	5.0	227	4.4
W12 × 16	W310 × 24	305	101	6.7	5.6	297	3.4	330	3.0	234	4.3	267	3.7
W10 × 30	W250 × 45	266	148	13.0	7.6	168	6.0	194	5.2	119	8.4	145	6.9
W10 × 26	W250 × 39	262	147	11.2	6.6	193	5.2	223	4.5	136	7.3	166	6.0
W10 × 22	W250 × 33	258	146	9.1	6.1	226	4.4	261	3.8	159	6.3	194	5.2
W10 × 19	W250 × 28	260	102	10.0	6.4	224	4.5	252	4.0	171	5.8	200	5.0
W10 × 17	W250 × 25	257	102	8.4	6.1	250	4.0	281	3.6	191	5.2	222	4.5
W10 × 15	W250 × 22	254	102	6.9	5.8	282	3.5	318	3.1	214	4.7	250	4.0
W8 × 21	W200 × 31	210	134	10.2	6.4	202	4.9	236	4.2	139	7.2	172	5.8
W8 × 18	W200 × 27	207	133	8.4	5.8	237	4.2	276	3.6	161	6.2	201	5.0

Australian Universal Beams

Section factor

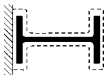
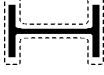
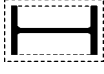
Size	Mass kg/m	Section depth mm	Section width mm	Thickness Flange mm	Web Thickness mm	t	Contour				Hollow			
							3 Sides		4 Sides		3 Sides		4 Sides	
							F/V	V/F	F/V	V/F	F/V	V/F	F/V	V/F
610 UB	125.0	612	229	19.6	11.9	mm	m ⁻¹	mm	mm	m ⁻¹	mm	mm	m ⁻¹	mm
610 UB	113.0	607	228	17.3	11.2	mm	118	8.5	7.6	91	11.0	105	9.5	9.5
610 UB	101.0	602	228	14.8	10.6	mm	129	7.7	6.9	99	10.1	115	8.7	8.7
530 UB	92.4	533	209	15.6	10.2	mm	144	7.0	6.2	110	9.1	128	7.8	7.8
530 UB	82.0	528	209	13.2	9.6	mm	142	7.1	6.3	108	9.3	126	8.0	8.0
460 UB	82.1	460	191	16.0	9.9	mm	140	6.3	5.6	120	8.3	140	7.1	7.1
460 UB	74.6	457	190	14.5	9.1	mm	154	7.1	6.3	106	9.5	124	8.1	8.1
460 UB	67.1	454	190	12.7	8.5	mm	170	6.5	5.7	116	8.6	136	7.4	7.4
410 UB	59.7	406	178	12.8	7.8	mm	174	5.9	5.2	128	7.8	150	6.7	6.7
410 UB	53.7	403	178	10.9	7.6	mm	192	5.7	5.1	130	7.7	153	6.5	6.5
360 UB	56.7	359	172	13.0	8.0	mm	168	5.2	4.6	143	7.0	169	5.9	5.9
360 UB	50.7	356	171	11.5	7.3	mm	187	5.9	5.2	123	8.1	147	6.8	6.8
360 UB	44.7	352	171	9.7	6.9	mm	210	5.3	4.7	136	7.3	163	6.1	6.1
310 UB	46.2	307	166	11.8	6.7	mm	185	4.8	4.2	153	6.5	183	5.5	5.5
310 UB	40.4	304	165	10.2	6.1	mm	209	5.4	4.7	132	7.6	160	6.3	6.3
310 UB	32.0	298	149	8.0	5.5	mm	253	4.8	4.1	148	6.7	180	5.6	5.6
250 UB	37.3	256	146	10.9	6.4	mm	197	4.0	3.5	183	5.5	219	4.6	4.6
250 UB	31.4	252	146	8.6	6.1	mm	232	5.1	4.4	139	7.2	169	5.9	5.9
250 UB	25.7	248	124	8.0	5.0	mm	262	4.3	3.7	162	6.2	199	5.0	5.0
						mm	300	3.8	3.3	190	5.3	228	4.4	4.4

(Continued)

Australian Universal Beams

Section factor

Size	Mass	Section depth	Section width	Thickness Flange	Web	t	Contour				Hollow			
							3 Sides		4 Sides		3 Sides		4 Sides	
							F/N	V/F	F/N	V/F	F/N	V/F	F/N	V/F
200 UB	29.8	207	134	9.6	6.3	210	4.8	245	4.1	143	7.0	179	5.6	
200 UB	25.4	203	133	7.8	5.8	246	4.1	287	3.5	167	6.0	208	4.8	
200 UB	22.3	202	133	7.0	5.0	276	3.6	323	3.1	187	5.3	233	4.3	
200 UB	18.2	198	99	7.0	4.5	295	3.4	338	3.0	213	4.7	256	3.9	
180 UB	22.2	179	90	10.0	6.0	218	4.6	250	4.0	159	6.3	191	5.2	
180 UB	18.1	175	90	8.0	5.0	265	3.8	304	3.3	191	5.2	230	4.3	
180 UB	16.1	173	90	7.0	4.5	298	3.4	342	2.9	214	4.7	258	3.9	
150 UB	18.0	155	75	9.5	6.0	227	4.4	260	3.8	167	6.0	200	5.0	
150 UB	14.0	150	75	7.0	5.0	289	3.5	331	3.0	211	4.7	253	4.0	



UK Universal Beams

Section factor

Size	Mass kg/m	Section depth mm	Section width mm	Thickness Flange mm	Web mm	t mm	Contour						Hollow					
							3 Sides		4 Sides		3 Sides		4 Sides		3 Sides		4 Sides	
							F/V	V/F										
686x254 UB	170	693	256	23.7	14.5	98	10.2	110	9.1	76	13.2	87	11.4					
686x254 UB	152	688	255	21.0	13.2	109	9.2	122	8.2	84	11.9	97	10.3					
686x254 UB	140	684	254	19.0	12.4	118	8.5	132	7.6	91	11.0	105	9.5					
686x254 UB	125	678	253	16.2	11.7	132	7.6	147	6.8	101	9.9	117	8.5					
610x305 UB	238	636	311	31.4	18.4	72	14.0	82	12.2	52	19.1	63	16.0					
610x305 UB	179	620	307	23.6	14.1	94	10.7	107	9.3	68	14.7	81	12.3					
610x305 UB	149	612	305	19.7	11.8	111	9.0	127	7.8	81	12.4	97	10.4					
610x229 UB	140	617	230	22.1	13.1	107	9.4	120	8.4	82	12.2	95	10.5					
610x229 UB	125	612	229	19.6	11.9	119	8.4	133	7.5	91	10.9	106	9.5					
610x229 UB	113	608	228	17.3	11.1	130	7.7	146	6.8	100	10.0	116	8.6					
610x229 UB	101	603	228	14.8	10.5	145	6.9	162	6.2	111	9.0	129	7.8					
533x210 UB	122	545	212	15.6	10.1	146	6.9	164	6.1	111	9.0	129	7.7					
533x210 UB	109	540	211	13.2	9.6	161	6.2	181	5.5	123	8.1	143	7.0					
533x210 UB	101	537	210	21.3	12.7	108	9.2	122	8.2	83	12.1	96	10.4					
533x210 UB	92	533	209	18.8	11.6	120	8.3	135	7.4	92	10.9	107	9.4					
533x210 UB	82	528	209	17.4	10.8	129	7.8	145	6.9	98	10.2	114	8.8					
457x191 UB	98	467	193	19.6	11.4	119	8.4	135	7.4	90	11.1	106	9.5					
457x191 UB	89	463	192	17.7	10.5	130	7.7	147	6.8	98	10.2	115	8.7					
457x191 UB	82	460	191	16.0	9.9	142	7.1	160	6.2	107	9.4	125	8.0					
457x191 UB	74	457	190	14.5	9.0	155	6.4	175	5.7	117	8.6	137	7.3					

(Continued)

UK Universal Beams

Section factor

Contour

Hollow

3 Sides 4 Sides 3 Sides 4 Sides



Size	Mass kg/m	Section depth mm	Section width mm	Thickness Flange mm	Web mm	t mm	Contour				Hollow											
							D mm	B mm	T mm	F/N m ⁻¹	V/F mm											
457×191 UB	67	453	190	12.7	8.5	8.5	171	193	5.9	128	193	5.2	128	193	5.2	128	193	7.8	150	7.8	150	6.6
457×152 UB	82	466	155	18.9	10.5	10.5	131	146	7.6	104	146	6.9	104	146	6.9	104	146	9.7	118	9.7	118	8.5
457×152 UB	74	462	154	17.0	9.6	9.6	145	161	6.9	114	161	6.2	114	161	6.2	114	161	8.8	130	8.8	130	7.7
457×152 UB	67	458	154	15.0	9.0	9.0	159	177	6.3	125	177	5.7	125	177	5.7	125	177	8.0	143	8.0	143	7.0
457×152 UB	60	455	153	13.3	8.1	8.1	177	197	5.6	139	197	5.1	139	197	5.1	139	197	7.2	159	7.2	159	6.3
457×152 UB	52	450	152	10.9	7.6	7.6	201	224	5.0	158	224	4.5	158	224	4.5	158	224	6.3	181	6.3	181	5.5
406×178 UB	74	413	180	16.0	9.5	9.5	142	161	7.0	106	161	6.2	106	161	6.2	106	161	9.4	125	9.4	125	8.0
406×178 UB	67	409	179	14.3	8.8	8.8	156	177	6.4	117	177	5.6	117	177	5.6	117	177	8.6	138	8.6	138	7.3
406×178 UB	60	406	178	12.8	7.9	7.9	174	197	5.7	130	197	5.1	130	197	5.1	130	197	7.7	153	7.7	153	6.5
406×178 UB	54	403	178	10.9	7.7	7.7	192	217	5.2	142	217	4.6	142	217	4.6	142	217	7.0	168	7.0	168	5.9
406×140 UB	46	403	142	11.2	6.8	6.8	208	232	4.8	162	232	4.3	162	232	4.3	162	232	6.2	186	6.2	186	5.4
406×140 UB	39	398	142	8.6	6.4	6.4	243	272	4.1	189	272	3.7	189	272	3.7	189	272	5.3	217	5.3	217	4.6
356×171 UB	67	363	173	15.7	9.1	9.1	144	164	7.0	105	164	6.1	105	164	6.1	105	164	9.5	126	9.5	126	8.0
356×171 UB	57	358	172	13.0	8.1	8.1	168	191	6.0	122	191	5.2	122	191	5.2	122	191	8.2	146	8.2	146	6.8
356×171 UB	51	355	172	11.5	7.4	7.4	186	213	5.4	136	213	4.7	136	213	4.7	136	213	7.4	162	7.4	162	6.2
356×171 UB	45	351	171	9.7	7.0	7.0	210	240	4.8	153	240	4.2	153	240	4.2	153	240	6.6	182	6.6	182	5.5
356×127 UB	39	353	126	10.7	6.6	6.6	215	240	4.6	167	240	4.2	167	240	4.2	167	240	6.0	193	6.0	193	5.2
356×127 UB	33	349	125	8.5	6.0	6.0	252	282	4.0	196	282	3.5	196	282	3.5	196	282	5.1	225	5.1	225	4.4
305×165 UB	54	310	167	13.7	7.9	7.9	161	185	6.2	114	185	5.4	114	185	5.4	114	185	8.7	139	8.7	139	7.2
305×165 UB	46	307	166	11.8	6.7	6.7	187	215	5.4	133	215	4.6	133	215	4.6	133	215	7.5	161	7.5	161	6.2

305×165 UB	40	303	165	10.2	6.0	212	4.7	245	4.1	150	6.6	183	5.5
305×127 UB	48	311	125	14.0	9.0	160	6.2	181	5.5	122	8.2	143	7.0
305×127 UB	42	307	124	12.1	8.0	182	5.5	205	4.9	138	7.2	162	6.2
305×127 UB	37	304	123	10.7	7.1	204	4.9	231	4.3	155	6.4	181	5.5
305×102 UB	33	313	102	10.8	6.6	220	4.5	244	4.1	174	5.7	199	5.0
305×102 UB	28	309	102	8.8	6.0	254	3.9	282	3.5	200	5.0	229	4.4
305×102 UB	25	305	102	7.0	5.8	286	3.5	318	3.1	225	4.4	257	3.9
254×146 UB	43	260	147	12.7	7.2	173	5.8	200	5.0	122	8.2	149	6.7
254×146 UB	37	256	146	10.9	6.3	199	5.0	230	4.4	139	7.2	171	5.9
254×146 UB	31	251	146	8.6	6.0	234	4.3	271	3.7	163	6.1	200	5.0
254×102 UB	28	260	102	10.0	6.3	226	4.4	254	3.9	173	5.8	201	5.0
254×102 UB	25	257	102	8.4	6.0	253	4.0	284	3.5	193	5.2	224	4.5
254×102 UB	22	254	102	6.8	5.7	286	3.5	323	3.1	218	4.6	254	3.9
203×133 UB	30	207	134	9.6	6.4	210	4.8	245	4.1	143	7.0	178	5.6
203×133 UB	25	203	133	7.8	5.7	248	4.0	290	3.4	169	5.9	210	4.8

Japanese H Sections

Section factor

Contour

Hollow

Size	Mass kg/m	Section depth mm	Section width mm	Thickness Flange mm	Web mm	3 Sides				4 Sides				3 Sides				4 Sides									
						F/N	V/F	F/V	V/F	F/N	V/F	F/V	V/F	F/N	V/F	F/V	V/F	F/N	V/F	F/V	V/F						
800×300 H	241	808	302	30.0	16.0	81	12.4	91	11.0	62	16.0	72	13.9	800×300 H	210	800	300	26.0	14.0	92	10.8	104	9.6	71	14.1	82	12.2
800×300 H	191	792	300	22.0	14.0	101	9.9	113	8.8	77	12.9	90	11.1	800×300 H	215	708	302	28.0	15.0	84	11.9	95	10.5	63	15.9	74	13.5
700×300 H	185	700	300	24.0	13.0	97	10.4	109	9.1	72	13.9	85	11.8	700×300 H	166	692	300	20.0	13.0	107	9.4	121	8.3	80	12.6	94	10.7
600×300 H	175	594	302	23.0	14.0	93	10.8	106	9.4	67	14.9	81	12.4	600×300 H	175	588	300	20.0	12.0	107	9.4	122	8.2	77	13.0	92	10.8
600×300 H	137	582	300	17.0	12.0	117	8.6	134	7.5	84	11.9	101	9.9	600×300 H	134	612	202	23.0	13.0	106	9.5	118	8.5	84	12.0	95	10.5
600×200 H	120	606	201	20.0	12.0	117	8.5	131	7.7	93	10.8	106	9.4	600×200 H	106	600	200	17.0	11.0	132	7.6	147	6.8	104	9.6	119	8.4
600×200 H	95	596	199	15.0	10.0	147	6.8	163	6.1	115	8.7	132	7.6	600×200 H	128	488	300	18.0	11.0	113	8.8	132	7.6	78	12.8	96	10.4
500×300 H	114	482	300	15.0	11.0	127	7.9	147	6.8	87	11.5	107	9.3	500×300 H	103	506	201	19.0	11.0	121	8.2	137	7.3	92	10.8	108	9.3
500×200 H	90	500	200	16.0	10.0	138	7.2	156	6.4	105	9.5	123	8.2	500×200 H	80	496	199	14.0	9.0	155	6.4	175	5.7	118	8.5	137	7.3
450×300 H	124	440	300	18.0	11.0	112	9.0	131	7.6	75	13.3	94	10.6														

450×300 H	106	434	299	15.0	10.0	129	7.7	151	6.6	86	11.6	109	9.2
450×200 H	76	450	200	14.0	9.0	153	6.5	174	5.8	114	8.8	134	7.4
450×200 H	66	446	199	12.0	8.0	175	5.7	198	5.0	129	7.7	153	6.5
400×300 H	107	390	300	16.0	10.0	122	8.2	144	6.9	79	12.6	101	9.9
400×300 H	94	386	299	14.0	9.0	137	7.3	162	6.2	89	11.2	114	8.8
400×200 H	66	400	200	13.0	8.0	165	6.1	188	5.3	119	8.4	143	7.0
400×200 H	57	396	199	11.0	7.0	191	5.2	218	4.6	137	7.3	165	6.1
350×250 H	80	340	250	14.0	9.0	139	7.2	164	6.1	92	10.9	116	8.6
350×250 H	69	336	249	12.0	8.0	159	6.3	187	5.3	104	9.6	133	7.5
350×175 H	50	350	175	11.0	7.0	192	5.2	220	4.6	139	7.2	166	6.0
350×175 H	41	346	174	9.0	6.0	228	4.4	261	3.8	164	6.1	197	5.1
300×200 H	65	298	201	14.0	9.0	143	7.0	168	6.0	97	10.3	121	8.3
300×200 H	57	294	200	12.0	8.0	162	6.2	190	5.3	109	9.2	137	7.3
300×150 H	37	300	150	9.0	6.5	222	4.5	254	3.9	160	6.2	192	5.2
300×150 H	32	298	149	8.0	5.5	253	4.0	289	3.5	183	5.5	219	4.6
250×175 H	44	244	175	11.0	7.0	178	5.6	209	4.8	118	8.5	149	6.7
250×125 H	30	250	125	9.0	6.0	229	4.4	262	3.8	166	6.0	199	5.0
250×125 H	26	248	124	8.0	5.0	263	3.8	300	3.3	190	5.3	228	4.4
200×150 H	31	194	150	9.0	6.0	212	4.7	250	4.0	138	7.3	176	5.7
200×100 H	21	200	100	8.0	5.5	254	3.9	291	3.4	184	5.4	221	4.5
200×100 H	18	198	99	7.0	4.5	295	3.4	338	3.0	214	4.7	256	3.9

IPe Narrow Flange Beams

Section factor

Contour

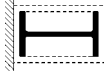
Hollow

3 Sides

4 Sides

3 Sides

4 Sides



Size	Mass kg/m	Section depth mm	Section width mm	Thickness Flange mm	Thickness Web mm	t mm	3 Sides		4 Sides		3 Sides		4 Sides	
							F/V m ⁻¹	V/F mm						
600R IPE	144.0	608	218	23.0	14.0	10.0	112	8.9	78	12.8	90	11.1		
600O IPE	155.0	610	224	24.0	15.0	10.6	106	9.4	73	13.6	85	11.8		
600A IPE	108.0	597	220	17.5	9.8	7.5	150	6.7	103	9.7	119	8.4		
600 IPE	122.0	600	220	19.0	12.0	8.5	132	7.6	91	11.0	105	9.5		
550R IPE	134.0	560	210	22.2	14.0	9.9	114	8.8	78	12.8	91	11.0		
550O IPE	123.0	556	212	20.2	12.7	9.1	124	8.1	85	11.8	98	10.2		
550A IPE	92.1	547	210	15.7	9.0	6.9	164	6.1	111	9.0	129	7.7		
550 IPE	106.0	550	210	17.2	11.1	7.8	143	7.0	98	10.2	113	8.8		
500R IPE	111.0	508	198	20.0	12.6	9.0	126	8.0	85	11.7	99	10.1		
500O IPE	107.0	506	202	19.0	12.0	8.6	131	7.6	89	11.3	103	9.7		
500A IPE	79.4	497	200	14.5	8.4	6.4	176	5.7	118	8.5	138	7.2		
500 IPE	90.7	500	200	16.0	10.2	7.3	153	6.5	103	9.7	121	8.3		
450R IPE	95.2	458	188	18.6	11.3	8.3	136	7.4	91	11.0	107	9.4		
450O IPE	92.4	456	192	17.6	11.0	8.0	141	7.1	94	10.7	110	9.1		
450A IPE	67.2	447	190	13.1	7.6	5.9	192	5.2	127	7.9	149	6.7		
450 IPE	77.6	450	190	14.6	9.4	6.8	166	6.0	110	9.1	130	7.7		
400R IPE	81.5	407	178	17.0	10.6	7.8	145	6.9	95	10.5	113	8.9		
400O IPE	75.7	404	182	15.5	9.7	7.2	157	6.4	103	9.7	122	8.2		
400A IPE	57.4	397	180	12.0	7.0	5.5	205	4.9	133	7.5	158	6.3		
400 IPE	66.3	400	180	13.5	8.6	6.4	178	5.6	116	8.6	137	7.3		
360R IPE	70.3	366	168	16.0	9.9	7.4	154	6.5	100	10.0	119	8.4		

360O IPE	66.0	364	172	14.7	9.2	146	6.9	166	6.0	107	9.3	127	7.8
360A IPE	50.2	357	170	11.5	6.6	189	5.3	216	4.6	138	7.2	165	6.1
360 IPE	57.1	360	170	12.7	8.0	167	6.0	190	5.3	122	8.2	146	6.9
330R IPE	60.3	336	158	14.5	9.2	147	6.8	167	6.0	108	9.3	129	7.8
330O IPE	57.0	334	162	13.5	8.5	157	6.4	179	5.6	114	8.7	137	7.3
330A IPE	43.0	327	160	10.0	6.5	205	4.9	234	4.3	149	6.7	178	5.6
330 IPE	49.1	330	160	11.5	7.5	180	5.6	205	4.9	131	7.6	157	6.4
300R IPE	51.7	306	147	13.7	8.5	157	6.4	180	5.6	115	8.7	137	7.3
300O IPE	49.3	304	152	12.7	8.0	167	6.0	191	5.2	121	8.3	145	6.9
300A IPE	36.5	297	150	9.2	6.1	222	4.5	254	3.9	160	6.3	192	5.2
300 IPE	42.2	300	150	10.7	7.1	193	5.2	220	4.5	139	7.2	167	6.0
270R IPE	44.0	276	133	13.1	7.7	167	6.0	191	5.2	122	8.2	146	6.8
270O IPE	42.3	274	136	12.2	7.5	175	5.7	200	5.0	127	7.9	152	6.6
270A IPE	30.7	267	135	8.7	5.5	237	4.2	272	3.7	171	5.8	206	4.9
270 IPE	36.1	270	135	10.2	6.6	203	4.9	232	4.3	147	6.8	176	5.7
240R IPE	37.3	245	118	12.3	7.5	175	5.7	199	5.0	128	7.8	153	6.5
240O IPE	34.3	242	122	10.8	7.0	191	5.2	219	4.6	139	7.2	167	6.0
240A IPE	26.2	237	120	8.3	5.2	247	4.0	283	3.5	178	5.6	214	4.7
240 IPE	30.7	240	120	9.8	6.2	212	4.7	242	4.1	153	6.5	184	5.4
220R IPE	31.6	225	108	11.8	6.7	189	5.3	216	4.6	139	7.2	166	6.0
220O IPE	29.4	222	112	10.2	6.6	205	4.9	235	4.3	149	6.7	179	5.6
220A IPE	22.2	217	110	7.7	5.0	266	3.8	305	3.3	192	5.2	231	4.3
220 IPE	26.2	220	110	9.2	5.9	227	4.4	260	3.8	165	6.1	198	5.1

References

- Aarnio, M. (1979) Glulam Timber Construction and the Fire Resistance of the Joints [in Finnish]. Helsinki School of Technology, Division of Building Engineering, Diploma Work. Otnas.
- Aarnio, M. and Kallioniemi, P. (1983) Fire Safety in Joints of Load Bearing Timber Construction [in Finnish]. VTT Research Report No. 233. Technical Research Centre of Finland.
- ABAQUS (2010) Version 6.10, Dassault Systèmes Simulia Corporation, Providence, RI.
- ABCB (2005) *International Fire Engineering Guidelines* (IFEG). Australian Building Codes Board, Canberra, ACT.
- ABCB (2015) *National Construction Code Series 2015 Volume 1, Building Code of Australia Class 2 to Class 9 Buildings*. Australian Building Codes Board, Canberra, ACT.
- Abrams, M.S. and Gustafarro, A.H. (1968) *Fire Endurance of Concrete Slabs as Influenced by Thickness, Aggregate Type and Moisture*. Research Bulletin 223. Research and Development Laboratories of the Portland Cement Association, Skokie, IL.
- Abrams, M.S. and Gustafarro, A.H. (1971) Fire tests of poke-through assemblies. *Fire Journal*, May.
- Abu, A.K. (2009) Behaviour of composite floor systems in fire. PhD thesis, University of Sheffield.
- Abu, A.K., Ramanitarivo, V. and Burgess, I.W. (2011) Collapse mechanisms of composite slab panels in fire. *Journal of Structural Fire Engineering*, **2**(3), 205–216.
- ACI (2007) Code Requirements for Determining the Fire Endurance of Concrete and Masonry Construction Assemblies. ACI 216.1-07. American Concrete Institute, Detroit, MI.
- Ahmed, G.N. and Hurst, J.P. (1995) Modelling the thermal behaviour of concrete slabs subjected to the ASTM E119 standard fire condition. *Journal of Fire Protection Engineering*, **7**(4), 125–132.
- AISI (1991) North American Specification for the Design of Cold-Formed Steel Structural Members. American Iron and Steel Institute, Washington, DC.
- Aldea, C.-M., Franssen, J.-M. and Dotrepe, J.-C. (1997) Fire test on normal and high strength reinforced concrete columns. Proceedings of the International Workshop on Fire Performance of High Strength Concrete, NIST Special Publication 919. National Institute of Standards and Technology, Gaithersburg, MD, pp. 109–124.
- Alfawakhiri, F. and Sultan, M.A. (1999) Fire resistance of load-bearing steel-stud walls protected with gypsum board: a review. *Fire Technology*, **35**(4), 308–335.
- Al-Jabri, K.S., Lennon, T., Burgess, I.W. and Plank R.J. (1998) Behaviour of steel and composite beam-column connections in fire. *Journal of Constructional Steel Research*, **46**, 1–3.
- Allen, L.W. (1970) *Fire Endurance of Selected Non-Loadbearing Concrete Masonry Walls*. DBR Fire Study No. 25. Division of Building Research, National Research Council of Canada, Ottawa.

- Almand, K. (1989) 'The Role of Passive Systems in Fire Safety Design in Buildings', *Fire Safety and Engineering - International Symposium Papers*. The Warren Centre, University of Sydney, Australia. pp 103–129
- Anderberg, Y. (1976) *Fire Exposed Hyperstatic Concrete Structures - An Experimental and Theoretical Study*. Division of Structural Mechanics and Concrete Construction. Lund Institute of Technology, Lund.
- Anderberg, Y. (1986) Measured and predicted behaviour of steel beams and columns in fire. Lund Institute of Technology, Lund.
- Anderberg, Y. (1988) Modelling steel behaviour. *Fire Safety Journal*, **13**(1), 17–26.
- Anderberg, Y. (1989) *Fire Engineering Design Based on PC*. Nordic Mini-Seminar on Fire Resistance of Concrete Structures, Trondheim. Fire Safety Design, Lund.
- Anderberg, Y. and Forsen, N.E. (1982) *Fire Resistance of Concrete Structures*. Nordic Concrete Research Publication No.1, Oslo. Reprinted as Report LUTVDG/(TVBB-3009). Lund University, Lund.
- Anderberg Y. and Thelandersson, S. (1976) Stress and deformation of concrete at high temperatures 2 – Experimental investigation and material behaviour. Bulletin 54. Lund Institute of Technology, Lund.
- Andersen, N.E. and Lauridsen, D.H. (1999) TT-Roof Slabs. Hollow Core Concrete Slabs. Technical Report X52650, Parts 1 and 2. Danish Institute of Fire Technology, Hvidovre.
- ANSYS (2009) Version 12.0, ANSYS Inc., Canonsburg, PA.
- Armer, G.S.T. and O'Dell, T. (eds) (1996) Fire, static and dynamic tests of building structures. Proceedings of the Second Cardington Conference. E & FN Spon, London.
- ASCE (2005) ASCE/SEI/SFPE 29-05: Standard Calculation Method for Structural Fire Protection. American Society of Civil Engineers, Reston, VA.
- ASCE (2010) Minimum Design Loads for Buildings and Other Structures. American Society of Civil Engineers, Reston, VA.
- ASFP (2014) *Fire Protection for Structural Steel in Buildings*, 5th edn. Association of Specialist Fire Protection Contractors and Manufacturers, Bordon.
- ASTM, (2005) ASTM C1396/C1396M - 11 Standard Specification for Gypsum Board. American Society for Testing and Materials, West Conshohocken, PA.
- ASTM (2012) Standard Test Methods for Fire Tests of Building Construction and Materials, ASTM E119. American Society for Testing and Materials, West Conshohocken, PA.
- ASTM (2015) Standard Test Method for Surface Burning Characteristics of Building Materials. ASTM E84-15a. ASTM International, West Conshohocken, PA.
- AWC (2012) National Design Specification (NDS) for Wood Construction. American Wood Council, Washington, DC.
- AWC (2015) Calculating the Fire Resistance of Exposed Wood Members. Technical Report No. 10. American Wood Council, Washington, DC.
- Babrauskas, V. (1979) *COMP2: A Program for Calculating Post-Flashover Fire Temperatures*, NBS Technical Note 991, National Bureau of Standards, Gaithersburg, MD.
- Babrauskas, V. (1981) A closed form approximation for post flashover compartment fires. *Fire Safety Journal*, **4**, 63–73.
- Babrauskas, V. (2008) Heat release rates, in *SFPE Handbook of Fire Protection Engineering*, 4th edn, Society of Fire Protection Engineers, Gaithersburg, MD.
- Babrauskas, V. and Grayson, S.J. (1992) *Heat Release in Fires*, Elsevier Applied Science, Amsterdam. Reprinted 2009 by Interscience Communications Ltd, London.
- Babrauskas, V. and Peacock, R. D. (1992) Heat release rate: The single most important variable in fire hazard. *Fire Safety Journal*, **18**, 255–272.
- Babrauskas, V. and Williamson, R.B. (1978a) Post-flashover compartment fires – basis of a theoretical model. *Fire and Materials*, **2**(2), 39–53.
- Babrauskas, V. and Williamson, R.B. (1978b) Temperature measurement in fire test furnaces. *Fire Technology*, **14**(3), 226–238.
- Bailey, C.G. (1995) Simulation of the structural behaviour of steel framed buildings in fire. PhD thesis, University of Sheffield.
- Bailey, C. G. (2000) Design of Steel Structures with Composite Slabs at the Fire Limit State, Final Report No. 81415, prepared for DETR and SCI. The Building Research Establishment, Garston, UK.
- Bailey, C. G. (2001) Membrane action of unrestrained lightly reinforced concrete slabs at large displacements. *Engineering Structures*, **23**, 470–483.
- Bailey, C. G. (2003) Efficient arrangement of reinforcement for membrane behaviour of composite floors in fire conditions. *Journal of Constructional Steel Research*, **59**, 931–949.

- Bailey, C. G. (2004) Membrane action of slab/beam composite floor systems in fire. *Engineering Structures*, **26**, 1691–1703.
- Bailey, C.G. and Khoury, G.A. (2011) Performance of Concrete Structures in Fire. MPA – The Concrete Centre, London.
- Bailey, C. G. and Lennon, T. (2008) Full-scale fire tests on hollowcore floors. *The Structural Engineer*, **86**(6), 33–39.
- Bailey, C. G. and Moore, D. B. (2000a) The structural behaviour of steel frames with composite floor slabs subject to fire: Part 1: Theory. *The Structural Engineer*, **78**(11), 19–27.
- Bailey, C. G. and Moore, D. B. (2000b) The structural behaviour of steel frames with composite floor slabs subject to fire: Part 2: Design. *The Structural Engineer*, **78**(11), 28–33.
- Bailey, C. G. and Toh, W. S. (2007) Behaviour of concrete floor slabs at ambient and elevated temperatures. *Fire Safety Journal*, **42**, 425–436.
- Bailey, C.G., Burgess, I.W. and Plank, R.J. (1996a) Analyses of the Effects of cooling and fire spread on steel-framed buildings. *Fire Safety Journal*, **26**, 273–293.
- Bailey, C.G., Burgess, I.W. and Plank, R.J. (1996b) The lateral torsional buckling of unrestrained steel beams in fire. *Journal of Constructional Steel Research*, **36**(2), 101–119.
- Barnfield, J.R. and Porter, A.M. (1984) Historic buildings and fire: fire performance of cast-iron structural elements. *The Structural Engineer*, **62A**(12), 373–380.
- Bathe K. (1991) *Finite Element Procedures*, Prentice-Hall, Upper Saddle River, NJ.
- Bazant, Z.P. and Kaplan, M.F. (1996) *Concrete at High Temperatures – Material Properties and Mathematical Models*. Concrete Design and Construction Series. Longman Group Ltd, UK.
- Beck, V.R. and Yung, D. (1994) The development of a risk-cost assessment model for the evaluation of fire safety in buildings. Proceedings of the Fourth International Conference on Fire Safety Science, Ottawa, Canada, pp. 817–828.
- Bennetts, I.D., Poh, K.W. and Thomas, I.R. (1999) *Economical Carparks - A Guide to Fire Safety*. BHP Steel, Melbourne.
- Berto, A.F. and Tomina, J.C. (1988) Lições de incêndio da sede administrativa da Cesp. Tecnologia de Edificações - Instituto de Pesquisas Tecnológicas do Estado de São Paulo, Brazil.
- Block, F.M. (2006) Development of a component-based finite element for steel beam-to-column connections at elevated temperatures. PhD thesis, University of Sheffield.
- Block, F.M., Burgess, I.W., Davidson, J.B. and Plank, R.J. (2007) The development of a component-based connection element for endplate connections in fire. *Fire Safety Journal*, **42**, 498–506.
- Bodig, J. and Jayne, B.A. (1982) *Mechanics of Wood and Wood Composites*, Van Nostrand Reinhold, New York.
- Bolonius Olesen, F. and König, J. (1992) Tests on glued laminated beams in bending exposed to natural fires. Proceedings of the CIB-W18 Meeting, Åhus, Sweden. Trätekt Report No. I9210061.
- Bolonius Olesen, F. and Toft Hansen, F. (1992) Full-Scale Tests on Loaded Glulam Beams Exposed to Natural Fires. Aalborg University, Aalborg.
- Bond, G.V.L. (1975) Fire and Steel Construction – Water Filled Hollow Columns. Constrado, Croydon.
- Both, C., van Foeken, R.J. and Twilt, L. (1996) Analytical aspects of the Cardington test programme. Proceedings of the Second Cardington Conference, Building Research Establishment, Watford.
- Botting, R. (1998) The Impact of Post Earthquake Fire on the Built Urban Environment. Fire Engineering Research Report 98/1. University of Canterbury, New Zealand.
- Bregulla, J., Mackay, S. and Matthews, S. (2010) Fire safety on timber frame sites during construction. Proceedings of the World Conference on Timber Engineering, Riva del Gardo, Italy.
- Bresler, B. and Iding, R.H.J. (1982) Effect of Fire Exposure on Steel Frame Buildings. Final Report to American Iron and Steel Institute. Wiss, Janney Elstner Associates, Emeryville, CA.
- BSI (1978) Code of Practice for the Structural Use of Timber. BS 5268, Section 4.1. Methods of Calculating the Fire Resistance of Timber Members. British Standards Institution, UK.
- BSI (1985) Structural Use of Concrete. BS 8110. British Standards Institution, UK.
- BSI (1987) Fire Tests on Building Materials and Structures, BS 476 (Parts 1 to 23). British Standards Institution, UK
- BSI (1990) BS 5268. Structural Use of Timber. Part 4, Section 4.2. Recommendations for Calculating the Fire Resistance of Timber Stud Walls and Joisted Floor Constructions. British Standards Institution, UK.
- BSI (2001) BS 7974. Application of Fire Safety Engineering Principles to the Design of Buildings – Code of Practice. British Standards Institution, UK
- BSI (2003a) Application of Fire Safety Engineering Principles to the Design of Buildings – Part 1: Initiation and Development of Fire Within the Enclosure of Origin (Sub-system 1) – Published Document PD7974-1. British Standards Institution, UK.

- BSI (2003b) BS 5950-8. Structural Use of Steelwork in Buildings - Part 8: Code of Practice for Fire Resistant Design. British Standards Institution, UK
- BSI (2007) Background paper to the UK National Annex to BS EN 1991-1-2, PD 6688-1-2. British Standards Institution, UK
- Buchanan, A.H. (1990) The bending strength of lumber. *Journal of Structural Engineering, USA*, **116**(5), 1213–1229.
- Buchanan, A.H. (1994) Structural design for fire in New Zealand. Proceedings of the Australasian Structural Engineering Conference, Sydney, Australia, pp. 643–649.
- Buchanan, A.H. (2015) Fire resistance of multi-storey timber buildings. Proceedings of the AOSFST Conference, Tsukuba, Japan.
- Buchanan, A.H. and Barber, D.J. (1994) Fire resistance of epoxied steel rods in glulam. Proceedings of the 1994 Pacific Timber Engineering Conference, Gold Coast, Australia. Vol. 1, pp. 590–598.
- Buchanan, A.H. and King, A.B. (1991) Fire performance of gusset connections in glue-laminated timber. *Fire and Materials*, **15**, 137–143.
- Buchanan, A.H., Östman, B. and Frangi, A. (2014) Fire Resistance of Timber Structures. International R&D Roadmap for Fire Resistance of Structures, pp. F66 – F91. NIST Special Publication 1188, National Institute of Standards and Technology, Washington, DC.
- Buchanan A.H., Palermo A., Carradine D. and Pampanin S. (2011) Post-tensioned timber frame buildings. *Journal of Structural Engineering, UK*, **89**(17), 24–30.
- Butcher, E.G., Chitty, T.B. and Ashton, L.A. (1966) The Temperature Attained by Steel in Building Fires, Fire Research Technical Paper No. 15. H.M. Stationery Office, London.
- Cachim, P. B. and Franssen, J. M. (2009) Numerical modelling of timber connections under fire loading using a component model. *Fire Safety Journal*, **44**, 840–853.
- Cadorin, J.F., Pinteá, D. and Franssen, J.-M. (2001) The Design Fire Tool OZone V2.0 – Theoretical Description and Validation on Experimental Fire Tests. University of Liege, Liege.
- Caldwell, C.A., Buchanan, A.H. and Fleischmann, C.M. (1999) Documentation for performance-based fire engineering design in New Zealand. *Journal of Fire Protection Engineering*, **10**(2), 24–31.
- Canadian Standards Association. (2009) Design of Steel Structures (CSA S16-09). Canadian Standards Association, Mississauga, ON.
- Carling, O. (1989) Fire Resistance of Joint Details in Load Bearing Timber Construction - A Literature Survey [Translated from Swedish]. BRANZ Study Report SR 18. Building Research Association of New Zealand.
- Carlson, C.C., Selvaggio, S.L. and Gustaferro, A.H. (1965) A Review of Studies of the Effects of Restraint on the Fire Resistance of Prestressed Concrete. PCA Research Department Bulletin 206. Portland Cement Association, Skokie, IL.
- CEN (2002a), *Eurocode 0: Basis of structural design. EN 1990*. European Committee for Standardization, Brussels.
- CEN (2002b) *Eurocode 1: Actions on structures - Part 1-2: General actions - Actions on structures exposed to fire. EN 1991-1-2*. European Committee for Standardization, Brussels.
- CEN (2004a) *Eurocode 2: Design of concrete structures - Part 1-2: General rules – Structural fire design. EN 1992-1-2*. European Committee for Standardization, Brussels.
- CEN (2004b) *Eurocode 5: Design of timber structures - Part 1-2: General – Structural fire design. EN 1995-1-2*. European Committee for Standardization, Brussels.
- CEN (2005a) *Eurocode 3: Design of steel structures - Part 1-1: General rules and rules for buildings. EN 1993-1-1*. European Committee for Standardization, Brussels.
- CEN (2005b) *Eurocode 3: Design of steel structures - Part 1-2: General rules – Structural fire design. EN 1993-1-2*. European Committee for Standardization, Brussels.
- CEN (2005c) *Eurocode 4: Design of composite steel and concrete structures – Part 1-2: General rules - Structural fire design. EN 1994-1-2*. European Committee for Standardization, Brussels.
- CEN (2005d) *Eurocode 6: Design of masonry structures – Part 1-2: General rules – Structural fire design, EN 1996-1-2*. European Committee for Standardization, Brussels.
- CEN (2012) Fire resistance tests – Part 1: General Requirements, EN 1363-1. European Committee for Standardization, Brussels.
- CEN (2015) Durability of reaction to fire performance - Classes of fire-retardant treated wood products in interior and exterior end use applications. FprEN 16755 Final Draft. European Committee for Standardization, Brussels.
- Chang, J. J. (2007) Computer simulation of hollowcore concrete flooring systems exposed to fire. PhD thesis, University of Canterbury, New Zealand

- CIB (1986) Design guide – Structural fire safety, CIB-W14. *Fire Safety Journal*, **10**(2), 75–138.
- Clancy, P. (1999) Time and probability of failure of timber framed walls in fire. PhD thesis, Victoria University of Technology, Victoria, Australia.
- Clifton, G.C. (1996) Fire Models for Large Firecells. HERA Report R4-83, New Zealand Heavy Engineering Research Association, Auckland.
- Clifton, G.C. (2001) Design of multi-storey steel framed buildings with unprotected secondary beams or joists for dependable inelastic response in severe fires. *Steel Design and Construction Bulletin*, **60**, 1–58.
- Clifton, G.C. (2006) Design of Composite Steel Floor Systems for Severe Fires. HERA Report R4-131, Manukau City, Auckland.
- Clifton, G.C., Gillies, A.G. and Mago N. (2010) The slab panel method: design of composite floor systems for dependable inelastic response to severe fires. Proceedings of the 6th International Conference on Structures in Fire (SiF'10), 2–4 June 2010, East Lansing, MI, USA, pp. 492–499.
- Coakley, D., Greenspun, H. and Gerard, G.C. (1982) *The Day the MGM Grand Hotel Burned*. Lyle Stuart Inc., Secaucus, NJ.
- Collier, P.C.R. (1991a) Design of Light Timber Framed Walls and Floors for Fire Resistance. BRANZ Technical Recommendation No. 9. Building Research Association of New Zealand.
- Collier, P.C.R. (1991b) Design of Loadbearing Light Timber Frame Walls for Fire Resistance: Part 1. BRANZ Study Report SR36. Building Research Association of New Zealand.
- Collier, P.C.R. (1992) Charring Rates of Timber. BRANZ Study Report No. 42. Building Research Association of New Zealand.
- Collier, P.C.R. (1996) A model for predicting the fire resisting performance of small scale cavity walls in realistic fires. *Fire Technology*, **32**(2), 120–136.
- Collins, M.J. (1983) Density Conversions for Radiata Pine. FRI Bulletin No. 49. Forest Research Institute, Rotorua, New Zealand.
- Collins, G. (1998) Fire resistance of inter-tenancy wall connections in multi-residential timber-frame buildings. Proceedings of the 4th World Conference on Timber Engineering, Montreux, Switzerland. Vol. 2, pp. 114–121.
- Comeau, E. (1999) Roof collapse kills three. *NFPA Journal*, **94**(4) 77–80.
- Cook, R.D. (1995) *Finite Element Modelling for Stress Analysis*. John Wiley & Sons., Inc, New York.
- Cooke, G.M.E. (1988) Thermal Bowing in Fire and How It Affects Building Design. BRE Information Paper IP 21/88. Building Research Establishment, Watford.
- Cooke, G.M.E. (1996) A review of compartment fire tests to explore the behavior of structural steel. Fire, static and dynamic tests of building structures. Proceedings of the Second Cardington Conference. E & F.N. Spon, London, pp. 17–32.
- Cooke, G.M.E. (1997) The behaviour of sandwich panels exposed to fire. *Building Engineer*, **72**(6), 14–29.
- Cooper, L.Y. (1997) The Thermal Response of Gypsum Panel Steel Stud Wall Systems Exposed to Fire Environments. NISTR 6027. National Institute of Standards and Technology, Gaithersburg, MD.
- Cosgrove, B.W. (1996) Fire Design of Single Storey Industrial Buildings. Fire Engineering Research Report No 96/3. University of Canterbury, New Zealand.
- Costello, R.S., Abu, A.K., Moss, P.J. and Buchanan, A.H. (2014) Full scale tests of timber box beams in fire conditions. Proceedings of the 8th International Conference on Structures in Fire, 11–13 June 2014, Shanghai, China.
- Craft, S.T., Desjardins, R. and Richardson, L.R. (2008) Development of small-scale evaluation methods for wood adhesives at elevated temperatures. Proceedings of the World Conference on Timber Engineering, Miyazaki, Japan, 2–5 June 2008, pp. 583–590.
- Cramer, S.M. (1995) Fire endurance modelling of wood floor/ceiling assemblies. Proceedings of the Fire & Materials Conference, Washington, DC, pp. 105–114.
- Cramer, S.M., Shrestha, D. and Mtenga, P.V. (1993) Computation of member forces in metal plate connected wood trusses. *Structural Engineering Review*, **5**(3), 209–217.
- Custer, R.L.P. and Meacham, B.J. (1997) *Introduction to Performance-based Fire Safety*. Society of Fire Protection Engineers and National Fire Protection Association, Gaithersburg, MD.
- Deal, S. (1993) *Technical Reference Guide for FPEtool Version 3.2*. NISTR 5486, National Institute of Standards and Technology, Gaithersburg, MD.
- de Feijter M.P. and Breunese M.P. (2007) Investigation of Fire in the Lloydstraat Car Park – Efectis Report – R0894(E). Efectis, Rotterdam.
- del Senno, M., Cont, S. and Piazza, M. (1998) Charring rate slowing by means of fibreglass-reinforcing coatings. Proceedings of the 4th World Conference on Timber Engineering, Montreux, Switzerland. Vol. 2, pp. 230–237.

- Drysdale, D. (2011) *An Introduction to Fire Dynamics*, 3rd edn. John Wiley & Sons, Ltd, Chichester.
- Duchow, M. and Abu, A.K. (2014) Collapse mechanisms of edge and corner slab panels in fire conditions. Proceedings of the 8th International Conference on Structures in Fire, 11–13 June 2014, Shanghai, China, pp. 335–342.
- Dunn, V. (1988) *Collapse of Burning Buildings; a Guide to Fireground Safety*. Fire Engineering, PenWell Books, New York.
- ECCS (1983) Calculation of the Fire Resistance of Composite Concrete Slabs with Profiled Steel Sheet Exposed to the Standard Fire. Publication No. 32. European Commission for Constructional Steelwork, Brussels.
- ECCS (1985) Design Manual on the European Recommendations for the Fire Safety of Steel Structures. European Commission for Constructional Steelwork, Brussels, Belgium
- ECCS (1988) Calculation of the Fire Resistance of Centrally-loaded Composite Steel-concrete Columns Exposed to the Standard Fire. Technical Note No. 55. European Commission for Constructional Steelwork, Brussels.
- ECCS (1995) Fire Resistance of Steel Structures. ECCS Technical Note No. 89. Technical Committee 3, European Commission for Constructional Steelwork, Brussels.
- El-Rimawi, J.A. (1989) The behaviour of flexural members under fire conditions. PhD thesis, University of Sheffield.
- El-Rimawi, J.A. Burgess, I.W. and Plank, R.J. (1996) The treatment of strain reversal in structural members during the cooling phase of a fire. *Journal of Constructional Steel Research*, **37**(2), 115–135.
- England, J.P., Young, S.A., Hui, M.C. and Kurban, N. (2000) *Guide for the Design of Fire Resistant Barriers and Structures*, Building Control Commission, Melbourne.
- Erchinger, C., Frangi, A. and Fontana, M. (2010) Fire design of steel-to-timber dowelled connections. *Engineering Structures*, **32**(2), 580–589.
- Espinos, A., Romero, M.L. and Hospitaler, A. (2012) Simple calculation model for evaluating the fire resistance of unreinforced concrete filled tubular columns. *Engineering Structures*, **42**, 231–244.
- Espinos, A., Romero, M. L. and Hospitaler, A. (2013) Fire design method for bar-reinforced circular and elliptical concrete filled tubular columns. *Engineering Structures*, **56**, 384–395.
- Fellinger, J. H. H. (2004) Shear and Anchorage Behaviour of Fire Exposed Hollow Core Slabs. DUP Science, Delft.
- Fleischmann, C.M., Buchanan, A.H. and Chang, J. (2008) Analytical methods for determining fire resistance of concrete members, in *SFPE Handbook of Fire Protection Engineering*, 4th edn, Society of Fire Protection Engineers, Gaithersburg, MD, Ch. 4-10.
- Fontana, M. and Borgogno, W. (1995) Brandverhalten von Slim-Floor-Verbunddecken, in *Stahlbau* Ernst+ Sohn, Berlin, Vol. **64**, pp. 168–174.
- Fontana, M. and Frangi, A. (1999) Fire behaviour of timber-concrete composite slabs. Proceedings of the Sixth International Symposium on Fire Safety Science, Poitiers, France.
- Forsen, N.E. (1982) A Theoretical Study of the Fire Resistance of Concrete Structures. FCB-SINTEF Report STF65 A82062, Trondheim, Norway.
- Foster, S., Chladna, M., Hsieh, C., Burgess, I. and Plank, R. (2007) Thermal and structural behaviour of a full-scale composite building subject to a severe compartment fire. *Fire Safety Journal*, **42**, 183–199.
- Frangi, A., Erchinger, C. and Fontana, M. (2009a) Experimental fire analysis of steel-to-timber connections using dowels and nails. *Fire and Materials*, **34**(1): 1–19.
- Frangi, A., Fontana, M., Hugi, E. and Jöbstl, R. (2009b) Experimental analysis of cross-laminated timber panels in fire. *Fire Safety Journal*, **44**, 1078–1087.
- Frangi, A., Knobloch, M. and Fontana, M. (2009c) Fire design of slabs made of hollow core elements. *Engineering Structures*, **31**, 150–157.
- Frangi, A., Knobloch, M. and Fontana, M. (2010) Fire design of timber-concrete composite slabs with screwed connections. *Journal of Structural Engineering*, **136**, 219–228.
- Franssen, J.-M. (1990) The unloading of building materials submitted to fire. *Fire Safety Journal*, **16**, 213–227.
- Franssen, J.-M. (2000) Design of concrete columns based on EC2 tabulated data: a critical review. Proceedings of the First International Workshop on Structures in Fire, Copenhagen, Denmark.
- Franssen, J.-M. (2003) A thermal/structural program modelling structures under fire. Proceedings of the NASCC 2003, 2–4 April 2003, Baltimore, MD.
- Franssen, J.-M. (2011) *User's Manual for SAFIR 2011: A Computer Program for Analysis of Structures Subjected to Fire*, University of Liege, Liege.
- Franssen, J.-M and Bruls, A. (1997) Design and tests of prestressed concrete beams. Proceedings of the Fifth International Symposium of Fire Safety Science, Melbourne, Australia, pp. 1081–1092.
- Franssen, J.-M., Cajot, L.-G. and Schleich, J.-B. (1998) Natural fires in large compartments: Effects caused on the structure by localised fires in large compartments. Proceedings of the Eurofire'98 Conference, 11–13 March, Brussels, Belgium.

- Franssen, J.-M., Kodur, V.K.R. and Mason, J. (2000) *User's Manual for SAFIR: A Computer Program for Analysis of Structures Submitted to Fire*. Internal Report SPEC/2000_03. University of Liege, Liege.
- Franssen, J.-M., Kodur, V.K.R. and Zaharia, R. (2009) *Designing Steel Structures for Fire Safety*, CRC Press, Leiden.
- Franssen, J.-M., Schleich, J.-B. and Cajot, L.-G. (1995) A simple model for the fire resistance of axially loaded members according to Eurocode 3. *Journal of Constructional Steel Research*, **35**, 49–69.
- Fredlund, B. (1979) Structural Design of Fire Exposed Rectangular Laminated Wood Beams with Respect to Lateral Buckling. Report No. 79-5. Department of Structural Mechanics, Lund University of Technology, Lund.
- Fredlund, B. (1993) Modelling of heat and mass transfer in wood structures during fire. *Fire Safety Journal*, **20**(1), 36–69.
- Friquin, K.L., Grimsbu, M. and Hovde, P.J. (2010) Charring rates for cross-laminated timber panels exposed to parametric and standard fires. Proceedings of the 12th World Conference on Timber Engineering, Riva del Garda, Italy.
- Fuller, J.J., Leichti, R.J. and White, R.H. (1992) Temperature distribution in a nailed gypsum-stud joint exposed to fire. *Fire and Materials*, **16**, 95–99.
- Gagnon, S. and Pirvu, C. (eds) (2011) *CLT Handbook: Cross-Laminated Timber*, FPInnovations, Quebec, QC.
- Gamble, W.L. (1989) Predicting Protected steel member fire endurance using spreadsheet programs. *Fire Technology*, **25**(3), 256–273.
- Gann, R. G. (2008) Final Report on the collapse of the World Trade Center Building 7. National Institute of Building and Technology, Washington, DC.
- Gerard, R., Barber, D. and Wolski, A. (2013) *Fire Safety Challenges of Tall Wood Buildings*, Arup North America Ltd, San Francisco, CA and Fire Protection Research Foundation, Quincy, MA.
- Gerard R.B., Carradine, D.M., Moss, P.J. and Buchanan, A.H. (2010) Fire performance of epoxied connections in heavy timber structures. Proceedings of the 6th International Conference on Structures in Fire (SiF'10), 2–4 June 2010, East Lansing, MI, USA.
- Gerhards, C.C. (1982) Effect of the moisture content and temperature on the mechanical properties of wood: an analysis of immediate effects. *Wood and Fibre*, **14**(1), 4–36.
- Gerlich, J.T., Collier, P.C.R. and Buchanan, A.H. (1996) Design of light steel framed walls for fire resistance. *Fire and Materials*, **20**, 79–96.
- Gillie, M (1999) Development of Generalized Stress Strain Relationships for the Concrete Slab in Shell Models. PIT Project Research Report SS1, The University of Edinburgh, Edinburgh.
- Glos, P. and Henrici, D. (1991) Bending strength and MOE of structural timber at temperatures up to 150°C [Translated from German by USDA Forest Products Laboratory, Madison, WI, 1992]. *Holz als Roh- und Werkstoff*, **49**, 417–422.
- Gustaferro, A. and Martin, L.D. (1988) *Design for Fire Resistance of Precast Prestressed Concrete*, 2nd edn. Prestressed Concrete Institute, Chicago, IL.
- Gypsum Association. (2012) *Fire Resistance Design Manual*, 20th edn. Gypsum Association, Hyattsville, MD.
- Hadvig, S. (1981) Charring of Wood in Building Fires. Report. Laboratory of Heating and Air Conditioning, Technical University of Denmark.
- Hanus, F. (2010) Analysis of simple connections in steel structures subjected to natural fires, PhD Thesis, University of Liege, Liege.
- Harmathy, T.Z. (1965) Ten rules of fire endurance rating. *Fire Technology*, **1**(2), 93–102.
- Harmathy, T.Z. (1993) *Fire Safety Design and Concrete*. Concrete Design and Construction Series. Longman Scientific and Technical, Harlow.
- Harris, S., Lane, W., Buchanan, A.H. and Moss, P.J. (2004) Fire Performance of Laminated Veneer Lumber (LVL) with Glued-in Steel Rod Connections. Proceedings of the 3rd International Conference on Structures in Fire (SiF'04), Ottawa, Canada, pp. 411–424.
- Hasemi, Y., Yokobayashi, S., Wakamatsu, T. and Ptchelintsev, A. (1995) Fire safety of building components exposed to a localised fire. Proceedings of the First Asia-Flam Conference, Kowloon, Hong Kong. Interscience Publications Ltd, London.
- Hayes, B. (1968) Allowing for membrane action in the plastic analysis of rectangular reinforced concrete slabs. *Magazine of Concrete Research*, **20**(65), 205–212.
- HERA (1996) HERA Fire Protection Manuals, Sections 7 and 8, Passive/Active Fire Protection of Steel. Report R4-89, New Zealand Heavy Engineering Research Association, Auckland.
- Hertz, K. (1981) Simple Temperature Calculations of Fire-Exposed Concrete Constructions. Report No. 159, Institute of Building Design, Technical University of Denmark, Kongens Lyngby.

- Hertz, K. (1982) The anchorage capacity of deformed reinforcing bars at normal temperature and high temperature. *Magazine of Concrete Research*, **34**(121).
- Hevia, A.R.M. 2014. Fire resistance of partially protected cross-laminated timber rooms. MEng. dissertation, Carleton University, Ottawa.
- HMSO (1961) Protection of Structural Steel Against Fire. Fire Research Station Note No. 2. Joint Fire Research Organisation. Her Majesty's Stationery Office, London.
- HMSO (1968) Report of the Inquiry into the Collapse of Flats at Ronan Point, Canning Town. Her Majesty's Stationery Office, London.
- Huang, Z., Burgess, I.W. and Plank, R.J. (1999) Nonlinear analysis of reinforced concrete slabs subjected to fire. *ACI Structures Journal*, **96**(1), 127–135.
- Huang, Z., Burgess, I.W. and Plank, R.J. (2000) Effective stiffness modelling of composite concrete slabs in fire. *Engineering Structures*, **22**, 1133–1144.
- Huang, Z., Burgess, I.W. and Plank, R.J. (2002) Modelling of six full-scale fire tests on a composite building. *The Structural Engineer*, **80**(19), 30–37.
- Huang, Z., Platten, A. and Roberts, J. (1996) Non-linear finite element model to predict temperature histories within reinforced concrete in fires. *Building and Environment*, **31**(2), 109–118.
- Hurley M.J. and Bukowski R.W. (2008) Fire hazard analysis and techniques, in *Fire Protection Handbook*, 20th edn, National Fire Protection Association, Gaithersburg, MD, Sect. 3, Ch. 7.
- ICC (2015) *International Building Code*. International Code Council, Washington, DC.
- Ingborg, S.H. (1928) Tests of the severity of building fires. *National Fire Protection Quarterly*, **22**(1), 43–61.
- Inwood, M. (1999) Review of NZS 3101 for High Strength and Lightweight Concrete Exposed to Fire. Fire Engineering Research Report 99/10. University of Canterbury, New Zealand.
- Iding, R., Bresler, B. and Nizamuddin, Z. (1977) FIRES-RC II. A Computer Program for the Fire Response of Structures – Reinforced Concrete Frames. Fire Research Group Report No. UCB FRG 77-8. University of California, Berkeley, CA.
- ISO (1999a) ISO 834-1:1999. Fire Resistance Tests – Elements of Building Construction – Part 1: General Requirements. International Organization for Standardization.
- ISO (1999b) ISO TR 13387-2. Fire Safety Engineering – Part 2: Design Fire Scenarios and Design Fires. International Organization for Standardization.
- ISO (2009) ISO 23932. Fire Safety Engineering – General Principles. International Organization for Standardization.
- ISO (2015) ISO 5660-1. Heat Release Rate (Cone Calorimeter Method) and Smoke Production Rate (Dynamic Measurement). International Organisation for Standardization.
- IStructE (1978) Design and Detailing of Concrete Structures for Fire Resistance. Institution of Structural Engineers, London.
- IStructE (2003) Introduction to the Fire Safety Engineering of Structures. Institution of Structural Engineers, London.
- IStructE (2007) Guide to the Advanced Fire Safety Engineering of Structures. Institution of Structural Engineers, London.
- Izzuddin, B.A. (1991) Nonlinear dynamic analysis of framed structures. PhD thesis, Imperial College, London.
- Izzuddin, B. A. and Elghazouli, A. Y. (2004a), Realistic modelling of composite and reinforced concrete floor slabs under extreme loading. I: Analytical method. *ASCE Journal of Structural Engineering*, **130**(12), 1972–1984.
- Izzuddin, B. A. and Elghazouli, A. Y. (2004b) Realistic modelling of composite and reinforced concrete floor slabs under extreme loading. II: Verification and Application. *ASCE Journal of Structural Engineering*, **130**(12), 1985–1996.
- James, M. and Buchanan, A.H. (2000) Fire resistance of seismic gaps. Proceedings of the 12th World Conference on Earthquake Engineering, Auckland, New Zealand.
- Janssens, M.L. (1994) Thermo-physical properties for wood pyrolysis models. Proceedings of the Pacific Timber Engineering Conference, Gold Coast, Australia, pp. 607–618.
- Janssens, M.L. (1997) A method for calculating the fire resistance of exposed timber decks. Proceedings of the Fifth International Symposium on Fire Safety Science, Melbourne, Australia, pp. 1189–1200.
- Janssens, M.L. and White, R.H. (1994) Temperature profiles in wood members exposed to fire. *Fire and Materials*, **18**, 263–265.
- Jansson, R. (2013) Fire spalling of concrete – theoretical and experimental studies. PhD thesis, KTH Royal Institute of Technology, Stockholm.

- Jansson, R. and Boström, L. (2008) Experimental study of the influence of polypropylene fibres on material properties and fire spalling of concrete. 3rd International Symposium on Tunnel Safety and Security (ISTSS), Stockholm, Sweden.
- Johansen, K.W. (1949) Theory of timber connections. *Forest Products Journal*, **25**(2), 249–262.
- Kawagoe, K. (1958) Fire Behaviour in Rooms. Report No. 27, Building Research Institute, Tokyo
- Karlsson, B. and Quintiere, J.G. (2000) *Enclosure Fire Dynamics*, CRC Press, Boca Raton, FL.
- Khoury, G.A. (2000) Effect of fire on concrete and concrete structures. *Progress in Structural Engineering and Materials*, **2**(4), 429–447.
- Khoury, G.A., Grainger, B.N. and Sullivan, P.J.E. (1985a) Strain of concrete during first heating to 600°C. *Magazine of Concrete Research*, **37**, 195–215.
- Khoury, G.A., Grainger, B.N. and Sullivan, P.J.E. (1985b) Transient thermal strain of concrete: Literature Review, conditions within specimen and behavior of individual constituents. *Magazine of Concrete Research*, **37**(132), 131–144.
- Khoury, G.A. and Sullivan, P.J.E. (1988) Research at Imperial College on the effect of elevated temperatures on concrete. *Fire Safety Journal*, **13**, 69–72.
- Kim, A.K., Taber, B.C. and Loughheed, G.D. (1998) Sprinkler protection of exterior glazing. *Fire Technology*, **34**(2), 116–138.
- Kinjo, H., Yusa, S., Horio, T., Hirashima, T., Matsumoto, T. and Saito, K. (2014) Fire performance including the cooling phase, of structural glued laminated timber beams. Proceedings of the 8th International Conference on Structures in Fire (SiF'14), 11–13 June 2014, Shanghai, China.
- Kirby, B.R. (1999) *The Behaviour of Multi-Storey Steel Framed Buildings*, Swinden Technology Centre, British Steel plc, Rotherham.
- Kirby, B.R., Lapwood, D.G. and Thomson, G. (1993) *The Reinstatement of Fire Damaged Steel and Iron Framed Structures*, Swinden Technology Centre, British Steel plc, Rotherham.
- Kirby, B.R. and Preston, R.R. (1988) High temperature properties of hot-rolled structural steels for use in fire engineering design studies. *Fire Safety Journal*, **13**, 27–37.
- Kirby, B.R., Wainman, D.E., Tomlinson, L.N., Kay, T.R. and Peacock, B.N. (1994) *Natural Fires in Large Scale Compartments*, A British Steel Technical, Fire Research Station Collaborative Project, Swinden Technology Centre, British Steel plc, Rotherham.
- Kirby, B.R., Wainman, D.E., Tomlinson, L.N., Kay, T.R. and Peacock, B.N. (1999) Natural fires in large scale compartments. *International Journal on Engineering Performance-Based Fire Codes*, **1**(2), 43–58.
- Klippel, M. (2014) Fire safety of bonded structural timber elements. PhD thesis. ETH Zurich, Zurich.
- Klippel, M., Leyder, C., Frangi, A., Fontana, M., Lam, F. and Ceccotti, A. (2014) Fire tests on loaded cross-laminated timber wall and floor elements. Proceedings of the Eleventh International Symposium on Fire Safety Science, 10–14 February 2014, University of Canterbury, New Zealand. International Association for Fire Safety Science. DOI: 10.3801/IAFSS.FSS.11-626.
- Klippstein, K.H. (1980) Behaviour of cold-formed steel studs in fire tests. Proceedings of the Fifth International Specialty Conference on Cold-Formed Steel Structures, 18–19 November 1980, St. Louis, MO, USA, pp. 275–300.
- Klote, J.H., Milke, J.A., Turnbull, P.G., Kasef, A. and Ferreira, M.J. (2012) *Handbook of Smoke Control Engineering*, American Society of Heating, Refrigerating, and Air-Conditioning Engineers (ASHRAE), Atlanta, GA.
- Knudsen, R.M. and Schniewind, A.P. (1975) Performance of wood structural members exposed to fire. *Forest Products Journal*, **25**(2), 23–32.
- Kodur, V.K.R. (1997) Studies on the fire resistance of high strength concrete at the National Research Council of Canada. Proceedings, International Workshop on Fire Performance of High Strength Concrete, NIST Special Publication 919. National Institute of Standards and Technology, Gaithersburg, MD, pp. 75–86.
- Kodur, V.K.R. (1999) Performance-based fire resistance design of concrete filled steel columns. *Journal of Constructional Steel Research*, **51**, 21–36.
- Kodur, V.K.R. and Sultan, M.A. (2000) Performance of wood stud shear walls exposed to fire. *Fire and Materials*, **24**(1), 9–16.
- Kodur, V.K.R., Sultan, M.A. and Alfawakhiri, F. (1999) Fire resistance tests on loadbearing steel stud walls. Proceedings of the Third International Conference on Fire Research and Engineering, Chicago, IL, USA. Society of Fire Protection Engineers, Gaithersburg, MD.
- Kolb, J. (2008) *Systems in Timber Engineering*. Birkhauser, Basel.
- Kollman, F.F.P. and Schulz, F. (1944) Versuche über den Einfluss der Temperatur auf die Festigkeitwerte von Flugzeugholzbaustoffen [in German]. Teilbericht 1 und 2, Eberswalde, 23 bzw. 25 S.

- König, J. (1995) Fire Resistance of Timber Joists and Load Bearing Wall Frames. Report No. I 9412071. TräteK, Swedish Institute for Wood Technology Research, Stockholm.
- König, J. (1998) Structural stability of timber structures in fire - Performance and requirements. Proceedings of the COST Action E5 Workshop on Timber Frame Building Systems. Building Research Establishment, Watford.
- König, J. and Walleij, L. (1999) One-Dimensional Charring of Timber Exposed to Standard and Parametric Fires in Initially Unprotected and Postprotected Situations. Report No. I 9908029. TräteK, Swedish Institute for Wood Technology Research, Stockholm.
- König, J. and Walleij, L. (2000) Timber Frame Assemblies Exposed to Standard and Parametric Fires. Part 2: A Design Model for Standard Fire Exposure. Report No. I0001001. TräteK, Swedish Institute for Wood Technology Research, Stockholm.
- Kordina, K. and Meyer-Ottens, C. (1983) *Holz Brandschutz Handbuch* [in German]. Deutsche Gesellschaft für Holzforschung. Ernst & Son, Berlin.
- Kordina, K. and Meyer-Ottens, C. (1995) *Holz Brandschutz Handbuch*, 2nd edn [in German]. Deutsche Gesellschaft für Holzforschung. Ernst & Son, Berlin.
- Kulak, G.L., Adams, P.F. and Gilmor, M.I. (1995) *Limit States Design in Structural Steel*, Canadian Institute of Steel Construction, Markham, ON.
- Lane, W., Buchanan, A.H. and Moss, P.J. (2004) Fire performance of laminated veneer lumber (LVL) Proceedings of World Conference on Timber Engineering, 14–17 June 2004, Lahti, Finland. Finnish Association of Civil Engineers RIL, Helsinki, Vol. 3, pp. 473–478.
- Lau, P.W.C. and Barrett, J.D. (1997) Modelling tension strength behaviour of structural lumber exposed to elevated temperatures. Proceedings of the 4th International Symposium on Fire Safety Science, Melbourne, Australia, pp. 1177–1188.
- Lau, P.W.C., White, R. and Van Zeeland, I. (1999) Modelling the charring behaviour of structural lumber. *Fire and Materials*, **23**, 209–216.
- Law, A. (2010) The assessment and response of concrete structures subject to fire. PhD thesis, University of Edinburgh.
- Law, M. (1971) A Relationship Between Fire Grading and Building Design and Contents. Fire Research Note No. 877. Fire Research Station, London.
- Law, M. (1973) Prediction of fire resistance. Paper in Symposium No. 5, Fire Resistance Requirements of Buildings, a New Approach. Department of the Environment and Fire Offices Committee Joint Fire Research Organisation. Her Majesty's Stationery Office, London.
- Law, M. (1983) A basis for the design of fire protection of building structures. *The Structural Engineer*, **61A**(1).
- Law, M. (1997) A review of formulae for T-equivalent. Proceedings of the 5th International Symposium on Fire Safety Science, Melbourne, Australia, pp. 985–996.
- Law, M. and O'Brien, T. (1989) *Fire Safety of Bare External Structural Steel*. Constrado, Croydon.
- Lawson, R.M. (1985) Fire Resistance of Ribbed Concrete Floors. CIRIA Report 107. Construction Industry Research and Information Association, London.
- Lawson, R. M. (1990) Behaviour of steel beam-to-column connections in fire. *The Structural Engineer*, **68**(14/17), 263–271.
- Leicester, R.H., Seath, C. and Pham, L. (1979) The fire resistance of metal connectors. Proceedings of the Nineteenth Forest Products Research Conference, 12–16 November 1979, Melbourne, Australia.
- Lennon, T. (2011) *Structural Fire Engineering*. ICE Publishing, UK
- Lennon, T., Bullock, M.J. and Enjily, V. (2000) The fire resistance of medium-rise timber frame buildings. Proceedings of the World Conference on Timber Engineering, Whistler, Canada.
- LeVan, S. and Winandy, J.E. (1990) Effects of fire retardant treatments on wood strength: A review. *Wood and Fiber Science*, **22**(1), 113–131.
- Lie, T.T. (1972) *Fire and Buildings*. Applied Science Publishers Ltd, London.
- Lie, T.T. (1977) A method for assessing the fire resistance of laminated timber beams and columns. *Canadian Journal of Civil Engineering*, **4**, 161–169.
- Lie, T.T. (ed.) (1992) Structural Fire Protection. ASCE Manuals and Reports of Engineering Practice, No. 78. American Society of Civil Engineers, New York.
- Lie, T.T. (1995) Fire temperature-time relations, in *SFPE Handbook of Fire Protection Engineering*, 2nd edn. Society of Fire Protection Engineers, Gaithersburg, MD.
- Lie, T.T. and Kodur, V.K.R. (1996) Fire resistance of steel columns filled with bar-reinforced concrete. *Journal of Structural Engineering*, **122**(1), 30–36.

- Lim, L. (2000) Stability of Precast Concrete Tilt Panels in Fire. Fire Engineering Research Report 00/12. University of Canterbury, Auckland.
- Lim, L. (2003) Membrane action in fire exposed concrete floor systems. PhD thesis, University of Canterbury, New Zealand.
- Lim, L., Buchanan, A., Moss, P., and Franssen, J. M. (2004) Numerical modelling of two-way reinforced concrete slabs in fire. *Engineering Structures*, **26**(8), 1081–1091.
- Liu, T.C.H. (1999) Moment-rotation-temperature characteristics of steel/composite connections. *Journal of Structural Engineering*, **125** (10), 1188–1197.
- Madsen, B. and Buchanan, A.H. (1986) Size effects in timber explained by a modified weakest link theory. *Canadian Journal of Civil Engineering*, **13**(2), 218–232.
- Magnusson, S.E. (1972) Probabilistic analysis of fire safety. ASCE-IABSE International Conference on Planning and Design of Tall Buildings. Conference Preprints Vol. DS, p. 424. Lehigh University, Bethlehem, PA.
- Magnusson, S.E. and Thelandersson, S. (1970) Temperature-time curves of complete process of fire development; theoretical study of wood fuel fires in enclosed spaces. *Acta Polytechnica Scandinavica. Civil Engineering and Building Construction Series* 65.
- Malhotra, H.L. (1984) Spalling of Concrete in Fires. CIRIA Technical Note No. 118. Construction Industry Research and Information Association, London.
- Malhotra, H.L. and Rogowski, B.F.W. (1970) Fire Resistance of Laminated Timber Columns. Fire and Structural Use of Timber in Buildings. Symposium No. 3. Her Majesty's Stationery Office, London, pp. 17–44.
- Marchant, E.W. (1972) *A Complete Guide to Fire and Buildings*. Medical and Technical Publishing Co Ltd., Lancaster.
- Martin, D.M. and Moore, D.B. (1997) Introduction and Background to the Research Programme and Major Fire Tests at BRE Cardington. Proceedings of the National Steel Construction Conference, May, London, UK.
- Martin, D.M. and Moore, D.B. (1999), *The behaviour of Multi-storey Steel Framed Buildings in fire: A European Joint Research Programme*. Cardington Test Report, prepared by British Steel plc.
- Martin, Z.A. and Tingley, D.A. (2000) Fire resistance of FRP reinforced glulam beams. Proceedings of the World Conference on Timber Engineering, Whistler, BC, Canada.
- Mayo, J. (2015) *Solid Wood: Case Studies in Mass Timber Architecture, Technology and Design*, Routledge, London.
- MBIE (2007) *New Zealand Building Code Handbook*, 3rd edn, Department of Building and Housing, Wellington, New Zealand.
- MBIE (2012) *CVM2 Verification Method: Framework for Fire Safety Design*, Department of Building and Housing, New Zealand.
- MBIE. (2014) Acceptable Solutions and Verification Methods for New Zealand Building Code Clause B1 Structure, Ministry of Business, Innovation and Employment, New Zealand.
- McCaffrey, B.J., Quintiere, J.G. and Harkleroad, M.F. (1981) Estimating room fire temperatures and the likelihood of flashover using fire test data correlations. *Fire Technology*, **17**(2), pp. 98–119.
- McGrattan, K., Hostikka, S., McDermott, R., Floyd, J., Weinschenk, C. and Overholt, K. (2015a) *Fire Dynamics Simulator Technical Reference Guide, Volume 1: Mathematical Model*, NIST Special Publication 1018-1, 6th edn, National Institute of Standards and Technology, Gaithersburg, MD.
- McGrattan, K., Hostikka, S., McDermott, R., Floyd, J., Weinschenk, C. and Overholt, K. (2015b) *Fire Dynamics Simulator User's Guide*, NIST Special Publication 1019, 6th edn, National Institute of Standards and Technology, Gaithersburg, MD.
- Meyer-Ottens, C. (1983) Junctions in Wood Structures - Total Construction. Proceedings, International Seminar on Three Decades of Structural Fire Safety. Building Research Establishment, Watford.
- Mikkola, E. (1990) Charring of Wood. VTT Research Report 689. Technical Research Centre of Finland.
- Milke, J.A. (2008) Analytical methods for determining fire resistance of steel members, in *SFPE Handbook of Fire Protection Engineering*, 4th edn, Society of Fire Protection Engineers, Gaithersburg, MD, Ch. 4-11. USA
- Min, J.-K. (2012) Numerical prediction of structural fire performance for precast prestressed concrete flooring systems. PhD thesis, University of Canterbury, New Zealand.
- Moore, D.B. and Lennon, T. (1997) Fire engineering design of steel structures. *Progress in Structural Engineering and Materials*, **1**(1), 4–9.
- Moss, P.J., Buchanan, A.H., Fragiocomo, M. and Austruy, C. (2010) Experimental testing and analytical prediction of the behaviour of timber bolted connections subjected to fire. *Fire Technology*, **46**, 129–148.
- NBCC (2010) *National Building Code of Canada*. National Research Council of Canada, Ottawa.
- Neville, A.M. (1997) *Properties of Concrete*, 4th edn, John Wiley & Sons, Inc., New York.

- Newman, G.M. (1990) *The Behaviour of Steel Portal Frames in Boundary Conditions*, 2nd edn, The Steel Construction Institute, U.K.
- Newman, G. M., & Lawson, R. M. (1991) Fire resistance of composite beams. Steel construction institute.
- Newman, G. M., Robinson, J. T. and Bailey, C. G. (2006) *Fire Safe Design: A New Approach to Multi-Storey Steel-Framed Buildings*. Second Edition, SCI Publication P288, The Steel Construction Institute, Ascot.
- NFPA (2003) *Fire Protection Handbook*, 19th edn, National Fire Protection Association, Quincy, MA.
- NFPA (2010a) *Fire Protection Handbook*, 20th edn, National Fire Protection Association, Quincy, MA.
- NFPA (2010b) Guideline on Fire Ratings of Archaic Materials and Assemblies. Appendix L. NFPA 909: Code for the Protection of Cultural Resource Properties – Museums, Libraries, and Places of Worship. National Fire Protection Association, Quincy, MA.
- Nielsen, P.C. and Olesen, F.B. (1982) Tensile Strength of Finger Joints at Elevated Temperatures. Report No. 8205. Institute of Building Technology and Structural Engineering, Aalborg.
- NKB (1994) Performance Requirements for Fire Safety and Technical Guide for Verification by Calculation. Report 1994:07 E. NKB Fire Safety Committee, Nordic Committee on Building Regulations, Helsinki.
- Norén, J.B. (1988) Failure of structural timber when exposed to fire. Proceedings of the International Conference on Timber Engineering, 19–22 September 1988, Seattle, WA, USA, pp. 5–14.
- Norén, J.B. (1996) Load-bearing capacity of nailed joints exposed to fire. *Fire and Materials*, **20**, 133–143.
- Nyman, C. (1980) The Effect of Temperature and Moisture on the Strength of Wood and Glue Joists [in Finnish]. VTT Forest Products Report No. 6. Technical Research Centre of Finland.
- O'Connor, M.A. and Martin, D.M. (1998) Behaviour of a multi-storey steel framed building subjected to fire attack. *Journal of Constructional Steel Research*, **1**(46), 295.
- O'Hara, M. (1994) Understanding through penetration protection systems. *NFPA Journal*, **Jan./Feb.**
- O'Meagher, A.J. and Bennetts, I.D. (1991) Modelling of concrete walls in fire. *Fire Safety Journal*, **17**, 315–335.
- O'Meagher, A.J., Bennetts, I.D., Dayawansa, P.H. and Thomas, I.R. (1992) Design of single storey industrial buildings for fire resistance. *Steel Construction*, **26**(2).
- O'Neill, J. (2013) The fire performance of timber floors in multi-storey buildings. PhD thesis, University of Canterbury, New Zealand.
- O'Neill J.W., Carradine D, Moss P.J., Fragiaco M., Dhakal R. and Buchanan A.H. (2011) Design of timber-concrete composite floors for fire resistance. *Journal of Structural Fire Engineering*, **2**(3), 231–242.
- Ohlemiller, T. J. (2008) Smoldering combustion, in *SFPE Handbook of Fire Protection Engineering*, 4th edn, Society of Fire Protection Engineers, Gaithersburg, MD, Ch. 2-9.
- Ohsawa, J. and Yoneda, Y. (1978) Shear test of woods as a model of defibration [in Japanese]. *Journal of the Japanese Wood Research Society*, **24**(4), 230–236.
- Okuyama, T., Suzuki, S. and Terazawa, S. (1977) Effect of temperature on orthotropic properties of wood. I. On the transverse anisotropy in bending [in Japanese]. *Journal of the Japanese Wood Research Society*, **23**(12), 609–616.
- Oleszkiewicz, I. (1991) Vertical separation of windows using spandrel walls and horizontal projections. *Fire Technology*, **27**(4), 334–340.
- Östman, B.A. (1985) Wood tensile strength at temperatures and moisture contents simulating fire conditions. *Wood Science and Technology*, **19**, 103–116.
- Östman, B.A., König, J. and Norén, J. (1994) Contribution to fire resistance of timber frame assemblies by means of fire protective boards. Proceedings of the Fire and Materials Conference, Washington, DC, USA. Trätekt Report No. I 9412074.
- Östman, B.A., Mikkola, E., Stein, R., Frangi, A., König, J., Dhima, D., Hakkarainen, T. and Bregulla, J. (2010) Fire Safety in Timber Buildings – Technical Guideline for Europe, SP Report 2010:19. SP Trätekt - SP Technical Research Institute of Sweden, Stockholm.
- Papaioannou, K. (1986) The conflagration of two large department stores in the centre of Athens. *Fire and Materials*, **10**, 171–177.
- Park, R. (1964) Tensile membrane behaviour of uniformly loaded rectangular reinforced concrete slabs with fully restrained edges. *Magazine of Concrete Research*, **16**(46), 39–44.
- Park, R. and Paulay, T. (1975) *Reinforced Concrete Structures*. John Wiley & Sons, Ltd, Chichester.
- Parker, W.J., Paabo, M., Scott, J.T., Gross, D. and Benjamin, I.A. (1975) Fire Endurance of Gypsum Board Walls and Chases Containing Plastic and Metallic Drain, Waste and Vent Plumbing Systems. NBS Building Science Series 72, National Bureau of Standards, Washington, DC.
- Peacock, R.D., Forney, G.P., Reneke, P.A., Portier, R.W. and Jones, W.W. (1993) CFAST, the Consolidated Model of Fire Growth and Smoke Transport. Technical Note 1299, National Institute of Standards and Technology, Gaithersburg, MD.

- Peng, L. (2010) Performance of heavy timber connections in fire. PhD Thesis, Carleton University, Ottawa.
- Peng, L., Hadjisophocleous, G., Mehaffey, J. and Mohammad, M. (2010) Fire resistance of wood-steel-wood bolted timber connections. Proceedings of the 6th International Conference on Structures in Fire, 2–4 June 2010, East Lansing, MI, USA, p. 552.
- Pettersson, O. (1973) The Connection between a Real Fire Exposure and the Heating Conditions according to Standard Fire Resistance Tests – with Special Application to Steel Structures. Document CECM 3-73/73. European Commission for Constructional Steelwork.
- Pettersson, O., Magnusson, S.E. and Thor, J. (1976) Fire Engineering Design of Steel Structures. Swedish Institute of Steel Construction Publication No. 50.
- Phan, L.T. (1996) Fire Performance of High Strength Concrete: A Report of the State-of-the-Art. NISTIR 5934. National Institute of Standards and Technology, Gaithersburg, MD.
- Pitts, D.R. and Sissom, L.E. (1977) *Schaum's Outline Series: Theory and Problems of Heat Transfer*, McGraw Hill, New York.
- Poh, K.W. (1996) Modelling Elevated Temperature Properties of Structural Steel. Report BHPR/SM/R/055. Broken Hill Proprietary Company Ltd, Perth.
- Poh, K.W. and Bennetts, I.D. (1995) Analysis of structural members under elevated temperature conditions. *Journal of Structural Engineering*, **121**(4), 664–675.
- Portier, R.W., Peacock, R.D. and Reneke, P.A. (1996) FASTLite: Engineering Tools for Estimating Fire Growth and Transport. Special Publication 899, National Institute of Standards and Technology, Gaithersburg, MD.
- Preusser, R. (1968) Plastic and elastic behaviour of wood affected by heat in open systems [in German]. *Holztechnologie*, **9**(4), 229–231.
- Purkiss, J.A. and Li, L.Y. (2013) *Fire Safety Engineering Design of Structures*, 3rd edn, CRC Press, Boca Raton, FL.
- Quintiere, J.G. (1998) *Principles of Fire Behaviour*, Delmar Publishers, Albany, NY.
- Quintiere, J.G. (2008) Compartment fire modelling, in *SFPE Handbook of Fire Protection Engineering*, 4th edn, Society of Fire Protection Engineers, Gaithersburg, MD, Ch. 3-5.
- Racher, P., Laplanche, K., Dhima, D. and Bouchaïr, A. (2010) Thermo-mechanical analysis of the fire performance of dowelled timber connection. *Engineering Structures*, **32**(4), 1148–1157.
- Rein, G., Zhang, X., Williams, P., Hume, B., Heise, A., Jowsey, A., Lane, B. and Torero, J.L. (2007) Multi-storey fire analysis for high-rise buildings. Proceedings of the 11th Interflam Conference, 3–5 September 2007, London, UK, pp. 605–615.
- Richardson, L.R. and McPhee, R.A. (1996) Fire resistance and sound-transmission-class ratings for wood frame walls. *Fire and Materials*, **20**, 123–131.
- Richardson, L.R., McPhee, R.A. and Batisita, M. (2000) Sound-transmission class and fire resistance ratings for wood frame floors. *Fire and Materials*, **24**(1), 17–28.
- Rose, P.S., Bailey, C.G., Burgess, I.W. and Plank, R.J. (1998) The influence of floor slabs on the structural performance of the Cardington frame in fire. *Journal of Constructional Steel Research*, **46**, 1–3, Paper 181.
- Rotter, J.M., Sanad, A.M., Usmani, A.S. and Gillie, M. (1999) Structural performance of redundant structures under local fires. Proceedings of the 8th Interflam Conference, 28 June–1 July, Edinburgh, UK, pp. 1069–1080.
- SA (2002) Structural Design Actions. AS/NZS 1170:2002. Standards Australia, Canberra, Standards New Zealand, Wellington.
- SA (2005) Methods for Fire Tests on Building Materials, Components and Structures - Fire Resistance Test of Elements of Construction. AS 1530.4. Standards Australia, Canberra.
- SA (2006) Timber Structures, Part 4: Fire Resistance for Structural Adequacy of Timber Members. AS 1720.4-2006. Standards Australia, Canberra.
- SA (2009) Concrete Structures. AS 3600-2009. Standards Australia, Canberra.
- Saito, Y., Harada, K., Sakaguchi, A., Nakae, K., Tsuchihashi, T., Tanaka, Y., Tasaka, S. and Yoshida, M. (2007) Burning of laminated wood assembly after intense heat exposure by fire resistance furnace. Proceedings of the 7th Asia-Oceania AOFST Symposium, 20–22 September 2007, Hong Kong.
- Sano, E. (1961a) Effects of temperature on the mechanical properties of wood. I. Compression parallel-to-grain [in Japanese]. *Journal of the Japanese Wood Research Society*, **7**(4), 147–150.
- Sano, E. (1961b) Effects of temperature on the mechanical properties of wood. II. Tension parallel-to-grain [in Japanese]. *Journal of the Japanese Wood Research Society*, **7**(5), 189–191.
- Sano, E. (1961c) Effects of temperature on the mechanical properties of wood. III. Torsion test [in Japanese]. *Journal of the Japanese Wood Research Society*, **7**(5), 191–193.
- Sarraj, M. (2007) The behaviour of steel fin plate connections in fire. PhD thesis, University of Sheffield.

- Scawthorn (1992) Fire following earthquake, in *Fire Safety in Tall Buildings*, Council on Tall Buildings and Urban Habitat, McGraw Hill Inc., New York, Ch. 4.
- SCI (1991) *Investigation of Broadgate Phase 8 Fire*, Structural Fire Engineering, Steel Construction Institute, Ascot.
- Schaffer, E.L. (1967) Charring Rate of Selected Woods – Transverse to Grain. US Forest Service Research Paper FPL69, US Forest Products Laboratory, Madison, WI.
- Schaffer, E.L. (1973) Effect of pyrolytic temperature on the longitudinal strength of dry Douglas fir. *Journal of Testing and Evaluation*, **1**(4), 319–329.
- Schaffer, E.L. (1977) State of structural timber fire endurance. *Wood and Fiber*, **9**(2), 145–190.
- Schaffer, E.L. (1984) Structural Fire Design: Wood. Research Paper FPL 450. US Forest Products Laboratory, Madison, WI.
- Schaffer, E.L. (1992) Fire-Resistive Structural Design. Proceedings, International Seminar on Wood Engineering. US Forest Products Laboratory, Madison, WI.
- Schaffer, E.L., Marx, C.M., Bender, D.A. and Woeste, F.E. (1986) Strength Validation and Fire Endurance of Glued Laminated Timber Beams. Research Paper FPL 467. US Forest Products Laboratory, Madison, WI.
- Schleich, J.B. (1996) A natural fire safety concept for buildings – 1. Fire, static and dynamic tests of building structures. Proceedings of the Second Cardington Conference. E & FN Spon, London, pp. 79–104
- Schleich, J.B. (1999) Competitive Steel Buildings through Natural Fire Safety Concept. Draft Final Report, Part 1. Profil Arbed Centre de Recherches, Luxembourg.
- Schleich, J. B., Cajot, L. G., Pierre, M., Brasseur, M., Franssen, J. M., Joyeux, D., Twilt, L., Oerle, J.V. and Aurtinetxe, G. (1999) Development of Design Rules for Steel Structures Subjected to Natural Fires in Large Compartments. Report EUR 18868. European Commission, Luxembourg.
- Schmid, J. and König, J. (2010) Cross Laminated Timber in Fire. SP Report 2010:11, Stockholm.
- Schmid, J., König, J. and Kohler, J. (2010) Fire-exposed cross laminated timber - modelling and tests. Proceedings of the World Conference on Timber Engineering, Riva del Garda, Italy.
- Schneider, U. (1986) Properties of Materials at High Temperatures – Concrete, Second Edition. RILEM Report, Paris.
- Schneider, U. (1988) Concrete at high temperatures - a general review. *Fire Safety Journal*, **13**, 55–68.
- Schneider U. and Horvath J. (2003), Behaviour of Ordinary Concrete at High Temperatures. Research Reports of Vienna University of Technology, Vienna.
- Schneider, U., Kersken-Bradley, M. and Max, U. (1990) Neuberechnung der Wärmeabzugsfaktoren w für die DIN V 18230 Teil 1-Baulicher Brandschutz im Industriebau. IRB-Verlag, Stuttgart.
- Schneider, U., Morita, T. and Franssen, J.-M. (1994) A concrete model considering the load history applied to centrally loaded columns under fire attack. Proceedings of the Fourth International Symposium on Fire Safety Science, 13–17 June 1994, Ottawa, Canada, pp. 1101–1112.
- Seigel, L.G. (1970) Designing for fire safety with exposed structural steel. *Fire Technology*, **6**(4), 269–278.
- SFPE (2000) *SFPE Engineering Guide to Performance-based Fire Protection Analysis and Design of Buildings*. Society of Fire Protection Engineers, Gaithersburg, MD.
- SFPE (2008) *SFPE Handbook of Fire Protection Engineering*, 4th edn, Society of Fire Protection Engineers, Gaithersburg, MD.
- Shrestha, D., Cramer, S.M. and White, R.H. (1994) Time temperature profile across a lumber section exposed to pyrolytic temperatures. *Fire and Materials*, **20**, 211–220.
- Shrestha, D., Cramer, S.M. and White, R.H. (1995) Simplified models for the properties of dimension lumber and metal plate connections at elevated temperatures. *Forest Products Journal*, **45**(7/8), 35–42.
- Shyam-Sunder, S. (2005) Federal Building and Fire Safety Investigation of the World Trade Center Disaster. Final Report of the National Construction Safety Team on the Collapses of the World Trade Center Towers (NIST NCSTAR 1). National Institute of Standards and Technology, Gaithersburg, MD.
- SNZ (1986) The design of fire walls and partitions to ensure stability and integrity. *Standards Magazine*, **32**(8), 14–19.
- SNZ (1991) MP9. Fire Properties of Building Materials and Elements of Structure. Miscellaneous Publication No. 9. Standards New Zealand, Wellington.
- SNZ (1993) Timber Structures Standard. NZS 3603:1993. Standards New Zealand, Wellington.
- SNZ (2006) Concrete Structures Standard Part 1 – The Design of Concrete Structures. NZS 3101. Standards New Zealand, Wellington.
- Song, Y.Y. (2009) Analysis of industrial steel portal frames under fire conditions. PhD thesis, University of Sheffield.
- Spearpoint, M.J. (2008) *Fire Engineering Design Guide*, 3rd edn. New Zealand Centre for Advanced Engineering, University of Canterbury, New Zealand.

- Srpic, S. (1995) The influence of the material hardening on the behaviour of a steel plane frame in fire. *Journal of Applied Mathematics and Mechanics*, **75**, 279–280.
- Steinbrugge, K.V. (1982) *Earthquakes, Volcanos and Tsunamis - An Anatomy of Hazards*. Skandia America Group.
- Sterner, E. and Wickstrom, U. (1990) TASEF - Temperature Analysis of Structures Exposed to Fire. Fire Technology SP Report 1990:05, Swedish National Testing Institute.
- Stern-Gottfried, J., Rein, G., Bisby, L.A. and Torero, J.L. (2010) Experimental review of the homogeneous temperature assumption in post-flashover compartment fires. *Fire Safety Journal*, **45**(4), 249–261.
- Stevens, W.C. and Turner, N. (1970) *Wood Bending Handbook*. Her Majesty's Stationery Office, London.
- Sullivan, P.J.E., Terro, M.J. and Morris, W.A. (1994) Critical review of fire-dedicated thermal and structural computer programs. *Journal of Applied Fire Science*, **3**(2), 113–135.
- Sultan, M.A. (1996) A model for predicting heat transfer through non-insulated unloaded steel-stud gypsum board wall assemblies exposed to fire. *Fire Technology*, **32**(3), 239–259.
- Sultan, M.A. (2000) Fire spread via wall/floor joints in multi-family dwellings. *Fire and Materials*, **24**(1), 1–8.
- Sultan, M.A. and Loughheed, G.D. (1997) Fire Resistance of Gypsum Board Wall Assemblies. Construction Technology Update No. 2. Institute for Research in Construction, National Research Council of Canada, Ottawa, pp. 1–4.
- Sun, R.R., Huang, Z. and Burgess, I.W. (2012), The collapse behaviour of braced steel frames exposed to fire. *Journal of Constructional Steel Research*, **72**, 130–142.
- SWRI (2012) *Directory of Listed Products for the Construction Industry*. Fire Technology Department, Southwest Research Institute, San Antonio, TX.
- Takeda, H. and Mehaffey, J.R. (1998) WALL2D: a model for predicting heat transfer through wood-stud walls exposed to fire. *Fire and Materials*, **22**, 133–140.
- Thomas, G.C. (1997) Fire resistance of light timber frame walls. PhD thesis: Fire Engineering Research Report 97-7, University of Canterbury, New Zealand.
- Thomas, G.C., Buchanan, A.H, Carr, A.J, Fleischmann, C.M. and Moss, P.J. (1995) Light timber framed walls exposed to compartment fires. *Journal of Fire Protection Engineering*, **7**(1), 25–35.
- Thomas, G.C., Buchanan, A.H. and Fleischmann, C.M. (1997) Structural fire design: the role of time equivalence. Proceedings of the 5th International Symposium on Fire Safety Science, 3–7 March 1997, Melbourne, Australia, pp. 607–618.
- Thomas, I.R. and Bennetts, I.D. (1999) Fires in enclosures with single ventilation openings - comparison of long and wide enclosures. Proceedings of the 6th International Symposium on Fire Safety Science, 5–9 July 1999, Poitiers, France.
- Thomas, P.H. and Heselden, A.J.M. (1972) Fully Developed Fires in Single Compartments. CIB Report No 20, Fire Research Note 923. Fire Research Station, London.
- Thomas, P.H., Hinkley, P.L., Theobald, C.R. and Simms, D.L. (1963) Investigations into the Flow of Hot Gases in Roof Venting. Fire Research Technical Paper No. 7. Fire Research Station, London.
- Tide, R.H.R. (1998) Integrity of structural steel after exposure to fire. *Engineering Journal*, **First Quarter**, 26–38.
- Tomasson, B. (1998) High Performance Concrete – Design Guidelines. Report, Department of Fire Safety Engineering, Lund University, Lund.
- TRADA (1976) The Fire at Morrison Printing Inks Machinery Ltd. Section 2d-1. Wood Products Design Manual. New Zealand Timber Research and Development Association, Wellington.
- Twilt, L. and Witteveen, J. (1974) The fire resistance of wood-clad steel columns. *Fire Prevention Science and Technology*, No. **11**, 14–20.
- UBC (1997) Uniform Building Code. International Conference of Building Officials, Whittier, CA.
- UL (2012) Fire Resistance Directory. Underwriters Laboratories Inc., Northbrook, IL.
- ULC (2007) Standard Methods of Fire Endurance Tests of Building Construction and Materials – Fourth Edition - CAN/ULC-S101-07. Underwriters Laboratories of Canada, Ontario.
- Van Acker, A. (2010) Fire safety of prestressed hollowcore floors. *Concrete Plant International*, **1**, 182–196.
- Van Oberbeek, T., Breunese, A., Gijsbers, J., Both, K., Maljaars, J. and Noordijk, L. (2010) New Regulations for hollowcore slabs after premature partial collapse. Proceedings of the 6th International Conference on Structures in Fire (SiF'10), 2–4 June 2010, East Lansing MI, USA, pp. 141–148.
- Wade, C., Baker, G., Frank, K., Robbins, A., Harrison, R., Spearpoint, M. and Fleischmann, C. (2013) *B-RISK User Guide and Technical Manual*, Building Research Levy, and the Ministry of Building, Innovation and Employment, BRANZ, Wellington.
- Wade, C.A. (1991) Method for Fire Engineering Design of Structural Concrete Beams and Floor Systems. BRANZ Technical Recommendation No. 8. Building Research Association of New Zealand.

- Wade, C.A. (1994) Performance of concrete floors exposed to real fires. *Journal of Fire Protection Engineering*, **6**(3), 113–124.
- Wade, C. A. (2004a) BRANZFIRE Software and User's Guide. BRANZ, Wellington.
- Wade, C. A. (2004b) BRANZFIRE Technical Reference Guide. BRANZ Study Report No. 92 (revised). BRANZ, Wellington.
- Wald, F., Simoes da Silva, L., Moore, D.B., Lennon, T., Chladna, M., Santiago, A., Benes, M. and Borges, L. (2006) Experimental behaviour of a steel structure under natural fire. *Fire Safety Journal*, **41**, 509–522.
- Walker, B. (1982) *Earthquake*. Time-Life Books, Amsterdam.
- Walton, W.D. and Thomas, P.H. (2008) Estimating temperatures in compartment fires, in *SFPE Handbook of Fire Protection Engineering*, 4th edn, Society of Fire Protection Engineers, Gaithersburg, MD, Ch. 3-6.
- Wang, Y.C. (2002) *Steel and Composite Structures: Behaviour and Design for Fire Safety*, Spoon Press, London.
- Wang, Y.C., Burgess, I.W., Wald, F. and Gillie, M. (2012) *Performance-based Fire Engineering of Structures*, CRC Press, Boca Raton, FL.
- Wang, Y.C., Lennon, T. and Moore, D.B. (1995) The behaviour of steel frames subjected to fire. *Journal of Constructional Steel Research*, **35**, 291–322.
- Watts, J.M. (2003) Probabilistic FIRE Models, in *Fire Protection Handbook*, 19th edn, National Fire Protection Association, Quincy, MA.
- Werther, N., O'Neill, J.W., Spellman, P.M., Abu, A.K., Moss, P.J., Buchanan, A.H. and Winter, S. (2012) Parametric study of modelling structural timber in fire with different software packages. Proceedings of the 7th International Conference on Structures in Fire (SiF'12), 6–8 June 2012, Zurich, Switzerland.
- White, R.H. (1984) Use of Coatings to Improve Fire Resistance of Wood. ASTM Special Technical Publication 826, ASTM, Philadelphia, PA.
- White, R.H. (1988) Charring rates of different wood species. PhD. thesis, University of Wisconsin, Madison.
- White, R.H. (2008) Analytical methods for determining fire resistance of timber members, in *SFPE Handbook of Fire Protection Engineering*, 2nd edn, Society of Fire Protection Engineers, Gaithersburg, MD, Ch. 4-11.
- White, R.H. (2009) Fire Resistance of Wood Members with Directly Applied Protection. Wood Design Focus, Summer 2009, pp. 13–19.
- White, R.H. and Cramer, S.M. (1994) Improving the fire endurance of wood truss systems. Proceedings of the Pacific Timber Engineering Conference, 11–15 July 1994, Gold Coast, Australia, pp. 582–589.
- White, R.H. and Nordheim, E.V. (1992) Charring rate of wood for ASTM E-119 exposure. *Fire Technology*, **28**(1), 5–30.
- White, R.H. and Schaffer, E.L. (1980) Transient moisture gradient in fire exposed wood slab. *Wood and Fiber*, **13**(1), 17–38.
- White, R.H., Schaffer, E.L. and Woeste, F.E. (1984) Replicate fire endurance tests of an unprotected wood joist floor assembly. *Wood and Fiber Science*, **16**(3), 374–390.
- Wickström, U. (1986) a very simple method for estimating temperatures in fire exposed structures, in *New Technology to Reduce Fire Losses and Costs* (eds S.J. Grayson and D.A. Smith), Elsevier Applied Science, London, pp. 186–194.
- Winandy, J.E. (1995) Effects of fire retardant treatments after 18 months of exposure at 150°F (66°C). Research Note FPL-RN-0264. US Forest Products Laboratory, Madison, WI.
- Winstone Wallboards (2012) *GiB Fire Rated Systems – Specification and Installation Manual*, Winstone Wallboards Ltd, Auckland.
- Woeste, F.E. and Schaffer, E.L. (1979) Second moment reliability analysis of fire-exposed wood joist floor assemblies. *Fire and Materials*, **3**(3), p. 126.
- Wood Handbook (2010) *Wood Handbook: Wood as an Engineering Material*. US Department of Agriculture, Forest Products Laboratory, Madison, WI.
- Young, S.A. (2000) Structural modelling of plasterboard-clad light timber framed walls in fire. PhD thesis, Victoria University of Technology, Victoria, Australia.
- Young, S.A. and Clancy, P. (1996) Compression load deformation of timber walls in fire. Proceedings of the Wood and Fire Safety Conference, 6–9 May 1996, The High Tatras, Slovak Republic, pp. 127–136.
- Young, S.A. and Clancy, P. (1998) Degradation of the mechanical properties in compression of Radiata Pine in fire. Proceedings of the 4th World Conference on Timber Engineering, 17–20 August 1998, Montreux, Switzerland, Vol. 2, pp. 246–253.
- Yu, C.M., Huang, Z., Burgess, I.W. and Plank, R.J. (2010), Development and validation of 3D composite structural elements at elevated temperatures. *Journal of Structural Engineering, ASCE*, **136**(3), 275–284.

- Yu, H.X., Burgess, I.W., Davison, J.B. and Plank, R.J. (2008) Numerical simulation of bolted steel connections in fire using explicit dynamic analysis. *Journal of Constructional Steel Research*, **64**, 515–525.
- Yu, H.X., Burgess, I.W., Davison, J.B. and Plank, R.J. (2009) Development of a yield-line model for endplate connections in fire. *Journal of Constructional Steel Research*, **65**(6), 1279–1289.
- Zhang, B., Su, M., Clifton, G.C., Abu, A.K. and Gu, T. (2014) Strength and stability of slab panel support beams. Proceedings of the 8th International Conference on Structures in Fire, 11–13 June 2014, Shanghai, China, pp. 255–264.
- Zienkiewicz, O.C. and Taylor, R.L. (1991) *The Finite Element Method*, 4th edn, McGraw-Hill, New York.

Index

- Ablation, 308
- Acceptable solution, 3
- Acoustic performance, 302, 331
- Active control, 12
- Active systems, 9, 17
- ADAPTIC, 370
- Additive method, 316
- Adhesives, 258, 296
- Adiabatic flame temperature, 38
- Advanced calculation methods, 340
- Advanced finite element modelling, 356
- Advanced hand calculation methods, 348
- After-fire stability, 149
- Allowable stress design, 117
- Alternative design, 3
- Anchorage failure, 200
- Applied loads, 101
- Approved fire resistance ratings, 103
- ASTM E119 standard fire, 61, 96, 149
- Auto-ignition, 39
- Automatic sprinkler systems, 12, 30, 38
- Axial restraint, 143, 220, 248

- Bailey-BRE method, 350, 353
- Batts, 309
- Blast, 101
- Bolted connections in steel, 188
- Bond failures, 200
- Boundary walls, 20
- Bricks, 33
- B-RISK, 48

- Broadgate, 349
- Buckling, 186, 245, 283
 - of timber studs, 322
- Building codes, 13, 37
- Burning period, 10, 50, 64
- Burning rates, 42
- Burnout, 20, 280

- Calorific values, 36, 42
- Cardington, 249, 310, 349
- Car parking buildings, 69, 251
- Cast-iron, 188
- Catenary action, 356
- Cavity insulation, 308
- Ceiling vents, 66
- Ceramic fibre, 309
- C-FAST, 48, 60
- Characteristic strength, 120, 265
- Charring rate, 262, 273
 - corner rounding, 275
 - protected timber, 276
 - realistic fires, 279
- Chemistry of gypsum, 306
- CIB formula, 92
- Cladding, 26
- Coefficient of convective heat transfer, 346
- Cold-rolled steel, 301
- Column buckling, 132, 359
- Combustible lining materials, 43
- Combustion, 37
- Component additive method, 295, 316

- Composite columns, 243
- Composite flooring, 235
- Composite slab design methods
 - Bailey-BRE method, 350
 - membrane action method, 350
 - slab panel method (SPM), 353
 - tensile membrane action, 349
- Composite steel-concrete structures, 234, 349
- Computational fluid dynamic (CFD), 48, 341, 343
- Computer fire models, 341
 - CFD models, 343
 - plume models, 342
 - post-flashover models, 343
 - zone models, 342
- Concealed spaces, 23
- Concepts tree, 14
- Concrete encasement, 167, 236
- Concrete filled tubes (CFT), 236, 247
- Concrete masonry, 199
- Concrete-steel composite structures, 234, 349
- Concrete tilt-panels, 252
- Concrete walls, 223
- Conduction, 69
- Cone calorimeter, 23, 39
- Confinement of concrete, 210
- Containment of fire, 17
- Continuity, 102
- Continuous steel beams, 185
- Convection, 69, 72
- Cooling phase, 356
- Corner rounding, 275
- Cover concrete, 201
- Cracking of concrete, 366
- Creep, 126, 273, 360
 - strain, 128, 173, 209
- Critical temperature method, 240
- Cross laminated timber (CLT), 257, 288
- Crushing of wood, 265
- Curtailment of reinforcing, 219

- Decay period, 10, 64
- Density, 69
 - concrete, 204
 - steel, 159
 - wood, 263
- Design equation, 84, 123
- Design fires, 60
- Disproportionate collapse, 136
- Doors, 9, 23, 110
- Dowel-type fasteners, 292
- Drywall, 301
- Ductility, 120, 248
- Duration-of-load factor, 266

- Earthquakes, 30
- Effective cross section method, 282

- Elastomeric adhesives, 302
- Electrical outlets, 332
- Emissivity, 73, 346
- Enthalpy approach, 347
- Environmental protection, 9
- Epoxied connections, 297
- Equal area concept, 90
- Equivalent fire severity, 90
 - equal area concept, 90
 - maximum load capacity concept, 92
 - maximum temperature concept, 91
 - time equivalent formula, 92
- Eurocode
 - formula, 93
 - parametric fires, 62
- European yield model, 293
- External fire, 62
- External steelwork, 165

- Fall-off time for gypsum board, 277
- Fibrous plaster, 305
- Field models, 48
- Finger joints in wood, 296
- Finish rating, 319
- Finite difference methods, 344
- Finite element methods, 344, 355
- Fire compartments, 20
- Fire design time, 20
- Fire detection, 12
- Fire development, 9
- Fire doors, 110
- Fire during construction, 29
- Fire Dynamics Simulator (FDS), 48, 343
- Fire endurance rating, 95
- Fire exposure models, 88
- Firefighters, 12
- Fire loads, 65
- Fire models, 341
- Fire resistance, 3, 17
 - rating, 95, 260, 311
 - tests, 61
 - applied loads, 101
 - failure criteria, 97
 - furnace pressure, 101
 - restraint and continuity, 102
 - small scale furnaces, 103
 - test equipment, 96
- Fire retardant chemicals, 261
- Fire spread, 22
- Fire stopping, 24, 334
- Fire suppression, 9
- Fire testing of floors, 100
- Flame spread, 22, 39, 43
- Flaming brands, 28
- Flashover, 9, 35, 48
- Foam plastic sandwich panels, 339

- Fuel, 35
 - controlled burning, 53, 59
 - fraction, 54
 - load, 22
 - energy density, 37
- Full room involvement, 10, 48
- Fully developed fire, 10, 48
- Furnace pressure, 101
- Furniture calorimeter, 40

- Gap width, 287
- Generic ratings, 95, 103, 157
- Glass, 112
- Glass fibre
 - batts, 309
 - reinforcing, 307
- Glazed doors, 110
- Glued timber connections, 296
- Glue laminated timber (glulam), 257
- Grillage models, 200
- Growth period, 10, 11
- Gypsum board, 34, 294, 301
- Gypsum chemistry, 306

- Harmathy's ten rules, 105
- Heat balance, 58
- Heated wood layer, 277
- Heat release rate, 22, 37, 40, 51
- Heat transfer
 - conduction, 69
 - convection, 72
 - radiation, 72
- Heat transfer model, 105
- Heavy timber, 257
- High strength concrete, 196
- Historical buildings, 112
- Hollow core
 - concrete slabs, 200
 - timber floors, 288
- Human behaviour, 11
- Hydrocarbon fire, 62

- Ignition, 10, 29, 39
- Impregnation of wood, 261
- Incipient period, 10
- In-grade tests, 266
- Insulation criterion, 99
- Integrity criterion, 99
- Intumescent paint, 9, 169
- ISO 834 standard fire, 61, 96

- Joule (J), 6
- Junctions and gaps, 110

- Kawagoe's equation, 51, 56
- Knots in wood, 265

- Laminated veneer lumber (LVL), 257
- Lateral torsional buckling, 134, 184, 283
- Law formula, 93
- Life safety, 8, 20
- Light steel
 - frame, 302
 - joists, 243
- Light timber frame, 257, 301
- Lightweight concrete, 198
- Lightweight sandwich panels, 335
- Light wood frame, 257, 301
- Limit states design, 117
- Load and resistance factor design (LRFD), 117
- Load combinations, 116, 124
- Load ratio, 125
- Loads for fire design, 124
- Local buckling, 249, 356
- Localized fires, 69

- Masonry, 33, 199
- Material properties in fire, 126
- Maximum load capacity concept, 92
- Maximum temperature concept, 91
- Mechanical properties
 - concrete, 207
 - steel, 171
 - wood, 264
- Megawatt (MW), 6
- Melting temperature, 32
- Membrane action method, 350
- Mesh sensitivity, 347
- Mill construction, 258
- Mineral wool insulation, 309
- Modulus of elasticity
 - concrete, 207
 - steel, 178
 - wood, 266
- Moisture content, 266, 347
- Moment redistribution, 140
- Multi-storey steel frame buildings, 248

- Nailed gusset connections, 295
- Nails, 293
- Numerical analysis, 355
- Numerical simulation, 348

- One-zone model, 343
- Onset of char method, 318
- Oxygen consumption calorimetry, 39
- OZONE model, 60, 344

- Parallel chord timber trusses, 310
- Parallel to grain wood properties, 267
- Parametric fires, 62
- Party walls, 333
- Passive control, 12

- Passive systems, 9, 17
- Peak heat release rate, 40
- Penetrations, 24, 109, 332
- Performance-based
 - codes, 13, 22
 - design, 2
- Perpendicular to grain wood properties, 269
- Pilot ignition, 39
- Plaster of Paris, 304
- Plastic design, 142
- Plastic foam, 335
- Plasticity, 121, 267
- Plume models, 342
- Portal frame buildings, 252
- Post-flashover fires, 35, 49, 54, 343
- Post-tensioned timber structures, 289
- Precast concrete, 254
- Pre-flashover fires, 12, 35, 40
- Prescriptive building codes, 2
- Pres-Lam timber structures, 289
- Prestressed concrete, 199
- Prestressing steel, 33, 200
- Probabilistic design, 13
- Probability of failure, 121
- Progressive burning, 66, 68
- Proof strength of steel, 174
- Property protection, 8, 20
- Proprietary ratings, 95, 104
- Protected timber, 276
- Pyrolysis of wood, 38, 51, 261

- Quality control, 4

- Radiant heat flux, 72
- Radiation, 69, 72
- Ramberg–Osgood relationship, 361
- Realistic fires, 279
- Redundancy, 135
- Reinforced concrete
 - columns, 223
 - walls, 223
- Reinforced glulam timber, 289
- Relaxation, 126
- Repair of fire damage, 22, 31, 260
- Resilient channels, 331
- Restrained thermal expansion, 359
- Restraint in fire tests, 102
- Risk assessment, 4, 13
- Rockwool insulation, 309
- Roof vents, 67, 252

- Safety factors, 13, 21
- SAFIR, 71, 237, 347, 370
- Sandwich panels, 335
- Scenario analysis, 13

- Screwed connections, 293
- Section factor, 157
- Seismic gaps, 110
- Separating function, 314
- Shear strength of wood, 271
- Sheetrock, 301
- Shrinkage, 199, 209, 259, 320
 - gap, 317
- Simplified calculation methods, 340
- Single-zone models, 60
- Size effects, 266
- Skylights, 252
- Slab panel method (SPM), 353
- Slim-floor beams, 243
- Small-scale furnaces, 103
- Smoke, 11, 17, 38
- Smouldering combustion, 38
- Software packages, 369
- Spalling, 123, 201
- Specific heat, 69
- Spontaneous combustion, 39
- Spray-on fire protection, 169
- Sprinklers, 12, 30, 38
- Stability criterion, 97
- Standard fire, 61, 96, 149
- Steam bending of wood, 267, 324
- Steel-concrete composite floors,
 - 349, 365
- Steel-fibre reinforced concrete, 199
- Steel protection systems
 - board systems, 167
 - concrete encasement, 167
 - concrete filling, 170
 - flame shields, 171
 - intumescent paint, 169
 - protection with timber, 170
 - spray-on systems, 169
 - water filling, 171
- Steel stud walls, 325
- Stone wool insulation, 309
- Strength domain, 86
- Stress related strain, 128, 209
- Stress–strain relationships, 121, 264
- Swedish fire curves, 56, 59

- Tabulated ratings, 103, 157, 340
- TASEF, 72, 240
- Temperature domain, 85
- Tenability limits, 12
- Tensile membrane action, 249, 349
- Tensile strength of concrete, 361
- Thermal bowing, 365
- Thermal conductivity, 58
- Thermal diffusivity, 70
- Thermal inertia, 39, 58, 70

- Thermal modelling, 344
- Thermal properties, 58, 70
 - concrete, 204
 - gypsum, 306
 - steel, 159
 - wood, 262
- Thermal response models, 344
- Thermal strain, 128, 172
- Thomas's flashover criterion, 49
- Three-dimensional models, 365, 368
- Tilt-panels, 252
- Timber beam-columns, 285
- Timber columns, 283
- Timber-concrete composite floors, 288
- Timber connections, 290
- Timber decking, 286
- Timber fire protection for steel, 170
- Timber joist floors, 327
- Timber stud walls, 320
- Timber trusses, 328
- Time domain, 85
- Time equivalent formula, 92, 279
- Time temperature curves, 9, 55, 65, 345
- To adjacent rooms, 23
- To other buildings, 27
- To other storeys, 25
- Trade-offs, 21
- Transient creep, 126
- Transient strain, 129, 209, 362
- Truss plates in wood, 296
- t-squared fires, 44
- Two-way concrete slabs, 350
- Two-zone models, 47, 343
- Type X gypsum board, 276, 305
- Ultimate strength design, 117, 119
- Units, 6
- Ventilation, 10, 43, 63
 - controlled burning, 49, 59
 - factor, 52
- Virtual work, 142
- VULCAN, 370
- Water of crystallization, 309
- Watt (W), 6
- Windows, 12, 26, 29, 49, 59
- Within room of origin, 22
- Wood frame construction, 301
- Working stress design, 117
- World Trade Center, 5, 39
- Yield-line theory, 354
- Yield strength, 174
- Zone models, 47, 342